Transcriptional Regulation of Gene Expression in Lung Carcinoma Cells

A thesis submitted for the degree of Ph.D.
Dublin City University
By

Padraig Doolan BSc. (Biotechnology)

VOLUME 1 (of 2)
Abstract, Introduction,
Materials & Methods, Results

The research work described in this thesis
was carried out under the supervision of

Professor Martin Clynes Ph.D.

National Cell & Tissue Culture Centre
School of Biological Sciences
Dublin City University

2001

I hereby certify that this material, which I now submit for assessment on the program of study leading to the award of Ph.D. is entirely my own work and has not been taken from the work of others save and to the extent that such work has been cited and acknowledged within the text of my work.

Signed: Padraig Doolan I.D. No.: 96970413

Date: 18 - 1 - 02

Abstract

Previous studies in this laboratory have demonstrated that exposure to 5-Bromo-2-deoxyuridine (BrdU) induces differentiation in the lung epithelial cancer cell lines DLKP and A549. This induction of differentiation was accompanied by increased protein expression of cytokeratins-8 and -18, $\alpha_2\beta_1$ integrin, cell-adhesion protein Ep-CAM, eukaryotic initiation factor eIF-4E and the transcription factors c-*myc* and YY1.

Following exposure to BrdU, RT-PCR analysis identified large increases in the mRNA levels of MRP1, MRP3, BCRP, BAXα, MRIT, COX-2 and eIF-2α, together with smaller gene expression increases for MRP2, α-catenin and E-cadherin, in the DLKP cell line. Survivin gene and protein expression was decreased. Increased gene expression of MRP1 and BCRP, as well as decreased MRP2, MRP4 and mdr-1 gene expression was observed in A549. DNA microarray analysis of BrdU-treated DLKP detected significantly increased gene expression of ETR103, p55CDC, Ini1, NSEP, EB1, RPS19 and FNRB, and significantly decreased gene expression of CREB2, c-*myc*, RPL6, TBP, CNBP, HIP116 and SOD1.

RT-PCR analysis of the DLKP cells identified increased expression of the MRP1, MRP2 and BCRP genes following exposure to cisplatin, of MRP2, α-catenin and E-cadherin following exposure to taxol and of MRP1, MRP2 and α-catenin following exposure to VP16. These results suggested that patterns of gene induction following exposure to an inducing agent are specific for that agent.

Transfac™ transcription factor analysis of the 5' promoter regions of MRPs 1-3, BCRP, MRIT, COX-2, eIF-2α, α-catenin and E-cadherin identified seven potentially shared factors. These factors were GATAs 1-3, MZF1, Ik-2, CdxA and AML-1a. RT-PCR analysis revealed increased GATA-2 and GATA-3 expression in BrdU-treated DLKP, but no change in BrdU-treated A549. RT-PCR analysis also revealed increased GATA-2 expression in VP16-treated DLKP.

Luciferase reporter plasmids attached to truncated regions of the MRP1 5' promoter identified the major regulatory region in normal DLKP cells. This region encompassed –91 to +103 bases relative to the transcriptional start site. When the DLKP cells were treated with BrdU, luciferase production increased dramatically in another area of the promoter (beween -91 and –411 bases, relative to the transcriptional start). This region of the MRP1 contains a single GATA-2 transcription factor recognition sequence. A similar result was observed following exposure to VP16. However, no significant change in luciferase readings was observed between BrdU-treated and untreated cells over the whole 2kb promoter, indicating that the major transcriptional target for BrdU is outside this region of the gene.

RT-PCR analysis on a number of human lung, breast and oesophageal tumour samples was carried out to examine the expression of MRPs 1-6, BCRP, mdr-1, mdr-3, COX-1, COX-2, MRIT, BAXα, Bcl-x_L, Bcl-x_S, Bcl-2α, Survivin, BAG, BAP, eIF-4E, eIF-2α and c-*myc*.

A novel ribozyme to MRP1 was designed and was observed to cleave its intended target in an *in vitro* cleavage assay. The ribozyme was successfully transfected into MRP1-expressing DLKP-SQ cells. However, the transfections did not affect significantly neither MRP1 RNA or protein expression nor the drug resistance profiles of the cells.

RNaseH activity assays for antisense oligonucleotides analyses were also successfully set up using an mdr-1 antisense. However, the identification of effective MRP1 antisense oligonucleotides was not made by either *in vitro* or *in vivo* studies.

Acknowledgements

I would like to thank Prof. Martin Clynes for his kindness, understanding and vision throughout the Ph.D. Especially in this last year, his guidance and help has been invaluable.

I would also like to thank Dr. William Beck and Dr. Kevin Scanlon, who provided plasmids used in the course of this work. Thanks also to Dr. Vincent Lynch and Dr. Enda McDermott of St. Vincent's hospital, Dublin, for providing clinical samples, and to Drs. Arnold Hill, Louise Kelly & Susan Kennedy for additional assistance.

A large thank you must go to Dr. Carmel Daly for all her efforts in proovreeding this thesis. Also thanks to Dr. Toni O'Doherty, my Postdoc. in the early days. Also, thanks to Rob for making sure the computers kept running to facilitate our e-mail, games,...oh, and the work as well!

Thanks to Carol, Yvonne and Mairead for keeping the whole place ticking over.

Also, thanks to all others in the Centre who contributed to this thesis. This not only includes the work done by Yizheng Liang, Niall Barron, John Cahill & Rasha Linehan, but all those who were available to give advice and guidance through the years. You are too numerous to mention, I've borrowed a lot! Thanks to Dee for the primers but more for the friendship through many a depressing evening. Thanks also to John for all the work he did and also for his completely uninteresting facts about football, of which he knows nowt. Also thanks to all the rest of the "buds" in the lab, for the craic in the good times and the merciless slagging in the bad, in no particular order; Rasha, Bella, Mick, Niall, Paddy, Helena, Finbar, Mary, Sharon and anyone else I've forgotten!

To Mam and Dad, who supported me through it all, this is definitely your moment as much as it is mine. To the bruds, Mike and Den, and my sister Rose, who all probably thought this day would never come, thanks for always being there, I'm lucky to have you all for my family. I owe you everything.

Thanks to the Grizzies, especially Anna, Dermo & Anne, who gave of their time to help complete this thesis and of their company too many times to mention over the years. Thanks also to the rest of the grizzie crew, Sinead, Sile, Ron & Ritchie.

Thanks to my out of work buddies – I won't mention you all here, you know who you are. Now you can all finally stop asking the "when are you going to finish?" question.

And last, but certainly not least, thanks to Kate, who has been through every step of this thesis with me and without whom not a move would have been made. Cheers babe, this one's for you.

For Mam, Dad,

Kate & Orla

Abbreviations

Ab	-	Antibody
ABC	-	ATP Binding Cassette
AMP	-	Adenosine Monophosphate
AS	-	Antisense
ATP	-	Adenosine-triphosphate
ATCC	-	American Tissue Culture Collection
BrdU	-	Bromodeoxyuridine
BSA	-	Bovine Serum Albumin
CAM	-	Cell Adhesion Molecule
cDNA	-	Complementary DNA
Da	-	Daltons
DEPC	-	Diethyl Pyrocarbonate
DMEM	-	Dulbecco's Minimum Essential Medium
DMSO	-	Dimethyl sulfoxide
DNase	-	Deoxyribonuclease
DNA	-	Deoxyribonucleic Acid
dNTP	-	Deoxynucleotide triphosphate (N= A, C, T, G or U)
DTT	-	Dithiothreitol
ECM	-	Extracellular matrix
EDTA	-	Ethylene diamine tetracetic acid
ELISA	-	Enzyme Linked Immuno Sorbent Assay
FCS	-	Fetal Calf Serum
GAPDH	-	Glyceraldehyde-6-phosphate dehydrogenase
GSH	-	Glutathione
GST	-	Glutathione-S-Transferase
GS-X Pump	-	GSH-conjugate export carrier
HEPES	-	N-[2-Hydroxyethyl]piperazine-N'-[2-ethanesulphonic acid]
HIV	-	Human Immunodeficiency Virus
H-SFM	-	Ham's F12 Serum Free Medium
IC_{50}	-	Inhibitory Concentration 50%
Ig	-	Immunoglobulin

IMS	-	Industrial Methylated Spirits
K	-	Keratin (cytokeratin)
kDa	-	Kilo Daltons
LRP	-	Lung Resistance-related Protein
MA	-	MRP1 Antisense
MAb	-	Monoclonal Antibody
MDR	-	Multiple Drug Resistance
MRP	-	Multidrug Resistance-associated Protein
MEM	-	Minimum Essential Medium
min	-	Minute(s)
MMLV-RT	-	Moloney Murine Leukemia Virus-Reverse Transcriptase
mRNA	-	Messenger RNA
MWM	-	Molecular Weight Marker
NCTCC	-	National Cell & Tissue Culture Centre
NRK	-	Normal Rat Kidney
NSCLC	-	Non-Small Cell Lung Carcinoma
OD	-	Optical Density
Oligos	-	Oligonucleotides
P	-	Passage
PBS A	-	Phosphate Buffered Saline A
PEG	-	Polyethylene Glycol
PCR	-	Polymerase Chain Reaction
Pgp	-	P-glycoprotein
pHβ	-	pHβApr-1-neo expression vector
PKA	-	cAMP-dependant protein kinase
PO	-	Phosphodiester
PS	-	Phosphorothioate
RA	-	Retinoic Acid
RNA	-	Ribonucleic Acid
RNase	-	Ribonuclease
RNase H	-	Ribonuclease H
RNasin	-	Ribonuclease Inhibitor
rpm	-	Revolution(s) Per Minute

RT-PCR	-	Reverse Transcriptase-PCR
Rz	-	Ribozyme
SCLC	-	Small Cell Lung Carcinoma
SDS	-	Sodium Doedecyl Sulphate
sec(s)	-	Second(s)
SF	-	Serum-Free
SFM	-	Serum-Free Medium
TBE	-	Tris-boric acid-EDTA buffer
TBS	-	Tris Buffered Saline
TE	-	Tris-EDTA
Topo II	-	Topoisomerase II
Td	-	Thymidine
TEMED	-	N, N, N', N'-Tetramethyl-Ethylenediamine
Tris	-	Tris(hydroxymethyl)aminomethane
UHP	-	Ultra high pure water
V-SCLC	-	Variant Small Cell Lung Carcinoma
v/v	-	volume/volume
w/v	-	weight per volume

Table of Contents Page

Volume 1:

Section 1.0

Introduction

1.1 General Introduction

One of the central goals of the gene expression field is understanding how a mammalian organism regulates transcription of approximately 30,000 genes in the proper spatial and temporal patterns. Knowledge of how transcription factors function during this "differential" gene expression can be applied to fundamental issues in the fields of biology and medicine. To decipher these mechanisms, we need to understand the numerous processes influencing transcription and develop technical and strategic approaches for addressing them. A gene's regulatory mechanisms may be of interest for a wide variety of reasons. The gene may be expressed with an interesting temporal or spatial pattern during the development of a cell or organism, suggesting that the gene's regulatory factors play an important developmental role. Alternatively, aberrant regulation of the gene may contribute to a particular disease, or the gene may be specifically expressed in a cell type associated with disease. In these instances, the regulatory factors may contribute to an understanding of disease pathogenesis or may provide targets for therapeutic intervention.

Lung cancers are of two principal types; Small Cell Lung Cancer (SCLC) and Non-Small Cell Lung Cancer (NSCLC). SCLC tends to spread rapidly, which normally discounts the use of surgery as an effective treatment. As a result, treatment normally consists of chemotherapy alone, or sometimes combined with radiation. NSCLC is normally refractory to chemotherapy, and so alternative combination treatments, such as surgery and radiotherapy, are usually employed. Strategies designed to treat lung cancers have been severely impaired by the lack of knowledge regarding the biological mechanisms controlling the differentiation and development of both normal and disease states of the lung. Despite recent advances in modern medical science little has been achieved in increasing the life expectancy of those diagnosed with lung cancer. Clearly, an alternative approach to the treatment of the disease in the lung would be of benefit, both to researchers and patients.

In the post-genome era it may soon be possible to associate a specific tumour type with a specific gene expression profile and to define each molecular lesion characteristic of any given cancer. It is intuitive that a successful therapeutic strategy for cancer should aim at elucidating the mechanisms underlying disease development and differentiation

which ultimately lead to full-blown neoplastic transformation. This approach is now rendered possible by major advances along several lines of investigation;

1. The possibility of analysing gene expression through high throughput methods
2. A more detailed knowledge of the regulatory regions and of the transcription factors that control gene expression also facilitated in the future by a comprehensive whole genome comparative analysis of these regulatory sequences
3. The ability of modulating gene expression at the single gene level through various approaches both pharmacological and biochemical

The purpose of this study is to advance the understanding of an alternative regimen of cancer treatment currently referred to as "Differentiation Therapy" (Roth, 1992; Lotan, 1996). Little is currently known of the transcriptional processes underlying differentiation in the lung. It is hoped from this analysis that a more detailed picture of transcriptional control in BrdU- and drug-induced lung cancer differentiation and gene expression may be postulated. This information may ultimately assist in identifying transcriptional targets for the therapeutic treatment of lung cancer.

1.2 Introduction to Cellular Differentiation and Stem Cell Theory

Cellular differentiation can be defined as the process leading to the expression of the phenotype characteristic of the functionally mature cell *in vivo*. Ham and Veomott (1980) described the process as "a cell acquires or displays a new phenotype without changing its genotype". As differentiation progresses, cell division is reduced and eventually lost (Davila *et al.*, 1990).

The principal cells that differentiate are stem cells, which are capable of rapid cell growth and division. These cells are multipotent and thus have the potential to differentiate into several different cell phenotypes. In general, they possess unlimited proliferative potential but they can remain quiescent under certain microenvironment conditions (Davila *et al.*, 1990). Differentiated cells are thought to be produced, not directly from stem cells, but rather via a committed progenitor or transit amplifying population (Watt, 1991). These cells continue and commit to differentiated cell types, allowing continual regeneration of the stem-cell population. It is important to note that although stem cells are capable of differentiating into multiple cell lineages, this is not their defining characteristic.

1.2.1 Gene expression and differentiation

The destiny of a cell during embryogenesis and development is regulated by gene expression which restricts the number of lineages that stem cells have the potential to form. Previous studies (Ham and Veomott, 1980) have proposed that "determination" is a process whereby a cell becomes committed to differentiate into a specific lineage. A determined or committed cell initially may not appear phenotypically different; this only occurs after the genetic blueprint has been implemented (Maclean and Hall, 1987). A cell can differentiate in a manner that results in either the irreversible loss of its proliferative properties (terminally differentiated), or in the retention of some of its proliferative capacity while the cell itself is fully differentiated (non-terminally differentiated). A number of other differentiation states are also well documented: dedifferentiation is the process by which a cell loses its differentiated phenotype and transdifferentiation occurs when a cell dedifferentiates and then redifferentiates into a

new and distinct phenotype (Davila *et al.*, 1990). It is apparent from this that as a cell undergoes differentiation, its gene expression profile will likewise change. This will be discussed in greater detail in later sections.

1.2.2 Differentiation mediated via tissue determined stem cells

A progenitor stem cell represents the progeny of stem cells which possess more limited proliferation and differentiation potential. This cell is usually only involved in a single cell lineage. Although stem cells in adult organs are pluripotent, the differentiated descendants are not usually expressed beyond the relevant organ in which the stem cell occurs, i.e. these stem cells are tissue determined stem cells (TDS cells) and are thus considered separate from embryonic stem cells (ES cells) (Sell, 1994).

1.2.3 The cell cycle and differentiation

TDS cells are believed to undergo a slow cell cycle in order to reduce the risk of errors during DNA replication. As TDS cells are present throughout the life of the organism, such errors could become amplified in the organism (Lajtha, 1982). Indeed it is proposed that most tumours contain TDS cell populations (Khan *et al.*, 1991) and that the overlapping expression of differentiation markers (Gazdar *et al.*, 1988) within cancer cells is indicative of a stem cell origin for most lung epithelial tumours.

1.2.4 Models of cell differentiation

During the differentiation process of TDS cells it is necessary that they maintain a constant cell number. One popular model for this is asymmetrical cell division. According to this model, when the stem cell divides one daughter cell remains a stem cell while the other becomes a transit cell and enters the differentiation process. This model suffers from a fundamental flaw in that it suggests that after receiving an appropriate stimulus it proceeds into a cell cycle that yields two different daughter cells (Lajtha, 1982). According to a model proposed by Holtzer *et al.* (1975), TDS cells are

only capable of binary decisions, e.g. stem cell A is capable of generating cells B or C, and cell B may then differentiate to cells D or E. As the transit cells pass through this hierarchy they go through cell division.

Although proliferation and differentiation appear to be interlinked processes during stem cell maturation, they are quite separate events that occur concomitantly. This suggests the whole differentiation process may be understood in terms of a spiral model (Potten and Loffler, 1990). Some TDS cells appear to be highly pluripotent giving rise to several different cell lineages, e.g. the haematopoietic system. Given this pluripotency, it can be envisaged that depending on the signal, a stem cell will adopt one direction of maturation over another.

1.3 Differentiation in the Lung

The lung is an extremely complex organ consisting of over 40 different cell types, allowing it to function as the principal gas exchange organ in the body. At least seven epithelial cell types lining the tracheobronchial airways have been identified. The lungs are organised into the intrapulmonary airways (bronchi and bronchioles) which account for 6-10% of the lungs volume, and the gas exchange area or parenchyma which accounts for approximately 80-90% of the lung volume.

1.3.1 Models of Lung differentiation

While the processes behind differentiation of epithelial and other cell systems are relatively well understood (Fuchs and Byrne, 1994), lung cell developmental biology lags behind. This is partly due to a failure to identify a stem cell of the lung. The principle of stem cells and their *in vitro* cultivation and manipulation is now well established for a number of tissue types. The existence of a stem cell in the lung is strongly suspected, given the ability of the lung to regenerate when exposed to local damage by atmospheric components (e.g. smoke, carbon black particles) and by lipophilic chemicals absorbed (e.g. through the gut) into the blood stream. However, identification of such a stem cell is hampered by the complexity of the respiratory system and the variety of cell types present (Plopper and Hyde, 1992; Paine and Simon, 1996; Mariassy, 1992).

1.3.2 Theory of common stem cell origin in lung cancer:

The most predominant hypothesis for stem cells *in vivo* in lung is that a different set of progenitor cells exist (including basal cells) each destined to give rise to a discrete differentiated cell type (Evans *et al.*, 1989; Jetten, 1991; Plopper *et al.*, 1992). In the case of type II cells, these cells proliferate and then differentiate into type I cells (Adamson and Bowden, 1979) and Clara cells can differentiate into ciliated cells (Jetten, 1991).

However, an alternative proposal is that there is a single pluripotent stem cell for generating ciliated cells, Clara cells and the other differentiated cell types (McDowell, 1987). This hypothesis suggests the existence of a monotypic stem cell, which is believed to be able to arise through dedifferentiation of any differentiated secretory cell type. There is some empirical evidence for this hypothesis as Clara cells are found to be positive for surfactant protein-A (SP-A) and surfactant protein-B (SP-B) which were originally described as specific products of type II pneumocyte cells. This suggests that Clara cells and type II pneumocytes are derived from the same stem cell.

Further tentative indications come from studies of fetal mouse lung where a definite population of progenitor cells co-express SP-A (type II cells), cc10 (Clara cells), and calcitonin gene-related protein (CGRP) (pulmonary neuroendocrine cells), each being a gene product used to indicate differentiated function in a different respiratory epithelial cell type (Wuenschell *et al.*, 1996). The studies reviewed by Emura (1997) suggest the possibility of a single population of pluripotent stem cells in the lung with the additional possibility of de-differentiation of ciliated, secretory and basal cells to provide the lung with regenerative capacity.

The presence of common overlapping features between lung cancer cell types supports the theory of a common stem cell origin for lung epithelial cancers. Gazdar *et al.* (1981) outlined how all the cells of the bronchial epithelium and the tumours which arise from them could have a common stem cell origin. The transforming events which lead to carcinogenesis affect undifferentiated or partially-differentiated cells. There are many reports in the literature of evidence for the presence of stem cell populations in tumour cell lines (Khan *et al.*, 1991). Gazdar *et al.* (1981) also suggested that the overlapping expression of markers between different tumour types is indicative of a common stem cell origin of lung epithelial cancers.

In summary, very little data exists about stem cells in the lung, the pathways they follow, their distribution and mechanism of action. No markers yet exist for lung stem cells. The idea of dedifferentiation is in contrast to the stem cell models developed in skin, liver and intestine in which the stem cell pre-exist in the epithelium (Emura, 1997). The lung is susceptible to local damage from a number of sources, as outlined. Therefore, it must possess some form of mechanism to regenerate itself, even if limited.

In attempting to identify if a cell is a stem cell, its native state is often altered during the investigation. This may result in loss of the stem cell or only a limited spectrum of responses being observed from the cell. Thus, due to the variety of cell types present and by the complexity of the respiratory system, identification of a lung stem cell is a difficult task.

1.3.3 Identification of a stem-like lung cell line, DLKP:

All of this has interesting implications with the isolation of a poorly-differentiated lung cell line, DLKP, at the NCTCC (Law *et al.,* 1992). Clones derived from this cell line exhibit the remarkable capacity to regenerate the mixed parental population over time. The DLKP novel cell line has been categorised as extremely poorly differentiated and consists of at least three subpopulations, termed SQ (Squamous), I (Intermediate) and M (Mesenchymal) (McBride *et al.,* 1998). These populations have shown the ability to interconvert and eventually, when cultured alone, replenish the parental phenotype. This, combined with the lack of expression of a number of differentiation-specific markers, has lead to the speculation that DLKP may represent a stem cell-like population. This has afforded a unique opportunity to study the process of lung cancer differentiation *in-vitro*, particularly the early stages of this process. Such studies will provide valuable insights into the mechanisms of early lung development, both in diseased and normal tissues, possibly identifying targets for therapeutic intervention and aiding in the design of strategies to treat lung cancers more effectively.

1.4 Cancer and Differentiation Therapy:

Cancer has been referred to as a "disease of abnormal differentiation" (Sporn and Roberts, 1983) and is theoretically a prime target for "Differentiation Therapy" (Roth, 1992; Lotan, 1996). Induction of differentiation has been considered as a possible component of therapy for cancer (Waxman *et al.*, 1988). The ultimate objective of this strategy is not aimed at killing the tumour so much as to induce the cancer cells, whose growth rate and cell cycle have become deregulated, to commit to differentiate into more "normal" cells in an attempt to slow and even halt growth and progression of the cancer. It is hoped that if differentiation-induced cancer cells lose their proliferative ability and cease to grow, then an examination of the molecular processes underlying this change would be of importance. It is this concept which formed the main objective of this study.

In vivo and *in vitro* studies support the role for differentiation defects early in the process of carcinogenesis. This may be due to the uncoupling of the integrated control of differentiation and proliferation in cancer cells, where such developments can result in a relative insensitivity to differentiation signals and increased sensitivity to proliferation signals. Two scenarios thus exist for the possible origins of cancer; from dedifferentiation of mature cells which retain the capacity to divide or from maturation arrest of immature cells. With increasing tumour progression, the histology of the tumour often indicates poorer differentiation and from a prognostic standpoint, patients with poorly differentiated tumours will generally have a lower survival rate than those with differentiated tumours (Behrens, 1994).

1.4.1 Physiological inducers of differentiation

A number of physiological agents involved in the modulation of lung differentiation *in vivo* have been identified, although their mechanisms of action remain largely unknown.

A number of studies using isolated lung cells (both adult and fetal) and cell lines have implicated a number of candidate factors including glucocorticoid steroids (Palmiter,

1972; Speirs *et al.*, 1991), chemokines (Sundell *et al.*, 1980; Lesur *et al.*, 1992), cell-matrix and cell-cell interactions (McCormick *et al.*, 1995; Speirs *et al.*, 1991).

Brurserud *et al.* (2000), reviewed that acute myelogenous leukaemia (AML) cells could be differentiated into further subsets following exposure to all trans-retinoic acid (ATRA) and several cytokines, such as IL-3 and GM-SCF. Thalidomide was also observed to be an effective differentiating agent on human leukaemia K562 cells by Hatfill *et al.* (1991). A combination of GM-CSF and 1,25-dihydroxy Vitamin D3 induced differentiation in human monoblast U937 leukaemia cells. A further differentiation study on the U937 cell investigating the differentative properties of low-dose ara-C line also included another leukaemic cell line, HL60 (Pinto *et al.*, 1988). Another study (Glazer *et al.*, 1986), observed induced differentiation in HL-60 cells following treatment with the cyclopentenyl analogue of cytidine. 1,25-dihydroxy Vitamin D3 also induced differentiation in two studies (Taoka *et al.*, 1993; Muto *et al.*, 1999). In the first study, Taoka *et al.* reported that interaction of the vitamin with HL60 cells induced differentiation of that cell line into monocyte cells. In the second study, Muto *et al.* examined the differentiation of a novel retinoic acid-resistant APL cell line (UF-1) following exposure to the vitamin. The vitamin induced growth inhibition and G1 arrest which resulted in differentiation of the cells towards granulocytes.

One of the first differentiation strategies to show promise in both *in vitro* and *in vivo* trials was that of the Vitamin A based differentiation-inducing compounds (Gendimenico and Mezich, 1993; Lotan, 1996). Natural retinoids have been found to play an important role in the maintenance of the normal differentiated state of the adult lung (Chytil, 1992). Retinoids thus play an important role in cancer differentiation and chemoprevention (Lotan, 1996). Retinoic acid (RA), has been implicated in the control of both cellular proliferation and differentiation, and has been shown to effect over 200 different gene products (Chytil, 1992). For example, RA regulates elastin production by lung fibroblasts during alveolar formation (McGowan *et al.*, 1995). In clinical trials, topical application of Retinoic Acid (RA) was shown to reduce the formation of skin papillomas (Tenenbaum *et al.,* 1998). Retinoic Acid has shown very strong potential as a therapeutic in cases of APL (Acute Promyelocytic Leukaemia) (Asou *et al.,* 1998) and AML (Acute Myeloid Leukaemia) (Tallman, 1996) reducing the risk of relapse and increasing the chance of long-term survival (Takeshita *et al.,* 1995; Degos, 1997).

Alternative approaches, including the development of novel RA metabolism blocking agents that increase endogenous levels of RA by inhibiting its breakdown in cancer cells (Sciarra *et al.,* 1998), are currently being applied to the treatment of prostate cancer.

1.4.2 Artificially-induced differentiation and gene expression

The gene expression profiles of cells change with the differentiation status of the cell. As a result, the cellular expression of certain genes and proteins may sometimes be used as markers to indicate the level or occurrence of differentiation in that cell. Although none of these gene changes may be defined as differentiation markers, there is enough evidence from differentiation studies to demonstrate the relevance of gene expression to the process of cellular differentiation.

c-fos mRNA expression was observed to be increased in a number of cell lines following exposure to the D vitamin analogue 1,25-dihydroxy Vitamin D3 (Kim *et al.*, 1991; Taoka *et al.*, 1993). c-*myc* gene expression was also decreased in both of these studies, which were associated with an induced differentiated phenotype of the cells. Pinto *et al.* (1988) also detected increased c-fos gene expression and decreased c-*myc* expression in the HL60 cell line following low-dose ara-C-induced differentiation. An increase in mRNA and protein expression levels of the cyclin-dependant kinase inhibitors p21 and p27 was observed by Muto *et al.* (1999) in the retinoic acid-resistant APL cell line (UF-1) following exposure to 1,25-dihydroxy Vitamin D3. An analogue of the D3 vitamin, EB 1089, was also observed to enhance the toxicity effect of adriamycin in MCF-7 breast tumour cells and also to promote apoptotic cell death in these cells (Sundaram *et al.*, 2000).

Retinoic acid (RA) also induces the differentiation of the murine P19 teratocarcinoma cell line (Scheibe *et al.*, 1991). In the same study, an increase in expression of alkaline phosphatase (ALP) mRNA and protein was also observed. RA also induces differentiation in human cancer cell lines, with a concomitant increase in expression of certain genes. Liu and Rabbani, (1995) observed an increase in expression of urinary plasminogen activator (uPA) mRNA and protein in the human prostate cancer cell line,

PC-3, following exposure to RA. Exposure to the chemical also resulted in increased invasiveness of the cell line.

Park *et al.* (1999) observed induced expression of the CCAAT/enhancer binding protein ε (C/EBPε) in the acute promyelocytic leukaemia (APL) cell line following exposure to retinoic acid (RA). The group observed that C/EBPε, a nuclear transcription factor expressed predominantly in myeloid cells, is a downstream target gene responsible for RA-induced granulocytic differentiation of APL cells.

Expression of the mdr-1 gene has also been examined following treatment of mdr-1-expressing cells with differentiating agents. Mickley *et al.* (1989) found that expression of mdr-1/Pgp correlated with the degree of differentiation in SW-620 and HCT-15 cell lines exposed to sodium butryate, dimethyl sulfoxide and dimethylformamide. However, the group also found that its induction was not always accompanied by expression of the multidrug-resistant phenotype. Zhou *et al.* (1993) induced a promyelocytic HL60/DNR cell line to differentiate using all-trans retinoic acid (ATRA) and dimethyl sulfoxide and observed that mdr-1 mRNA and protein expression levels remained unaffected.

1.4.3 Use of Bromodeoxyuridine (BrdU) to induce differentiation in human cells

5-Bromo-2'-deoxyuridine (BrdU) has been used for twenty years as a tool for measuring DNA synthesis in isolated chromosomes and in cells and tissues. BrdU is a thymidine (Td) analogue which can compete with Td for incorporation into DNA. It appears to be capable of modulating differentiation in a number of cell lineages. Its activity is reversible if removed from the culture medium or if thymidine is added to the growth medium in equimolar concentrations (Ashman and Davidson, 1980). This indicates that BrdU is not acting as a mutagen, but is reversibly blocking specific differentiation pathways.

1.4.3.1 Examples of BrdU-induced differentiation

Low levels of BrdU have been shown to alter the differentiation status of different kinds of cells. It is best referred to as a differentiation modulating agent since it has been shown to be a potent inducer of differentiation in some cell lines (Yen *et al.,* 1987; Sugimoto *et al.,* 1988; Valyi-Nagy *et al.,* 1993), while it can inhibit the differentiation of others (Seecoff and Dewhurst, 1976, Tapscott *et al.,* 1989). The exact mechanism by which BrdU exerts its differentiation-modulating effects is unclear but incorporation into DNA is seen as essential. This involves BrdU being converted to bromodeoxyuridine monophosphate, which competes with thymidine for incorporation into DNA (O'Neill and Stockdale, 1974). Experimental evidence for this hypothesis comes from a study by Keoffler *et al.* (1983) which showed that a thymidine kinase-deficient human myeloid cell line (HL-60) was unable to incorporate BrdU into its DNA and subsequently failed to respond to the ability of BrdU to modulate its differentiation status.

BrdU has also been found to induce differentiation of melanoma cells, with a resultant change in morphology. Flattening of the cells, with a 20-fold increase in cell surface area and a 17-fold increase in nuclear area was observed (Valyi-Nagi *et al.*, 1993). Tumourigenicity of these cells in nude mice was suppressed when the cell lines were treated with BrdU. Colony formation in soft agar of these BrdU-treated cells was also decreased by more than 10% at a 10μM concentration compared to untreated cells (Valyi-Nagi *et al.*, 1993).

BrdU has been shown to induce terminal differentiation in HL60 leukaemic cells (Yen and Forbes, 1990). BrdU induces the early events, leading to precommitment to the onset of terminal differentiation along the myeloid or monocytic pathways. BrdU has also been found to induce differentiation in human myeloid leukaemia cells (Koeffler *et al.*, 1983).

BrdU has also been observed to induce Schwannian differentiation in neuroblastoma (Sugimoto *et al.*, 1988). BrdU treatment of neuroblastoma cells has been shown to upregulate expression of human melanoma-associated antigen (Feyles *et al.*, 1991a).

Feyles *et al.* (1991b) examined the effects of BrdU on a SCLC cell line with features of neuroendocrine differentiation. Treatment resulted in induction of substrate-adherent growth, along with an epithloid morphology and increased expression of neuroendocrine markers.

1.4.3.2 Models of BrdU-induced differentiation:

A number of models exist to explain the ability of BrdU to modulate differentiation. The first envisages that BrdU induces chromosomal breakages and incorporates into DNA in a non-random fashion at sequences termed "fragile sites" (Hecht *et al.,* 1988; Sutherland, 1988; Sutherland, 1991). These fragile sites have recently been correlated with predisposition to colon cancer (Tunca *et al.*, 2000). These breakages and the associated chromosomal aberrations can be associated with stepwise changes in the differentiation of a cell. Some corroboration for this model comes from a study by Schwartz and Snead (1982) which found that BrdU seemed to concentrate within repetitive DNA nucleotide sequences rather than randomly throughout the nuclear DNA. However, such selective incorporation would suit the other models also. This explains the reproducibility of the effects observed with BrdU-induced differentiation. O'Neill and Stockdale (1973) developed a model for BrdU-induced modulation of differentiation that assumes that BrdU "sensitivity" resides on a single pair of chromosomes, suggesting the presence of a "master gene" or target through which BrdU exerts its effects. In this model, inhibition of differentiation occurs in a dominant fashion if approximately 30% or more of naturally occurring thymidine is replaced by BrdU in the readout strand of either chromosome. This sort of model agrees with the predicted mechanisms of action of a number of DNA-intercalating agents. BrdU substitution into DNA and intercalation of such agents may have similar effects, thought to be through direct DNA bending at either major or minor grooves, thereby altering promoter structure and availability to transcription factors. BrdU has been demonstrated to decrease c-*myc* expression at the transcriptional level in the leukaemic cell line, HL60 (Yen and Forbes, 1990) and in human melanoma lines (Valyi-Nagyi *et al.,* 1993). This result would appear to suggest that the c-*myc* promoter regions are susceptible to modulation by agents that disrupt promoter structure through thymidine substitution. The incorporation of BrdU into DNA may also affect the ability of the cell to methylate

guanine residues near genes. Such inhibition of methylation could lead to increased transcription of those genes. Kresnak and Davidson, (1993) observed an inverse relationship between the susceptibility of various guanine residues to dimethylsulphate (DMS) methylation and the susceptibility of those residues to mutagenesis by BrdU.

Alternatively, BrdU may directly influence the ability of proteins to associate with DNA. The second model proposes that BrdU alters the affinity of DNA sequences for regulatory proteins. Studies on the *lac* operon with BrdU incorporated showed that the *lac* suppressor was bound with greater affinity (Lin and Riggs, 1972).

In the third model, BrdU has been found to exert its effects on differentiation by alteration of a key regulatory gene(s) that alters transcription of genes involved in differentiation (Arnold *et al.*, 1988; Rauth and Davidson, 1993). In BrdU inhibition of myoblast differentiation, such an alteration occurs with the down-regulation or complete inhibition of the key regulatory gene, MyoD1 (Tapscott *et al.*, 1989; Nanthakumar and Henning, 1995). It could be envisaged that BrdU-induced alteration of differentiation in other tissues e.g. inhibition in mammary epithelial cells and pancreatic acinar cells, could be by a similar mechanism. This is strengthened by the homology of MyoD1 to the *myc* family of proteins, which have an important role in differentiation. Indeed, in BrdU-induced differentiation of neuroblastoma, a decrease of both N-*myc* protein and mRNA levels occur (Ross *et al.*, 1995).

Finally, it is possible that BrdU incorporation causes an alteration in the reading frame of the DNA template resulting in the formation of an abnormal mRNA, which is incapable of synthesising the correct differentiation products (Hill *et al.*, 1974).

1.4.3.3 BrdU-induced differentiation and gene expression

While the effects of BrdU on the differentative properties of different cell lines has been demonstrated, less is known of the molecular bases underlying such changes. As the ability of BrdU to modulate differentiation may be related to its incorporation into DNA, this may implicate the involvement of inhibition of expression of differentiation-specific genes (Harding *et al.*, 1978). Induction or inhibition of differentiation depends on the particular cell type and the target genes. Decreased c-*myc* gene expression levels as a result of BrdU treatment has been demonstrated in terminally differentiated

leukaemic cells (Yen and Forbes, 1990) and in differentiating melanoma cells (Valyi-Nagi *et al.*, 1993).

Horii *et al.* (1989) observed decreased gene expression of the N-myc and c-src transcription factors in human neuroblastoma cells following BrdU-induced differentiation. BrdU has also been shown to decrease expression of the c-jun gene in human melanoma cells (Rieber and Rieber, 1994), as well as c-myb gene expression in HL60 cells (Yen *et al.*, 1992). Additional studies have identified the ability of BrdU to induce expression of the following genes; prolactin (Wilson *et al.*, 1983), numerous glycolipid antigens (Andrews *et al.*, 1990), neuronal kinesin (Vignali *et al.*, 1996) and endothelin A (Ohtani *et al.*, 1997).

In addition, BrdU has also been shown to upregulate expression of the actin gene and increase cell adhesiveness in B16 melanoma cells (Gomez *et al.*, 1995). Actin may be an important gene in melanoma growth where actin expression appears to be inversely correlated with melanoma metastatic potential (Shimokawa-Kuroki *et al.*, 1994).

1.4.3.4 BrdU: Differentiating agent or inducer of pre-commitment?

BrdU is considered by some scientists to be an inducer of pre-commitment to differentiation rather than an actual differentiation inducing agent. This was highlighted by the findings that BrdU treatment of HL60s for 24 hours, followed by treatment with Retinoic Acid resulted in a faster response to Retinoic Acid (RA) than the single addition of RA alone (Yen *et al.*, 1990). It would appear that BrdU can initiate some of the early changes induced by RA in HL60 differentiation, including early c-*myc* downregulation. However, the same author reported previously (Yen *et al.*, 1987) that pre-commitment to differentiation involves an early increase in c-*myc* levels in the same leukaemic line, as induced by RA. This suggests that pre-commitment to differentiation in these cells involves increased expression of c-*myc*. It therefore appears that the true mechanisms of induction and commitment to differentiation remain unclear, even in individual cell types.

1.4.3.5 BrdU as an inhibitor of differentiation:

BrdU has been found to suppress differentiation and promote invasiveness of melanoma cells (Thomas *et al.*, 1994). The integrin repertoire expressed by melanoma cells is relevant to their invasive phenotype. Expression of $\alpha_2\beta_1$, $\alpha_5\beta_1$ and $\alpha_6\beta_1$ integrins and metalloproteinases were found to be increased, while induction of α_3 and $\alpha_v\beta_3$ integrins was shown in these cells. The production of melanin was repressed by BrdU. BrdU-treated cells were found to cause extensive invasion of Matrigel (Thomas *et al.*, 1994). BrdU has been found to block myogenesis and differentiation through a myogenic regulatory gene, MyoD1, in a mouse myoblast cell line (Tapscott *et al.*, 1989). It appears that although BrdU was incorporated into the muscle structural genes, these genes were apparently transcribed normally.

1.4.3.6 Use of BrdU as an antitumour agent

As already outlined, BrdU competes with naturally occurring Thymidine for incorporation into DNA during replication and as such it, and other similar compounds, should be ideal candidates for anti-tumour agents, since they require cell division and DNA synthesis to exert their effects (Bick and Devine, 1977). While few clinical trials are based on the differentiation-modulating properties of this drug (Freeman, 1969; Ameye *et al.*, 1989), BrdU has been used widely as a radiosensitiser in an attempt to improve radiological treatments (Lawrence *et al.*, 1992; McGinn and Kinsella, 1993). Radiosensitisation trials to date include the treatment of malignant glioma (Vander *et al.*, 1990), ulcerative herpetic keratitis (van Bijsterveld *et al.*, 1989), malignant astrocytomas (Greenberg *et al.*, 1988) and malignant brain tumours (Matsutani *et al.*, 1988). Administration of BrdU is normally by controlled perfusion (Doirion *et al.*, 1999), and has been used in combination with radiolabelled monoclonal antibodies (Buchsbaum *et al.*, 1994). While radiolabelled antibody approaches offer the potential of targeted chemotherapy, they are limited by low dose-relate deliverable. As such, the trials of Buchsbaum *et al.* (1994) may offer a means of enhancing the efficacy of low dose radiolabelled monoclonal antibody approaches.

1.4.3.7 BrdU-induced differentiation in the NCTCC

Recent work in the NCTCC has shown that BrdU induces differentiation in the poorly differentiated lung carcinoma cell line, DLKP, and in the lung adenocarcinoma cell line, A549 (P. Meleady, PhD. Thesis, 1997; F. O' Sullivan, PhD. Thesis, 1999; D. Walsh, PhD. Thesis, 1999). The morphological effects of BrdU-induced differentiation included cell flattening and enlargement, accompanied by a decreased growth rate. Removal of BrdU resulted in a gradual reversion towards the parental undifferentiated phenotype, indicating that the exposed cells were not terminally differentiated by the agent. This indicated that BrdU exposure did not result in fully differentiated cells but possibly that the agent induced a pre-commitment to differentiate in the DLKP cell line. BrdU has been suggested to induce pre-commitment to differentiation in a leukaemic cell line (Yen and Forbes, 1987). However, removal of BrdU after seven days exposure to DLKP cells did not affect expression levels of cytokeratin-8 three months later (D. Walsh, PhD. Thesis, 1999). This result indicated that BrdU is an "irreversible" mutational inducer of DLKP, in agreement with findings reported by Feyles *et al.* (1991a), using a SCLC cell line, NCI-H69.

Previous work carried out in the NCTCC (P. Meleady, PhD. Thesis, 1997) examined the effect of BrdU exposure on the DLKP cell line. Treatment of the cells with BrdU resulted in the induction of the $\alpha_2\beta_1$ integrin and upregulation of $\alpha_2\beta_1$ integrin expression. Associated with this change in integrin expression was a functional change in the properties of the cells themselves with BrdU treatment. The cells developed different adhesive properties showing more rapid attachment to the extracellular matrix proteins, collagen, laminin and fibronectin, and to basement membrane compared to untreated cells. Addition of an anti-antigen blocking antibody to BrdU-treated cells reversed the changes in adhesive properties of the cells. BrdU treatment also induced the expression of a number of epithelial antigens, including Epithelial Specific Antigen (a cellular adhesion molecule) and keratin 19 (K19) filaments in DLKP. In order to demonstrate that these results were not due to a "cloning" effect of BrdU, two of the clonal populations described by McBride *et al.* (1998) were exposed to BrdU and assessed for keratin expression (D. Walsh, PhD. Thesis, 1999). Both DLKP-SQ and DLKP-I clonal cell lines proved to be inducible for the cytokeratins. A significant

upregulation of keratin 19 protein expression was also observed in the human adenocarcinoma cell line, A549, after BrdU treatment (P. Meleady, PhD. Thesis, 1997). Preliminary RT-PCR analysis, however, failed to show any effect on expression of keratin 19 mRNA.

Further work on the DLKP cell line (F. O' Sullivan, PhD. Thesis, 1999), identified that BrdU increased expression of the non-calcium dependent, homophilic cell-adhesion protein, Ep-CAM as well as decreasing expression of the focal adhesion proteins α-actinin and α-catenin. The Ca^{2+}-dependent cell-cell adhesion protein, E-cadherin, is believed to be affected by BrdU exposure through the elevated expression of these two genes. mRNA expression of the Ep-CAM homologue GA733-1 was also upregulated in DLKP, but not A549 cells, following BrdU exposure.

Protein expression studies (D. Walsh, PhD. Thesis, 1999) revealed increased expression of cytokeratins K8 and K18 in BrdU-exposed DLKP. No change in mRNA expression was observed following treatment with the agent, which indicated that these proteins may be translationally regulated by BrdU. Expression of the eukaryotic initiation factors eIF-4E and 2α as well as the transcription factor Yin-Yang 1 (YY1) and c-Myc1 proteins were also observed to increase in BrdU-treated DLKP and A549 cells. A BrdU-induced translational cascade was posited from these results, utilising the c-myc and YY1 transcription factors as targets for BrdU action, through which all subsequent protein upregulation was mediated. This has been backed up by a previous finding that a major function of transcription factors is to indirectly regulate the translational efficiency of the cell (Grandori *et al.*, 1996). This theory possibly explains the lack of transcriptional targets identified for c-*myc* to date.

1.5 Selection of agents which may induce similar effects to BrdU in lung cell lines

From the results presented here, it was apparent that the differentiating agent, BrdU, was capable of inducing a host of gene and protein expression changes in lung epithelial cell lines. It was therefore considered interesting to examine whether other agents were capable of inducing a similar response. To this end, three chemotherapeutic drugs were chosen, cisplatin, taxol and VP16 which may be capable of mimicking the gene induction and differentiation-inducing effects of BrdU.

1.5.1 Use of chemotherapy in the treatment of cancer

Surgery, radiotherapy and chemotherapy are all effective treatments for cancer and have been used alone and in combination. Surgery and radiotherapy can often eradicate primary or localised disease but may ultimately fail because the cancer has metastasised to other areas of the body. In such instances, chemotherapy may control or eliminate metastatic disease and reduce mortality. Chemotherapy combined with surgery or radiotherapy or both, known as adjuvant therapy, has increased survival rates for a number of solid tumours that were previously treated by only one therapeutic modality.

Chemotherapy remains the main form of drug treatment at all stages of cancer development. The chemicals involved are directed at disrupting the cell cycle, with RNA, DNA and protein molecules as the targets. Synthetic chemotherapeutic agents currently in use can be categorised according to whether they alkylate DNA (alkylating agents) or antagonise metabolites required for DNA synthesis (antimetabolites). A third group are natural products from plants and fungi.

The ultimate clinical effectiveness of any anticancer drug requires that it kill malignant tumour cells *in vivo* at doses that allow enough cells in the patient's critical tissues (e.g. bone marrow, gastrointestinal tract) to survive so that recovery can occur. In general, anticancer drugs are most useful against malignant tumours with a high proportion of dividing cells. Thus, in practical terms, drugs alone are primarily effective against the leukaemias and lymphomas. The most common malignant tumours, however, are "solid" tumours, including those of the colon, rectum, lung and breast. These tumours

usually have a low proportion of dividing cells and therefore are less susceptible to treatment by drugs alone.

1.5.2 Introduction to chemotherapeutic drugs

A total of six separate chemotherapeutic drugs were utilised in this study to examine the effect of various therapies on lung cancer cells. Details on each of the drugs is provided in Section 2.3, although a general introduction to their mode of action will be included here. The six drugs utilised here are Adriamycin (Doxorubicin), Cisplatin, Taxol (Paclitaxel), VP16 (Etoposide), Vinblastine and Vincristine. In Section 3.3, reference is made to a separate study carried out by Dr. Yizheng Liang, in which additional drugs were used.

1.5.2.1 Adriamycin (Doxorubicin)

Adriamycin is a natural product drug, a multi-ring fungal anthracycline and a related compound to epirubicin. Both drugs have several effects on DNA (and RNA). They intercalate and cause partial unwinding of the DNA helix but they also generate single- and double-strand breaks. Intercalation between adjacent pairs in the double helix results in the inhibition of replication, transcription and replication. Adriamycin also binds to the enzyme DNA topoisomerase II. This enzyme is needed for the cleavage, unwinding and rejoining of DNA strands during DNA synthesis. Adriamycin blocks the religation step but it can also generate free radicals, which may contribute to its strand-breaking action (Carter *et al.*, 1981; Niedle and Waring, 1983). All the effects of adriamycin on DNA contribute to the drug being an S-phase-specific agent.

Adriamycin is widely used in the treatment of leukaemias and solid cancers such as those of the breast, lung and ovary (Carter *et al.*, 1981; King, 2000; Schiller, 2001; Schuette, 2001). Its main side effect is on heart function and this is dose limiting. Drug resistance results from overproduction of P-glycoprotein and decreased efficiency in repairing DNA strand breaks. Topoisomerase II mutations have been detected in

experimentally induced adriamycin-resistant cell lines (King, 2000) but the clinical relevance of this observation is uncertain.

1.5.2.2 Cisplatin

Cisplatin, and its analogue Carboplatin, are platinum-containing alkylating chemotherapeutic agents. Alkylating agents form adducts with DNA bases that disrupt DNA synthesis. Most alkylating agents have two functional groups, each of which can react with a DNA base and form interstrand and intrastrand cross-links within the DNA double-helix. These links can be formed at any stage of the cell cycle, so alkylating agents are not phase-specific. Cisplatin and its analogue are converted to alkylating species in the body, preferentially forming adducts at the N-7 position of guanine and adenine. These adducts can interact with adjacent bases on the same strand (intrastrand adducts) or on separate strands (interstrand adducts). The order of formation for adduct formation is G:G > A:G > others. Intrastrand adducts distort the DNA helix whilst interstrand links prevent strand separation so that replication is inhibited or abnormal. Cisplatin is particularly effective against ovarian and testicular cancers (Einhorn, 1997; Gregory *et al.*, 2000; Nardi *et al.*, 2001) although it is also a common choice for the chemotherapeutic treatment of some lung cancers (Novello and Chevalier, 2001; Schiller, 2001; Schuette, 2001). It has an advantage over other chemotherapeutic agents in that it has minimal effect on the bone marrow. Its main toxicities are nausea, renal dysfunction (nephrotoxicity) and neural effects. Carboplatin has a similar anti-tumour profile to Cisplatin but it has greatly reduced side effects, especially nephrotoxicity (King, 2000).

Resistance to Cisplatin can result from its altered cellular transport, enhanced repair of damaged or inactivating reactions of the cisplatin with sulphydryl groups in proteins and glutathione (King, 2000). Cisplatin derivatives are also substrates for glutathione-S-transferase, the detoxifying enzyme which conjugates the drug with reduced glutathione, leading to cisplatin-resistant cancers overexpressing the enzyme (Liu *et al.*, 2001). The drug also upregulates metallothionine (Aubrecht *et al.*, 1999), whose sulphydryl groups interact with the drug by a reaction analogous to that of glutathione.

1.5.2.3 Taxol (Paclitaxel)

The importance of microtubules as a target for taxol was suggested by its ability to induce G_2/M cell cycle arrest under conditions that had minimal effect on DNA, RNA or protein synthesis (Pratt *et al.*, 1994). However, in contrast to other known microtubule antagonists, taxol disrupts the equilibrium between free tubulin and microtubules by shifting it in the direction of assembly, rather than disassembly. As a result, taxol treatment causes both the stabilisation of ordinary cytoplasmic microtubules and the formation of abnormal bundles of microtubules (Schiff and Horwitz; 1979; Schiff and Horwitz; 1980). In a study of human leukaemic cell lines, the reversibility of bundle formation was correlated with resistance to taxol cytotoxicity (Rowinsky *et al.*, 1988).

Paclitaxel is a novel anticancer agent with activity in a broad range of epithelial cancers, including carcinomas of the ovary, breast, head, neck, bladder, lung and prostate (Schiller, 2001; Schuette, 2001). The efficacy of the drug is limited by the development of drug resistance in a population of malignant surviving cells. Defined molecular mechanisms for acquired tumour cell resistance to taxol include overexpression of mdr-1 (Chen *et al.*, 1994; Lin *et al.*, 1999) and differential expression of β-tubulin isotypes or β-tubulin gene point mutations (Dumontet *et al.*, 1996; Giannakakou *et al.*, 1997). Recent data also suggest that p53 status and mitosis checkpoint control is important in determining the sensitivity of the cells to Taxol (Li and Benezera, 1996). Further studies, reviewed in Blagosklonny and Fojo, (1999), have outlined numerous additional cellular and molecular effects, such as induction of cytokines and tumour-suppressor genes, indirect cytotoxicity due to secretion of tumour necrosis factor, vast activation of signal-transduction pathways and selective activity against cells lacking functional p53. All of these effects have been noted only with taxol concentrations 1,000-fold higher than that required for mitotic arrest and apoptosis.

1.5.2.4 Vinca alkaloids (Vinblastine; Vincristine)

Vincristine and Vinblastine are complex plant alkaloids isolated from the periwinkle plant *Catharanthus roseus*. They are members of a general class of drugs that act as mitotic inhibitors which act by interfering with the function of microtubules, a class of long, tube-like cellular organelles approximately 250nm in diameter (Pratt and Ruddon, 1979). Microtubules and microfilaments play an important role in the movement of cells relative to each other and in the movement of organelles within the cytoplasm of a single cell. The cytotoxicity of vincristine and vinblastine is attributed to their ability to interrupt cell division in metaphase (Bruchovsky *et al.*, 1965), but other effects could also contribute to cell death. Their action is M phase specific.

The vinca alkaloids specifically exert their effect by binding to tubulin and prevent its polymerisation (King, 2000). As polymerised tubules form the spindles that retract chromosomes into daughter cells at mitosis, their disruption results in blocked mitosis. Exposure of mitotic cells to the drugs is followed by the rapid disappearance of the spindle apparatus and the maintenance of the chromosomes in the condensed state. Although the effects are seen at the time, the actual vincristine-tubulin interaction occurs during interphase. Although chemically unrelated, the terpene taxol (from yew trees) acts at the same locus but prevents tubulin depolymerisation.

Although vincristine and vinblastine have very similar chemical structures and behave in essentially the same way at the level of drug-tubulin interaction, there are differences in the spectrum of the antitumour activity of the two drugs in both experimental animal tumours and clinical cancer. No reason for these differences is currently known. These compounds are effective against a broad spectrum of cancers such as lung, ovarian and testicular cancer (Culine *et al.*, 1994; Einhorn, 1997; Schiller, 2001; Schuette, 2001). They have bone marrow and neural toxicities, and development of drug resistance to both agents is via overproduction of P-glycoprotein (Bradley *et al.*, 1989).

1.5.2.5 VP16

Etoposide (VP16) is a semisynthetic derivative of the mitotic inhibitor Podophyllotoxin, which acts by binding to tubulin. The end result of such tubulin binding by Podophyllotoxin is microtubule dissolution and mitotic arrest (Pratt and Ruddon, 1979) and it was originally thought that VP16 exerted its effect in a similar fashion. However, VP16 does not induce microtubule dissolution and the drug reduces the mitotic index rather than produce mitotic arrest. Instead, the drug appears to have its primary effect in G_2 or perhaps late S phase, and prevents the entry of the cell cycle into mitosis (Huang *et al.*, 1973; Grieder *et al.*, 1974). In various systems, VP16 has been shown to decrease nucleotide uptake into cells (Loike and Horwitz, 1976a) and to increase intracellular DNA degradation (Loike and Horwitz, 1976b). More recently, (Van Maanen *et al.*, 1988) it has been shown to be a inhibitor of DNA topoisomerase II (Topo II). Topo II interacts with DNA in the process of DNA unwinding and the sealing of DNA strand breaks (Pratt *et al.*, 1994). VP16 inhibits the ability of Topo II to repair these strand breaks, leading to the generation of unrepairable double-strand breaks at critical sites (Smith, 1994). Smith *et al.* (1994) also showed that etoposide can induce cell cycle delay and modulation of topo II in small cell lung cancer (SCLC). However, the exact biological mechanism of action of VP16 remains unclear.

VP16 and the other epiodophyllotoxin analogue, VM 26 are active against Hodgkins disease, non-Hodgkin's lymphoma, acute leukaemias and small cell lung cancer (Fitoussi *et al.*, 1999; Schiller, 2001; Schuette, 2001).

1.5.3 Differentiation induced by exposure to chemotherapeutic drugs

Murine erythroleukaemia cells (MELC) selected for resistance to vincristine were more easily induced to differentiate by hexamethylenebisacetamide (HMBA) (Richon *et al.*, 1991). This group observed that drug-selected cells differentiated far more quickly than non-drug-selected and that this change may be due to gene expression changes caused by the selection process. 5-fluorouracil was also found to induce differentiation in K562 cells (Yang and Chang, 1995). Adriamycin (doxorubicin) has been shown to induce differentiation in human breast tumour MCF-7 cells (Fornari *et al.*, 1994). This

differentiated phenotype was also associated with a decrease in c-*myc* mRNA levels in the cell line. Doxorubicin also induced a senescence-like phenotype in colon carcinoma cell lines HCT116 and HT1080, which was accompanied by a knock-out of expression of p53 and p21 (Chang *et al.*, 1999).

1.5.4 Gene induction response to chemotherapy

1.5.4.1 Gene induction response to Cisplatin:

Gately *et al.* (1994), observed increased expression of the growth arrest and DNA damage-inducible gene GADD-153 in human ovarian 2008 carcinoma cells, when the tumour cells were grown both in vitro and in tumour xenografts in nude mice. Further work on this subject carried out by Delmastro *et al.* (1997), indicates that this response is more directly correlated with downstream biologic effects of cisplatin damage than with actual Pt-DNA adduct levels. The induction of expression of c-jun in the human melanoma cell line RPMI8322 following exposure to cisplatin was observed by Zhao *et al.* (1995). Cisplatin and VP-16 were used to study the induction of apoptosis in Panc-1 cells, and its outcome relative to the expression of BAX and Bcl-2 (Lee *et al.*, 1997). The group found upregulation of BAX expression, but no change in the expression of Bcl-2 in the cells. Expression of p53 is the gene studied most often in cells following exposure to cisplatin (Lee *et al.*, 1997; Siddik *et al.*, 1998; Zamble *et al.*, 1998; Jones *et al.*, 1998; Hagopian *et al.*, 1999). Lee *et al.* (1997) found that mutated p53 was required for the induction of apoptosis in PANC-1 cells in the study already mentioned, although no upregulation in expression of the gene was observed following exposure to cisplatin. Siddik *et al.* (1998) observed increases in p53 expression which were found to be cisplatin dose-dependent in human A2780 ovarian cancer cells. Induction of p53 and p21 in the cisplatin-resistant ovarian cancer cell line OVCA-429 by cisplatin and another platinum analogue, DACH-acetato-Pt was observed by Hagopian *et al.* (1999). Jones *et al.* (1998) found upregulated expression of Bak and 21-kDa BAX in human A2780 cells following exposure to cisplatin. Exposure to taxol was also observed to increase expression of these genes in A2780, but it was also found to increase expression of Bak and 21-kDa BAX in a cisplatin-resistant, p53-null variant of the cell

line. No change in expression levels of Bcl-2, Bcl-x_L, or 24-kDa BAX was observed in either of the cell lines during the experiment. This result indicated that functional p53 may be required for the cisplatin effects and not for the taxol-related effects. p53 gene responses to cisplatin has also been examined in mouse testicular teratocarcinoma cells (Zamble *et al.*, 1998). This group observed p53 protein accumulation through transcriptional mechanisms, followed by induction of p53-target genes. Cisplatin exposure also caused prolonged cell cycle arrest followed accompanied by induction of the p21 gene. Cisplatin was also observed to induce expression of the ERCC-1 gene, which is important in nucleotide excision repair, following exposure to the drug in human ovarian A2780 cells (Li *et al.*, 1998).

1.5.4.2 Gene induction response to Taxol (Paclitaxel):

The resistance mechanisms utilised by human MES-SA sarcoma cells in response to exposure to taxol were examined by Dumontet *et al.* (1996). The group found that taxol exposure resulted in activation of expression of the mdr-1 gene in this cell line, which yielded a broad resistance to vinblastine, adriamycin and etoposide (VP16). Taxol was also observed to increase expression of the growth arrest and DNA damage-inducible gene GADD-153 in the human ovarian 2008 carcinoma cell line (Gately *et al.*, 1996), and to induce apoptosis in human ovarian carcinoma SKOV3 cells, (Ling *et al.*, 1998), with an attendant induction of c-Mos gene expression. In the same study, Ling *et al.* also observed an induction of c-Mos protein expression following exposure to vinblastine in the SKOV3 cell line, but no change following exposure to camptothecin, etoposide and cisplatin. Examination of gene expression in a taxol-selected SKOV3 cell line using cDNA microarray technology revealed increased expression of mdr-1 but not MRP1 (Duan *et al.*, 1999). The taxol-resistant cell line was also observed to be cross-resistant to adriamycin and vincristine. Overall, twelve genes were observed to be overexpressed in the resistant subline; these included the cytokines interleukin 6, interleukin 8 and monocyte chemotactic protein 1. Induction of expression of mdr-1 mRNA was also observed in a number of human ovarian cell lines by Yamamoto *et al.* (2000), following exposure of the cell lines to taxol.

1.5.4.3 Gene induction response to VP-16 (Etoposide):

Jaffrezou *et al.* (1994) examined the effect of VP-16 on human sarcoma MES-SA cells. They observed a significant decrease in the expression of both topoisomerase II α and β mRNA (Topo II is the natural target enzyme for etoposide) in six out of seven stably established mutant cell lines. No change in expression of MRP1 was observed. The effect of VP16 in mouse L fibroblasts was examined by Sacchi and Schiaffonati, (1996), in which the authors looked at expression levels of three classes of genes: stress-response, growth- and cycle-related and apoptosis-related. The group observed repression of the c-myc, c-fos and c-jun genes, as well as transient induction of the apoptotic tTG gene. Etoposide-exposed A549 cells revealed an increase in expression of MRP1, a decrease in LRP expression and no change in expression levels of the mdr-1 gene (Trussardi *et al.*, 1998). Gibson *et al.* (1999) examined the gene expression of BAXα and Bcl-2 in a number of cell lines exposed to a combination dose of VP-16 followed by cyclophosphamide. Increased BAXα expression was first observed in three breast cancer cell lines; MCF-7, MDA-MB-435S and MDA-MB-A231 following exposure to VP-16 alone. An additional dose of cyclophosphamide induced higher levels of BAXα expression than were observed with just VP-16. This combination of chemotherapeutic agents also resulted in reduced Bcl-2 expression, whereas exposure to VP-16 alone had no effect.

1.5.4.4 Gene induction following exposure to other chemotherapeutic drugs

Exposure to the DNA-damaging agent 5-fluorouracil (5-FU) has been shown to induce an increase in thymidylate synthase (TS) gene expression in the human colon cancer H630 cell line when combined with interferon-gamma (Chu *et al.*, 1993). 5-fluorouracil on its own was also found to induce differentiation in K562 cells (Yang and Chang, 1995), although no change in c-*myc* mRNA or protein expression levels was observed. 5-FU was also found to induce expression of the carcinoembryonic antigen (CEA) in the human colon carcinoma cell line HT-29 (Prete *et al.*, 1996). Finally, p53 mRNA and protein expression in a number of p53-expressing clonal cell lines was examined following exposure to the drug (Mirjolet *et al.*, 2000). The group found that p53 mRNA

expression varied according to the clone under examination, but that in all clones, 5-FU altered transcriptional and translational regulation leading to up-regulation of the p53 protein.

Adriamycin (doxorubicin) has been shown to induce differentiation in human breast tumour MCF-7 cells (Fornari *et al.*, 1994). This differentiated phenotype was also associated with a decrease in c-*myc* mRNA levels in the cell line. A single-step adriamycin selection was attempted by Chen *et al.* (1994), in which a number of clones were isolated from the human sarcoma cell line MES-SA and analysed for mdr-1 expression. Elevated levels of mdr-1 mRNA were found in all clones tested as well as increased P-glycoprotein expression. Expression levels of topoisomerase II α and β, MRP1, glutathione and p110 were unaffected. Doxorubicin also induced a senescence-like phenotype in colon carcinoma cell lines HCT116 and HT1080, which was accompanied by a knock-out of expression of p53 and p21 (Chang *et al.*, 1999). Exposure to related anthracyclines also resulted in induced gene expression. Nielsen *et al.* (1998) observed significant increases in P-glycoprotein expression in murine Ehrlich ascites tumour cells (EHR2) after exposure to daunorubicin, a related analogue. Two other analogues, 4-demethoxydaunorubicin and MX2, a morpholino-anthracycline, were also observed to induce mdr-1 expression in a low-level human multidrug-resistant leukaemia cell line, CEM/A7R (Hu *et al.*, 1999).

The chemotherapeutic drug cytarabine (ara-C) induced LRP gene expression (Komarov *et al.*, 1998) (although no consequent increase in LRP protein was reported), as well as inducing apoptosis in HL-60 cells (Bouffard and Momparler, 1995). Other chemotherapeutic drugs which have been found to induce gene expression include gemcitabine, which has been shown to induce c-jun and c-fos gene expression in the HL-60 cell line (Bouffard and Momparler, 1995), as well as inducing p53 and p21 expression in the human lung cancer cell line H460 (Tolis *et al.*, 1999). The chemotherapeutic drug Topotecan has also been shown to have the same effect in this latter study (Tolis *et al.*, 1999). Mitoxantrone, a novel antineoplastic drug, has also been shown to induce apoptosis in human myeloid leukaemia HL-60 and KG-1 cells as well as increasing c-jun gene expression and repressing the expression of c-myc and Bcl-2 (Bhalla *et al.*, 1993).

Christodoulopoulos *et al.* (1999) found that chlorambucil induced expression of the human homologue of Rad51 (HsRad51) in lymphocytes from patients with B-cell chronic lymphocytic leukaemia (B-CLL). Chlorambucil is the standard alkylating agent used to treat patients with B-CLL, while HsRad51 may be implicated in recombination repair and induction of DNA repair enzymes.

Tamoxifen is a nonsteroidal antiestrogen which is widely used in breast cancer treatment and is currently under evaluation as a chemopreventative agent for individuals at high risk of contracting the disease. Examination of the effects of Tamoxifen on the expression of xenobiotic metabolising enzymes in F344 rat liver cells was also investigated (Nuwaysir *et al.*, 1995). The group observed increases in expression of CYPIIB1, CYPIIB2, CYPIIBA and microsomal epoxide hydrolase mRNA and protein levels in both male and females.

1.5.4.5 Gene induction following exposure to other agents

Induced gene expression has been observed in a number of cell types following exposure to different agents. The range of gene-altering substances is very wide, incorporating chemical agents which differ vastly in terms of their mode of activity and make-up (e.g. chemotherapeutic drugs), as well as physical agents which induce a more corporeal effect, such as UV irradiation, and heat shock.

Expression of the mdr-1 and p53 genes are the two most studied genes following induction by various external agents. Mdr-1 gene expression has been found to be upregulated in the human renal adenocarcinoma cell line HTB-46 following exposure to heat-shock and arsenite (Chin *et al.*, 1990). Further work on this area identified the presence of heat-shock responsive elements in the promoter sequence of the mdr-1 gene which were responsible for the heat-shock-mediated increase in expression (Kioka *et al.*, 1992). Expression of the mdr-1 gene has also been found to be induced in human cancer KB cells following exposure to UV light irradiation (Uchiumi *et al.*, 1993). Two sequences in the mdr-1 promoter were found be essential for the stress induction of the mdr-1 gene promoter activity. Chaudhary and Roninson, (1993) also observed increases in expression of the mdr-1 gene following treatment with a variety of chemotherapeutic

drugs, a number of which will be discussed later. Mdr-1 expression has also been induced in rat liver tumours following injection of diethylnitrosamine (Fardel *et al.*, 1994), a treatment which also induced mdr-3 gene expression in two clones isolated from one of the treated tumours. Sodium butyrate, a differentiating agent, induced mdr-1 gene expression in the human colon carcinoma cell lines Clone-A (Kramer *et al.*, 1993), as well as SW 620, HCT-15, DLD-1 and LS 180 (Frommel *et al.*, 1993). Other genes found to be induced by chemical means in cancer cells include COX-2-induced protein expression in human colon carcinoma cell line HT-29 by carbachol, a stable receptor agonist (Yang and Frucht, 2000), as well as c-myc mRNA, induced in rat livers by aflatoxin B1 and age (Larson *et al.*, 1993) and suppressed in MCF-7 human breast tumour cells by the anthracycline analogue, idarubicin (Gewirtz *et al.*, 1998). Both mRNA and protein expression of the breast cancer resistance gene BRCA-1 was inhibited in the human breast MCF-7 and ovary BG-1 cell lines by exposure to the polycyclic aromatic hydrocarbon Benzo[*a*]pyrene. This hydrocarbon has also been found to induce expression of the p53 gene in A549 and NIH 3T3 cells (Pei *et al.*, 1999). p53 protein expression has also been induced in normal lymphocyte cells following exposure to the alkylating agent nitrogen mustard (Bhatia *et al.*, 1995), while suppression of the gene has been observed in human chronic lymphocytic leukaemia (CLL) cells following exposure to the synthetic flavone Flavopiridol (Byrd *et al.*, 1998).

A number of other agents have been found to induce gene expression following exposure in certain cell lines. Oltipraz is a synthetic dithiolethione with chemopreventative activity against carcinogen-induced neoplasia of liver, lung and colon in several animal model systems. Delivery of oltipraz to patients at high risk of colorectal cancer resulted in the induction of mRNA for the detoxifying enzymes γ-glutamylcysteine synthase (γ-GCS) and DT-diphorase taken from colon mucosal biopsies (O'Dwyer *et al.*, 1996). Further work on this dithiolethione by this group identified the induction of DT-diaphorase mRNA in the human colon adenocarcinoma cell line HT-29, following exposure to oltipraz (O'Dwyer *et al.*, 1997). Asbestos has been found to induce c-fos and c-jun gene expression in rat pleural mesothelial cells (Heintz *et al.*, 1993). Asbestos has also been shown to induce an extended lifespan in normal human mesothelial cells with a concomitant increase in expression of the SV40 T antigen (Xu *et al.*, 1999). The phorbol ester TPA (phorbol 12-myristate 13-acetate)

has been shown to induce c-fos and c-myc gene expression in mononuclear blood cells taken from patients with B-chronic lymphocytic leukaemia (B-CLL) (Drexler *et al.*, 1989), as well as inducing LRP gene expression in HL-60 and K562 cells (Komarov *et al.*, 1998) and ERCC-1 protein in human ovarian A2780 cells (Li *et al.*, 1998).

1.6 Eukaryotic gene transcription

In eukaryotes, DNA is assembled into chromatin, which maintains genes in an inactive state by restricting access to RNA polymerases and its accessory factors. During the process of development, genes are turned on and off in a pre-programmed fashion, a process which eventually generates cell specificity. This developmental program is orchestrated by transcription factors which bind to specific DNA recognition sites near the genes they control. A single transcription factor is not dedicated to each regulatory event. Instead, a mechanism called combinatorial control is employed (Carey and Smale, 2000). In combinatorial control, different combinations of ubiquitous and cell-type-specific regulatory proteins are used to turn genes on and off in different regulatory contexts. The ability of an organism to employ small numbers of regulatory proteins to elicit a larger number of regulatory decisions is one of the major strengths of eukaryotic transcriptional control.

1.6.1 General overview of gene structure and activation

In a typical gene, a DNA sequence called the core promoter is located immediately adjacent to and upstream of the gene. The core promoter binds RNA polymerase II (Pol II) and its accessory factors and directs Pol II to begin transcribing at the correct start site. *In vivo*, in the absence of regulatory proteins, the core promoter is generally inactive and fails to interact with the general transcription machinery. Immediately upstream of the core promoter is a regulatory promoter, and farther away either upstream or downstream are enhancer sequences. Regulatory promoters and enhancers bind proteins called activators, which "turn on" or activate transcription of the gene. Activation generally occurs by recruitment of the general machinery to the core promoter via interactions between the activator bound to promoter DNA and the general machinery in solution. Some activators are ubiquitously expressed, whereas others are restricted to certain cell types, regulating genes necessary for a particular cell's function.

To activate a gene, the chromatin encompassing that gene and its control regions must be altered or "remodelled" to permit transcription. The mechanisms of remodelling are unclear, but they involve changes in the structure of chromatin and in modification of

histones that somehow increase accessibility to transcription factors. Remodelling achieved at a local level affects only the chromatin close to a gene. In some instances, however, a single gene or locus of related genes may spread over 100kb or more. In these cases, genes might be under the control of not simply specific enhancers and regulatory promoters but also of locus control regions (LCRs), which remodel chromatin and control global access activators over an extended region (Carey and Smale, 2000).

Once enhancers are accessible, they can stimulate transcription of a gene. However, because enhancers are known to activate transcription when they are positioned large distances from a gene, they could inadvertently activate other nearby genes in the absence of appropriate regulation. To focus the action of the enhancer or LCR on the appropriate gene or set of genes, the gene and its regulatory regions are thought to be assembled into a domain. Domain formation appears to involve boundary elements and matrix attachment regions (MARs). Boundary or insulator elements are thought to flank both sides of an individual gene or gene locus. These elements bind proteins that prevent the enhancer from communicating with genes on the opposite side of the insulator. MARs also flank some active genes and tether them as loops to the nuclear periphery or matrix although a gene function has not been established (Carey and Smale, 2000).

The current view is that once the enhancer and promoter are acccesible, they bind to combinations of activators. Binding of activators is generally cooperative, where one protein binds weakly, but multiple activators engage in protein-protein interactions that increase each of their affinities for the regulatory region. The nucleoprotein structures comprising these combinatorial microarrays of activators are called enhanceosomes (Carey and Smale, 2000). The enhanceosome interacts with the general transcription machinery and recruits it to a core promoter to form "the Pre-Initiation Complex" or PIC (see Section 1.6.1.1). The enhanceosome, the general machinery and the core promoter form a complicated network of protein-protein and DNA-protein interactions that dictate the frequency of transcription intiiation. The interactions between the enhanceosome and components of the general machinery are rarely direct but are bridged or linked by proteins called coactivators.

1.6.2 Transcription Initiation

Eukaryotic gene transcription occurs in three stages; initiation, promoter clearance, elongation and termination. The main target for regulation appears to be the process of RNA polymerase binding and transcription initiation. RNA polymerase is the enzyme that reads the DNA code and convert it into an RNA "message". This is then transported from the nucleus to the cytoplasm where it can be translated into protein. The three RNA polymerases lack the intrinsic ability to interact specifically with DNA sequences but they acquire specificity through interaction with cellular proteins called transcription factors. These place the RNA polymerase enzyme in the correct position on the DNA to begin transcription. There are three different RNA polymerase enzymes which carry out distinct functions: RNA polymerase I (Pol I) transcribes ribosomal RNA (rRNA), RNA polymerase II (Pol II) transcribes protein-encoding messenger RNAs (mRNAs) and RNA polymerase III (Pol III) transcribes genes coding for amino acid transfer RNAs (tRNAs) (Geiduschek and Kassavetis, 2001; Landick, 2001). As a result, Pol II is the focus of most of the discussion which will take place here.

1.6.2.1 Initiation and the formation of the Pre-Initiation Complex (PIC)

The promoter region of eukaryotic protein-coding genes is arbitrarily divided into two segments: a core promoter region of encompassing DNA sequences between approximately –40 and +50 bases relative to a transcriptional start site and an enhancer region consisting of either positive or negative regulatory elements (Fig. 1.6.1) (Carey and Smale, 2000). The two key genetic elements within the core promoter are the TATA box and the initiator (Inr) element. Core promoter structures contain combinations of these elements, termed $TATA^{+}$ Inr^{-}, $TATA^{+}$ Inr^{+} and $TATA^{-}$ Inr^{+} (Novina and Roy, 1996). The majority of cellular promoters contain a TATA box. Recently, a number of genes have been identified that do not contain a TATA motif and appear to be predominantly housekeeping genes.

Fig. 1.6.1 Model of typical gene and components involved in gene activation

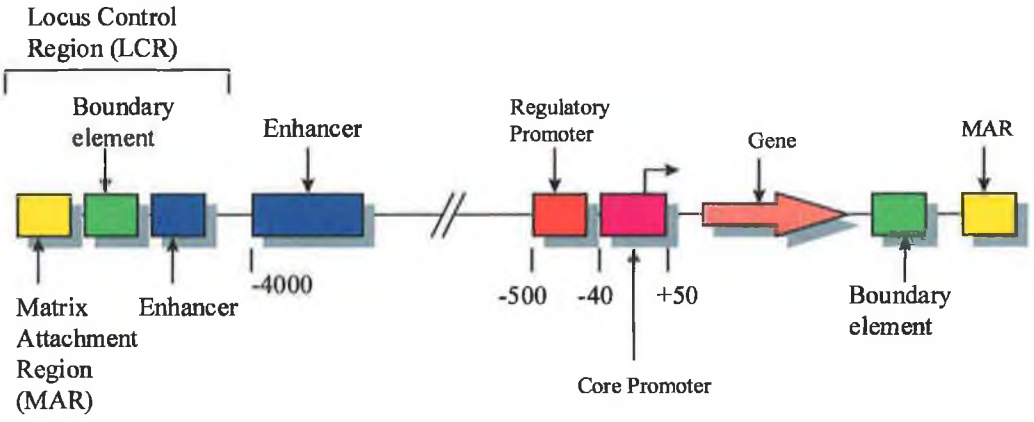

Core promoter DNA elements;

1. Bind to and control assembly of the preinitiation complex containing Pol II, the general transcription factor, and coactivators
2. Position the transcription start site and control the directionality of transcription
3. Respond to nearby or distal activators and repressors in a cell

(Carey and Smale, 2000).

In most cases, the core promoter elements do not play a direct role in regulated transcription. The core promoter alone is generally inactive *in vivo*, but *in vitro* it can bind to the general machinery and support low levels of transcription. This amount of basal transcription is dictated by the DNA sequences in the core promoter. Activators greatly stimulate transcription levels, and the effect is called activated transcription (Carey and Smale, 2000).

The basic process of transcription initiation involves the recruitment of RNA polymerase II to the transcriptional start site via tethering to various General Transcription Factors (GTFs) that recognise the promoter region and begin assembly of the "pre-intiation complex" (PIC). This is a giant complex estimated to consist of approximately 50 components adding up to a molecular weight of more than 3 MDa (Halle and Meisterernst, 1996). The PIC that binds the core promoter consists of two classes of factors; the GTFs including Pol II, TFIIA (Transcription Factor IIA), TFIIB, TFIID, TFIIE, TFIIF and TFIIH and coactivators and corepressors that mediate response to regulatory signals (Myer and Young 1998).

1.6.3 Transcriptional Enhancers

Transcriptional regulation is controlled by the binding of sequence-specific DNA-binding proteins to regulatory promoters and enhancers (reviewed in Blackwood and Kadonaga, 1998). The regulatory promoter is normally defined as the region surrounding the core promoter and within a few hundred base pairs of the transcription start site, either upstream or downstream of the gene or within an intron. The distinctions between regulatory promoters and enhancers have even become blurred over time because control elements found in an enhancer can often function in the context of a promoter (Blackwood and Kadonaga, 1998). Conversely, individual promoter elements can often impart enhancer activity if multimers of that element are inserted at a more distant location.

Currently, the specific properties that permit an enhancer to function from a great distance have not been determined. Current models for enhancer action have been reviewed recently (Kadonaga, 1998). The current view is that enhancers bind activators and other sequence-specific proteins that are involved in chromatin remodelling. Once bound, these activators loop out the intervening DNA to interact with proteins bound to the regulatory or core promoters. These interactions are believed to stabilise transcription factor assembly.

1.6.4 Regulation of Gene Transcription from TATA-less promoters

In recent years there have been a growing number of reports of promoter elements that lack any discernible TATA box motif, originally thought to be a critical control point in the initiation process. Surprisingly, many of these, including creatine kinase, dihydrofolate reductase, cytochrome c oxidase and a number of ribosomal proteins (Azizkhan *et al.,* 1993; Basu *et al.,* 1993), are "housekeeping" genes. In the case of cytochrome c oxidase (COX-1, COX-2), the –17 to +20 region of the promoter contains fused binding sites for two enhancer proteins, NF-E1 (also called YY1) and SP1 (Basu *et al.,* 1993). The transcription start site at position –8 to +9 is flanked by a 17 base initiator element (Inr). Mutation studies showed that basal transcription from this Inr element did not involve SP1 binding but was completely dependent on YY1 binding.

The importance of SP1 sites in the regulation of TATA-less promoter initiation may actually depend more upon the presence of immediately adjacent YY1 binding. This is highlighted by the findings of Basu *et al.* (1993) above, together with the demonstration that SP1 and YY1 physically interact to form a protein complex (Lee *et al.*, 1993) suggesting a synergistic effect on TATA-less promoter activity in the presence of both factors. The role of this interaction with SP1 is still unclear, however, since SP1 actually counters YY1-mediated transcriptional activation of the TATA-less dihidrofolate reductase gene in *Drosophila* (Azizkhan *et al.*, 1993).

1.7 Gene expression profiles examined in this study

From the results already obtained by other researchers, as well as the previous findings in this laboratory (Section 1.4.3.7), the cell systems of DLKP and A549 were chosen to study the effects of BrdU-induced differentiation in lung epithelial cell lines. As has been already shown, a significant level of induced protein expression in response to BrdU has already been demonstrated in these cell lines (Section 1.4.3.7). It was considered interesting to examine the expression levels of a number of functionally diverse genes during BrdU-induced differentiation in these cells. The rest of this Introduction deals with a discussion of these genes, the expression of which was examined in the BrdU-treated lung cell lines using RT-PCR analysis.

Broadly, there were six classes of genes examined;

1. Genes associated with mediating multidrug resistance (MDR); this group was the most populous, incorporating mdr-1, mdr-3, MRPs 1-6, and BCRP
2. Apoptotic genes; the pro-apoptotic MRIT, BAXα, Bcl-x_S and BAP and the anti-apoptotic Bcl-x_L, Bcl-2α, Survivin and BAG genes
3. Eukaryotic initiation factor genes, eIF-2α and eIF-4E
4. Genes involved in tumour progression; COXs-1 and COX-2
5. Cell adhesion genes; E-cadherin, α-catenin and β-catenin
6. The transcription factor gene; c-*myc*

Each of these genes are discussed in greater detail in the following subsections, which will provide the main reasons these genes were selected for analysis in this study.

1.7.1 Introduction to multidrug resistance (MDR)

Multidrug Resistance (MDR) severely compromises the efficacy of cancer chemotherapy in the clinic. It occurs when tumours that may initially have been sensitive, become resistant to a variety of therapeutically important anticancer drugs that are structurally unrelated and have diverse cellular targets. MDR may be observed in primary therapy (inherent resistance) or be acquired during or after treatment (acquired resistance) (Yu *et al.,* 1999). Although the majority of tumours do show an initial

response to chemotherapy, a relapse that neither responds to the drugs initially used nor to other anticancer drugs often follows. *In-vitro* studies have shown that MDR is accompanied by reduced intracellular drug accumulation due to increased drug efflux by energy-dependant trans-membrane drug transport proteins (Endicott and Ling, 1989).

One major mechanism of resistance to such drugs is linked to decreased cellular accumulation of anticancer drugs through enhanced cellular efflux of the anti-tumour compounds. Such multidrug resistance can be conferred *in vivo* and *in vitro*, by a number of proteins. The most important genes mediating drug resistance *in vivo* are the M_r 170,000 P-glycoprotein (encoded by the *MDR*1 gene) (Gottesman and Pastan, 1993), and the more recently identified 190kDa MRP1 (Cole *et al.,* 1992) and its homologues (Kool *et al.*, 1997). All of these proteins are members of the ABC (ATP-binding cassette) transporter family and function as ATP-dependent active transporters.

1.7.1.1 P-glycoprotein (Pgp)

Pgp is a plasma membrane efflux pump with ATPase activity and a molecular weight of 170 kDa. It is composed of two similar halves, each containing six putative transmembrane domains and one nucleotide-binding site consensus sequence. This unique structural characteristic of Pgp has been conserved in a large number of membrane associated transporters from bacteria to higher eukaryotes, forming a novel superfamily of proteins called the ATP binding cassettes (ABC) transporters (Higgins, 1992). The ATP-binding cassette (ABC) transporters, present in organisms ranging from bacteria to man, are involved in the ATP-dependent transport of a wide variety of compounds, ranging from inorganic ions to large polypeptides (Tusnady *et al.,* 1997), and are involved in the tolerance to a wide diversity of cytotoxic agents in both prokaryotes and eukaryotes (Higgins, 1992).

Pgp acts to promote the efflux of a variety of drugs with resultant reduction in intracellular drug concentration (Clynes, 1993). The physiological function of Pgp is not, however, completely understood. Detoxification of naturally occurring compounds and excretion of endogenous metabolites, e.g. steroid hormones, are possibilities, while

there is evidence that it is an essential component of a volume-regulated chloride channel (Gottesmann and Pastan, 1993).

1.7.1.2 Multidrug resistance-associated Protein 1 (MRP1) and MRP homologues

Studies of a Pgp negative multidrug resistant cell line led to the identification of another transmembrane protein, the p-190 multidrug resistance-associated protein (MRP) (Cole *et al.*, 1992). MRP is a 1531 amino acid protein that was predicted to be a member of the ABC transporter superfamily (Loe *et al.*, 1996). This protein is now recognised as MRP1 (Hipfner *et al.*, 1999). Despite their similar function, MRP1 and Pgp show little sequence homology, which is restricted to the ATP binding site. Drug cross-resistance profiles are similar but not identical for MRP1 and Pgp overexpressing cells (Lautier *et al.*, 1996) and agents that reverse Pgp are usually less effective on MRP1.

1.7.1.2.1 MRP1 Protein structure

Most ABC transporters are comprised of two polytopic MSDs (Membrane Spanning Domain) and two NBDs (Nucleotide Binding Domain) (Higgins, 1992). The predicted topology of MRP1 is inconsistent with the typical four-domain structure. A schematic outline of the protein topology of MRP1 is provided in Fig. 1.7.1.

Fig. 1.7.1 Predicted MRP1 protein structure

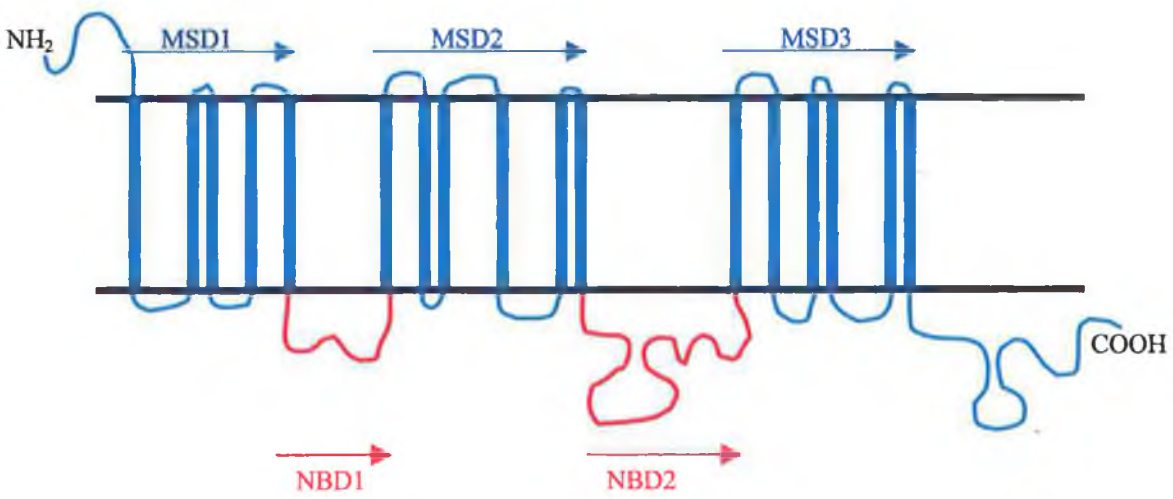

1.7.1.2.2 Investigation of important regions of MRP1 protein structure

Gao *et al.* (1998), investigated the possible role of the third MSD of MRP1 and its related transporters and their results demonstrated that two truncated molecules (MRP229-1531 and MRP281-1531) lacking MSD1 can be expressed in Sf21 cells as efficiently as the full length protein. They then examined the ability of various MRP1 fragments, expressed individually and in combination, to transport the MRP substrate, Leukotriene C_4 (LTC_4). It was found that elimination of the entire NH_2 terminal MSD, or just the first putative transmembrane helix, or substitution of the MSD with the comparable region of the functionally and structurally related transporter, the canalicular multispecific organic anion transporter (cMOAT/MRP2), had little effect on protein accumulation in the membrane. However, all three modifications decreased LTC_4 transport activity by at least 90%. Transport activity could be reconstituted by co-expression of the NH_2-terminal MSD with a fragment corresponding to the remainder of the MRP molecule, but this required both the region encoding the transmembrane helices of the NH_2 terminal MSD and the cytoplasmic region (L_0) linking it to the next MSD. In contrast, a major part of the cytoplasmic region linking the NH_2-proximal nucleotide binding domain of the protein to the COOH-proximal MSD was not required for active transport of LTC_4.

In most ABC transporters, the binding and the subsequent hydrolysis of ATP by the NBDs is believed to be coupled to, and provide the energy for substrate transport (Hipfner *et al.,* 1999). These domains are highly conserved, typically showing 30-40% identity among different superfamily members in a core region of about 200 amino acids. The NBDs of ABC superfamily members share two sequence motifs, designated "Walker A" and "Walker B", with many other nucleotide binding proteins (Walker *et al.,* 1982). Mutational analysis of a number of ABC proteins indicates that these two regions are critical for ATPase function (Hipfner *et al.,* 1999). Another feature that distinguishes MRP1-like transporters from other ABC superfamily members is a difference in the structure of the NH_2-proximal NBD (NBD1). Alignment of the primary sequences of MRP1, LtPgpA, and CFTR with the human Pgp encoded by the MDR1 gene revealed that, in comparison to P-glycoprotein, these transporters all contain a "deletion" of 13 amino acids located between the Walker A and B motifs of NBD1.

1.7.1.2.3 Identification of homologues of MRP1

The first transport protein to be recognised as a member of the MRP family was cMOAT (Taniguchi *et al.,* 1996). A full length human cMOAT cDNA was isolated which was highly homologous to rat cMOAT. Sequencing of cMOAT revealed an open reading frame coding for 1545 amino acids that showed 46% similarity to that of human MRP1. Taniguchi *et al.* (1996), estimated the size of cMOAT to be approx. 4.5kb, similar to that of MRP1 mRNA but larger than the human mdr-1 mRNA.

To date five human MRP1-related proteins, designated MRP2, MRP3, MRP4, MRP5 and MRP6 have been discribed (Kool *et al.,* 1997; Taniguchi *et al.,* 1996; Konig *et al.,* 1999; Kool *et al.,* 1999a and 1999b and Kiuchi *et al.,* 1998). A search of the human Expressed Sequence Tag (EST) database by Allikmets *et al.* (1996), yielded 21 new ABC genes, including genes for transporters related to MRP1. In an independent search, Kool *et al.* (1997), found four transporters related to MRP1 and cMOAT and analysed the expression of these genes, called MRP3-6, in normal tissues and tumour cell lines. A fifth homologue of MRP1 was also identified as the human SUR (sulfonyl urea receptor) gene. The percentages of homology for the COOH-terminal 124 amino acids are shown in Table 1.6.1. Percentages of identity were determined using the GAP program of GCG (Kool *et al.,* 1997). The highest homology is found between MRP1 and MRP3 (83% similarity) and the lowest between SUR and any of the MRPs (59% similarity).

Table 1.7.1: Homology between the COOH terminal 124 amino acids of the six human MRP homologues and human SUR

	MRP1	**MRP2**	**MRP3**	**MRP4**	**MRP5**	**MRP6**	**HSUR**
MRP1	100						
cMOAT	73	100					
MRP3	83	73	100				
MRP4	69	65	64	100			
MRP5	66	65	62	66	100		
MRP6	69	64	67	62	57	100	
HSUR	59	57	57	58	57	46	100

The existence of a seventh family member, MRP7, has only been inferred from a database search and so far there is no other information available (Borst *et al.,* 1999). The sMRP has been reported by Suzuki *et al.* (2000), to be a spliced variant of the MRP5 gene, expressed in various human tissues. ARA represents the 3'end of the MRP6 gene that is incidentally co-amplified with MRP1 in cells selected for adriamycin resistance (Kool *et al.,* 1999). Within the group of mammalian ABC transporters the MRPs form a cluster that is clearly demarcated from the other known groups, such as Pgp, CFTR and the sulphonylurea receptors.

1.7.1.2.4 Function /Transport by MRP1 and MRP homologues

In 1994 two groups independently demonstrated that MRP1 is able to transport glutathione (GSH) conjugates of drugs (Leier *et al.,* 1994 and Jedlitschly *et al.,* 1994). Leier *et al.* (1994), demonstrated that the MRP1 gene encodes a primary-active ATP dependent export pump that can transport the cysteinyl leukotriene, LTC_4 and glutathione conjugates such as glutathione disulphate (GSSG). Elevated levels of ATP-dependent transport of LTC_4 and certain other GSH conjugates were also demonstrated by Jedlitschly *et al.* (1994). The findings that MRP1 can transport cysteinyl leukotrienes (e.g. LTC_4) as well as other GSH conjugates suggest that this protein may be a GSH conjugate/organic anion transporter, a GSH-X pump. Therefore, it appears that MRP1 is a transporter of multivalent organic anions, preferably glutathione S-conjugates (Loe *et al.,* 1996b; Jedlitsky *et al.,* 1996; Muller *et al.,* 1994), but also of sulphate conjugates (Jedlitsky *et al.,* 1996).

The mechanism of MRP1-mediated transport of chemotherapeutic drugs is presently unclear. Although MRP1 has been shown to reduce cellular accumulation of at least some of the drugs to which it confers resistance, such as adriamycin, daunorubicin, vincristine and VP-16, it has previously not been possible to demonstrate direct transport of these compounds or other unmodified chemotherapeutic drugs by MRP1-enriched membrane vesicles (Cole *et al.,* 1998; Jedlitschky *et al.,* 1996; Loe *et al.,* 1996 and Muller *et al.,* 1994), and contrary reports claiming to have shown direct transport of these compounds have recently been retracted (Cole *et al.,* 1998). A number of authors have also reported the ability of the MRP1 protein to mediate the active transport of

neutral (etoposide (VP-16)) and cationic (adriamycin, vincristine, daunorubicin and rhodamine 123) lipophilic drugs as well as anions (e.g. dinitrophenyl-S-glutathione and calcein) (Broxterman *et al.,* 1996).

Jedlitschy *et al.* (1997), demonstrated that bilirubin glucuronides were better substrates for MRP2 than MRP1, which are transported by both proteins in an ATP dependent manner. MRP2 is also reported to be the predominant export pump responsible for hepatobiliary excretion of the amphiphilic anion Fluo-3 (Keppler *et al.*, 1999 and Konig *et al.*, 1999). MRP3 expression has been correlated with doxorubicin resistance and a weaker, but still highly significant connection with resistance to vincristine, etoposide and cisplatin (Young *et al.*, 1999). Bakos *et al.* (1998), reported that MRP4 expressed the basic structure required for GS-X pump activity as does MRP1, however characterisation of MRP4 substrates remains to be elucidated. Suzuki *et al.* (2000), reported that MRP5 mRNA was detected in a large number of human tissues. Kool *et al.* (1999b), reported that their analysis of a number of MDR and cisplatin resistant cell lines provided no evidence for the involvement of MRP6 in drug resistance.

1.7.1.2.5 MRP1 and MRP homologue expression in cell lines and human tissues

Since the discovery of MRP1 in the small cell lung cancer cell line, H69AR (Cole *et al.*, 1992), MRP1 has been identified in non-Pgp multidrug resistant cell lines from a variety of tumour types, including leukemias, fibrosarcoma, non-small cell lung, human small cell lung, breast, cervix, prostate, and bladder carcinomas (Izquierdo *et al.,* 1996). MRP1 has also been detected either at the protein or mRNA level in normal human tissues including lung, stomach, colon, peripheral blood macrophages, thyroid, testis, nerve, bladder, adrenal, ovary, pancreas, gall-bladder, duodenum, heart, muscle, placenta, brain, kidney, liver and spleen (Loe *et al.,* 1996a; Zaman *et al.,* 1993; Cole *et al.,* 1992 and Kool *et al.,* 1997).

MRP2 (cMOAT) is found predominantly in the liver, duodenum and, in low levels, in the kidney (Kool *et al.,* 1997; Schaub *et al.,* 1997). Kool *et al.* (1997) and Kiuchi *et al.* (1998), reported that MRP3 mRNA is mainly expressed in the liver, colon, intestine and adrenal gland, and to a lesser extent in several other tissues. Kool *et al.* (1997), reported

that MRP4 was found only in a small number of tissues at very low levels. However, Lee *et al.* (1998), demonstrated, using RNA blot analysis, the expression of MRP4 in a wide range of tissues, with particularly high levels in prostate, but almost undetectable levels in the liver. MRP5, like MRP1, is readily detected in several tissues with highest levels in skeletal muscle, intermediate levels in kidney, testis, heart and brain and low levels in most other tissues, including lung, liver, spleen, thymus, prostate, ovary and placenta (Belinsky *et al.,* 1998). Recent investigations have shown that MRP6 is predominantly expressed in liver and kidney cells and to a lesser extent in other tissues (Kool *et al.,* 1999b).

1.7.1.2.6 MRP1 and clinical multidrug resistance

The expression of MRP1 protein and/or mRNA has been detected in almost every tumour type examined, including both solid tumours (lung, gastrointestinal and urothelial carcinomas, neuroblastoma, glioma, retinoblastoma, melanoma, cancers of the breast, endometrium, ovary, prostate and thyroid) (Ito *et al.*, 1998; Canitrot *et al.*, 1998; Chan *et al.*, 1997; Nanashima *et al.*, 1999; Hipfner *et al.*, 1999; Oshika *et al.*, 1998; Loe *et al.*, 1996), and hematological malignancies (Filipits *et al.*, 1997; Abbaszadegan *et al.*, 1994; Loe *et al.*, 1996b). Among the common tumour types, expression of high levels of MRP1 is particularly frequent in the major histologic forms of non-small cell lung cancer (Nooter *et al.*, 1996; Giaconne *et al.*, 1996; Hipfner *et al.*, 1999).

A number of authors have reported that the expression levels of MRP1 are of prognostic significance. Chan *et al.* (1997), reported that MRP1 expression in retinoblastoma (RB) was associated with the rare failures of chemotherapy in RB. Canitrot *et al.* (1998), and Campling *et al.* (1997), reported that the expression of MRP1 mRNA was a negative determinant of the chemotherapeutic response of untreated Small Cell Lung Cancer (SCLC). MRP1 was also reported by Ito *et al.* (1999), to have prognostic value in primary breast cancer and might be used as one of the markers for poor prognosis in patients with this disease (Huang *et al.*, 1998). Oda *et al.* (1996), also suggested a link between MRP1 expression and poor prognosis in Ewings sarcoma and malignant peripheral neuroectodermal tumour of bone (MPNT).

1.7.1.2.7 Additional genes thought to be associated with MDR

BCRP was first identified in the human MCF-7 breast cancer cell line which displayed an ATP-dependant reduction in intracellular anthracycline accumulation (Doyle *et al.*, 1998). Since then, it has been characterised and identified in a number of human tissues (Maliepaard *et al.*, 2001a). BCRP mRNA encodes a protein of 663 amino acids which was also identified as a member of the ABC family of transporters that encompass the MRP homologues. A previous study by Ma *et al.* (1998) had identified a novel mechanism of multidrug resistance in the ovarian cancer cell line IGROV1 selected in topotecan. Further research (Maliepaard *et al.*, 1999; Scheffer *et al.*, 2000; Yang *et al.*, 2000) confirmed the expression of the BCRP gene in the IGROV1 and MCF-7 cell lines following selection in topotecan. Scheffer *et al.* (2000) also localised the protein in the plasma membrane of the IGROV1 cell line. BCRP expression has also been observed in cell lines following exposure to mitoxantrone (Maliepaard *et al.*, 1999; Ross *et al.*, 1999), and the BCRP gene is sometimes referred to as the Mitoxantrone resistance gene (MXR). Further studies identified expression of BCRP in a flavopiridol-resistant MCF-7 subline (Robey *et al.*, 2001).

Expression of BCRP has been linked with resistance to mitoxantrone, methotrexate (MTX), adriamycin, daunorubicin bisantrene and topotecan (Doyle *et al.*, 1998; Volk *et al.*, 2000; Litman *et al.*, 2000). A clinical study (Ross *et al.*, 2000), observed a sufficiently high level of BCRP gene expression in patients with AML to warrant additional investigation. Little is currently known of how BCRP mediates cross-resistance to these drugs.

Despite its close sequence similarity to mdr-1 (75%) (reviewed in Klein *et al.*, 1999), mdr-3 is not implicated in multidrug resistance. However, the absence of mdr-3 protein expression has been identified as the cause of progressive familiar intrahepatic cholestasis in both rats and humans (PFIC2 and 3, respectively) (reviewed in Klein *et al.*, 1999). Mdr-3 is a phospholipid (phosphatidyl choline) translocator (van Helvoort *et al.*, 1996), with a highly specific expression pattern in the canalicular membrane of the liver (Smith *et al.*, 1994).

1.7.2 COX-1 and COX-2

As outlined in Section 1.7.1, COX-1 and COX-2 refer to two isoforms of the enzyme prostaglandin endoperoxide synthase (PGE). This enzyme transforms arachidonic acid, liberated by phospholipase A_2, to prostaglandins. PGE is a dual function enzyme, incorporating both a cyclooxygenase and a peroxidase activity (Vane *et al.*, 1996).

Human COX-1, a 22kb gene, is a membrane bound hemo-and glyco-protein with a molecular weight of 71kD. It is found in greatest amounts in the endoplasmic reticulum of prostanoid-forming cells. The three-dimensional structure, determined by Picot *et al.* (1994), shows that COX-1 comprises three independent folding units: an epidermal growth factor like domain, a membrane binding motif and an enzymatic domain. COX-1 is constitutively produced and is believed to be involved in regulating normal cellular processes, such as gastro intestinal (GI) cytoprotection, vascular homeostasis, and renal function. The concentration of the enzyme remains largely stable, but small increases of expression of two-to four-fold can occur in response to stimulation with hormones or growth factors (DeWitt *et al.*, 1991).

In contrast, COX-2, identified by Fu *et al.* (1990), as an inducible synthase and a distinct isoform of cyclooxygenase encoded by a different gene from COX-1, is undetectable in most normal tissue. However, the expression of COX-2 can be increased dramatically after exposure of fibroblasts, vascular smooth muscle or endothelial cells to growth factors, hypoxia, phorbol esters or cytokines and by lipopolysaccharides (LPS) in monocytes/macrophages (Bolten, 1998, Vane *et al.*, 1996). The human COX-2 gene is 8.3kb in size, smaller than COX-1 but with a similar molecular weight. The amino acid sequence of its cDNA shows only a 60% homology with COX-1. COX-2 and COX-1 also have similar active sites for the attachment of arachidonic acid or NSAIDs, although the active site of COX-2 is larger than that of COX-1 and can accept a wider range of structures as substrates (Meade *et al.*, 1993). Both enzymes have similar Km and Vmax values for the metabolism of arachidonic acid. (Meade *et al.*, 1993).

1.7.3 Introduction to translation initiation

Initiation is the primary target for the control of translation, with the binding of the ribosomal pre-initiation complex to the mRNA and the scanning process being controlled through a number of mechanisms including RNA-binding repressors, modulation of the Initiation Factors involved, and the effects of secondary structure adopted by a particular mRNAs 5'-UTR.

The basic process of translation initiation involves the binding of the 40S Ribosomal subunit complexed with a charged initiator tRNA (tMet) to the 5' Cap from where it scans the 5' UTR in search of an in-frame AUG start codon. tRNAs (transfer RNAs) carry the Amino Acids to the actively translating ribosome during protein synthesis. The Eukaryotic signal to begin translation is an AUG codon in a particular context, and as such, all proteins begin with a Methionine (encoded by AUG and recognised by t-Met) that is later cleaved. The 40S ribosomal subunit is guided onto the correct region of the mRNA to begin translation by numerous Initiation Factors, known as eIFs (eukaryotic translation Initiation Factors), that catalyse various stages of the binding, scanning and initiation processes (Kleijn, 1998).

1.7.3.1 Eukaryotic Initiation Factor 2 (eIF-2)

With their individual roles the eukaryotic translation Initiation Factors (eIFs) act in concert to assemble the ribosome on the 5' end of the mRNA and begin the scanning process in search of the initiator AUG codon. eIF-2 recruits the initiator tRNA (Met-tRNA) and conducts it as a Met tRNA-eIF2-GTP complex to the 40S Ribosomal subunit, to form the 43S pre-initiation complex (Colhurst *et al.,* 1987; Altman and Trachsel, 1993).

eIF-2 is a multimeric protein comprising of three dissimilar polypeptide chains, α, β and γ, which are thought to remain associated throughout the process of initiation (Proud *et al.,* 1991). The α-subunit is the site for regulation of eIF-2 activity, via phosphorylation. The β-subunit is involved in the interaction of eIF-2 with eIF-2B, which recycles eIF-2

via GDP-nucleotide exchange, and with eIF-5, which catalyses GTP-hydrolysis to release the tRNA during initiation. The γ-subunit is the actual "carrier" of the GTP/GDP molecule (Asano and Hinnesbuch, 1998).

1.7.3.2 Eukaryotic Initiation Factor 4E (eIF-4E)

eIF4E, otherwise known as eIF4α or the small cap binding protein, binds directly to the 5' 7-Methyl-Gppp cap in an ATP-dependent manner, and is thought to be the first factor to interact with the mRNA to initiate translation. eIF-4E is a 25 kDa phospho-protein responsible for Cap-binding specificity in eIF-4F complexes during eukaryotic translation initiation events. eIF-4E consists of a single αβ domain which contains 8 antiparallel β strands forming a curved β sheet (Sonenberg and Gingras, 1998). Phosphorylation of eIF-4E occurs as part of the eIF-4F complex (Tauzon *et al.,* 1990) greatly enhancing and stabilising its association with the cap (Minich *et al.,* 1994).

eIF-4E is widely accepted as the limiting factor in translation initiation, particularly for mRNAs with complex 5' UTRs (Hentze, 1997). It is present in molar levels significantly lower than that of other initiation factors (Sonenberg, 1996). It is the most specifically targeted mRNA-binding eIF and is an essential component of the cytoplasmic cap-binding complex. The cap-binding activity of the eIF-4E peptide is thought to reside in a highly evolutionarily conserved placement of tryptophan residues in both yeast and mammals (Altmann *et al.,* 1988). This factor therefore plays a critical role in the regulation of translation, particularly of specific mRNA species, and the levels and activity of eIF-4E are critical to the control of cellular proliferation and differentiation (Jaramillo *et al.,* 1991). A rather novel and as-yet to be proven additional function for eIF-4E has been suggested, namely that it may play some part in the transport of mRNAs from the nucleus (Rom *et al.,* 1998).

1.7.4 Introduction to transcription factors

1.7.4.1 c-*myc*

c-*myc* is a member of a multigene family consisting of two other members, L-*myc* (identified in SCLC) and N-*myc* (expressed in neuroblastomas) (Erisman and Astrin, 1988). It is one of the immediate early growth response genes and is rapidly, but transiently, induced in quiescent cells upon mitogenic stimulation; mRNA and protein levels are sustained throughout the cell cycle in proliferating cells (Evan *et al.*, 1992). The gene is frequently seen translocated to the heavy chain locus of the immunoglobulin gene in Burkitt's lymphoma suggesting that c-*myc* has a primary role in the transformation of some human haematopoietic cells (Watt *et al.*, 1983).

The c-Myc protein is a member of the nuclear oncoproteins and acts as a transcription factor to promote cell proliferation and has an elusive role to play in control of the cell cycle (Pardee, 1989). C-Myc usually stimulates proliferation, but if growth is inhibited by other factors, Myc-induced apoptosis will occur. Myc therefore has a dual role to play in the cell: myc stimulates growth in the presence of survival factors and induces apoptosis in the presence of growth inhibiting factors (Mihich and Schimke, 1994).

Expression of the c-*myc* gene occurs in most cell types and is detectable in almost all proliferating cells and is vital for normal cell development. Deregulated c-*myc* expression in found in a wide variety of malignancies. Overexpression of both the gene and protein has been associated with early relapse and poor prognosis in clinical breast tumours (Kreipe *et al.*, 1993).

1.7.5 Introduction to cell adhesion and cell adhesion molecules (CAMs)

Cell adhesion is crucial for the assembly of individual cells into the three-dimensional tissues of animals. Cells do not simply "stick together" to form tissues, but rather are organised into very diverse and highly distinctive patterns. A variety of cell adhesion mechanisms are responsible for assembling cells together and, along with their

connections to the internal cytoskeleton, determine the overall architecture of the tissue. Thus, cell adhesion systems should be regarded as mechanisms that help translate basic genetic information into the complex three-dimensional patterns of cells in tissues (Gumbiner, 1999). The expression on the surface of cells of various types of cell adhesion molecules influences cell-cell sorting, tissue architecture and cellular differentiation. Cell adhesion molecules carry out these functions by binding other cell adhesion molecules or by binding to the extra-cellular matrix (ECM).

The ability to recognise similar (homotypic) or dissimilar (heterotypic) cell types or ECM proteins is mediated by four classes of membrane receptor; integrins, selectins, cadherins and the immunogloblulin cell adhesion molecules. All these CAMs are in effect membrane receptors whose extracellular domains bind ligands that generate conformational change in the cytoplasmic tail, enabling it to bind cytoplasmic proteins (Gumbiner, 1999). These adaptor molecules link with various signalling pathways that influence cell proliferation, migration, differentiation and apoptosis. Cell-cell adhesion seems to be a static process but dynamic rearrangements of adhesion should occur during the various cellular processes, such as epithelial cell scattering (metastasis), dispersal of cancer cells, or differentiation (Kaibuchi *et al.*, 1999).

1.7.5.1 E-cadherin

There are at least twelve known members of the cadherin family, which are divided into subclasses, sharing a common basic structure. The three main subclasses are E-Cadherin (found on many types of epithelial cells), P-Cadherin (found in the placenta and epidermis), and N-Cadherin (found on nerve, heart and lens cells) (Takeichi, 1991). Cadherins are the "glue" by which adjacent epithelial cells are attached to each other; they are important in determining the pattern of cells in a tissue. They function as Ca^{2+}-dependent homophilic cell-cell binding proteins (Nose *et al.*, 1990). They are believed to modulate differentiation by co-signalling with other cell adhesion molecules e.g. E-cadherin and the integrins act together to modulate glandular differentiation in colorectal cells (Pignatelli *et al.*, 1992)

The cadherin molecules interact with the actin cytoskeleton via the catenins (α, β, and γ) located in the focal adhesion complexes (Ozawa *et al.*, 1990). The cytoplasmic domain of E-cadherin interacts with β-catenin or γ-catenin directly, which then interact with α-catenin, which has been thought to directly or indirectly link the complex composed of E-cadherin, β-catenin and α-catenin with the actin cytoskeleton. Through these interactions with the catenins to the cytoskeleton, the cadherins form cell junctions in epithelial cells (Ranscht, 1994). A disruption of these catenins leads to a disruption of cadherin function (Ozawa *et al.*, 1990).

Down-regulation of the E-cadherin/catenin complex has been implicated in oesophageal cancer (Kadowaki *et al.*, 1994), gastric cancer (Streit *et al.*, 1996) and colon cancer (Vermeulen *et al.*, 1995). At present, little is known about cadherin expression in SCLC (Shimoyama *et al.*, 1989). E-cadherin suppression is also associated with various stages of differentiation and development (Christofori and Semb, 1999).

1.7.5.2 α-catenin

The interaction of cadherin-catenin complex with the actin-based cytoskeleton through α-catenin is indispensable for cadherin-based cell adhesion activity (Imamura *et al.*, 1999). Fusion studies involving the COOH portion of α-catenin and mutant non-functional E-cadherin as expressed in mouse L cells (Nagafuchi *et al.*, 1994), indicated that α-catenin, especially the COOH-terminal half, is crucial for the full cadherin-based cell adhesion activity as well as cadherin-cytoskeleton interaction.

1.7.5.3 β-catenin

β-catenin, the vertebrate homologue of armadillo protein in *Drosophila*, is a multifactorial protein involved in two apparently independent processes; cell-cell adhesion and signal transduction via transcriptional activation. The role of β-catenin in adhesion has already been outlined; in the adherens junctions of epithelial cells, the cytoplasmic domain of E-cadherin organises a peripheral protein complex, including α-

catenin, β-catenin and γ-catenin that is necessary for adhesion to occur. Recently, studies have implicated mutations in the β-catenin gene with a characteristic phenotype in ovarian malignant transformation; endometroid ovarian carcinoma (Palacios and Gamallo, 1998).

1.7.6 Introduction to apoptosis

Apoptosis is a mechanism of cell death whereby a cell actively participates in its own destruction. "Apoptosis" was a term used by Kerr *et al.* (1972), to describe a series of morphological changes shared by dying cells in various biological systems. These morphological changes include cell shrinkage, membrane blebbing, chromatin condensation and endonucleolytic cleavage of DNA into nucleosomal-length fragments, and finally the production of budding "apoptotic-bodies". The process does not induce an inflammatory response.

Apoptosis is regulated by many genes in normal tissues, some of which are normal cellular counterparts of genes influential in the transformation of normal to malignant cells. The protein products of these genes can influence cell viability either by promoting or inhibiting cell death and it is the balance or interplay of this myriad of proteins which influences a cell's susceptibility to death.

1.7.6.1 The Bcl-2 Gene family:

The study of the Bcl-2 family as genes that influence cell viability and death independent of cell division represents a vast area of research in the whole field of cancer biology. Analysis by Tsujimoto and Croce (1986) indicated that the Bcl-2 gene consists of at least two exons that produce three transcripts of 8.5kb, 5.5kb and 3.5kb long mRNAs. The Bcl-2 cDNA sequence was analysed, from which two protein products were postulated; Bcl-2α (239 amino acids) and Bcl-2β (205aas), that differ only at their carboxy terminus. The Bcl-2α mRNA encodes a 26kDa protein that is homologous to the hypothetical Epstein-Barr virus protein BHFR1 (Cleary *et al.*, 1986).

The anti-apoptotic activity of the Bcl-2 gene has been reviewed by Reed (1994). Evidence has been found to suggest that Bcl-2 functions as an apoptosis-repressing gene primarily by inhibiting the cell death function of pro-apoptotic proteins such as BAX (Hunter and Parslow, 1996). Craig (1995) also indicated that Bcl-2 may inhibit apoptosis by altering Ca^{2+} fluxes through intracellular organelles. As calcium can function as a second messenger in intracellular signalling, this may be how Bcl-2 exerts its effect on cell death signal transduction pathways.

A number of other genes have been discovered recently as members of this group; among them, Bcl-x (Boise *et al.*, 1993), BAX and BAG (Takayama *et al.*, 1995). These proteins can homo- or hetero-dimerise and the balance of the pro- or anti-apoptotic effect determines whether a cell should live or die.

Bcl-2 has been found to associate *in vivo* with a Bcl-2-associated X protein (BAX). BAX was identified as a 21kDa protein with extreme amino acid homology with Bcl-2, and which forms homo- or hetero-dimers with Bcl-2 *in vivo*. When BAX predominates, apoptosis is increased and the repressive activity of Bcl-2 is countered. Three alternative transcripts of the gene have been identified - α, β and γ. BAXα codes for the 21kDa protein product of the gene. RNA splicing may act as a differential regulator of BAX activity and localisation with BAXβ providing an additional level of regulation. No function for BAXγ has yet been elucidated. BAX was first reported to act as a tumour suppressor (Yin *et al.*, 1997). The group observed that p53-induced expression of BAX stimulated apoptosis in slow-growing mouse tumours. An antisense oligonucleotide directed against the gene in a rat sympathetic neuron cell line promoted growth of the cell line (Gillardon *et al.*, 1996). Expression of BAX has also been correlated with intracellular accumulation of taxol in SW626 ovarian cancer cells (Strobel *et al.*, 1998). Expression of the gene has also been correlated with differential regulation in tumours of the central and peripheral nervous system (Krajewski *et al.*, 1997) and in uterine cancer (Saitoh *et al.*, 1999).

Boise *et al.* (1993), isolated the Bcl-x gene from libraries by hybridisation with a Bcl-2 probe. Two distinct Bcl-x mRNAs can form as a result of alternative splicing – the long form Bcl-x_L, (233 amino acids) and the short form, Bcl-x_S (170 amino acids). The

shorter form lacks two domains, BH1 and BH2, commonly found in most proteins of the Bcl-2 family. Bcl-x can function as a Bcl-2-independent regulator of apoptosis but both transcripts work in a reciprocal fashion to one another, i.e. Bcl-x_L confers resistance to apoptosis (anti-apoptotic) whereas Bcl-x_S, in a dominant manner, prevents increased levels of Bcl-2 from inducing apoptosis. Both Bcl-x_L and Bcl-x_S can form heterodimers and/or multidimers with Bcl-2 (Sato *et al.*, 1994). A heteromeric complex between Bcl-x_S and Bcl-2 is normally inactive, whereas Bcl-x_L normally mediates apoptosis by binding to the same downstream regulators of apoptosis as Bcl-2. To date, Bcl-x expression has been detected in a number of clinical studies, including primary colorectal cancers (Krajewska *et al.*, 1996) and esophageal squamous cell carcinoma (Takayama *et al.*, 2001).

BAG (or Bag-1) was identified by Takayama *et al.* (1995). The group found that the BAG-1 protein shares no significant homology with Bcl-2 or other Bcl-2 family proteins, which can form homo- and heterodimers. In gene transfer experiments using a human lymphoid cell line, Jurkat, coexpression of BAG-1 and Bcl-2 provided markedly increased protection from cell death induced by several stimuli, including staurosporine, anti-Fas antibody, and cytolytic T cells, relative to cells that contained gene transfer-mediated elevations in either BAG-1 or Bcl-2 protein alone. BAG-transfected 3T3 fibroblasts also exhibited prolonged cell survival in response to an apoptotic stimulus. These findings indicated that Bag-1 represented a novel type of anti-cell death gene and suggest that some routes of apoptosis induction previously ascribed to Bcl-2-independent pathways may instead reflect a need for the combination of Bcl-2 and BAG-1. Further studies Takayama *et al.* (1997) showed that the protein inhibits expression of the heat-shock protein Hsp70/Hsc70 and thus may provide a link between cell signalling, cell death and the stress response. BAG-1 protein was also observed to inhibit retinoic acid (RA)-induced apoptosis in MCF-7 breast cancer cells (Liu *et al.*, 1998), and expression of the gene was correlated with cell survival and enhancement of Bcl-2 activity in hydridoma cells (Terada *et al.*, 1997).

1.7.6.2 Introduction to other genes involved in modulating apoptosis

1.7.6.2.1 Survivin

Survivin is the most recently discovered, and also the smallest member of a group of anti-apoptotic genes (IAPs). It consists of 12 amino acids and has a molecular weight of 16.4 kDa. In contrast to the other described IAPs, Survivin displays regulation at the transcriptional level. It is abundant during development in proliferating tissues and in tissues in which apoptosis is evident, but is low or absent in terminally differentiated adult tissues (Kobayashi *et al.*, 1999). Most importantly, Survivin is upregulated in a number of common cancers and transformed cell lines (Ambrosini *et al.*, 1997). Additional evidence suggesting that Survivin may play an important anti-apoptotic role in cell proliferation and cancer progression comes from the findings that Survivin is upregulated in G2/M (Li *et al.*, 1998; Kobayashi *et al.*, 1999) and that it is associated with spindle microtubules and seems to require this association for anti-apoptotic activity at least with respect to the apoptosis inducer taxol (Li *et al.*, 1998). Also, overexpression of the gene encoding Survivin blocks cell death in response to a number of different stimuli (Li *et al.*, 1998; Kobayashi *et al.*, 1999) and Survivin binds, although not well, to processed forms of caspase-3 and caspase-7 (Kobayashi *et al.*, 1999). An antisense oligonucleotide directed at Survivin promoted caspase activation and cell death in HeLa cells (Ambrosini *et al.*, 1998).

1.7.6.2.2 MRIT

There is a paucity of information on the pro-apoptotic MRIT gene. MRIT or "MACH-related inducer of toxicity" has been observed to interact with Bcl-x_L and FLICE (MACH) simultaneously and independently (Han *et al.*, 1997). MACH is a large prodomain caspase that links the aggregated complex of the death domain receptors of the tumor necrosis factor receptor family to downstream caspases which trigger apoptosis. However, unlike FLICE, the C-terminal domain of MRIT lacks the caspase catalytic consensus sequence (Han *et al.*, 1997). This group also showed that MRIT associates with caspases possessing large and small prodomains (FLICE, and

CPP32/YAMA), as well as with the adaptor molecule FADD. Thus, MRIT is a mammalian protein that interacts simultaneously with both caspases and a Bcl-2 family member. Thus the gene may function as a crucial link between cell survival and cell death pathways in mammalian cells.

1.7.6.2.3 BAP

BAP (or Bap31) has been defined as a human Bcl-2-interacting protein (Ng *et al.*, 1997). It is a 28-kD (p28) polytopic integral protein of the endoplasmic reticulum whose COOH-terminal cytosolic region contains overlapping predicted leucine zipper and weak death effector homology domains (anti-apoptotic), flanked on either side by identical caspase recognition sites. Ng *et al.* (1997) also showed that Bap is part of a complex that includes Bcl-2/Bcl-XL and procaspase-8. Bax, a pro-apoptotic member of the Bcl-2 family, does not associate with the complex; however, it prevents Bcl-2 from doing so. In the absence of elevated Bcl-2 levels, apoptotic signaling by adenovirus E1A oncoproteins promote cleavage of p28 at the two caspase recognition sites. The resulting NH2-terminal p20 fragment induces apoptosis when expressed ectopically in otherwise normal cells. Taken together, the results suggest that Bap is part of a complex in the endoplasmic reticulum that mechanically bridges an apoptosis-initiating caspase, like procaspase-8, with the anti-apoptotic regulator Bcl-2 or Bcl-x_L (Ng and Shore, 1998).

1.8 DNA microarrays

Nucleic acid microarrays provide a powerful methodology for studying biological systems on a genomic scale. Microarray technology has enabled the modern science of gene expression profiling in which the expression state of hundreds to thousands of genes may be summarised in a single experiment. This high throughput analysis of gene expression has revolutionised traditional methods of basic science research, disease investigation, drug discovery and toxicity testing.

A standard microarray consists of hundreds of long oligonucleotides immobilised by UV irradiation on a plastic, glass or membrane support. Each gene on a microarray is represented by one of these oligos. Standard oligos are 80 bases in length. This length is chosen to combine the high hybridisation efficiency of a lengthy cDNA fragment with a short oligo's ability to distinguish between different genes. These microarrays are probed with radiolabelled cDNA generated from the target RNA samples of interest. Once hybridised, excess label is rinsed away and the microarray is examined using specific instruments and software. Computer analysis specially designated for a selected microarray then decides if alterations in gene expression have been observed, and if so, by how much. With an optimised system, the examination of expression of thousands of genes may be examined in any system.

Although the technology is relatively novel, it has been extensively utilised already in a large number of studies. It has recently been used in lung cancer cell lines to examine expression of apoptotic gene expression (Kannan *et al.*, 2001) as well as general genetic profiling of squamous lung cell carcinomas (Wang *et al.*, 2000) and in bronchial epithelial cells (Hellmann *et al.*, 2001). However, this is just a small number of the instances of usage of the technology; a current literature search revealed over 3500 published articles featuring microarray analysis.

1.9 Aims of thesis

Previous work by a number of researchers in this laboratory had identified that exposure of the lung epithelial cell lines DLKP and A549 to the differentiating agent 5'-Bromo-2-deoxyuridine (BrdU) induced expression of a number of diverse proteins including cytokeratins-8 and -18, $\alpha_2\beta_1$ integrin, cell-adhesion protein Ep-CAM, eukaryotic initiation factor eIF-4E and the transcription factors c-*myc* and YY1. The mRNA levels for α_2 integrin was increased in the DLKP cells following exposure to BrdU, However, mRNA expression levels for the other proteins remained unaffected by exposure to BrdU (P. Meleady, PhD. Thesis, 1997).

As BrdU has been postulated to integrate into the DNA of exposed cells, it was expected that the agent exerted at least part of its differentiation and gene-inducing effects transcriptionally. In order to investigate this hypothesis, it was necessary to elucidate the effects of BrdU on gene expression levels in differentiating cells. As there is a significant dearth of evidence for transcriptional regulation of gene expression by BrdU, it was decided to examine the expression of several genes in BrdU-differentiated DLKP and A549 cells. Performing these experiments formed the starting point for the project described in this thesis.

A transcriptional model of BrdU-induced gene expression does not currently exist. In order to create a potential model, a numbers of questions needed to be answered;

1. What genes are induced by BrdU in differentiated cells?
2. Are there any common factors which may mediate BrdU-induced transcriptional upregulation in these cells?

To address the first question, RT-PCR was chosen as the initial method of analysis, although DNA microarray analysis was included at a later stage. This latter method would be the preferred initial gene identification procedure for future studies, due to the wide number of genes which may be assayed for expression rapidly and easily. The type of genes chosen for examination were selected from functionally diverse groups, some of whom have already been shown to be induced during differentiation. Several genes were identified as being affected, the bulk of these in the DLKP cell line.

Once several genes identified affected by BrdU had been identified, it was hypothesised that BrdU may mediate induction of gene expression in DLKP by utilising a common transcription factor, or group of factors. 5' promoter analysis of several of these affected genes was carried out and which identified a number of common transcription recognition sites shared by all genes. RT-PCR analysis on these common factors was then carried out to investigate if expression of these factors was affected in BrdU-treated DLKP.

The DLKP cell line was also exposed to a variety of chemotherapeutic drugs both in short-term assays (two weeks or less) and in the selecting-out of drug-resistant DLKP sublines. The gene expression profiles of these cells was then examined by RT-PCR.

Gene expression studies by RT-PCR was also carried out on a number of human lung tumour tissue samples to identify potential clinically relevant gene expression markers in lung cancer.

Finally, the use of gene therapy techniques to modify expression of the MRP1 gene in a subline of DLKP, DLKP-SQ was carried. This was attempted using both antisense and ribozymes to downregulate MRP1 gene and protein expression. This was carried out to investigate if expression of this potentially clinically important gene could be decreased in lung cancer cell lines by such methods.

Section 2.0

Materials and Methods

2.1 Preparation for cell culture

2.1.1 Water

Ultrapure water was used in the preparation of all media and 1x solutions. Pre-treatment, involving activated carbon, pre-filtration and anti-scaling was first carried out. The water was then purified by a reverse osmosis system (Millipore Milli-RO 10 Plus, Elgastat UHP). This system is designed to produce purified water from a suitable municipal water supply. The system utilises a semi-permeable reverse osmosis membrane to remove contaminants from the feed water. This results in water which is low in organic salts, organic matter, colloids and bacteria with a standard of 12-18 MΩ/cm resistance.

2.1.2 Glassware

Solutions pertaining to cell culture and maintenance were prepared and stored in sterile glass bottles. Bottles (and lids) and all other glassware used for any cell-related work were prepared as follows; all glassware and lids were soaked in a 2% (v/v) solution of RBS-25 (AGB Scientific) for at least 1 hour. This is a deproteinising agent which removes proteinaceous material from the bottles. Following scrubbing and several rinses in tap water, the bottles were washed twice by machine (Miele G7783 washer/disinfecter) using Neodisher GK detergent and sterilised by autoclaving. Waste bottles containing spent medium from cells were autoclaved, rinsed in tap water and treated as above. Glassware used for large-scale cell production were treated specially, as outlined in Section 2.2.4.1.

2.1.3 Sterilisation

Water, glassware and all thermostable solutions were sterilised by autoclaving at 121°C for 20 min under 15 p.s.i. pressure. Thermolabile solutions were filtered through a

0.22μm sterile filter (Millipore, millex-gv, SLGV-025BS). Low protein-binding filters were used for all protein-containing solutions. Acrodisc (Pall Gelman Laboratory, C4187) 0.8/0.2μm filters were used for non-serum/protein solutions.

2.1.4 Media Preparation

The basal media used during routine cell culture were prepared according to the formulations shown in Table 2.1.1. 10x media were added to sterile ultrapure water, buffered with HEPES (Sigma, H-9136) and $NaHCO_3$ (BDH, 30151) and adjusted to a pH of 7.45 - 7.55 using sterile 1.5M NaOH and 1.5M HCl. The media were filtered through sterile 0.22 μm bell filters (Gelman, 121-58) and stored in 500ml sterile bottles at 4°C. Sterility checks were carried out on each 500ml bottle of medium as described in Section 2.2.8.

The basal media were stored at 4°C up to their expiry dates as specified on each individual 10x medium container. Prior to use, 100ml aliquots of basal media were supplemented with 2mM L-glutamine (Gibco, 25030-024) and 5% foetal calf serum (PAA laboratories, A15-042) and this was used as routine culture medium. This was stored for up to 2 weeks at 4°C.

Table 2.1.1 Preparation of basal media

	DMEM (Dulbecco's Modified Eagle Medium) (mls) (Sigma, D-5648)	**Hams F12 (mls) (Sigma, N-6760)**
10X Medium	500	Powder
Ultrapure H_2O (UHP)	4300	4700
1M HEPES[1]	100	100
7.5% $NaHCO_3$	45	45

[1] The weight equivalent of 1M N- (2-Hydroxyethyl) piperazine-N'- (2-ethanesulfonic acid) (HEPES) was dissolved in an 80% volume of ultra-pure water and autoclaved. The pH was adjusted to 7.5 with 5M NaOH.

Ham's F12 medium was supplemented with 5% FCS. For most cell lines, (DLKP, DLKP-A2B, DLKP-SQ, A549 and A549 C9) ATCC (Ham's F12/ DMEM (1:1)) supplemented with 5% FCS and 2mM L-glutamine was routinely used. For the COR L23S/R cell lines, RPMI 1640 media (Gibco, 52400-025), was routinely used. This was supplied as a 1X stock and supplemented with 10% FCS and 2mM L-glutamine. Also, in order to maintain the strongly MRP1-overexpressing character of COR L23R, this cell line was fed once every two-three weeks with media containing Adriamycin at a concentration of 0.2 μg/ml. For these cells, Adriamycin was dissolved in sterile distilled water at 500 μg/ml and aliquoted into 500 μl aliquots. These could be stored for up to one year at -20^0C. The working concentration of Adriamycin in media was taken to be 0.2 μg/ml.

2.2 Routine management of cell lines

2.2.1 Safety Precautions

All routine cell culture work was carried out in a class II down-flow re-circulating laminar flow cabinet (Nuaire Biological Cabinet). Any work which involved toxic compounds was carried out in a cytoguard (Gelman). Strict aseptic techniques were adhered to at all times. Both laminar flow cabinets and cytoguards were swabbed with 70% industrial methylated spirits (IMS) before and after use, as were all items used in the experiment. Each cell line was assigned specific media and waste bottles and only one cell line was worked with at a time in the cabinet which was allowed to clear for 15min between different cell lines. The cabinet itself was cleaned each week with industrial detergents (Virkon, Antec. International; TEGO, T.H.Goldschmidt Ltd.), as were the incubators. A separate Laboratory coat was kept for aseptic work and gloves were worn at all times during cell work.

2.2.2 Cell Lines

The cell lines used during the course of this study, their sources and their basal media requirements are listed in Table 2.2.1. Lines were maintained in 25cm^2 flasks (Costar, 3050), 75cm^2 flasks (Costar, 3075) or 175cm^2 flasks (Nulge Nunc, 156502) at 37°C and fed every two to three days.

Table 2.2.1 Cell Lines used in study

Cell Line	Source of Cell Line	Media	Cell Type
DLKP	NCTCC	ATCC*	Poorly differentiated human Lung squamous carcinoma
DLKP-SQ	NCTCC	ATCC*	Squamous clonal sub-population of DLKP
A549	ATCC$^{\Psi}$	ATCC*	Human Lung adenocarcinoma
A549 C9	NCTCC	ATCC*	Clonal sub-population of A549
COR L23S	Dr. P. Twentyman	RPMI 1640	Large cell lung cancer cell line
COR L23R	Dr. P. Twentyman	RPMI 1640	Adr-resistant variant of CORL23 (S)

ATCC* = Basal media consists of a 1:1 mixture of DMEM and Hams F12.

ATCC$^{\Psi}$ = American Tissue Culture Collection.

NCTCC = National Cell and Tissue Culture Centre.

2.2.3 Subculture of Adherent Lines

During routine subculturing or harvesting of adherent lines, cells were removed from their flasks by enzymatic detachment.

Cell culture flasks were emptied of waste medium and rinsed with a pre-warmed (37°C) trypsin/EDTA (Trypsin Versene - TV) solution (0.25% trypsin (Gibco, 25090-028), 0.01% EDTA (Sigma, E-5134) solution in PBS (Oxoid, BR14a)). The purpose of this was to inhibit any naturally occurring trypsin inhibitor which would be present in residual serum. Fresh TV was then placed on the cells (4ml/25cm^2 flask, 7ml/75cm^2 flask or 10ml/175 cm^2 flask) and the flasks incubated at 37°C until the cells were seen to have detached (5-10 min). The flasks were struck once, roughly, to ensure total cell detachment. The trypsin was deactivated by addition of an equal volume of growth medium (*i.e.* containing 5% serum). The entire solution was transferred to a 20ml sterile universal tube (Greiner, 201151) and centrifuged at 1,200 rpm for 3 min. The resulting cell pellet was resuspended in pre-warmed (37°C) fresh growth medium,

counted (Section 2.2.5) and used to re-seed a flask at the required cell density or to set up an assay.

2.2.4 Subculture of suspension cells

Large amounts of cells (e.g. DLKP-SQ) were sometimes required for certain assays, such as for the Inside-Out Vesicle (IOV) assays described in Section 2.3.2. Although these cells are normally adherent, they are grown in suspension in order to maximise cell growth in large numbers (e.g.1 x 10^8 cells).

Cell lines growing in suspension did not require enzymatic detachment. Sometimes it was necessary to detach some of the cells, which had become loosely adhered to the flask surface by gently tapping the flask. The cell suspension was removed to a sterile universal centrifuged at 1200rpm for 3 min and used to re-seed fresh flasks or set up assays. 500ml glass spinner flasks from Techne (Cambridge, UK) were used for the majority of the Inside-Out Vesicle (IOV) culture experiments, although 500ml spinner flasks from Bellco (New Jersey, USA) were also used. Before glass spinner flasks could be used for any cell work they needed to be siliconised to prevent cells adhering to the glass.

2.2.4.1 Siliconisation of spinner flasks

1. Spinner flasks were soaked in a warm solution of 2% RBS-25 for one hour and then scrubbed vigorously with a scrubbing brush.
2. After treatment with RBS, the flasks were soaked in 0.1 M NaOH overnight. This is a depyrogenation step, which removes excess dimethyldichlorosilane from previous treatments and also any contaminating proteins.
3. Flasks were rinsed three times in tap water and three times in UHP water and were allowed to dry overnight @ 37°C.
4. A small amount (approximately 10-15mls) of 2% dimethyldichlorosilane in 1,1,1 trichloroethane (BDH, 33164) was added to the flasks. They were then rotated by hand to ensure even coating of all surfaces (including the agitator and inside the

lids). This procedure was carried out with care in a fume hood. The flasks were allowed to air-dry overnight, after which time they were rinsed three times in ultrapure (UHP) water. A small amount of UHP water was left in the flask after the final rinse and the two side arm caps left a little open to allow steam ventilation during autoclaving.

5. Flasks were loosely covered with tin foil and sterilised at 121°C at 15 p.s.i. absolute pressure for 20 minutes.

2.2.4.2 Culturing in spinner flasks

1. After sterilisation, flasks were rinsed with pre-warmed medium and incubated at 37°C ready for use.
2. Cells in the exponential phase of growth were trypsinised in the normal manner. 250ml of medium containing cells harvested from a 175cm^2 flask (Nulge Nunc, 156502) were inoculated into the spinner.
3. Flasks were incubated at 37°C on a magnetic spinner unit (Techne, MCS-104L) at an average speed of 25rpm. After a period of 24 hours, the agitation rate was increased to 35rpm.
4. After three days of growth in the spinner flasks, the cells were fed with 100 mls media. Cells were harvested after seven days at which time the cell number was approximately 1.5 x 10^8 cells per flask.

2.2.4.3 Sampling from spinner flasks

Sampling was carried out in the laminar flow cabinet making sure to keep the agitator rotating to ensure a representative sample from the spinner flask was being obtained. Usually, a 1ml sample was taken and centrifuged at 1200rpm for 3 minutes. The supernatant was then carefully removed and 1ml of pre-warmed trypsin was added to the cells and incubated at 37°C for 5-10 minutes. The cells were pipetted gently to obtain a single cell suspension and counted as described in Section 2.2.5. Trypsin was added to try to break up cell aggregates.

2.2.5 Cell Counting

Cell counting and viability determinations were carried out using a trypan blue (Gibco, 15250-012) dye exclusion technique.

1. An aliquot of trypan blue was added to a sample from a single cell suspension in a ratio of 1:5.
2. After 3 min incubation at room temperature, a sample of this mixture was applied to the chamber of a haemocytometer over which a glass coverslip had been placed.
3. Cells in the 16 squares of the four outer corner grids of the chamber were counted microscopically. An average number per corner was calculated with the dilution factor being taken into account and final cell numbers were multiplied by 10^4 to determine the number of cells per ml. The volume occupied by sample in chamber is 0.1cm x 0.1cm x 0.01cm *i.e.* 0.0001cm^3 (therefore cell number x 10^4 is equivalent to cells per ml). Non-viable cells were those which stained blue while viable cells excluded the trypan blue dye and remained unstained.

2.2.6 Cell Freezing

To allow long term storage of cell stocks, cells were frozen and cryo-preserved in liquid nitrogen at temperatures below –180°C. Once frozen properly, such stocks should last indefinitely.

1. Cells to be frozen were harvested in the log phase of growth (*i.e.* actively growing and approximately 50 - 70% confluent) and counted as described in Sections 2.2.5.
2. Pelleted cells were re-suspended in serum and an equal volume of a DMSO/serum (1:9, v/v) (Sigma, D-5879). This solution was slowly added dropwise to the cell suspension to give a final concentration of at least $5x10^6$ cells/ml. This step was very important, as DMSO is toxic to cells. When added slowly, the cells had a period of time to adapt to the presence of the DMSO, otherwise cells may have lysed.
3. The suspension was aliquoted into cryovials (Greiner, 122 278) which were quickly placed in the vapour phase of liquid nitrogen containers (approximately

-80°C). After 2.5 to 3.5 hours, the cryovials were lowered down into the liquid nitrogen where they were stored until required.

2.2.7 Cell Thawing

1. Immediately prior to the removal of a cryovial from the liquid nitrogen stores for thawing, a sterile universal tube containing growth medium was prepared for the rapid transfer and dilution of thawed cells to reduce their exposure time to the DMSO freezing solution which is toxic at room temperature.
2. The cryovial was removed and thawed quickly under hot running water.
3. When almost fully thawed, the DMSO-cell suspension was quickly transferred to the media-containing universal.
4. The suspension was centrifuged at 1,200 rpm. for 3 min, the DMSO-containing supernatant removed, and the pellet re-suspended in fresh growth medium.
5. A viability count was carried out (Section 2.2.5) to determine the efficacy of the freezing/thawing procedures.
6. Thawed cells were then placed into 25cm^2 tissue culture flasks with 7mls of the appropriate type of medium and allowed to attach overnight.
7. After 24 hours, the cells were re-fed with fresh medium to remove any residual traces of DMSO.

2.2.8 Sterility Checks

Sterility checks were routinely carried out on all media, supplements and trypsin used for cell culture. Samples of basal media were inoculated either into TSB (Oxoid CM129) (incubated at 20-25°C) or thioglycollate broth (Oxoid, CM173) (and incubated at 30-35°C). Both sets were incubated at their specific temperature for up to 2 weeks checking for turbidity and sedimentation. TSB supports the growth of yeasts, moulds and aerobes, while thioglycollate supports the growth of anaerobes and aerobes. Growth media (*i.e.* supplemented with serum and L-glutamine) were sterility checked at least 2 days prior to use by incubating samples at 37°C and checking as before.

2.2.9 *Mycoplasma* Analysis

Mycoplasma examinations were carried out routinely (at least every 3 months) on all cell lines used in this study.

2.2.9.1 Indirect Staining Procedure

In this procedure, *Mycoplasma*-negative NRK cells (a normal rat kidney fibroblast line) were used as indicator cells. These cells were incubated with supernatant from test cell lines and examined for *Mycoplasma* contamination. NRK cells were used for this procedure because cell integrity is well maintained during fixation. A fluorescent Hoechst stain was utilised which binds specifically to DNA and so will stain the nucleus of the cell in addition to any *Mycoplasma* DNA present. A *Mycoplasma* infection would thus be seen as small fluorescent bodies in the cytoplasm of the NRK cells and sometimes outside the cells.

1. NRK cells were seeded onto sterile coverslips in sterile Petri dishes (Greiner, 633185) at a cell density of $2x10^3$ cells per ml and allowed to attach overnight at 37°C in a 5% CO_2 humidified incubator.
2. 1ml of cell-free (cleared by centrifugation at 1,200 rpm for 3 min) supernatant from each test cell line was inoculated onto an NRK Petri dish and incubated as before until the cells reached 20 - 50% confluency (4 - 5 days).
3. After this time, the waste medium was removed from the Petri dishes, the coverslips washed twice with sterile PBS, once with a cold PBS/Carnoys (50/50) solution and fixed with 2ml of Carnoys solution (acetic acid:methanol-1:3) for 10 mins.
4. The fixative was removed and after air drying, the coverslips were washed twice in deionised water and stained with 2 mls of Hoechst 33258 stain (BDH) (50ng/ml) for 10 mins.

From this point on, work proceeded in the dark to limit quenching of the fluorescent stain.

1. The coverslips were rinsed three times in PBS.

2. They were then mounted in 50% (v/v) glycerol in 0.05M citric acid and 0.1M disodium phosphate.
3. Examination was carried out using a fluorescent microscope with a UV filter.

Prior to removing a sample for mycoplasma analysis, cells should be passaged a min. of 3 times after thawing to facilitate the detection of low level infection.

- Cells should be subcultured for 3 passages in antibiotic free medium (as antibiotics may mask the levels of infection).
- Cell lines routinely cultured in the presence of drugs should be sub-cultured at least once in drug free medium before analysis (some drugs such as adriamycin lead to background level of autofluorescence).
- Optimum conditions for harvesting supernatant for analysis occur when the culture is in log-phase near confluency and the medium has not been renewed in 2-3 days.

2.2.9.2 Direct Staining

The direct stain for *Mycoplasma* involved a culture method where test samples were inoculated onto an enriched *Mycoplasma* culture broth (Oxoid, CM403) - supplemented with 20% serum, 10% yeast extract (Oxoid L21, 15% w/v) and 10% stock solution (12.5g D-glucose, 2.5g L-arginine and 250mls sterile-filtered UHP). This medium optimised growth of any contaminants and incubated at 37°C for 48 hours. Sample of this broth were streaked onto plates of *Mycoplasma* agar base (Oxoid, CM401) which had also been supplemented as above and the plates were incubated for 3 weeks at 37°C in a CO_2 environment. The plates were viewed microscopically at least every 7 days and the appearance of small, "fried egg" -shaped colonies would be indicative of a mycoplasma infection.

2.3 Specialised techniques in cell culture

2.3.1 Miniaturised *in vitro* toxicity assays

2.3.1.1 *In vitro* toxicity assay experimental procedure

Due to the nature of the compounds tested in the assays, precautions were taken to limit the risks involved in their handling and disposal. All work involving toxic compounds was carried out in a Gelman "Cytoguard" laminar air flow cabinet (CG Series). All chemotherapeutic drugs used by this researcher were stored and disposed of as described in Table 2.3.1. A number of additional drugs were used by Dr. Yizheng Liang in the selecting-out of drug-resistant DLKP cell lines (Section 3.3).

Table 2.3.1 Chemotherapeutic drugs used in study

Cytotoxic drug	Supplier	Inactivation	Storage
Vinblastine	David Bull Laboratories Ltd.	Autoclave	Store at 4^0C
Vincristine	David Bull Laboratories Ltd.	Autoclave	Store at 4^0C
Adriamycin	Farmitalia	Hyperchlorite inactivation followed by autoclaving	Store at 4^0C
VP16 (Etoposide)	Bristol-Meyers squib, Pharm. Ltd.	Incineration	Store at RT
Cisplatin	David Bull Laboratories Ltd.	Incineration	Store at RT
Taxol	Bristol-Meyers squib, Pharm. Ltd.	Incineration	Store at 4^0C

1. Cells in the exponential phase of growth were harvested by trypsinisation as described in Section 2.2.3.
2. Cell suspensions containing $1x10^4$ cells/ml were prepared in cell culture medium. Volumes of 100 µls of these cell suspensions were added in to 96 well plates

(Costar, 3599) using a multichannel pipette. The plates were divided so that each variable was set up with 8 repeats and 12 variables per plate. A control lane, one to which no drug would be added, was included on all plates. Plates were agitated gently in order to ensure even dispersion of cells over a given well. Cells were incubated overnight at 37°C in an atmosphere containing 5% CO_2.

3. Cytotoxic drug dilutions were prepared at their final concentration in cell culture medium. The plates were emptied of media and 100 µl volumes of the drug dilutions were added to each well using a multichannel pipette. Plates were mixed gently as above.
4. Cells were incubated for 6 days at 37°C and 5% CO_2. At this point the control wells would have reached approximately 80% confluency.
5. Assessment of cell survival in the presence of drug was determined by acid phosphatase assay (Section 2.3.1.4). The concentration of drug which caused 50% cell kill (IC_{50} of the drug) was determined from a plot of the % survival (relative to the control cells) versus cytotoxic drug concentration.

2.3.1.2 NSAID mediated drug toxicity combination assays

1. Cells were trypsinised from the flask in the exponential phase of growth as described in Section 2.2.3.
2. Cell suspensions containing 1 x 10^4 cells /ml were prepared in cell culture medium. Volumes of 100µl of this cell suspension were added into 96-well plates (Costar, 3599) using a multichannel pipette. Plates were agitated gently in order to ensure even dispersion of cells over a given well. Cells were incubated overnight at 37°C in an atmosphere containing 5% CO_2.
3. Cytotoxic drug dilutions and Indomethacin NSAID dilutions were prepared at 4X their final concentration in media. Volumes of 50 µls of the drug dilution and 50 µls of the NSAID dilution were added to each relevant well so that a total final volume of 200 µls was present in each well. Stock Indomethacin solutions were prepared at approximately 15mg/10ml media, filter sterilised with a 0.22µm filter (Millipore, millex-gv, SLGV-025BS) and were then used for all subsequent dilutions. All potential toxicity-enhancing agents were dissolved in DMSO, ethanol

or media as appropriate. Solvent control experiments showed that no toxicity enhancement effects were due to the presence of DMSO or ethanol.

4. Cells were incubated for 6 days at 37°C in an atmosphere containing 5% CO_2. At this point the control wells would have reached approximately 80% confluency.
5. Cell number was assessed using the acid phosphatase assay (Section 2.3.1.4) and the relevant efficiency of each NSAID tested was elucidated.

2.3.1.3 *In-vitro* Antisense Toxicity assays

1. Cells were trypsinised from the flask in the exponential phase of growth as described in Section 2.2.3.
2. Cell suspensions containing 1 x 10^4 cells /ml were prepared in cell culture medium. Volumes of 100µl of this cell suspension were added into 96-well plates (Costar, 3599) using a multichannel pipette. Plates were agitated gently in order to ensure even dispersion of cells over a given well. Cells were incubated overnight at 37°C in an atmosphere containing 5% CO_2.
3. Antisense oligonucleotides at different concentrations were combined with a transfection agent (as outlined in Section 2.4.4.4) and added to media. 100 µls of this oligo:media mix was added to each well and the plates were incubated overnight at 37°C and 5% CO_2.
4. After 24 hours, this media was removed from the plates and fresh media containing antisense oligos and transfection reagents were added. The cells were re-incubated for 48 hours at 37°C and 5% CO_2.
5. After 48 hours, the media was removed from the plates, the wells were rinsed once with fresh media and re-incubated with 100 µls fresh media per well for 4 hours.
6. Cytotoxic drug dilutions were prepared at their final concentration in cell culture medium. The plates were emptied of media and 100 µl volumes of the drug dilutions were added to each well using a multichannel pipette.
7. Cells were incubated for 4 days at 37°C and 5% CO_2. At this point, the plates were taken down and assayed for confluency using the acid phosphatase assay (Section 2.3.1.4).

2.3.1.4 Assessment of cell number - Acid Phosphatase assay

1. Following the incubation period of 6 days, media was removed from the plates.
2. Each well on the plate was washed with 100 µls PBS. This was removed and 100 µls of freshly prepared phosphatase substrate (10mM *p*-nitrophenol phosphate (Sigma 104-0) in 0.1M sodium acetate (Sigma, S8625), 0.1% triton X-100 (BDH, 30632), pH 5.5) was added to each well. The plates were wrapped in tinfoil and incubated in the dark at 37°C for 2 hours.
3. The enzymatic reaction was stopped by the addition of 50 µls of 1M NaOH to each well.
4. The plate was read in a dual beam plate reader at 405 nm with a reference wavelength of 620 nm.

2.3.2 Inside-out Vesicle (IOV) assays

2.3.2.1 Isolation of IOVs

The isolation of IOVs from various cell lines was performed as described by Ishikawa *et al.* (1994) and was carried out as follows;

1. Approximately 7 x 10^8 cells were pelleted at 5,000 rpm (1,200 x g) for 10 mins. at 4°C in a Sorvall refrigerated centrifuge.
2. The supernatant was decanted and the pellets resuspended in 50ml ice cold PBS. The combined pellets were transferred to a 50 ml tube (Corning, 430921) and spun at 4,000 rpm for 5 mins.
3. The resulting cell pellet was resuspended in 230 mls hypotonic buffer (Table 2.3.2). The PMSF was added to the buffer immediately before use.
4. Cells were lysed by gentle agitation at 4^0C for 1.5 hours.
5. The cell lysate was centrifuged at 28,000 rpm (100,000 x g) for 35 mins. at 4°C in a Beckman SW28 rotor in a Beckman XL-80 ultracentrifuge.

6. The resulting pellets were resuspended in 10 mls of hypotonic buffer and homogenised for 15 mins at 4°C with a Braun Potter S886 homogeniser.
7. The homogenised cell extract was diluted to a final volume of 20 mls with incubation buffer which was prepared as shown in Table 2.3.3.
8. This crude membrane fraction (roughly 10 mls) was layered over 28.5 mls 38% sucrose/10mM Tris-HCl pH 7.4, (38g sucrose in 100ml 10mM Tris-HCl pH 7.4) and centrifuged at 28,000 rpm (100,000 x g) for 35 mins. at 4°C in an SW28 rotor. The interface was marked to specify the location of the plasma membrane band which developed after the sucrose centrifugation step.
9. A thin white band became localised at the interface after centrifugation and this was removed with a pasteur pipette and diluted to a total volume of 20 mls with incubation buffer.
10. The suspension was centrifuged at 38,200 rpm (100,000 x g) for 35 mins. at 4°C using a Beckman 70/70.1 Ti rotor.
11. The pellets were resuspended in 0.2 mls incubation buffer. Vesicles were formed by passing resuspended pellets through a 27-guage needle 20 times using a 1ml syringe.
12. To determine the protein concentration, a Bradford assay was carried out (Section 2.4.1.2) and the IOV preparation was diluted to a concentration of 5mg protein/ml with incubation buffer. Volumes of 50 µls IOVs were frozen at -80^{0}C.

Table 2.3.2 Hypotonic buffer for IOV isolation

Buffer Constituent	Preparation Instructions
0.5mM Sodium Phosphate (pH 7.0)	30 mg NaP in 500 ml UHP
0.1 mM EGTA	19.2 mg EGTA added to NaP solution
0.1 mM PMSF	100 mM stock prepared in EtOH

Table 2.3.3 Incubation buffer for IOV isolation

Buffer Constituent	Preparation instructions
10 mM Tris-HCl (pH 7.4)	1.211g Tris in 1L UHP water
250 mM Sucrose	42.79g Sucrose in 500 ml 10 mM Tris-HCl (pH 7.4)

2.3.2.2 Transport assays with IOVs

Transport assays with IOVs were performed as described by Ishikawa *et al.* (1994). The protocol used is described below;

1. A number of solutions were prepared in advance of the assay. The protocol used for the preparation of the incubation buffer has already been described in Table 2.3.3. An ATP/creatine phosphate/$MgCl_2$/10mM Tris-HCl (pH 7.4) solution is prepared as outlined in Table 2.3.4. Volumes of 200µls were frozen at -80°C.

Table 2.3.4 ATP/Creatine phosphate/$MgCl_2$/10mM Tris-HCl preparation protocol

Buffer constituent	Preparation instructions
$MgCl_2$ $6H_20$	203.3mg in 30 mls Incubation buffer
ATP (Disodium salt)	6.05 mg ATP in 3 mls $MgCl_2$ $6H_20$ solution
Creatine phosphate	32.7 mg in 3mls ATP solution

2. For the AMP solution, 4.99mg AMP (Sigma, A1752) was substituted for the ATP (Sigma A7699). Once prepared, 100 µl volumes were frozen at -80°C.
3. A creatine kinase solution (2mg/ml), (Sigma, C5755) was prepared in incubation buffer and 50µl aliquots frozen at -80 °C.
4. Prior to performing the assay, filters (Millipore, GSWP-02500) were soaked in the incubation buffer for 1 hour at 4°C. Once soaked, the filters were applied to the filter apparatus (Millipore, 12-25 Sampling Manifold) and vacuum was applied to the system.
5. An eppendorf thermomixer (Eppendorf, 5436) was allowed to equilibrate at 37°C and once at temperature, the ATP, AMP, creatine kinase and IOV solutions were thawed rapidly at 37°C. After thawing, solutions were immediately placed on ice.
6. An eppendorf was placed in the thermomixer and the following added sequentially: 60 µls incubation buffer, 30 µls ATP, 5 µls creatine kinase, 5 µls [3H]-LTC4 (DuPont NEN, NET-1018, 0.01 mCi/ml) and 10 µls IOVs. After every sequential addition the thermomixer was adjusted to half speed mixing to allow agitation of the various components of the mixture.

7. Aliquots of 20 µls were removed at appropriate timepoints and added in to 1ml of ice cold incubation buffer.
8. These were then washed through the filter apparatus. The eppendorf was washed out with 1 ml of ice cold incubation buffer. The filter was finally washed with 2 mls of ice cold incubation buffer.
9. Filters were removed and placed in 8 mls scintillation cocktail (ICN, 882475) in a scintillation vial. After allowing 12 hours for the filters to fully dissolve, the vials were counted for [^{3}H] content using a Beckman LS-6500 scintillation counter using a 1 minute count time.
10. For an AMP negative control, the above procedure was repeated with ATP replaced by AMP. For a total negative control, neither ATP nor AMP were included but were instead replaced with 30 µls incubation buffer.
11. For assessment of a compound's ability to inhibit LtC_4 transport ability, the compound of interest was dissolved in incubation buffer at the desired concentration. 5 µls of this was added to an eppendorf in the thermomixer. 55 µls of incubation buffer was then added. The standard volumes of ATP, AMP, creatine kinase, LtC_4 and IOV were added to a total final volume of 110 µls.

2.3.3 Differentiation Studies

Differentiation studies were carried out using 5-bromodeoxyuridine (BrdU) (Sigma, B5002). BrdU powder was reconstituted in UHP water to a stock concentration of 10mM and the resultant solution was filter sterilised through a sterile 0.22µm filter, aliquoted into sterile Eppendorfs and stored at -20^{0}C for up to 1 year.

2.3.3.1 Differentiation assays

All differentiation assays were carried out on adherent A549 and DLKP cells. In all experiments, cells were plated onto 6-well plates (Costar, 3516) at densities of $5x10^3$ per well. 1.5ml of medium was sufficient for each well. The cells were allowed to attach and form colonies by incubating at 37°C, 5% CO_2 for 48 hours. The plates were covered

with parafilm to prevent contamination. The medium was removed and replaced with BrdU-containing medium at 10μM concentration. The length of time the flasks were exposed to BrdU is as outlined here;

2-day exposure flask

5-day exposure flask

7-day exposure flask

15-day exposure flask

Plates were wrapped in aluminium foil because of the light-sensitive nature of BrdU and incubated for up to 21 days. Medium was replaced every 2-3 days over the course of the assay. All waste medium was retained for disposal by incineration.

2.3.3 Exposure of DLKP cells to chemotherapeutic drugs

24 x 175cm^2 flasks were set up with DLKP cells at a concentration of 9 x 10^5 cells per flask (30 mls per flask, 3 x 10^4 cells/ml) and incubated o/night at 37°C. There were eight flasks per drug type per experiment, making up the total number of flasks; one flask each for RT-PCR analysis, Western blotting and *in-vitro* toxicity testing, respectively. The length of exposure times for each flask was as follows:

3 x 2-day exposure flask

3 x 5-day exposure flask

3 x 7-day exposure flask

3 x 15-day exposure flask

The cells were separately exposed to three drugs, cisplatin, taxol and VP16. The concentrations were calculated from preliminary in vitro toxicity assays and RT-PCRs on exposed cells. These concentrations are listed in Table 3.2.1.

2.4 Analytical Techniques

2.4.1 Western Blot analysis

2.4.1.1 Sample preparation

Cells were grown in flasks until they reached 80-90% confluency. They were then trypsinised and centrifuged at 1,200 rpm. for 5 min. The pellet was washed in PBS and re-pelleted twice. The tube was inverted and drained of supernatant. Further treatment of the cell pellet depended on the type of extract required; lysed or sonicated.

2.4.1.1.1 Lysis of cell pellet

1ml of lysis buffer (PBS, 1% NP-40 (Sigma; N-3516), 1X protease inhibitors and 0.2mg/ml PMSF (Sigma, P7626)) was added to the pellet and left on ice for 20 min. A 100X stock solution of protease inhibitors consisted of 400mM DTT (Sigma, D5545), 1mg/ml aprotonin (Sigma, A1153), 1mg/ml leupeptin (Sigma, L2884), 1mg/ml soybean trypsin inhibitor (Sigma, T9003), 1mg/ml pepstatin A (Sigma, P6425) and 1mg/ml benzamidine (Sigma, B6506). If cell lysis had not occurred after 20 min the cells were subjected to sonication. Whole cell extracts were aliquoted and stored at -80°C.

2.4.1.1.2 Sonication of cell pellet

One protease inhibitor tablet from Complete™ Protease Inhibitor (Boehringer Mannheim, 1 697 498) was added to 2 mls UHP. This was then diluted 1/25 and 200 µls of this diluted solution was added to the pellet. The mix was sonicated in a Labsonic U (Braun) 2-3 times at a repeating duty cycle of 0.5s, while checking under a microscope to make sure all the cells had been lysed. Before loading on to an SDS-PAGE gel, 2 µls of the sonicated sample was removed and diluted to 10 µls with UHP for protein quantification.

Sonicated cell extracts were either used immediately in Westerns or were stored at –80°C.

2.4.1.2 Quantification of Protein

Protein levels were determined using the Bio-Rad protein assay kit (Bio-Rad; 500-0006) with a series of bovine serum albumin (BSA) (Sigma, A9543) solutions as standards. A stock solution of 25 mg/ml BSA was used to make a standard curve. 10 µl samples were diluted into eppendorfs in a stepwise fashion from 0 – 2 mg/ml BSA. The Biorad was first filtered through 3MM filter paper (Schleicher and Schuell, 311647) and then diluted 1/5 with UHP as it was supplied as a 5-fold concentrate. The diluted dye reagent (490 µls) was added to each standard and sample eppendorf and the mixtures vortexed. The 500 µl samples were diluted out in 100 µl aliquots onto a 96-well plate (Costar, 3599). After a period of 5 min to 1h, the OD_{570} was measured, against a reagent blank. From the plot of the OD_{570} of BSA standards versus their concentrations, the concentration of protein in the test samples was determined. From this, a relative volume for each protein sample was determined for loading onto the gels. Usually 10-20 µg protein per lane was loaded.

2.4.1.3 Gel electrophoresis

Proteins for western blot analysis were separated by SDS-polyacylamide gel electrophoresis (SDS-PAGE). Resolving and stacking gels were prepared as outlined in Table 2.4.1 and poured into clean 10cm x 8cm gel cassettes which consisted of 1 glass and 1 aluminium plate, separated by 0.75cm plastic spacers. The plates were cleaned by first rinsing in RBS, followed by tap water and finally UHP. After drying, the plates were wiped down in one direction using tissue paper soaked in 70% Industrial Methylated Spirits (IMS). The spacers and comb used were also cleaned in this way. After these had dried, the resolving gel was poured first and allowed to set for 1 hour at room temperature. The stacking gel was then poured and a comb was placed into the stacking gel in order to create wells for sample loading. Once set, the gels could be used immediately or wrapped in aluminium foil and stored at 4°C for 24 hours.

1X running buffer (14.4g Glycine, 3.03g Tris and 1g SDS in 1L) was added to the running apparatus before samples were loaded. The samples were loaded onto the stacking gels, in equal amounts relative to the protein concentration of the sample. The loading buffer (New England Biolabs, 7709) was prepared by adding 1/10 volume 30X Reducing agent to 1 volume 3X loading buffer, and this mix was added at ½ volume to each of the test samples. The samples were loaded including 7µl of molecular weight colour protein markers (New England Biolabs, 7708S). The gels were run at 250V, 45mA for approximately 1.5 hours. When the bromophenol blue dye front was seen to have reached the end of the gels, electrophoresis was stopped.

Table 2.4.1 Preparation of electrophoresis gels

Components	Resolving gel (7.5%)	Resolving gel (12%)	Stacking gel
Acrylamide stock[*2]	3.8 mls	5.25 mls	0.8 mls
Ultrapure water	8.0 mls	6.45 mls	3.6 mls
1.875M-Tris/HCl, pH 8.8	3.0 mls	3.0 mls	-
1.25M-Tris/HCl, pH 6.8	-	-	0.5 mls
10% SDS (Sigma, L-4509)	150 µls	150 µls	50 µls
10% Ammonium persulphate (Sigma, A-1433)	60 µls	60 µls	17 µls
TEMED (Sigma, T-8133)	10 µls	10 µls	6 µls

[2] Acrylamide stock solution consists of 29.1g acrylamide (Sigma, A8887) and 0.9g NN'-methylene bis-acrylamide (Sigma, 7256) dissolved in 60ml UHP water and made up to 100ml final volume. The solution was stored in the dark at 4°C for up to 1 month. All components were purchased from Sigma, SDS (L-4509), NH_4-persulphate (A-1433) and TEMED, N,N,N,N'-tetramethylethylenediamine (T-8133).

2.4.1.4 Western blotting

Following electrophoresis, the acrylamide gels were equilibrated in transfer buffer (25mM Tris, 192mM glycine (Sigma, G-7126) pH 8.3-8.5 without adjusting) for 10 min. Protein in gels were transferred onto PVDF membranes (Boehringer Mannheim, 1722026) by semi-dry electroblotting. Eight sheets of Whatman 3mm filter paper (Whatman, 1001824) were soaked in transfer buffer and placed on the cathode plate of a semi-dry blotting apparatus (Biorad). Excess air was removed from between the filters by rolling a universal over the filter paper. A piece of PVDF membrane, cut to the same size of the gel, was prepared for transfer (soaked for 30 secs. in methanol, 2 mins. in UHP and finally 5 mins. in transfer buffer) and placed over the filter paper, making sure there were no air bubbles. The acrylamide gel was placed over the PVDF membrane and eight more sheets of presoaked filter paper were placed on top of the gel. Excess air was again removed by rolling the universal over the filter paper. The proteins were transferred from the gel to the nitrocellulose at a current of 34mA at 15V for 24-25 mins.

All incubation steps from now on, including the blocking step, were carried out on a revolving apparatus (Stovall, Bellydancer) to ensure even exposure of the blot to all reagents. The PVDF membranes were blocked for 2 hours at room temperature with fresh filtered 5% non-fat dried milk (Cadburys, Marvel skimmed milk) in Tris-buffered saline (TBS) with 0.5% Tween (Sigma, P-1379) pH 7.5. After blocking, the membranes were rinsed once in 1X TBS and incubated with 10 mls primary antibody. The specific conditions for the MRP1 antibody are outlined in Section 2.4.1.4.1, below. Bound antibody was detected using enhanced chemiluminescence (ECL).

2.4.1.4.1 MRP1

Protein samples assayed for the presence of MRP1 were treated with a 1/50 dilution of anti-human MRP1 Rat Mab (MRP1 R1) (TCS, ZUMC-201). The MRP1 antibody was diluted 1:50 in 1X TBS with 0.1% Tween and the membranes were incubated shaking overnight at 4°C. The primary antibody was removed and the membranes rinsed 3 times with TBS/0.5% Tween. The secondary antibody was a 1/10,000 dilution of rabbit

anti-rat-HRP immunoglobulin (Dako, P450). The membranes were washed 3 times in TBS/0.5% Tween and developed as outlined in Section 2.4.1.5.

2.4.1.5 Enhanced chemiluminescence detection

Protein bands were developed using the Enhanced Chemiluminescence Kit (ECL) (Amersham, RPN2109) according to the manufacturer's instructions.

The blot was removed to a darkroom for all subsequent manipulations. A sheet of parafilm was flattened over a smooth surface, *e.g.* a glass plate, making sure all air bubbles were removed. The membrane was placed on the parafilm, and excess fluid removed. 1.5mls of ECL detection reagent 1 and 1.5mls of reagent 2 were mixed and covered over the membrane. Charges on the parafilm ensured the fluid stayed on the membrane. The reagent was removed after one minute and the membrane wrapped in cling film. The membrane was exposed to autoradiographic film (Boehringer Mannheim, 1666916) in an autoradiographic cassette for various times, depending on the signal (30s – 5 mins.). The autoradiographic film was then developed.

The exposed film was developed for 5min in developer (Kodak, LX24, diluted 1:6.5 in water). The film was briefly immersed in water and fixed (Kodak, FX-40, diluted 1:5 in water), for 5min. The film was transferred to water for 5 min and then air-dried.

2.4.2 RNA Analysis

2.4.2.1 Preparation for RNA Analysis

Due to the labile nature of RNA and the high abundance of RNase enzymes in the environment a number of precautionary steps were followed when analysing RNA throughout the course of these studies.

- All solutions (which could be autoclaved) that came into contact with RNA were all

prepared from sterile ultra-pure water and treated with 0.1% diethyl pyrocarbonate (DEPC) (Sigma, D5758) before autoclaving (autoclaving inactivates DEPC), with the exception of Tris-containing solutions (DEPC reacts with amines and so is inactivated by Tris). The Tris-containing solutions were made with DEPC-treated ultra-pure water.

- Disposable gloves were worn at all times to protect both the operator and the experiment (hands are an abundant source of RNase enzymes). This prevented the introduction of RNases and foreign RNA/DNA into the reactions. Gloves were changed frequently.

2.4.2.2 RNA Isolation

Total RNA was extracted from cultured cell lines, antisense-, ribozyme- and plasmid-transfected cell lines, as well as BrdU-treated cell lines. Human tumour and normal specimens throughout the course of these studies were also analysed using the technique outlined below. The size of the flasks varied, but the method remained the same.

A standard method of extracting RNA from cells was as follows: cells were seeded into 175cm^2 flasks (Nulge Nunc, 156502) at a density of approximately 2x10^6 per flask and allowed to attach and form colonies for 48-72 hours at 37^{0}C. The cells were trypsinised and the pellet was washed once with PBS. The cells were pelleted and lysed using 1ml of TRI REAGENT™ (Sigma, T-9424). The following procedure is that outlined in the protocol for TRI REAGENT™. The samples were allowed to stand for 5 mins. at room temperature to allow complete dissociation of nucleoprotein complexes. 0.2 mls of chloroform was added per ml of TRI REAGENT™ used and the sample was shaken vigorously for 15 sec and allowed to stand for 15 min at room temperature. The sample was centrifuged at 13000rpm for 15 mins. at 4°C in a microfuge. This step separated the mixture into 3 phases with the RNA contained in the colourless upper aqueous layer. The DNA and protein fractions resulting from the total RNA isolation were retained in case they were required at some future date. The aqueous layer was transferred to a new Eppendorf and 0.5 mls of 100% isopropanol was added per ml of TRI REAGENT™ originally used. The sample was mixed and allowed to stand at room temperature for

10-15 mins. before being centrifuged again at 13000rpm for 10 min at 4°C. The RNA formed a precipitate at the bottom of the tube. The supernatant was removed and the pellet was washed with 1ml of 75% ethanol per ml of TRI REAGENT™ used and centrifuged at 4°C for 5 mins. at 13000rpm. The supernatant was removed and the pellet was allowed to air-dry for 10-15 mins. 20-30 µls of DEPC water was added to the RNA to resuspend the pellet.

2.4.2.3 RNA Quantitation

RNA was quantified spectrophotometrically at 260nm using the following formula:

$$OD_{260nm} \times \text{Dilution factor} \times 40 = \mu g/ml \text{ RNA}$$

An A_{260}/A_{280} ratio of 1.8-2 is indicative of pure RNA, although RNA with ratios from 1.7 – 2.1 were routinely observed and used in subsequent experiments. Partially solubilised RNA has a ratio of <1.6 (Ausubel *et al.*, 1991). The yield of RNA from most lines of cultured cells is 100-200µg/90mm plate (Sambrook *et al.*, 1989). In these studies 200 µg RNA per 175cm^2 flask was retrieved. RNA samples were diluted to 500 ng/µl and stored at –80°C.

2.4.2.4 Micropipette Accuracy Tests

Accuracy and precision tests were carried out routinely on all micropipettes used in all steps of the RT-PCR reactions. The accuracy and precision of the pipettes was determined by standard methods involving repeatedly pipetting specific volumes of water and weighing them on an analytical balance. The specifications for these tests were supplied by Gilson.

2.4.2.5 Reverse-Transcription Polymerase Chain Reaction (RT-PCR) analysis of isolated RNA

2.4.2.5.1 Reverse Transcription of isolated RNA

Reverse transcriptase (RT) reactions were set up on benches using micropipettes, which were specifically allocated to this work.

To form the cDNA, the following reagents were mixed in a 0.5ml eppendorf (Eppendorf, 0030 121 023), heated to 72°C for 5 min and then chilled on ice.

2µl of a 5x buffer (100mM-Tris/HCl, pH 9.0, 50mM-KCl, 1% Triton X-100) (Sigma, P-2317)
1.2µl 25mM-$MgCl_2$ (Sigma, M-8787)
1µl oligo (dT) primers (1µg/µl)
1µl RNasin (40U/µl) (Sigma, R-2520)
0.4µl dNTPs (10mM of each dNTP) (Sigma, DNTP-100)
2µl total RNA (500ng/µl)
7.4µl DEPC water

To this, 4µl water and 1µl Moloney murine leukaemia virus-reverse transcriptase (MMLV-RT) (40,000U/µl) (Sigma, M-1302) were added. The solutions were mixed and the RT reaction was carried out by incubating the Eppendorfs at 37°C for 1 hour. The MMLV-RT enzyme was inactivated by heating to 95°C for 3 mins. The cDNA was stored at -20°C until required for use in PCR reactions as outlined in Section 2.4.2.6.2.

2.4.2.5.2 Polymerase Chain Reaction (PCR) amplification of cDNA

The cDNA formed in the above reaction was used for subsequent analysis by PCR

A standardised polymerase chain reaction (PCR) procedure was followed in this study. Standard Eppendorf tubes were used, as for the RT reactions. All reagents had been aliquoted and were stored at -20°C and all reactions were carried out in a laminar flow cabinet. A complete list of all PCR primers and reaction conditions are included in Appendix A.

A typical PCR reaction contained the following:

9µl UHP

5µl 5x buffer (100mM-Tris/HCl, pH 9.0, 50mM-KCl, 1% Triton X-100)

2µl 25mM-$MgCl_2$

1µl each of first and second strand target primers[3] (250ng/ml)

1µl each of first and second strand endogenous control primer (250ng/ml) (β-actin)

10µl cDNA

Taq/dNTP mixture 1µl dNTPs (10mM each of dATP, dCTP, dGTP and dTTP)

0.5µl of 5U/µl *Taq* DNA polymerase enzyme (Sigma, D-4545)

18.5µl UHP

The samples were mixed by pipetting two or three times. A typical reaction would be:

	95°C for 3 min	-	denaturation
Taq/dNTP mixture added here			
30 cycles:	95°C for 30 sec.	-	denaturation
	X[4]°C for 30 sec.	-	annealing
	72°C for 30 sec.	-	extension
And finally,			
	72°C for 7 min.		extension

Following amplification, the PCR products were stored at 4°C for analysis by gel electrophoresis

[3] All oligonucleotide primers used throughout the course of this thesis were made to order on an "Applied BioSystems 394 DNA/RNA Synthesiser" by Oswel DNA service, Lab 5005, Medical and Biological Services building, University of Southampton, Boldrewood, Bassett Cresent East, Southampton, SO16 7PX.
[4] Temperature dependent on primer type

2.4.2.6 Electrophoresis of PCR products

A 2% agarose gel (Sigma, A-9539) was prepared in 1X TBE (10.8g Tris base, 5.5g Boric acid, 4 mls 0.5M EDTA, 996mls UHP) and melted in a microwave oven. After allowing to cool, 4 µls of a 10mg/ml ethidium bromide solution was added per 100mls of gel which was then poured into an electrophoresis apparatus (BioRad). Combs were placed in the gel to form wells and the gel was allowed to set.

4µl of 6X loading buffer loading buffer (50% glycerol, 1mg/ml bromophenol blue, 1mM EDTA) was added to 20µl PCR of each sample and this was run on the gel at 80-90mV for approximately 2 hours. When the dye front was seen to have migrated the required distance, the gel was removed from the apparatus and examined on a transilluminator and photographed.

2.4.2.7 Densitometric analysis

Densitometric analysis was carried out using the MS Windows 3.1 compatible Molecular Analyst software/PC image analysis software available for use on the 670 Imaging Densitometer (Bio-Rad. CA) Version 1.3. Developed negatives of gels were scanned using transmission light and the image transferred to the computer. The amount of light blocked by the DNA band is in direct proportion to the intensity of the DNA present. A standard area was set and scanned and a value was taken for the Optical Density (O.D.) of each individual pixel on the screen. The average value of this O.D. (within a set area, usually cm^2) is normalised for background of an identical set area. The normalised reading is taken as the densitometric value used in analysis. As a result, these O.D. readings were unitless.

2.4.3 Northern Analysis

The RNA samples to be analysed were first separated by Formaldehyde-Agarose Electrophoresis.

2.4.3.1 Formaldehyde-Agarose gel Electrophoresis

A 100ml 1% agarose gel was prepared by dissolving 1g of agarose in 73.4 ml UHP. The gel was cooled to around 60°C and 10ml of 10X MOPS buffer (0.25M MOPS, 0.05M Na acetate, 0.01 EDTA, pH 7.0) was added along with 16.6 ml formaldehyde and mixed well before pouring. The running buffer for the gel was 1X MOPS containing 12.9 ml formaldehyde/300ml. 1 or 2μg of mRNA was freeze-dried overnight in a 500 μl eppendorf and dissolved in 5μl of UHP, to allow equal loading volumes. The RNA samples were mixed with RNA loading buffer (2.9μl 10X MOPS, 5μl formaldehyde, 14.3 μl formamide, 1.43μl tracking buffer and heated to 65°C for 15min, placed on ice and loaded onto the gel. The RNA samples were run on the gels at 10 V/cm for 2 hours alongside RNA size markers (Promega, G3191). The gels were washed in 3 changes of UHP over 30 minutes.

2.4.3.2 Northern Blotting

A sheet of Hybond-N (Amersham, RPN 303N) was cut to the same size as the RNA gel. A tray or glass dish was half filled with the transfer buffer (20X SSC (8.823 % (w/v) tri-sodium citrate, 17.532 % (w/v) NaCl, pH 7-8)). A platform was made to stand in the tray above the level of the transfer buffer and a wick (3MM filter paper) was placed over the platform into the transfer buffer. The RNA gel was placed loading side down on the wick platform without trapping air bubbles. The Hybond-N was placed on top of the RNA gel and three sheets of 3MM filter paper placed upon the Hybond-N. A stack of absorbent tissue paper over 5cm high was placed on top of the filter paper and was covered with a glass plate. Finally, a glass plate with a 750g weight was placed on top of the paper stack and the transfer was carried out overnight. After blotting, the transfer apparatus was dismantled and the wells were marked on the Hybond-N to allow identification by hand. The nucleic acid was fixed to the membrane by baking at 80°C for 2 hours and stored until use between two sheets of dry filter paper.

After blotting, the gel was soaked in a 1 μg/ml EtBr solution with agitation and was then viewed under a UV lamp. The efficiency of RNA transfer to the membrane could

then be assessed by looking for remaining traces of 28S and 16S ribosomal bands. The lane on the gel containing the RNA markers was removed from the gel before blotting and stained with EtBr alongside the blotted gel. The position of the RNA markers were photographed and used as a reference to size bands on the developed Northern Blots.

2.4.3.3 Preparation of MRP1 Hybridisation probe

The MRP1 probe was prepared from a MRP1 cDNA plasmid (pHβ-Apr-neo) kindly donated by Dr. Susan Cole. A 1kb fragment of the MRP1 cDNA was cut from the plasmid using two restriction enzymes. The fragment was electrophoresed on a 1% low-melting point agarose gel containing ethidium bromide at 75mV for 1 to 2 hours along with the molecular weight size markers IX and III (Boehringer Mannheim, 558 552 and 1 449 460) to check for the correct fragment size. The gel was viewed under a UV illuminator and the fragment band cut out of the gel with a scalpel. The 1 kb fragment was extracted from the agarose using the Qiaex II Agarose Gel Extraction kit according to the manufacturer's protocol (Qiagen, 20021).

2.4.3.4 Radioactive Labelling of Probes

All DNA probes were random prime labelled with [α-^{32}P]dCTP (Amersham) using the Prime-a-gene labelling kit (Promega : U1100) according to the supplied protocol. Riboprobes (RNA) were generated with [α-^{32}P]CTP (Amersham) using the Riboprobe *In Vitro* Transcription Systems kit (Promega: P1440) according to the supplied protocol. The T7 promoter and RNA polymerase were used in this labelling reaction. 20 to 40 ng of cDNA fragment and 5μl of [α-^{32}P]dCTP or [α-^{32}P]rCTP was used to make each probe.

To test the percentage incorporation of nucleotides into the DNA probes, TCA precipitation was performed. 1 μl out of the 50μl reaction mix was diluted 1 in 100 with water. 1μl of the diluted probe was blotted onto four 1cm^2 pieces of filter paper and air-dried. Two of these pieces of filter paper were washed twice for 10 minutes in 10% Tri-

chloro Acetic Acid (Riedel-del Haen: UN-No-1839), rinsed in 100% ethanol and air-dried. The counts on the two washed and unwashed pieces of filter were measured using a scintillation counter. The filter paper was placed in scintillation counter tubes with 10ml of scintillation fluid (Ecolite) (ICN, 882475) and the Counts per minute (CPM) read. The CPM of the washed pieces of filter paper as a percentage of the unwashed pieces of filter paper gave the percentage incorporation of the probe. Probes with less than 50% incorporation were purified using NAP10 columns (Amersham, 17-0854-01) according to the manufacturer's protocol.

2.4.3.5 Hybridisation of labelled probes to RNA membranes

The Northern membranes were prehybridised overnight at 65°C in 10ml of hybridisation buffer (In 100ml : 43ml 1 M Sodium phosphate pH 7.2, 33 ml 20% Sodium Dodecyl Sulphate (SDS), 20 ml 5% BSA, 4ml 0.5 M EDTA) per membrane. The hybridisation was carried out in glass hybridisation tubes in a hybridisation oven. The appropriate probe was heated to 100°C for 5 min before addition to 10ml of preheated (65°C) hybridisation buffer. Sufficient probe was used to give $3x10^6$ CPM/ml hybridisation buffer. The pre-hybridisation buffer was discarded from the hybridisation tubes and replaced with the fresh hybridisation buffer containing the denatured probe. Hybridisation was carried out at 65°C overnight. The membranes were then washed at 65°C for 5 min in 2X SSC, followed by 2 x 15 min washes in 0.5X SSC, 0.1% SDS and 2 x 15 min washes in 0.1X SSC, 0.1% SDS. The membranes were wrapped in cling film and exposed to X-ray film at -80°C for the desired length of time (typically 24h to 5 days).

2.4.4 Plasmid DNA manipulation

2.4.4.1 Plasmids and oligonucleotides used

The MRP1 ribozyme was cloned into the pHβApr-1-neo expression plasmid and was a

generous gift from Dr. Kevin Scanlon. All standard[5] antisense molecules used were phosphorothioate oligonucleotides, all other antisense were Second-Generation™ chimera[6] oligos. A list of all phosphorothioate antisense sequences is included in Appendix A (Table 7.5A), while the designed Second-Generation™ chimera sequences are listed in Table 3.10.1.

2.4.4.2 Production of unique plasmid DNA samples

In certain cases, as in the event of the *in-vitro* ribozyme cleavage experiment (Section 2.4.7), plasmid DNA expressing the correct sequence of interest in the right orientation was manufactured in the lab. In these cases, the target DNA fragment (e.g. the ribozyme *in-vitro* cleavage (IVC) target fragment) experiment was amplified in a standard RT-PCR reaction (Section 2.4.2.5), cloned into a suitable vector (Section 2.4.4.2.1) and analysed using restriction digest (Section 2.4.4.5) and sequencing reactions (Section 2.4.4.6). The protocols following on from this Section can be regarded as examples of the actual protocols used.

2.4.4.2.1 Ligation of target DNA into a suitable vector

The procedure followed for ligating the all vectors with their corresponding target DNA was that as outlined in the pTarget™ Mammalian Expression Vector System (Promega, A1410) and all manipulations carried out were as outlined in the pTarget™ Mammalian Expression Vector System Technical Manual (Promega, TM044). All necessary ingredients were supplied with the kit.

1. The vector ratio calculation was carried out for the insert:vector involved as follows:

[5] Made to order on an "Applied BioSystems 394 DNA/RNA Synthesiser" by Oswel DNA service, Lab 5005, Medical and Biological Services building, University of Southampton, Boldrewood, Bassett Cresent East, Southampton, SO16 7PX.
[6] Manufactured by Oligos Etc. Inc., 172 Main St., P.O. Box 309, Bethel, ME, 04217, USA

$$\frac{60ng\ Vector\ X\ 0.476\ kb\ Insert}{5.67kb\ vector} \quad X \quad \frac{2}{1} = 10\ \eta g\ insert$$

2. The pTarget™ vector and Control insert tubes were first centrifuged to collect the contents at the bottom of the tube.
3. Ligation reactions were set up as described in Table 2.4.2.

Table 2.4.2 List of standard components for ligation reaction

	Standard Reaction	Positive Reaction
T4 DNA Ligase 10X Buffer	1 µl	1 µl
Vector (60ng)	1 µl	1 µl
Target PCR product	1 µl	-
Control Insert DNA	-	2 µl
T4 DNA Ligase	1 µl	1 µl
UHP	6 µl	5 µl

4. The tubes were incubated overnight at 4^0C.
5. The DNA was stored at -20^0C after ligation. The DNA is now ready for transformation into bacteria (Section 2.4.4.3).

2.4.4.3 Transformation of Bacteria

100µl of competent JM109 bacterial cell suspension (Promega, L2001) was mixed with 20ng DNA and placed on ice for 40min after which the mixture was heat-shocked at 42°C for 90sec and then placed on ice for 3min. 1ml of LB broth ((10g Tryptone (Oxoid, L42), 5g Yeast Extract (Oxoid, L21) 5g NaCl (Merck, K1880814))/litre LB, autoclaved before use) was added to the competent cell suspension and incubated at 37°C for 40min. 400µl of this suspension was spread on a selecting agar plate (LB agar containing appropriate antibiotic conc.) and incubated overnight at 37°C. Single colonies, which grew on these selecting plates, were further streaked onto another selecting plate and allowed to grow overnight at 37°C.

2.4.4.4 DNA miniprep of plasmid DNA

This was carried out in order to determine the orientation of the inserted DNA sequence in the transformed plasmid. Only plasmids with the insert in the correct orientation could be used in the *in-vitro* cleavage (IVC) experiment.

1. Single colonies were selected off the plates and incubated in universals containing 5 mls LB/Amp shaking at 180rpm at 37^0C overnight. White colonies generally contain inserts, but inserts may also be present in blue colonies. For this reason, a number of white colonies, blue colonies and white-blue colonies (white colonies with a blue centre) were selected for incubation. The positive control reaction yielded all blue colonies, which were too numerous to count.
2. After 16-24 hours incubation, 1.5 mls of culture was removed from each of the incubated samples and spun down at 8500rpm in a microfuge. The supernatant was decanted and another 1.5 mls of culture was added and again spun down.
3. The samples were subjected to a plasmid miniprep, as outlined in the Stratagene Clearcut™ Miniprep kit (Stratagene, 400732). The cell preps were each resuspended in three 105 µls of Solution 1.
4. 125 µls of Solution 2 was added, and the eppendorf was mixed gently by inversion.
5. 125 µls of Solution 3 was added, and the eppendorf was mixed gently by inversion. The eppendorf was then placed on ice for 5 mins.
6. The eppendorf tubes were then spun down in a microfuge at 8500rpm and the supernatants were carefully transferred to fresh tubes, leaving cell debris behind.
7. The kit-supplied DNA binding resin was mixed by vortexing until resuspended. 15 µls of this resin was added to each collected supernatant. The tubes were then mixed by inversion.
8. The samples were loaded into kit-supplied spin cups. The cups were spun down in a microfuge at 13,000rpm for 30 secs., which retained the resin and plasmid DNA.
9. A kit-supplied wash buffer was prepared for each sample by diluting 200 µls of 2X wash buffer with 200 µls of 100% (v/v) ethanol. 400 µls of this wash buffer was added to the spin cup and the cups spun at 13,000rpm again for 30 secs. This step was repeated for all samples.

10. The spin cups were transferred to fresh eppendorfs. 50 µls of UHP was loaded into each spin cup to elute the DNA and the samples spun down at 13,000rpm again for 30 secs. The plasmid DNA was stored at -20^0C in the eppendorfs.

2.4.4.5 Restriction enzyme digestion of plasmid DNA

5 µls of each isolated plasmid sample was run out on a 2% agarose gel to check for degradation. Restriction digestion was then carried out to confirm orientation of the insert. All digestions were carried out using the recipe as outlined in Table 2.4.3.

Table 2.4.3 Standard DNA digestion mix

Component	Volume (µls)
DNA sample	10
undiluted enzyme	1
10X Multi-core reaction buffer (Promega, R9991)	1.5
UHP	2.5

All 15 µls were run out on a 1% agarose gel, together with 3 µls loading dye. From the banding patterns observed, the orientation of the insert was correctly discerned. From this information, samples were selected for large-scale plasmid preparation.

2.4.4.6 Plasmid DNA Sequencing

In order to fully confirm the orientation of the inserted DNA in the plasmid, certain samples which had been indicated as being of desired orientation from the restriction digest were sequenced using the following procedures.

2.4.4.6.1 Preparation/Purification of plasmid DNA prior to Sequencing

1. From the appropriate culture universal from Section 2.4.4.3, 50µls of culture was removed and spread on LB/Ampicillin plates. The plates were incubated at 37^0C overnight.
2. The following day, single colonies were selected and were incubated shaking in universals containing 10 mls LB/Ampicillin media at 37^0C overnight.
3. Plasmid DNA was isolated using the Wizard™ *Plus* Minipreps DNA Purification System (Promega, A7100). 3 mls of the culture was pelleted at 1,400 x g for 10 mins. The pellet was resuspended in 400 µls cell resuspension solution and then in 400 µls Cell Lysis solution in an eppendorf. The tube was mixed and 400 µls Cell Neutralisation solution was added. The lysate was centrifuged at 13,000rpm in a microfuge for 30 mins. The plasmid was then purified without using a vacuum manifold.
4. A Wizard™ minicolumn was set up in the usual way and the cleared lysate from the cleaned plasmid samples was added to the barrel of the minicolumn/syringe assembly. The lysate was pushed into the column using the plunger. The lysate was then washed in 2 mls column wash solution and centrifuged at 13,000rpm in a microfuge for 2 mins. The plasmid DNA was eluted by the addition of 50 µls UHP followed by centrifugation at 13,000rpm in a microfuge for 2 mins.

2.4.4.6.2 Sequencing of plasmid DNA

The plasmid DNA was sequenced using the ^{T7}Sequencing™ Kit (Pharmacia Biotech, 27-1682-01). The sequencing gel was poured as outlined in Section 2.4.7.8.

1. 10 µls of template DNA, 2 µls of diluted (2.5 µM) T7 primer, and 2 µls of annealing buffer were added together in an eppendorf, mixed, centrifuged and incubated at 60^0C for 10 mins. These were then left at room temperature for 10 mins. and centrifuged again.
2. To this mix was added 3 µls of labelling mix (dATP), 1 µl of labelled dATP (S_{35}) and 2 µls of diluted T7 DNA polymerase. These were mixed and left at room temperature for 5 mins.

3. Four eppendorfs were labelled A,C,G,T for each template, 2.5 µls of each of the "read short mixes" were added to their corresponding tube and incubated for 1 min. at 37^0C.
4. To each of the pre-warmed sequencing mixes, 4.5 µls of the labelling reaction was added, mixed by gentle pipetting and incubated at 37^0C for 5 mins.
5. 5 µls of stop solution was added and mixed gently.

4 µls of each reaction was added to a fresh tube and incubated at 75-80^0C for 2 mins. And immediately loaded on the sequencing gel. The remainder of the sequencing reactions was stored at –20^0C.

Once orientation had been confirmed by sequencing, large-scale preparation was carried out.

2.4.4.7 Large scale plasmid preparation

A single colony (Section 2.4.4.3) was inoculated into 10ml of LB Amp 50µg/ml and grown overnight; 2ml of this suspension (1% inoculum) was added to 200ml of TB (2.4g Tryptone, 4.8g Yeast Extract, 0.8 mls Glycerol, 0.17M KH_2PO_4 and 0.72M K_2HPO_4) Amp 50µg/ml and left to grow overnight at 37°C for large scale isolation of plasmid from JM109 cells. The following day the cells were pelleted and lysed in 20ml of an ice-cold solution containing 50mM glucose, 25mM Tris-Cl, 10mM EDTA, pH8.0 and 5mg/ml lysozyme (Sigma, L6876) at room temperature for 10-15min. 40ml of a 0.2N NaOH and 1.0% SDS solution was gently mixed with the lysate until the suspension became clear and incubated on ice for 10min. 30ml of 3M K-Acetate, pH5.2 was added to the above and mixed gently until a flocculent precipitate appeared at which stage the mixture was stored on ice for at least 10min. The sample was centrifuged at 35,000xg. for 1h at 4°C. The supernatant was then recovered and added to 0.6 volume of 100% Isopropanol, mixed gently and left at room temperature for 20-30min. The suspension was then centrifuged at 35,000xg. for 30min at 20°C after which the supernatant was discarded. The pellet was washed in ice-cold 70% ethanol and resuspended in 5ml of TE, pH8.0. To remove any contaminating RNA, the plasmid solution was treated with RNase Plus (5 Prime → 3 Prime Inc.; 5-461036) (to a final dilution of 1:250) for 30min at 37°C followed

by phenol:chloroform:isoamyl alcohol extractions (25:24:1). 10M ammonium acetate was added to the aqueous phase to a final concentration of 2.0M. 0.6 volume of 100% Isopropanol was added to the sample, mixed and stored at room temperature for 20-30min. The sample was centrifuged at 13,000rpm and the DNA pellet was washed in 70% ethanol and resuspended in 3.6ml of 10mM Tris-Cl, 1mM EDTA, and 1.0M NaCl, pH8.0. 1.8ml of this sample was loaded into one of two pZ523 columns (following the manufacturer's instructions) and the column effluent was precipitated with 0.6 volume 100% Isopropanol, as described previously. The DNA was pelleted at 13,000rpm in an epifuge, washed in 70% ethanol and resuspended in TE. The DNA concentration was determined by measuring the OD_{260nm}.

2.4.5 Transfection of mammalian cells with exogenous DNA

2.4.5.1 Optimisation of plasmid/antisense transfection protocol

Before full transfections involving the various DNA fragments into the different cell lines could proceed, transfection protocols were first optimised for each of the parameters involved. The DNA used was the pCH110 plasmid which codes for beta-galactosidase activity.

The target cell line was trypsinised in the usual fashion (Section 2.2.3) and set up in the container of interest (i.e. 24/6-well plate, 25-75 cm^2 flask) at several different cell concentrations, which were arbitrarily chosen. Following incubation overnight at 37°C, the cells were transfected according to the transfection protocol for the transfectant used. Only the volumes of transfectant and conc. of DNA were altered to ascertain the most efficient combination. Cells were transfected either in the presence of serum overnight or for four hours in the absence of serum, both at 37°C. After transfection, the cells were washed 2X with PBS and fixed by the addition of fix solution (0.4mls 25% glutaraldehyde (Sigma, G-7526), 10mls 0.5M Sodium Phosphate buffer (pH 7.3), 2.5mls 0.1 EGTA (pH 8.0)(Sigma, E-0396), 0.1mls 1.0M $MgCl_2$ (Sigma, M-8266), 37mls UHP) for 10 mins. The cells were then washed for 10 mins. in wash solution (40mls 0.5M Phosphate buffer (pH 7.3), 10mls 1.0M $MgCl_2$ (Sigma, M-8266), 20mg

Sodium deoxycholate (Sigma, D-4297), 40µls Nonidet P-40 (Sigma I-3021), 160mls UHP). Staining was carried out on the cells using 2.5mls of stain solution (10mls rinse solution, 0.4mls X-gal (Sigma, B-4252) (25mg/ml in dimethylformamide), 16.5mg potassium ferricyanide (Sigma, P-8131), 16.5mg potassium ferrocyanide (Sigma, P-9387)) overnight at 37°C. After staining, the cells were washed with 10mls rinse solution and examined microscopically. Positive cells were those stained blue - the combination resulting in the most blue colonies was adjudged to be the most efficient association and was thereafter used for that cell line.

2.4.5.2 Transfection of DNA using lipofection reagents

On the day prior to transfections, the cells to be transfected were plated from a single cell suspension (Section 2.2.3) and seeded into 25cm^2 flasks at 3x10^5 cells per flask. On the day of the transfection, the plasmids to be transfected were prepared along with the lipid transfection reagents according to the manufacturers protocols (DOTAP - Boehringer Mannheim, 1 202 375; Lipofectin – GibcoBRL, 18292-011; Lipofectamine, GibcoBRL, 10964-013; Fugene6 - Boehringer Mannheim, 1 814 443). The cells were either transfected for four hours in the absence of serum after which the media was replaced with serum containing media, or for 24h to 48h in the presence of 10% FCS. For all transfections the cells were incubated at 37°C. This procedure is the same for plasmids coding for ribozyme expression as well as normal gene expression. For transfection of antisense oligonucleotides, cells were set up in duplicate 25cm^2 flasks and treated on days one and two in exactly the same way as for ribozyme transfections. However, on the third day, cells were again transfected with fresh media supplemented with transfection mix. The cells were then reincubated at 37°C. After 24 hours, one set of cells was taken down for analysis by RT-PCR (Section 2.4.1), and the second set was removed after 48 hours for analysis by Western blotting (Section 2.1.4.6). Cells were also transfected with antisense in 96-well plates for the purpose of determining the effect on their drug resistance profiles (Section 2.3.1.2).

2.4.5.3 Estimation of transfection effect

Examining the effect of transfections took different forms regarding the type of DNA used. Ribozyme transfections involved the selection and establishment of stably-transfected clonal cell lines, where RNA, protein and drug profiles were only assayed once the new cell line(s) were obtained. Antisense transfections differed in that they were treated as transient transfections and results were obtained from the transfected cells immediately, without the cloning out of transfected cells.

For expression plasmids, (pCH110), as has already been explained, effect detection was achieved by staining for the plasmid, in which transfected colonies stained blue. These could then be counted and the relative efficiency of the transfection calculated from the number of transfected vs. untransfected cells. Other expression plasmids used were pTarget™ and pGL3.

In the case of ribozyme transfections, single colonies of stably transfected cells were selected and isolated. The selection process was carried out by feeding the "transfected" cells with media containing geneticin (Sigma; G9516) - the plasmids used had a geneticin-resistant gene, therefore, only those cells containing the plasmid will survive treatment with geneticin. 2 days after transfection, the flask of cells was fed with 3-4 times the levels of geneticin normally required to kill 50% of the cells transfected (e.g. IC_{50} for DLKP-SQ cells is 65μg/ml; cells were fed with media containing 200μg/ml geneticin). In complete media, when the cells grew readily in this concentration of selecting agent, the concentration was increased step-wise to a final concentration of 600μg/ml. At this stage the cells were plated out in 96-well plates (Costar, 3596) at a clonal density of one cell/well. Clonal populations were propagated from these wells, as transfected cells were periodically challenged with geneticin to maintain stability of transfectants and prevent cross-contamination with non-transfected cells.

Cells treated with antisense were taken down as outlined in Section 2.4.4.4. RT-PCR analysis, Western blotting was carried out to determine the effect, if any, of the transfection on a given gene. *In-vitro* Toxicity assays were also carried out (Section 2.3.1.2) to determine effect on drug resistance.

2.4.6 Isolation of RNA from Tumour/Normal Samples

1. Breast and Lung samples (both Tumour (T) and Normal (N)) were obtained from Drs. Enda McDermott and Vincent Lynch, respectively. Both work at St. Vincent's hospital, Mount Merrion.
2. Samples arrived within 4 hours of the operation via courier. They were transported in a 50ml tube in a sealed clear plastic bag to prevent contamination contained inside a padded envelope. Tubes were filled with *RNAlater* (Ambion, 7021) to prevent degradation by RNases. Upon arrival, tubes were stored at -80^0C until RNA isolation.
3. All manipulations of the human material was carried out inside a class II down-flow re-circulating laminar flow cabinet (Nuaire Biological Cabinet) to prevent contamination. The floor of the cabinet was lined with two sheets of tin foil and then covered with two large plastic autoclavable sheets.
4. All implements (e.g. scissors, forceps, tin foil, etc.) used in the RNA isolation were baked @ 200^0C overnight prior to use.
5. The Tumour/Normal sample was removed from the 50ml tube and squeezed using the forceps to remove any excess RNAlater solution. This is carried out as the presence of excess RNAlater alters the pH of the solution, which affects the subsequent yield of RNA.
6. A piece of tin foil was folded into a cup shape and ~20mls of liquid N_2 was added. The liquid N_2 was allowed to boil off, allowing it time to permeate to the centre of the tissue sample.
7. The tin foil was folded over and the frozen tumour was struck roughly several times with a hammer. Extra liquid N_2 was added if sample began to thaw.
8. Broken pieces of tissue were removed with a forceps to a Braun potter S886 homogenisation chamber. 2 mls of Tri Reagent was added, the pestle was inserted and the cells were homogenised on ice for ~5 mins. at medium speed.
9. After homogenisation, the cell homogenate was removed to two eppendorfs. These were spun @ 1300 rpm for 2 mins. in a bench-top microcentrifuge to remove large cell debris.
10. The samples then underwent the TRI REAGENT™ protocol for RNA isolation (Section 2.4.2.2).

2.4.7 RNase H assay

1. An antisense sequence was chosen from the literature or designed from the coding strand of the gene of interest. This sequence is included in the Appendix.
2. Two primers were selected which were complementary to each other. One of these primers was attached to a T7 RNA polymerase promoter and Leader sequence and when amplified, yielded a DNA product complementary to the chosen antisense sequence. These primer sequences are also included in the Appendix.
3. The two primers were amplified together in a typical PCR reaction (Section 2.4.2.6.2), except that there was no template DNA. The mix used was therefore as outlined in Table 2.4.4.

Table 2.4.4 List of components for IVC-PCR

Item	Volume (µls)
$MgCl_2$ (Sigma, M-8787)	3
10X Buffer (Sigma, P-2317)	5
Primer A	2
Primer B	2
H_2O	36.5
dNTPs (10mM) (Sigma, DNTP-100)	1
Taq (Sigma, D-4545)	0.5 (2 units)

The PCR was cycled for 35 cycles at an appropriate Tm (^{0}C).

4. The PCR product was run out on a 1% agarose gel (Section 2.4.2.6.3). The visualised gel was excised from the gel using a sharp blade and purified using a QIAEX II gel extraction kit (Qiagen, 20021) according to the manufacturers instructions.
5. Using a T7 Riboprobe kit (Promega, Cat. # P1440), the target DNA was converted to RNA, which was used to bind to the Antisense. The kit utilises the T7 RNA polymerase promoter to transcribe RNA from the DNA. Transcription takes place in the presence of a limiting amount of unlabelled rCTP and an excess of radioactively labelled rCTP ([α-^{32}P]rCTP (Amersham)) which ensures the incorporation of this label into the RNA product. The transcription mix was as outlined in Table 2.4.5.

Table 2.4.5 List of components for T7-riboprobe [α-^{32}P]rCTP transcription

Item	Volume (µls)
Transcription Optimised 5X Buffer	4
DTT, 100mM	2
Rnasin	1
ATP, GTP and UTP (2.5mM each)	4
100µM CTP	2.4
Template DNA	1
[α-^{32}P]CTP (400Ci /mmol, 10mCi / ml)	5
T7 RNA Polymerase	1

6. The transcription mix was incubated @ 37^{0}C for 60 mins. After transcription, the tubes were spun down to gather all of the reaction mix at the bottom. 1µl of RQ1 DNase (Promega, M6101, supplied with kit) was then added and the mix was re-incubated @ 37^{0}C for 15 mins.
7. The transcription mix was extracted once with 24:24:1 Phenol:Chloroform: Isolamylalcohol and once with 24:1 Chloroform:Isoamylalcohol, before 0.5 volumes of 7.5M Sodium Acetate and 2.5 volumes 100% Ethanol were added. The RNA was left to precipitate for 60 mins. at –80^{o}C.
8. The RNA pellet was spun down at 13,000rpm in a bench-top microfuge and air-dried for 10 – 15 mins. The pellet was resuspended in 20 – 30 µls UHP.
9. This RNA product was added to an RNA Quick-Spin Column (Boehringer, 1273990) which had been prepared according to the manufacturer's instructions and the purified product was collected after centrifugation at 2600rpm for 4mins. in an SW28 bucket rotor.
10. A cleavage mix was set up as outlined in Table 2.4.6.

Table 2.4.6 List of components for RNase H-mediated cleavage of RNA

Item	Volume (µls)
20mM HEPES-KOH, pH 8.0	1
50mM KCl (Promega, L4591)	1
4mM $MgCl_2$	1
1mM DTT (Promega, P1171)	1
Radioactively Labelled Target RNA	5
Antisense	5
50 µg/ml BSA (Promega, R9461)	1
Ribonuclease H (Promega, M4281)	1

Prior to addition of RNase H, the labelled target and antisense were incubated together @ 95^{0}C for 3 mins. before incubation on ice for 1 min. The enzyme was then added and the tubes are placed @ 37^{0}C for 20 mins. The reaction was stopped by addition of 1µl of 0.5 M EDTA (Sigma, E-5134).

11. This reaction mix was run on a 12% Polyacrylamide Gel. The mix for the gel is as outlined in Section 2.4.8.5. Before loading onto the gel, the samples were incubated @ 95^{0}C for 3 mins. before incubation on ice for 1 min. The gel was run @ 40V/cm for 45 mins. The gel was then removed and covered in clingfilm. X-OMAT AR film (Kodak, 1651512) was exposed to the gel overnight and developed as usual.

2.4.8 *In-vitro* cleavage of MRP1 Ribozyme

2.4.8.1 Generation and purification of the Ribozyme and target DNA templates:

1. Two primers were chosen which would anneal to each other and amplify up a DNA copy of the Ribozyme together with a T7 RNA polymerase Promoter and Leader sequence. Another pair of MRP1 primers were selected which amplified up a stretch of the MRP1 cDNA that contained the Rz cleavage site. The sequence of the primers is included in the Appendix.
2. A standard PCR protocol was carried out using both sets of primers separately as outlined in Section 2.4.2.6.2.

3. The PCR samples containing the Ribozyme were freeze-dried for two hours until completely desiccated. The dried samples were resuspended in a smaller volume of UHP and purified using a Qiagen kit (Qiagen, 20021).
4. The PCR samples containing the target DNA for cleavage were purified directly using the Qiagen kit.

2.4.8.2 Isolation of cell extract

MRP1 ribozyme-expressing clones were harvested in the usual manner (Section 2.2.3) and then resuspended in 1ml 5% SDS solution per 75cm^2 flask of confluent cells. This cell extract, or lysate, was agitated for 30 mins. at 4°C. The cell extract was stored at -20°C and used at roughly ten times the volumes of the purified ribozyme RNA in the IVC reaction (Section 2.4.8.5).

2.4.8.3 Ribozyme in-vitro Cleavage assay (IVC):

All radiolabelled RNA sequences were generated using the T7 Riboprobe® system (Promega, P1440).

1. The plasmid DNA was first linearised using a standard Sma I restriction enzyme which cut only once in the vector and not at all in the insert.
2. The DNA was cleaned up using the Wizard™ *Plus* Minipreps DNA Purification System (Promega, A7100).
3. The mix for the transcription protocol was made up as outlined in Table 2.4.7

Table 2.4.7 Components for transcription of [α-^{32}P]rCTP-labelled ribozyme

Component	Volume (µls)
Transcription optimised 5X Buffer	4
DTT, 100mM	2
Recombinant RNasin® Ribonuclease Inhibitor	0.5
rATP, rGTP and rUTP[7] (2.5 mM each)	4
100 µM rCTP	2.4
Linearised target plasmid DNA[8]	1
[α-^{32}P] rCTP (50 µCi at 10 µCi/µl)	5
T7 RNA Polymerase	1

4. The eppendorf was incubated for 1 hour at 37^{0}C.
5. 1 µl of RQ1 DNase (Promega, M6101) was added to the tube and incubated for 15 mins. at 37^{0}C.

2.4.8.4 Purification of target DNA for Ribozyme cleavage

1. 25 µls TE-saturated phenol:chloroform was added to the tube. The tube was vortexed and spun down at 13,000rpm in a microfuge.
2. The yellow upper aqueous phase was then transferred to a fresh tube and 25 µls of chloroform:isoamylalcohol (24:1) was added. The tube was vortexed, spun down and the upper phase transferred to a fresh tube as before.
3. 12.5 µls of 7.5M ammonium acetate and 75 µls of 100% ethanol were added. The tube was mixed and placed at –70^{0}C for 30 mins.
4. The tube was then centrifuged at 13,000rpm for 20 mins.
5. The supernatant was removed and the pellet was washed with 0.5 mls 70% ethanol. The pellet was dried at room temperature for 10-15 mins. and finally resuspended in 20 µls UHP.

[7] Prepared by adding 1 µl of each of 10mM rATP, rGTP, rUTP and UHP.
[8] Plasmid DNA must have a conc. of at least 0.5 µg/µl.

6. A Quick Spin™ column (Boehringer Mannheim, 1273990) was removed from packaging and prepared as instructed. The contents of the tube were added to the column, which was placed in a collection tube.
7. The column was spun down in a Beckman SW28 rotor at 2600rpm for 2 mins.
8. The eluate was stored at -20^0C and the column was discarded.

2.4.8.5 *In-vitro* Cleavage reactions with Ribozyme and Target DNA:

1. Cleavage reactions were set up in four eppendorfs as outlined in Table 2.4.8

Table 2.4.8 List of components for ribozyme *in-vitro* cleavage (IVC) reactions

Component	Volume (µls)
Target RNA	1
50mM Tris pH 8.0	1
Ribozyme	4
$MgCl_2$	1
Recombinant RNasin® Ribonuclease Inhibitor	1
UHP	2

2. The UHP, 50mM Tris, target RNA and Ribozyme were added together first. The tubes were heated to 90^0C for 3 mins. and placed on ice for 1 min.
3. $MgCl_2$ and RNasin® were added to the tubes, and the samples were incubated at 37^0C.
4. The tubes were taken off the heating block at different time points and 10 µls of sample loading dye was added to them to stop the reaction. The time points chosen were (mins.) 0, 30, 60, 180. All samples were stored at -20^0C.

2.4.8.6 Polyacrylamide gel analysis for Sequencing/RNase H/*in vitro* Cleavage reactions:

The products of the Ribozyme *in-vitro* cleavage reactions were run out on 12% Acrylamide gels as outlined here.

2.4.8.6.1 Preparation of gel apparatus

Before pouring, the plates were washed in RBS to remove all traces of gel, rinsed firstly with tap water and then UHP. These were then dried with tissue, treated with 10% SDS, followed by more UHP and wiped again. The plates were then wiped in one direction using 70% Industrial Methylated Spirits (IMS). The plastic seal (for RNase H/*in vitro* cleavage gels) and comb were also rinsed in tap water, UHP and then 70% IMS.

2.4.8.6.2 Gel composition (for all gels):

63g Urea (Sigma, U-5378) was dissolved in 15 mls 10X TBE in a microwave, together with 10 mls UHP and heated to 60°C. Once in solution, 30 mls 40% Acrylamide (Gibco BRL, 35722-024) was added and this was made up to 150 mls with UHP. Once gel cast had been assembled, to 50 mls gel of this gel mix was added 250 µls of freshly made 10% APS (Reidel de Haen, 11222) and 50 µls TEMED. The gel mix was then ready to pour.

2.4.8.6.3 Assembly, Pouring and running of gels:

For sequencing gels, a plastic sealing strip was lined on both sides of the casting tray. The gel tray was laid flat, and the gel mix was poured onto it, starting from the bottom. The front plate was gently pushed forward from the bottom, while continuously adding the gel mix, until both plates were laid exactly on top of each other. The gel cast was then fully assembled, with the gel sealed in using clips on both sides. The comb was

then inserted and the gel was left to set for 30 mins. 2l of 1X TBE was heated to 60^0C and added to the gel apparatus. The comb was removed after the gel had set and a syringe was used to wash the wells of residual urea. Sample running buffer (Section 2.4.3.1) was added to a number of the wells and the gel was pre-run at 1700 volts for 1-1.5 hours or until the temperature of the gel reached 40-50^0C, after which it was ready for loading of sequencing samples. The samples were heated to 90^0C for 3 mins. before being loaded on the gel. The gel was run for 2hrs, or until the loading dye (bromophenol blue/xylene cyanol) had reached the bottom of the gel.

For RNase H/*in-vitro* cleavage gels, the base plate was laid flat and the outside was lined with the plastic seal. The front plate was placed directly over the base plate. The cast was kept in place with the use of bullclips. The seal was tested by the addition of UHP into the cast to check for leaks. Once no leaks were detected, the gel was poured, the comb was inserted and left to set. Once set, the bullclips were removed and the gel was placed upright in the running apparatus. 1X TBE was used as the gel running buffer, the comb was removed and a syringe was used to wash the wells of residual urea. The sample running buffer was added to a number of the wells and the gel was pre-run at 1700 volts for 20 mins., after which it was ready for loading of cleavage reaction samples. The samples were heated to 90^0C for 3 mins. before being transferred to ice for 1 min., after which they were loaded on the gel. The gel was run at 1700 volts for 1 hour, or until the loading dye had approached (within 2 cm of) the bottom of the gel.

2.4.8.6.4 Disassembly and Developing of acrylamide gels:

For sequencing gels, the plates were separated and 3MM filter paper (cut to size) was placed on top of the gel, avoiding bubbles. The paper was lifted gently, taking the gel with the paper. This was then covered with cling film and placed on top of another sheet of 3MM filter paper in the gel drier, with the cling film facing up. The gel was dried at 80^0C for 2 hours. When dry, the gel was placed in a cassette and in the darkroom the cling film was removed and a sheet of X-ray film was placed on the gel (Kodak, X-OMAT S, 500 9907). The cassette was sealed shut and the gel was exposed to the film for 48 hours. The film was removed from the cassette in the darkroom, placed (and agitated) in developer (Kodak, 5070933) for 5 mins., UHP (1 min.), fixer (3 mins.)

(Kodak, 5211412) and finally UHP again for 1 min. before being left to drip-dry overnight.

For RNase H/*in-vitro* cleavage gels, the plates were separated and a sheet of cling film was placed over the gel. The gel was placed behind a perspex screen and put inside a cupboard in the darkroom. A sheet of X-ray film (Kodak, 5211412) was placed over the cling film and exposed for 48 hours. After exposure, the film was developed in the same way as for the sequencing gels.

2.4.9 DNA microarray analysis on BrdU-treated DLKP cells

RNA isolated from DLKP cells which had been exposed to BrdU for one week (Section 2.3.3) and untreated control DLKP cells was used in the DNA microarray analysis. The procedure followed was as outlined by the manufacturer, "Atlas Human Cancer 1.2 Array Gene" (Clontech, 7851-1). In brief, the procedure involved the generation of a radioactively-labelled complementary DNA (cDNA) copy of the isolated RNA samples. These labelled cDNA samples were each hybridised to a separate DNA array membrane (Clontech, PT3547-3) and the membranes were rinsed of excess label. These hybridised membranes were then read using a Cyclone™ Phosphorimager and analysed with AtlasImage™ 2.01 software. Altered expression of genes observed between the two membranes were identified and quantified by computer analysis.

2.4.10 Luciferase transfections and monitoring of expression results

Plasmids containing the luciferase gene attached to truncated forms of the MRP1 promoter and a full-length CMV promoter were transfected overnight into DLKP cells as outlined in Section 2.4.5. A at 1μg/μl working concentration of the plasmids was used, of which 1μg was used per $5X10^5$ cells (except the Positive plasmid, of which 10ηg was used per $5X10^5$ cells). The following procedure for analysing luciferase levels in transfected cells was the same as that outlined in the Luciferase Assay System™ (Promega, E1500). After 24hrs, the cells were washed twice with 1X PBS and then left

to lyse in 1X lysis buffer (5X supplied with kit, diluted to 1X with UHP) at 4°C for 20mins. The lysis buffer, containing lysed cells, was removed to an eppendorf, vortexed for 30s and immediately placed in liquid N_2. The eppendorf was then quickly thawed and the cells were spun at 13,000rpm in a bench-top microfuge (Hereaus). The supernatant was removed to a fresh eppendorf and the cell debris discarded. 10µls of this supernatant was then added to 50µls 1X luciferase substrate (5X supplied with kit, diluted to 1X with UHP) and the luciferase levels analysed using a standard luminometer.

Section 3.0

Results

3.1 Analysis of cells exposed to BrdU

A549 and DLKP cells were cultured as outlined in Section 2.2.3, and set up for BrdU treatment (Section 2.3.3). Cells were continuously exposed to BrdU over different intervals as outlined in Table 3.1.1

Table 3.1.1 Breakdown of timepoints for drug-exposed DLKP cells

Time Point (Days)	Sample Name	Assay conditions
0	C7	No BrdU exposure, Control sample
2	Br2	BrdU exposure for 2 days
5	Br5	BrdU exposure for 5 days
7	Br7	BrdU exposure for 7 days
15	Br15	BrdU exposure for 15 days

Initially, RT-PCR was used to analyse whether exposure to the differentiating agent resulted in any differences in RNA expression. *In-vitro* toxicity assays were also used to examine if exposure to the differentiating agent resulted in a change in the drug resistance profile of the cell line.

3.1.1 Analysis of BrdU-exposed A549 and DLKP cells using RT-PCR

Cells were taken down after the course of exposure to the differentiating agent and RNA was extracted using the TRI Reagent™ method as outlined in Section 2.4.2.2. Initially, RT-PCR was utilised to examine differences in the expression of various genes at the RNA level following exposure to BrdU.

All PCRs were duplicated in order to maximise accuracy of the results. Initially PCRs were carried out on two separate isolations of BrdU-exposed cell samples. If the expression pattern of a particular gene was observed to be significantly altered in both isolations, the process was repeated on a third, separate isolate for confirmation, again in duplicate. If this third result confirmed the earlier two, it was deemed significant and repeatable and only results which conformed to this criterion were examined

individually in the following Sections. The results obtained for the other genes have been summarised in Table 3.1.3.

Expression levels of a total of twenty-five genes were successfully examined over the course of the study (Table 3.1.2). Positive controls were unavailable for many of these samples and even when available, the resultant product was often of unsatisfactory quality. In order to provide positive samples to validate the PCRs, PCR products which were deemed to be of the correct size for the relevant gene (and therefore the correctly amplified product), were purified using a Qiagen kit (Qiagen, 20021) and used as positive samples. In some cases, these samples did not work as planned and in those gel photos the positive and negative lanes are not shown. The negative control used in all cases was filter-sterilised water.

Table 3.1.2 List of genes examined for expression in BrdU-exposed cells

Gene
MRP1
MRP2 (cMOAT)
MRP3
MRP4
MRP5
MRP6
Mdr-1
Mdr-3
BCRP
COX-1
COX-2
BAXα
MRIT
Survivin
BAG
BAP
Bcl-2α
Bcl-x_L
Bcl-x_S
eIF-4E
eIF-2α
c-*myc*
α-catenin
β-catenin
E-cadherin

3.1.1.1 MRP1

MRP1 expression in A549 was found to increase with increasing days of exposure to BrdU up until Day 7, whereafter expression returned to its normal resting state (Fig. 3.1.1). The approximate increase was 74% at day seven.

In DLKP, BrdU also induced MRP1 upregulation. A twelve-fold increase in MRP1 expression is observed after seven days (Fig. 3.1.1).

3.1.1.2 MRP2 (cMOAT)

MRP2 expression was observed to decrease in BrdU-treated cell line A549 over all fifteen days of treatment (Fig. 3.1.2). This expression decrease was not felt to be of significance in this cell line.

By contrast, MRP2 expression was upregulated in DLKP cells after treatment with BrdU (Fig. 3.1.2). DLKP expresses very low levels of MRP2 normally, and the increase in expression was could only accurately be determined by densitometry. However, while the increase in expression appeared significant, MRP2 expression increasing 29-fold after BrdU treatment, the overall increase was not large.

3.1.1.3 MRP3

As can be seen from Fig. 3.1.3, MRP3 expression is almost undetectable in the control DLKP sample. However, after exposure to BrdU, expression levels are observed to rise to over 300-fold excess after fifteen days. No data exists for MRP 3 expression levels after fifteen days.

Fig. 3.1.1: MRP1 RT-PCR on BrdU-treated cells

Fig. 3.1.1a:

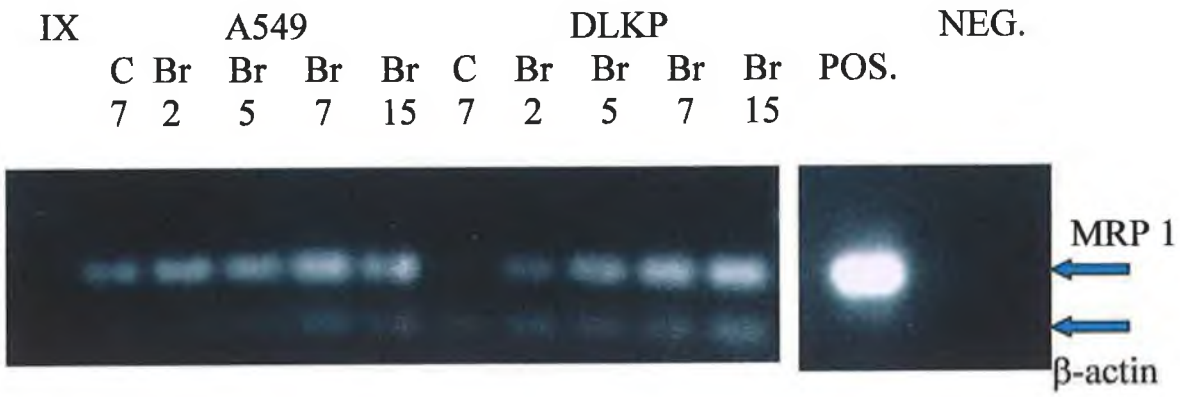

Fig. 3.1.1b:

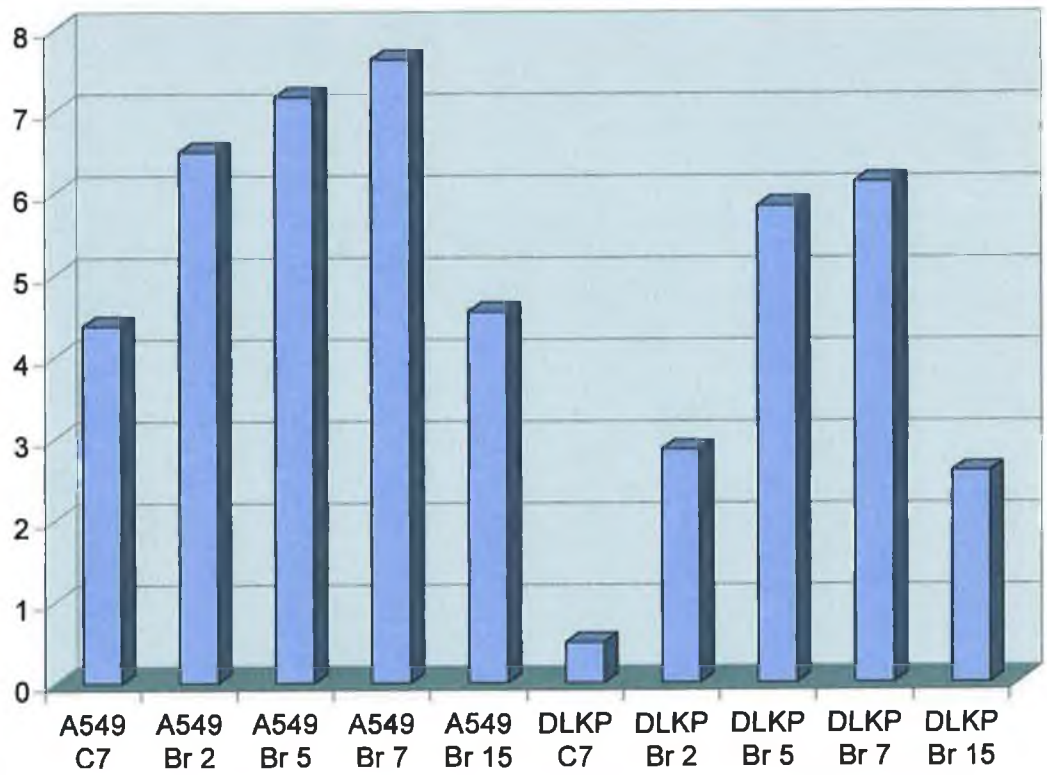

Fig. 3.1.1a: Gel electrophoresis photograph of MRP 1 RT-PCR results on BrdU-treated A549 & DLKP cells; Fig. 3.1.1b: Densitometric analysis of RT-PCR results.

Fig. 3.1.2: MRP2 RT-PCR on BrdU-treated cells

Fig. 3.1.2a:

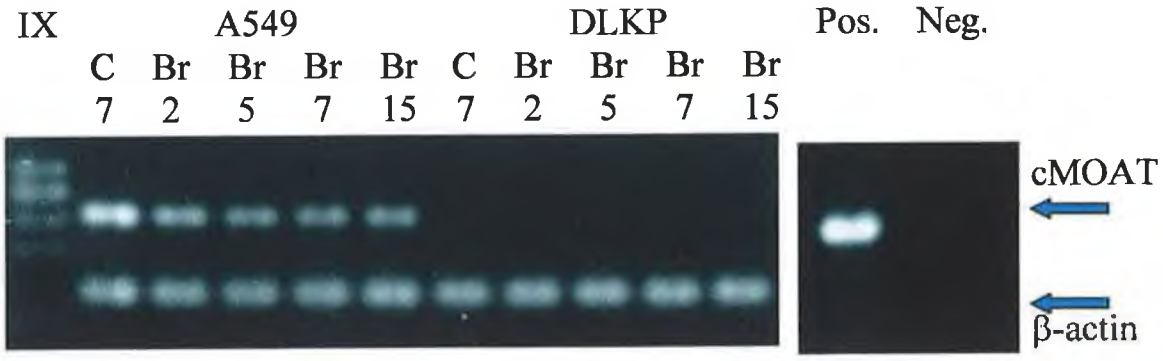

Fig. 3.1.2b:

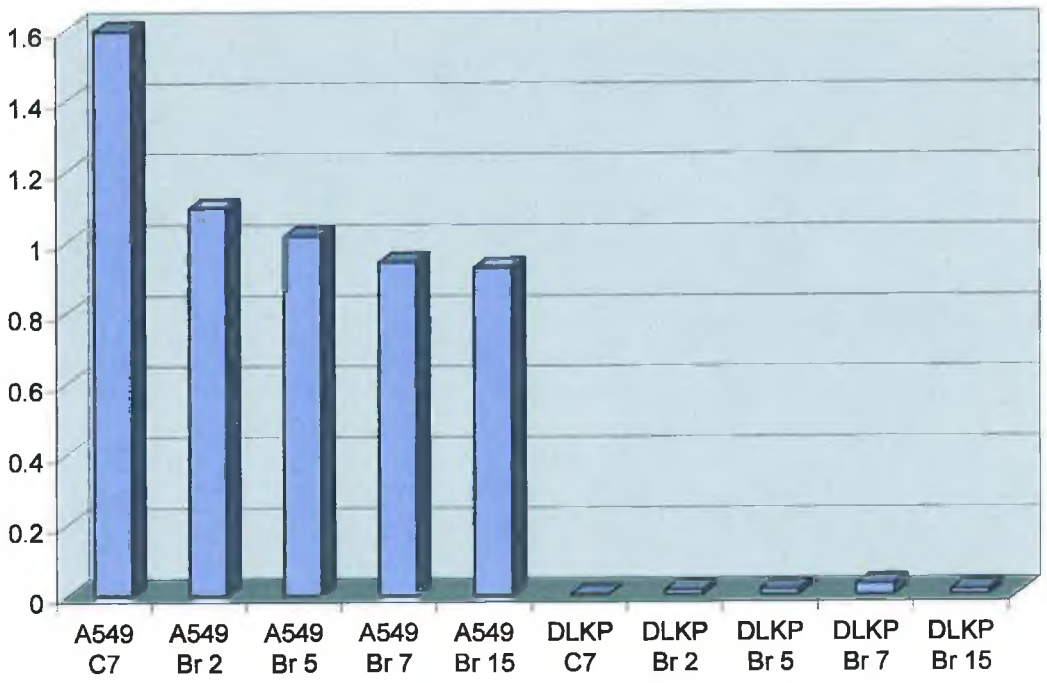

Fig. 3.1.2a: Gel electrophoresis photograph of MRP2 (cMOAT) RT-PCR results on BrdU-treated A549 & DLKP cells; Fig. 3.1.2b: Densitometric analysis of RT-PCR results.

Fig. 3.1.3: MRP3 RT-PCR on BrdU-treated DLKP cells

Fig. 3.1.3a:

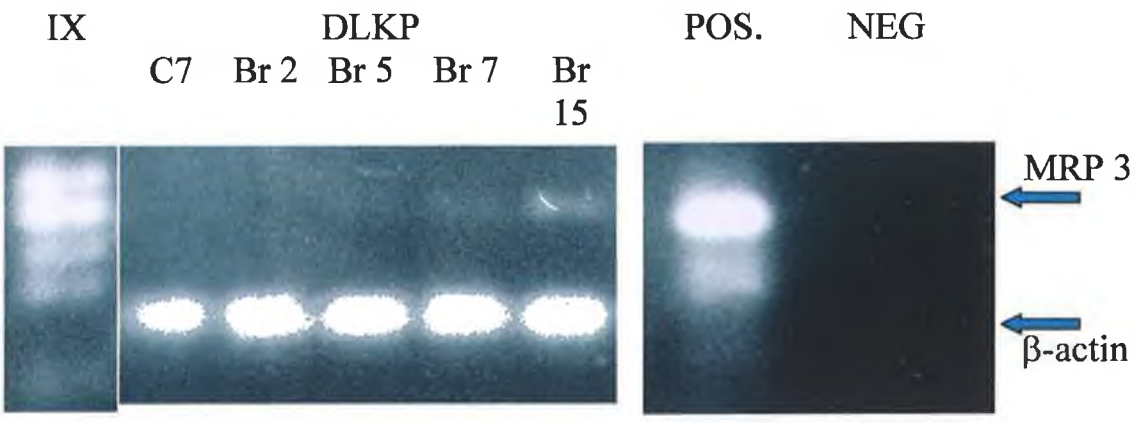

Fig. 3.1.3b:

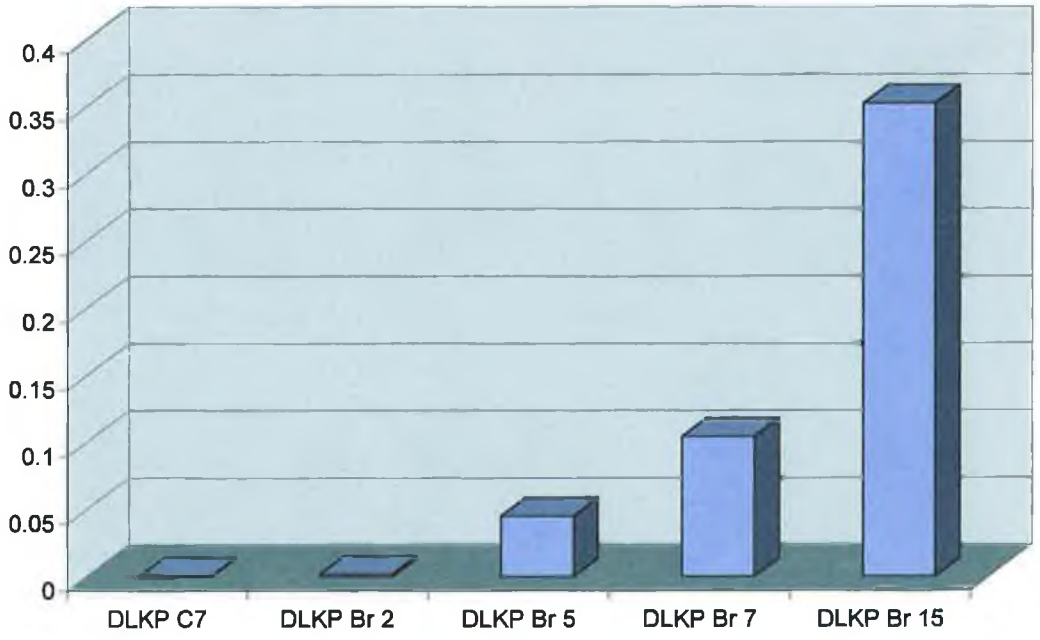

Fig. 3.1.3a: Gel electrophoresis photograph of MRP3 RT-PCR results on BrdU-treated DLKP cells; Fig. 3.1.3b: Densitometric analysis of RT-PCR results.

3.1.1.4 MRP4

MRP4 expression was observed to decrease in a logarithmic fashion following BrdU treatment in the A549 cell line (Fig. 3.1.4). Like cMOAT and MRP3, MRP4 is expressed in A549 at relatively high levels in its normal state. The decrease in expression was largest after fifteen days, when expression levels were observed to be at 12% that of normal. In DLKP, MRP4 increased in expression over the course of BrdU treatment, peaking at day seven with an increase of over 250-fold, before returning to near-normal levels.

3.1.1.5 mdr-1

mdr-1 expression was observe to decrease dramatically in A549 cells only after just one day of BrdU treatment, after which levels did not rise significantly over the course of treatment (Fig. 3.1.5).

3.1.1.6 BCRP

BCRP expression in A549 was observed to increase gradually with increasing BrdU exposure over the whole course of treatment (Fig. 3.1.6). As with mdr-1, BCRP is normally expressed at very low levels in DLKP. However, increasing expression of BCRP was observed in this cell line with increasing BrdU exposure up to seven days, at which an overall 44-fold increase was observed. Thereafter, expression decreased slightly.

3.1.1.7 COX-2

Initially, COX-2 expression in DLKP increased rapidly, reaching a 65-fold increase after only five days exposure to BrdU (Fig. 3.1.7). Expression peaked at seven days after which it was seen to subside slightly (roughly 44-fold). The gene was found to be expressed at very low levels in untreated DLKP cells (by contrast normal A549

Fig. 3.1.4: MRP4 RT-PCR on BrdU-treated cells

Fig. 3.1.4a:

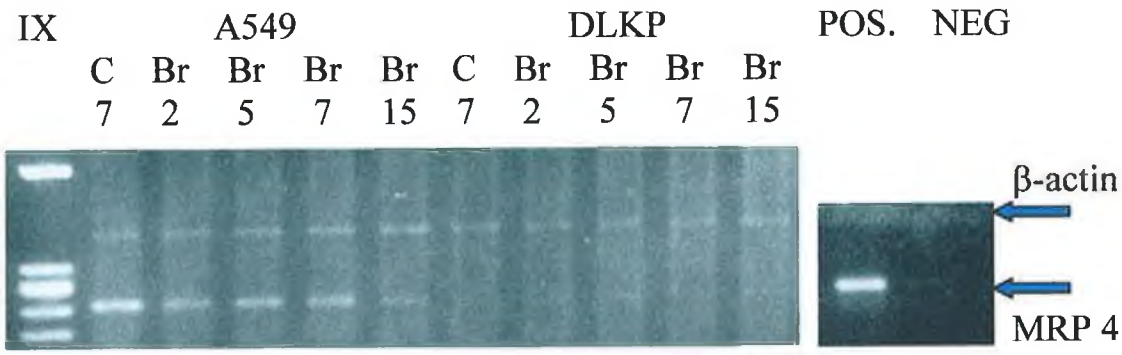

Fig. 3.1.4b:

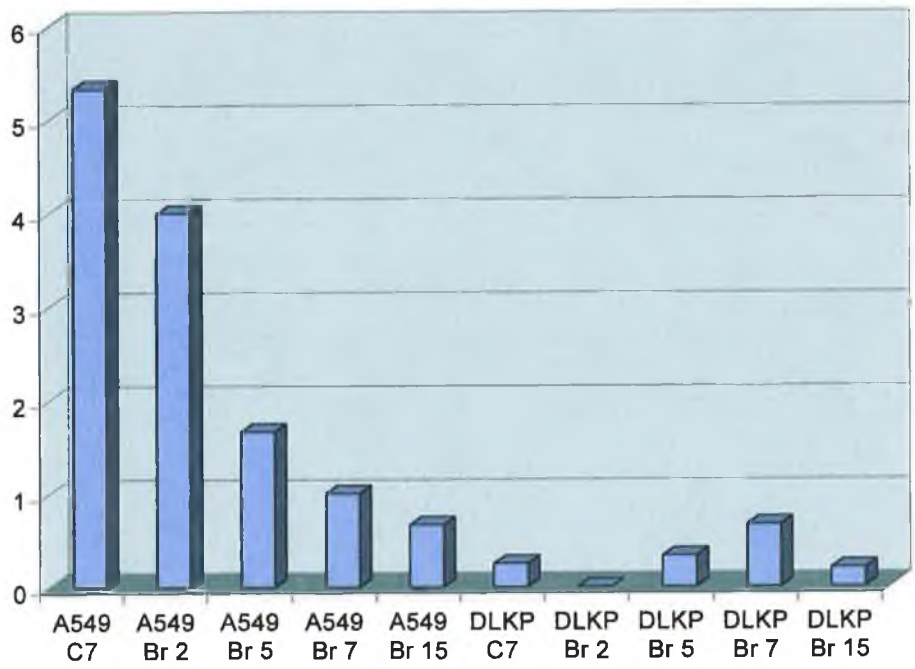

Fig. 3.1.4a: Gel electrophoresis photograph of MRP4 RT-PCR results on BrdU-treated A549 & DLKP cells; Fig. 3.1.4b: Densitometric analysis of RT-PCR results.

Fig. 3.1.5: mdr-1 RT-PCR on BrdU-treated A549 cells

Fig. 3.1.5a:

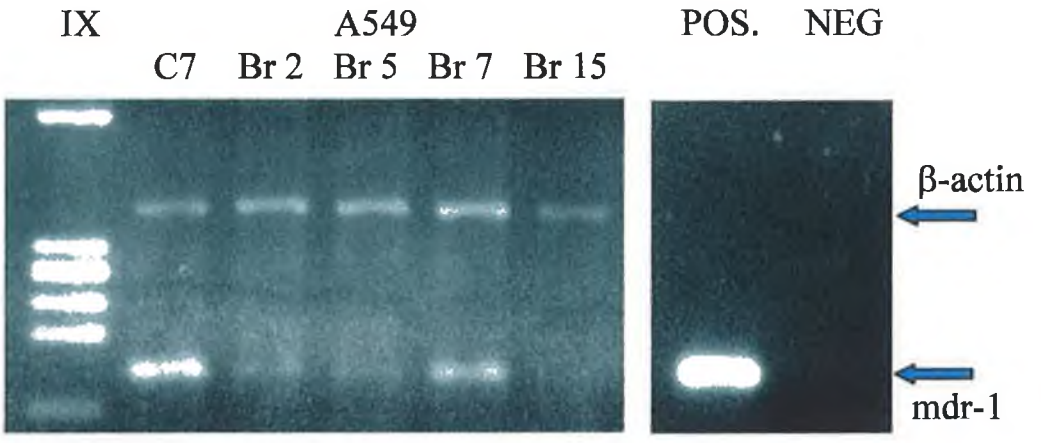

Fig. 3.1.5b:

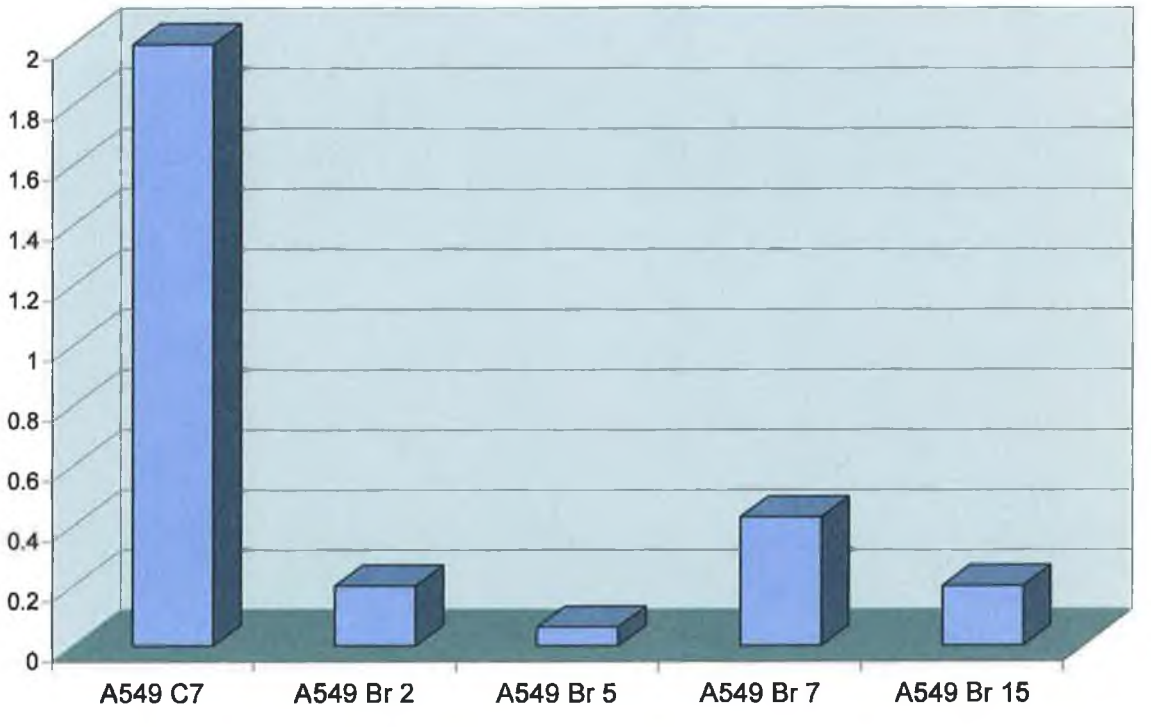

Fig. 3.1.5a: Gel electrophoresis photograph of mdr-1 RT-PCR results on BrdU-treated A549 cells; Fig. 3.1.5b: Densitometric analysis of RT-PCR results.

Fig. 3.1.6: BCRP RT-PCR on BrdU-treated cells

Fig. 3.1.6a:

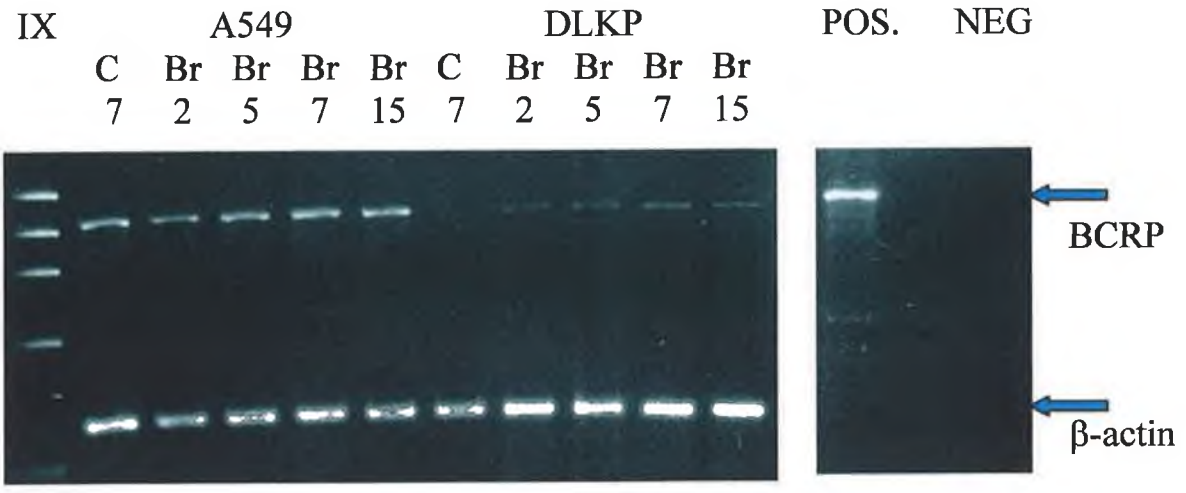

Fig. 3.1.6b:

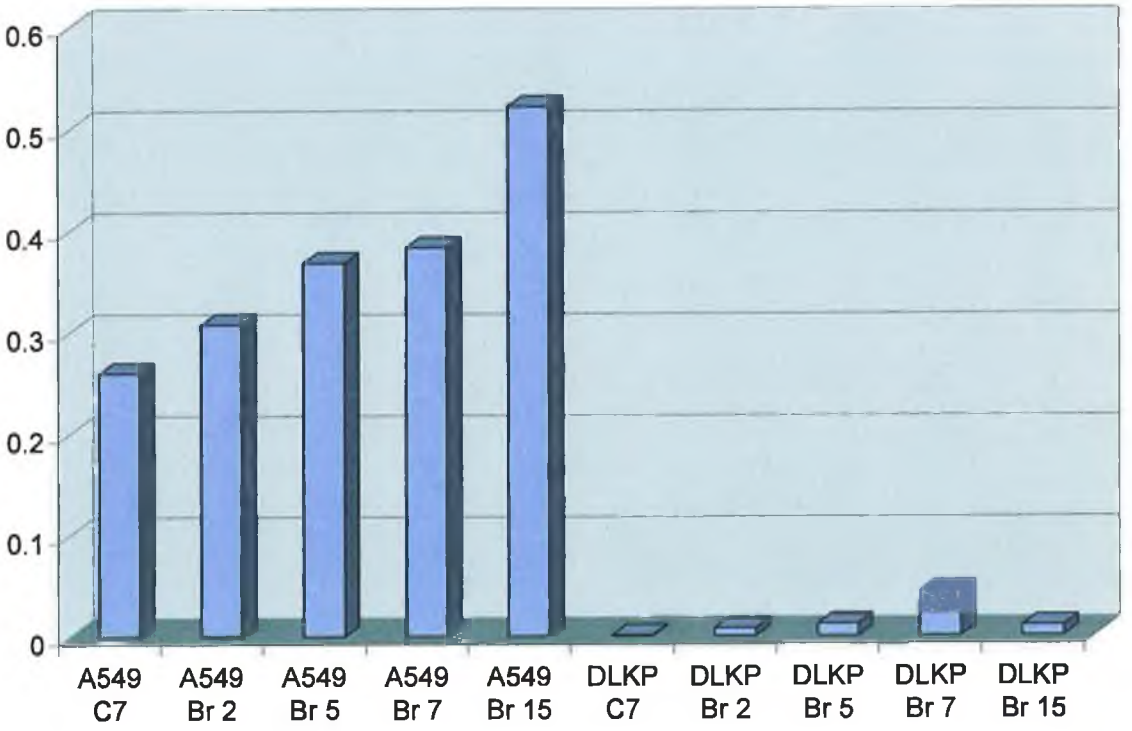

Fig. 3.1.6a: Gel electrophoresis photograph of BCRP RT-PCR results on BrdU-treated A549 & DLKP cells; Fig. 3.1.6b: Densitometric analysis of RT-PCR results.

Fig. 3.1.7: COX-2 RT-PCR on BrdU-treated DLKP cells

Fig. 3.1.7a:

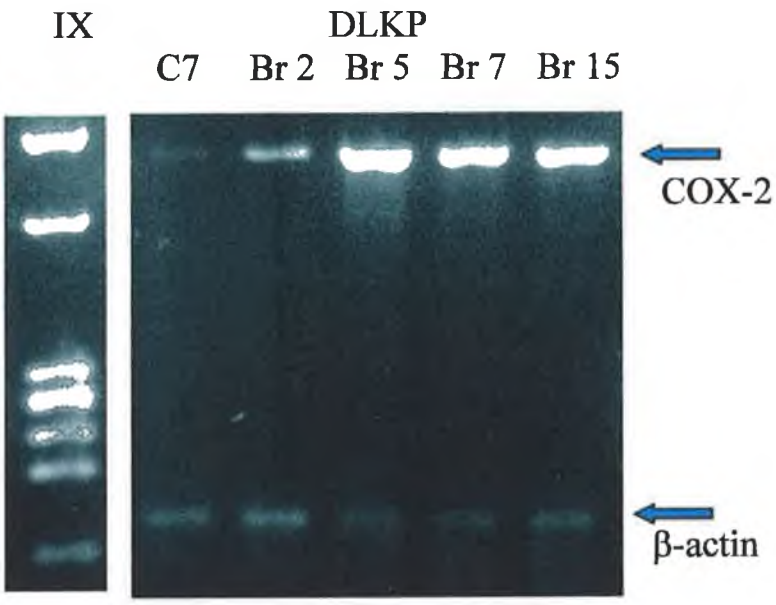

Fig. 3.1.7b:

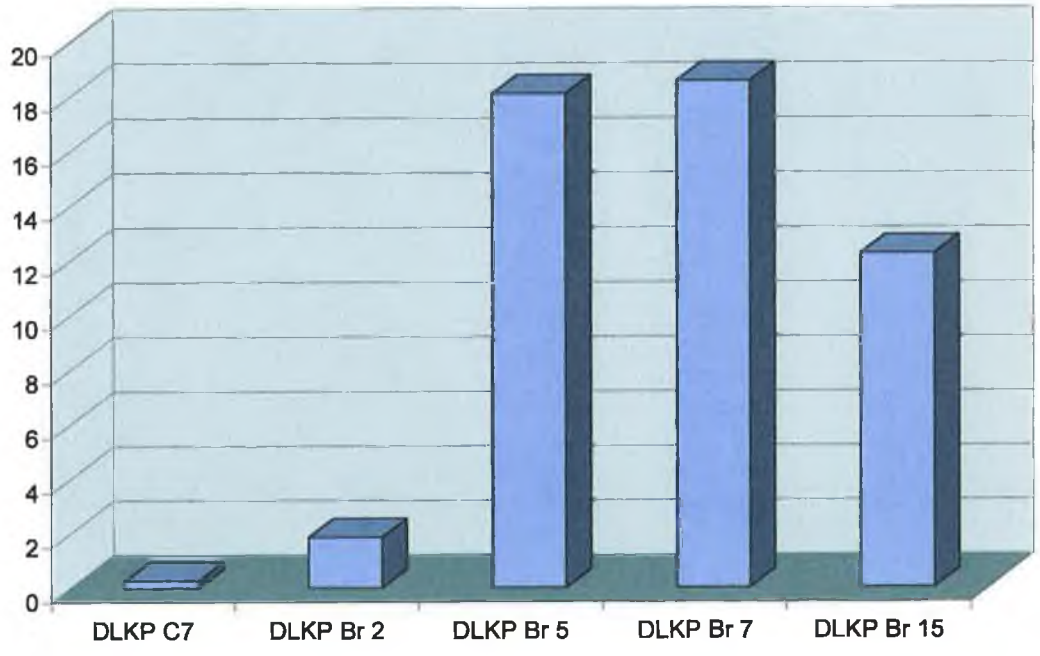

Fig. 3.1.7a: Gel electrophoresis photograph of COX-2 RT-PCR results on BrdU-treated DLKP cells; Fig. 3.1.7b: Densitometric analysis of RT-PCR results.

expressed over 30 times this amount), so the increase in this gene was found to be among the most significant of all the genes surveyed.

3.1.1.8 eIF-2α

eIf-2α expression was found to increase in DLKP cells over the course of BrdU treatment (Fig. 3.1.8). Expression was observed to peak after five days exposure to the agent, with a three-fold upregulation. Thereafter, expression of the gene did not alter much for the following ten days of treatment.

3.1.1.9 BAX α

A six-fold increase in BAX α gene expression after five days exposure to BrdU was observed in the DLKP cell line (Fig. 3.1.9). This level of expression remained constant until after seven days of exposure, when it decreased dramatically to 10% that of normal levels. Expression levels of the gene in untreated cells are normally at a low level.

3.1.1.10 MRIT

As can be seen in Fig. 3.1.10, exposure to BrdU resulted in an increase in expression of the MRIT gene in the DLKP cell line. Initially, expression increased rapidly and was observed to increase over three-fold after two days of exposure. This level of increased expression persisted until after five days of exposure, after which levels decreased to near-normal amounts. This expression pattern for MRIT was markedly dissimilar to the other patterns, as the expression increase was most noted after only two days exposure to the differentiating agent.

Fig. 3.1.8: eIf-2α RT-PCR on BrdU-treated DLKP cells

Fig. 3.1.8a:

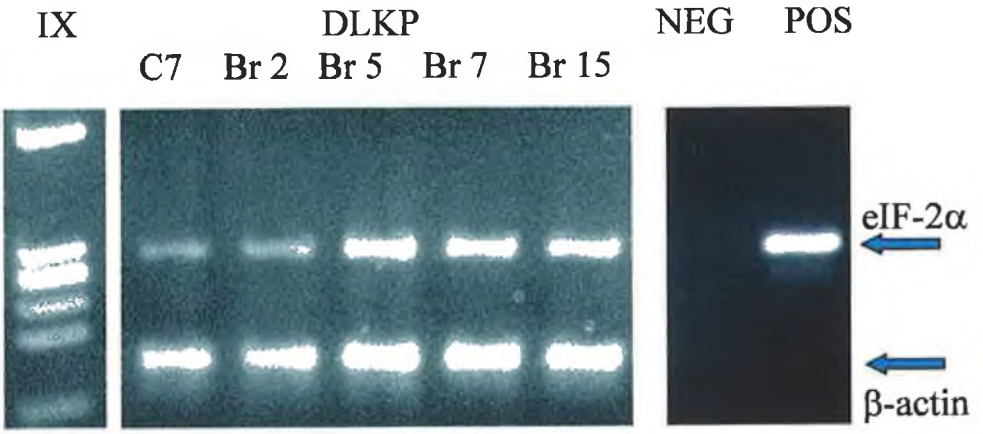

Fig. 3.1.8b:

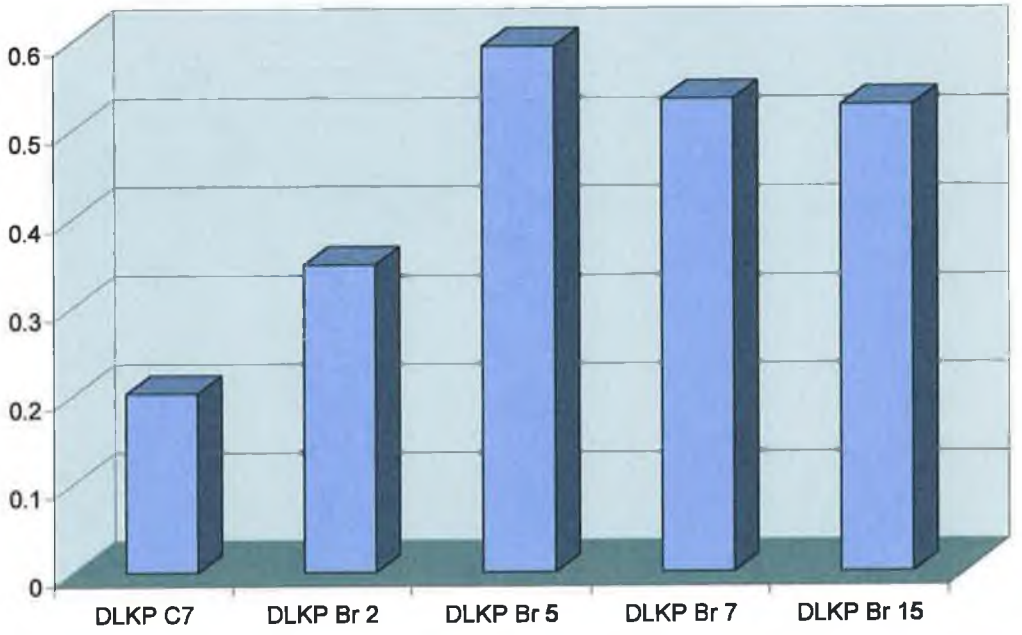

Fig. 3.1.8a: Gel electrophoresis photograph of eIF-2α RT-PCR results on BrdU-treated DLKP cells; Fig. 3.1.8b: Densitometric analysis of RT-PCR results.

Fig. 3.1.9: BAXα RT-PCR on BrdU-treated DLKP cells

Fig. 3.1.9a:

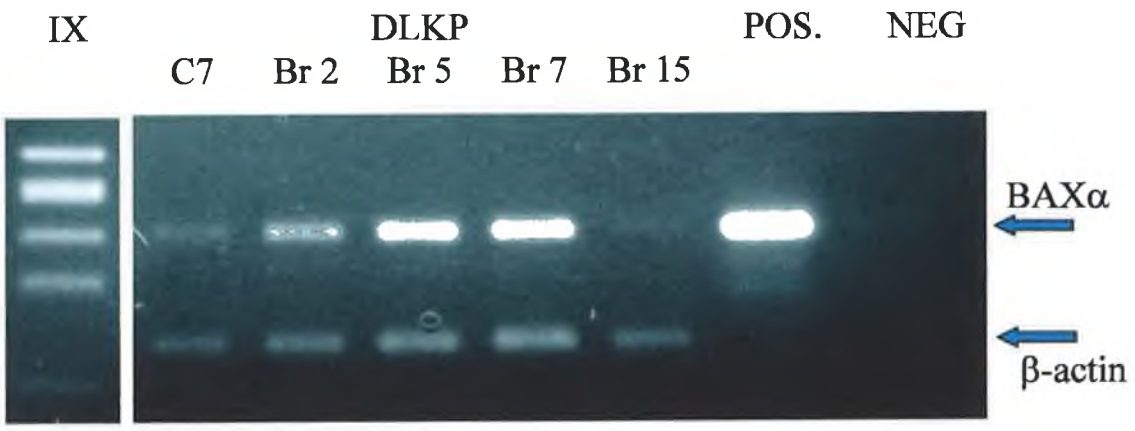

Fig. 3.1.9b:

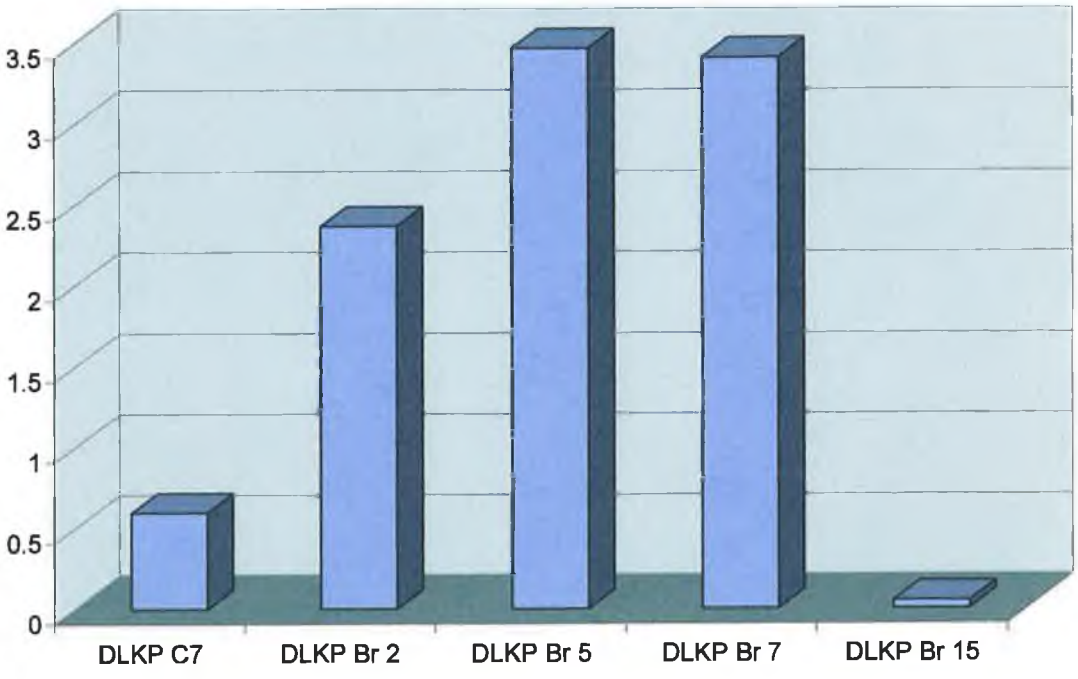

Fig. 3.1.9a: Gel electrophoresis photograph of BAXα RT-PCR results on BrdU-treated DLKP cells; Fig. 3.1.9b: Densitometric analysis of RT-PCR results.

Fig. 3.1.10: MRIT RT-PCR on BrdU-treated DLKP cells

Fig. 3.1.10a:

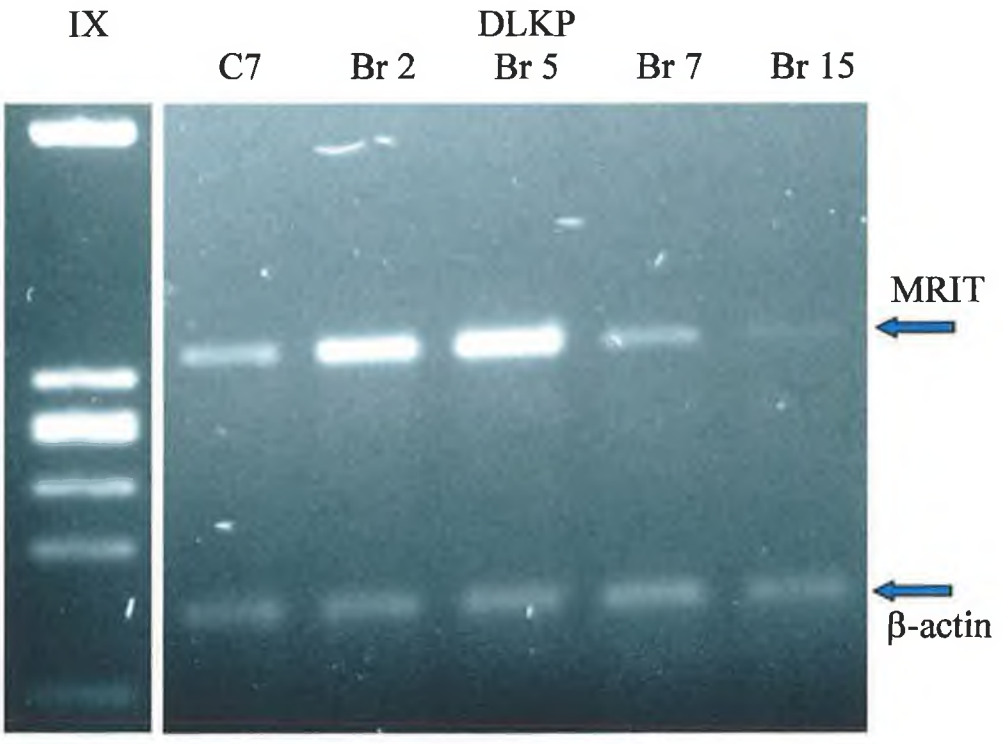

Fig. 3.1.10b:

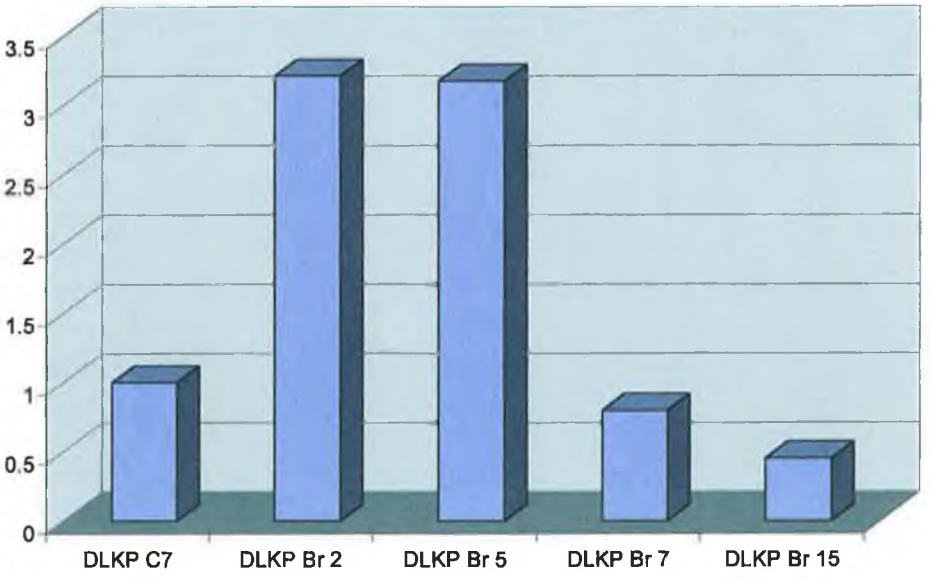

Fig. 3.1.10a: Gel electrophoresis photograph of MRIT RT-PCR results on BrdU-treated DLKP cells; Fig. 3.1.10b: Densitometric analysis of RT-PCR results.

3.1.1.11 Survivin

Expression of the Survivin gene was observed to decrease in the DLKP cell line following exposure to the differentiating agent, BrdU (Fig. 3.1.11). This was the only gene studied in DLKP whose expression was observed to consistently and significantly decrease in the cell line.

3.1.1.12 α-catenin

α-catenin expression in DLKP cells was observed to increase slightly in the cells tested following exposure to the differentiating agent BrdU. As can be seen in Fig. 3.1.12, the degree of increase was not very large, as the maximum increase was roughly 66% of normal basal levels.

3.1.1.13 E-cadherin

The expression of the E-cadherin gene was observed to increase in BrdU-exposed DLKP cells (Fig. 3.1.13). The expansion in expression was at its optimum at day five, with a roughly 2.5 fold increase, after which expression levels decreased to near-normal amounts after fifteen days of treatment.

3.1.1.14 Summary of RT-PCR results for BrdU-exposed cells: significant and non-significant

For purposes of clarity, the RT-PCR results for the expression profiles of genes considered affected significantly by BrdU exposure in DLKP and A549 cells have been summarised in Table 3.1.3. The expression of a number of other genes in these cells was also examined using RT-PCR. The results of these PCRs were not included in the earlier Section due to either a lack of consistency or a lack of significance. The results of these PCRs are summarised in Table 3.1.4.

Fig. 3.1.11: Survivin RT-PCR on BrdU-treated DLKP cells

Fig. 3.1.11a:

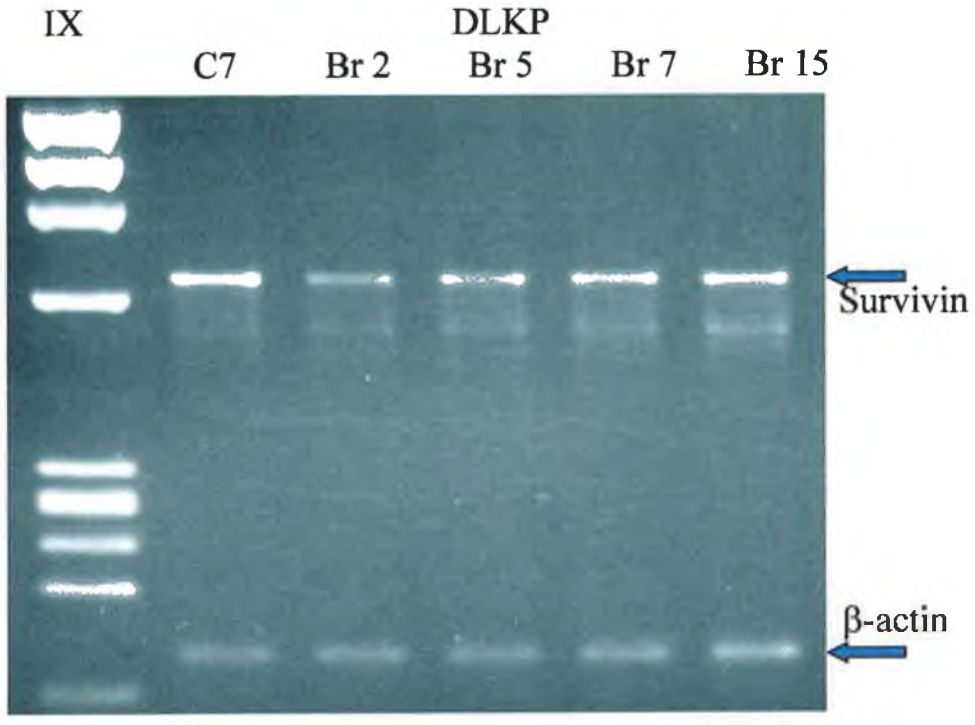

Fig. 3.1.11b:

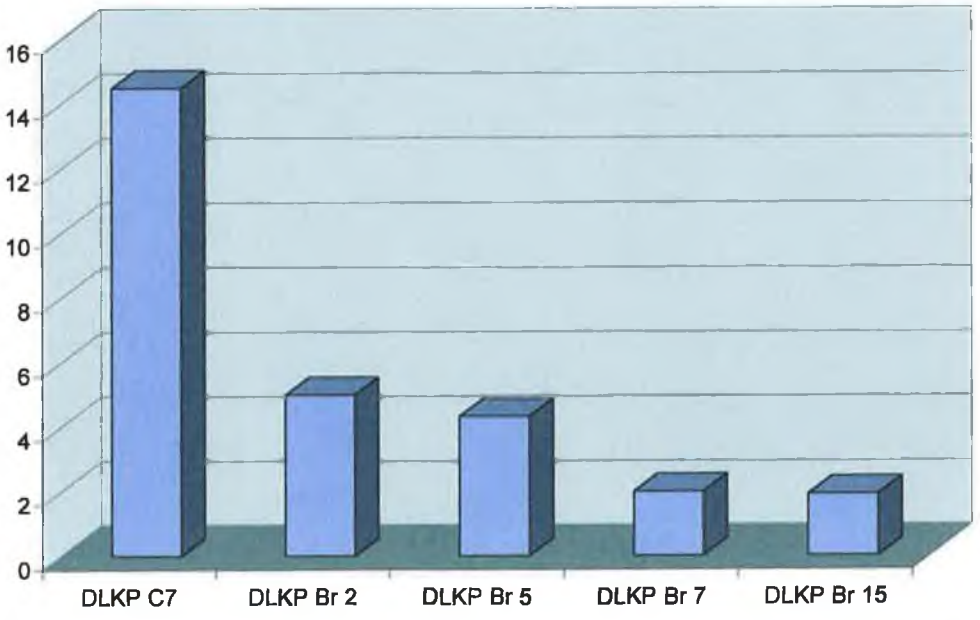

Fig. 3.1.11a: Gel electrophoresis photograph of Survivin RT-PCR results on BrdU-treated DLKP cells; Fig. 3.1.11b: Densitometric analysis of RT-PCR results.

Fig. 3.1.12: α-catenin RT-PCR on BrdU-treated DLKP cells

Fig. 3.1.12a:

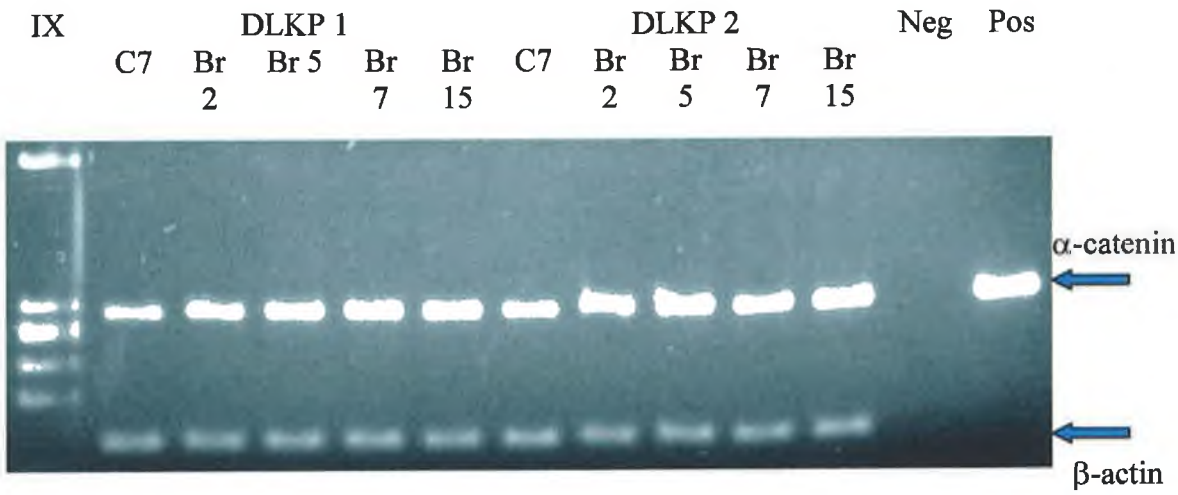

Fig. 3.1.12b:

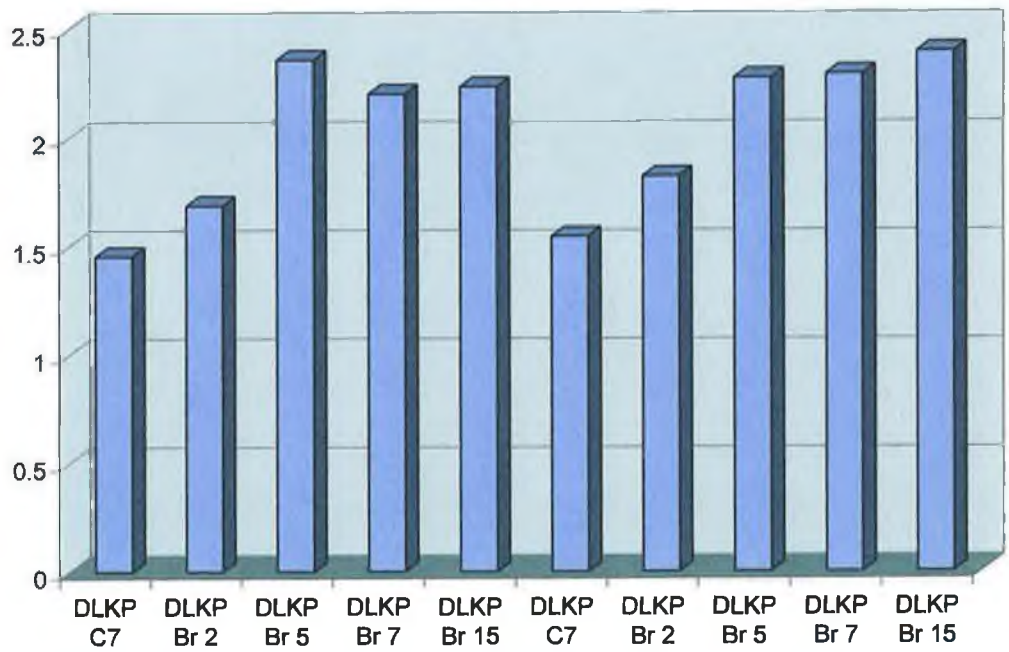

Fig. 3.1.12a: Gel electrophoresis photograph of α-catenin RT-PCR results on BrdU-treated DLKP cells; Fig. 3.1.12b: Densitometric analysis of RT-PCR results.

Fig. 3.1.13: E-cadherin RT-PCR on BrdU-treated DLKP cells

Fig. 3.1.13a:

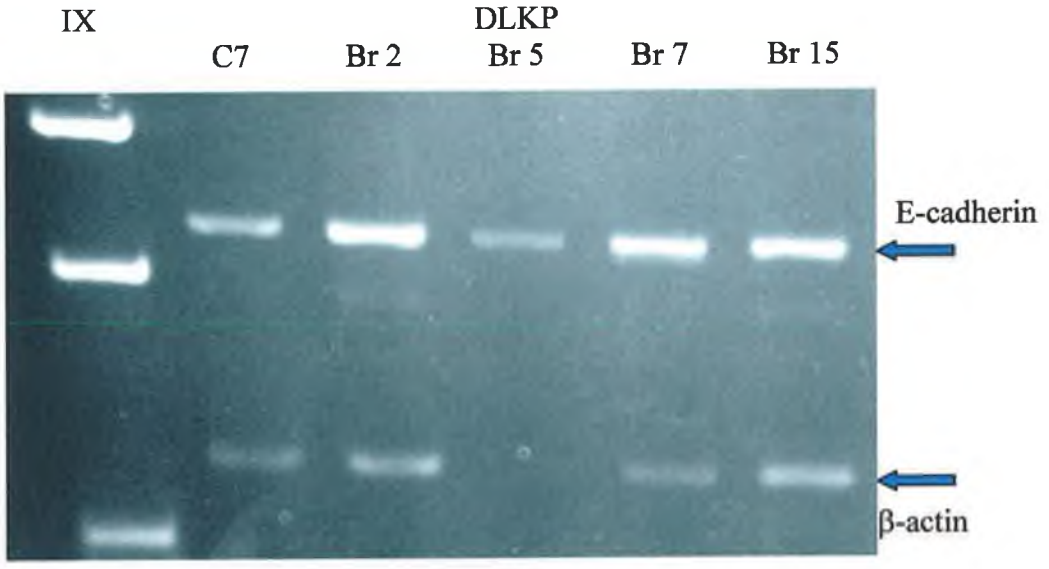

Fig. 3.1.13b:

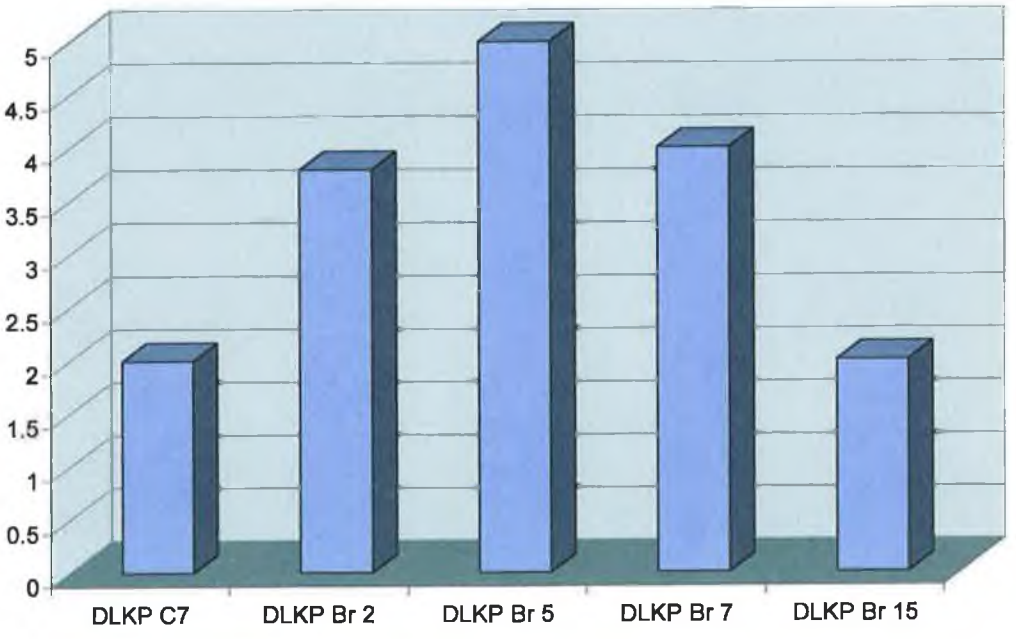

Fig. 3.1.13a: Gel electrophoresis photograph of E-cadherin RT-PCR results on BrdU-treated DLKP cells; Fig. 3.1.13b: Densitometric analysis of RT-PCR results.

Table 3.1.3 Summary of significant BrdU RT-PCR results

Gene	Cell Line	Effect of BrdU on gene expression
MRP1	A549	Slight increase in expression (<two-fold)
	DLKP	Significant increase in expression (>twelve-fold after seven days
MRP2	A549	Slight decrease in expression
	DLKP	Significant increase in expression (>29-fold after seven days
MRP3	DLKP	Significant increase in expression (>300-fold after seven days
MRP4	A549	Significant decrease in expression up to fifteen days
	DLKP	Overall slight increase in expression
Mdr-1	A549	Significant decrease in expression
BCRP	A549	Slight increase in expression (two-fold)
	DLKP	Significant increase in expression (44-fold after seven days)
COX-2	DLKP	Significant increase in expression (67-fold after seven days)
EIF-2α	DLKP	Significant increase in expression (three-fold after five days)
BAXα	DLKP	Significant increase in expression (six-fold after five days)
MRIT	DLKP	Significant increase in expression (three-fold after five days)
Survivin	DLKP	Significant decrease in expression
α-catenin	DLKP	Slight increase in expression (<two-fold)
E-cadherin	DLKP	Slight increase in expression (>two-fold)

Table 3.1.4 Summary of non-significant BrdU RT-PCR results

Gene	Cell Line	Effect of BrdU on gene expression
MRP3	A549	Slight decrease in expression, result not significance
MRP5	DLKP	No change in already low level of gene expression
MRP6	A549	No consistent trend, up- and down-regulation observed over the course of the experiment
	DLKP	Overall decrease in expression, however bands were too faint to be certain of an accurate result
Mdr-1	DLKP	BrdU had very little effect on the expression of this gene
Mdr-3	A549	No mdr-3 expression observed in any of the samples
	DLKP	No mdr-3 expression observed in any of the samples
COX-1	A549	No COX-1 expression observed in any of the samples
	DLKP	No COX-1 expression observed in any of the samples
COX-2	A549	Inconsistent pattern of upregulation, not repeatable
BAX α	A549	Slight decrease in expression, result not felt to be of significance
BAG	A549	Slight increase in expression, result not felt to be of significance
	DLKP	Slight decrease in expression, result not felt to be of significance
BAP	A549	Slight decrease in expression, result not felt to be of significance
	DLKP	Slight decrease in expression, result not felt to be of significance
Survivin	A549	Inconsistency in results; one isolate revealed a strong decrease in expression, the other a strong increase
MRIT	A549	Overall slight increase in expression, however expression pattern was inconsistent over different isolates
Bcl-2α	A549	No gene expression observed in BrdU-treated cells
	DLKP	No gene expression observed in BrdU-treated cells

Table 3.1.3 Cont'd.

Gene	Cell Line	Effect of BrdU on gene expression
Bcl-$x_{L/S}$	A549	Inconsistent and unrepeatable expression trends observed
	DLKP	Inconsistent and unrepeatable expression trends observed
c-*myc*	A549	Slight increase observed overall, however, this result was not felt to be of significance
	DLKP	Slight decrease observed in expression, however the result is not repeatable
eIF-4E	A549	No clear pattern, change in expression varies for each isolate
	DLKP	Overall increase in expression, not consistently repeatable
eIF-2α	A549	Slight decrease in expression, however not consistently repeatable
α-catenin	A549	Slight rise in expression levels, unrepeatable
β-catenin	A549	Slight decrease in expression, not significant
	DLKP	Slight increase in expression, not significant
E-cadherin	A549	No significant alteration in gene expression

3.1.2 Analysis of BrdU-exposed DLKP cells using *in vitro* toxicity testing

In the previous Section, RT-PCR analysis was used to examine the roles played by a number of genes in the BrdU-differentiated cell lines A549 and DLKP. The expression of a number of genes thought to be important in cancer progression and resistance to chemotherapy were observed to be altered in both of these cell lines following exposure to BrdU. The greater number of gene expression changes, however, were seen in the DLKP cell line. As a result, this cell line was chosen for further analysis.

In order to examine the effect of up- and down-regulation of a number of these genes in the BrdU-treated cells, these treated cells were exposed *in-vitro* to a selection of

chemotherapeutic drugs. The chemotherapeutic drugs chosen for *in-vitro* toxicity testing were drugs which are routinely used in the treatment of lung cancer in the clinical setting and which have been used in the characterisation of numerous lung cancer cell lines in our own laboratory. The four drugs chosen were

- Adriamycin (Doxorubicin),
- Cisplatin,
- Taxol
- VP16 (VP16).

The cells were set up for drug treatment as outlined in Section 2.3.1. A second assay was also set up exactly one week after the first, in order to provide a duplicate set of results. Five time points were then chosen[1] for the analysis and treated with BrdU as outlined in Section 3.1.

Once the cells had been exposed for the required amount of time, they were harvested and set up for *in-vitro* toxicity testing as outlined in Section 2.3.1.2. Four separate standard toxicity assays involving the four chosen individual chemotherapeutic drugs were set up in 96-well tissue culture plates, with one plate for each time point examined, giving a total of 20 plates per experiment.

The cells were then exposed to the various drugs over a range of concentrations, which encompassed the IC_{50} values for each drug for the DLKP cell line. At the end of the seven-day toxicity assay, the cells were taken down and analysed using the acid-phosphatase assay (Section 2.3.1.4). The results for the first set of toxicity experiments were then compared with those obtained for the duplicate set for accuracy. If any discrepancies were observed at this stage, the experiment was repeated. The results presented here are from one individual experiment which were successfully repeated.

[1] These are the same time points which were selected for analysis in the BrdU RT-PCR analyses (Section 3.1.1).

3.1.2.1 Effect of BrdU-exposure on the drug-resistance of DLKP cells

As can be seen from Figs. 3.1.14 – 3.1.17, exposure to the differentiating agent BrdU over several of the selected timepoints does not affect greatly the resistance profile of the DLKP cells. A very slight decrease in drug resistance is revealed with increasing length of exposure to BrdU. However, this decrease is extremely small and is not considered significant.

After seven days exposure to BrdU, the growth rate of the cells was observed to be severely interrupted, which facilitated the elimination of the cells at a far lower drug concentration than that previously determined by toxicity analysis. This result was observed to be generally the same over the range of drugs studied. By day fifteen, the growth rate of the cells had returned to normal.

These results indicate that, in spite of changes in gene expression (at the mRNA level) of several genes which may be expected to confer drug resistance, no significant change in resistance to the drugs is observed. However, at day seven, exposure to BrdU resulted in a significant interruption of cell survival which was not observed at any of the other time points.

3.1.3 Analysis of BrdU-treated DLKP cells using Western blotting

These western blots were carried out by Rasha Linehan. The BrdU-exposed DLKP cells were also analysed using Western blotting. Analysis with this technique was limited to the number of antibodies currently available for analysis in the NCTCC. Western blot analysis on whole-cell protein preparations was carried out on the cells for Survivin and MRP1. No expression of the MRP1 protein was detected in these preparations of DLKP. However, expression of the Survivin protein was observed to decrease slightly in the DLKP cells following treatment with BrdU. Fig. 3.1.18 shows the results of the Survivin western blot as well as an α-tubulin western blot which was used to normalise the Survivin results. From the data presented in the densitometry, it can be seen that Survivin expression levels decrease slightly after two days exposure to the agent before increasing again up to seven days. After fifteen days exposure, expression levels have again decreased to less than half that of normal cells.

Fig. 3.1.14 Effect of BrdU exposure on Adriamycin resistance in DLKP cells

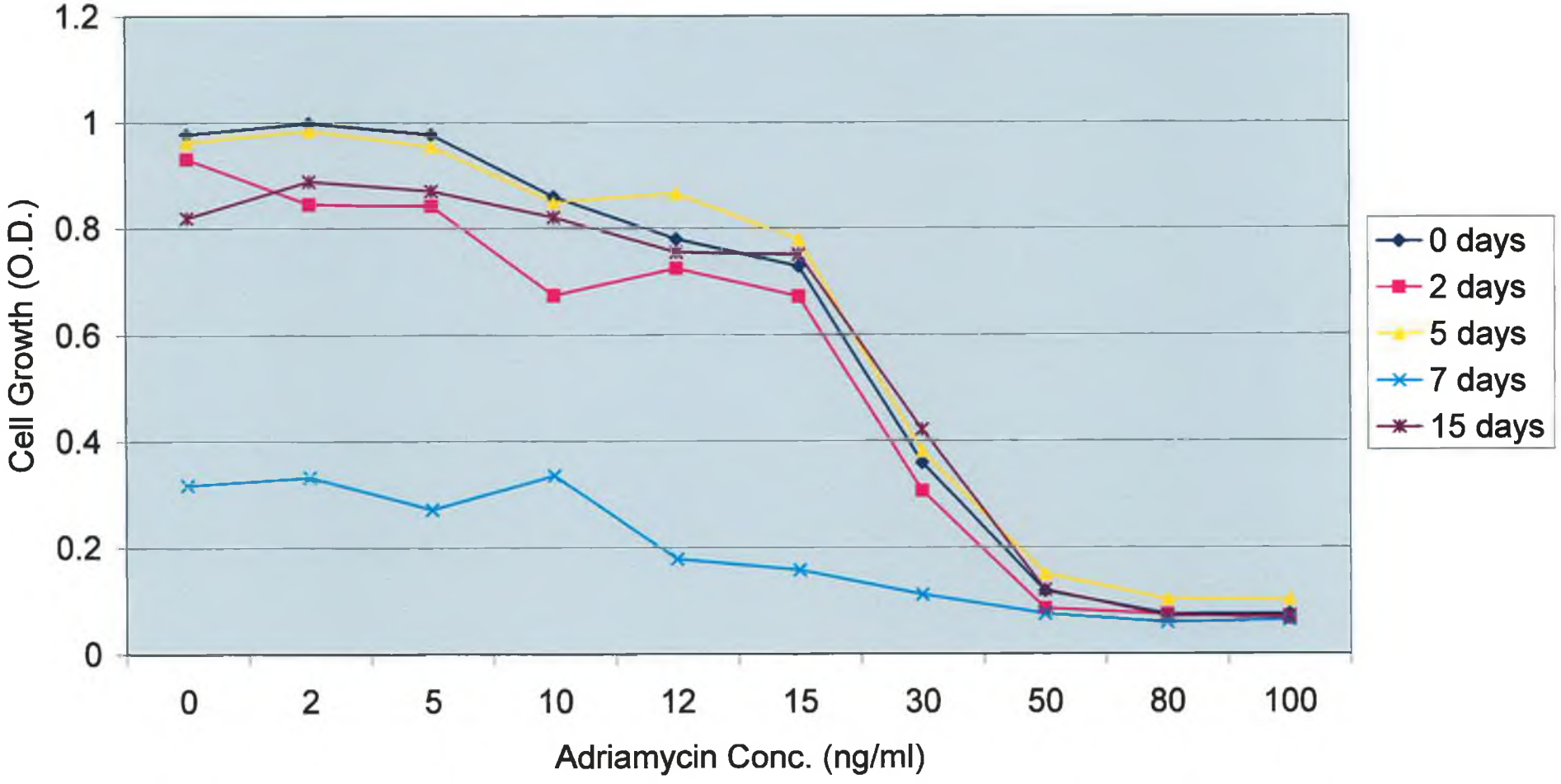

Fig. 3.1.15 Effect of BrdU exposure on Cisplatin resistance in DLKP cells

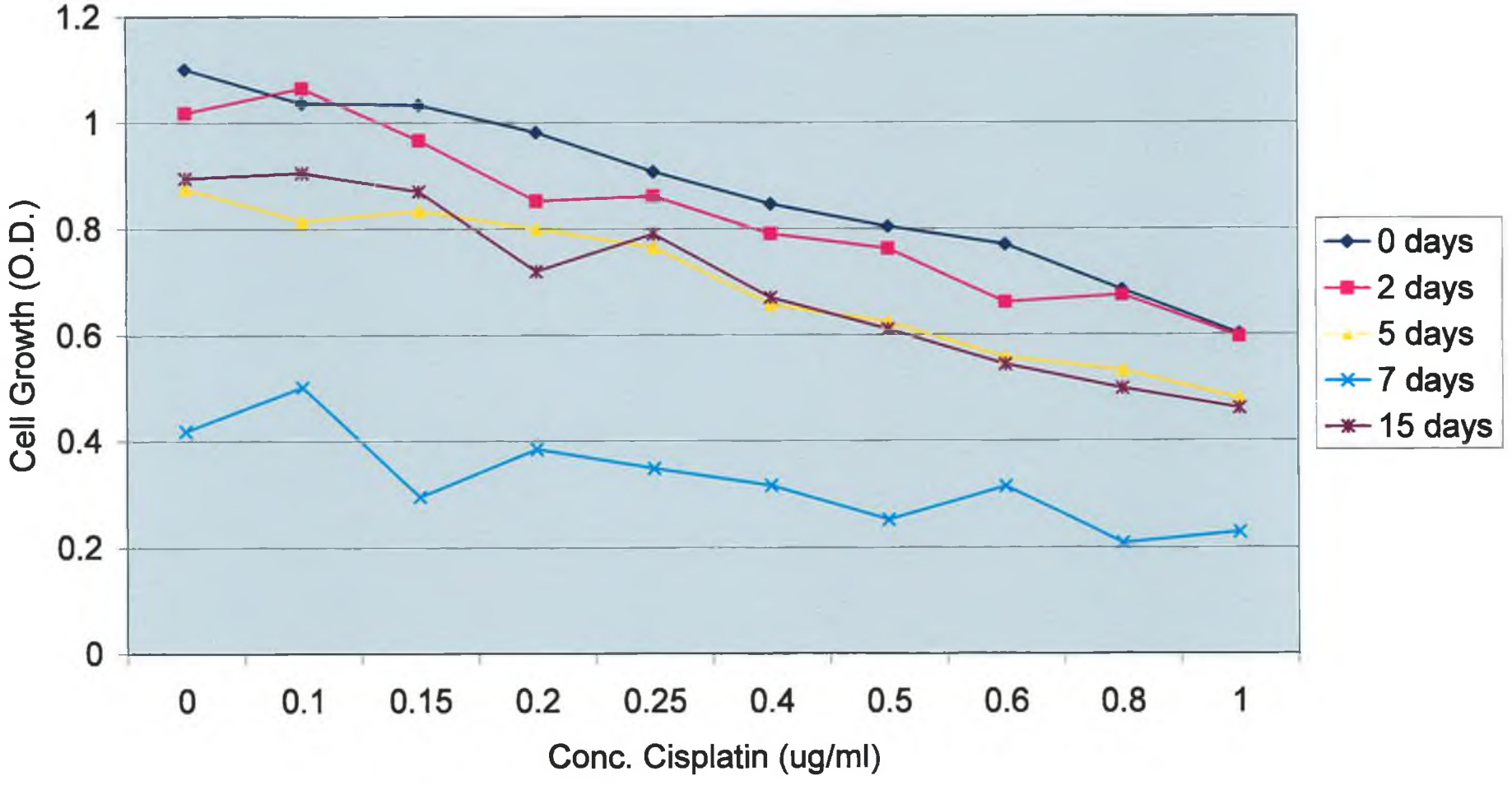

Fig. 3.1.16 Effect of BrdU exposure on Taxol resistance in DLKP cells

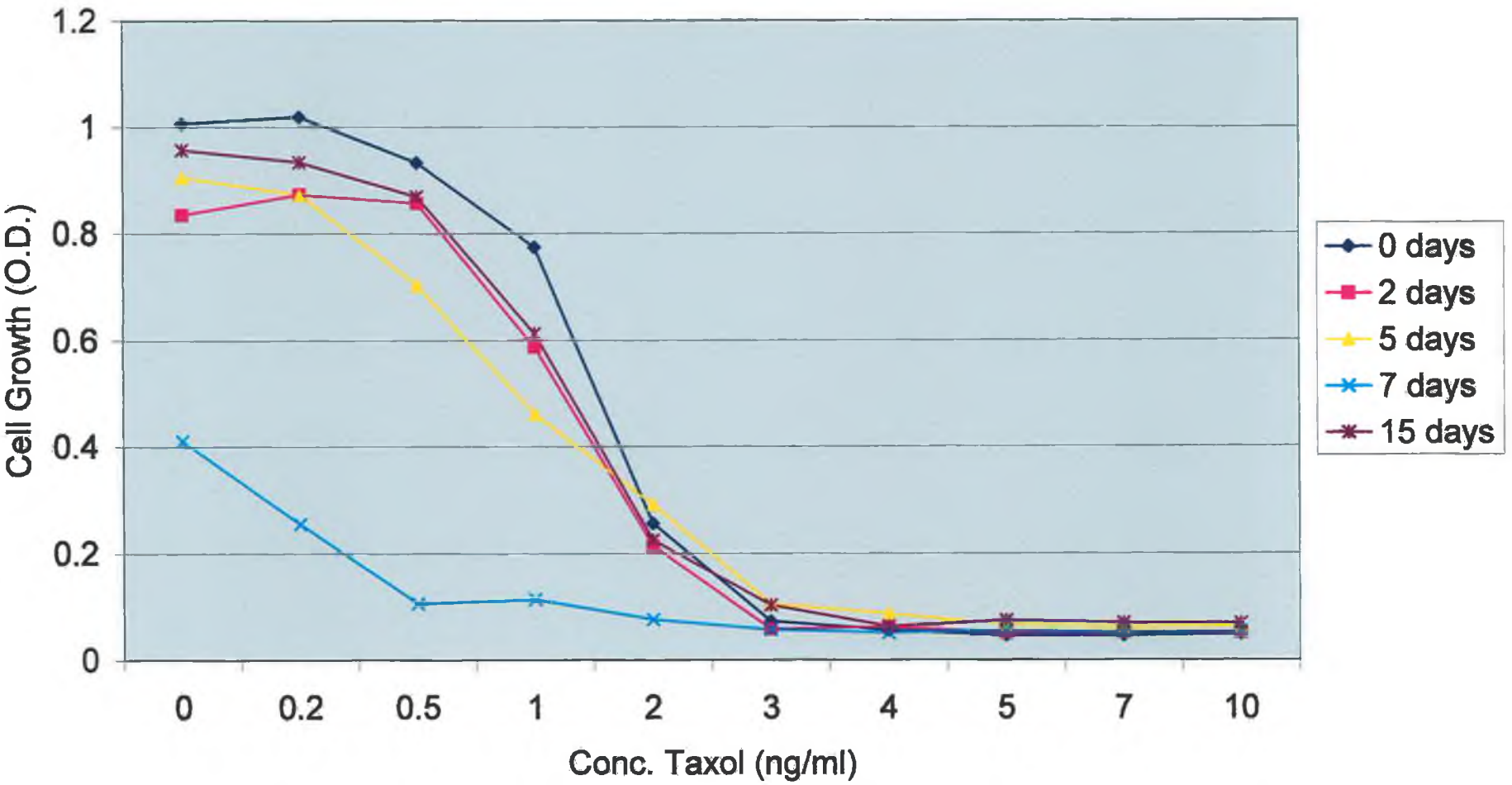

Fig. 3.1.17 Effect of BrdU exposure on VP16 resistance in DLKP cells

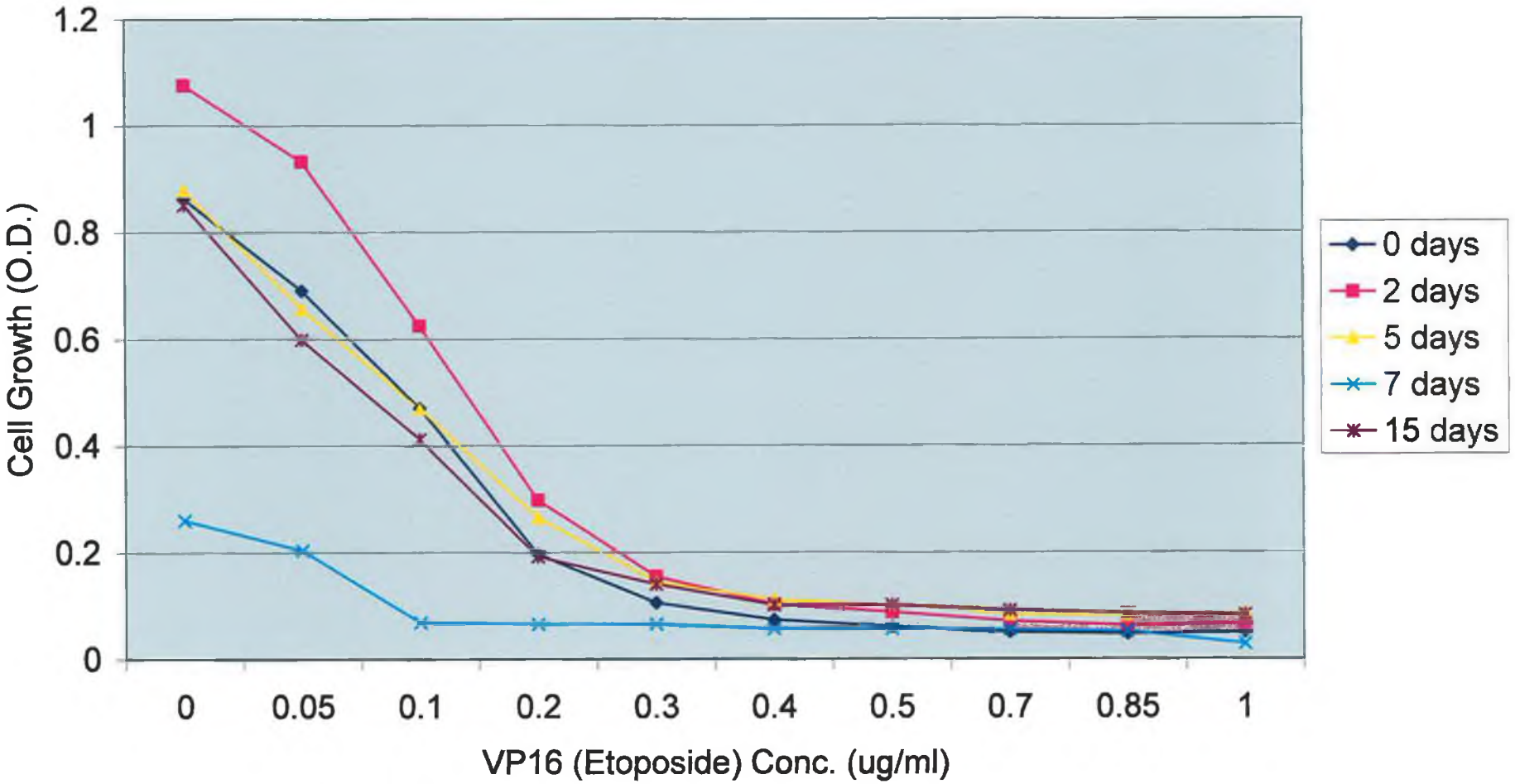

Fig. 3.1.18: Survivin Western on BrdU-treated DLKP cells

Fig. 3.1.18a:

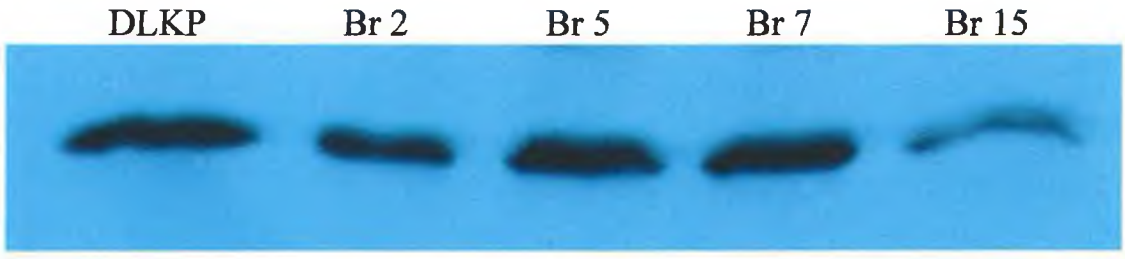

Fig. 3.1.18b:

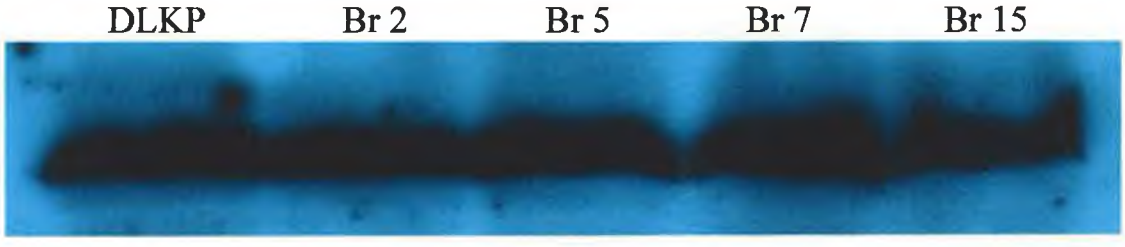

Fig. 3.1.18c:

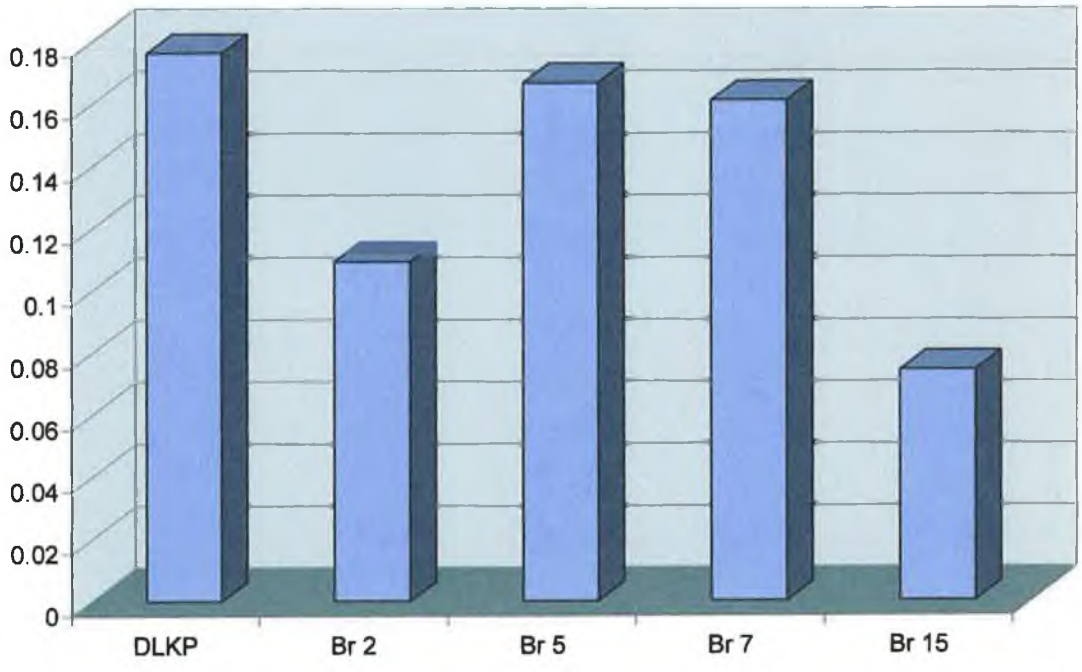

Fig. 3.1.18a: Survivin Western blot analysis of BrdU-treated DLKP cells; Fig. 3.1.18b: α-tubulin Western blot on BrdU-treated DLKP cells; Fig. 3.1.18c: Densitometric analysis of Western blot results.

Fig. 3.1.18: Survivin Western on BrdU-treated DLKP cells

Fig. 3.1.18a:

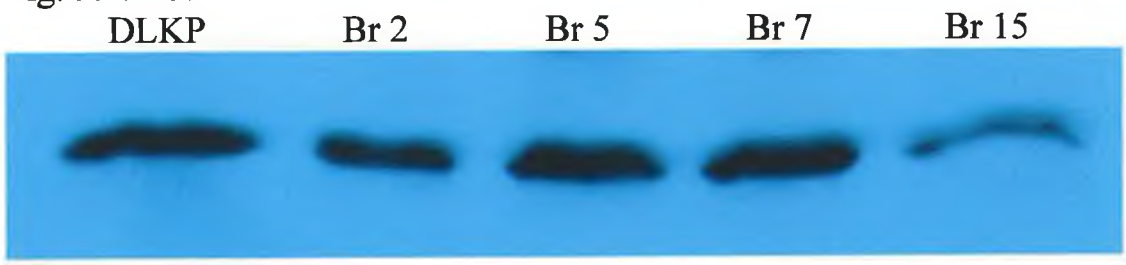

Fig. 3.1.18b:

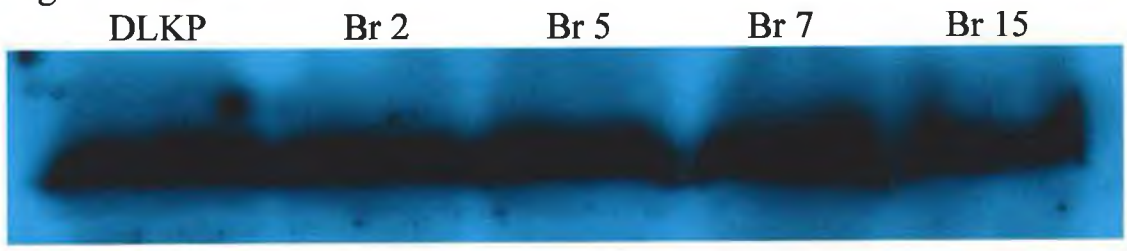

Fig. 3.1.18c:

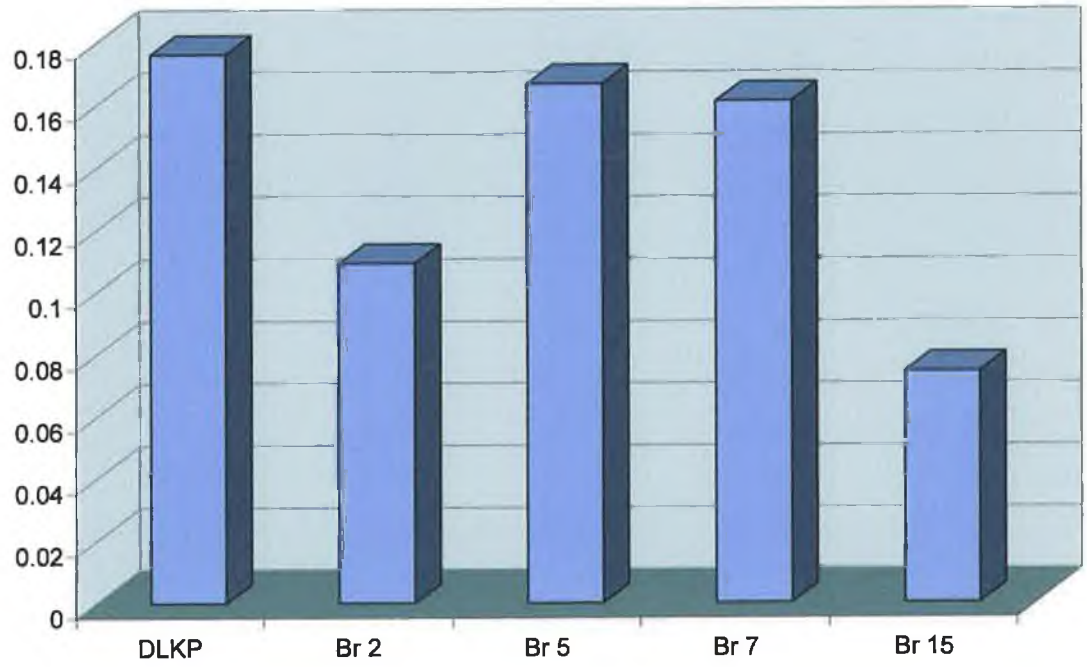

Fig. 3.1.18a: Survivin Western blot analysis of BrdU-treated DLKP cells; Fig. 3.1.18b: α-tubulin Western blot on BrdU-treated DLKP cells; Fig. 3.1.18c: Densitometric analysis of Western blot results.

3.2 Analysis of cells continuously exposed to chemotherapeutic drugs

DLKP was exposed to a variety of chemotherapeutic drugs to ascertain if these drugs could, like BrdU, cause significant alterations in gene expression. The drugs selected for exposure, VP16, Taxol and Cisplatin, are commonly used in the treatment of lung cancer. As outlined in Section 1.5.4 of the introduction, exposure of cells to these drugs as well as drug-selection has resulted in increased expression of several cancer-related genes. The cells were exposed to a sub-lethal concentration of each drug which was chosen to ensure maximum cell survival while not affecting the inducible gene response already observed. The concentration of each drug used is listed in Table 3.2.1. The procedure for setting up this assay has already been outlined in Section 2.3.4. The cells were exposed to the relevant concentration of each drug at the same specified intervals as those for the BrdU assays and were finally taken down two weeks after the exposure has commenced and subjected to analysis by RT-PCR and *in-vitro* toxicity testing. Two separate control cell lines were used in the analyses in order to increase the accuracy of the assay.

Table 3.2.1Concentrations of drug used to induce gene expression in DLKP cells

Drug Type	Stock Concentration (ηg/μl)	Working Concentration (ηg/ml)
Cisplatin	1000	125
Taxol	6000	0.15
VP16	20000	30

3.2.1 Analysis of drug-exposed DLKP cells using RT-PCR analysis

Cells were taken down after the course of exposure to each chemotherapeutic drug and RNA was extracted using the TRI Reagent™ method as outlined in Section 2.4.2.2. Each time course corresponded to a time point already examined in the BrdU exposure assays (Section 3.1) and are represented on the graphical plots here by those chronological divisions (i.e. VP16 2 – two days exposure to VP16, VP16 5 – five days, etc.). Standard RT-PCR analysis was carried out on all RNA samples isolated as outlined (Section 2.4.2.5). All PCRs were duplicated in order to maximise accuracy of

the results. Duplicate untreated DLKP control samples were also included to check reproducibility.

All twenty-five genes whose expression was studied by RT-PCR in the BrdU-treated cells were also examined for altered expression in the drug-exposed DLKP cells. The negative control used in all cases was filter-sterilised water. Only results which were considered significant will be examined in detail in this Section.

3.2.1.1 MRP1

MRP1 expression was observed to be strongly upregulated following short-term exposure to the drugs cisplatin and VP16 (Figs. 3.2.1 and 3.2.2). Exposure of the DLKP cells to taxol did not result in increased MRP1 expression (data not shown).

3.2.1.2 MRP2 (cMOAT)

MRP2 expression was observed increased in the DLKP cell line following exposure to all three selected chemotherapeutic drugs (Figs. 3.2.3 – 3.2.5).

3.2.1.3 BCRP

BCRP expression was observed increased in the DLKP cell line following exposure to cisplatin (Fig. 3.2.6). However, the expression increase was not exactly the same for both sets of samples. In the first set, a strong difference in expression levels of the gene was observed between the two control samples. Also, in this set, BCRP expression increased roughly two-fold by day seven only to decrease to near-normal levels by day fifteen. In the second set, expression of the gene followed the same pattern, although increasing by a higher amount and ending at over two-fold the normal expression levels by day fifteen. However, it was felt that, in both cases, the increase in expression was repeatable and consistent with exposure to the chemotherapeutic agent, cisplatin.

Fig. 3.2.1: MRP1 RT-PCR on Cisplatin-treated DLKP cells

Fig. 3.2.1a:

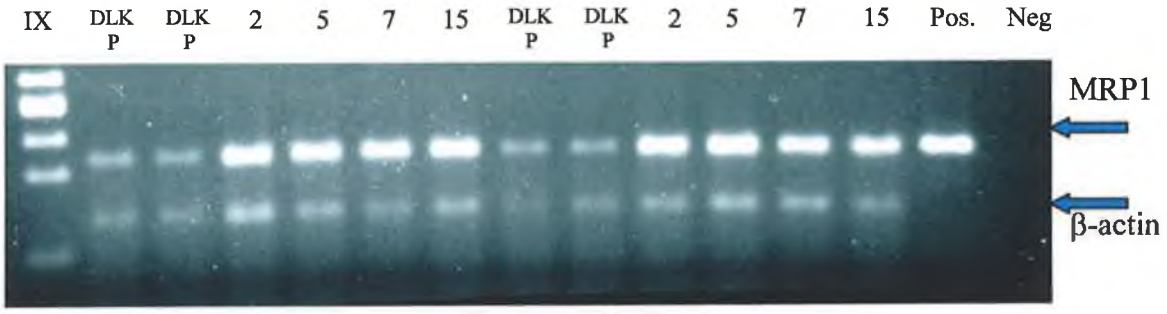

Fig. 3.2.1b:

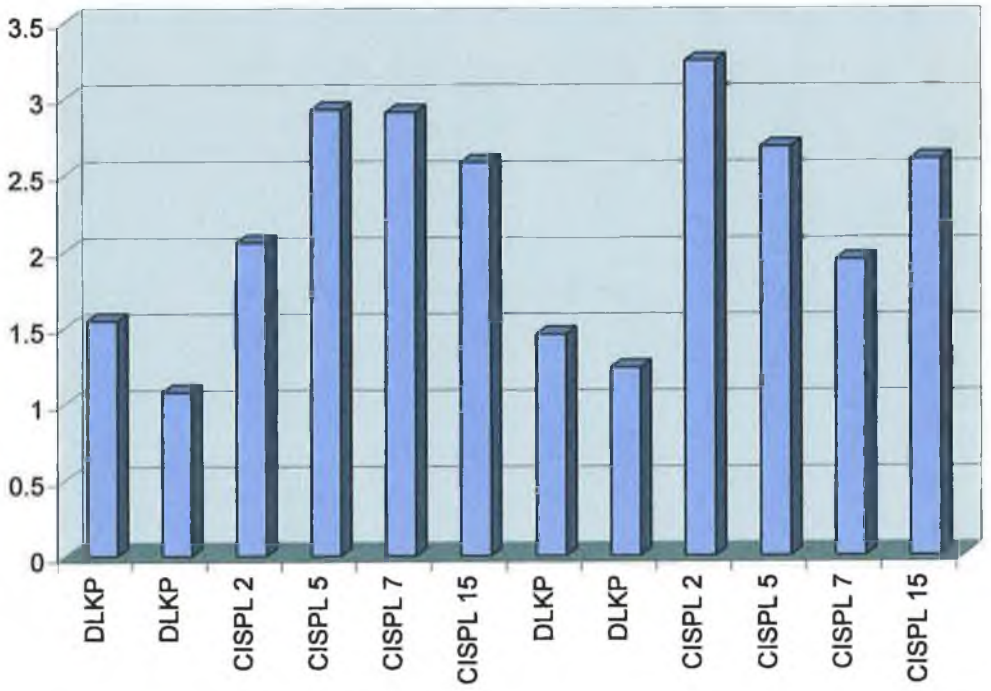

Fig. 3.2.1a: Gel electrophoresis photograph of MRP1 RT-PCR results on Cisplatin-exposed DLKP cells; Fig. 3.2.1b: Densitometric analysis of RT-PCR results.

Fig. 3.2.2: MRP1 RT-PCR on VP16-treated DLKP cells

Fig. 3.2.2a:

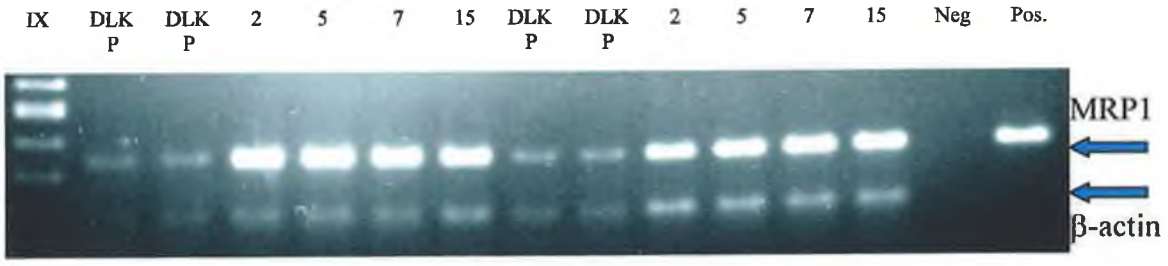

Fig. 3.2.2b:

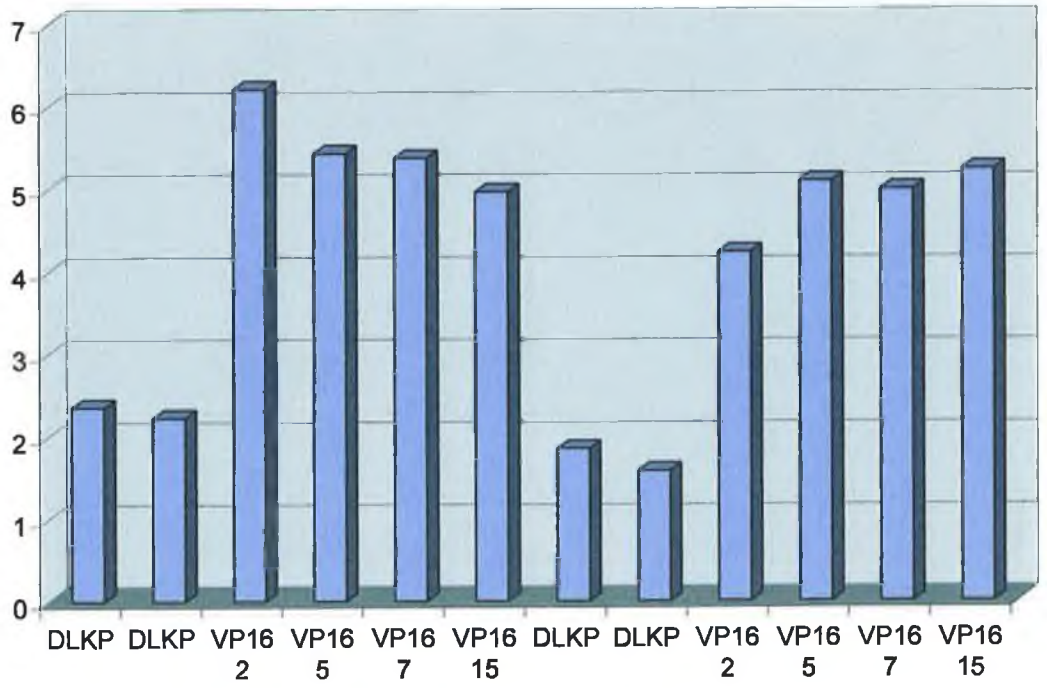

Fig. 3.2.2a: Gel electrophoresis photograph of MRP1 RT-PCR results on Etoposide-exposed DLKP cells; Fig. 3.2.2b: Densitometric analysis of RT-PCR results.

Fig. 3.2.3: MRP2 RT-PCR on Cisplatin-treated DLKP cells

Fig. 3.2.3a:

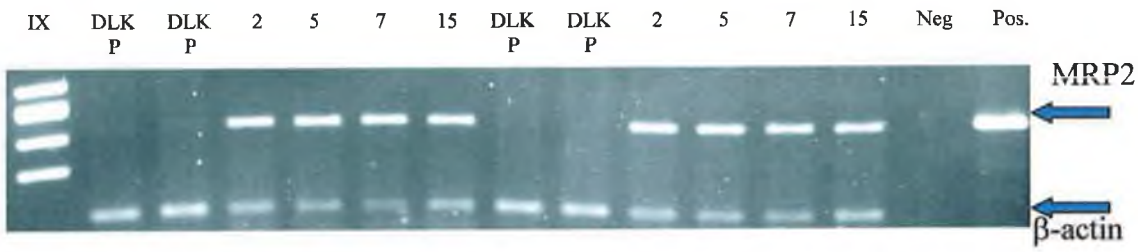

Fig. 3.2.3b:

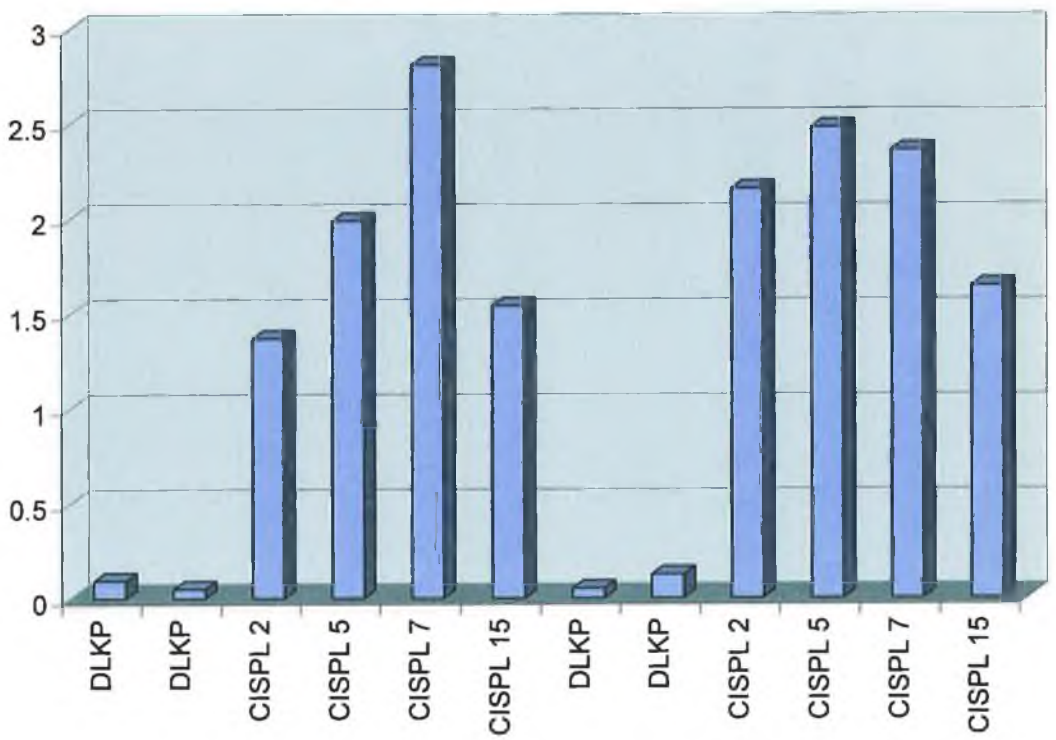

Fig. 3.2.3a: Gel electrophoresis photograph of MRP2 RT-PCR results on Cisplatin-exposed DLKP cells; Fig. 3.2.3b: Densitometric analysis of RT-PCR results.

Fig. 3.2.4: MRP2 RT-PCR on Taxol-treated DLKP cells

Fig. 3.2.4a:

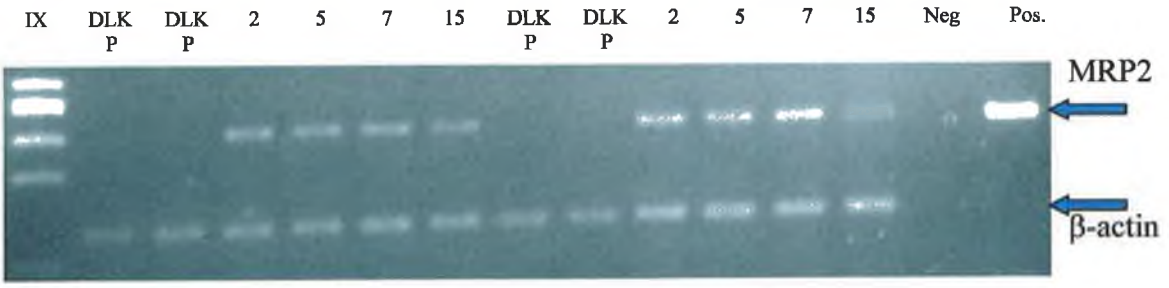

Fig. 3.2.4b:

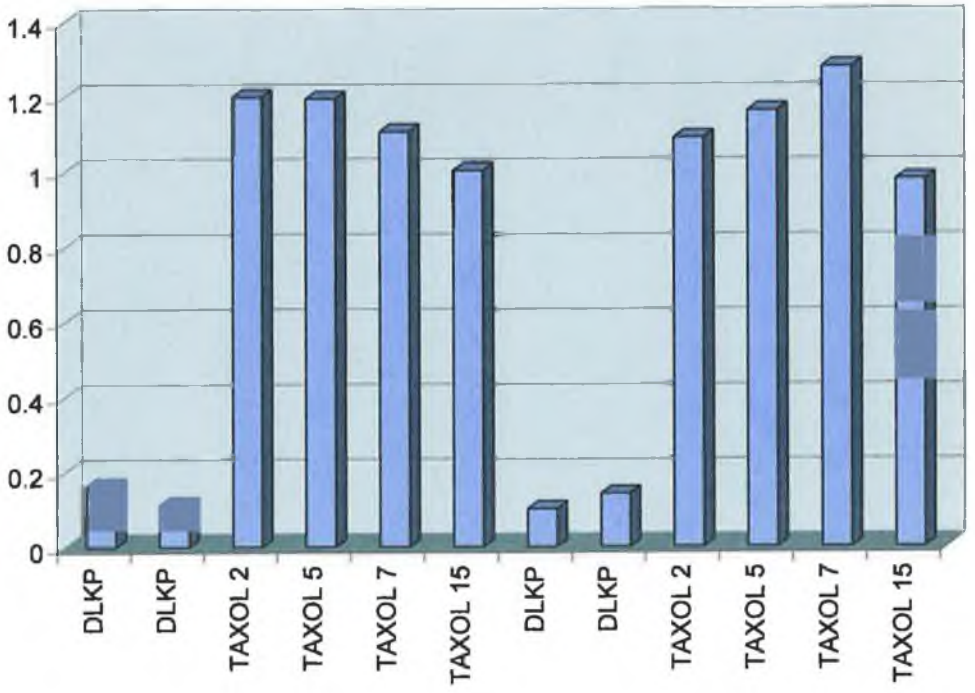

Fig. 3.2.4a: Gel electrophoresis photograph of MRP2 RT-PCR results on Taxol-exposed DLKP cells; Fig. 3.2.4b: Densitometric analysis of RT-PCR results.

Fig. 3.2.5: MRP2 RT-PCR on VP16-treated DLKP cells

Fig. 3.2.5a:

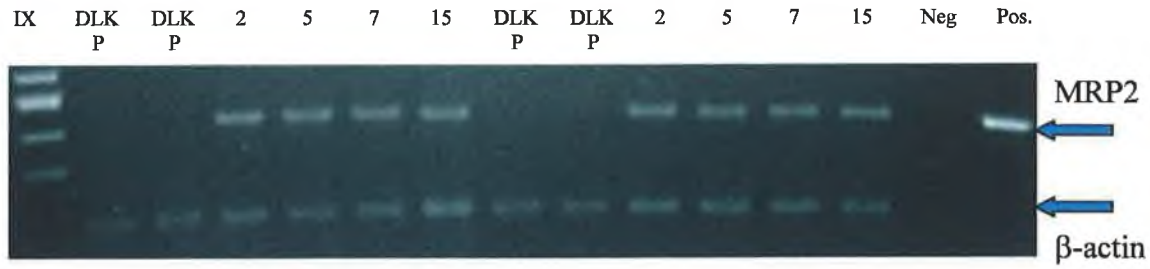

Fig. 3.2.5b:

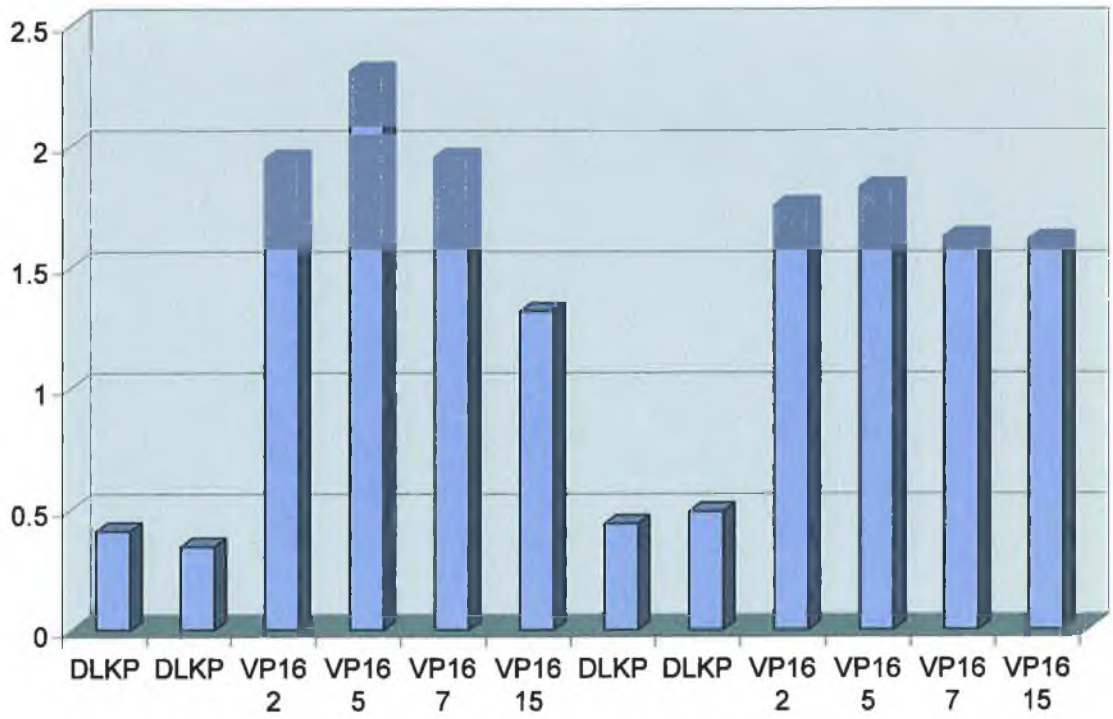

Fig. 3.2.5a: Gel electrophoresis photograph of MRP2 RT-PCR results on VP16-exposed DLKP cells; Fig. 3.2.5b: Densitometric analysis of RT-PCR results.

Fig. 3.2.6: BCRP RT-PCR on Cisplatin-treated DLKP cells

Fig. 3.2.6a:

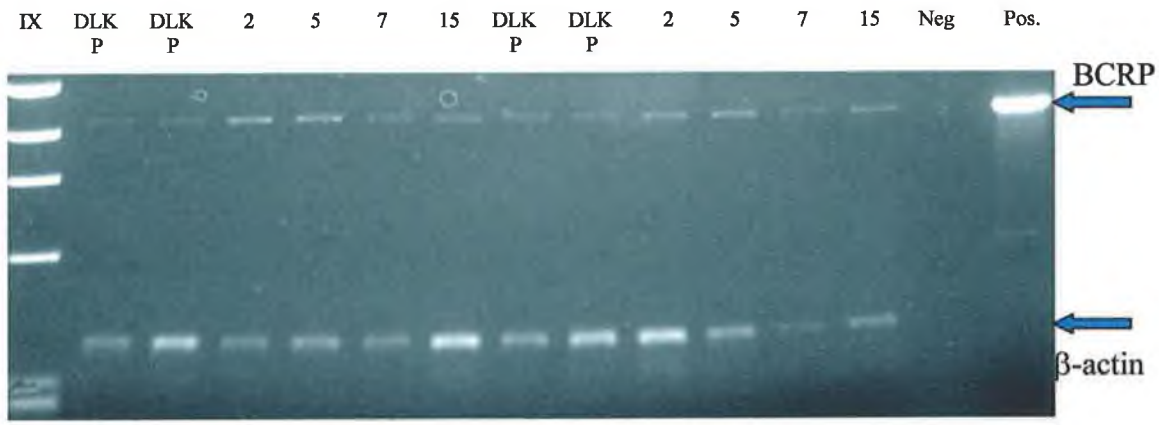

Fig. 3.2.6b:

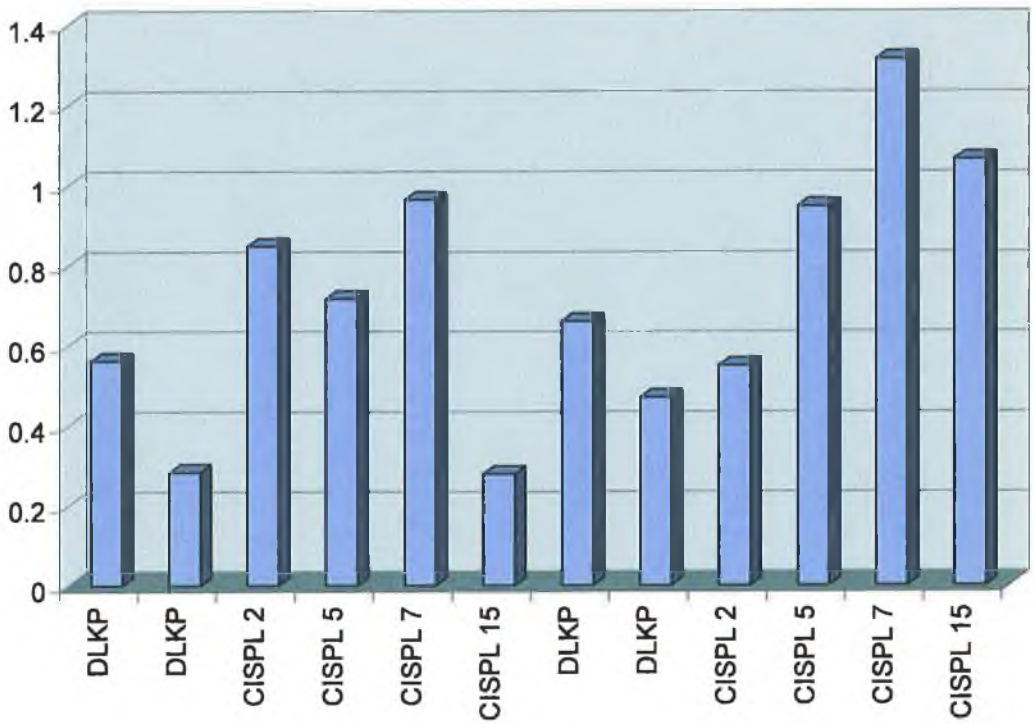

Fig. 3.2.6a: Gel electrophoresis photograph of BCRP RT-PCR results on Cisplatin-exposed DLKP cells; Fig. 3.2.6b: Densitometric analysis of RT-PCR results.

Exposure of the DLKP cells to taxol and VP16 did result in some slight expression changes of BCRP. However, these were not felt to be of significance (data not shown).

3.2.1.4 α-catenin

Exposure of DLKP cells to two of the chemotherapeutic drugs tested (taxol and VP16) increased α-catenin expression (Figs. 3.2.7 and 3.2.8). In the case of the VP16-treated cells, the expression increase was highly significant, with an overall increase of over seven-fold after five days exposure to the drug. For the taxol-exposed cells, the result was far less impressive. Treatment with cisplatin was also observed to increase expression of α-catenin in one of the sample sets but not in the duplicate (data not shown).

3.2.1.5 E-cadherin

Exposure of the DLKP cell line to taxol was observed to result in a small increase in expression of the E-cadherin gene (Fig. 3.2.9). Although the pattern of expression increase was not identical in both sample sets, the increase in both was deemed significant at day fifteen.

3.2.1.6 Summary of RT-PCR results for drug-exposed DLKP cells: significant and non-significant

For purposes of clarity, the RT-PCR results for the expression profiles of genes considered affected significantly by drug exposure in DLKP cells have been summarised in Table 3.2.2.

Fig. 3.2.7: α-catenin RT-PCR on Taxol-treated DLKP cells

Fig. 3.2.7a:

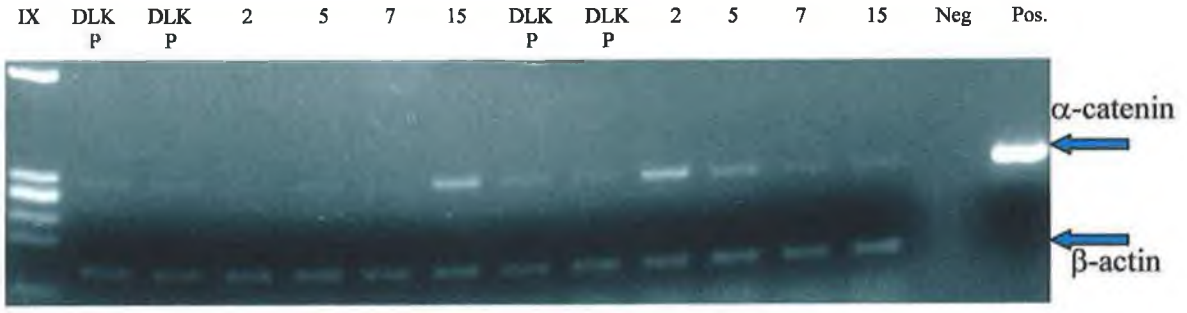

Fig. 3.2.7b:

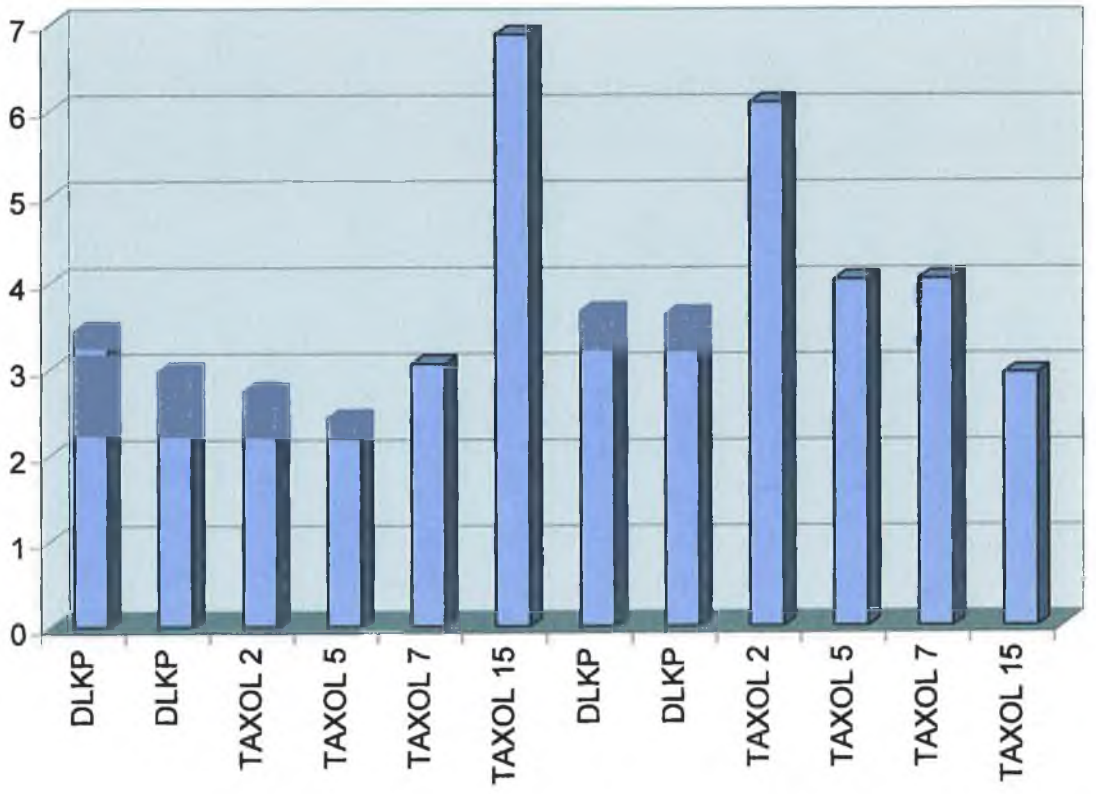

Fig. 3.2.7a: Gel electrophoresis photograph of α-catenin RT-PCR results on Taxol-exposed DLKP cells; Fig. 3.2.7b: Densitometric analysis of RT-PCR results.

Fig. 3.2.8: α-catenin RT-PCR on VP16-treated DLKP cells

Fig. 3.2.8a:

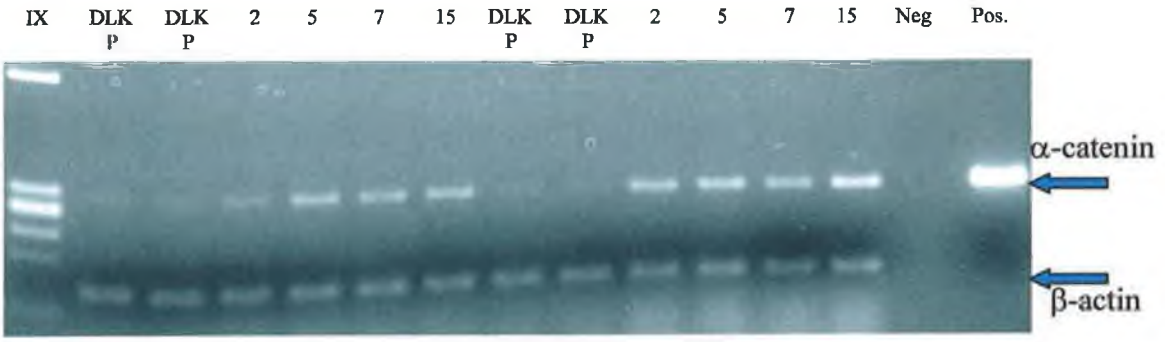

Fig. 3.2.8b:

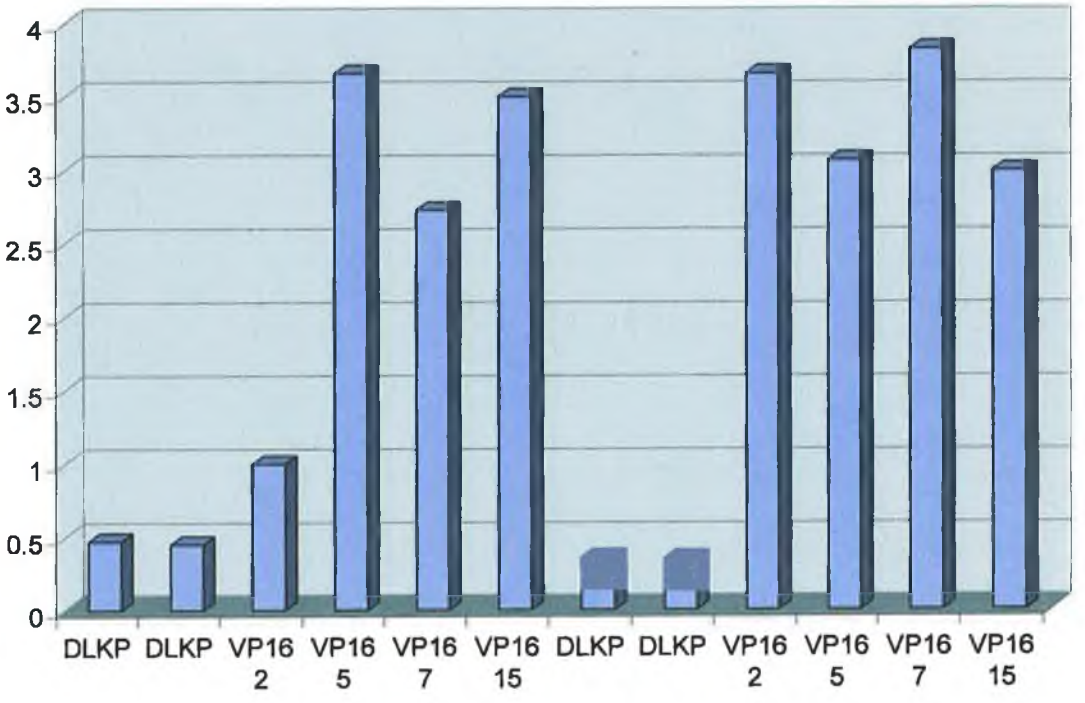

Fig. 3.2.8a: Gel electrophoresis photograph of α-catenin RT-PCR results on VP16-exposed DLKP cells; Fig. 3.2.8b: Densitometric analysis of RT-PCR results.

Fig. 3.2.9: E-cadherin RT-PCR on Taxol-treated DLKP cells

Fig. 3.2.9a:

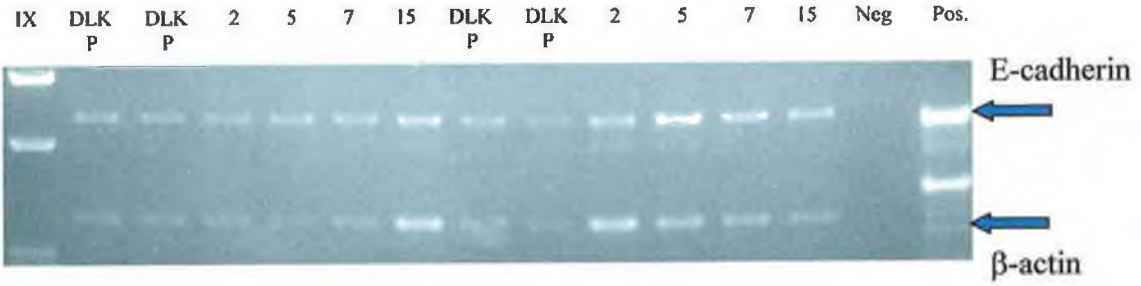

Fig. 3.2.9b:

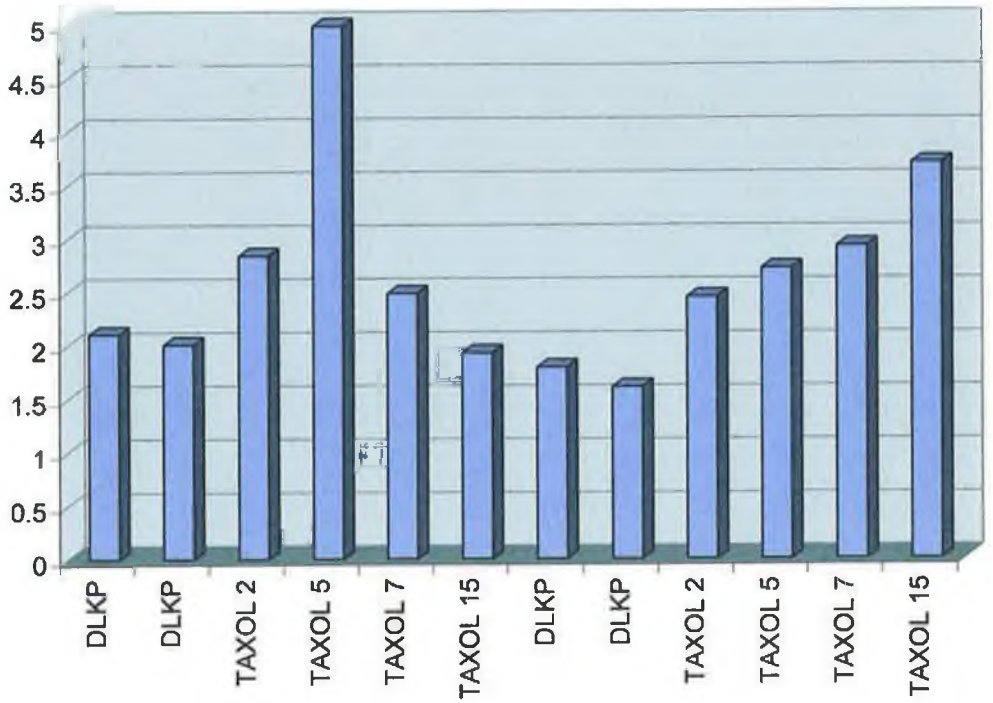

Fig. 3.2.9a: Gel electrophoresis photograph of E-cadherin RT-PCR results on Taxol-exposed DLKP cells; Fig. 3.2.9b: Densitometric analysis of RT-PCR results.

Table 3.2.2 Summary of significant RT-PCR results for drug-exposed DLKP

Gene	Drug Used	Effect of drug exposure on gene expression
MRP1	Cisplatin	Significant increase in expression (>three-fold)
	VP16	Significant increase in expression (>three-fold)
MRP2	Cisplatin	Significant increase in expression (>thirty-fold)
	Taxol	Significant increase in expression (>six-fold)
	VP16	Significant increase in expression (>four-fold)
BCRP	Cisplatin	Small increase in expression (two-fold)
α-catenin	Taxol	Small increase in expression (two-fold)
	VP16	Significant increase in expression (>seven-fold)
E-cadherin	Taxol	Small increase in expression (two-fold)

Of the thirteen expression RT-PCRs carried out on the drug-exposed DLKP cells however, only five were observed to yield significant increases in gene expression following exposure to the chemotherapeutic agents. In no sample set was a significant decrease in gene expression observed. The results of the non-significant PCR results are summarised in Table 3.2.3.

Table 3.2.3 Summary of non-significant RT-PCR results for drug-exposed DLKP

Gene	Drug type	Result
MRP1	Taxol	No change in expression profile
MRP3	Cisplatin	No change in expression profile
	Taxol	No change in expression profile
	VP16	No change in expression profile
MRP4	Cisplatin	Slight increase in expression, unrepeatable
	Taxol	No change in expression profile
	VP16	No change in expression profile
MRP5	Cisplatin	Slight decrease in expression
	Taxol	No change in expression profile
	VP16	No change in expression profile
MRP6	Cisplatin	No gene expression detected
	Taxol	No gene expression detected
	VP16	No gene expression detected
Mdr-1	Cisplatin	Little change in expression
	Taxol	Slight decrease in expression
	VP16	No change in expression profile
Mdr-3	Cisplatin	No gene expression detected
	Taxol	No gene expression detected
	VP16	No gene expression detected
BCRP	Taxol	Variation in expression profile, very inconsistent
	VP16	Same as for taxol-exposed DLKP
COX-1	Cisplatin	No change in expression profile
	Taxol	No change in expression profile
	VP16	No change in expression profile
COX-2	Cisplatin	No change in expression profile
	Taxol	No change in expression profile
	VP16	No change in expression profile
BAXα	Cisplatin	No change in expression profile
	Taxol	No change in expression profile
	VP16	No change in expression profile

Table 3.2.3 Cont'd.

Gene	Drug type	Result
MRIT	Cisplatin	No change in expression profile
	Taxol	No change in expression profile
	VP16	No change in expression profile
Survivin	Cisplatin	No change in expression profile
	Taxol	No change in expression profile
	VP16	No change in expression profile
BAG	Cisplatin	No change in expression profile
	Taxol	No change in expression profile
	VP16	No change in expression profile
BAP	Cisplatin	No change in expression profile
	Taxol	No change in expression profile
	VP16	No change in expression profile
Bcl-2α	Cisplatin	No change in expression profile
	Taxol	No change in expression profile
	VP16	No change in expression profile
Bcl-x_L	Cisplatin	No change in expression profile
	Taxol	No change in expression profile
	VP16	No change in expression profile
Bcl-x_S	Cisplatin	No change in expression profile
	Taxol	No change in expression profile
	VP16	No change in expression profile
eIF-4E	Cisplatin	No change in expression profile
	Taxol	No change in expression profile
	VP16	No change in expression profile
eIF-2α	Cisplatin	No change in expression profile
	Taxol	No change in expression profile
	VP16	No change in expression profile
c-myc	Cisplatin	No change in expression profile
	Taxol	No change in expression profile
	VP16	No change in expression profile
α-catenin	Cisplatin	Slight increase in one sample

Table 3.2.3 Cont'd.

Gene	Drug type	Result
β-catenin	Cisplatin	No change in expression profile
	Taxol	No change in expression profile
	VP16	No change in expression profile
E-cadherin	Cisplatin	Slight increases in some samples
	VP16	Same as for cisplatin-exposed DLKP

3.2.2 Analysis of drug-exposed DLKP cells using *in vitro* toxicity testing

3.2.2.1 Effect of Cisplatin exposure on DLKP drug-resistance profiles

As can be seen from Figs. 3.2.10 – 3.2.13, continuous exposure (as described in Section 3.2.1) to a selected sub-lethal concentration of cisplatin did not elicit any great change in the toxicity profile of the DLKP cells, nor the resultant IC_{50} values. Of the four drug types chosen for examination, cisplatin did not affect very much the expected dose-response curve. However, in all cases, the level of growth for the day five-treated sample was slightly higher than for all the other treatments, including the untreated controls. This increase ranged from 20-40% of the initial level of growth for the control cells. Overall, the toxicity profiles did not appear to match those of the BrdU samples, as the dose-response curve obtained for the day seven sample resembled for the greater part those of the other treatments.

3.2.2.2 Effect of Taxol exposure on the drug-resistance profiles of DLKP cells

The results from these toxicity assays can be seen in Figs. 3.2.14 – 3.2.17. The drug profile results for the taxol-exposed DLKP cells did not differ greatly from those obtained for the cisplatin-exposed cells. As seen for the cisplatin-treated DLKP, the exposure of the cells to low continuous-doses of Taxol did not appear to alter the dose-response curves for any of the treated samples. As can be seen from the dose-response curves, the pattern of response does not differ much from treatment to treatment. Also,

Fig. 3.2.10: Effect of Cisplatin exposure on Adriamycin resistance in DLKP cells

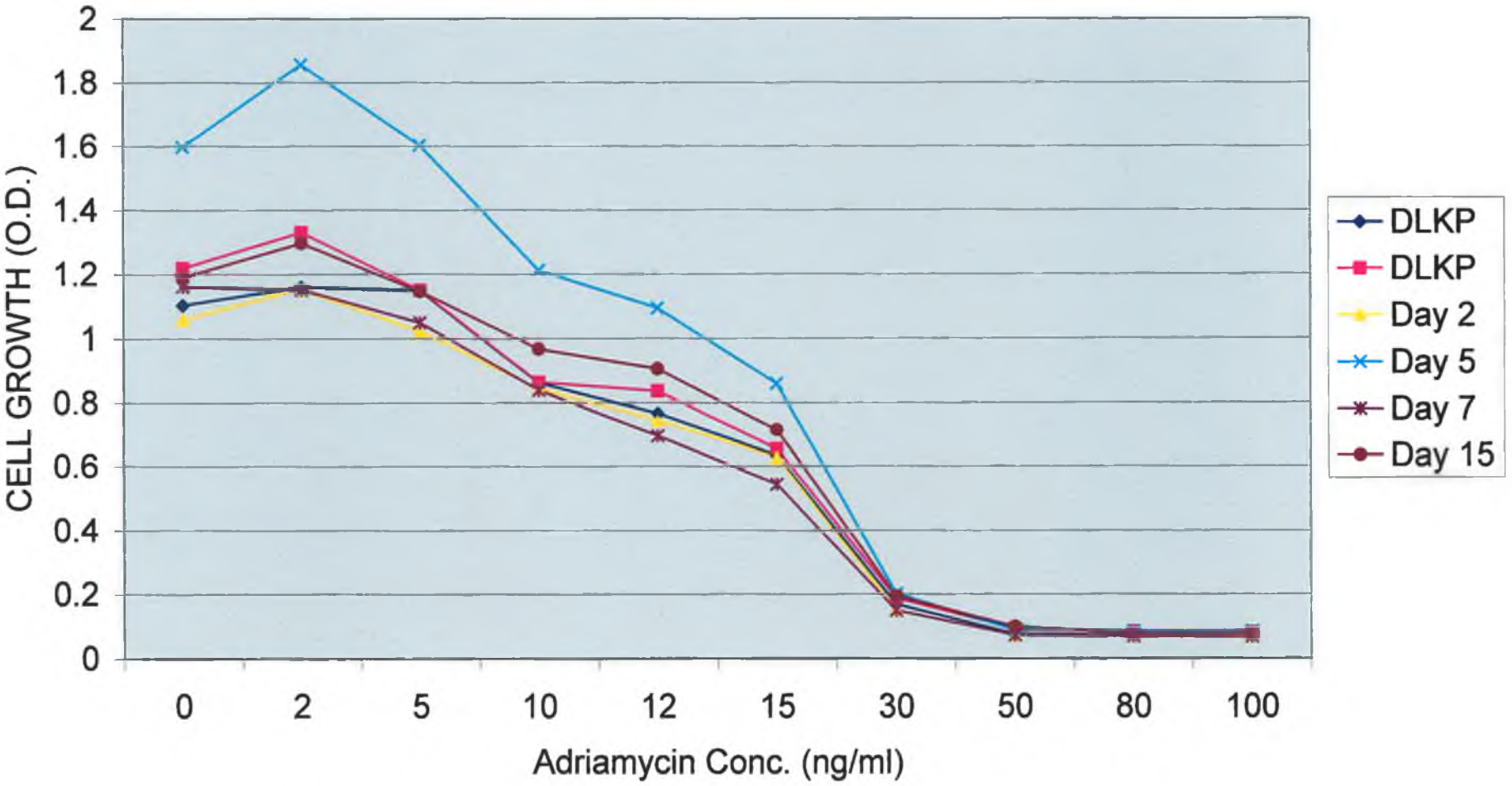

Fig. 3.2.11: Effect of Cisplatin exposure on Cisplatin resistance in DLKP cells

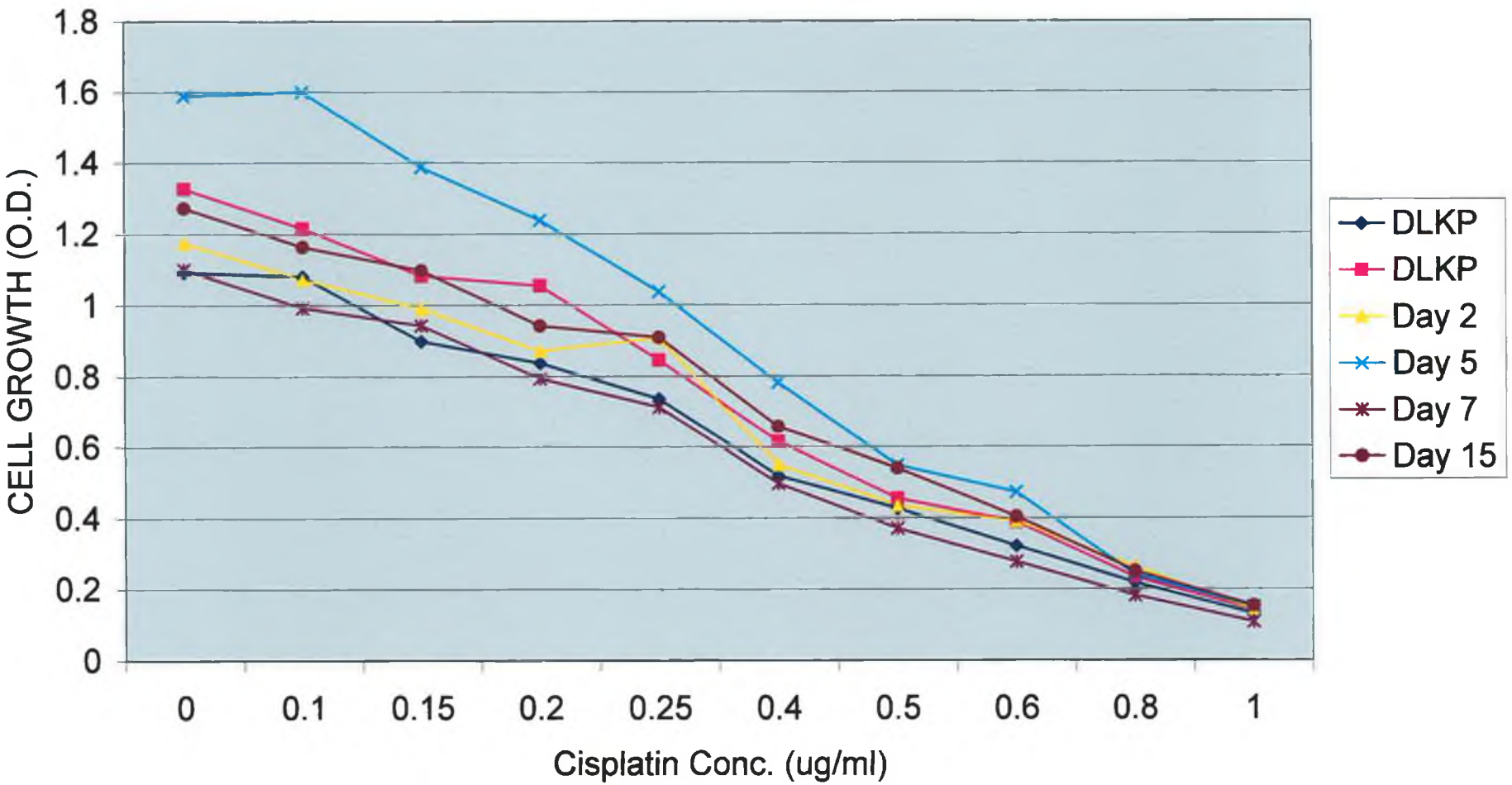

Fig. 3.2.12: Effect of Cisplatin exposure on Taxol resistance in DLKP cells

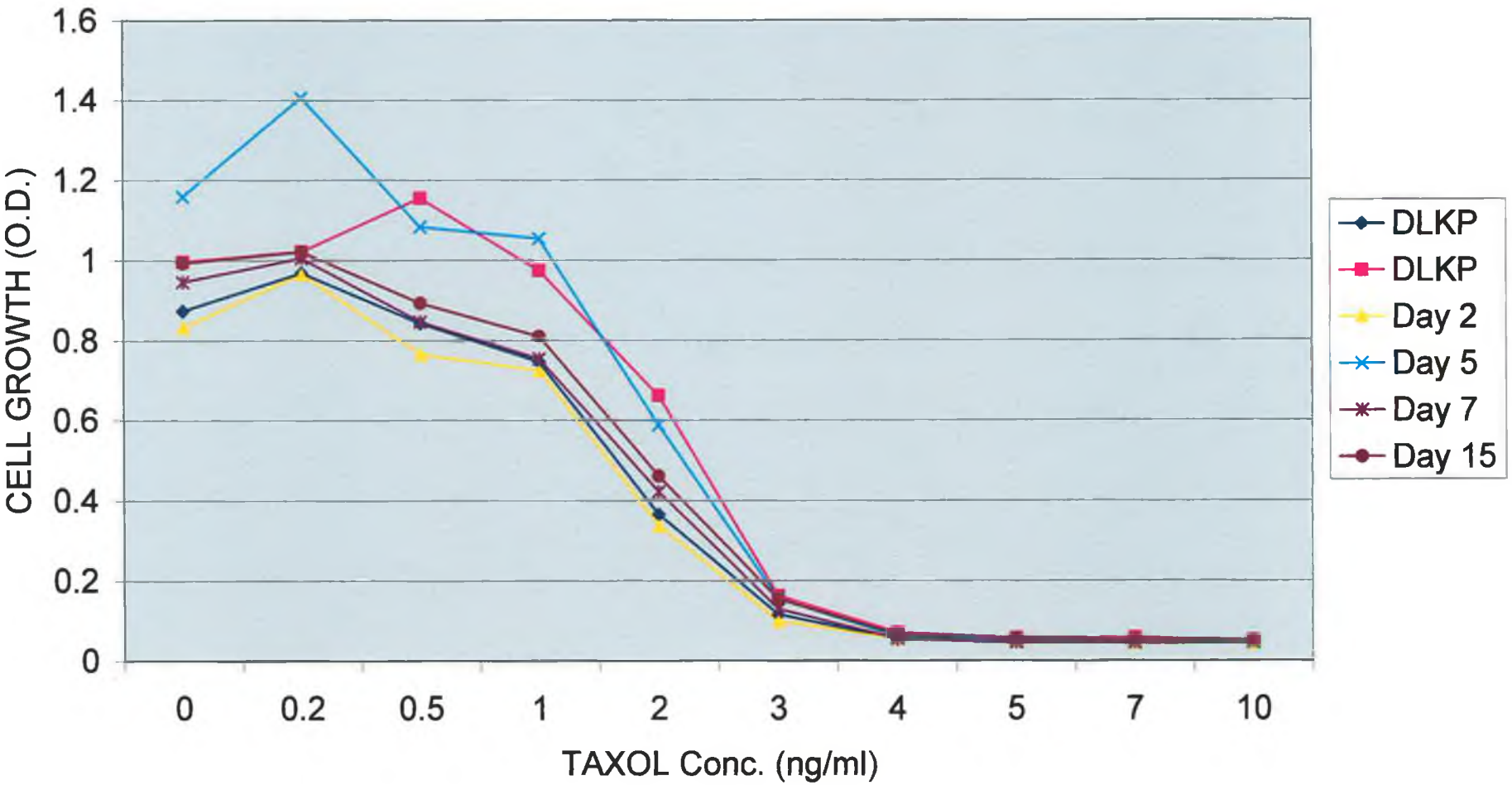

Fig 3.2.13: Effect of Cisplatin exposure on VP16 resistance in DLKP cells

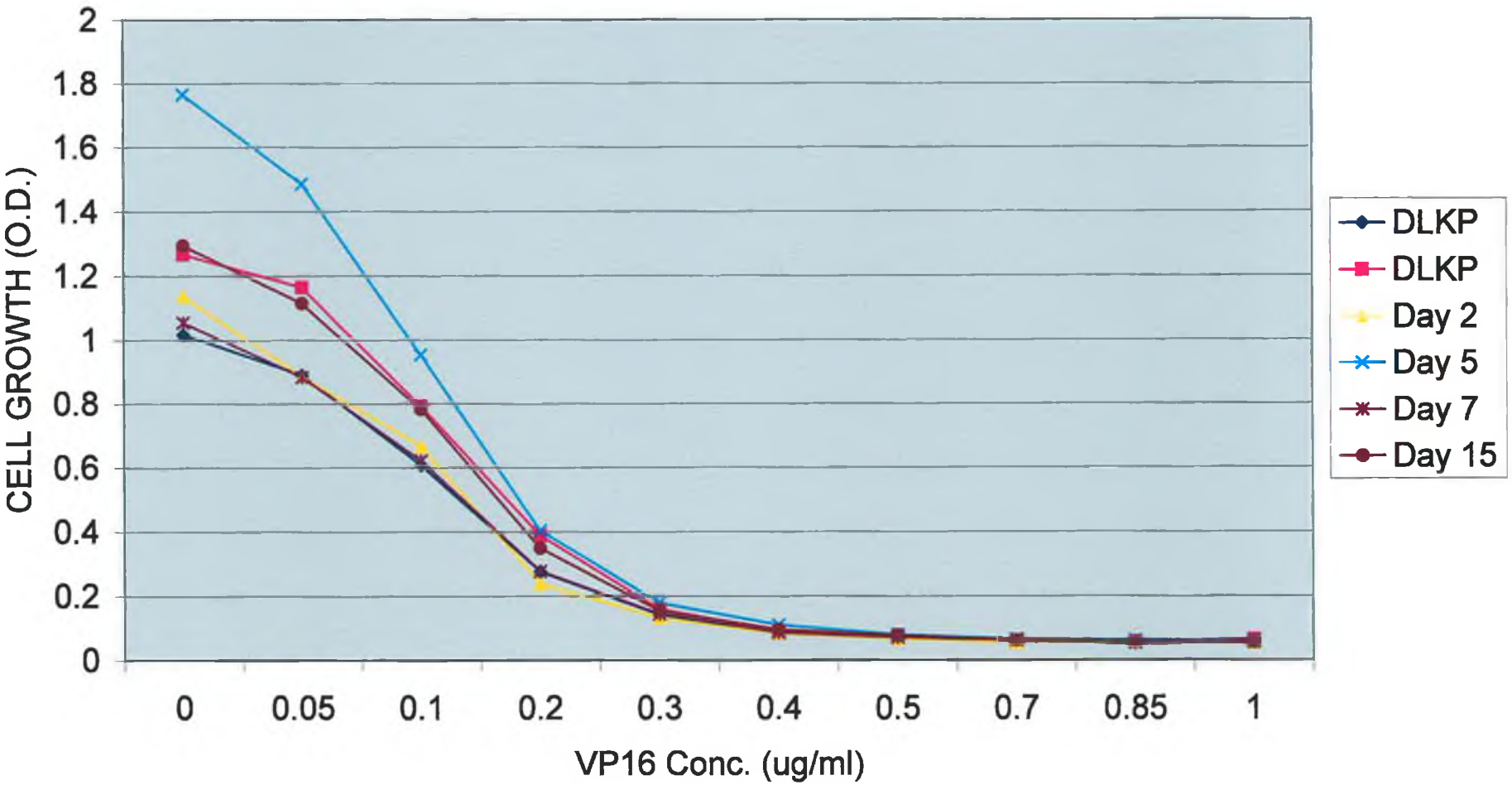

Fig. 3.2.14: Effect of Taxol exposure on Adriamycin resistance in DLKP cells

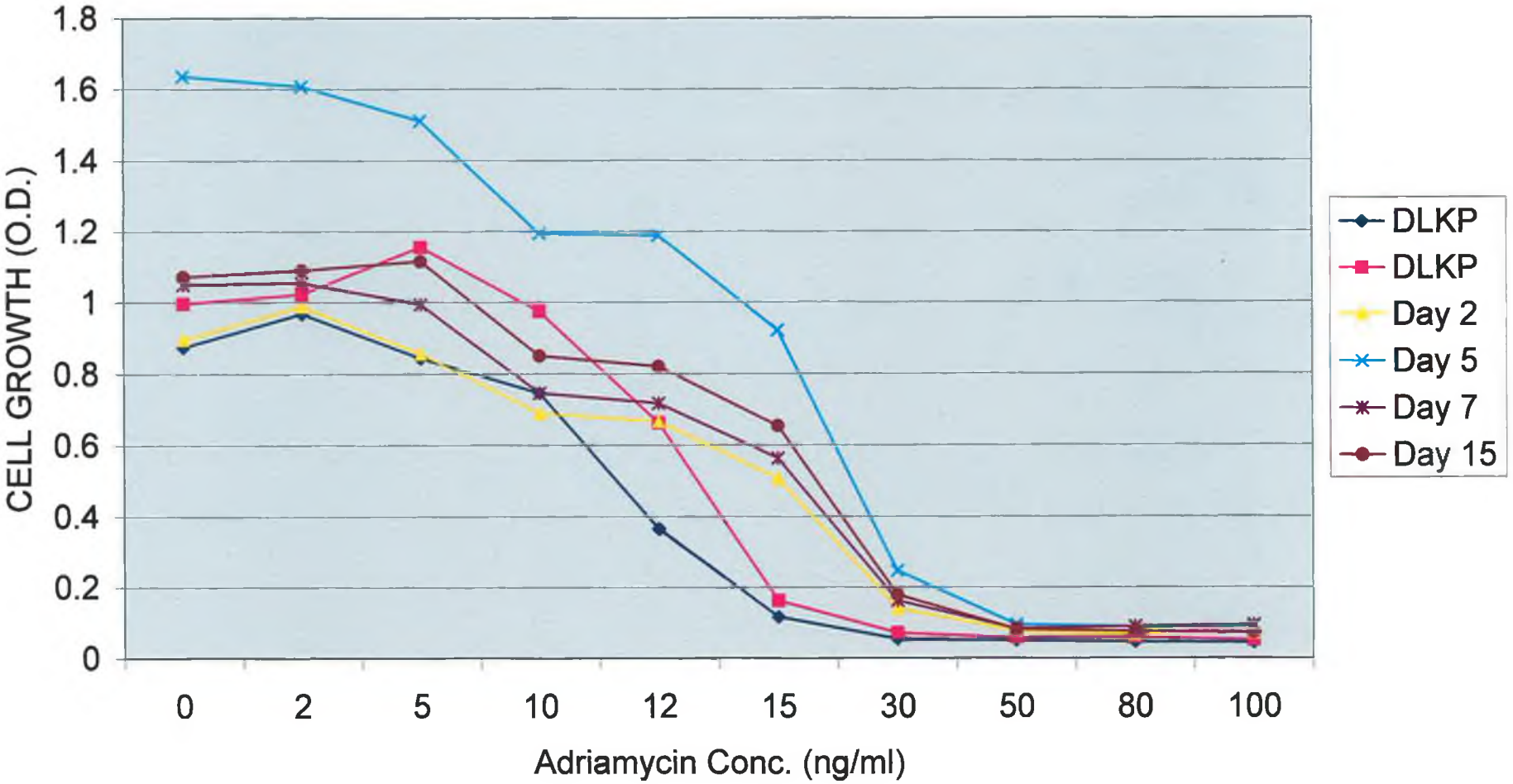

Fig. 3.2.15: Effect of Taxol exposure on Cisplatin resistance in DLKP cells

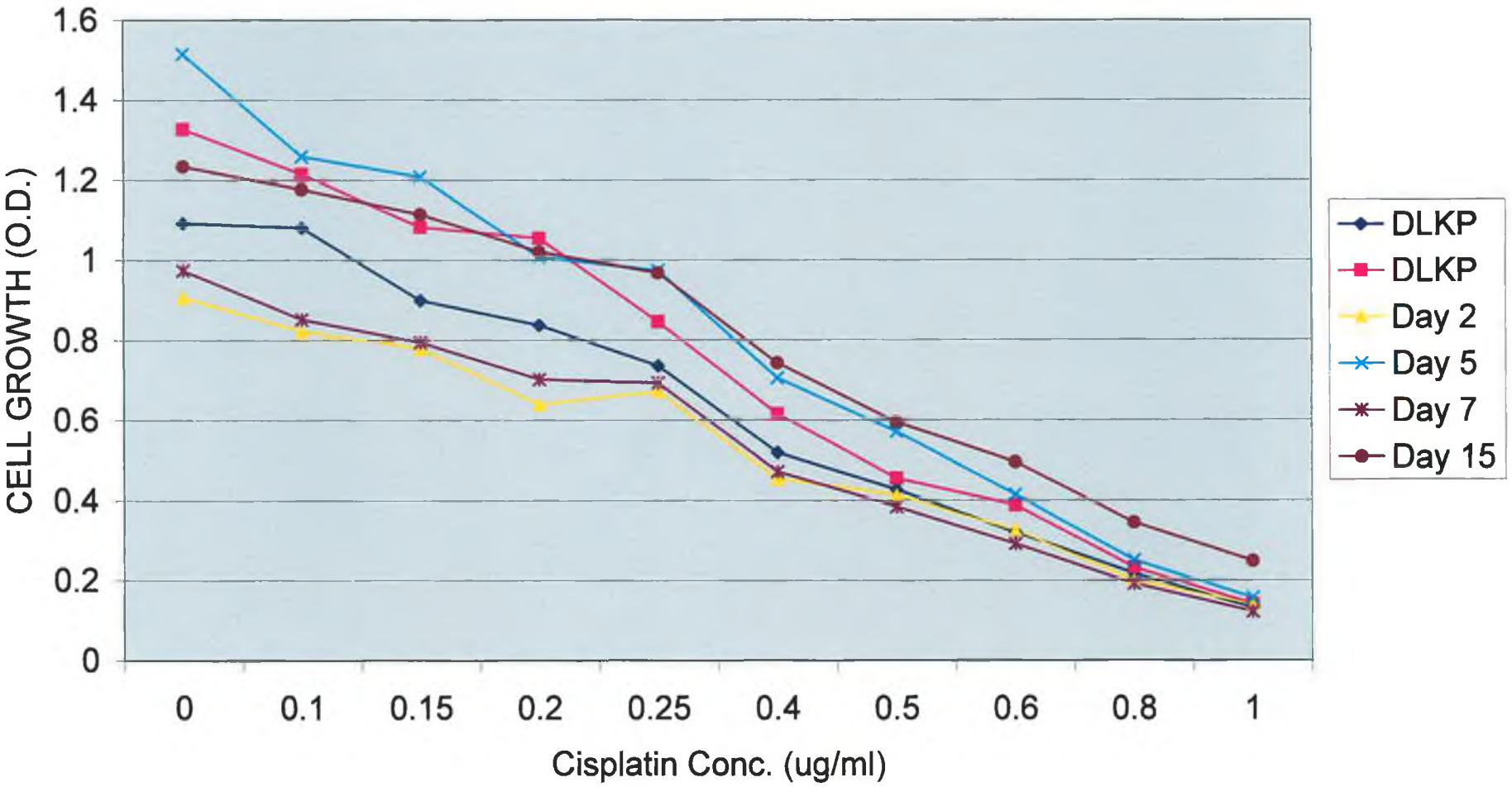

Fig. 3.2.16: Effect of Taxol exposure on Taxol resistance in DLKP cells

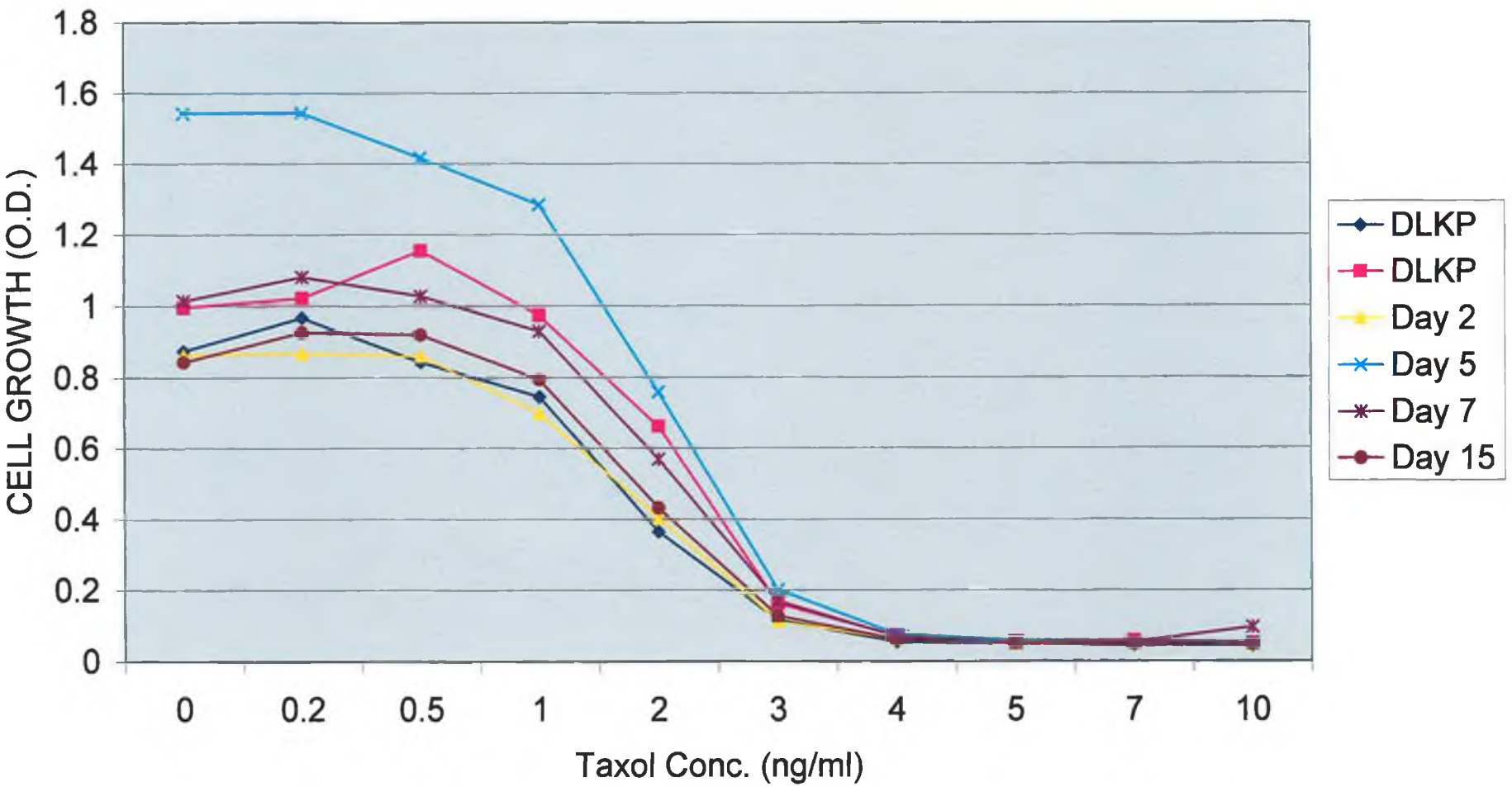

Fig. 3.2.17: Effect of Taxol exposure on VP16 resistance in DLKP cells

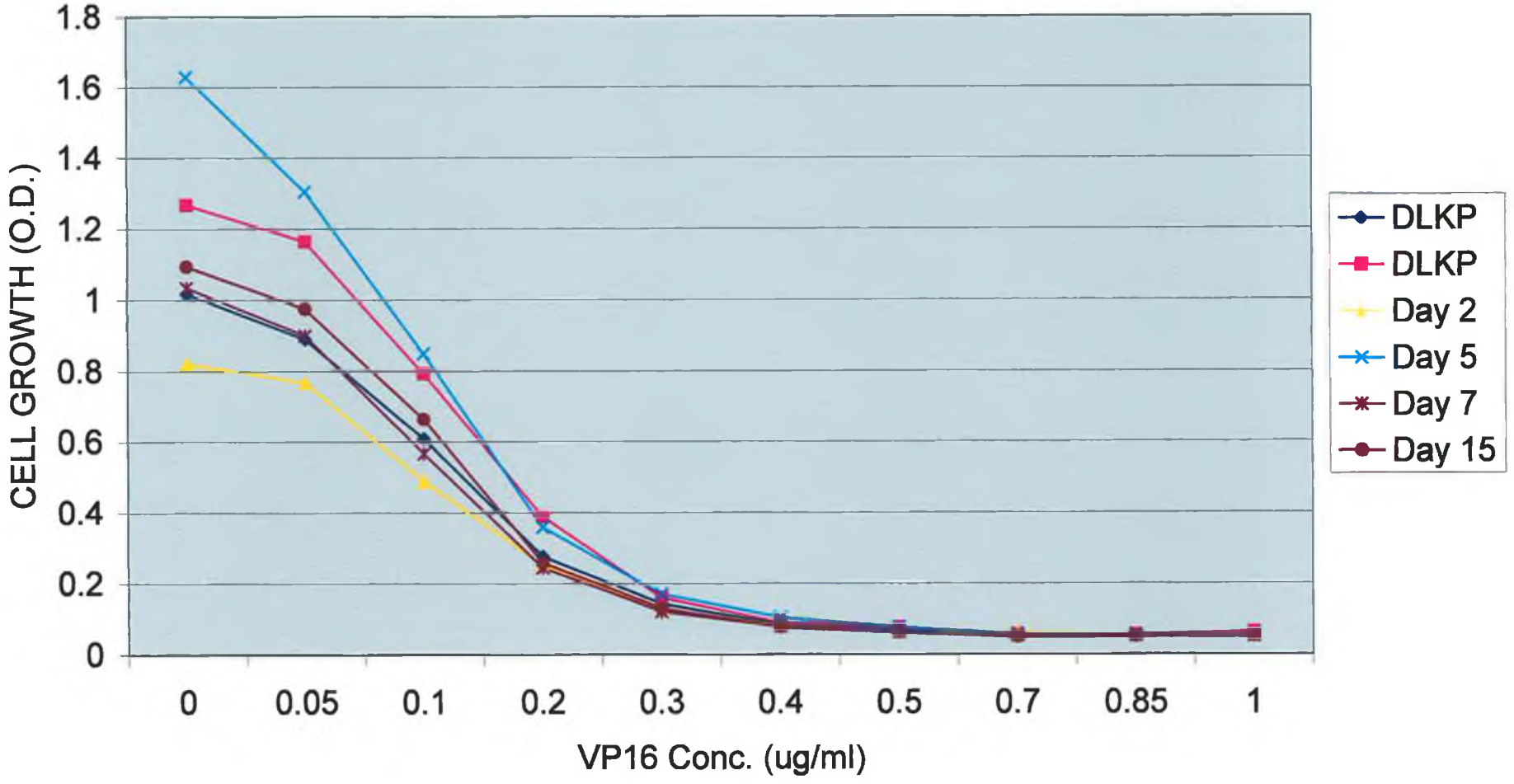

as observed for the cisplatin-exposed cells, the dose-response curve for the day five sample was consistently higher than for the other samples, varying between 20 and 60% more than that of the nearest untreated control growth sample. A comparison of the relevant IC_{50} values, however, reveals no significant change in the drug-resistance profiles of the cells. The profiles also did not match those obtained for the BrdU-treated samples, as the day seven-treated sample did not exhibit a lowered dose-response curve than those obtained for the other treatments.

3.2.2.3 Effect of VP16 exposure on DLKP drug-resistance profiles

The drug-resistance profiles of the VP16-exposed DLKP cells differed significantly from their control samples (Figs. 3.2.18 – 3.2.21), and also from the samples observed already. In each of the four toxicity assays, the dose-response curves of the VP16-treated cells were significantly lower than those obtained for the untreated control cells. It would appear from the plots that exposure to the drug caused a general disruptive effect on the growth of the cell which hinders the cell's ability to respond to a toxicity assay with other, structurally unrelated, drugs. Furthermore, the debilitating effect on the growth of the cell appears to worsen with increasing length of exposure to VP16, and as such the dose-response pattern differs very significantly both from the patterns observed for the other treatments, as well as for the BrdU-exposed cells. While the general debilitative effect of VP16 on the growth of DLKP resembled slightly that obtained for the day seven BrdU-treated sample, none of the other BrdU treatments resulted in this effect. An examination of the relative IC50s also reveals no significant change for the VP16-exposed samples relative to the control cells for each of the different drugs.

Fig. 3.2.18: Effect of VP16 exposure on Adriamycin resistance in DLKP cells

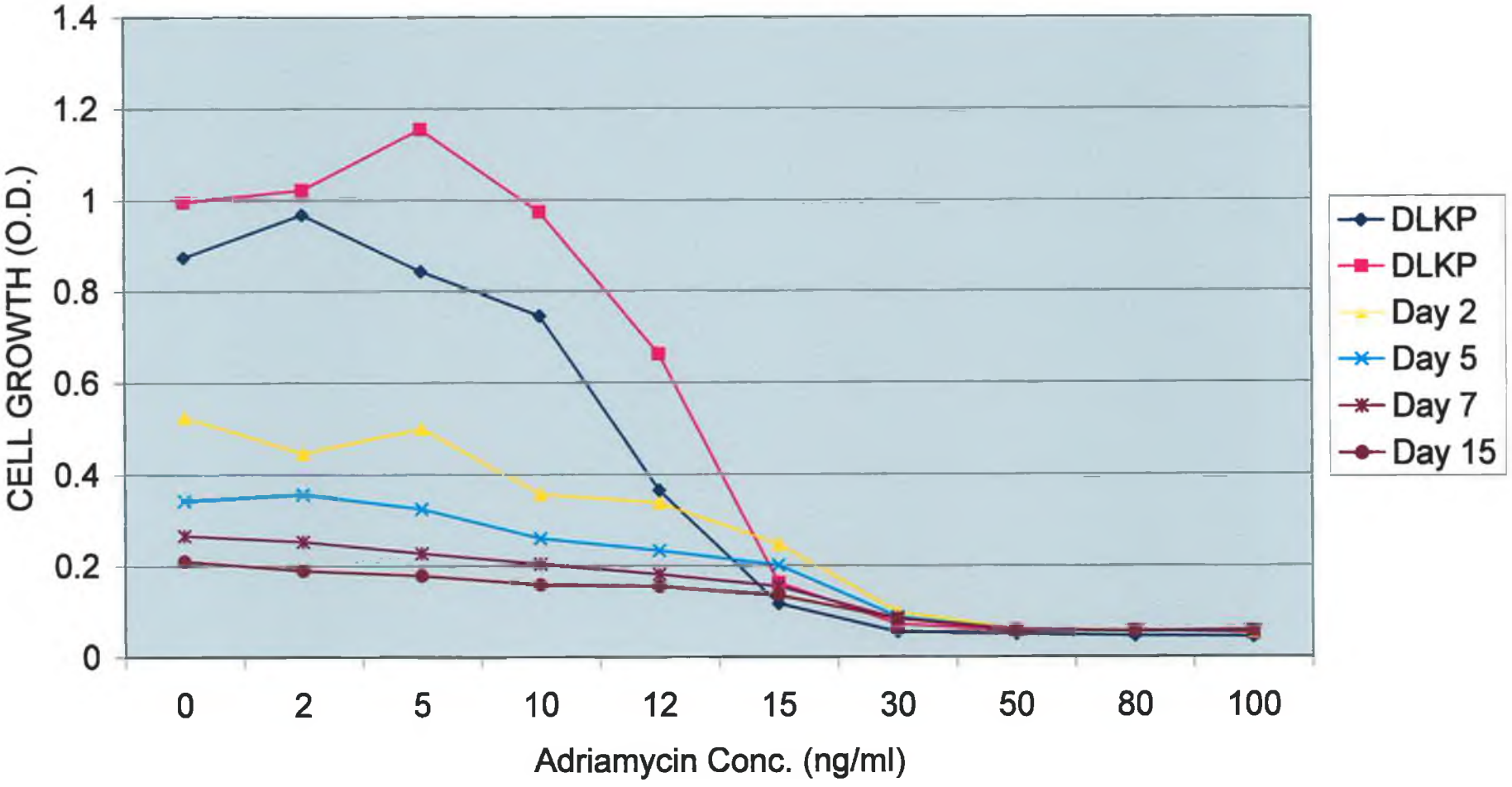

Fig. 3.2.19: Effect of VP16 exposure on Cisplatin resistance in DLKP cells

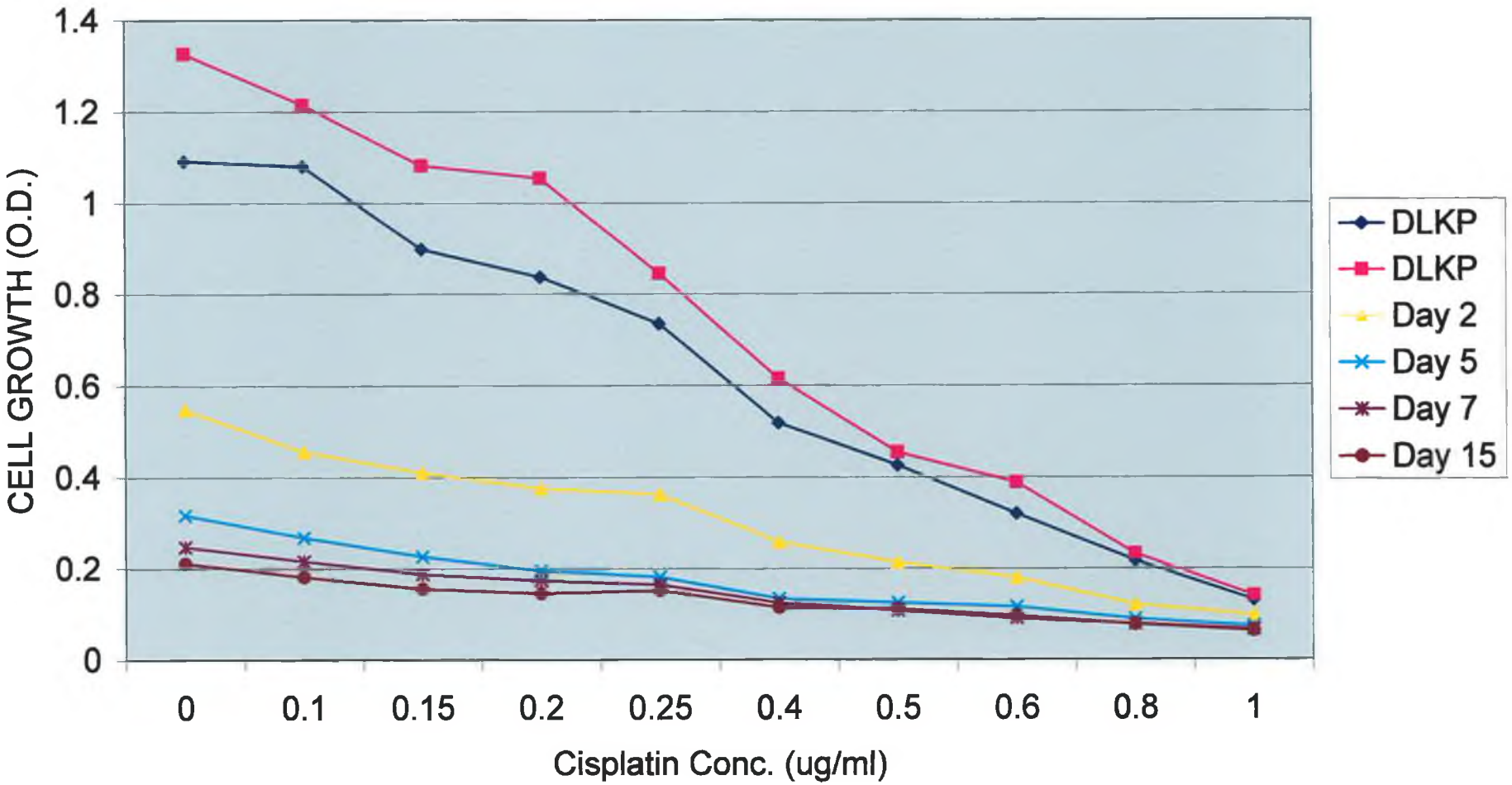

Fig. 3.2.20: Effect of VP16 exposure on Taxol resistance in DLKP cells

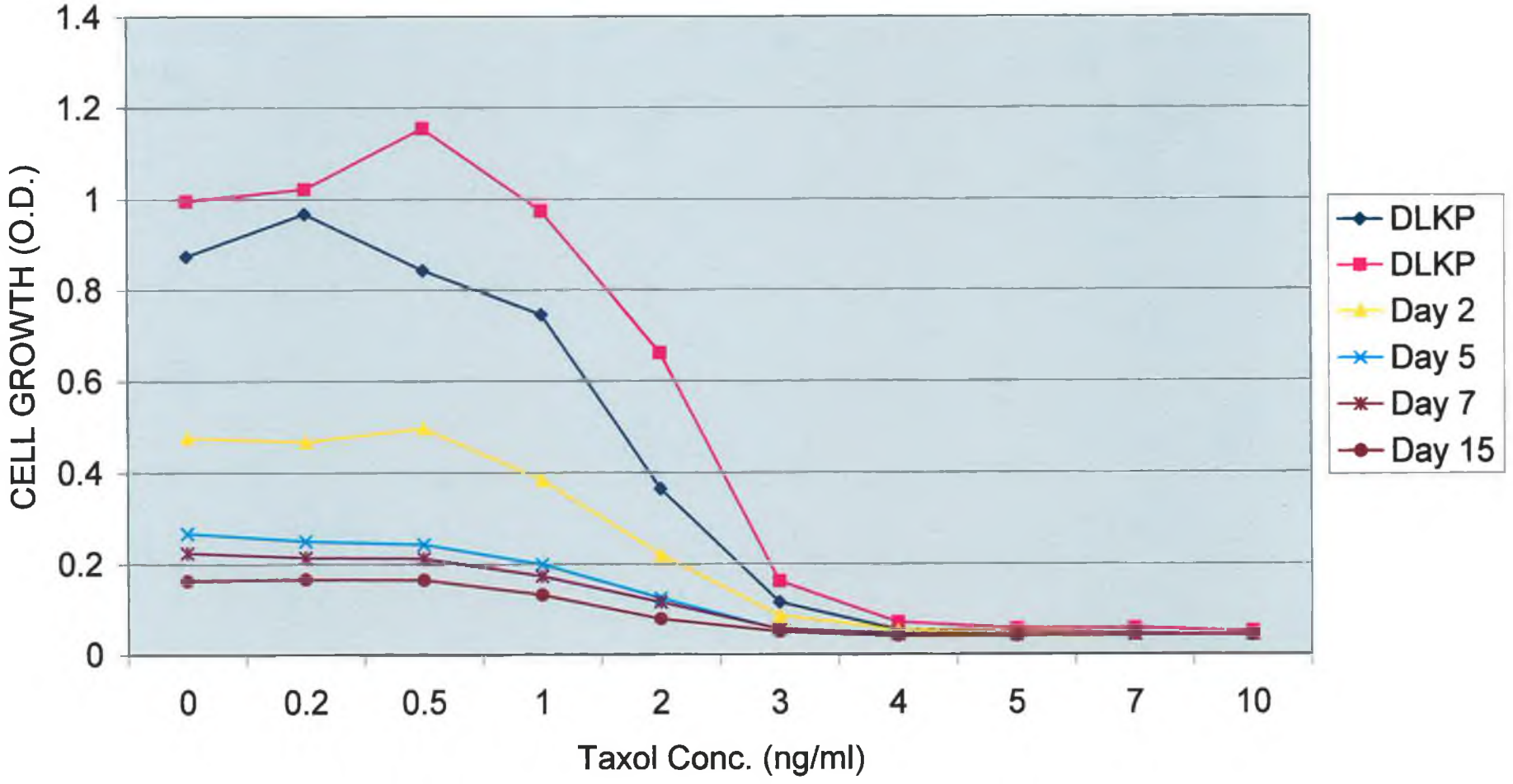

Fig. 3.2.21: Effect of VP16 exposure on VP16 resistance in DLKP cells

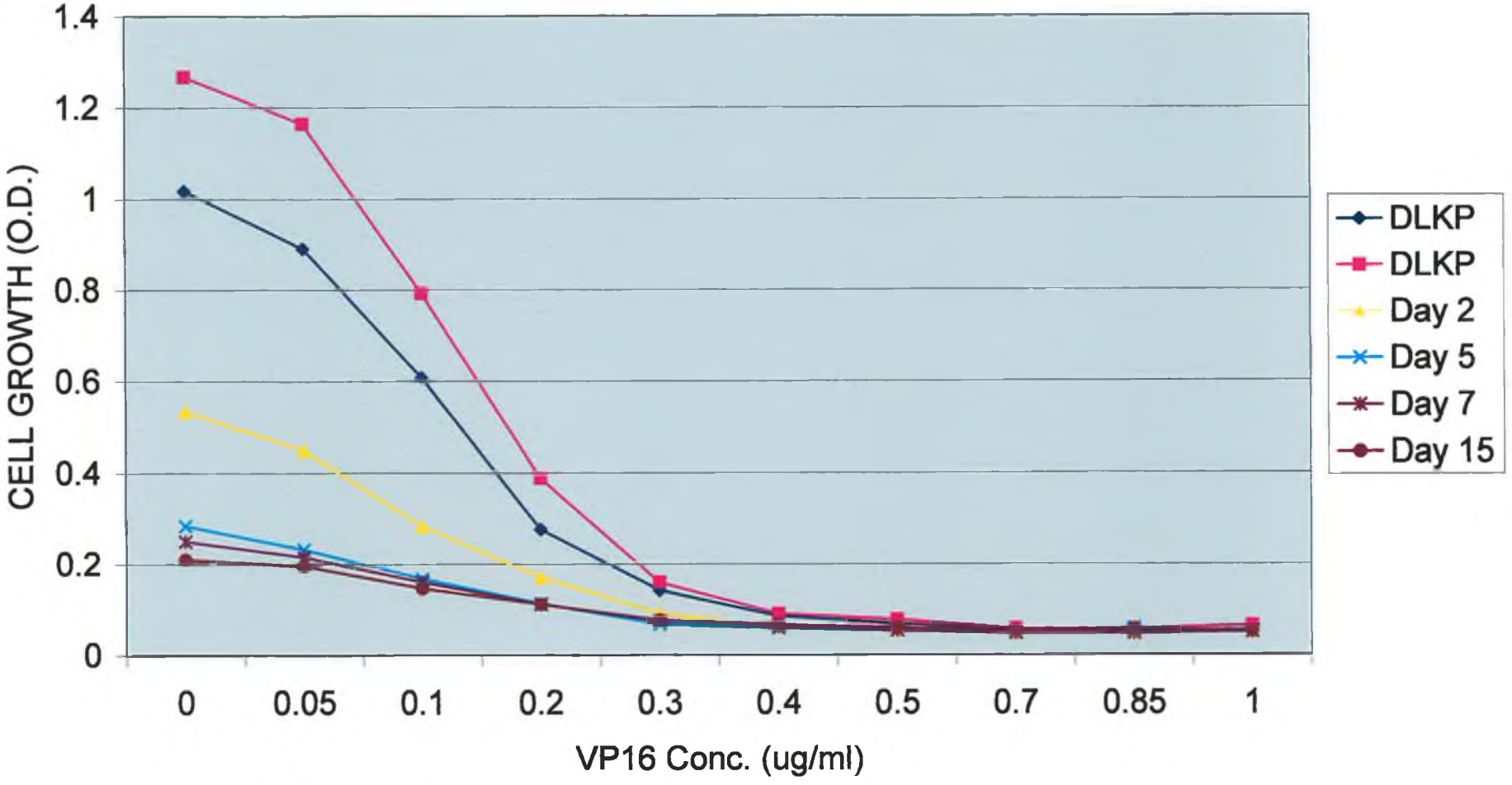

3.3 Analysis of drug-selected DLKP cell lines using RT-PCR

The DLKP cell line was continuously pulse-selected (four to ten times) in a number of sub-lethal drug concentrations over a number of weeks by Dr.Yizheng Liang. This procedure resulted in the selection out of a number of cell lines which displayed an increased resistance profile to the drug of selection relative to the parent DLKP.

It was thought that an analysis of the gene expression profiles of these drug-selected cell lines would be useful in that it may provide certain correlations between the expression of certain genes relevant to continuous long- and short-term exposures to chemotherapeutic drugs. The effect of short-term exposure of DLKP cells to a smaller number of drugs has already been examined (Section 3.2.1); this Section will deal with the effect of long-term selection of the DLKP cell line in the presence of a larger number of chemotherapeutic agents.

The cells were set up and harvested as for a standard drug-exposure assay (Section 2.3.3) by Dr. Liang and RNA was harvested and quantified in the usual manner (Section 2.4.2). This RNA was then used in RT-PCR reactions using all the available primers for multidrug resistance-related genes, as well as the α- and β-catenins as well as E-cadherin. Expression levels of the apoptotic genes were not examined for the drug-selected DLKP. The PCR products were run out on 2% agarose gels and photographed using film negatives for densitometric analysis. A total of ten chemotherapeutic drugs were used in the selection process; these are listed, along with their abbreviations and method of action in Table 3.3.1.

Table 3.3.1 List of all drugs used in long-term selection from DLKP

Name of Drug	Abbreviation	Method of action
Vincristine	*VCR*	Inhibitor of chromatin function
VP16	*VP16*	Inhibitor of chromatin function
Taxotere	*Taxot*	Inhibitor of chromatin function
Mitoxantrone	*Mitox*	Inhibitor of chromatin function
Lomustine	*CCNU*	Covalent DNA binding drug
Carmustine	*BCNU*	Covalent DNA binding drug
Chlorambucil	*Chlor*	Covalent DNA binding drug
Cisplatin	*Cispl*	Non-covalent DNA binding drug
5-fluorouracil	*5-FU*	Anti-metabolic drug
Methotrexate	*MTX*	Anti-metabolic drug

3.3.1 MRP 1

MRP1 expression was increased in most of the drug-selected cell lines (Fig. 3.3.1). No change in expression was observed after selection in 5-fluorouracil and expression was slightly lowered in the Mitoxantrone-selected cell line. All other selections showed a slight increase in MRP1 gene expression following selection, most significant of which was observed in the Vincristine- and VP16-selected cell lines (roughly two-fold). Short-term exposures to cisplatin and VP16 (Section 3.2.1) also revealed increased MRP1 expression following exposure to VP16.

Fig. 3.3.1: MRP1 RT-PCR results on drug-selected cell lines

Fig. 3.3.1a:

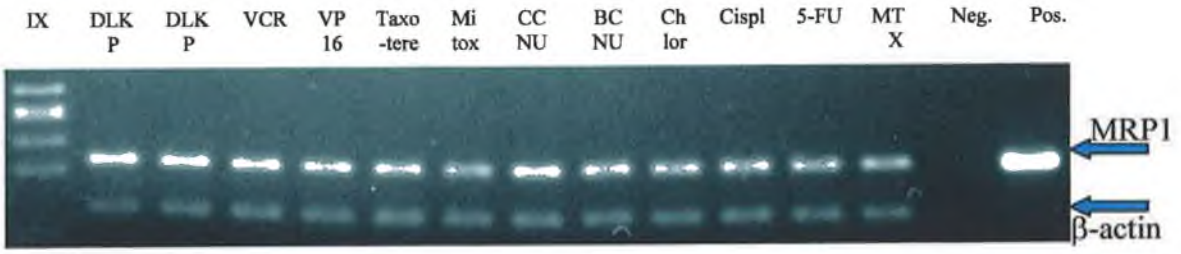

Fig. 3.3.1b:

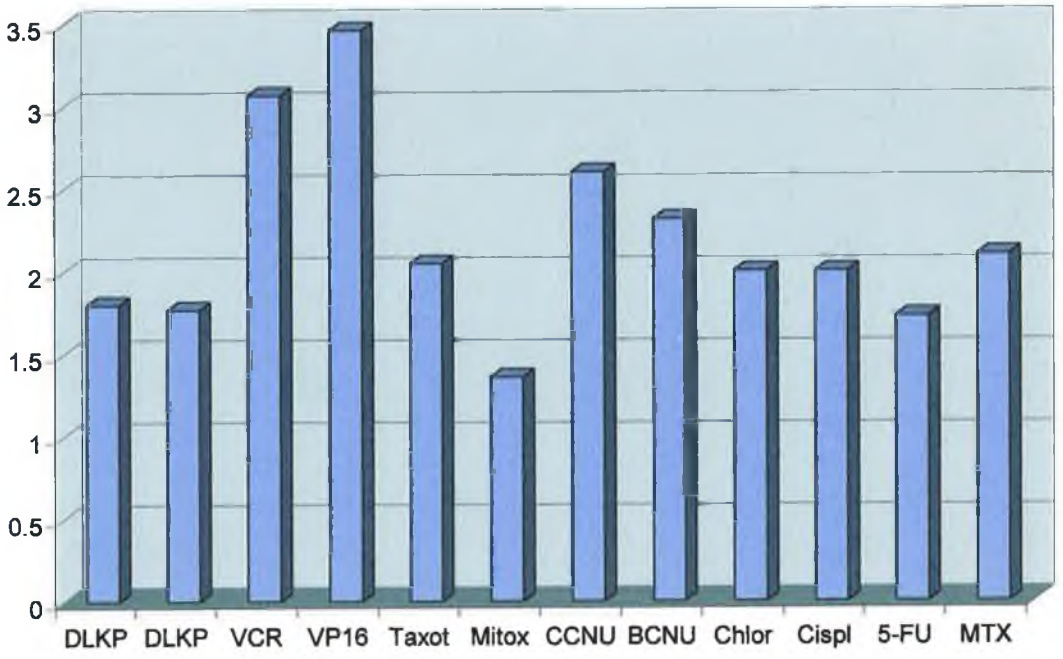

Fig. 3.3.1a: Gel electrophoresis photograph of MRP1 RT-PCR results on drug-selected DLKP cells; Fig 3.3.1b: Densitometric analysis of RT-PCR results.

3.3.2 MRP 2 (cMOAT)

Only continuous selection in Vincristine resulted in an increased level of expression of the MRP2 gene in these cell lines (>two-fold) (Fig. 3.3.2). All other selections resulted in slight decreases in the level of cMOAT gene expression. This is in marked contrast to the short-term exposure results, where exposure to all three drugs resulted in significant upregulation of cMOAT gene expression (Section 3.2.1).

3.3.3 MRP3

MRP3 expression was decreased in most of the drug-selected DLKP cell lines studied (Fig. 3.3.3). Expression of the gene was observed increased in only two of the drug-selected cell lines; those selected in Taxotere and Methotrexate. Short-term exposure of DLKP to cisplatin, taxol and VP16 also revealed no change in MRP3 expression (Section 3.2.1).

3.3.4 MRP4

MRP4 expression either decreased or remained unaffected in most of the drug-selected cell lines studied (Fig. 3.3.4). MRP4 expression increased 2-fold in response to selection to the drugs CCNU, Cisplatin and Methotrexate. Expression of the gene was increased in excess of three-fold in response to selection in BCNU. Gene expression had decreased following selection in Chlorambucil, Vincristine and VP16. All other results were deemed insignificant. Short-term exposure of DLKP to cisplatin, taxol and VP16 also revealed no change in MRP4 expression (Section 3.2.1).

3.3.5 MRP5

MRP 5 expression was increased in the majority of the drug-selected cell lines (Fig. 3.3.5). Only selection in Vincristine and CCNU appeared to result in decreased or

Fig. 3.3.2: MRP2 RT-PCR results from drug-selected cell lines

Fig. 3.3.2a:

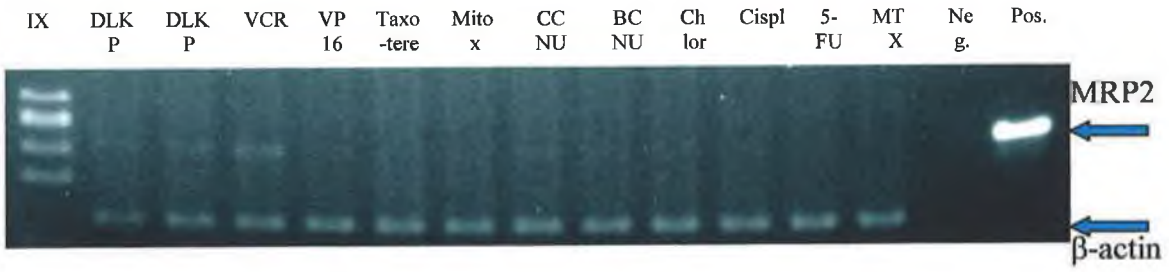

Fig. 3.3.2b:

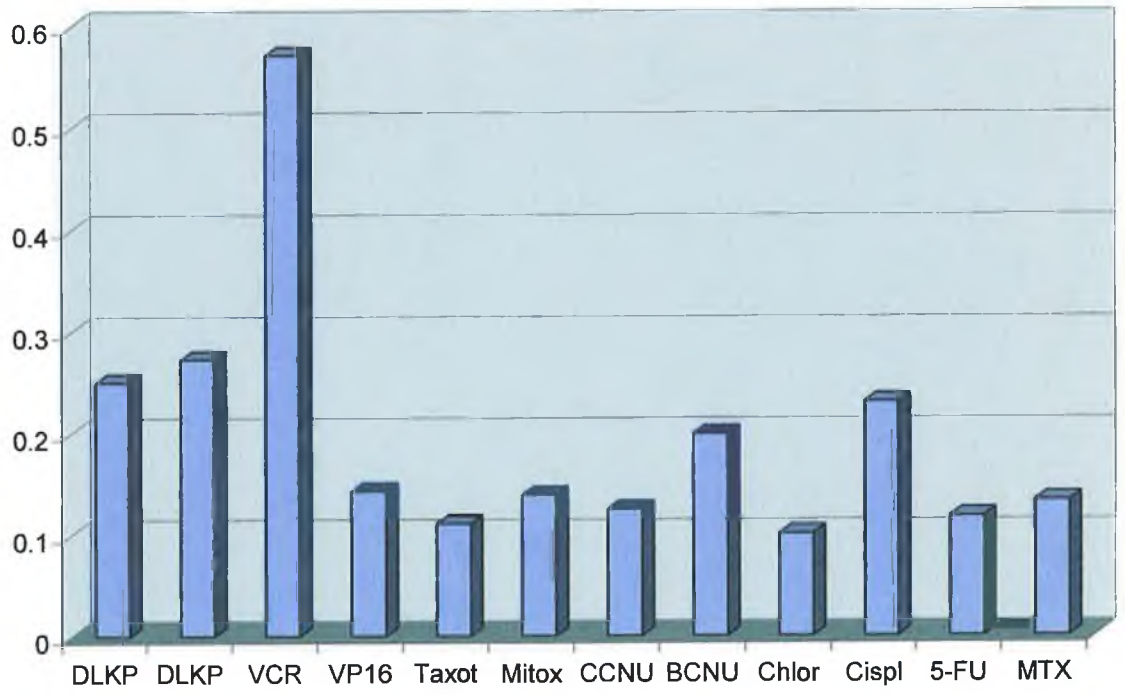

Fig. 3.3.2a: Gel electrophoresis photograph of MRP2 RT-PCR results on drug-selected DLKP cells; Fig 3.3.2b: Densitometric analysis of RT-PCR results.

Fig. 3.3.3: MRP3 RT-PCR results from drug-selected cell lines

Fig. 3.3.3a:

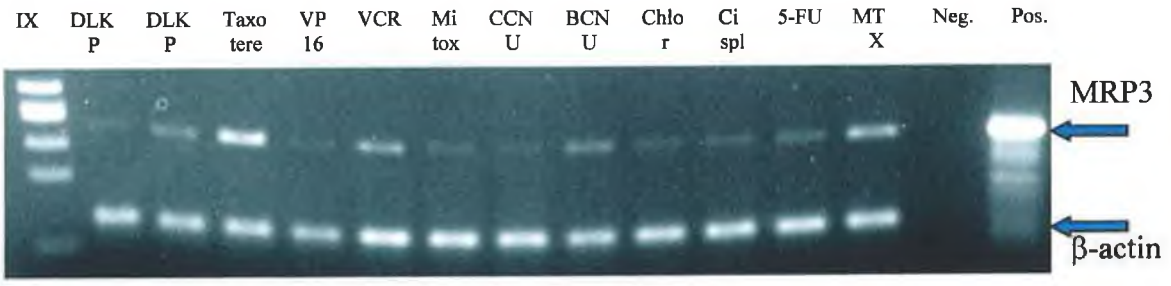

Fig. 3.3.3b:

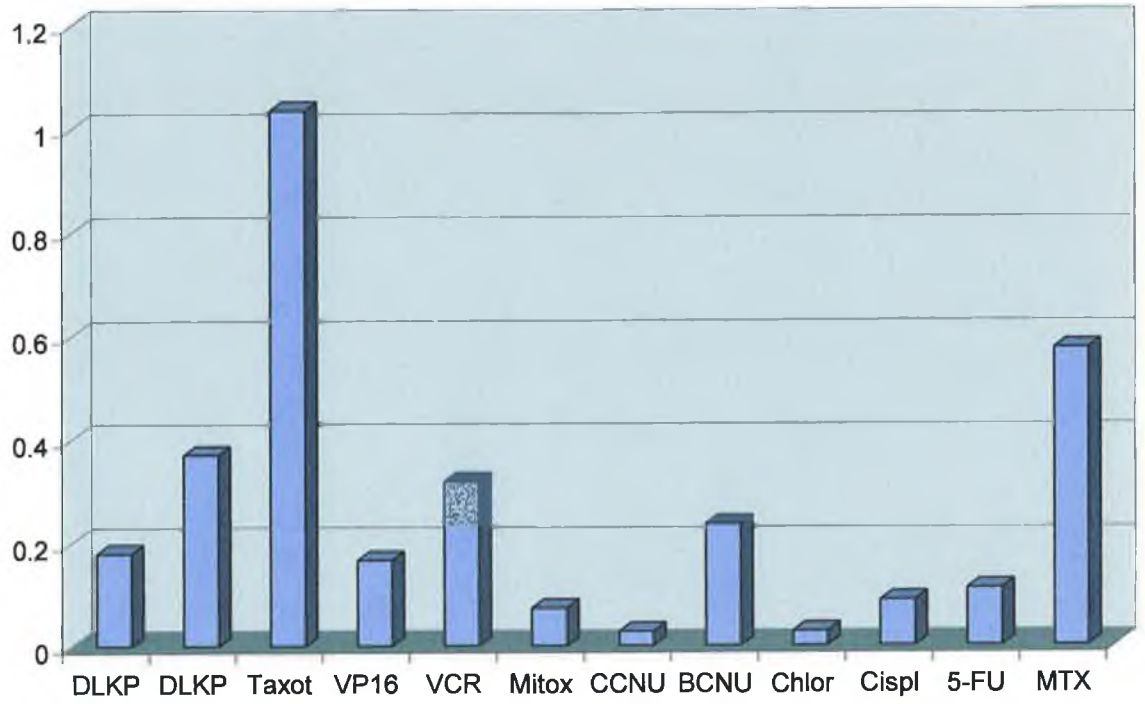

Fig. 3.3.3a: Gel electrophoresis photograph of MRP3 RT-PCR results on drug-selected DLKP cells; Fig 3.3.3b: Densitometric analysis of RT-PCR results.

Fig. 3.3.4: MRP4 RT-PCR results from drug-selected cell lines

Fig. 3.3.4a:

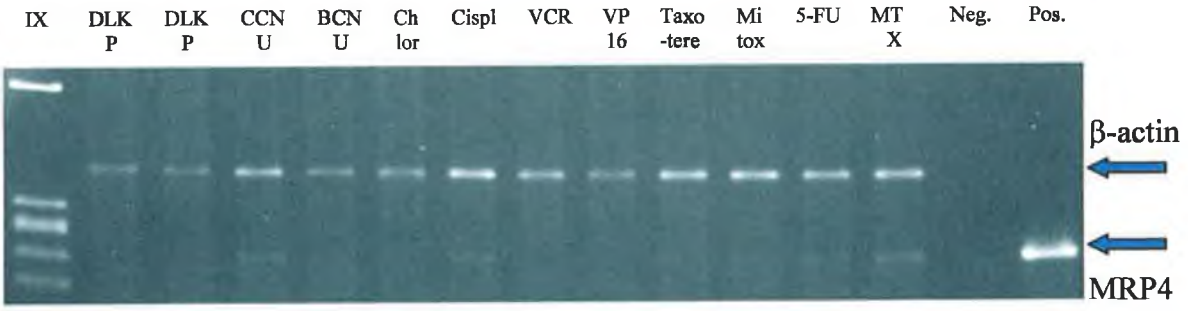

Fig. 3.3.4b:

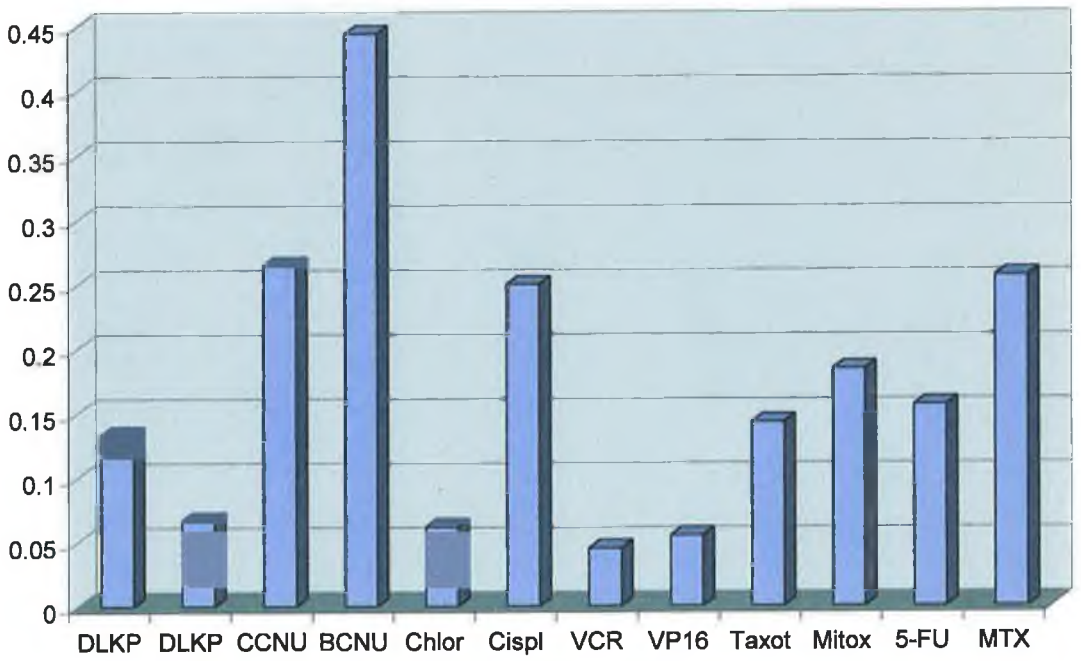

Fig. 3.3.4a: Gel electrophoresis photograph of MRP4 RT-PCR repeat results on drug-selected DLKP cells; Fig 3.3.4b: Densitometric analysis of RT-PCR results.

Fig. 3.3.5: MRP5 RT-PCR results from drug-selected cell lines

Fig. 3.3.5a:

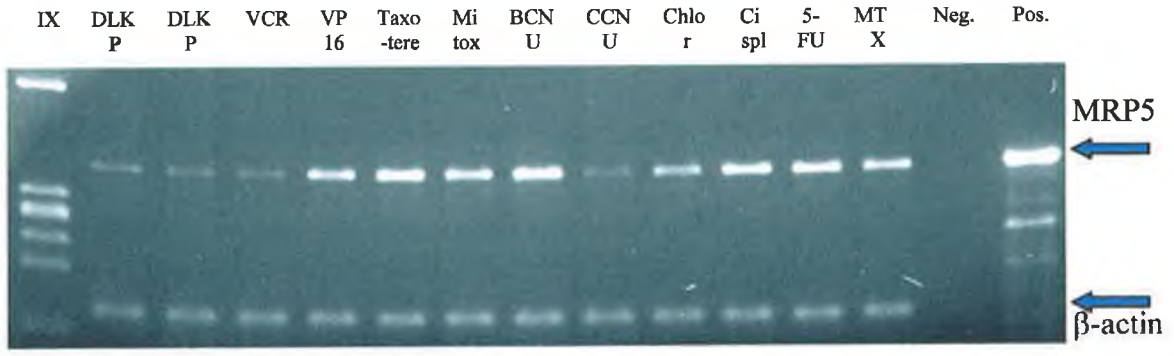

Fig. 3.3.5b:

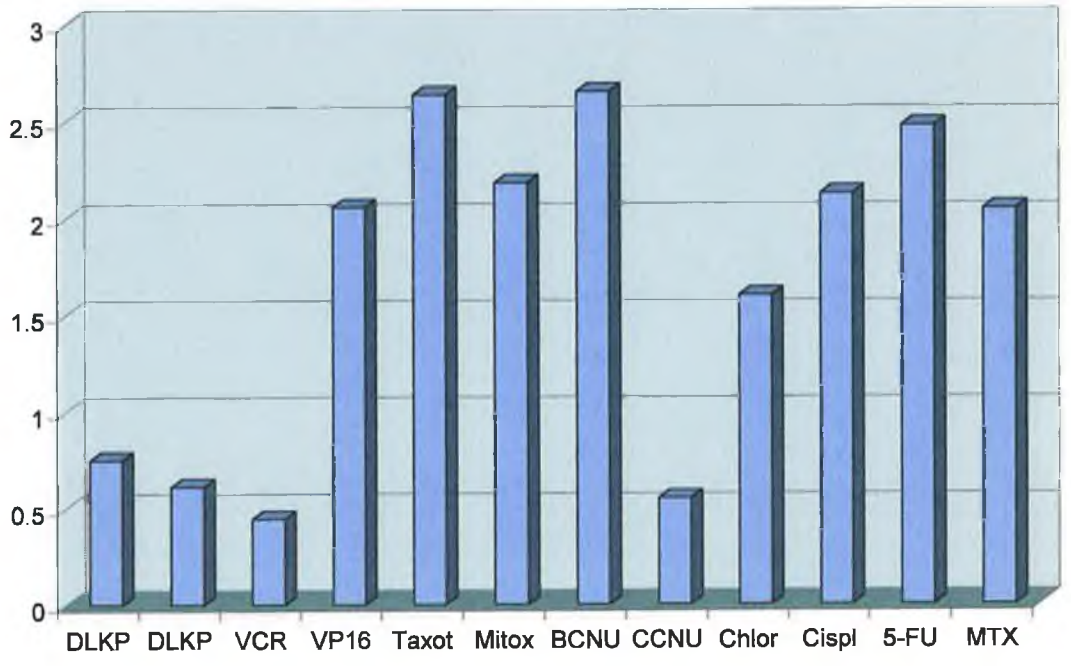

Fig. 3.3.5a: Gel electrophoresis photograph of MRP5 RT-PCR results on drug-selected DLKP cells; Fig 3.3.5b: Densitometric analysis of RT-PCR results.

unaffected expression. Short-term exposure to cisplatin, taxol and VP16 did not result in increased MRP5 expression (Section 3.2.1).

3.3.6 mdr-1

DLKP expresses very low levels of mdr-1 basally, and this is borne out by the control samples. Overall, mdr-1 expression was not altered significantly in most of the drug-selected cell lines (Fig. 3.3.6). Only selection in Vincristine and Taxotere resulted in an increased expression level of the gene. Vincristine increased expression levels roughly four-fold, whereas selection in Taxotere increased levels almost 35-fold. No change in mdr-1 expression in DLKP was observed using short-term exposure to cisplatin, taxol, or VP16.

3.3.7 BCRP

BCRP expression was observed to be decreased in most of the drug-selected cell lines (Fig. 3.3.7). The only significant increase was observed in the Mitoxantrone-selected cell line, which yielded a BCRP expression increase over eight-fold that of normal DLKP cells. In contrast to the short-term exposure result (Section 3.2.1), in which BCRP expression was observed increased following exposure to cisplatin, selection in the drug resulted in decreased expression of the gene.

3.3.8 Summary of genes showing increased expression following selection in drug

As already outlined, this study had a dual purpose; to reveal if selection of DLKP in different drugs revealed similar gene expression results to short-term exposure of the cell line to those drugs and also to indicate potential drug substrates for the multidrug resistance-associated genes currently under examination. The results for this second purpose are listed in Table 3.3.2.

Fig. 3.3.6: mdr-1 RT-PCR results from drug-selected cell lines

Fig. 3.3.6a:

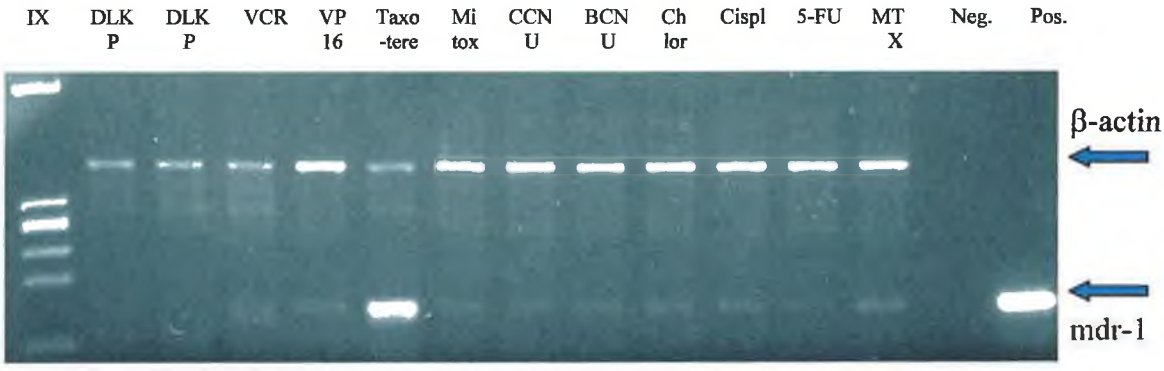

Fig. 3.3.6b:

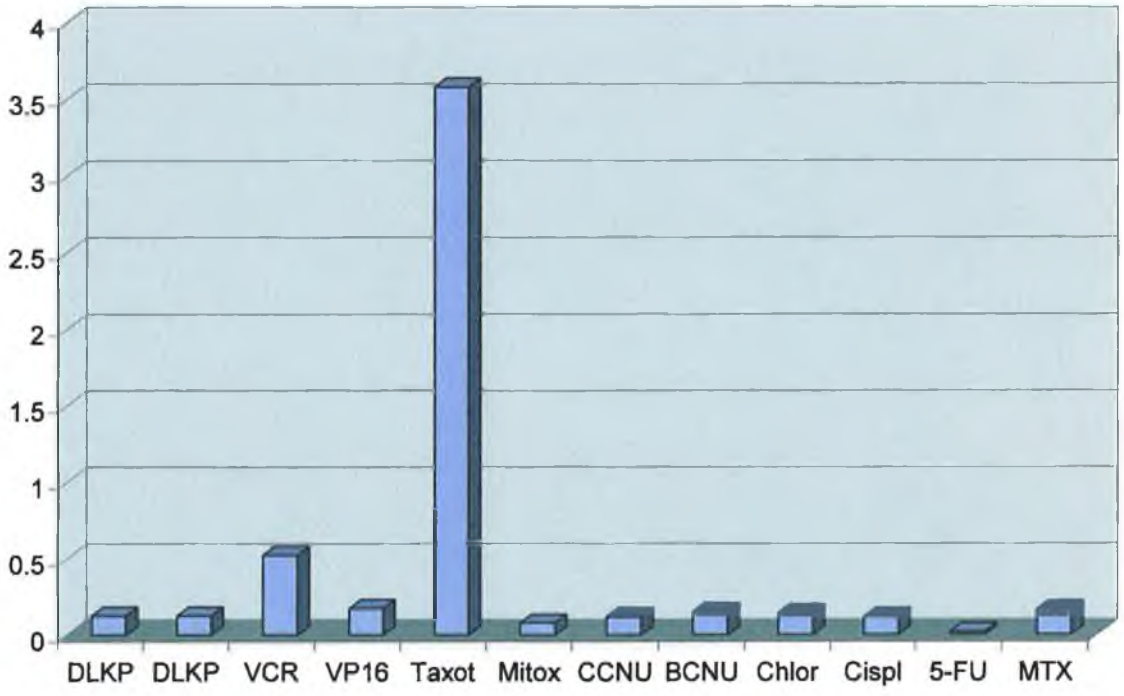

Fig. 3.3.6a: Gel electrophoresis photograph of mdr-1 RT-PCR results on drug-selected DLKP cells; Fig 3.3.6b: Densitometric analysis of RT-PCR results.

Fig. 3.3.7: BCRP RT-PCR results from drug-selected cell lines

Fig. 3.3.7a:

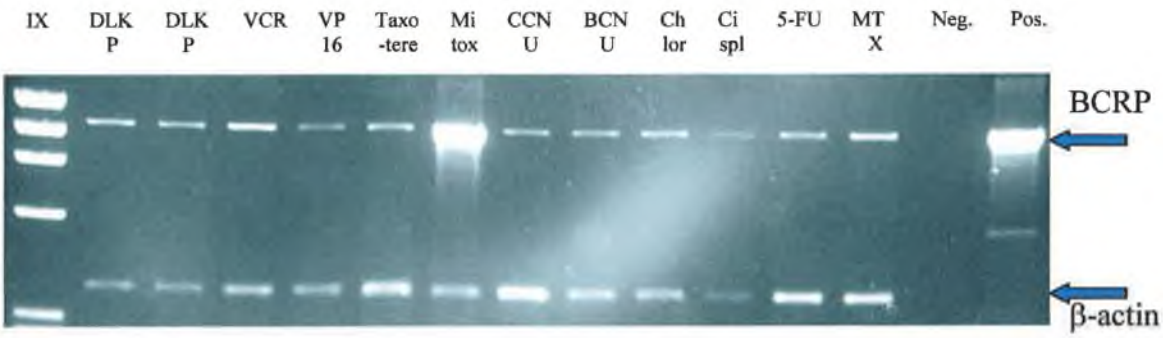

Fig. 3.3.7b:

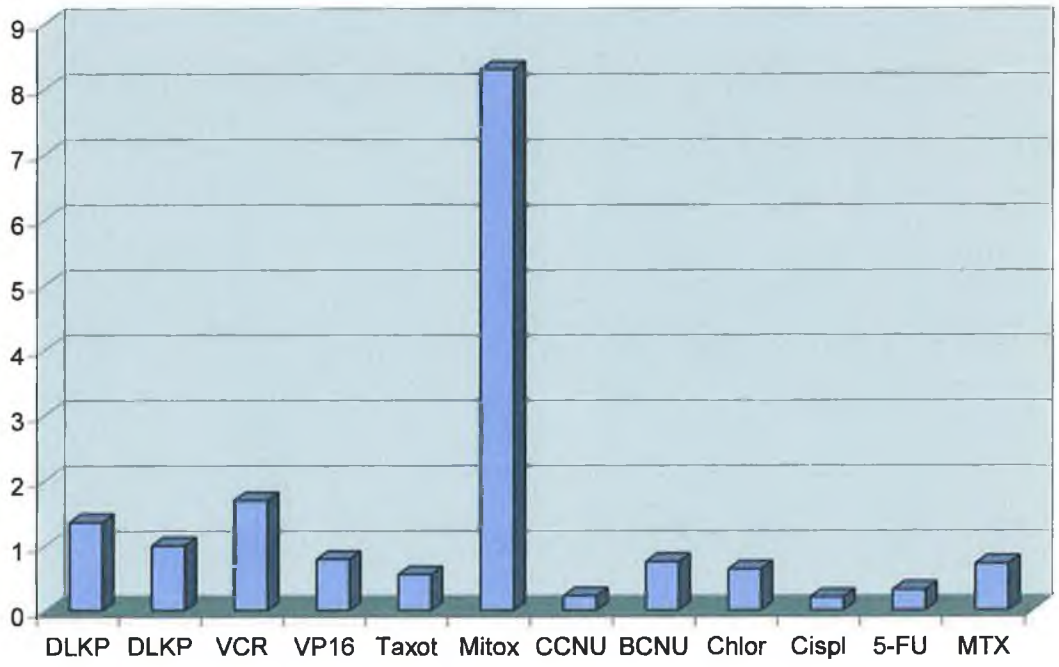

Fig. 3.3.7a: Gel electrophoresis photograph of BCRP RT-PCR results on drug-selected DLKP cells; Fig 3.3.7b: Densitometric analysis of RT-PCR results.

Table 3.3.2 List of genes with increased expression following selection in drug

Drug Name	Genes Upregulated	Amount of increase
Vincristine	MRP1	2-fold
	MRP2	>2-fold
	Mdr-1	4-fold
VP16 (VP16)	MRP1	2-fold
	MRP5	4-fold
Taxotere	MRP3	4-fold
	MRP5	5-fold
	mdr-1	35-fold
Mitoxantrone	MRP5	4-fold
	BCRP	>8-fold
CCNU	MRP1	1.5-fold
	MRP4	2-fold
BCNU	MRP1	1.5-fold
	MRP4	>3-fold
	MRP5	5-fold
Chlorambucil	MRP5	3-fold
Cisplatin	MRP4	2-fold
	MRP5	4-fold
5-fluorouracil	MRP 5	5-fold
Methotrexate	MRP3	>2-fold
	MRP4	2-fold
	MRP5	4-fold

3.4 Analysis of promoter regions of genes affected by BrdU exposure

3.4.1 Transcription factor analysis of promoter regions

From the results presented in Section 3.1.1, it was seen that exposing actively growing cells to the differentiating agent BrdU alters the mRNA expression levels of a number of specific genes. It was hypothesised from this observation that BrdU may affect expression of these genes at the transcriptional level, although the possibility that alterations in mRNA stability may be responsible could not be disregarded. It was also hypothesised that if BrdU were affecting expression of these genes transcriptionally, it may mediate this effect through a common transcription factor.

In order to test the BrdU-regulated common-transcription factor hypothesis, a sequence analysis of the 5' promoter regions of genes whose expression increased in BrdU-treated DLKP cells was carried out using a specific computer package which searches these sequences for known transcription factor binding sites. Once found and collated, the obtained transcription factors for each gene could be compared to each other in order to identify common transcription factors.

As the bulk of the upregulated gene results were observed in DLKP, it was felt that analysis of results in this cell line would be the most productive, although, as shall be demonstrated, the analysis was also extended to the A549 cell line as well. From the results presented in Section 3.1.1, a total of twelve genes were observed to display increased expression in the DLKP cell line following exposure to BrdU. Nine of these genes, MRPs 1-3, BCRP, COX-2, eIF-2α, MRIT, α-catenin and E-cadherin were chosen as the genes which would be subjected to the transcription factor analysis which will be outlined here.

Up to 3kb of sequence data from the promoter regions of these six genes was obtained from GENBANK (http://www.ncbi.nlm.nih.gov/80/) using BLAST searches and entered into the *Transfac*™ (http://www.transfac.gbf.de) database. The choice of 3kb of promoter sequence was an arbitrary one; previous characterisations of the promoter

regions of the MRP genes 1, 2 and 3 (Zhu and Center, 1994; Stockel *et al.*, 2000, Fromm *et al.*, 1999) used between 1kb and 2kb of promoter sequence for analysis. (This 3kb of promoter sequence denotes 3kb of data in reverse from the translational start site of the gene). The database is web-based and analyses sequence for known transcription factor recognition sequences (motifs). The recognition sequences for these factors often vary by a few bases even within the same gene sequence. For this reason, a sample sequence motif only is shown in Table 3.4.1 for each transcription recognition site, as to include all possible sequences would be impractical.

Once the promoter regions of the six genes had been analysed, a total of one hundred and forty-seven different potential transcription factor recognition sequences were identified on a combination of all six promoter regions. These recognition sequences, as well as their attendant classification numbers and an example of each of their recognition sequences are shown in Table. 3.4.1. Obviously, these sites are merely putative, the database has identified recognition sequences which could possibly be utilised; most of these potential sites will not be utilised by any transcription factor. Also, the level of suitability of factors to their relevant recognition sequences had to be arbitrarily chosen. For this experiment, a suitability percentage of 85% was considered to allow for a level of variation in the recognition motifs while also providing a large enough margin of error to encapsulate all possible putative transcription factors.

Table 3.4.1 List of *Transfac*™ transcription factor recognition motifs

Classification No.	Name	Sample Sequence
M00001	MyoD	GGTCAGGTGGGG
M00002	E47	GCGGCCACCCGCCGG
M00003	v-Myb	TTCAGTTATA
M00005	AP-4	CTGCCCGCCGCTGGGTCC
M00008	Sp1	ACCACGGCCG
M00009	Ttk 69K	GTTCCTGC
M00011	Evi-1	ATTCTCTTGT
M00019	Dfd	AATTCAATTACAGTTC
M00020	Ftz	CTTACTTGCTTT
M00021	Kr	ATAATCCGGT
M00022	Hb	TTTTTTTTTG
M00025	Elk-1	GCGCTTCCGGAAGG
M00027	AbaA	CCTTCCTCCTTCCCTCGCT
M00028	HSF	TTTCT
M00029	HSF	GGAAT
M00030	MATa1	TGATGAACAT
M00031	MATalpha2	GATTACATGC
M00032	c-Ets-1(p54)	GGCCTCCGGC
M00033	p300	CCCAGGAGTTGGAG
M00037	NF-E2	GGCTGAGTCAC
M00039	CREB	TGAGGTCA
M00040	CRE-BP1	CGGGCTTACGC
M00041	CRE-BP1/c-Jun	TGAGGTCA
M00042	Sox-5	TTATTGTTAG
M00046	GCR1	GACTTCCTG
M00048	ADR1	TGGAGA
M00050	E2F	GGGCCAAA
M00051	NF-kappaB (p50)	GGGTCTCCCC
M00052	NF-kappaB (p65)	GGGGATTCCC
M00053	c-Rel	GGGGATTCCC
M00054	NF-kappaB	GGGACTACCC
M00055	N-Myc	GGACACGTGTGC
M00059	YY1	ATTAAAAAATGGAATCA
M00060	Sn	AAGTTCCTTTGA
M00063	IRF-2	GGGTTCCCTTTTC
M00066	Tal-1alpha/E47	GTCAACAGCT
M00071	E47	GTCAACAGCT
M00072	CP2	TTGGCATGTGC
M00073	DeltaEF1	ATTAGGTGTTA
M00074	c-Ets-1(p54)	AAGTTCCTTTGA
M00075	GATA-1	CGTGATACGC
M00076	GATA-2	ACGGATACTG
M00077	GATA-3	CCTGATAGC
M00079	Evi-1	TTATCTTGTTC
M00080	Evi-1	AATTTTCTTA
M00081	Evi-1	TTATCTACTGA
M00082	Evi-1	TTATCATGTCT
M00083	MZF1	TCCCCTCC

Table 3.4.1 Cont'd

Classification No.	Name	Sample Sequence
M00084	MZF1	TGGGGAGGGGCCA
M00087	Ik-2	AGCTGGGACTAC
M00091	BR-C Z1	TAATTTTTTTATTATTA
M00092	BR-C Z2	TTATTATTATTTTTT
M00093	BR-C Z3	TCTTTTAATTTATTT
M00094	BR-C Z4	TTTTCTTTTTTT
M00096	Pbx-1	TTGATTTTT
M00098	Pax-2	CGTCGTCTTGCATTATTCA
M00099	S8	GCAATTCAATTACAGT
M00100	CdxA	TTTATTGCAC
M00101	CdxA	TTTATTGCAC
M00104	CDP CR1	AATGGATCGC
M00105	CDP CR3	CAATAAATATTTGTT
M00106	CDP CR3+HD	AATGGATCGC
M00108	NRF-2	CTCTTCTGGTG
M00109	C/EBPbeta	TTGTTAGGAAAGA
M00111	CF1 / USP	GGGTTCACG
M00112	CF1 / USP	GGGTTCACG
M00113	CREB	GGGGTGACGCGG
M00116	C/EBPalpha	CTTTAAGCAACTTG
M00117	C/EBPbeta	AAGTTCTGCAACTC
M00120	Dl	AATTTTTCTCT
M00121	USF	AGGACACGTGTGCG
M00122	USF	TAGTCACATGTCCA
M00123	c-Myc/Max	AAGCACCTGTGA
M00126	GATA-1	AACCTCATCTCTCT
M00127	GATA-1	AACCTCATCTCTCT
M00128	GATA-1	AACCTCATCTCTC
M00129	HFH-1	TCTTGTTTATCT
M00130	HFH-2	GTTGTTTTTTT
M00131	HNF-3beta	TTCTATTTGTTC
M00132	HNF-1	GGTTAACGATTAAAT
M00133	Tst-1	ATTCAATTACAGTTC
M00136	Oct-1	TGAATGCATATTAAT
M00137	Oct-1	TTTTGATTACTTA
M00140	Bcd	GGGATTAC
M00141	Lyf-1	TCTCTCAAA
M00142	NIT2	TATCTA
M00145	Brn-2	TCATATTTACAATGCC
M00146	HSF1	GGAAGGTTCT
M00147	HSF2	TTGATTTTTCT
M00148	SRY	AAACTTA
M00154	STRE	GCCCCTGC
M00156	RORalpha1	TTGACCTTATATT
M00157	RORalpha2	AGAAGTATGTCAG
M00158	COUP-TF / HNF-4	TGAACTTTAAAACT
M00159	C/EBP	TCTTTGGAAAAGT
M00160	SRY	TCTCTTGTTTAT

Table 3.4.1 Cont'd

Classification No.	Name	Sample Sequence
M00162	Oct-1	CCAATTTACATTTC
M00163	HSF	TTTCTTTTCTTTTTT
M00164	HSF	CTGAGATTTCTTTTCT
M00167	HSF	TTTCTTTTCTTTTTT
M00172	AP-1	GCTGAGTCACT
M00173	AP-1	TTTTAGTCACA
M00174	AP-1	GCTGAGTCACT
M00175	AP-4	TGCAGCTGTT
M00176	AP-4	TTCCTGCTGA
M00183	c-Myb	AGCAGTTTGG
M00184	MyoD	CACAGCTGAC
M00187	USF	GTCACTTGGC
M00188	AP-1	GCTGAGTCACT
M00190	C/EBP	CTTTAAGCAACTTG
M00192	GR	ACAGAACAGAGCGTTGCCG
M00199	AP-1	CTGAGTCAC
M00203	GATA-X	CAAACTTATCT
M00204	GCN4	TGAGTCACTC
M00209	NF-Y	CGACTAACCGACTC
M00211	PolyA downstream element	CGTGATCTC
M00216	TATA	ATTTTATACT
M00217	USF	GCAGGTGG
M00220	SREBP-1	CTCAAGTGATC
M00221	SREBP-1	GTGGCGTGATC
M00222	Th1/E47	ACAGCCAGACGCCCTC
M00223	STATx	TTCTCAGAA
M00226	P	TCCTACCAC
M00227	v-Myb	TCTAACTGT
M00228	VBP	TTTACATCAT
M00230	Skn-1	ATGATGGAGAAACTGC
M00231	MEF-2	TCTTGTACTAAAAATACAAAAT
M00232	MEF-2	TCTTGTACTAAAAATACAAAAT
M00235	AhR/Arnt	TGAGGGGAGCGTGCCC
M00236	Arnt	CAGGACACGTGTGCGC
M00239	v-ErbA	CCATGAGGTCAAGGCT
M00240	Nkx-2.5	TCAAGTG
M00241	Nkx-2.5	CTTACTTG
M00247	PacC	CAGTGCCAAGAGAAGTA
M00248	Oct-1	ACTATGGTAATA
M00249	CHOP-C/EBPα	GAGGATGCACAA
M00250	Gfi-1	CTGGTTCCTGCTGAGATTTCTT
M00252	TATA	GTTGGCCATTTATAT
M00253	Cap	TCATCCCC
M00254	CCAAT box	CCGGGCCAATAA
M00257	RREB-1	GGGTGTGGTTGGGG
M00258	ISRE	AGCAGAAGCGAAACTG

Table 3.4.1 Cont'd

Classification No.	Name	Sample Sequence
M00263	StuAp	CACCGCGCCC
M00266	Croc	TAATTTATTTATTAAA
M00267	XFD-1	CATCTAAATAATCC
M00268	XFD-2	TTTATGTGTATACT
M00269	XFD-3	TTTTTGATTACTTA
M00271	AML-1a	TGGGGT

3.4.2 Identification of common potential transcription factors

The number of sequences outlined in Table 3.4.1 was obtained from of a total of two hundred and seventy-one known vertebrate transcription recognition factor sequences, a complete list of which may be obtained at the following web address, (http://pdap1.trc.rwcp.or.jp/htbin/show_tfmatrix). The *Transfac*™ sequence analysis for each promoter was then compared by hand to the complete list of known transcription factor motifs in order to identify any common transcription factors that may exist between the six sequences. This was carried out as follows; if the *Transfac*™ sequence analysis of MRP1, for example, indicated that the recognition sequence for a particular transcription factor was contained within the promoter sequence of the MRP1 gene, a note was made by hand beside that transcription factor on the above-mentioned list. This was carried out for all six genes, at the end of which the recognition motifs of a number of common transcription factors had been identified as being present on the promoter sequences of these six genes. Several motifs were repeated many times in different sequences, indicating that these factors may be important in regulating separate genes. Also, as evinced by Table 3.4.1, a far larger number of potential transcription factors were identified on the promoter sequences of the genes. Obviously, the more gene promoter sequences which were analysed for common transcription factors increased, the probability of finding common sequence motifs decreased. This, however, does not mitigate against the identification of other transcription factors as being important or even essential in the regulation of those genes. This study was designed only to identify common transcription recognition sites.

As a result, only seven recognition sequences were identified as being common to all nine genes. These are summarised in Table 3.4.2.

Table 3.4.2 Common transcription factors for genes induced by BrdU

Classification No.	Name
M00075	GATA-1
M00076	GATA-2
M00077	GATA-3
M00083	MZF1
M00087	Ik-2
M00101	CdxA
M00271	AML-1a

3.4.3 RT-PCR analysis of expression of transcription factors in BrdU-treated cells

The analysis was begun by examining whether the agent affected mRNA expression levels of any of the various transcription factors. From the literature, PCR primers were chosen to amplify each of these nine transcription factors. A list of these primer sequences can be found in Appendix A (Table 7.2A). RT-PCR was carried out on the nine transcription factors using the BrdU-treated DLKP and A549 RNA samples (as outlined in Section 2.2.2.5). The amplified fragments were visualised using agarose gel electrophoresis.

Seven of the nine transcription factor primer sets (C/EBP, GATA-1, IK-2, AML-1a, CdxA, Nkx-2.5 and MZF1) yielded either very weak signal or no signal at all for both cell lines and were discarded. This result does not, however, indicate that these transcription factors were not utilised in these cells. It is possible that the PCR primers or regimens selected were not optimal for gene amplification. The GATA-2 and GATA-3 PCRs however, yielded a clean reproducible product for both the A549 and DLKP cell lines. The results for these RT-PCRs are presented here.

3.4.3.1 GATA-2 gene expression in BrdU-treated A549 and DLKP cell lines

The results of the duplicate GATA-2 RT-PCRs on DLKP and A549 cells are shown in Figs. 3.4.1 and 3.4.2. As can be seen, GATA-2 gene expression is strongly increased in

the DLKP cell line following exposure to BrdU (Fig. 3.4.1). The pattern of upregulation of expression appeared to differ slightly, however, between the two preparations of DLKP cells. In the first sample set, expression of the gene was increased up to a maximum of over eight-fold that of normal DLKP after seven days exposure to BrdU. It is interesting to note that all of the genes used in the identification of the GATA-2 and -3 transcription factors also reached a maximum level of gene expression after seven days exposure to BrdU. Thereafter, expression of the gene decreased to roughly three times that of normal cells after fifteen days. In the second sample set, a higher level of basal GATA-2 expression was observed in the control DLKP sample. The subsequent increases in GATA-2 gene expression following BrdU treatment were, as a result, slightly lower with respect to this control sample. However, the expression increases were roughly similar when compared to the first sample set control, for all samples up to, and including, day seven. A final difference between the two was the observation of a very high level of expression of GATA-2 after fifteen days exposure to BrdU.

In the BrdU-treated A549 cells (Fig. 3.4.2), expression of the GATA-2 gene was observed to increase in both preparations, although in an irregular fashion. A significant increase in expression of the gene (~fifty-fold) after two days treatment was observed in one set of A549 cells examined. However, the increase was only significant against the very low level of expression of the gene in the control sample. Also, GATA-2 expression was observed to decrease after this date, although it remained higher than untreated expression levels. The second sample set yielded a different pattern of expression increase, this time yielding a maximum expression increase of three-fold at day fifteen. Again, expression levels of GATA-2 remained slightly higher throughout than for untreated A549.

3.4.3.2 GATA-3 gene expression in BrdU-treated A549 and DLKP cell lines

Similar to the results obtained for GATA-2 expression in the BrdU-treated DLKP cells, GATA-3 expression was also observed upregulated in the DLKP cell line following exposure to the agent (Fig. 3.4.3). In both sample preparations, the highest level of GATA-3 expression occurred after seven days of exposure to BrdU, which was also the

Fig. 3.4.1: GATA-2 RT-PCR on BrdU-treated DLKP cells

Fig. 3.4.1a:

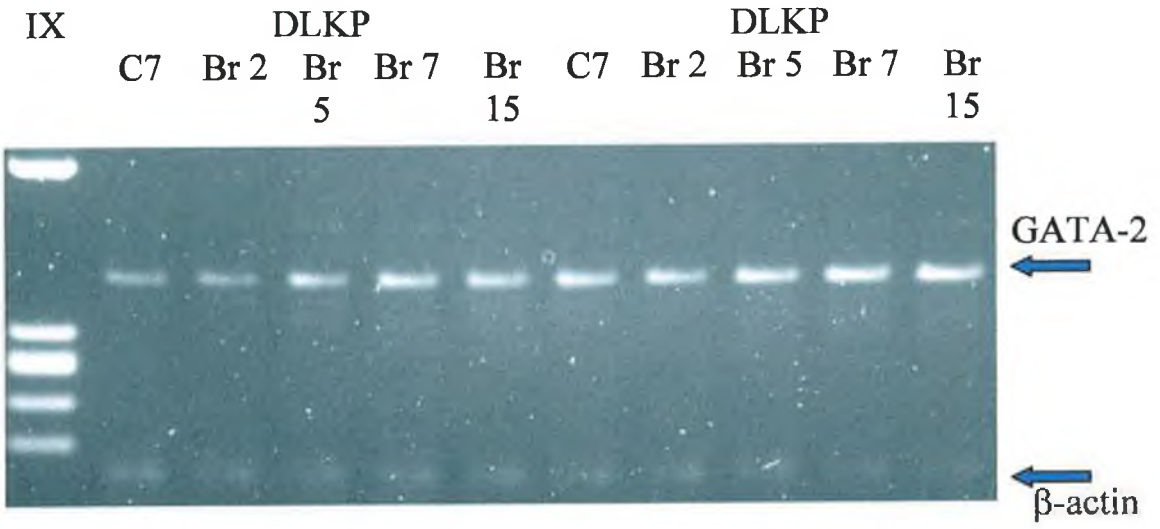

Fig. 3.4.1b:

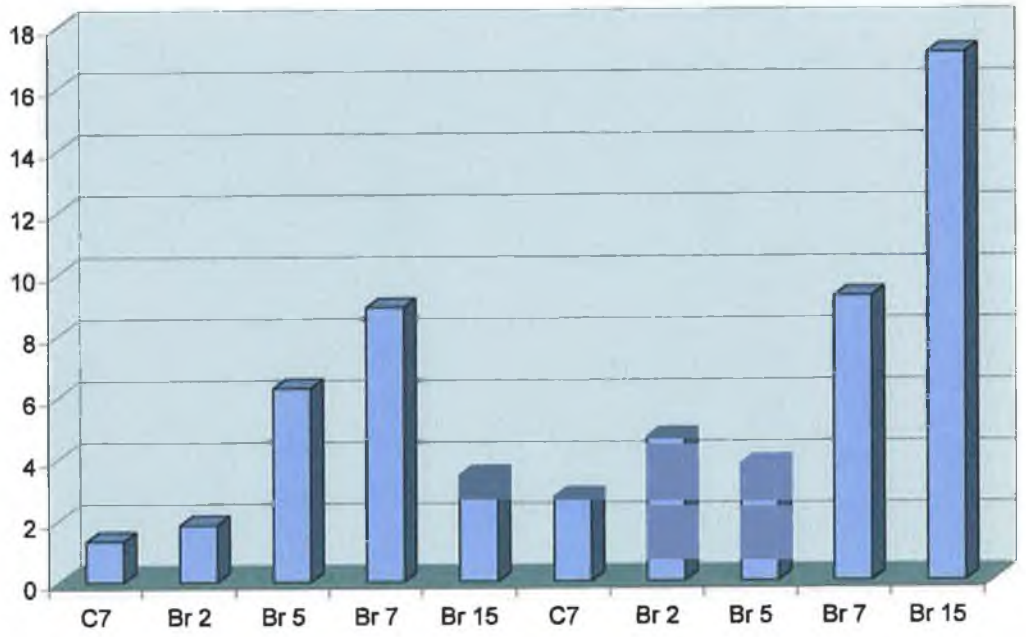

Fig. 3.4.1a: Gel electrophoresis photograph of GATA-2 RT-PCR results on BrdU-treated DLKP cells; Fig. 3.4.1b: Densitometric analysis of RT-PCR results.

Fig. 3.4.2: GATA-2 RT-PCR on BrdU-treated A549 cells

Fig. 3.4.2a:

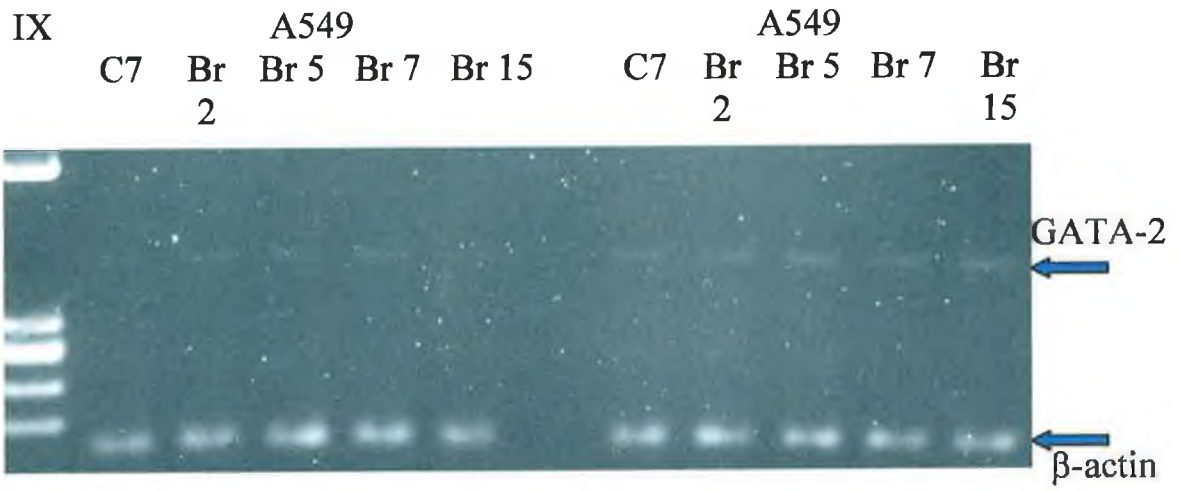

Fig. 3.4.2b:

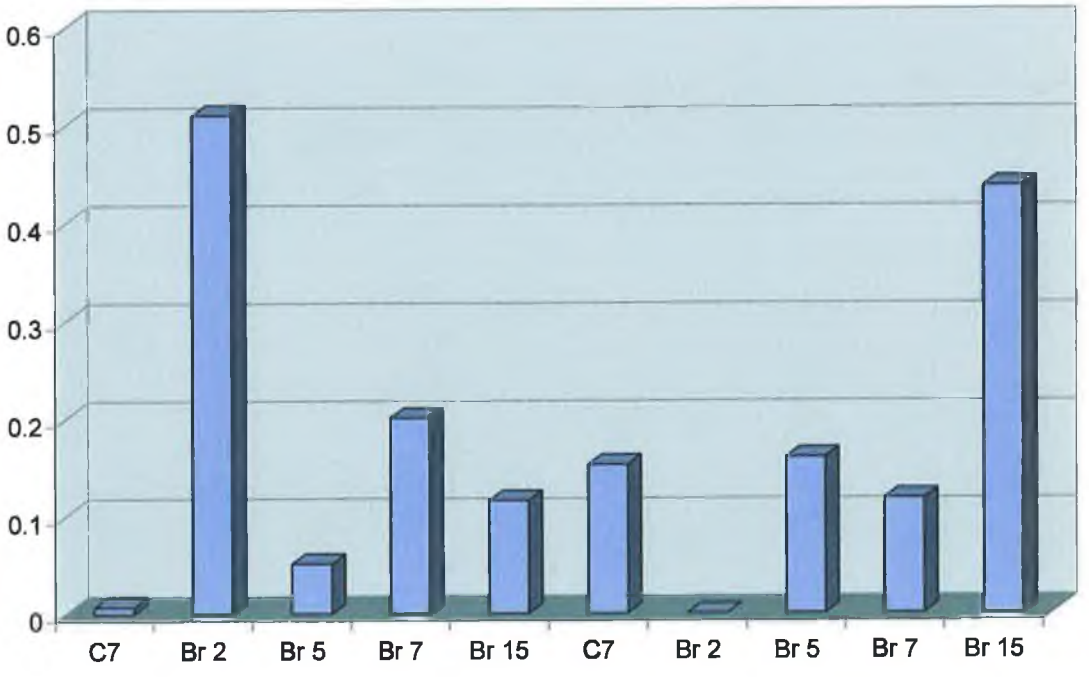

Fig. 3.4.2a: Gel electrophoresis photograph of GATA-2 RT-PCR results on BrdU-treated A549 cells; Fig. 3.4.2b: Densitometric analysis of RT-PCR results.

Fig. 3.4.3: GATA-3 RT-PCR on BrdU-treated DLKP cells

Fig. 3.4.3a:

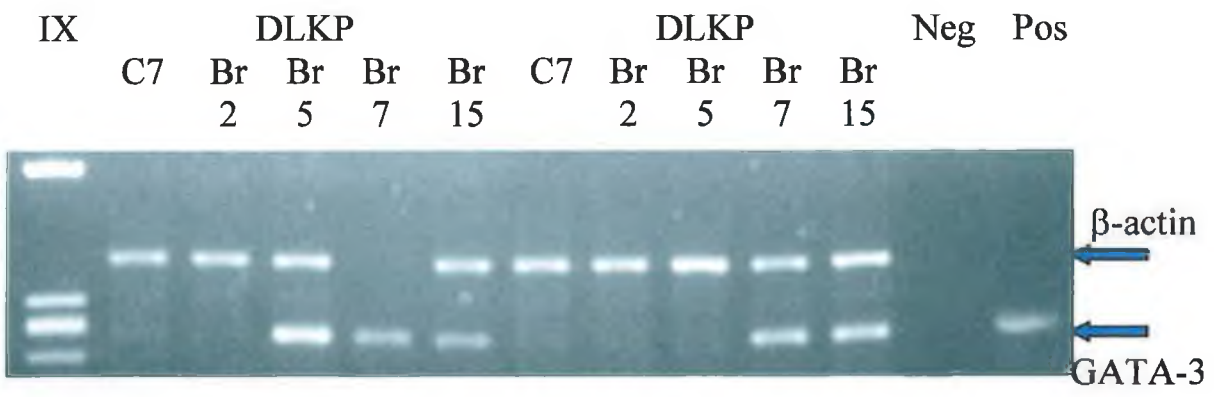

Fig. 3.4.3b:

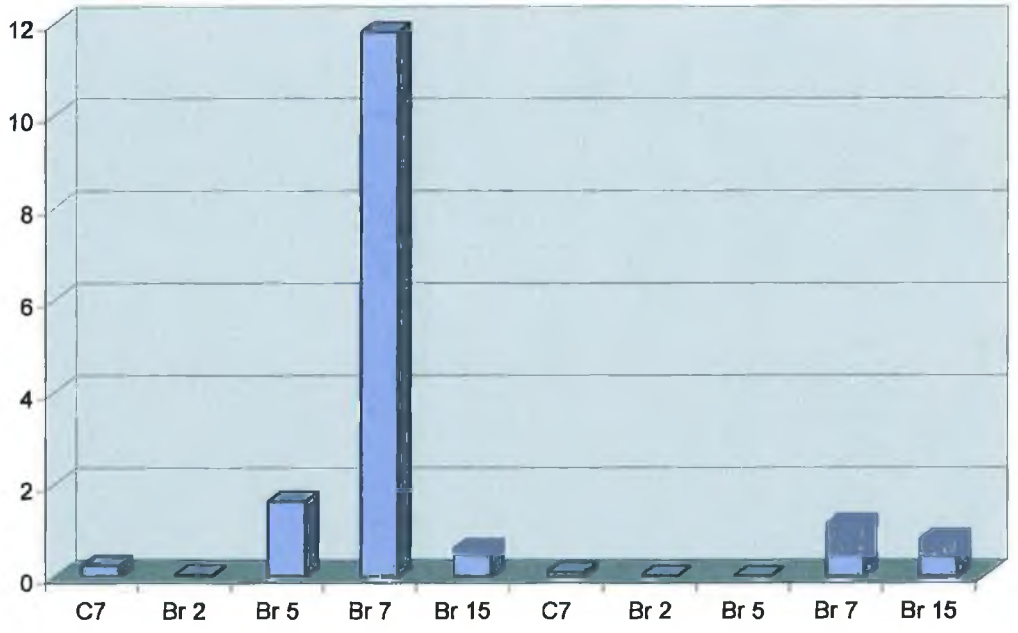

Fig. 3.4.3a: Gel electrophoresis photograph of GATA-3 RT-PCR results on BrdU-treated DLKP cells; Fig. 3.4.3b: Densitometric analysis of RT-PCR results.

time point at which most of the genes upregulated in expression by BrdU reached their maximum expression potential. The level of expression for the first sample set was also observed to be far higher than the second, although, as already outlined, the pattern of expression remained identical.

The picture was significantly different for the BrdU-exposed A549 cells. Expression of the GATA-3 gene in both sample preparations was significantly decreased following exposure to the differentiating agent (Fig. 3.4.4).

3.4.3.3 Summary of GATA-2 and GATA-3 RT-PCR results

From these results, it is apparent that exposure of the DLKP cell line to the differentiating agent BrdU results in increased expression of the transcription factors GATA-2 and GATA-3. These two transcription factors are potential transcriptionally regulating elements of the six genes chosen for analysis due to their increased expression following exposure to BrdU. It is therefore possible that BrdU positively affects the expression of these six genes by increasing the expression of one or more of the transcription factors responsible for the positive regulation of these genes.

By contrast, the expression patterns of both GATA-2 and GATA-3 factors in the BrdU-treated A549 cells were far more irregular. GATA-2 expression does increase in A549 following BrdU treatment, although this increase does not follow a linear pattern, and so may be directly correlated with increases observed for BrdU-upregulated genes in this cell line. For GATA-3, overall expression is observed to decrease in A549 cells following exposure to BrdU.

3.4.4 RT-PCR analysis of expression of transcription factors in drug-exposed DLKP

Following on from the analysis of the short-term drug-exposure assays carried out on DLKP cell line, it was thought relevant to investigate the gene expression profiles in the drug-treated DLKP cells, of the GATA-2 and GATA-3 transcription factors already examined in the BrdU-exposed cells. Standard RT-PCRs, as outlined in Section 2.4.2.5,

Fig. 3.4.4: GATA-3 RT-PCR on BrdU-treated A549 cells

Fig. 3.4.4a:

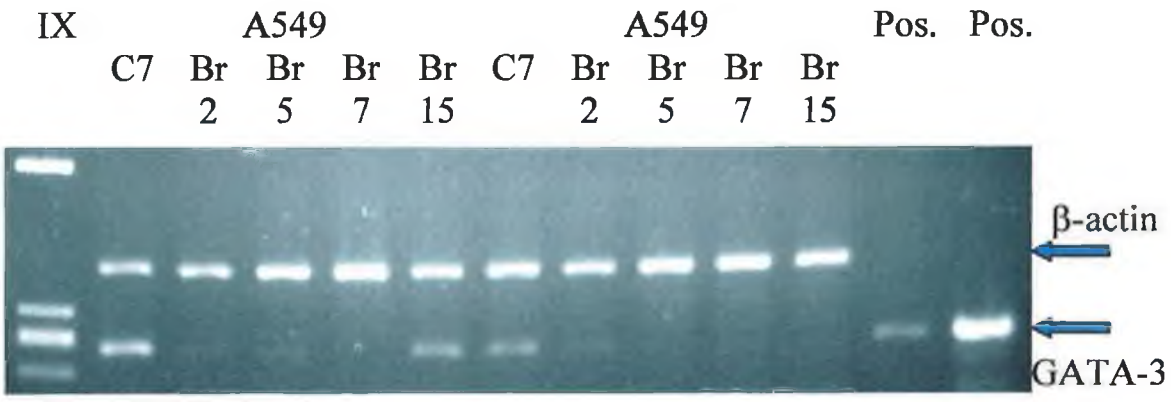

Fig. 3.4.4b:

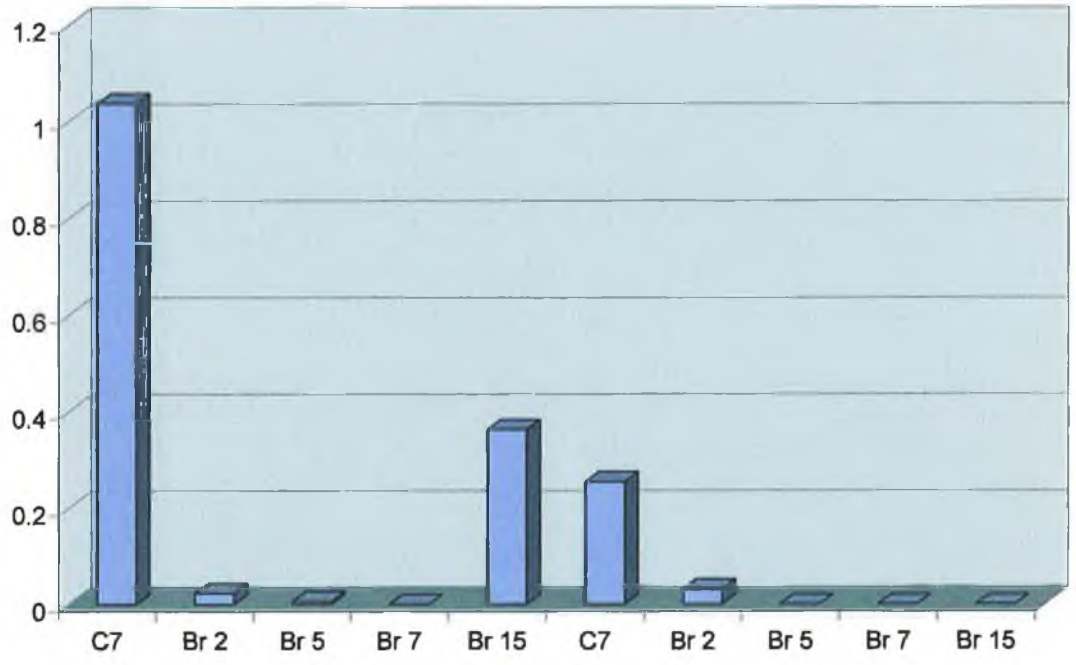

Fig. 3.4.4a: Gel electrophoresis photograph of GATA-3 RT-PCR results on BrdU-treated A549 cells; Fig. 3.4.4b: Densitometric analysis of RT-PCR results.

were carried out on the isolated RNA samples and the resulting PCR products eluted on a 2% agarose gel.

GATA-2 expression was significantly increased in the DLKP cells exposed to VP16 (Fig. 3.4.5), with an overall three-fold increase in expression of the gene following exposure to the drug. However, no significant effect on GATA-2 expression was observed following exposure to cisplatin or taxol (Figs. 3.4.6 and 3.4.7, respectively). By contrast, GATA-3 expression was not significantly altered in DLKP cells exposed to any of the three chemotherapeutic drugs (Figs. 3.4.8 – 3.4.10).

3.4.5 Transcription factor analysis of the 5' promoter regions of genes with increased expression following exposure to chemotherapeutic drugs

Exposure of the DLKP and A549 cell lines to the differentiating agent BrdU had helped identify a number of genes whose expression was positively regulated by the agent (Section 3.1.1). This, in turn led to the identification of the GATA-2 and -3 transcription factors, which may be involved in the BrdU-mediated regulation of those genes (Section 3.4.2). It was considered that a similar approach to the analysis of the promoter regions of genes whose expression was observed increased following exposure to chemotherapeutic drugs may yield a similar discovery. DLKP cells were exposed to three chemotherapeutic drugs (cisplatin, taxol and VP16) (Section 3.2.) and a number of genes were observed to be increased in expression following exposure to the different drugs (Section 3.2.1). As the method of drug action differs from one to another, it was considered prudent to analyse the promoter regions of genes influenced by each drug in turn, i.e. the promoter regions of the MRP genes 1 and 2, and the BCRP gene, all increased in expression in DLKP cells following exposure to cisplatin, would be compared to each other to identify common transcription factors. Likewise, the promoter regions of MRP2, α-catenin and E-cadherin (expression increase following exposure to taxol) and MRPs1 and 2 and α-catenin (induced by VP16) would be compared for the same reason. The analysis and comparison of the promoter regions was carried out as outlined in Section 3.4.1.

Fig. 3.4.5: GATA-2 RT-PCR on VP16-treated DLKP cells

Fig. 3.4.5a:

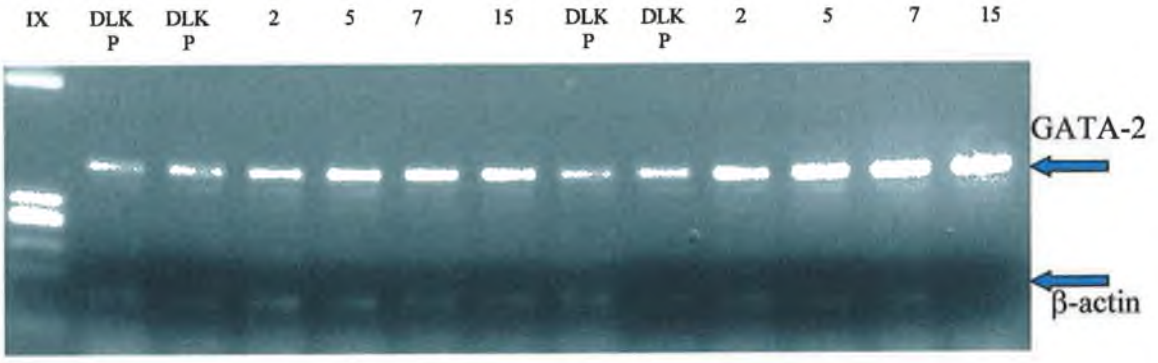

Fig. 3.4.5b:

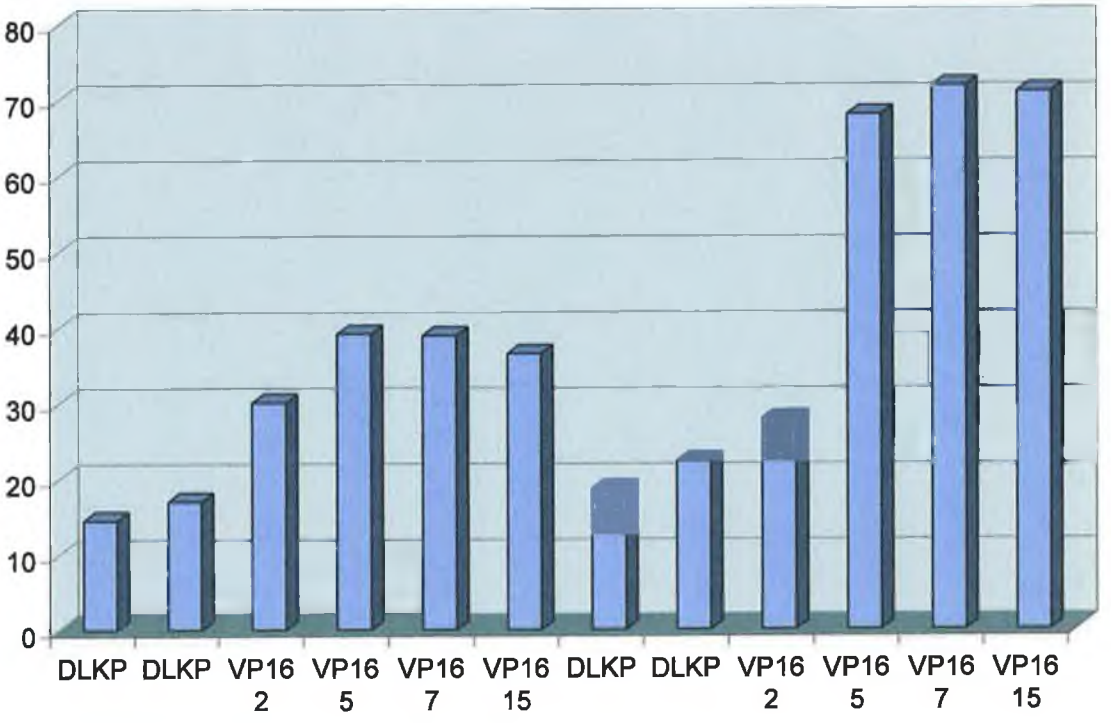

Fig. 3.4.5a: Gel electrophoresis photograph of GATA-2 RT-PCR results on VP16-exposed DLKP cells; Fig. 3.4.5b: Densitometric analysis of RT-PCR results.

Fig. 3.4.6: GATA-2 RT-PCR on Cisplatin-treated DLKP cells

Fig. 3.4.6a:

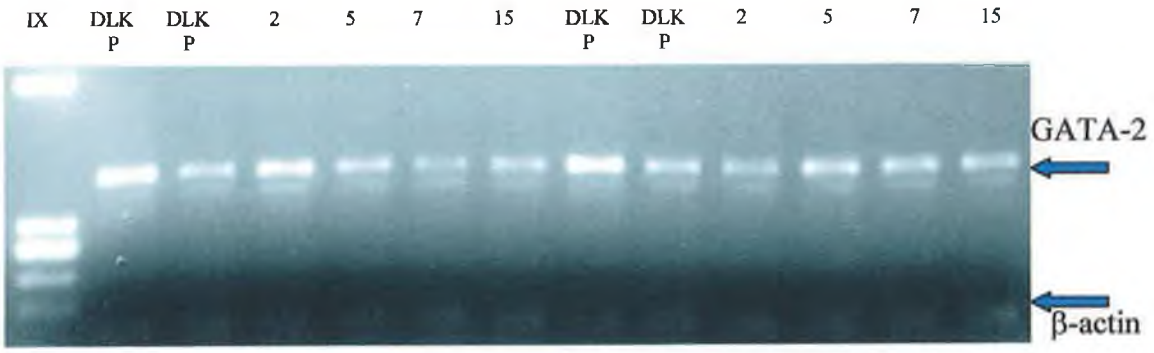

Fig. 3.4.6b:

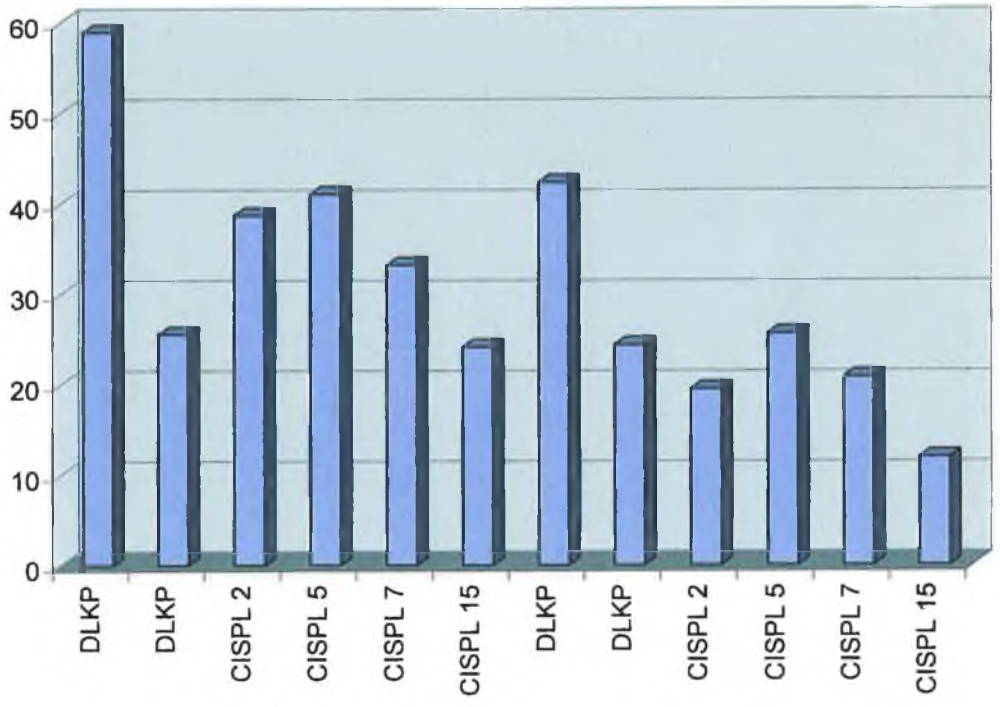

Fig. 3.4.6a: Gel electrophoresis photograph of GATA-2 RT-PCR results on Cisplatin-exposed DLKP cells; Fig. 3.4.6b: Densitometric analysis of RT-PCR results.

Fig. 3.4.7: GATA-2 RT-PCR on Taxol-treated DLKP cells

Fig. 3.4.7a:

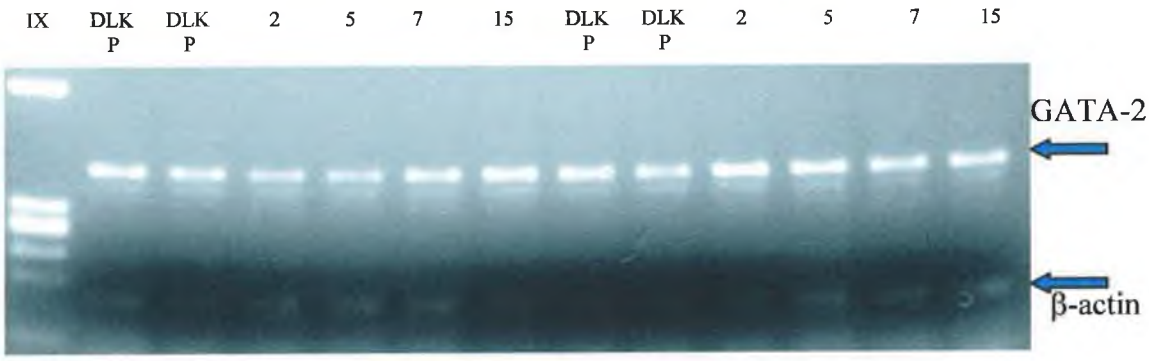

Fig. 3.4.7b:

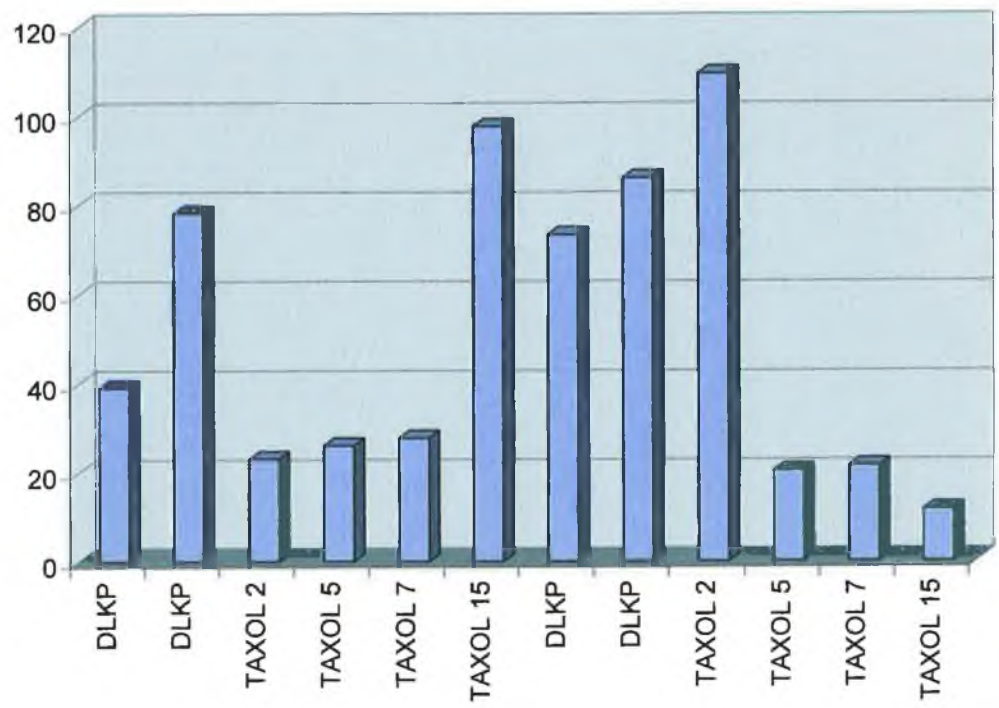

Fig. 3.4.7a: Gel electrophoresis photograph of GATA-2 RT-PCR results on Taxol-exposed DLKP cells; Fig. 3.4.7b: Densitometric analysis of RT-PCR results.

Fig. 3.4.8: GATA-3 RT-PCR on Cisplatin-treated DLKP cells

Fig. 3.4.8a:

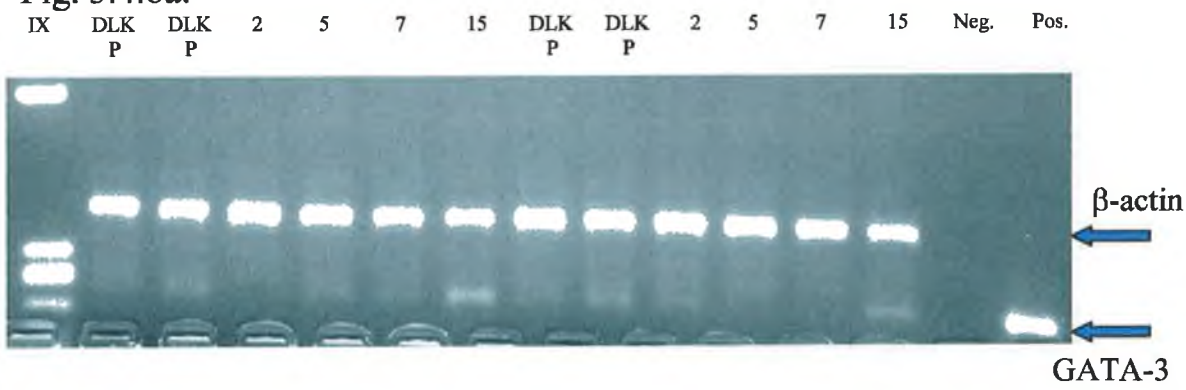

Fig. 3.4.8b:

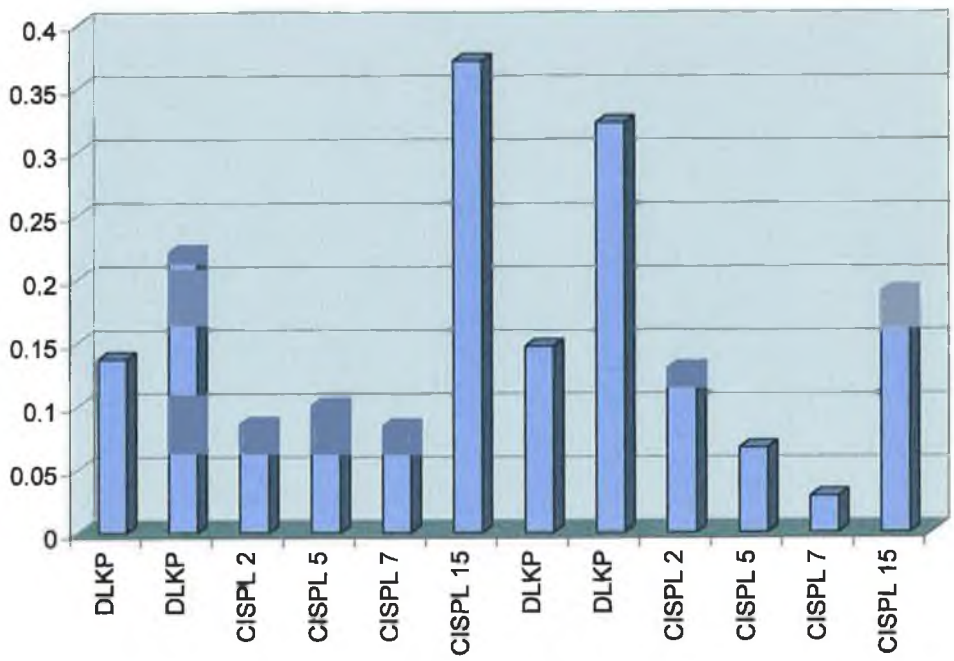

Fig. 3.4.8a: Gel electrophoresis photograph of GATA-3 RT-PCR results on Cisplatin-treated DLKP cells; Fig. 3.4.8b: Densitometric analysis of RT-PCR results.

Fig. 3.4.9: GATA-3 RT-PCR on Taxol-treated DLKP cells

Fig. 3.4.9a:

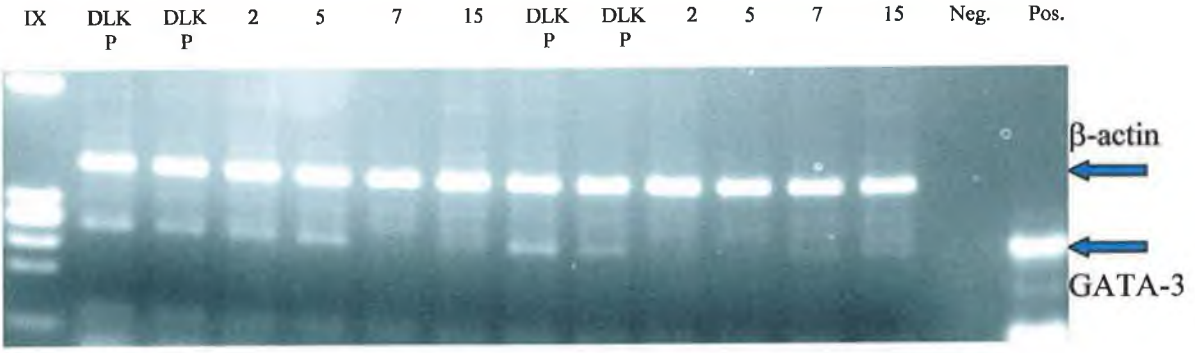

Fig. 3.4.9b:

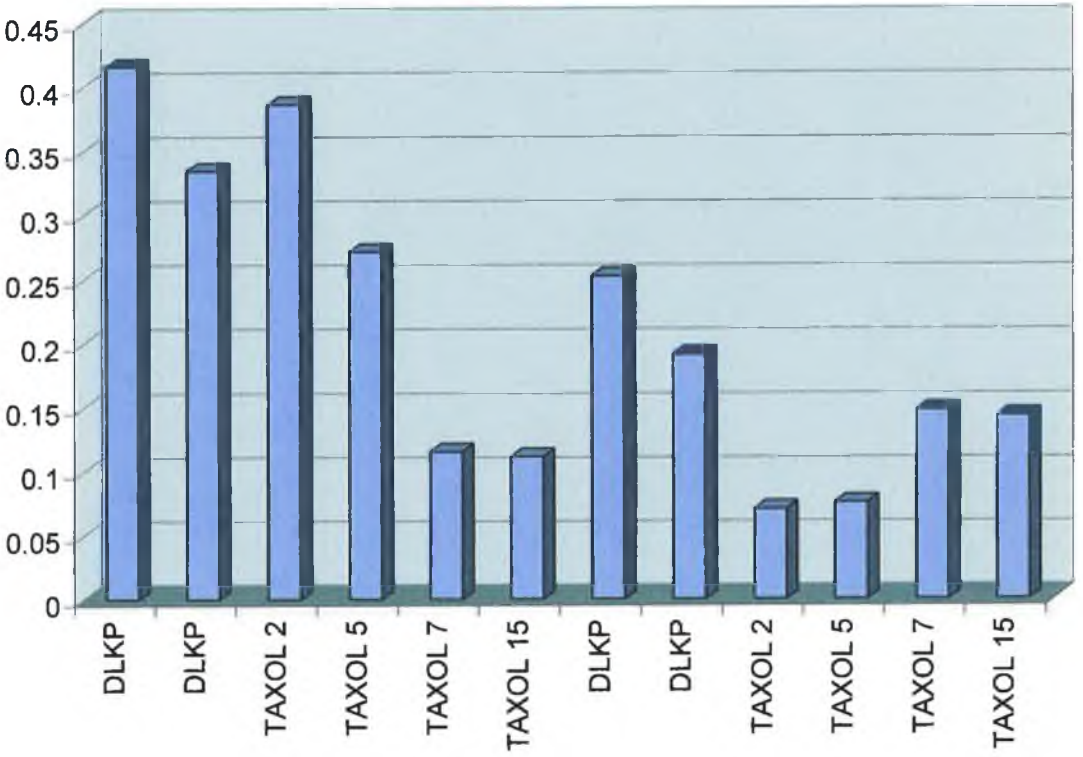

Fig. 3.4.9a: Gel electrophoresis photograph of GATA-3 RT-PCR results on Taxol-treated DLKP cells; Fig. 3.4.9b: Densitometric analysis of RT-PCR results.

Fig. 3.4.10: GATA-3 RT-PCR on VP16-treated DLKP cells

Fig. 3.4.10a:

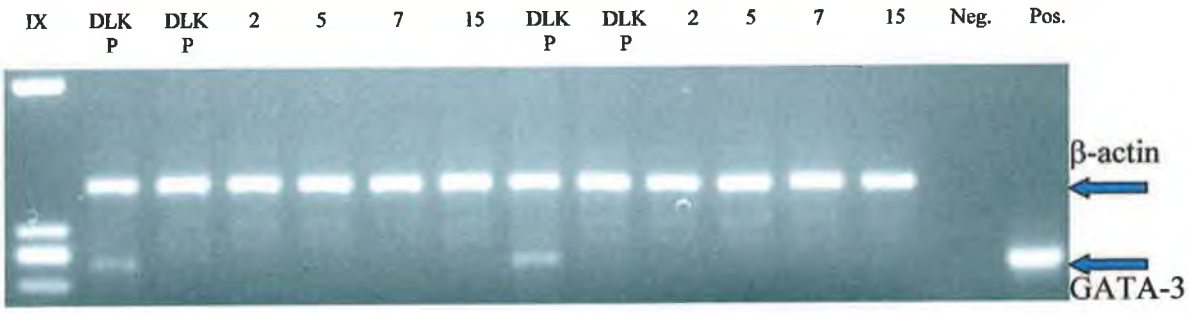

Fig. 3.4.10b:

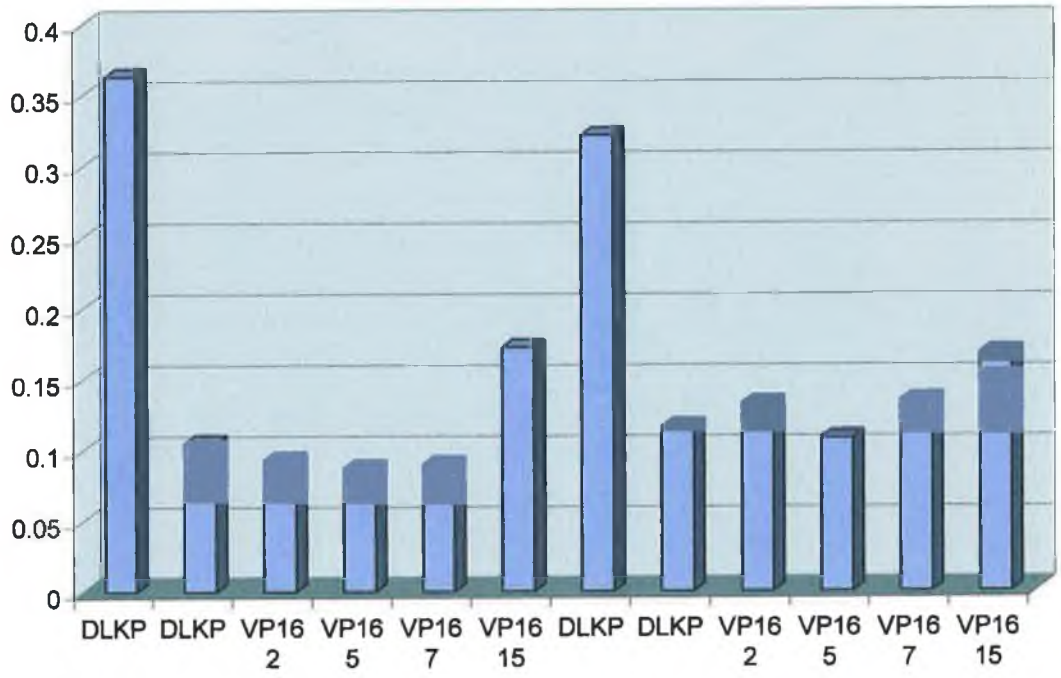

Fig. 3.4.10a: Gel electrophoresis photograph of GATA-3 RT-PCR results on Taxol-treated DLKP cells; Fig. 3.4.10b: Densitometric analysis of RT-PCR results.

3.4.5.1 Transcription factor analysis of the promoter regions of Cisplatin-induced genes

As already outlined (Section 3.4.1), the expression of MRP1, MRP2 and BCRP of the examined genes was upregulated following exposure to the chemotherapeutic drug, cisplatin. Transcription factor analysis as outlined in Section 3.4.1 was carried out which identified a total of one hundred and thirty potential transcription factors which were located on the 5' promoter regions of the three induced genes. These transcription factors are listed among the 147 transcription factors shown in Table 3.4.1. A list of the common potential transcription factors was subsequently drawn up from this total list of 130. These twenty-three common factors, together with a sample recognition sequence and the classification number of each, are listed in Table 3.4.3.

Table 3.4.3. Common transcription factors for genes induced by Cisplatin

Classification No.	Name	Sample Sequence
M00033	P300	CCCAGGAGTTGGAG
M00075	GATA-1	CGTGATCCGC
M00076	GATA-2	CAGCATCTCC
M00077	GATA-3	CCTTATCTC
M00083	MZF1	TCCCCTCC
M00087	Ik-2	AGCTGGGACTAC
M00099	S8	GCAATTCAATTACAGT
M00100	CdxA	ATTTCTG
M00101	CdxA	AATTACA
M00106	CDP CR3+HD	AATGGATCGC
M00122	USF	TAGTCACATGTCCA
M00127	GATA-1	AACCTCATCTCTCT
M00141	Lyf-1	TCTCTCAAA
M00148	SRY	AAACTTA
M00159	C/EBP	TCTTTGGAAAAGT
M00162	Oct-1	CCAATTTACATTTC
M00173	AP-1	TTTTAGTCACA
M00174	AP-1	GCTGAGTCACT
M00203	GATA-X	CAAACTTATCT
M00217	USF	GCAGGTGG
M00240	Nkx-2.5	TCAAGTG
M00241	Nkx-2.5	CTTACTTG
M00271	AML-1a	TGTGGT

As can be seen, all nine common potential transcription factors identified from the six BrdU-upregulated genes are observed here, along with fourteen other factors potentially utilisable by cisplatin in upregulating expression of the three genes under examination.

3.4.5.2 Transcription factor analysis of the promoter regions of Taxol-induced genes

As already outlined (Section 3.4.1), the expression of MRP2, α-catenin and E-cadherin of the examined genes was upregulated following exposure to taxol. Transcription factor analysis as outlined in Section 3.4.1 was carried out which identified a total of one hundred and twenty-two potential transcription factors which were located on the 5' promoter regions of the three induced genes. These transcription factors are listed among the 147 transcription factors shown in Table 3.4.1. A list of the common potential transcription factors was subsequently drawn up from this total list of 122. These eighteen common factors, together with a sample recognition sequence and the classification number of each, are listed in Table 3.4.4.

Table 3.4.4. Common transcription factors for genes induced by Taxol

Classification No.	Name	Sample Sequence
M00001	MyoD	GGTCAGGTGGGG
M00008	Sp1	ACCACGGCCG
M00033	P300	CCCAGGAGTTGGAG
M00073	DeltaEF1	ATTAGGTGTTA
M00075	GATA-1	CGTGATCCGC
M00076	GATA-2	CAGCATCTCC
M00077	GATA-3	CCTTATCTC
M00083	MZF1	TCCCCTCC
M00087	Ik-2	AGCTGGGACTAC
M00100	CdxA	ATTTCTG
M00101	CdxA	AATTACA
M00130	HFH-2	GTTGTTTTTTT
M00131	HNF-3beta	TTCTATTTGTTC
M00141	Lyf-1	TCTCTCAAA
M00148	SRY	AAACTTA
M00160	SRY	TCTCTTGTTTAT
M00217	USF	GCAGGTGG
M00271	AML-1a	TGTGGT

3.4.5.3 Transcription factor analysis of the promoter regions of VP16-induced genes

As already outlined (Section 3.4.1), the expression of MRP1, MRP2 and α-catenin of the examined genes was observed upregulated following exposure to VP16. Transcription factor analysis as outlined in Section 3.4.1 was carried out which identified a total of one hundred and thirty-five potential transcription factors which

were located on the 5' promoter regions of the three induced genes. These transcription factors are listed among the 147 transcription factors shown in Table 3.4.1. A list of the common potential transcription factors was subsequently drawn up from this total list of 122. These twenty-seven common factors, together with a sample recognition sequence and the classification number of each, are listed in Table 3.4.5.

Table 3.4.5. Common transcription factors for genes induced by VP16

Classification No.	Name	Sample Sequence
M00001	MyoD	GGTCAGGTGGGG
M00008	Sp1	ACCACGGCCG
M00033	P300	CCCAGGAGTTGGAG
M00037	NF-E2	GGCTGAGTCAC
M00073	DeltaEF1	ATTAGGTGTTA
M00075	GATA-1	CGTGATCCGC
M00076	GATA-2	CAGCATCTCC
M00077	GATA-3	CCTTATCTC
M00083	MZF1	TCCCCTCC
M00087	Ik-2	AGCTGGGACTAC
M00100	CdxA	ATTTCTG
M00101	CdxA	AATTACA
M00106	CDP CR3+HD	AATGGATCGC
M00109	C/EBPbeta	TTGTTAGGAAAGA
M00127	GATA-1	AACCTCATCTCTCT
M00130	HFH-2	GTTGTTTTTTT
M00131	HNF-3beta	TTCTATTTGTTC
M00137	Oct-1	TTTTGATTACTTA
M00141	Lyf-1	TCTCTCAAA
M00148	SRY	AAACTTA
M00159	C/EBP	TCTTTGGAAAAGT
M00160	SRY	TCTCTTGTTTAT
M00173	AP-1	TTTTAGTCACA
M00199	AP-1	CTGAGTCAC
M00203	GATA-X	CAAACTTATCT
M00217	USF	GCAGGTGG
M00271	AML-1a	TGTGGT

3.4.6 Analysis of promoter regions of the MRP1 gene in the DLKP cell line

MRP1 expression was observed increased by the action of the differentiating agent BrdU, in both the DLKP and A549 cell lines; the only gene studied here to do so (Section 3.1.1). MRP1 expression was also increased in the short-term cisplatin- and VP16-exposed DLKP cells (Section 3.2.1) as well as in the vincristine- and VP16-

selected cell lines (Section 3.3.1). As a result, it was considered useful to examine more closely the effect on the 5' promoter region of the gene of the agents examined here (e.g. BrdU, Cisplatin, Taxol, VP16).

Computer-aided transcription factor analysis carried out here (Section 3.4.1), has already identified a number of common transcription factors as being potentially involved in the BrdU-mediated regulation of the MRP1 gene in the DLKP cell line, while RT-PCR of those factors has identified two factors observed to be upregulated following exposure to BrdU (Section 3.4.2). Further transcription factor analysis examining the upregulation of MRP1 by the chemotherapeutic drugs cisplatin and VP16 has also identified additional common potential transcription factors which may be utilised by these agents in the positive regulation of MRP1 (Section 3.4.5).

A complementary approach to examining the effect of these agents on specific regions of the 5' promoter of the MRP1 gene in the DLKP cell line would be useful in identifying which regions of the MRP1 promoter region were utilised by the various agents employed to produce the upregulated MRP1 gene response. As a result, it was considered necessary to examine the action of these agents on the promoter region of the MRP1 gene specifically.

A number of pGL2 (Promega, E1621) plasmid constructs containing truncated Sections of the 5' MRP1 promoter region attached to the luciferase gene were obtained from Dr. William Beck (Wang and Beck, 1998). The 5' promoter region of the human MRP1 gene was cloned from drug-resistant HL-60 cells and the 2.1kb (-2008 to +103bp, relative to the transcription start site) promoter fragment was fused to the luciferase gene in the pGL2-Basic (Promega, E1611) plasmid. Deletion mutants were generated by restriction digestion of p-2008 with *Bsu*36I (at –1123bp), *Pvu*II (at –660bp), *Bst*EII (at –411bp), *Sma*I (at –91bp) and at 3' of the promoter with *Hind*III (at +103bp). The promoter fragments were then cloned into pGL2-Basic to generate p-1123, p-660, p-411 and p-91, respectively. A schematic linear map of each of the pGL2 plasmids used is shown in Fig. 3.4.11.

The five constructs were then transiently transfected in DLKP cells as outlined in Section 2.4.5. The cells were then either taken down at the prescribed day or treated

Fig. 3.4.11: MRP1 gene promoter-luciferase reporter plasmids

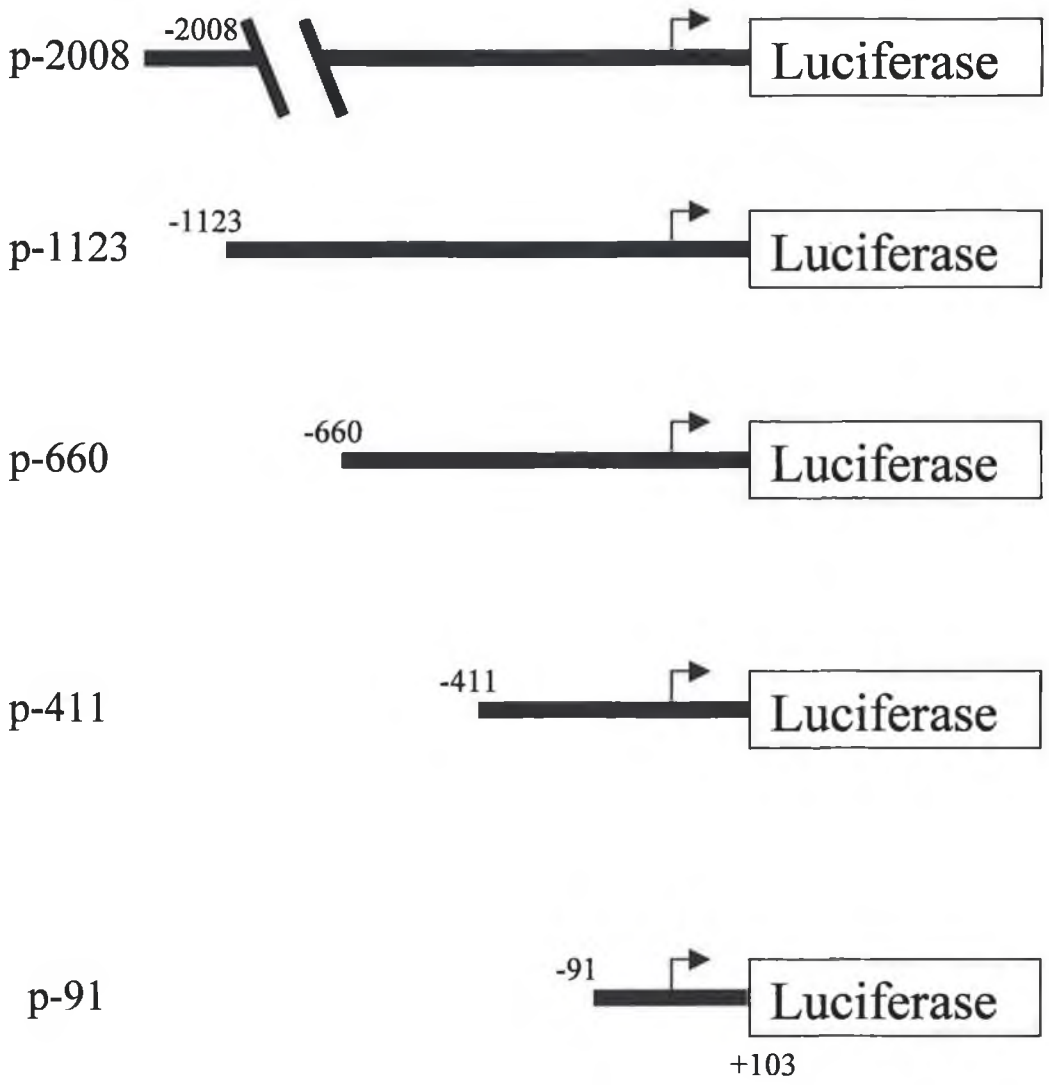

Fig. 3.4.11: Schematic linear map of pGL2 plasmids containing various lengths of the human MRP1 gene promoter 5' to the luciferase gene. Numbered DNA sequences in the above maps correspond to those in the published sequence (Zhu & Center, 1994), relative to the transcriptional start (*arrow*).

with one of four agents; BrdU, Cisplatin, Taxol or VP16 before being taken down and assayed for luciferase expression.

The experiment took the form of six separate transfection experiments. The first (Untreated 0 hrs) was the standard luciferase transfection protocol; the cells were transfected overnight with the various plasmids, taken down and the luciferase readings obtained. This was intended as a dual control; one to indicate which parts of the MRP1 promoter were normally utilised in normal DLKP cells and two, to provide a basal level of luciferase expression against which all other treatments could be compared. The (Untreated 24 hrs) sample refers to a second control where after the overnight transfection with the MRP1 promoter plasmids, the cells were re-fed with ordinary media and then left for a further 24 hrs. This was carried out to indicate any alterations in luciferase expression following removal of the transfecting agent and plasmids. The BrdU and three drug treatments illustrated in Figs. 3.4.13 to 3.4.16 refer to DLKP cells transfected overnight with the MRP1 promoter plasmids, then exposed to one of four agents (BrdU, Cisplatin, Taxol and VP16) for a further 24 hrs. This was carried out to investigate which area of the MRP1 promoter, if any, is affected by these chemicals in upregulating expression of the MRP1 gene as has already been demonstrated in this cell line. Although Taxol was not observed to influence MRP1 expression in DLKP cells, previous work carried out in this laboratory had indicated that it may induce expression of the gene at near-fatal doses to the cells and so it was considered prudent to include the drug in our analysis.

The transfections displayed in Figs. 3.4.12 to 3.4.16 are identified by the region of the truncated MRP1 promoter each plasmid contains. Four additional internal transfection controls were also included in the experiment. These are listed as "DLKP", "DLKP-F", "BASIC" and "Positive" and refer to, respectively, untransfected DLKP cell line, untranfected DLKP in the presence of the transfecting agent, Fugene, DLKP transfected with the empty, or basic, pGL2 plasmid and DLKP transfected with the Positive pGL2 plasmid, which is the luciferase gene attached to a full-length cytomegalovirus (CMV) promoter. Cells were transfected overnight and luciferase readings obtained as outined in Section 2.4.10.

While the "Untreated 0 hrs" transfection was carried out in duplicate, all other transfections were only carried out once. As such these results are, as yet, purely an indication of the action of the agents examined on the promoter region of the MRP1 gene. The actual luciferase readings obtained for each transfection, including the average obtained for the duplicate untreated 0hrs transfections, and the results for the positive PGL2 transfection controls are shown in Table 3.4.6.

Table 3.4.6 List of luciferase readings obtained from plasmid transfections

	U 0hrs	U 24hrs	BrdU	Cispl	Taxol	VP16
DLKP	4.325	0	0	5.112	0	0
DLKP-F	0	3.32	1.178	7.899	4.444	0
PBasic	2.803	0	6.2	3.4	0	4
p-2008	1060	1021	998	406	451	1196
p-1123	899	625	462	642	396	865
p-660	755	309	288	332	263	754
p-411	574	479	1944	264	357	1894
p-91	2490	1484	380	295	141	767
Positive	35300	23700	19170	13800	12300	14700

3.4.6.1 Basal expression of the MRP1 gene in the DLKP cell line

Overnight transient transfection of the MRP1 promoter-containing plasmids identified the –91 region of the MRP1 promoter as being the primary region of the gene normally utilised in DLKP cells (Fig. 3.4.12). This region contains a large number of transcriptional regulators, the most numerous being the Sp1 transcriptional promoter and was also the region identified by Zhu and Center (1994) as containing the major promoter of the MRP1 gene in the Chinese hamster ovary (CHO) cell line. In this experiment, luciferase expression readings for the plasmid incorporating this fragment was roughly 2.5 times that of the plasmid encoding the next highest fragment, that of the complete –2008 promoter segment. Also, it may be noted that luciferase expression decreases to one fifth that obtained for the –91 plasmid if the region of promoter examined is increased to –411 bases. These results indicate that in the DLKP cell line, the main promoter for the MRP1 gene lies in the first ninety bases back from the

Fig. 3.4.12: Examination of MRP1 promoter regulation in the DLKP cell line using luciferase expression

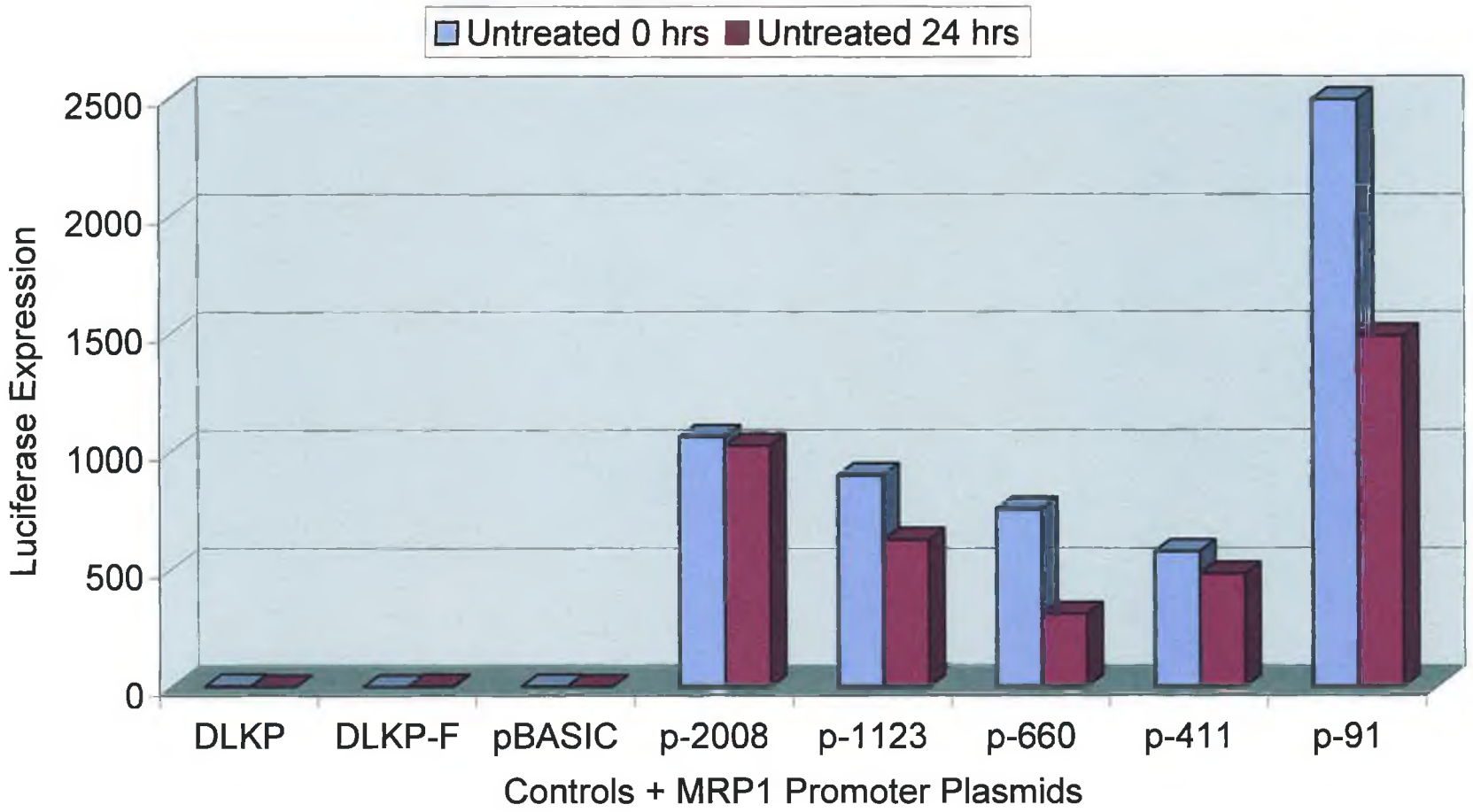

transcriptional start site of the MRP1 gene and that there is potentially a major transcriptional repressor coded between the –91 and –411 bases of the promoter sequence.

The following Figs. (Figs. 3.4.13 – 3.4.16) all include the luciferase results from the Untreated 0hrs (BLUE) and Untreated 24hrs (RED) controls which were obtained as controls for the other treatments as already outlined (Section 3.4.6). As was seen for the normal, untreated DLKP (Untreated 0hrs) (see above), the -91 bases of the MRP1 promoter was also the most productive region of the promoter used in positively-regulating expression of the MRP1 gene after a further 24hrs in ordinary media (Untreated 24hrs), although expression levels are observed to decrease slightly for most plasmids. For instance, the decrease is roughly 3% for p-2008, but almost 60% for p-660. These two control transfections will be referred to in all treatments for comparative purposes. The gene-inducing agent in all subsequent plots (Figs. 3.4.13 – Fig. 3.4.16) is represented by the yellow plot.

3.4.6.2 Expression of the MRP1 gene in DLKP following exposure to BrdU

Fig. 3.4.13 shows the effect of exposure to BrdU on the expression of luciferase in the transfected cells. BrdU was exposed to the cells at a 10μM concentration overnight – this is also the concentration at which BrdU has previously increased expression of several genes (Section 3.1). As can be seen, exposure to BrdU increases expression of luciferase four-fold in the -411 transfected DLKP, while expression levels are markedly decreased in the -91 transfected cells. This result would appear to indicate that BrdU targets this area of the MRP1 promoter in positively regulating expression of the gene, with the subsequent decrease in transcriptional utilisation of the recognition site within the –91 region of the promoter sequence. No significant changes were observed for the other fragments.

Fig. 3.4.13: Effect of BrdU exposure on lucifrase expression in MRP1 Promoter-transfected DLKP cells

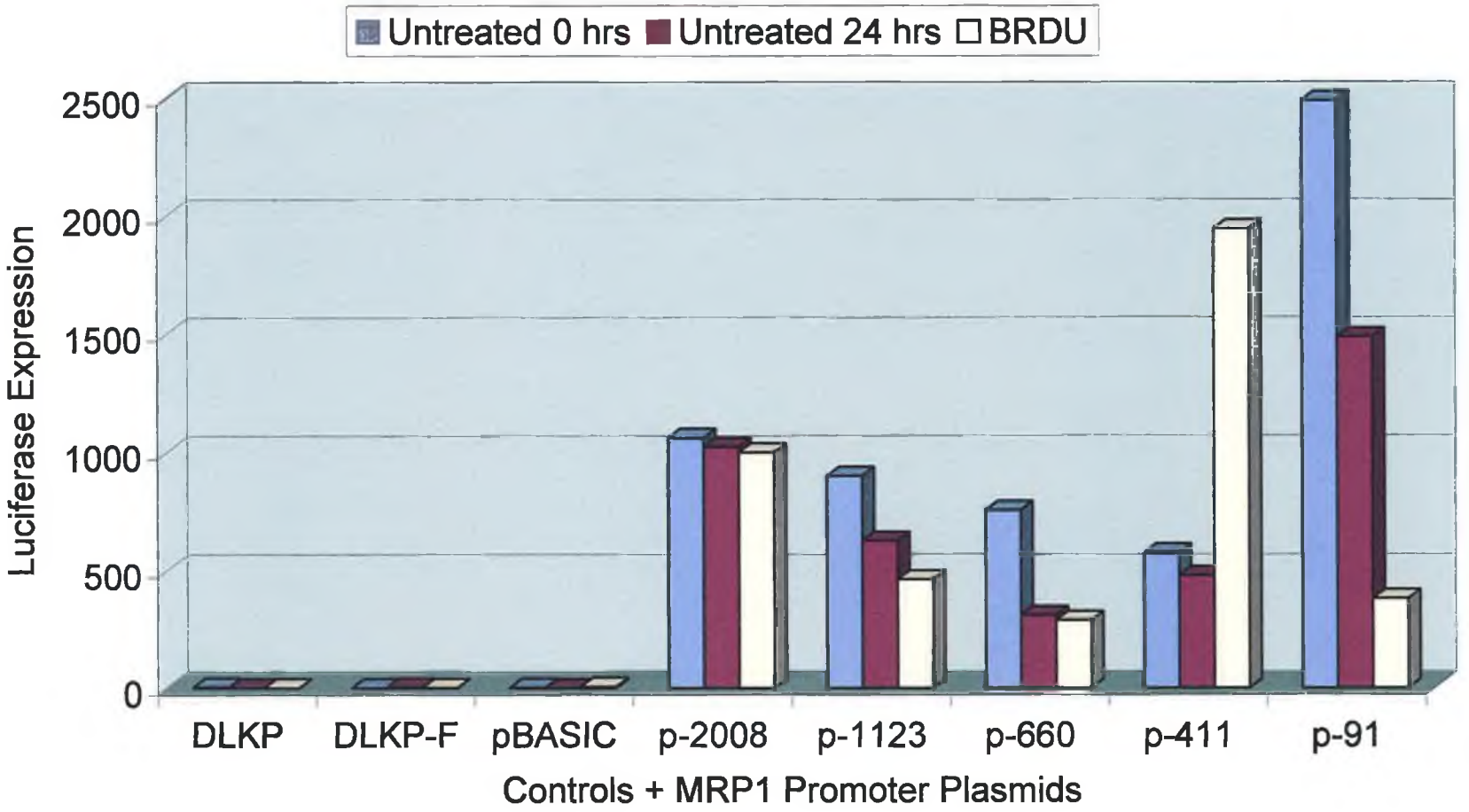

3.4.6.3 Expression of the MRP1 gene in DLKP following exposure to Cisplatin

The effect of cisplatin on the expression of luciferase in the transfected cells is shown in Fig. 3.4.14. Cisplatin was exposed to the cells at a 125ηg/ml concentration overnight – this is also the concentration at which cisplatin has previously increased expression of several genes (Section 3.2). As can be seen, the expression of luciferase was lowered following exposure to the drug. No clear increase in expression was observed for any of the plasmid transfections, and it would appear, from this transfection at least, that cisplatin is not a potential agent for the transcriptional induction of MRP1 gene expression.

This result is quite surprising, as exposure to cisplatin has previously been demonstrated here to induce expression of MRP1 in DLKP (Section 3.2). It is possible that this *in vitro* assay does not mimic exactly the effects of the drug *in vivo*. Also, this difference in expression levels could be due to the fact that these cells were taken down and expression was analysed after only 24hrs of exposure. In the previous results demonstrating MRP1 induction following cisplatin exposure, the earliest assay time point was 48hrs.

3.4.6.4 Expression of the MRP1 gene in DLKP following exposure to Taxol

The effect of taxol on the expression of luciferase in the transfected cells was observed to be almost identical to the effect obtained following exposure to cisplatin, the results of which may be seen in Fig. 3.4.15. Taxol was exposed to the cells at a 0.15ηg/ml concentration overnight – this is also the concentration at which taxol has previously increased expression of several genes (Section 3.2). Again, the expression of luciferase was observed to be lowered for all transfections following exposure to the drug. No clear increase in expression was observed for any of the plasmid transfections, and it would appear again, from this transfection, that taxol is not a potential agent for the transcriptional induction of MRP1 gene expression.

Fig. 3.4.14: Effect of Cisplatin exposure on luciferase expression in MRP1 Promoter-transfected DLKP cells

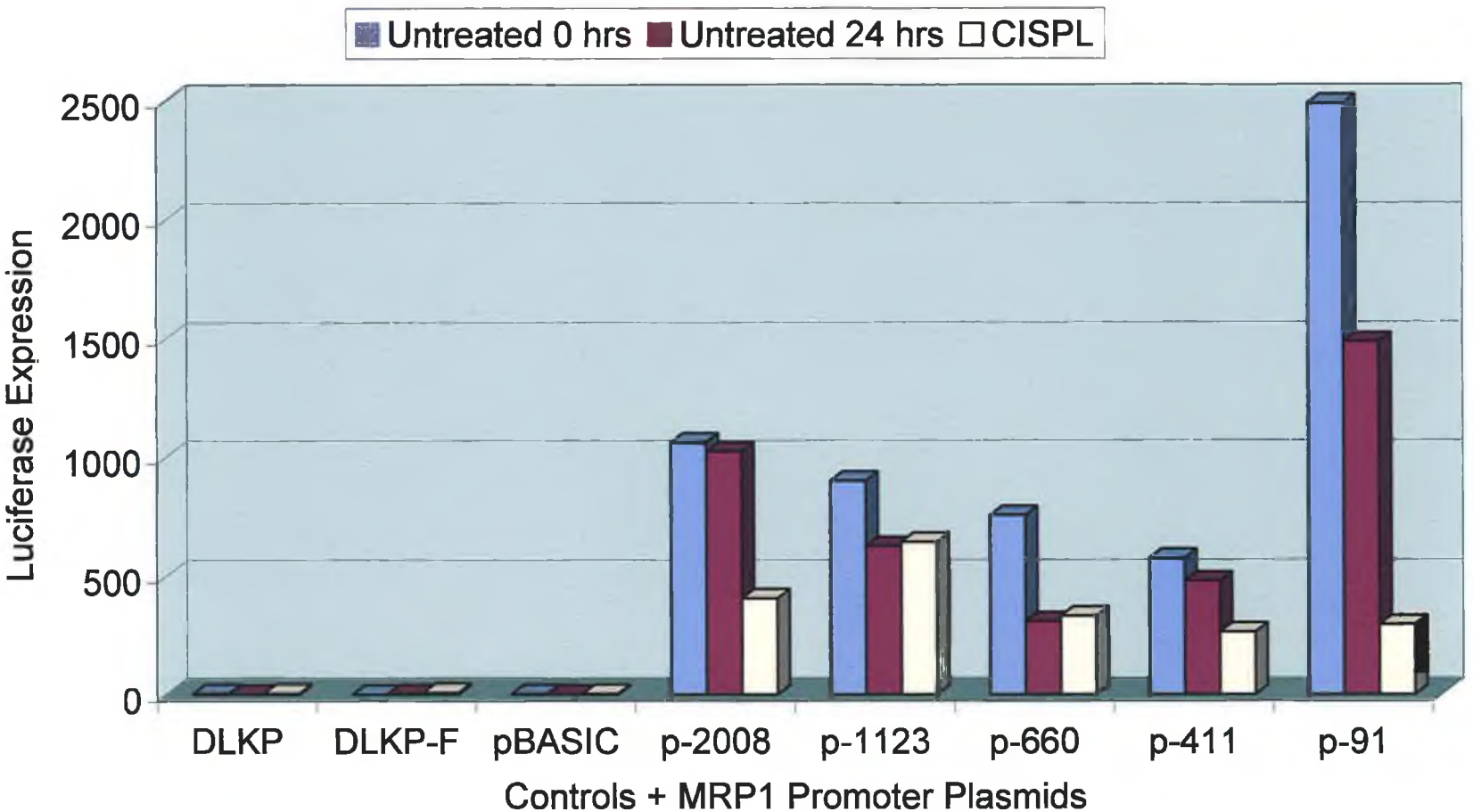

Fig. 3.4.15: Effect of Taxol exposure on luciferase expression in MRP1 Promoter-transfected DLKP cells

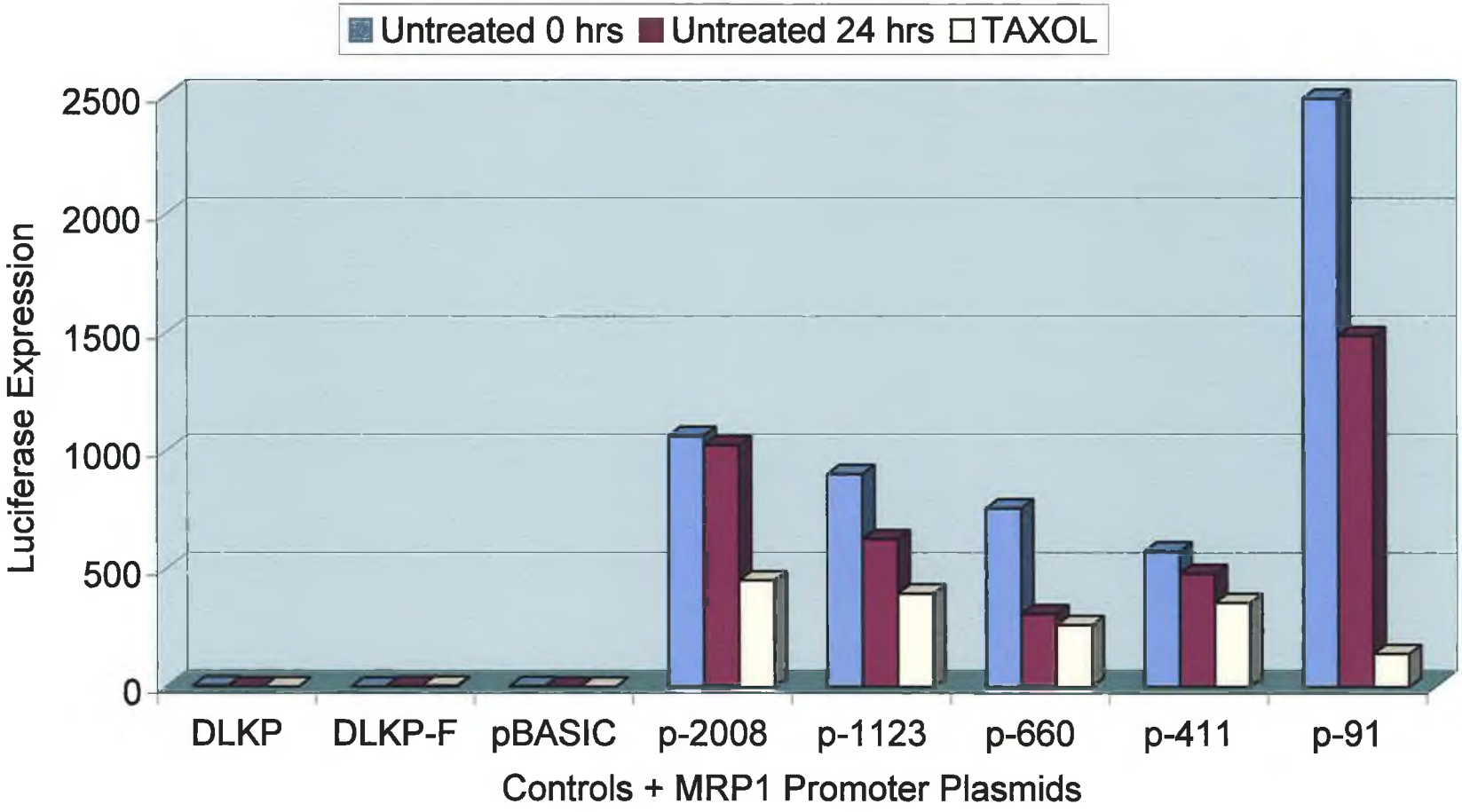

3.4.6.5 Expression of the MRP1 gene in DLKP following exposure to VP16

Fig. 3.4.16 shows the effect of exposure to VP16 on the expression of luciferase in the transfected DLKP cells. VP16 was exposed to the cells at a 30ηg/ml concentration overnight – this is also the concentration at which VP16 has previously increased expression of several genes (Section 3.2). As for the BrdU-treated cells, expression of luciferase increased four-fold in the -411 transfected DLKP, while expression levels were markedly decreased in the -91 transfected cells. This result would appear to indicate that VP16 also targets this area of the MRP1 promoter in positively regulating expression of the gene, again accompanied by the attendant decrease in luciferase production from the –91 promoter plasmid. No significant changes were observed for the other fragments.

3.4.7 Correlation of *Transfac*™ data, MRP1 promoter transfections and RT-PCR results

From the results shown in this Section on the BrdU-affected genes, it was hypothesised that BrdU may be exerting an upregulation effect on the expression of GATA-2 or GATA-3 leading to an increase in expression of, among others, the MRP1 gene. The MRP1 promoter transfections localised the most likely site targetted by the BrdU to a region of the MRP1 promoter between –91 and –411 bases back from the transcriptional start site. A re-examination of the *Transfac*™ recognition site data for this 320 base region revealed a solitary potential recognition site for the GATA-2 transcription factor (M00076), as well as other potential binding sites for the common factors MZF1 (M00083), CdxA (M00101) and AML-1a (M00271). A schematic map of this area of the 5' MRP1 promoter showing the location and orientation of the potential relevant binding sites for transcription factors is displayed in Fig. 3.4.17.

Fig. 3.4.16: Effect of VP16 exposure on luciferase expression in MRP1 Promoter-transfected DLKP cells

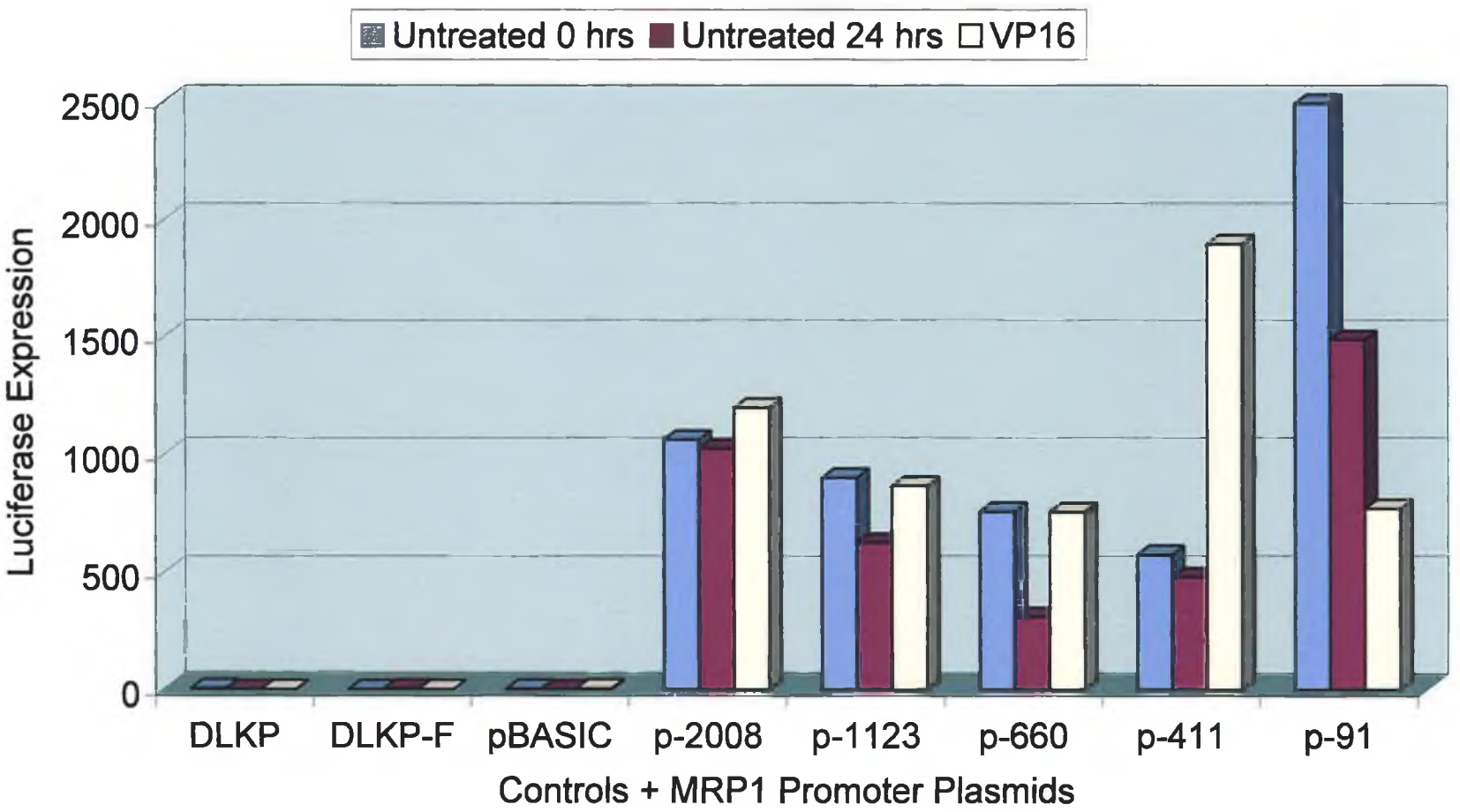

Fig. 3.4.17: MRP1 5' Promoter sequence

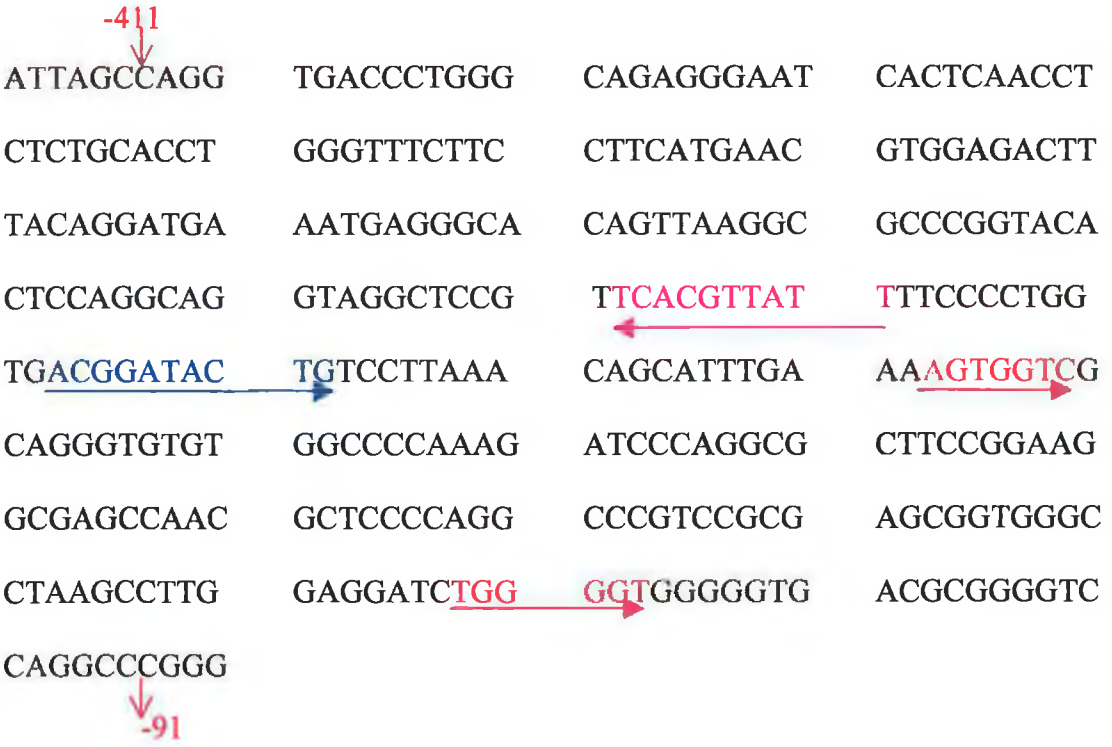

Fig. 3.4.17: Sequence of MRP1 5' promoter from bases –91 to –411 (relative to the transcriptional start) containing transcription recognition sequences for AML-1a (RED), CdxA (PINK) and the solitary GATA-2 recognition factor (BLUE).

3.5 Analysis of BrdU-treated DLKP cells by DNA microarray

From the results presented here (Section 3.1), it is apparent that exposure of cell lines, most notably DLKP, to the differentiating agent BrdU, results in fluctuation of expression of a number of genes normally expressed in that cell line. All of these results were obtained from first optimising PCRs for the different genes, and then carrying out these RT-PCRs on RNA extracted from the BrdU-exposed cells. The choice of genes surveyed was based on "educated guesses" for the identification of genes which may be relevant to drug resistance or differentiation.

The emergence recently, of DNA array technology (see Section 1.8), has made possible the examination of gene expression for a wide variety of genes and proteins with a standardised labour-saving protocol. It was felt that this new technology would be the next logical approach to extend the analysis of the BrdU-treated cell lines in our possession. By using DNA arrays to examine gene expression levels in BrdU-exposed cells, a much larger number of genes could be identified as being either up- or downregulated following treatment with the agent. These results would then be complemented by RT-PCR analysis to confirm gene up- or downregulation. It was felt that this step would be necessary to confirm the efficacy of any results received from the array.

A standard DNA array kit (Clontech, 7851-1) was obtained and used to examine changes in gene expression between normal control DLKP cells and DLKP cells which had been exposed to BrdU for seven days. The seven day sample was chosen for comparison with untreated DLKP cells. The same isolated RNA samples used in the RT-PCRs were used in the DNA array experiment, which was carried out as outlined in Section 2.4.9.

A schematic map of the array and its organisation is provided in Fig. 3.5.1. The type of array used in this experiment was the "Atlas Human Cancer 1.2 Array Gene" array (Clontech, PT3547-3). A total of 597 genes were examined on this array. A complete list of these genes may be obtained from the Clontech website (www. atlas.clontech.com). These genes were divided into roughly six classes, although there

Fig. 3.5.1: Layout of DNA array

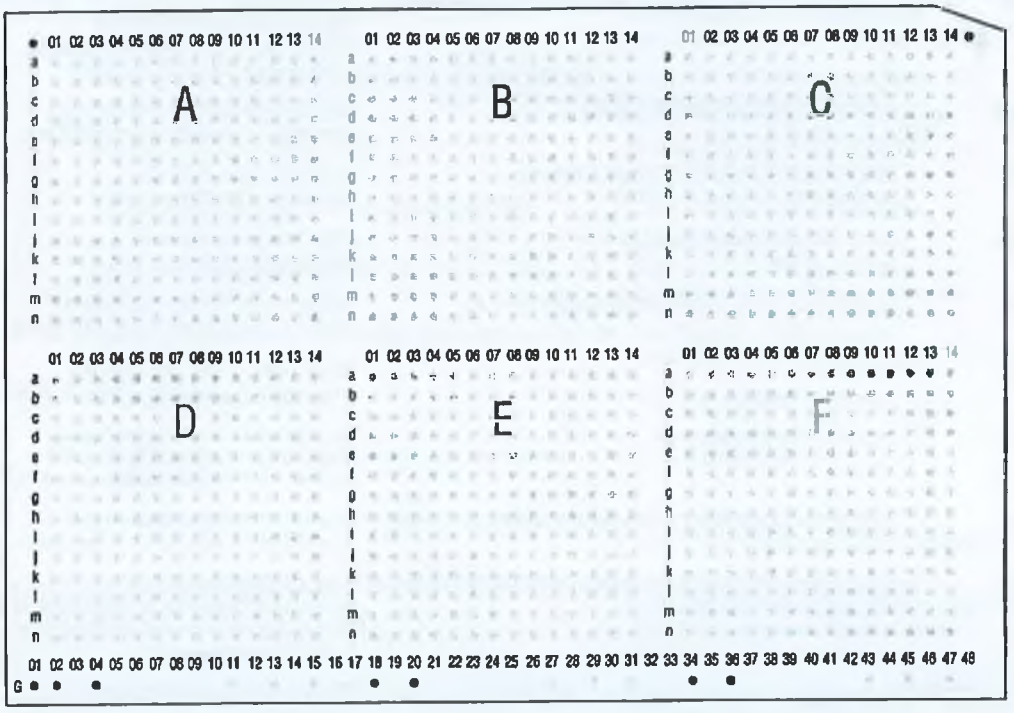

Fig. 3.5.1: Scanned photograph of layout of DNA array.

was a lot of overlap between Sections, arranged by letters, for the experiment. The six classes are outlined in Table 3.5.1:

Table 3.5.1 Groups of genes analysed in BrdU-exposed DLKP RNA

Group	Genes/Proteins
A	Oncogenes, Tumour suppressors and Cell cycle proteins
B	Intracellular kinases and Phosphatases
C	Apoptoic regulators and Transcriptional activators and repressors
D	Cell adhesion receptors and Surface antigens
E	Interleukins, Interferons and Growth factors
F	Functionally unclassified proteins and Housekeeping genes

The results for genes observed to be upregulated in expression, as well as the level of upregulation, is shown in Table 3.5.2. The genes downregulated in expression, again together with the degree of downregulation, are shown in Table 3.5.3. For the sake of simplicity, the level of change in expression has been rounded off to the nearest whole number, which represents 2-, 3- or 4-fold, etc. change in expression of the gene. Also, results of changes in expression which were less than a two-fold increase or decrease following BrdU treatment are not displayed, since these were not considered to be of significance. A scan of the two analysed arrays is provided, for illustration, in Fig. 3.5.2.

This experiment was only carried out once, without duplicates. It is the opinion of this researcher that these results are representative only, and require the repetition of both this array experiment as well as confirmation via RT-PCR of the mentioned changes in gene expression before they may be taken seriously. All lab manipulations were carried out by John Cahill and I. All computer analysis was carried out by Dr. Niall Barron.

Fig. 3.5.2: Scan of DNA array of BrdU-treated DLKP cells

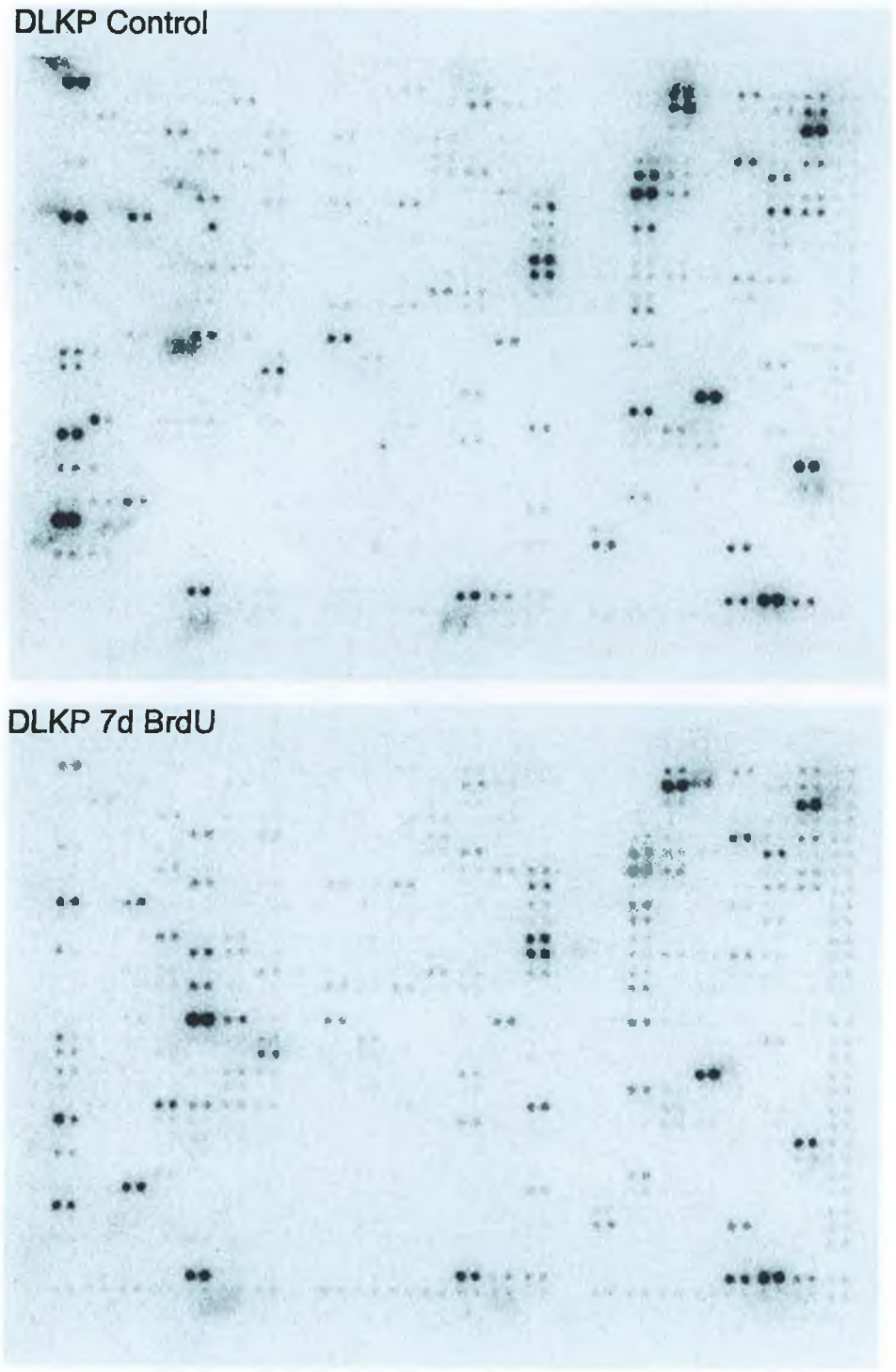

Fig. 3.5.2: Scanned photograph of DNA array results on BrdU-treated DLKP cells at Day 0 (DLKP Control) and Day seven (DLKP 7d BrdU).

Table 3.5.2 Genes upregulated in DLKP after seven days BrdU exposure

Protein/Gene	-Fold Increase
Early growth response protein 1 (hEGR1); transcription factor ETR103; KROX24; zinc finger protein 225; AT225	11
p55CDC	8
Ini1	8
Nuclease-sensitive element DNA-binding protein (NSEP)	7
EB1 protein	7
40S ribosomal protein S19 (RPS19)	4
Fibronectin receptor beta subunit (FNRB); integrin beta 1 (ITGB1); VLA4 beta subunit; CD29 antigen	3
DNA-binding protein inhibitor ID-1; Id-1H	2
70-kDa heat shock protein 1 (HSP70.1; HSPA1)	2
Mitogen-activated protein kinase p38 (MAP kinase p38); cytokine suppressive anti-inflammatory drug binding protein (CSAID binding protein; CSBP); MAX-interacting protein 2 (MXI2)	2
Growth arrest and DNA-damage-inducible protein 153 (GADD153); DNA-damage-inducible transcript 3 (DDIT3); C/EBP homologous protein (CHOP)	2
Glutathione S-transferase pi (GSTP1; GST3)	2
Alpha1-catenin (CTNNA1); cadherin-associated protein; alpha E-catenin	2
27-kDa heat-shock protein (HSP27); stress-responsive protein 27 (SRP27); estrogen-regulated 24-kDa protein; HSPB1	2
Hepatoma-derived growth factor (HDGF)	2
Guanine nucleotide-binding protein G-s alpha subunit (GNAS); adenylate cyclase-stimulating G alpha protein	2

Table 3.5.2 shows the genes upregulated in the DLKP cells following seven days exposure to BrdU. As can be seen, a total of sixteen genes out of 597 were upregulated in response to the differentiating agent. The most significant increase was in the transcription factor ETR103, whose expression increased eleven-fold after seven days

exposure to BrdU. Other highly significant increases were observed for p55CDC and Ini1 (both eight-fold) and for the Nuclease-sensitive element DNA-binding protein (NSEP) and EB1 protein (both seven-fold).

Table 3.5.3 Genes downregulated in DLKP after seven days BrdU exposure

Protein/Gene	-Fold Decrease
CAMP-dependent transcription factor ATF-4; DNA-binding protein TAXREB67; cAMP-response element binding protein (CREB2)	7
c-*myc* oncogene	7
60S ribosomal protein L6 (RPL6); TAX-responsive enhancer element binding protein 107 (TAXREB107); neoplasm-related protein C140	5
Transcription initiation factor IID; TATA-box factor; TATA sequence-binding protein (TBP)	4
Cellular nucleic acid binding protein (CNBP); sterol regulatory element-binding protein	3
DNA-binding protein HIP116; ATPase; SNF2/SWI2-related protein	3
GA-binding protein beta-2 subunit (GABP-beta2); transcription factor E4TF1-60	3
Cytosolic superoxide dismutase 1 (SOD1)	2
Activator 1 37-kDa subunit; replication factor C 37-kDa subunit (RFC37); RFC4	2
N-ras; transforming p21 protein	2
DNA-dependent protein kinase (DNA-PK) + DNA-PK catalytic subunit (DNA-PKCS)	2
Octamer-binding transcription factor 2 (oct-2; OTF2); lymphoid-restricted immunoglobulin octamer binding protein NF-A2; POU2F2	2
Vascular endothelial growth factor precursor (VEGF); vascular permeability factor (VPF)	2
CACCC-box DNA-binding protein	2
Signal transducer and activator of transcription 6 (STAT6); IL-4 STAT	2
v-erbA related protein (EAR3); COUP transcription factor (COUP-TF)	2
Glutathione S-transferase mu1 (GSTM1; GST1); HB subunit 4; GTH4	2
Neuroleukin (NLK); glucose-6-phosphate isomerase (GPI); phosphoglucose Isomerase (PGI); phosphohexose isomerase (PHI)	2
ERBB-3 receptor protein-tyrosine kinase precursor; epidermal growth factor receptor	2
acyl-CoA-binding protein (ACBP); diazepam binding inhibitor (DBI)	2

Table 3.5.3 shows the genes downregulated in the DLKP cells following seven days exposure to BrdU. As can be seen, twenty genes out of a total of 597 were decreased in expression in response to the differentiating agent. The most significant decreases were in cAMP-response element binding protein (CREB2) and the c-*myc* oncogene (both seven-fold) after seven days exposure to BrdU. Other significant decreases were in the 60S ribosomal protein L6 (RPL6) (five-fold) and Transcription initiation factor IID (four-fold).

Only five genes assayed for changes in expression in the BrdU-exposed DLKP using RT-PCR (Section 3.1.1) were also analysed using the array. These five genes, along with their fold increase (+) or decrease (-) in expression and location within the DNA array can be seen in Table 3.5.4.

Table 3.5.4Genes examined in BrdU-DLKP array also examined using RT-PCR

Array Position	Protein/Gene	-Fold Change
A1a	c-myc oncogene	7 (-)
C2h	Apoptosis regulator bax	-
C3e	Apoptosis regulator bcl-x	-
C4b	Apoptosis regulator bcl-2	-
E5g	alpha1 catenin (CTNNA1)	2 (+)

Finally, a number of housekeeping genes were included on the array to standardise the amount of RNA analysed on each array, and also to provide a control for those samples against which changes in gene expression could be compared. While the majority of the housekeeping genes remained the same from the first array to the second, two of these genes were observed upregulated in expression in the seven-day BrdU-treated DLKP RNA sample. These two genes, along with their respective degree of upregulation are listed in Table. 3.5.5.

Table. 3.5.5 Housekeeping genes upregulated by BrdU in DLKP cells

Housekeeping gene	-Fold Increase
Ubiquitin (Stress response protein)	3
Cytoplasmic beta-actin (ACTB) (Cytoskeleton protein)	2

3.6 Analysis of gene expression in human clinical tissue samples

3.6.1 Introduction to the clinical study group

It has been shown from the literature that the expression of certain genes may play a significant role in tumour growth and progression (e.g. Nooter *et al.*, 1998, etc.). The purpose of this study was twofold:

1. To ascertain if a reliable method of RNA isolation from human tumours could be achieved and also if subsequent analysis of that RNA using RT-PCR and/or other methods yielded results which were clear-cut and reproducible.
2. To investigate the clinical importance of the genes examined in the BrdU- and drug-exposed DLKP and A549 cells.

The types of tissue examined were primary lung, breast and oesophageal tumour samples with accompanying normal controls. A number of lymph node samples were also investigated, so as to correlate the expression results of metastasised tissue compared to their corresponding unmetastasised primary tumour. To this end, the lymph node samples required were those from patients whose primary tumours had already been donated. It is important to not at this point that tissue samples were not microdissected upon delivery, so the analysed tissues may comprise a mix of tumourigenic and non-tumourigenic material.

A total of fifty human tissue samples were obtained from St. Vincent's Hospital, Dublin over the months January to May 1999. The tissue breakdown was: eighteen single tumour samples, two mediastinal lymph node samples and fifteen tumour/normal sample pairs. The samples were stored at $-80^{\circ}C$ until ready for RNA isolation. RNA was isolated as described in Section 2.4.6. and the samples subjected to RT-PCR analysis. RT-PCR results were visualised using gel electrophoresis and densitometry.

In order that the study be as unbiased as possible, the samples were received without any form of clinical information and as such were analysed on agarose electrophoresis gels without regard to their origin or tumour type. As a result, the gel photographs presented here display the gene expression results of the different types of tissue which

were supplied. There were a number of different tissue types supplied, which for clarity, have been divided here into five distinct classes, in descending order of importance to this survey. These classes of tissue are:

- Primary lung
- Primary breast
- Primary oesophageal
- Metastasised lung tumour tissue, mediastinal lymph node samples, metastasised breast tumour tissue
- Normal non-carcinoma tissue.

A large number of the tissue samples (seventeen) supplied were from secondary (metastasised) tumours. As such, these tumours could not be classified as being of lung, breast or oesophageal origin and were classified separately to the primary tissue samples obtained. As well, neither of the mediastinal lymph node samples corresponded to any primary tumours supplied and as such, these tissues constitute another group of metastasised tissue. Finally, a total of five tissue samples were classified as non-carcinoma in origin.

Therefore, the survey group comprises the following five categories:

1. Four single primary lung tumour samples and ten primary lung tumour/normal sample pairs.
2. Two single primary breast tumour samples.
3. Two single primary oesophageal tumour samples.
4. Metastasised lung tumour (five single tumour samples, two mediastinal lymph nodes, three tumour/normal sample pairs) and metastasised breast tumour (two single tumour samples, one tumour/normal sample pair),
5. Tissue of non-carcinoma origin (one duodenal tissue sample, one empyema strip decortication sample, three non-malignant bronchial resection samples from pneumonal patients).

As a result, the study group comprised a total of twenty-two separate RT-PCRs carried out on fifty tissue samples, which yielded a total of eleven hundred individual results. These are broken up into the various categories as illustrated in Table 3.6.1.

Table 3.6.1 Amounts of PCR results obtained per analysis category

Analysis Category	No. of samples	RT-PCR results per category
Primary Lung	24	528
Primary Breast	2	44
Primary Oesophageal	2	44
Metastasised tissue	17	374
Non-carcinoma tissue	5	110

Each tissue sample was given a particular nomenclature indicating in what order it was received and whether the reference pertains to a single tumour sample (T), a tumour/normal sample pair (T/N), oesophageal primary sample (O) or a mediastinal lymph node (LN) sample. Other classifications include; ESD - empyema strip decortication and D – Duodenal sample).

Also, the relative expression level of each gene was determined by densitometry, which is unitless (as explained in Section 2.4.2.7). For reasons of simplicity, the levels of gene expression observed were divided into Low, Medium and High ranges, which reflect the densitometric levels measured. Average expression levels for each gene were surveyed and these divisions were decided upon arbitrarily. The limits of these ranges are outlined in Table 3.6.2.

The criteria for estimation of mdr-3 expression are not available as no sample was observed to express this gene. The gene expression and clinical data for all twenty-two genes is included in Tables 7.1B - 7.10B in Appendix B. The expression data for the normal samples is printed in bold lettering to distinguish these samples from tumourigenic tissue. In sample pairs which differ in expression levels but not by a large enough margin to exceed the ranges decided here, a "+" will denote which of the two tissues was expressed to a higher level.

Also, in Figs. 3.6.1 – 3.6.42, the different classes of tissue were assigned colours to distinguish one from another. Lung primary tissue samples are RED, Breast primary are BLUE, Oesophageal primary are ORANGE, Metastasised tissue is GREY and Non-carcinoma tissue is NAVY.

Table 3.6.2 Criteria for identifying the different categories of gene expression

	LOW	MEDIUM (MED)	HIGH
MRP1	<0.15	0.15-0.4	>0.4
MRP2	<0.1	0.1-0.3	>0.3
MRP3	<2	2-4	>4
MRP4	<0.5	0.5-1	>1
MRP5	<0.1	0.1-0.2	>0.2
MRP6	<1	1-2	>2
Mdr-1	<0.2	0.2-0.4	>0.4
BCRP	<0.04	0.04-0.1	>0.1
Mdr-3	N/A	N/A	N/A
COX-1	<0.2	0.2-0.4	>0.4
COX-2	<0.2	0.2-1	>1
BAP	<1	1-4	>4
BAXα	<0.2	0.2-0.6	>0.6
MRIT	<1	1-1.5	>1.5
Bcl-x_S	<0.1	0.1-0.15	>0.15
Bcl-x_L	<1.5	1.5-2	>2
Bcl-2α	<0.5	0.5-1	>1
BAG	<2	2-4	>4
Survivin	<1	1-1.5	>1.5
eIF-4E	<2	2-6	>6
eIF-2α	<5	5-15	>15
c-*myc*	<0.015	0.015-0.03	>0.03

3.6.2 RT-PCR expression results for Primary Human Lung Tissue samples

This was the most important study group as it was the only sample group of reasonable size composed solely of confirmed primary tumour samples. The group comprised of ten lung tumour samples with normal controls, and four lung tumour samples without controls. The gene expression data for these samples is included in Table 7.1B in

Appendix B. A complete list of these sample numbers as used in the survey is provided in Table 3.6.3.

Table 3.6.3 List of Primary Lung tissue samples

Sample Name	Sample Tissue Type
1 T	Single Tumour only
2 T	Single Tumour only
3 T	Single Tumour only
12 T	Single Tumour only
16 T/N	Tumour with Normal tissue control
17 T/N	Tumour with Normal tissue control
18 T/N	Tumour with Normal tissue control
19 T/N	Tumour with Normal tissue control
21 T/N	Tumour with Normal tissue control
22 T/N	Tumour with Normal tissue control
23 T/N	Tumour with Normal tissue control
25 T/N	Tumour with Normal tissue control
B5 T/N	Tumour with Normal tissue control
B6 T/N	Tumour with Normal tissue control

3.6.2.1 MRP1

The results of these RT-PCRs can be seen in Figs. 3.6.1 and 3.6.2. MRP1 expression was detected in twenty-two of the twenty-four primary lung tissue samples assayed (>91%). Expression was detected in three of the four tumour samples without controls. In the tumour/normal sample set, MRP1 expression was detected in every sample except one. Overall, MRP1 expression was observed to be higher in the tumour sample relative to the normal in five of the ten tumour/normal sample pairs (50%). Another sample pair expressed identical amounts of the gene in both tissues, while the remaining four pairs (40%) express higher amounts of the gene in the normal tissue.

Fig. 3.6.1: MRP1 RT-PCR on Tumour tissue samples

Fig. 3.6.1a:

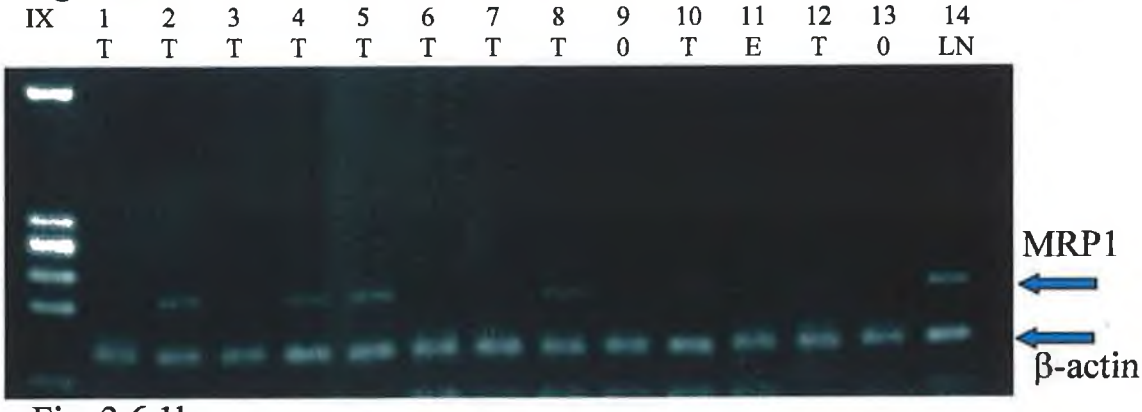

Fig. 3.6.1b:

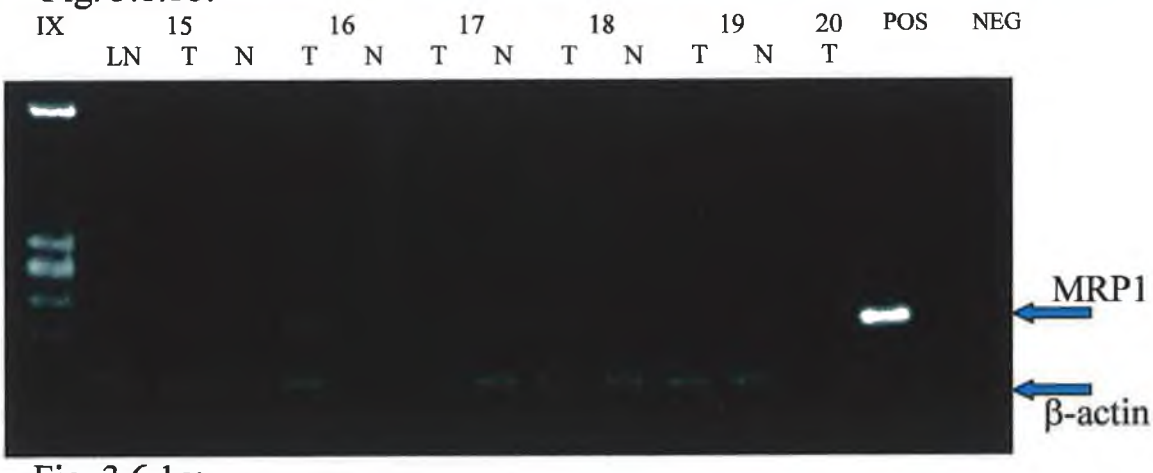

Fig. 3.6.1c:

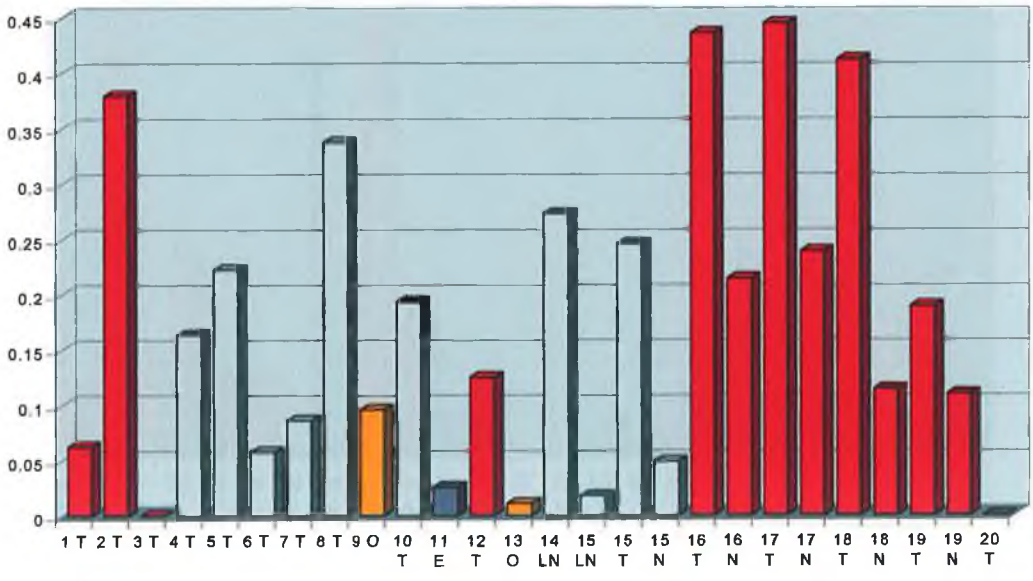

Figs. 3.6.1a & b: Gel electrophoresis photographs of MRP1 RT-PCR results on Lung Primary (RED), Oesophagus Primary (ORANGE), Metastatic (GREY) & Non-carcinoma (NAVY) tissue samples; Fig. 3.6.1c: Densitometry of RT-PCR results.

3.6.2.2 MRP2 (cMOAT)

The results of these RT-PCRs can be seen in Figs. 3.6.3 and 3.6.4. MRP2 expression was observed at a mainly low level in nineteen of the twenty-four samples studied (>71%). Three of the four tumour samples without controls were observed to express the MRP2 gene at a low level. Expression levels of the gene were higher in the tumour samples relative to their normal controls in four (40%) tumour/normal sample pairs. Normals expressed higher amounts of the gene in three sample pairs (30%), while three other sample pairs (30%) expressed identical amounts of the gene in both tissues.

3.6.2.3 MRP3

The results of these RT-PCRs can be seen in Figs. 3.6.5 and 3.6.6. MRP3 expression was detected in twenty-three of the twenty-four lung tissue samples assayed (96%). Expression was generally observed to be of a low level in most of these samples. All four lung tumour samples without controls expressed the gene at this low level. Four of the ten tumour/normal sample pairs (40%) expressed higher amounts of the gene in the tumour sample relative to their corresponding normal equivalent, while three pairs (30%) expressed higher amounts in the normal sample. A further three sample pairs (30%) expressed identical amounts of the gene in both tissues.

3.6.2.4 MRP4

The results of these RT-PCRs can be seen in Figs. 3.6.7 and 3.6.8. MRP4 expression was observed in fifteen of the twenty-four (>62%) lung tissue sample specimens. Expression of the gene was observed in all four of the tumour specimens without normals. In the tumour/normal sample pairs, three pairs (30%) did not express the gene in either sample. In the seven sample pairs which were observed to express MRP4, expression was observed to be higher in the tumour sample in five of these seven pairs (>70%). In only two sample pairs (<30%) was expression of the gene higher in the normal sample relative to the tumour.

Fig. 3.6.3: MRP2 RT-PCR on Tumour tissue samples

Fig. 3.6.3a:

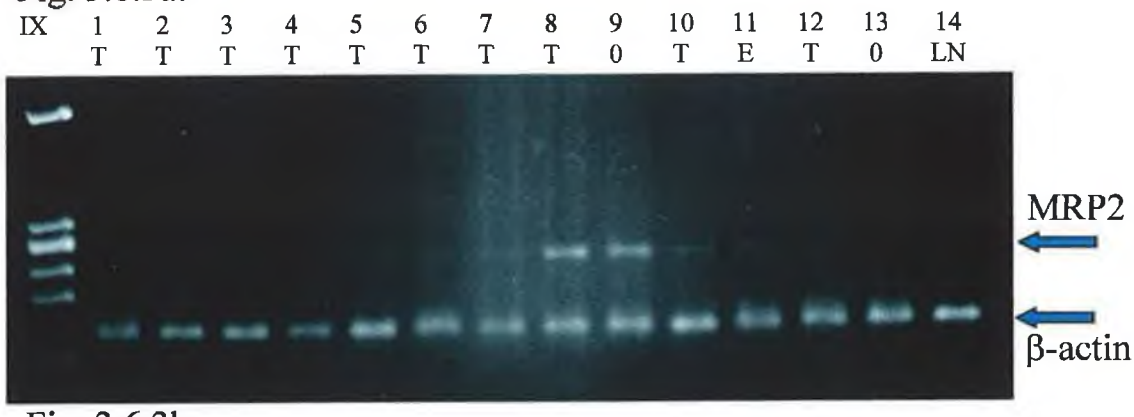

Fig. 3.6.3b:

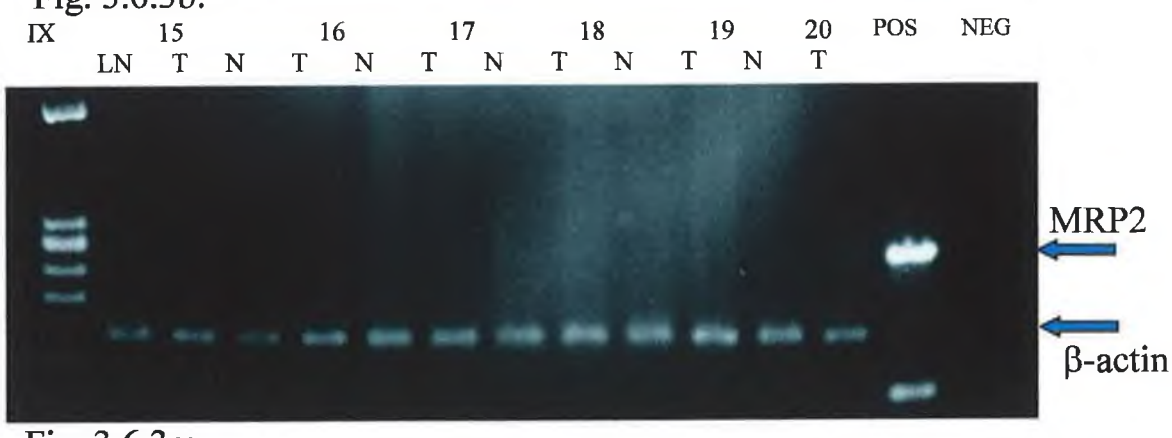

Fig. 3.6.3c:

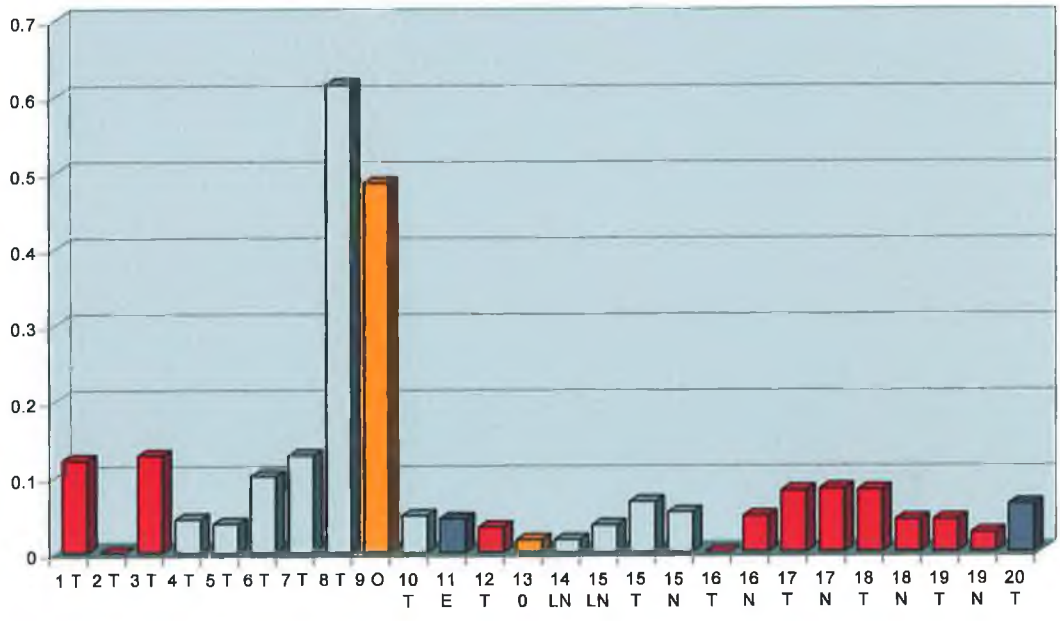

Figs. 3.6.3a & b: Gel electrophoresis photographs of MRP2 RT-PCR results on Lung Primary (RED), Oesophagus Primary (ORANGE), Metastatic (GREY) & Non-carcinoma (NAVY) tissue samples; Fig. 3.6.3c: Densitometry of RT-PCR results.

Fig. 3.6.4: MRP2 RT-PCR on Tumour tissue samples

Fig. 3.6.4a:

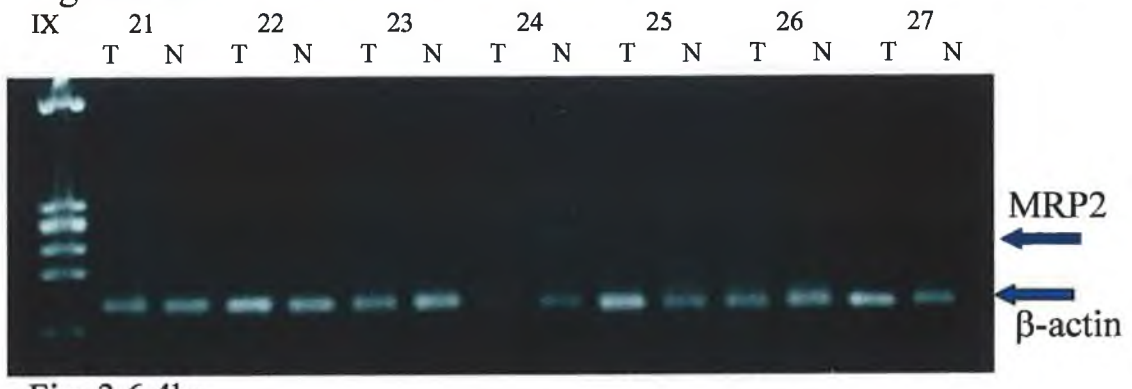

Fig. 3.6.4b:

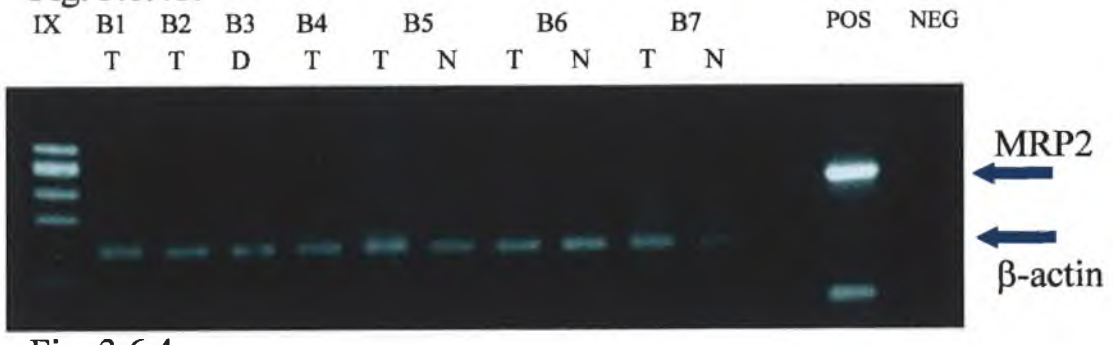

Fig. 3.6.4c:

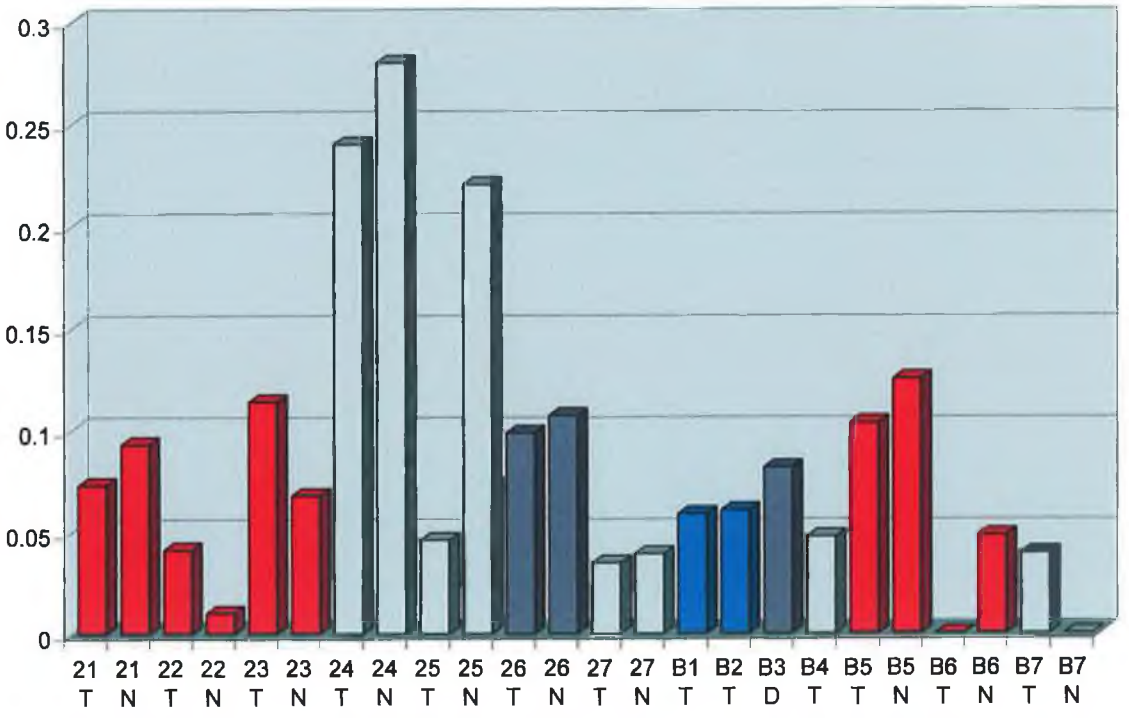

Figs. 3.6.4a & b: Gel electrophoresis photographs of MRP2 RT-PCR results on Lung Primary (RED), Breast Primary (BLUE), Metastatic (GREY) tissue samples & Non-carcinoma (NAVY) tissue samples; Fig. 3.6.4c: Densitometry of RT-PCR results.

Fig. 3.6.5: MRP3 RT-PCR on Tumour tissue samples

Fig. 3.6.5a:

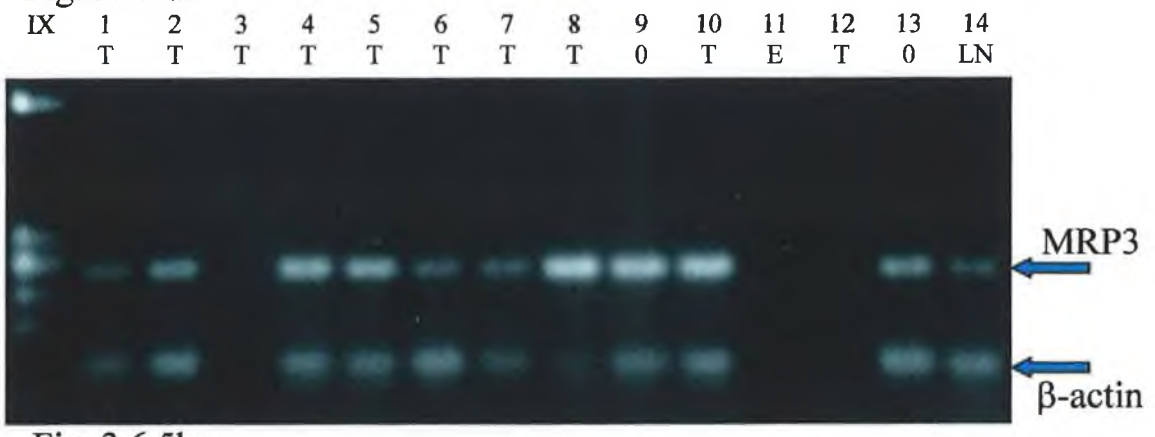

Fig. 3.6.5b:

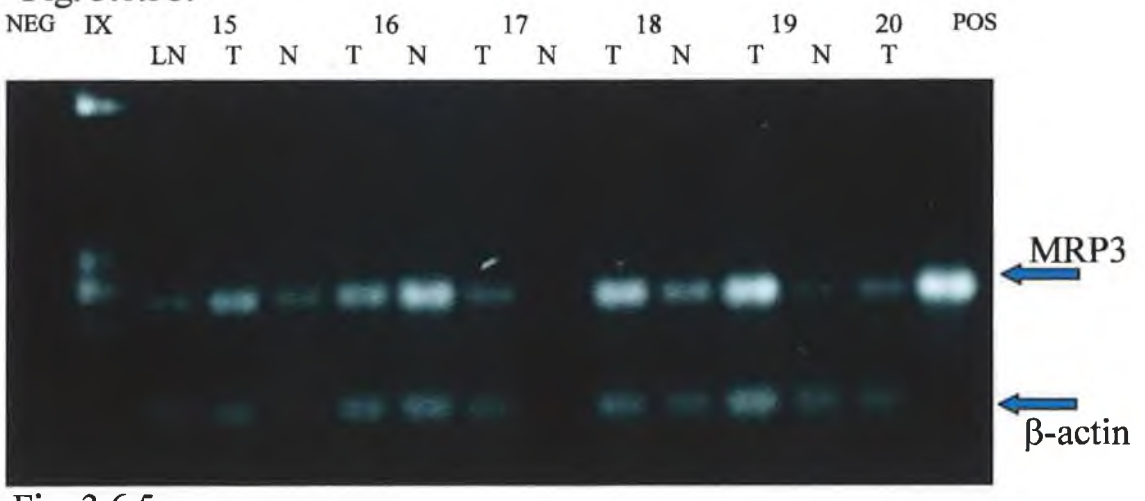

Fig. 3.6.5c:

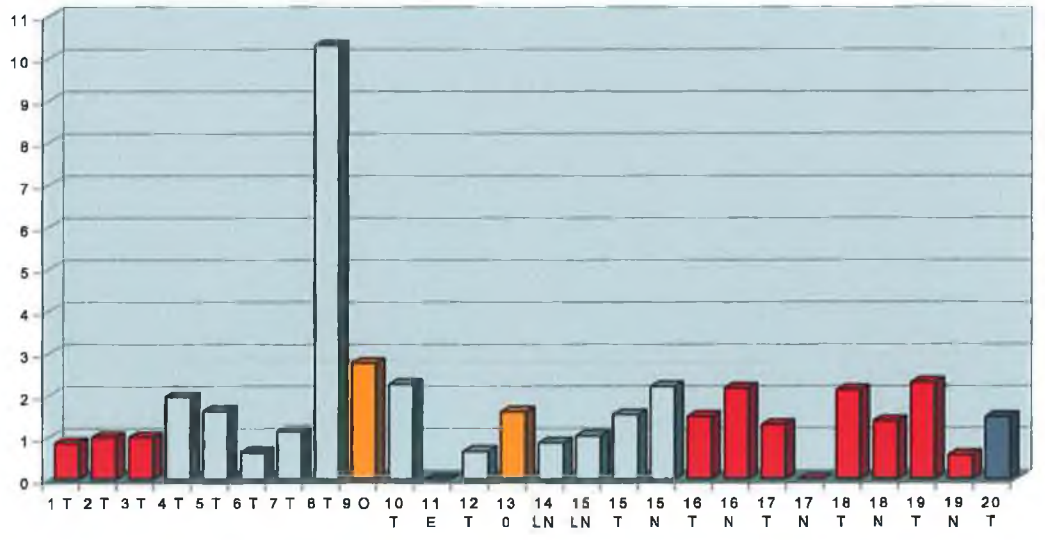

Figs. 3.6.5a & b: Gel electrophoresis photographs of MRP3 RT-PCR results on Lung Primary (RED), Oesophagus Primary (ORANGE), Metastatic (GREY) & Non-carcinoma (NAVY) tissue samples; Fig. 3.6.5c: Densitometry of RT-PCR results.

Fig. 3.6.6: MRP3 RT-PCR on Tumour tissue samples

Fig. 3.6.6a:

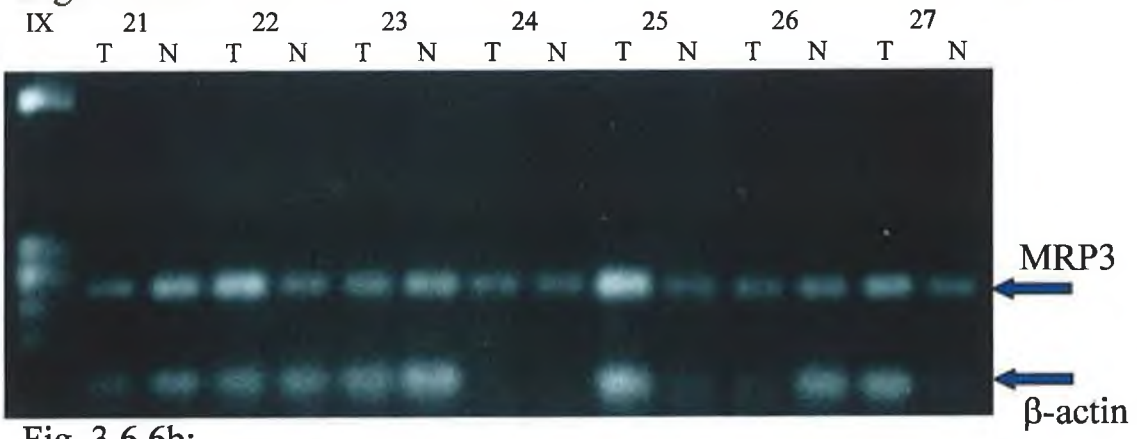

Fig. 3.6.6b:

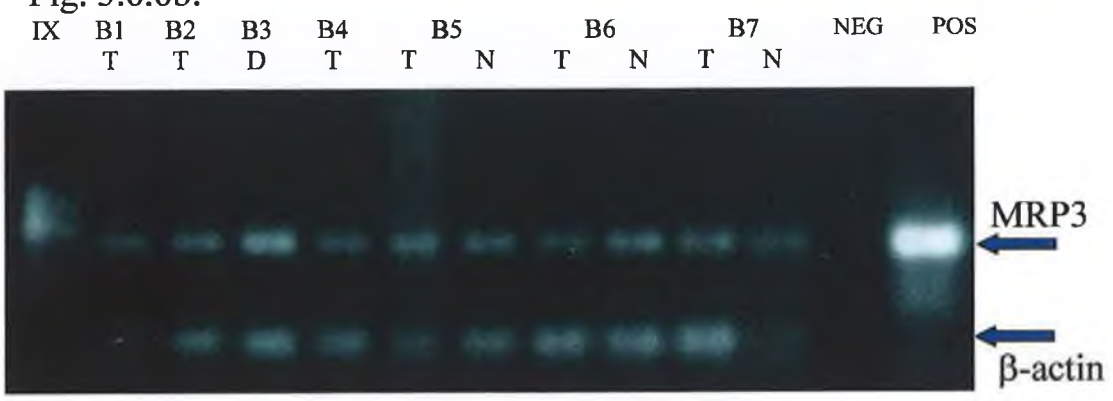

Fig. 3.6.6c:

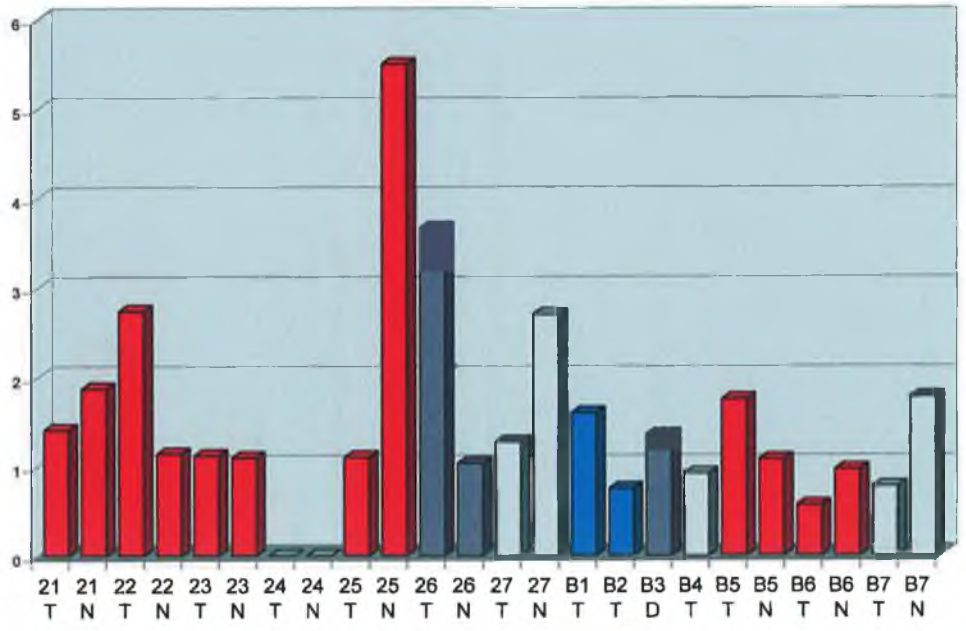

Figs. 3.6.6a & b: Gel electrophoresis photographs of MRP3 RT-PCR results on Lung Primary (RED), Breast Primary (BLUE), Metastatic (GREY) & Non-carcinoma (NAVY) tissue samples; Fig. 3.6.6c: Densitometry of RT-PCR results.

Fig. 3.6.8: MRP4 RT-PCR on Tumour tissue samples

Fig. 3.6.8a:

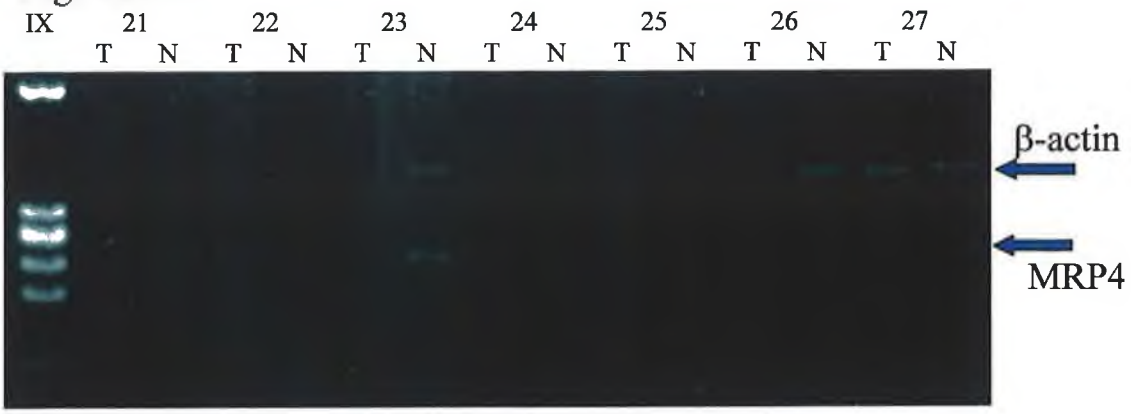

Fig. 3.6.8b:

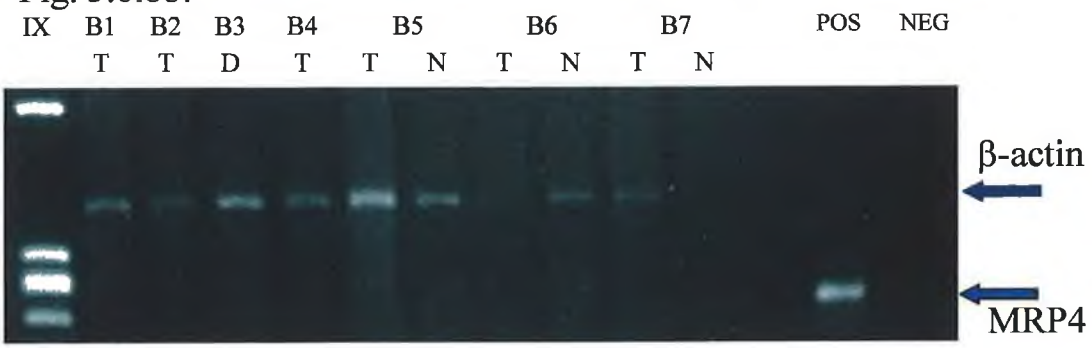

Fig. 3.6.8c:

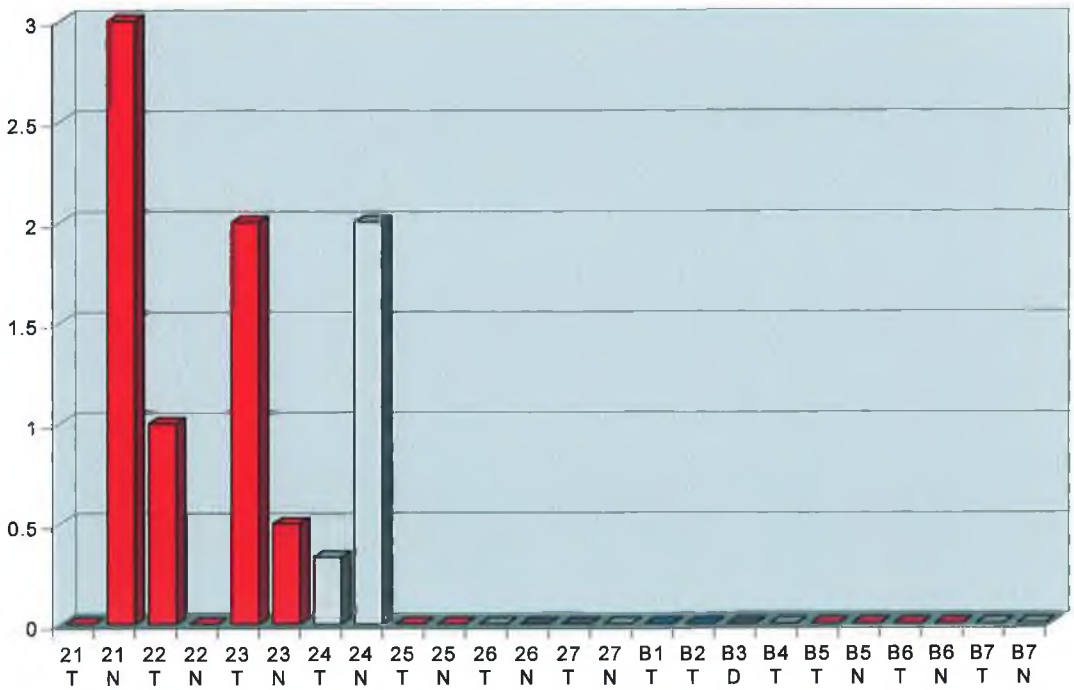

Figs. 3.6.8a & b: Gel electrophoresis photographs of MRP4 RT-PCR results on Lung Primary (RED), Breast Primary (BLUE), Metastatic (GREY) & Non-carcinoma (NAVY) tissue samples; Fig. 3.6.8c: Densitometry of RT-PCR results.

3.6.2.5 MRP5

The results of these RT-PCRs can be seen in Figs. 3.6.9 and 3.6.10. Twenty-two of the twenty-four (>91%) lung tissue samples were observed to express the MRP5 gene. High levels of expression of the gene were observed in two of the four (50%) tumour samples without controls as well as lower expression in a third sample. All of the tumour/normal sample pairs expressed the gene in at least one of the tissues. In these sample pairs, six of the ten pairs (60%) expressed higher amounts of the gene in the tumour sample relative to the normal, while only three pairs (30%) did the opposite. The remaining sample pair expressed identical amounts of the gene in both tissues.

3.6.2.6 MRP6

The results of these RT-PCRs can be seen in Figs. 3.6.11 and 3.6.12. MRP6 expression was observed in twenty-one of the twenty-four (>87%) lung tissue specimens studied. Expression of the gene was observed in all the unpaired tumour samples. All of the tumour/normal sample pairs expressed the gene in at least one of the paired tissues. Of these sample pairs, only two (20%) expressed higher amounts of the gene in the tumour sample relative to the normal control. One other sample pair expressed identical amounts of the gene in both tissues, while the remaining seven sample pairs (70%) expressed more MRP6 in the normal tissue. However, the quality of these PCRs is questionable and care would need to be taken in relying too much on the results obtained for expression of this gene.

3.6.2.7 mdr-1

The results of these RT-PCRs can be seen in Figs. 3.6.13 and 3.6.14. mdr-1 expression was observed in twenty-one of the twenty-four (>87%) lung tissue specimens studied. Expression of the gene was detected in all four of the tumour samples studied without controls. All of the tumour/normal sample pairs expressed the gene in at least one of the tissues. Of these pairs, mdr-1 overexpression in the tumour sample relative to the

Fig. 3.6.9: MRP5 RT-PCR on Tumour tissue samples

Fig. 3.6.9a:

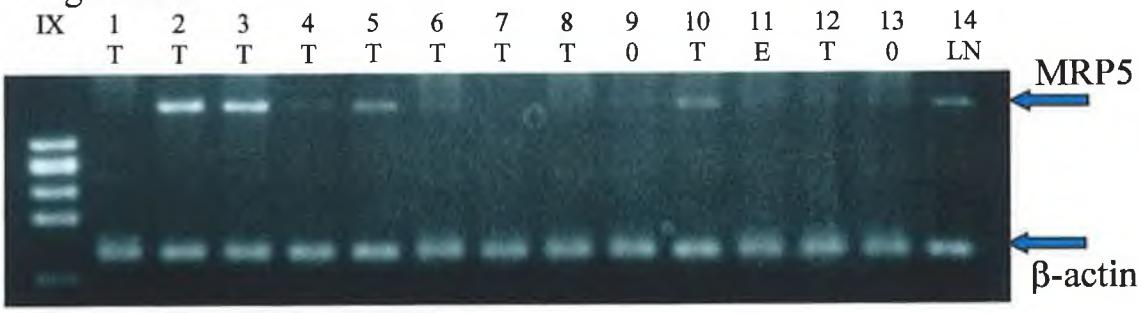

Fig. 3.6.9b:

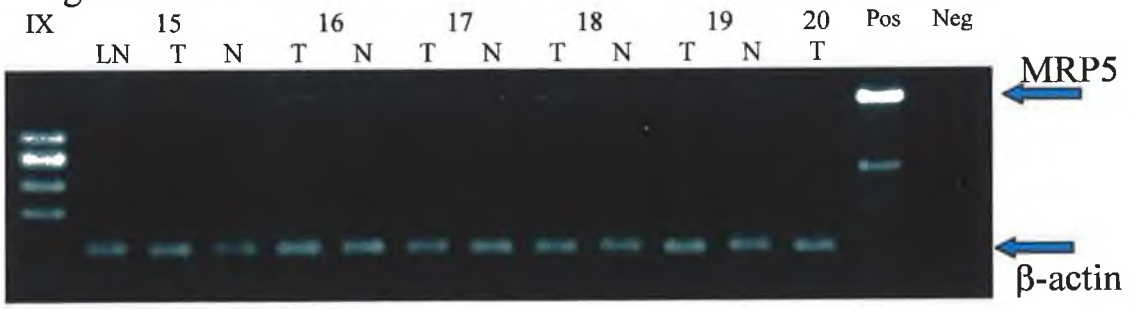

Fig. 3.6.9c:

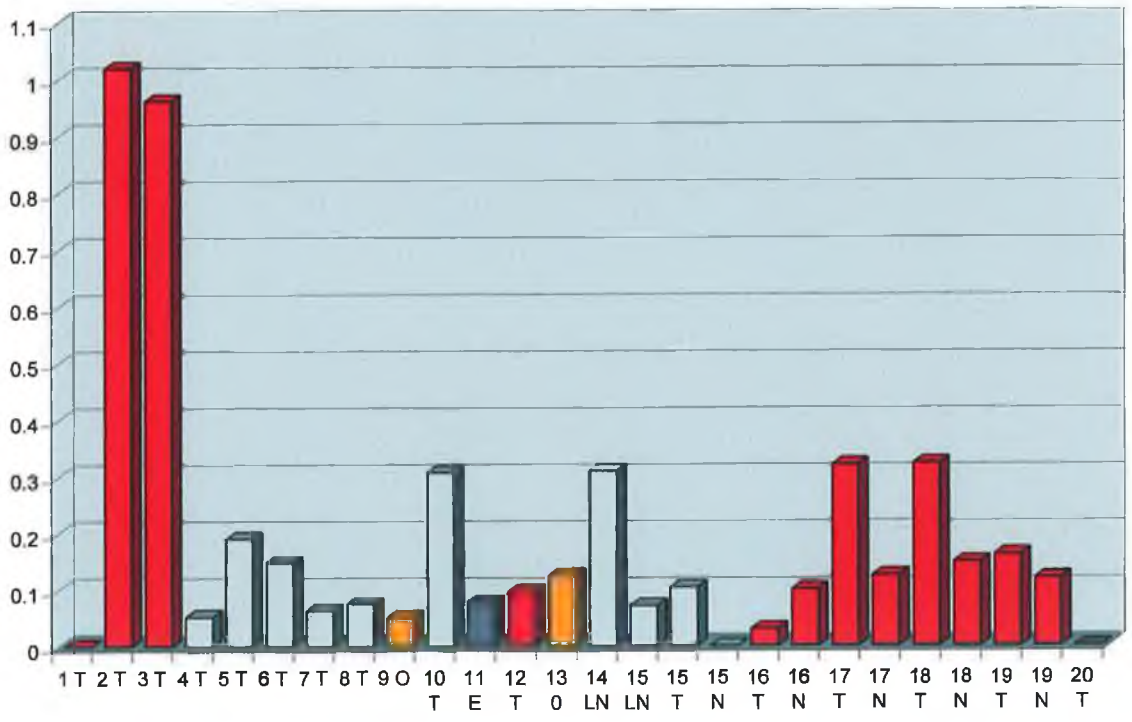

Figs. 3.6.9a & b: Gel electrophoresis photographs of MRP5 RT-PCR results on Lung Primary (RED), Oesophagus Primary (ORANGE), Metastatic (GREY) & Non-carcinoma (NAVY) tissue samples; Fig. 3.6.9c: Densitometry of RT-PCR results.

Fig. 3.6.10: MRP5 RT-PCR on Tumour tissue samples

Fig. 3.6.10a:

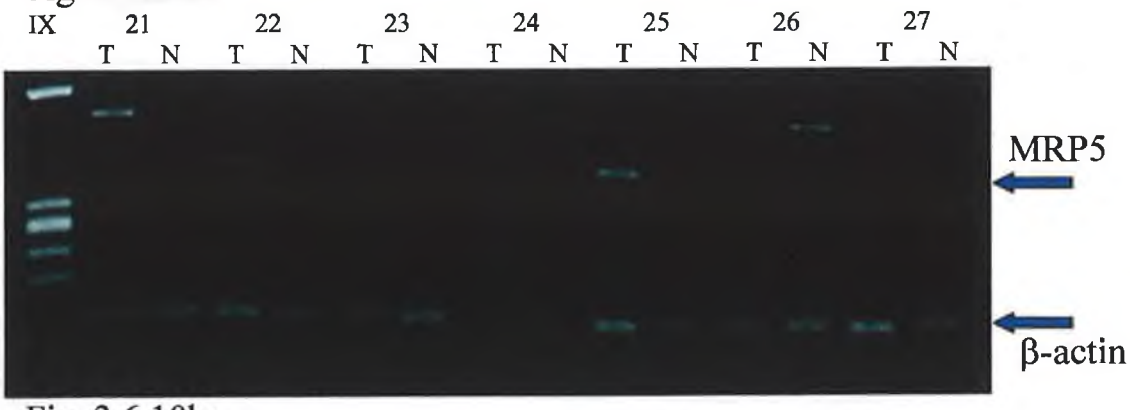

Fig. 3.6.10b:

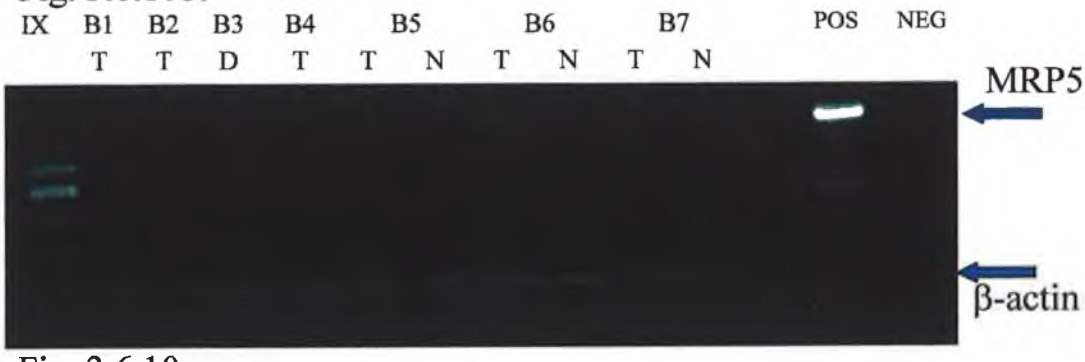

Fig. 3.6.10c:

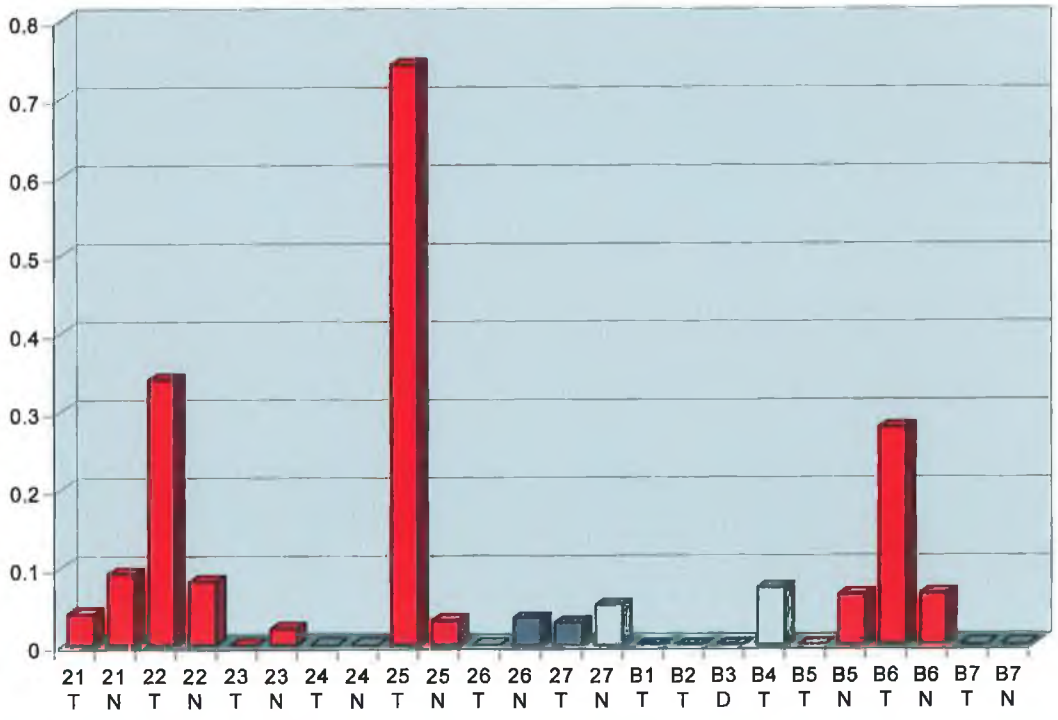

Figs. 3.6.10a & b: Gel electrophoresis photographs of MRP5 RT-PCR results on Lung Primary (RED), Breast Primary (BLUE), Metastatic (GREY) & Non-carcinoma (NAVY) tissue samples; Fig. 3.6.10c: Densitometry of RT-PCR results.

Fig. 3.6.11: MRP6 RT-PCR on Tumour tissue samples

Fig. 3.6.11a:

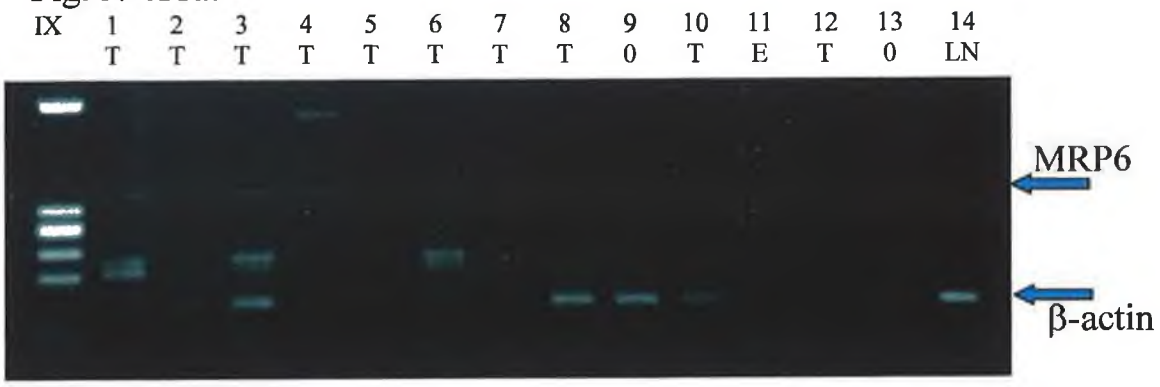

Fig. 3.6.11b:

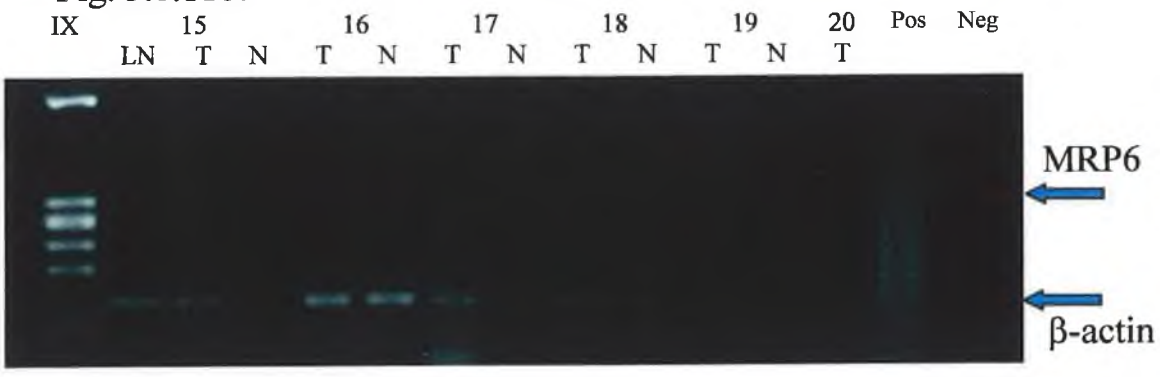

Fig. 3.6.11c:

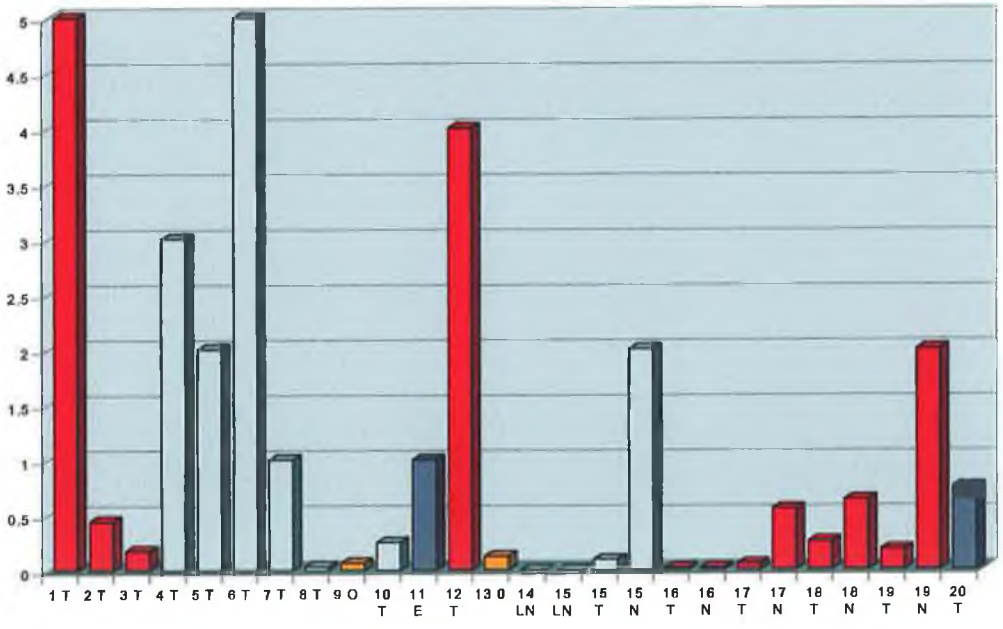

Figs. 3.6.11a & b: Gel electrophoresis photographs of MRP6 RT-PCR results on Lung Primary (RED), Oesophagus Primary (ORANGE), Metastatic (GREY) & Non-carcinoma (NAVY) tissue samples; Fig. 3.6.9c: Densitometry of RT-PCR results.

Fig. 3.6.12: MRP6 RT-PCR on Tumour tissue samples

Fig. 3.6.12a:

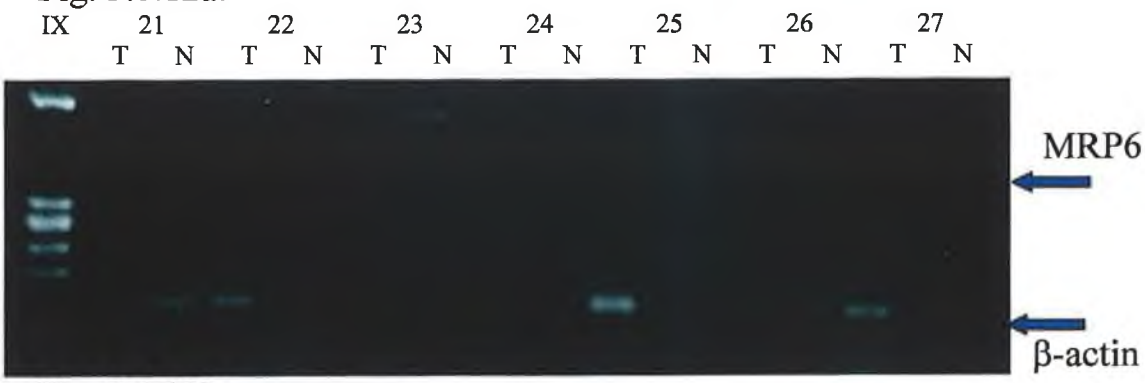

Fig. 3.6.12b:

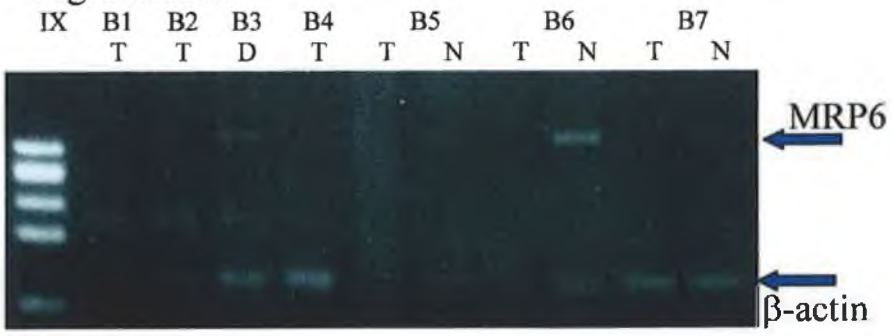

Fig. 3.6.12c:

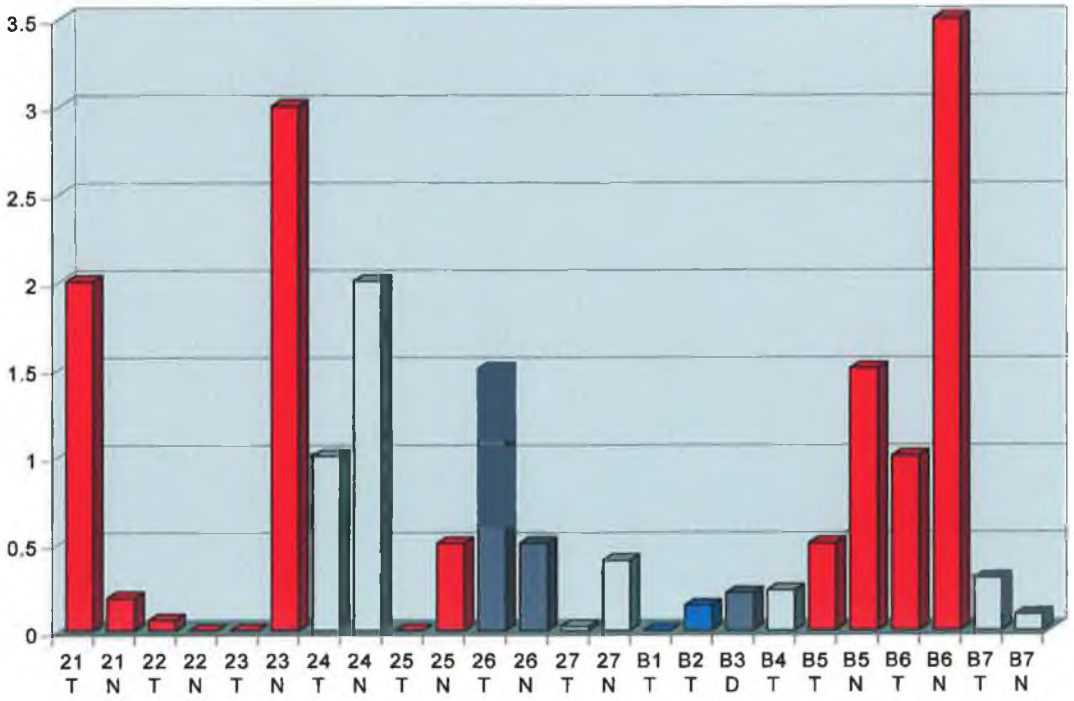

Figs. 3.6.12a & b: Gel electrophoresis photographs of MRP6 RT-PCR results on Lung Primary (RED), Breast Primary (BLUE), Metastatic (GREY) & Non-carcinoma (NAVY) tissue samples; Fig. 3.6.12c: Densitometry of RT-PCR results.

Fig. 3.6.13: mdr-1 RT-PCR on Tumour tissue samples

Fig. 3.6.13a:

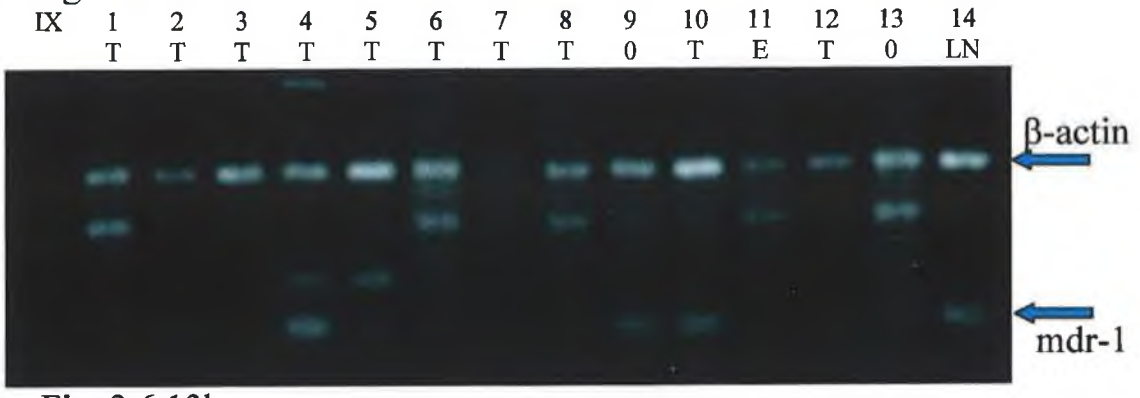

Fig. 3.6.13b:

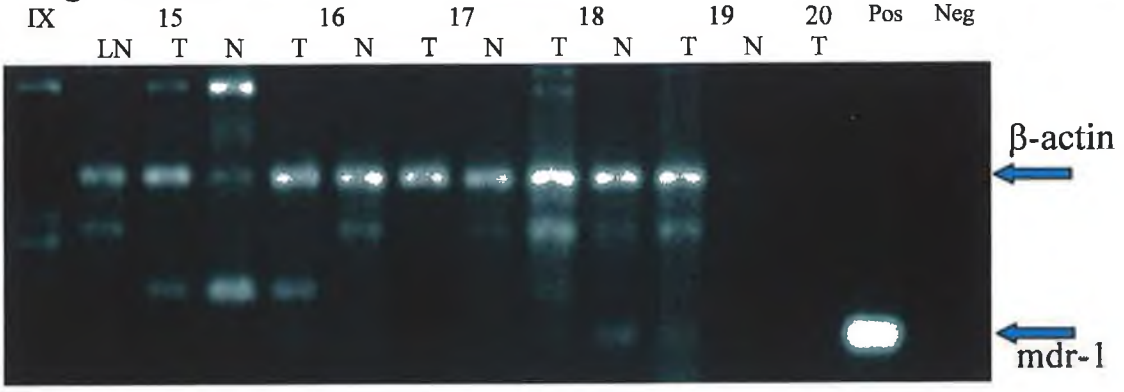

Fig. 3.6.13c:

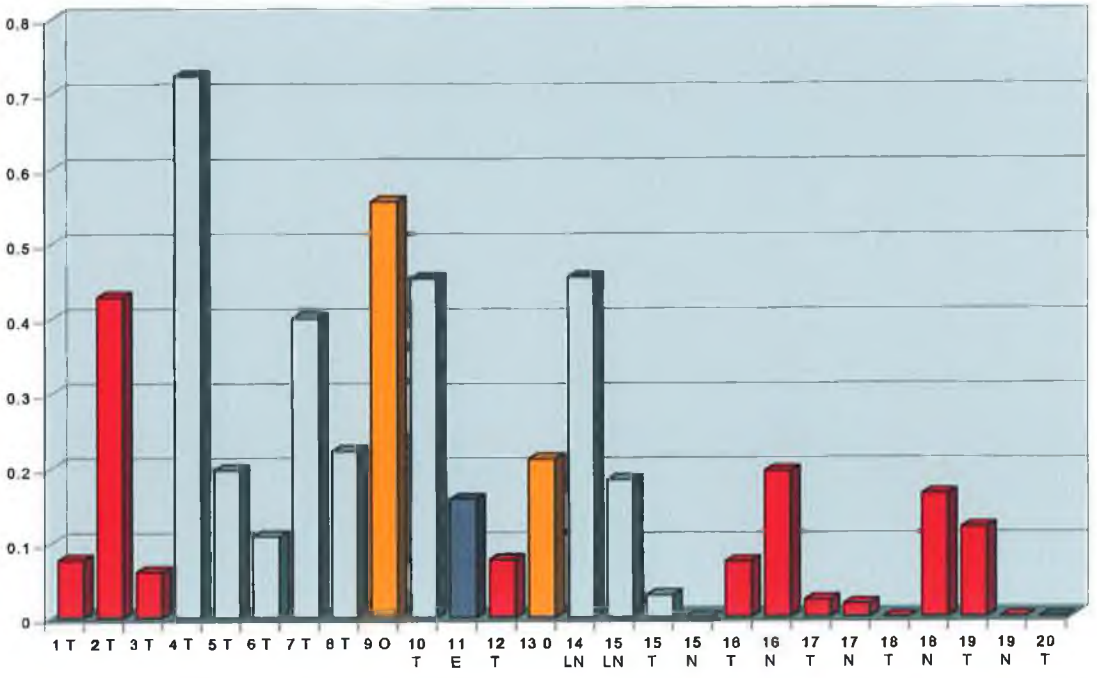

Figs. 3.6.13a & b: Gel electrophoresis photographs of mdr-1 RT-PCR results on Lung Primary (RED), Oesophagus Primary (ORANGE), Metastatic (GREY) & Non-carcinoma (NAVY) tissue samples; Fig. 3.6.13c: Densitometry of RT-PCR results.

Fig. 3.6.14: mdr-1 RT-PCR on Tumour tissue samples

Fig. 3.6.14a:

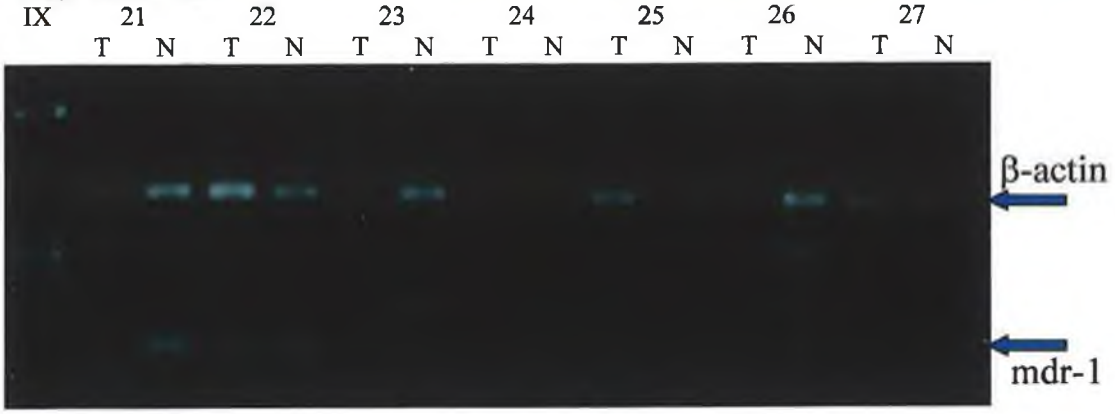

Fig. 3.6.14b:

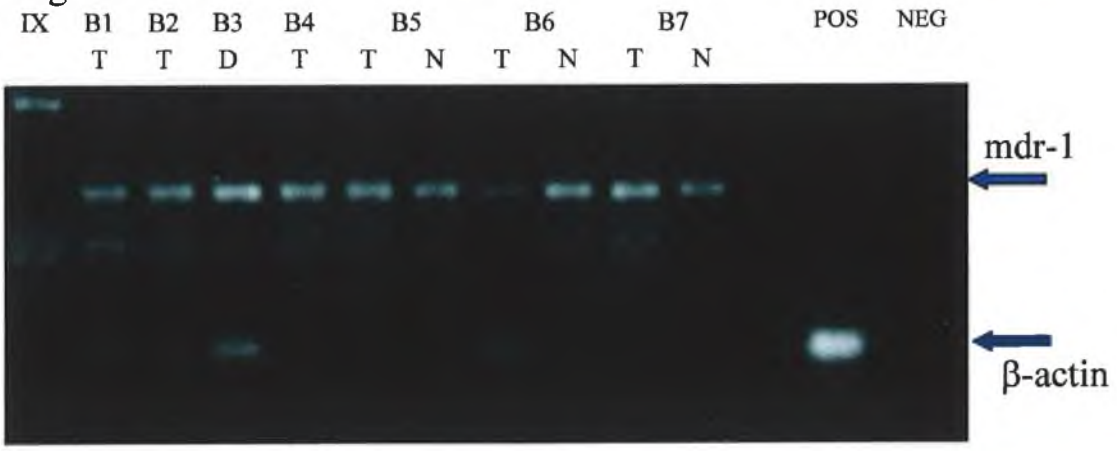

Fig. 3.6.14c:

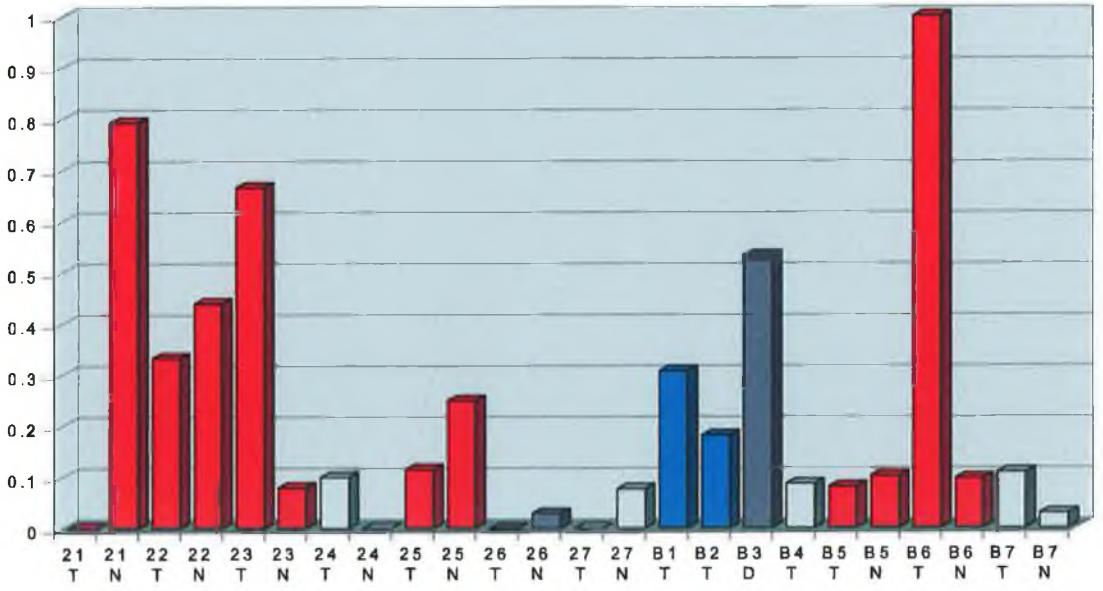

Figs. 3.6.14a & b: Gel electrophoresis photographs of mdr-1 RT-PCR results on Lung Primary (RED), Breast Primary (BLUE), Metastatic (GREY) & Non-carcinoma (NAVY) tissue samples; Fig. 3.6.14c: Densitometry of RT-PCR results.

normal was only observed in three (30%) sets. A total of five (50%) sample pairs expressed higher amounts of the gene in the normal sample relative to the tumour, while a further two pairs (20%) expressed similar amounts of mdr-1 in both tissues.

3.6.2.8 BCRP

The results of these RT-PCRs can be seen in Figs. 3.6.15 and 3.6.16. Twenty of the twenty-four lung tissue samples (>83%) assayed for BCRP expression were observed to be positive for the gene. Medium to high levels of expression were observed for the unpaired tumour samples. Nine of the ten tumour/normal sample pairs were observed to express the gene in at least one of the tissue samples. Of these nine sample pairs, only three (33%) expressed higher amounts of the gene in the tumour sample relative to its normal control. Two other sample pairs expressed similar amounts of the gene, while four (>44%) of the pairs expressed higher amounts in the normal tissue sample.

3.6.2.9 mdr-3

mdr-3 was not expressed in any of the lung tissue samples assayed for expression. A positive level of expression was observed for the PCR positive control, which indicated that the PCR had been carried out correctly. This result indicated that, in these samples at least, mdr-3 is not a factor to be considered in the prognosis of this disease (data not shown).

3.6.2.10 COX-1

The results of these RT-PCRs can be seen in Figs. 3.6.17 and 3.6.18. COX-1 was expressed in nine (37.5%) of the twenty-four lung tissue samples assayed. Expression was detected in two (50%) of the four unpaired tumour samples. Five (50%) of the following ten tumour/normal sample pairs were observed to express the gene in at least one of the tissue samples. Of these samples, COX-1 expression was observed

Fig. 3.6.15: BCRP RT-PCR on Tumour tissue samples

Fig. 3.6.15a:

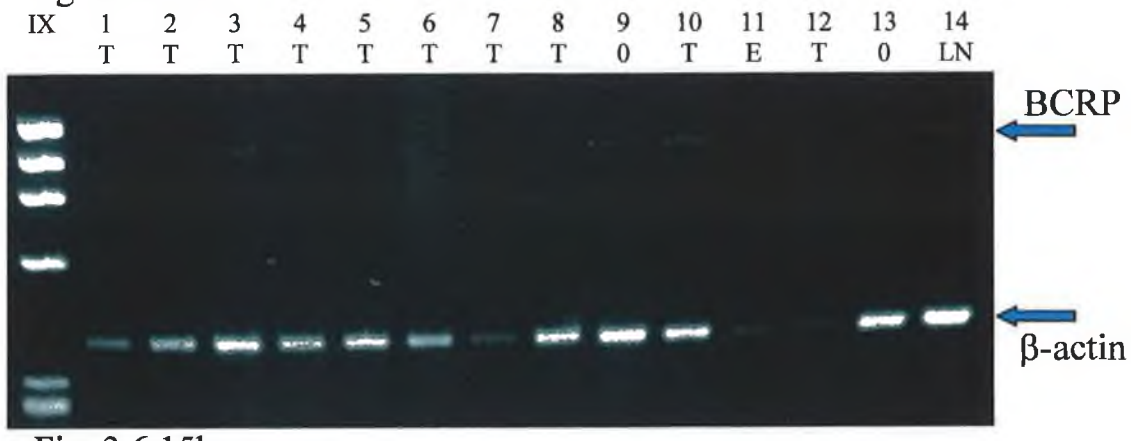

Fig. 3.6.15b:

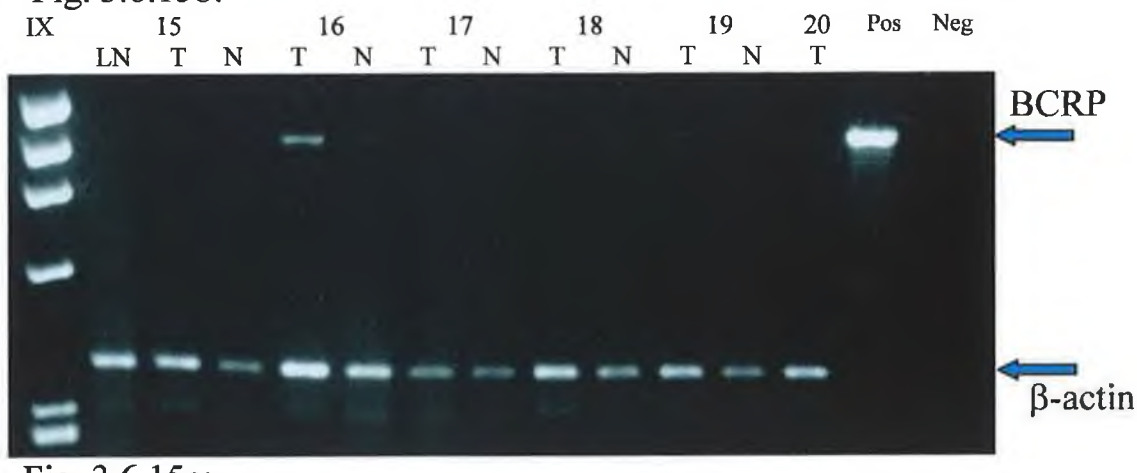

Fig. 3.6.15c:

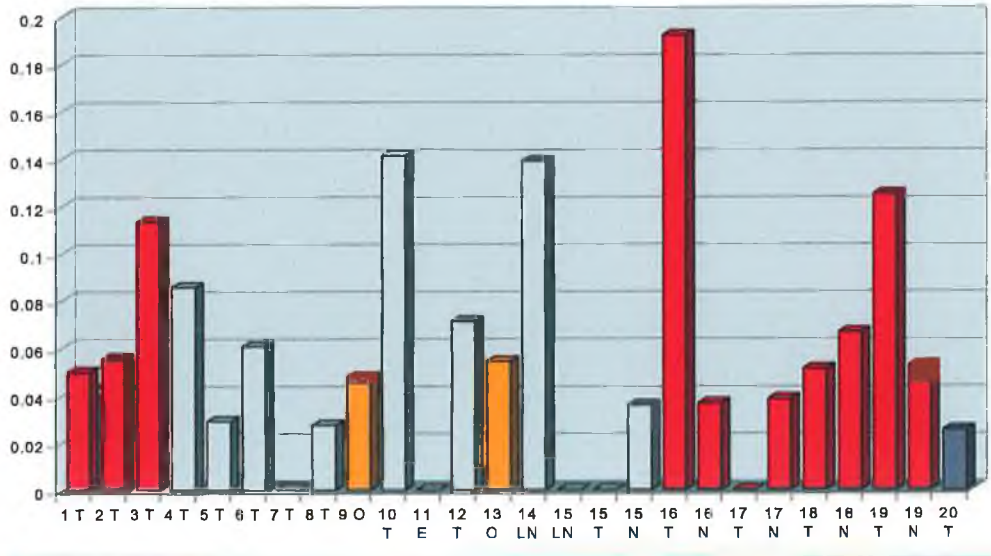

Figs. 3.6.15a & b: Gel electrophoresis photographs of BCRP RT-PCR results on Lung Primary (RED), Oesophagus Primary (ORANGE), Metastatic (GREY) & Non-carcinoma (NAVY) tissue samples; Fig. 3.6.15c: Densitometry of RT-PCR results.

Fig. 3.6.16: BCRP RT-PCR on Tumour tissue samples

Fig. 3.6.16a:

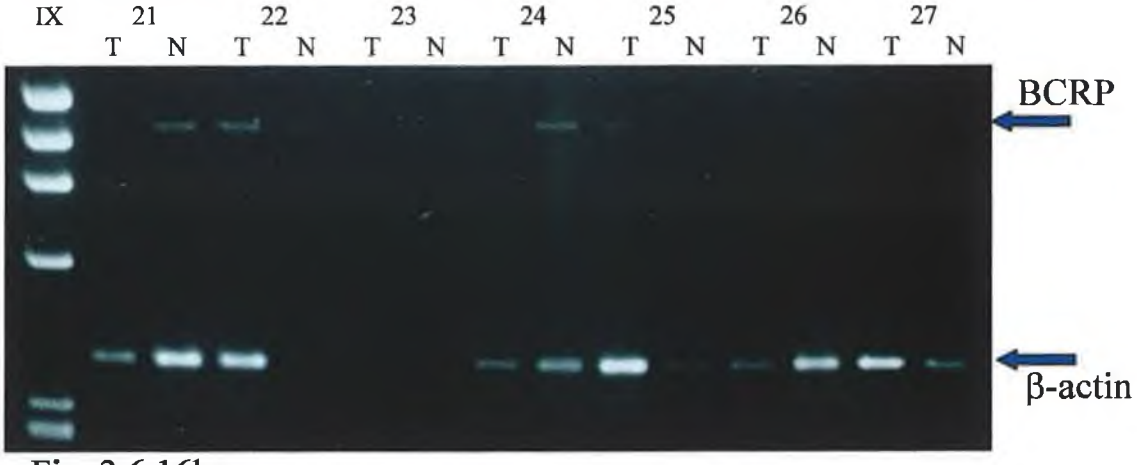

Fig. 3.6.16b:

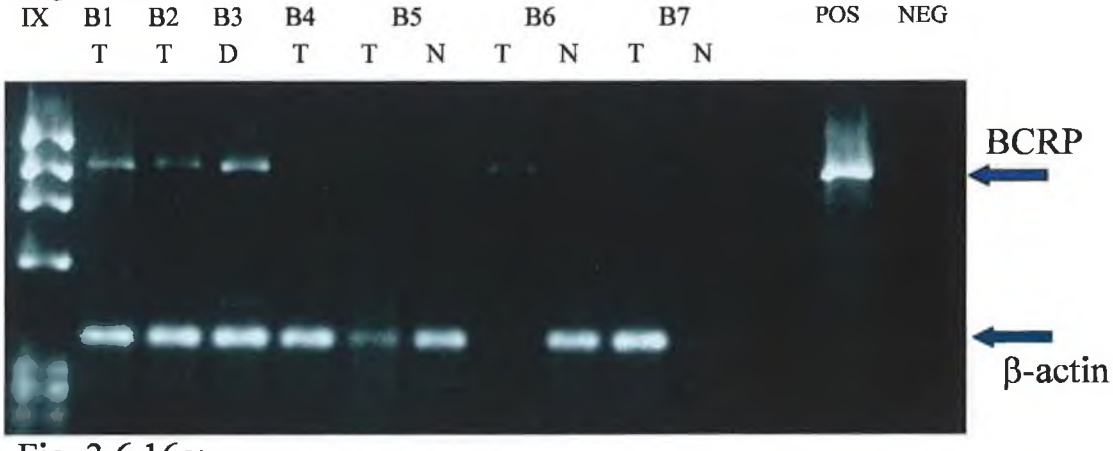

Fig. 3.6.16c:

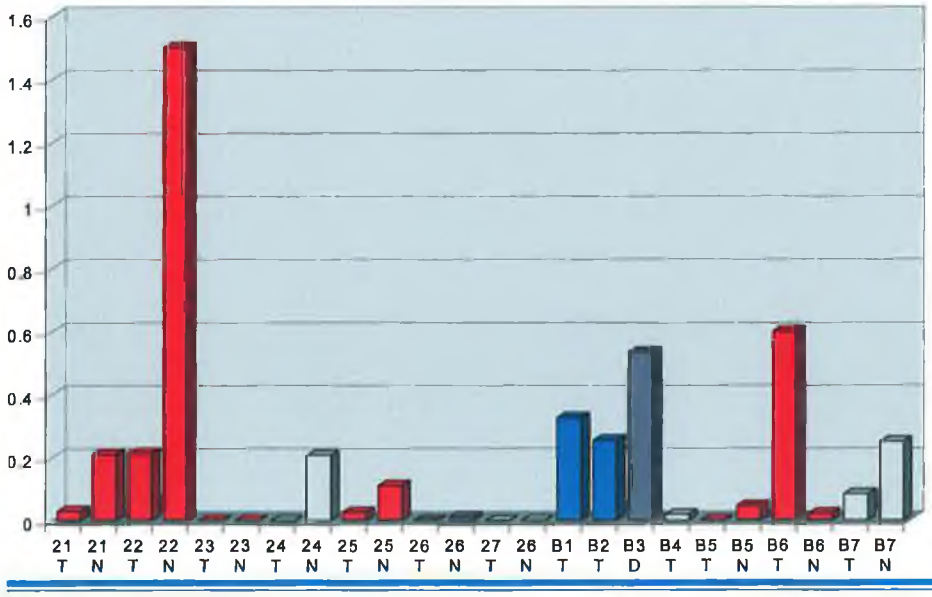

Figs. 3.6.16a & b: Gel electrophoresis photographs of BCRP RT-PCR results on Lung Primary (RED), Breast Primary (BLUE), Metastatic (GREY) & Non-carcinoma (NAVY) tissue samples; Fig. 3.6.16c: Densitometry of RT-PCR results.

Fig. 3.6.17: COX-1 RT-PCR on Tumour tissue samples

Fig. 3.6.17a:

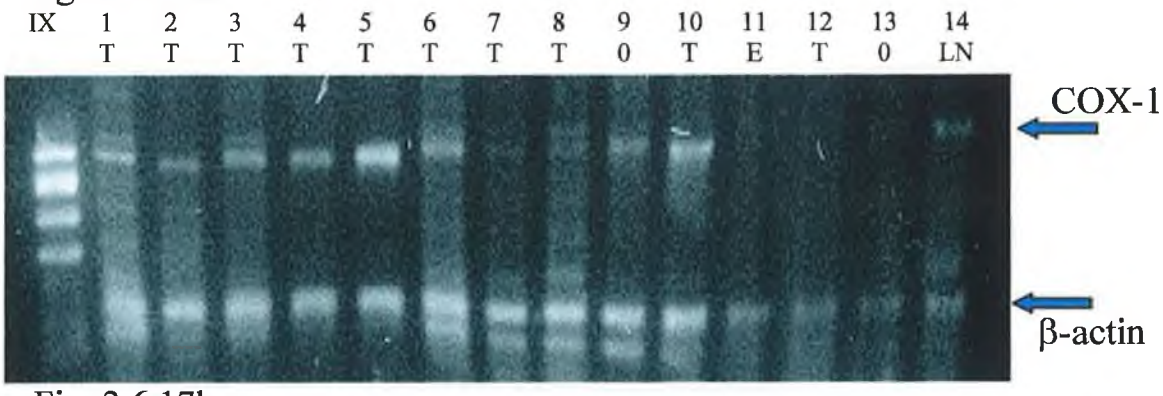

Fig. 3.6.17b:

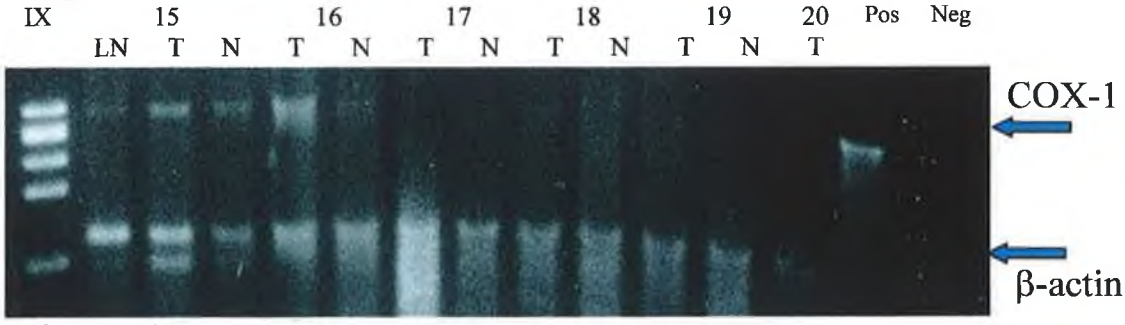

Fig. 3.6.17c:

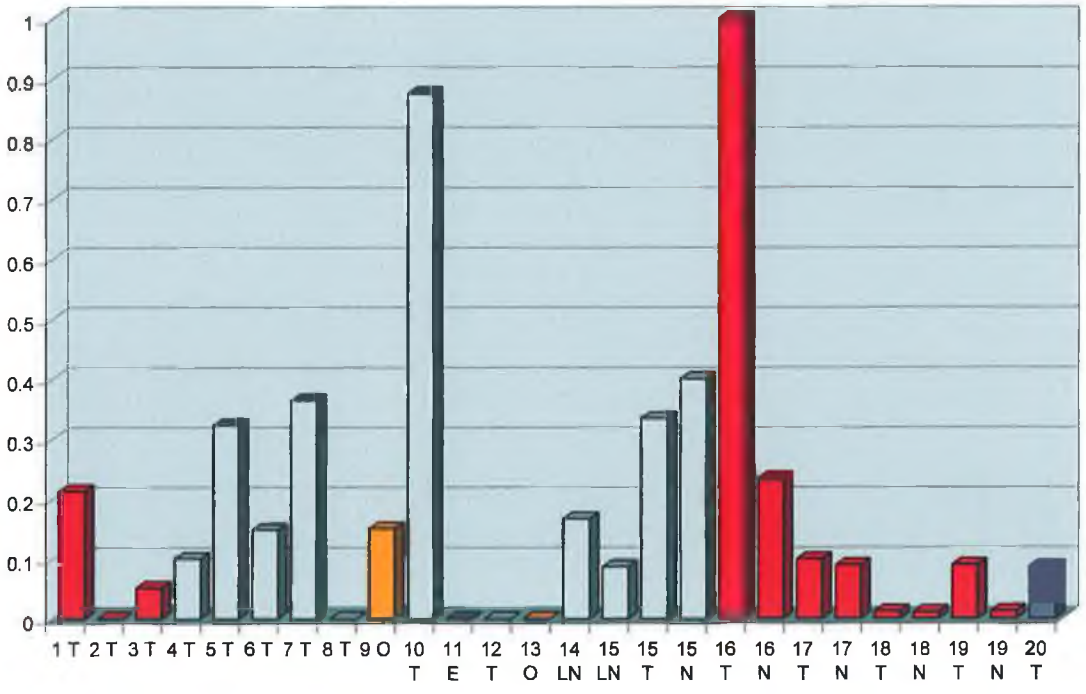

Figs. 3.6.17a & b: Gel electrophoresis photographs of COX-1 RT-PCR results on Lung Primary (RED), Oesophagus Primary (ORANGE), Metastatic (GREY) & Non-carcinoma (NAVY) tissue samples; Fig. 3.6.17c: Densitometry of RT-PCR results.

Fig. 3.6.18: COX-1 RT-PCR on Tumour tissue samples

Fig. 3.6.18a:

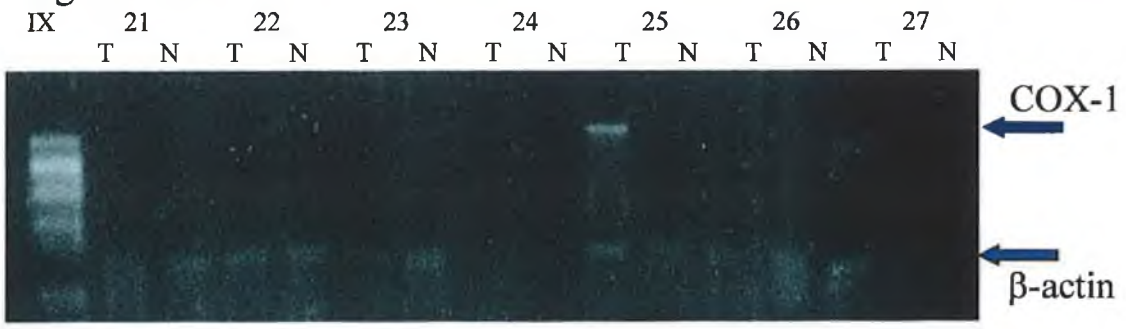

Fig. 3.6.18b:

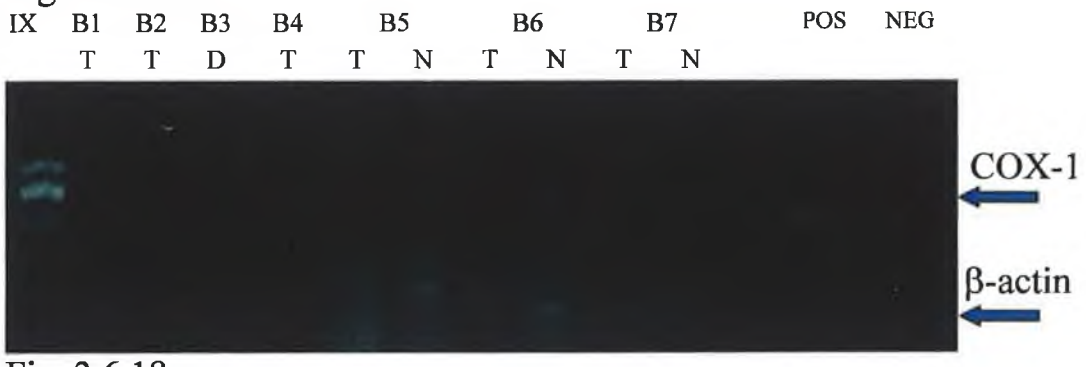

Fig. 3.6.18c:

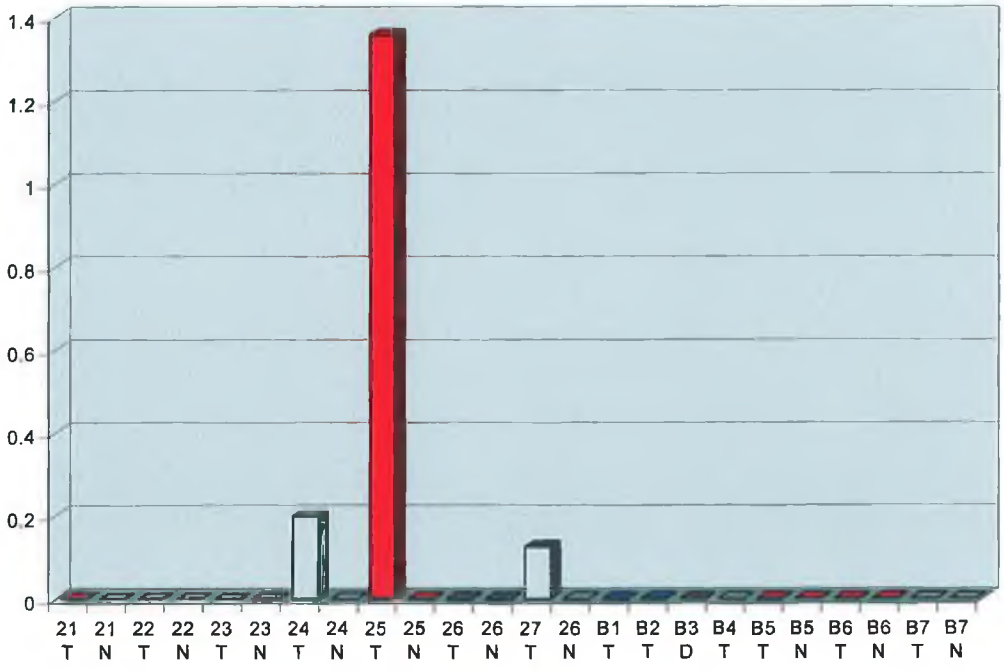

Figs. 3.6.18a & b: Gel electrophoresis photographs of COX-1 RT-PCR results on Lung Primary (RED), Breast Primary (BLUE), Metastatic (GREY& Non-carcinoma (NAVY) tissue samples; Fig. 3.6.18c: Densitometry of RT-PCR results.

overexpressed in the tumour sample relative to the normal control in three (60%) sample pairs. Also, the highest expression levels observed for these tissues was recorded in the tumour samples. As with MRP6, however, the quality of the RT-PCRs is poor, and the results questionable.

3.6.2.11 COX-2

The results of these RT-PCRs can be seen in Figs. 3.6.19 and 3.6.20. Expression of the COX-2 gene was observed in fourteen (>58%) of the twenty-four lung tissue specimens inspected. Expression was detected in only one of the four unpaired tumour samples. Two tumour/normal sample pairs did not express the gene in either tissue. Of the remaining eight sample pairs that did express the gene, six (75%) expressed higher amounts of COX-2 in the tumour sample relative to the normal tissue.

3.6.2.12 BAP

The results of these RT-PCRs for the pro-apoptotic BAP gene can be seen in Figs. 3.6.21 and 3.6.22. BAP expression was observed in all twenty-four lung tissue samples studied, the first gene studied here to do so. However, only four (40%) of the ten tumour/normal sample pairs overexpress the gene in the normal tissue, while five (50%) pairs overexpress the gene in the tumour sample. The remaining sample pair expresses identical amounts of BAP in both tissues while the gene is expressed in all four unpaired tumour samples.

3.6.2.13 BAXα

The results of these RT-PCRs can be seen in Figs. 3.6.23 and 3.6.24. BAXα is also a pro-apoptotic gene and, like BAP, is observed expressed in all twenty-four of the lung samples assayed. Expression of the gene is also observed to be high in most of these samples. In the paired tumour/normal samples, expression of the gene is observed to be

Fig. 3.6.19: COX-2 RT-PCR on Tumour tissue samples

Fig. 3.6.19a:

Fig. 3.6.19b:

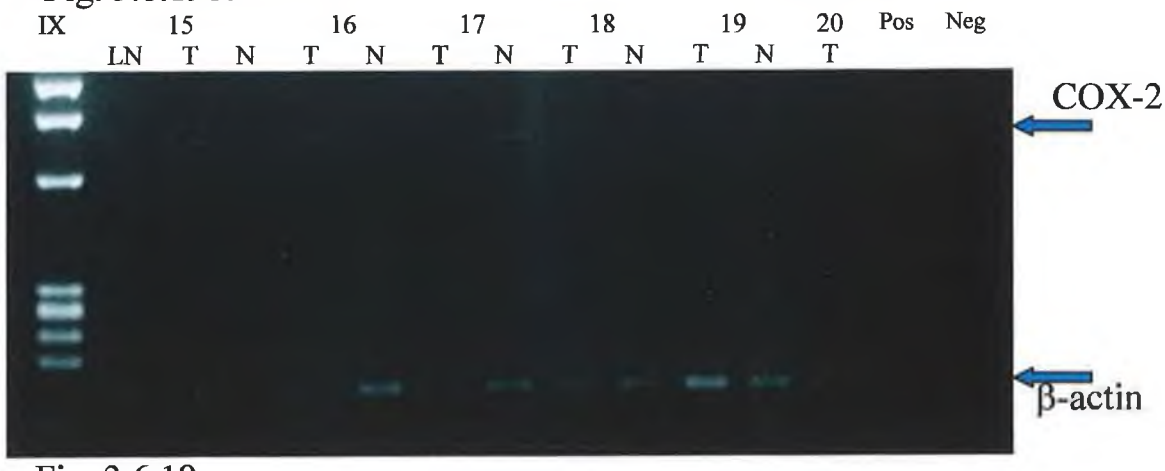

Fig. 3.6.19c:

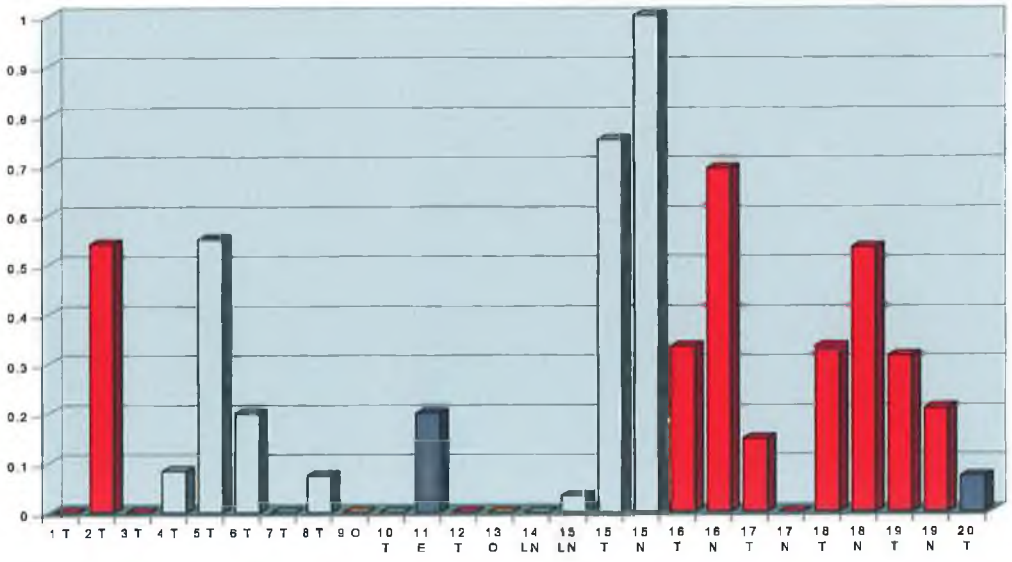

Figs. 3.6.19a & b: Gel electrophoresis photographs of COX-2 RT-PCR results on Lung Primary (RED), Oesophagus Primary (ORANGE), Metastatic (GREY) & Non-carcinoma (NAVY) tissue samples; Fig. 3.6.19c: Densitometry of RT-PCR results.

Fig. 3.6.20: COX-2 RT-PCR on Tumour tissue samples

Fig. 3.6.20a:

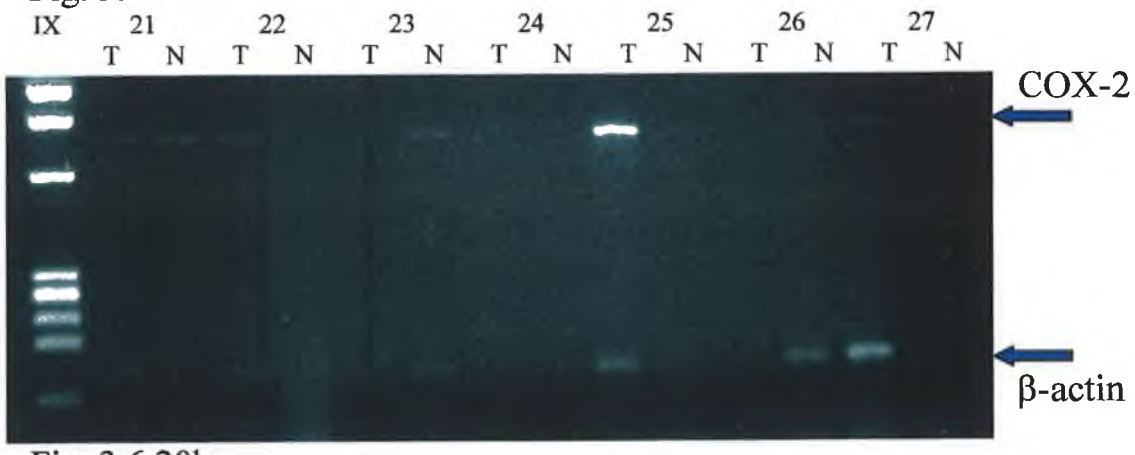

Fig. 3.6.20b:

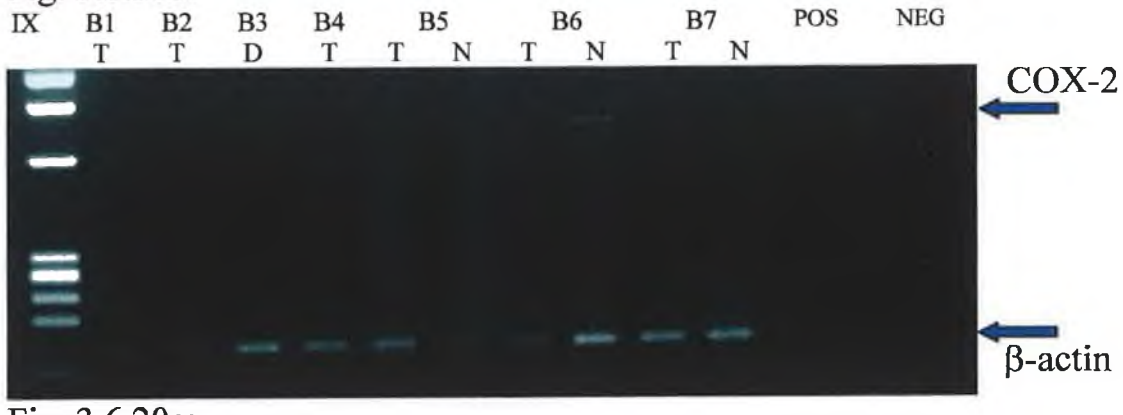

Fig. 3.6.20c:

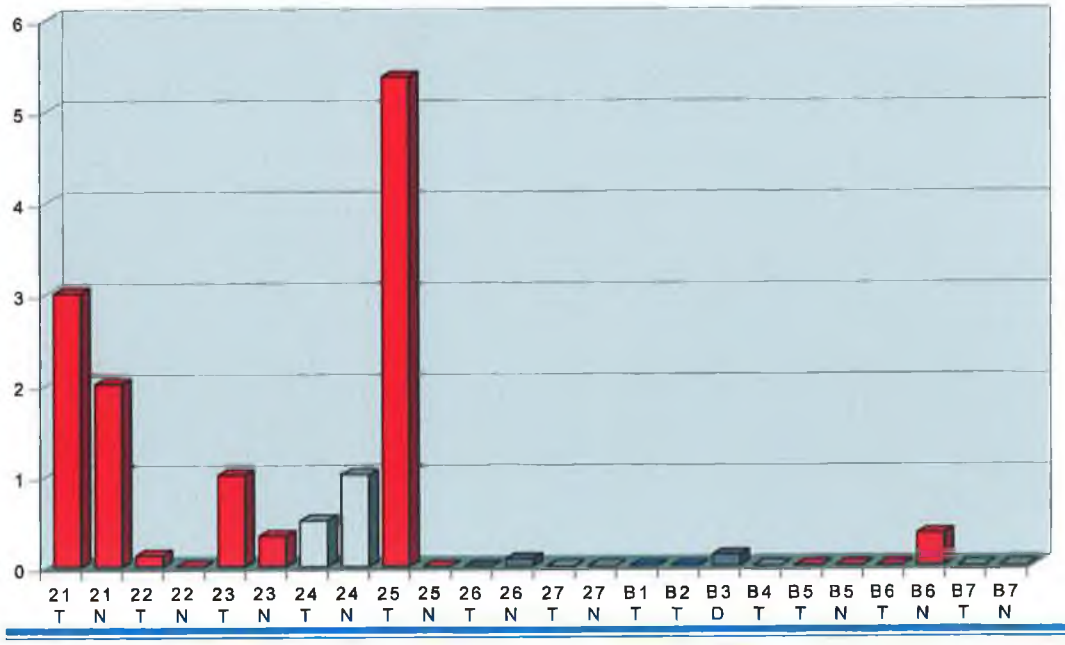

Figs. 3.6.20a & b: Gel electrophoresis photographs of COX-2 RT-PCR results on Lung Primary (RED), Breast Primary (BLUE), Metastatic (GREY) & Non-carcinoma (NAVY) tissue samples; Fig. 3.6.20c: Densitometry of RT-PCR results.

Fig. 3.6.21: BAP RT-PCR on Tumour tissue samples

Fig. 3.6.21a:

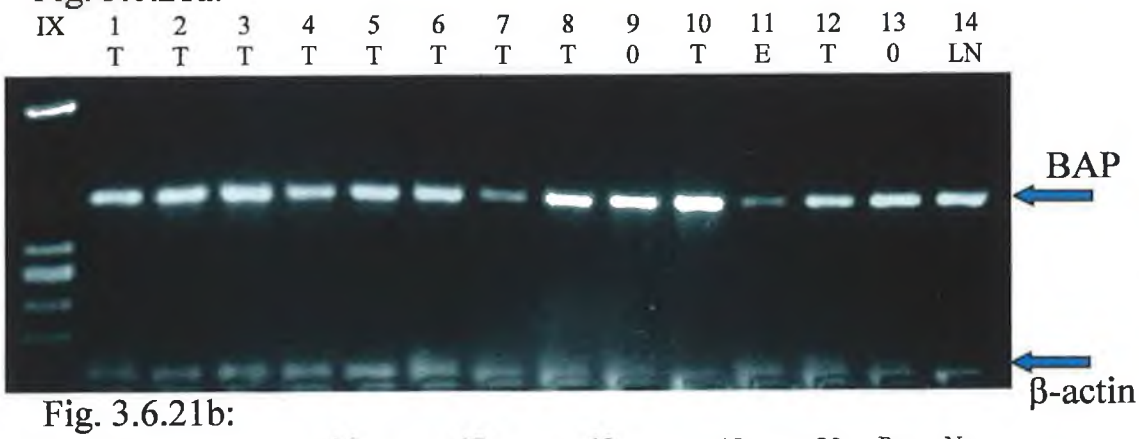

Fig. 3.6.21b:

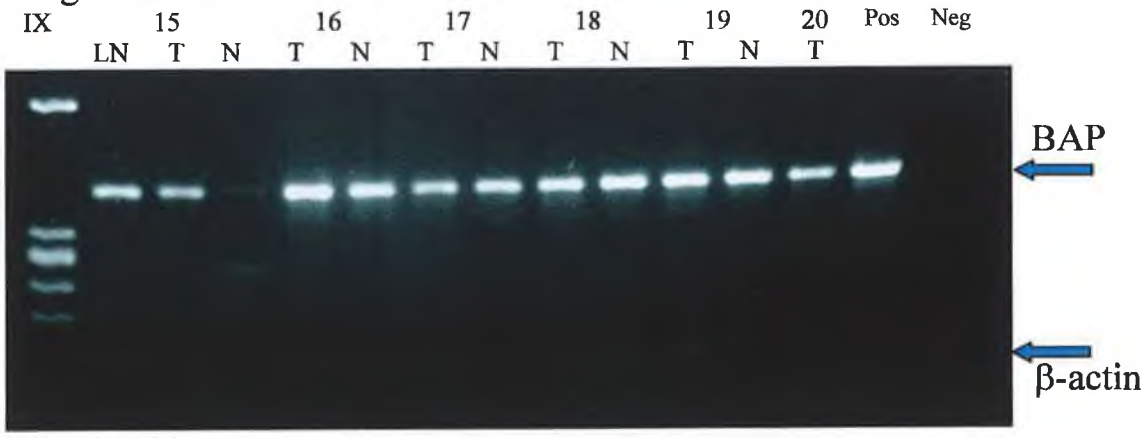

Fig. 3.6.21c:

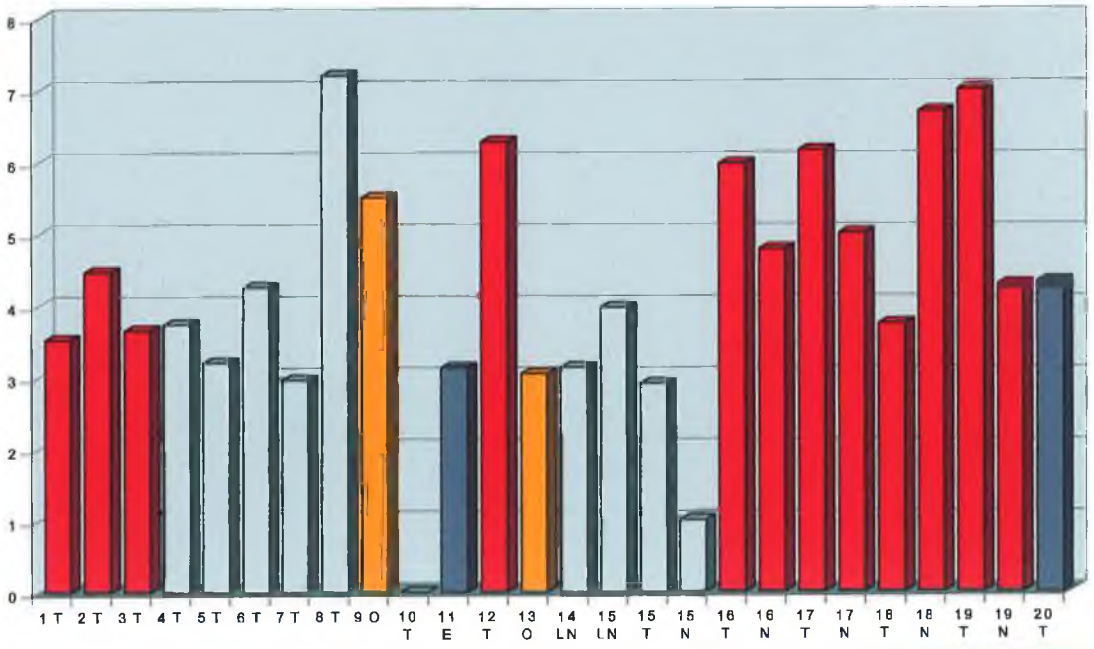

Figs. 3.6.21a & b: Gel electrophoresis photographs of BAP RT-PCR results on Lung Primary (RED), Oesophagus Primary (ORANGE), Metastatic (GREY) & Non-carcinoma (NAVY) tissue samples; Fig. 3.6.21c: Densitometry of RT-PCR results.

Fig. 3.6.22: BAP RT-PCR on Tumour tissue samples

Fig. 3.6.22a:

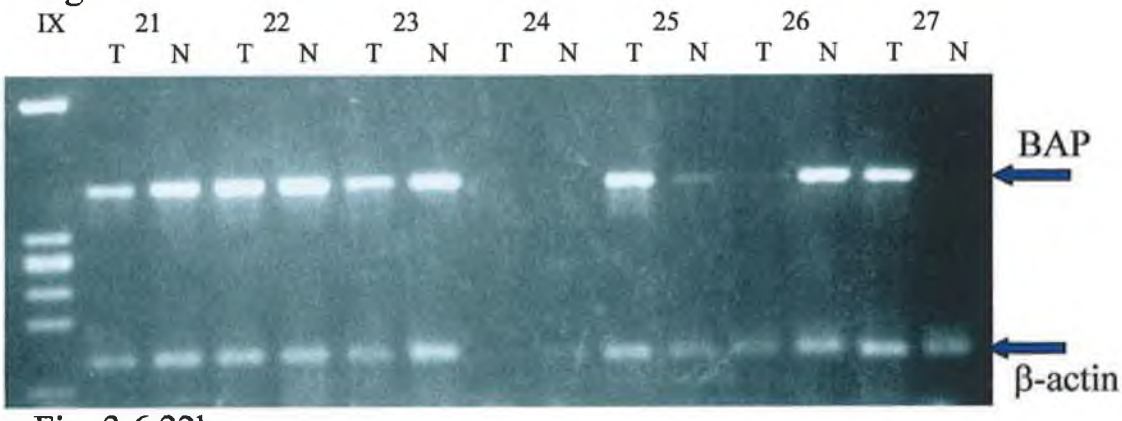

Fig. 3.6.22b:

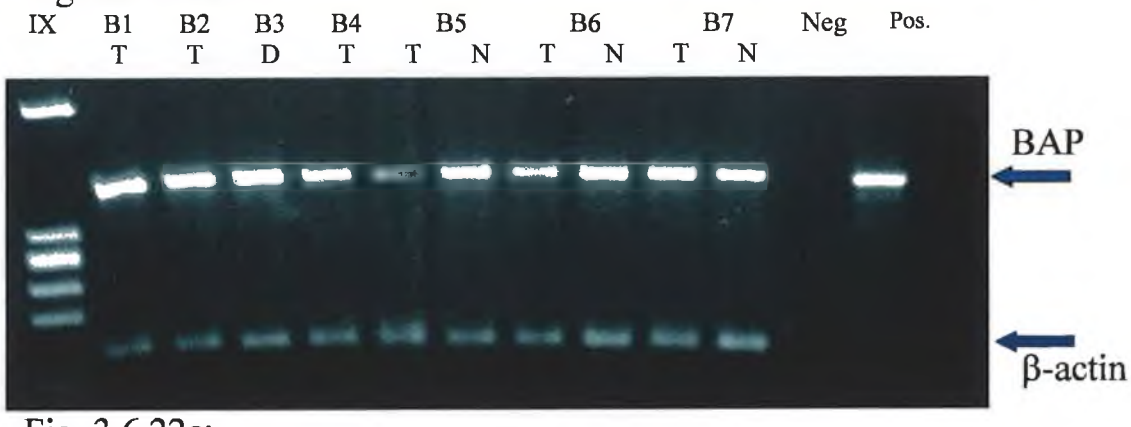

Fig. 3.6.22c:

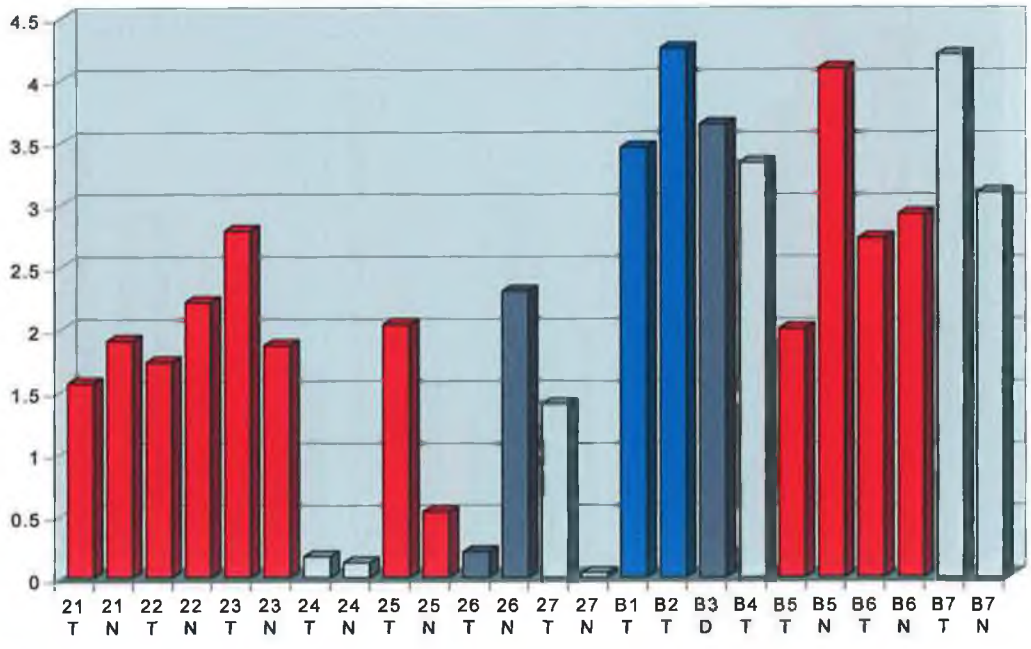

Figs. 3.6.22a & b: Gel electrophoresis photographs of BAP RT-PCR results on Lung Primary (RED), Breast Primary (BLUE), Metastatic (GREY) & Non-carcinoma (NAVY) tissue samples; Fig. 3.6.22c: Densitometry of RT-PCR results.

higher in the normal sample of only four pairs (40%). The remaining six pairs all express higher amounts of the gene in the tumour sample.

3.6.2.14 MRIT

The results of these RT-PCRs for the pro-apoptotic MRIT gene can be seen in Figs. 3.6.25 and 3.6.26. MRIT was found to be expressed in twenty-three of the twenty-four lung samples studied (>95%). Eight (80%) of the paired tumour/normal tissue samples expressed higher amounts of the gene in the normal sample relative to the tumour sample. Although expression of the gene was also observed in the four unpaired samples, it was felt that the former result was of significance.

3.6.2.15 Bcl-x_S/ Bcl-x_L

The results of these RT-PCRs can be seen in Figs. 3.6.27 to 3.6.30. Bcl-x_S, also a pro-apoptotic gene, was found to be expressed in nineteen (>70%) out of the twenty-four tissue samples. Overall, expression was generally in the medium to high range. All four unpaired tumour samples were observed to express the gene. Also, eight of the tumour/normal sample pairs (80%) expressed the gene to some degree in at least one of the tissue samples. Of these eight sample pairs, only two (25%) expressed higher amounts of the gene in the normal tissue, while another sample pair expressed identical amounts of the gene in both tissues. The remaining five sample pairs (62.5%) expressed higher amounts of the gene in the tumour tissue.

The anti-apoptotic Bcl-x_L gene was expressed in twenty out of twenty-four lung tissue samples (>80%) studied. High levels of expression were detected in the four unpaired tumour samples. Of the ten tumour/normal sample pairs, eight were observed to express the gene in both tissues, while the remaining two pairs did not express Bcl-x_L at all. Of these eight, Bcl-x_L was observed overexpressed in the tumour sample in five (62.5%) pairs. Another pair expressed identical amounts of the gene in both tissues, while the

Fig. 3.6.25: MRIT RT-PCR on Tumour tissue samples

Fig. 3.6.25a:

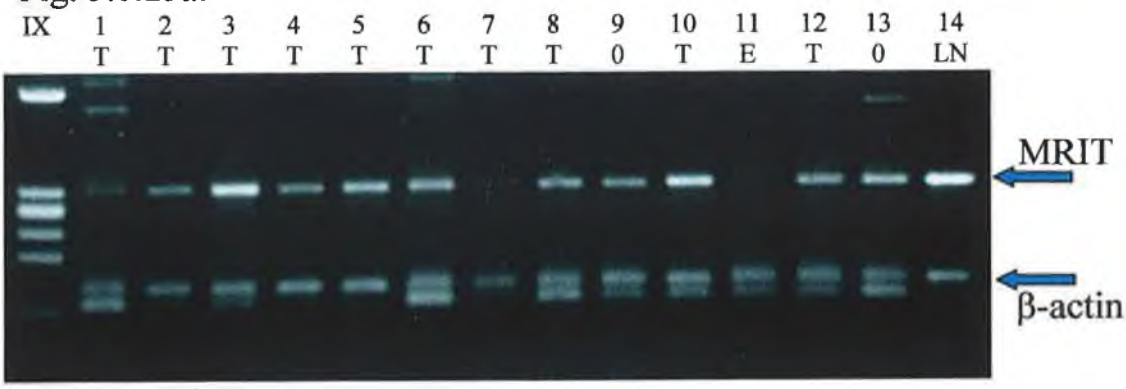

Fig. 3.6.25b:

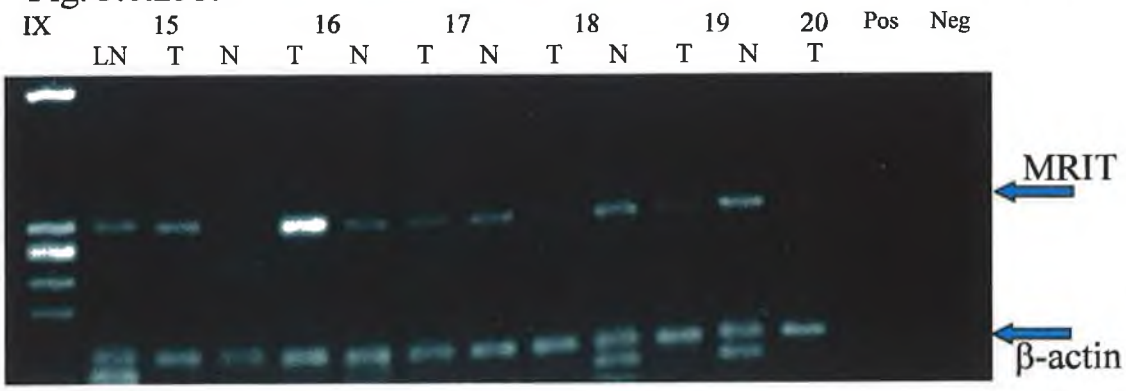

Fig. 3.6.25c:

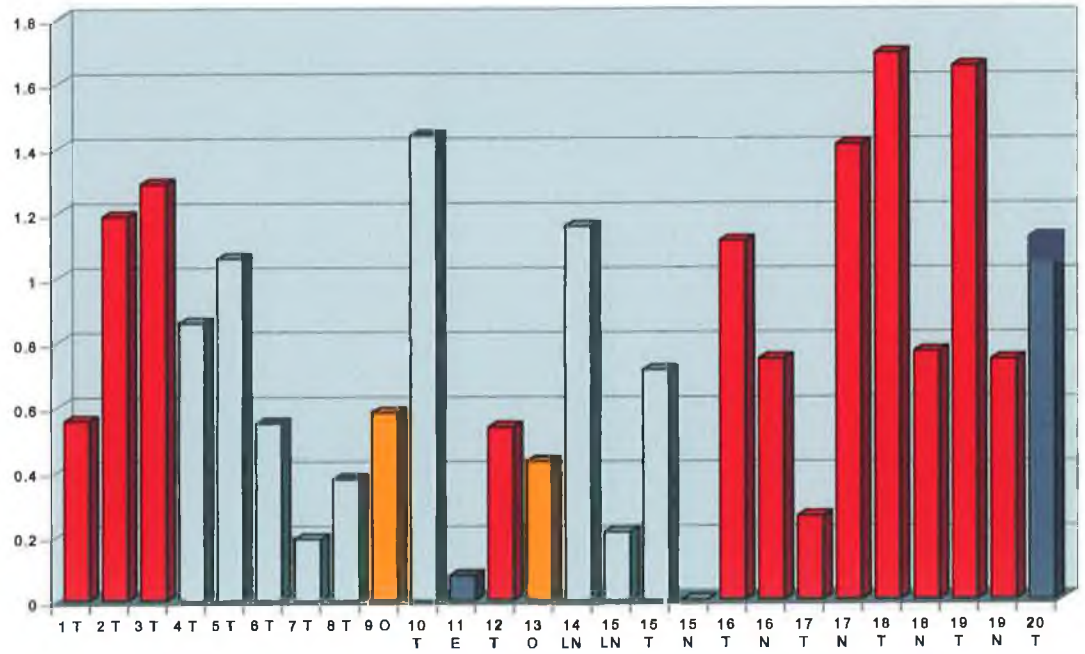

Figs. 3.6.25a & b: Gel electrophoresis photographs of MRIT RT-PCR results on Lung Primary (RED), Oesophagus Primary (ORANGE), Metastatic (GREY) & Non-carcinoma (NAVY) tissue samples; Fig. 3.6.25c: Densitometry of RT-PCR results.

Fig. 3.6.26: MRIT RT-PCR on Tumour tissue samples

Fig. 3.6.26a:

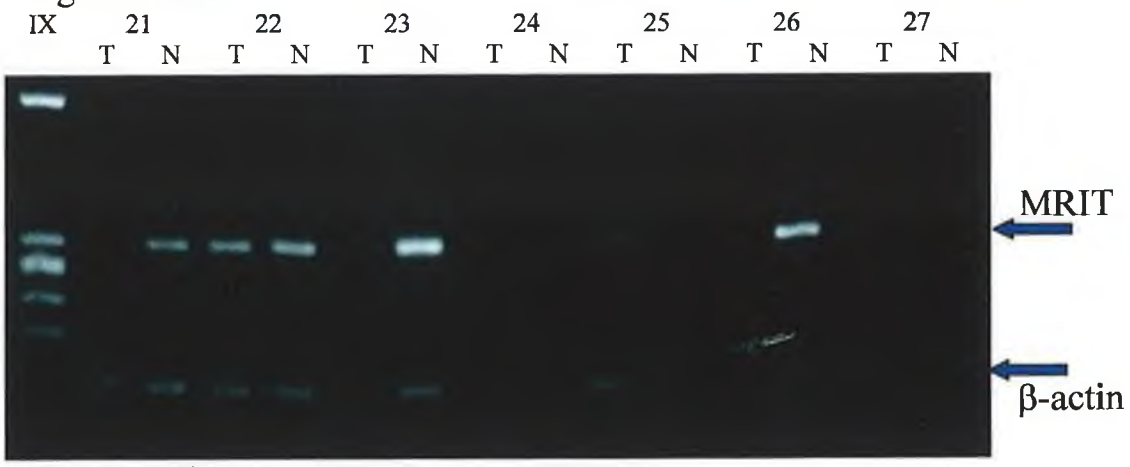

Fig. 3.6.26b:

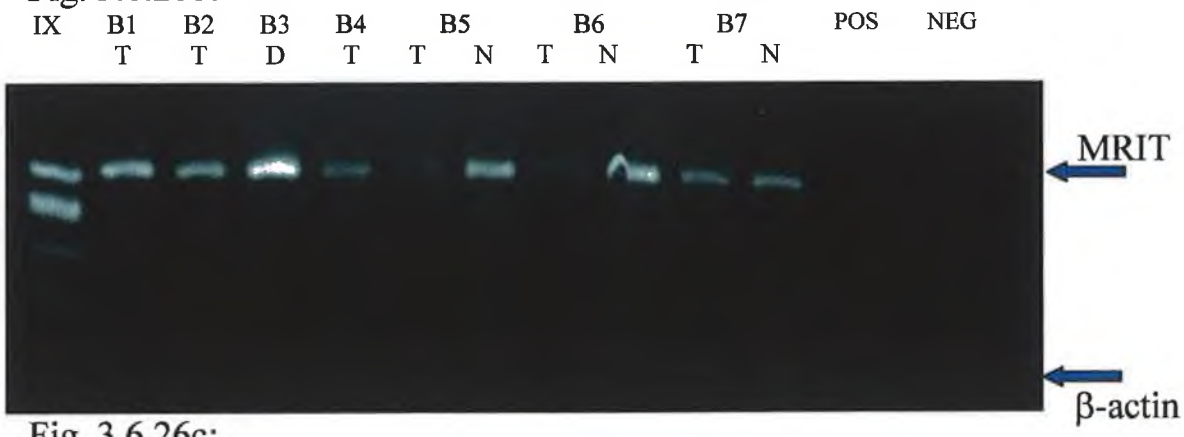

Fig. 3.6.26c:

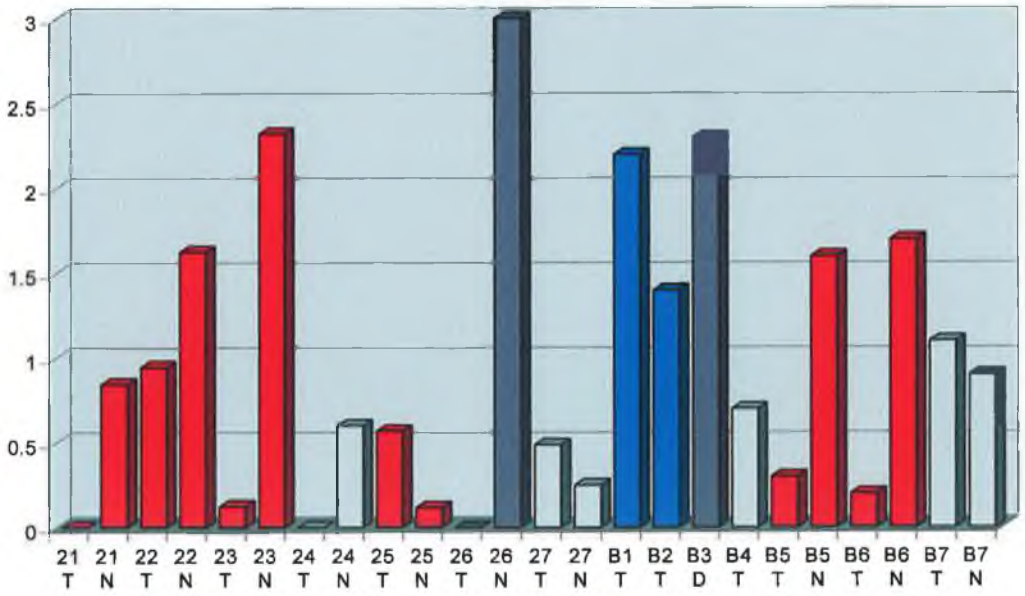

Figs. 3.6.26a & b: Gel electrophoresis photographs of MRIT RT-PCR results on Lung Primary (RED), Breast Primary (BLUE), Metastatic (GREY) & Non-carcinoma (NAVY) tissue samples; Fig. 3.6.26c: Densitometry of RT-PCR results.

Fig. 3.6.27: Bcl-$x_{S/L}$ RT-PCR on Tumour tissue samples

Fig. 3.6.27a:

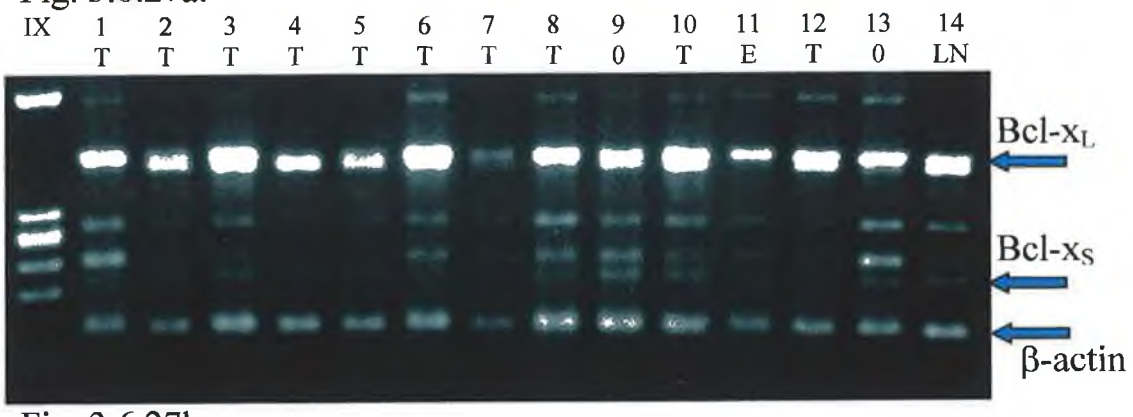

Fig. 3.6.27b:

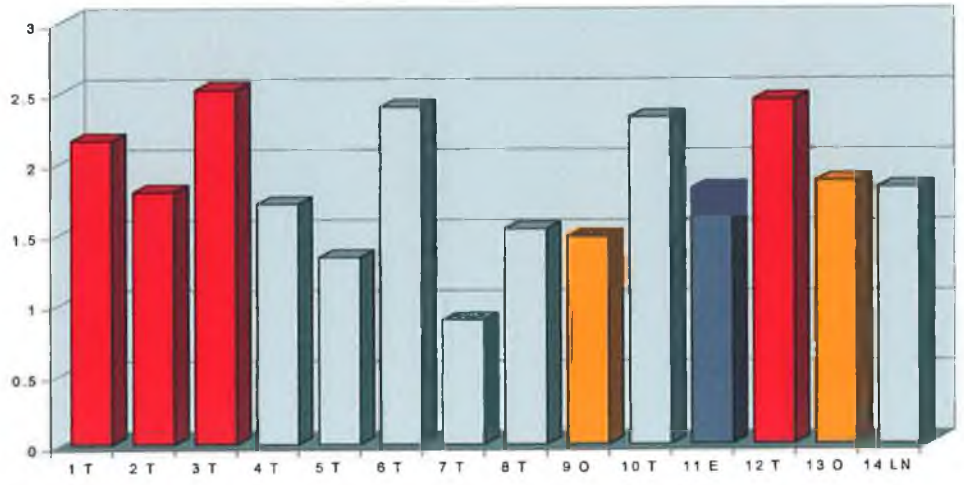

Fig. 3.6.27c:

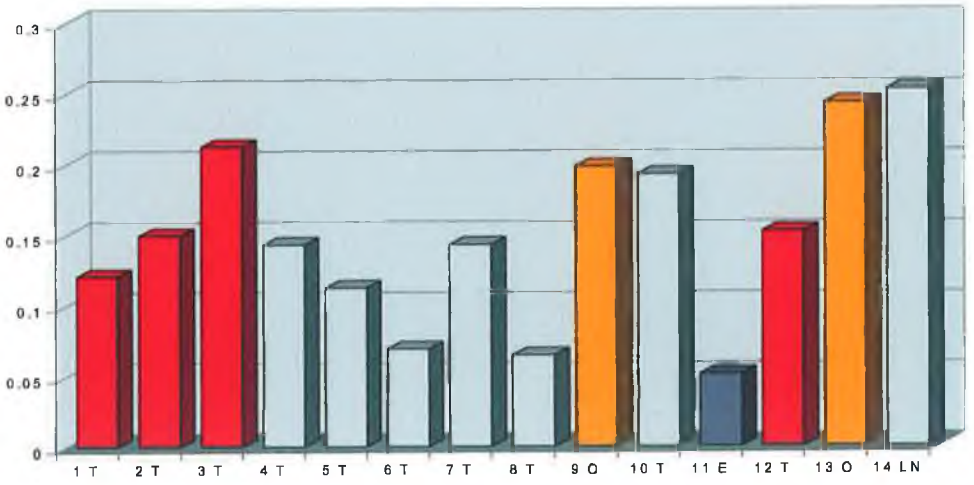

Fig. 3.6.27a: Gel electrophoresis photograph of Bcl-$x_{L/S}$ RT-PCR results on Lung Primary (RED), Oesophagus Primary (ORANGE), Metastatic (GREY) & Non-carcinoma (NAVY) tissue samples; Fig. 3.6.27b: Densitometric analysis of Bcl-x_L RT-PCR results; Fig. 3.6.27c: Densitometric analysis of Bcl-x_S RT-PCR results.

Fig. 3.6.28: Bcl-$x_{S/L}$ RT-PCR on Tumour tissue samples

Fig. 3.6.28a:

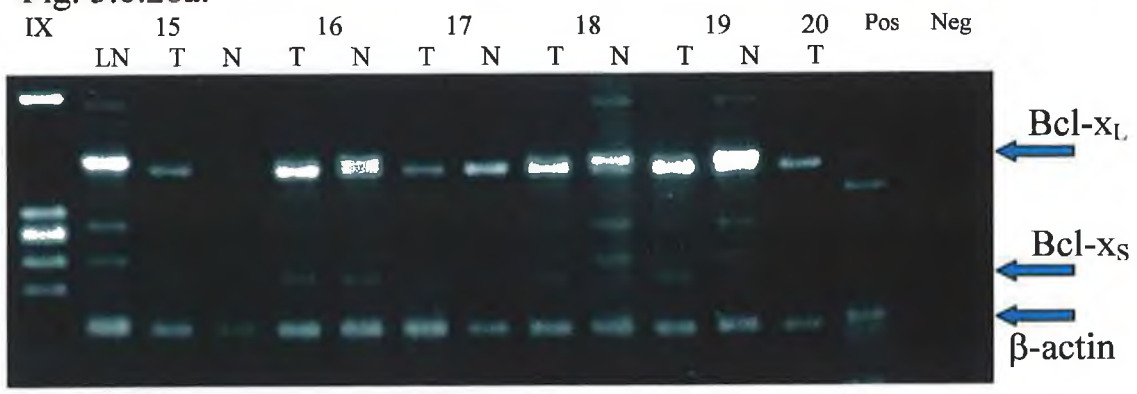

Fig. 3.6.28b:

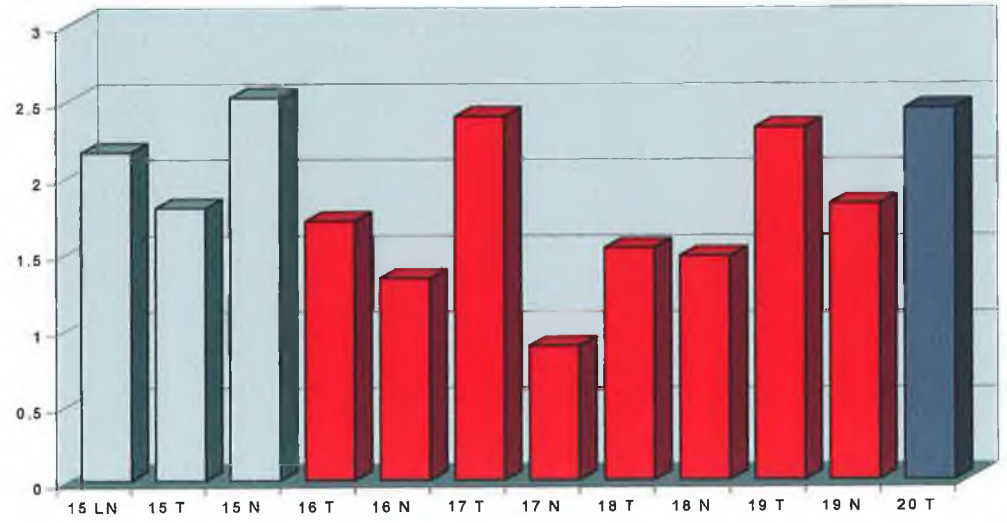

Fig. 3.6.28c:

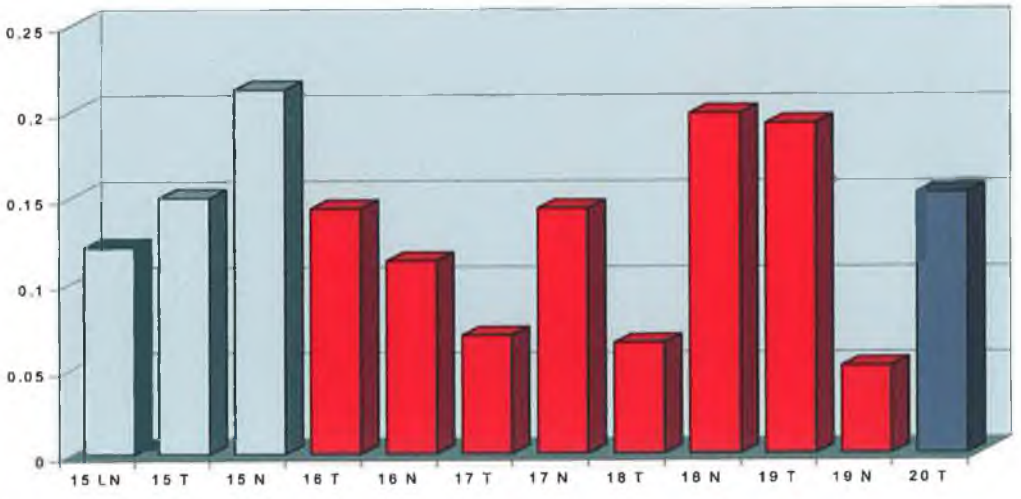

Fig. 3.6.28a: Gel electrophoresis photograph of Bcl-$x_{L/S}$ RT-PCR results on Lung Primary (RED), Oesophagus Primary (ORANGE), Metastatic (GREY) & Non-carcinoma (NAVY) tissue samples; Fig. 3.6.28b: Densitometric analysis of Bcl-x_L RT-PCR results; Fig. 3.6.28c: Densitometric analysis of Bcl-x_S RT-PCR results.

Fig. 3.6.29: Bcl-$x_{S/L}$ RT-PCR on Tumour tissue samples

Fig. 3.6.29a:

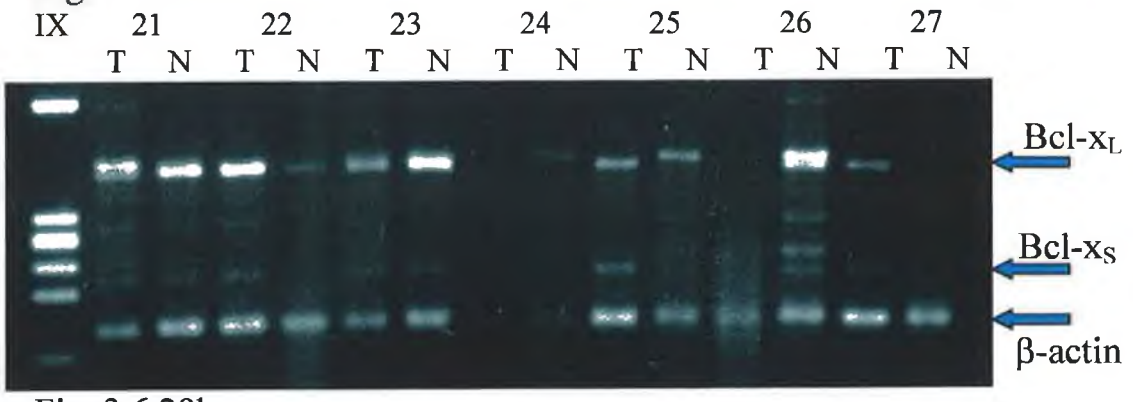

Fig. 3.6.29b:

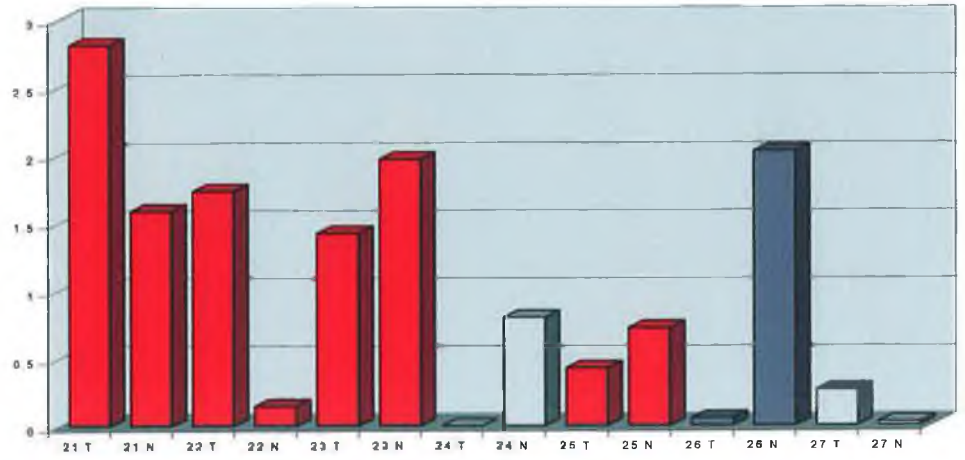

Fig. 3.6.29c:

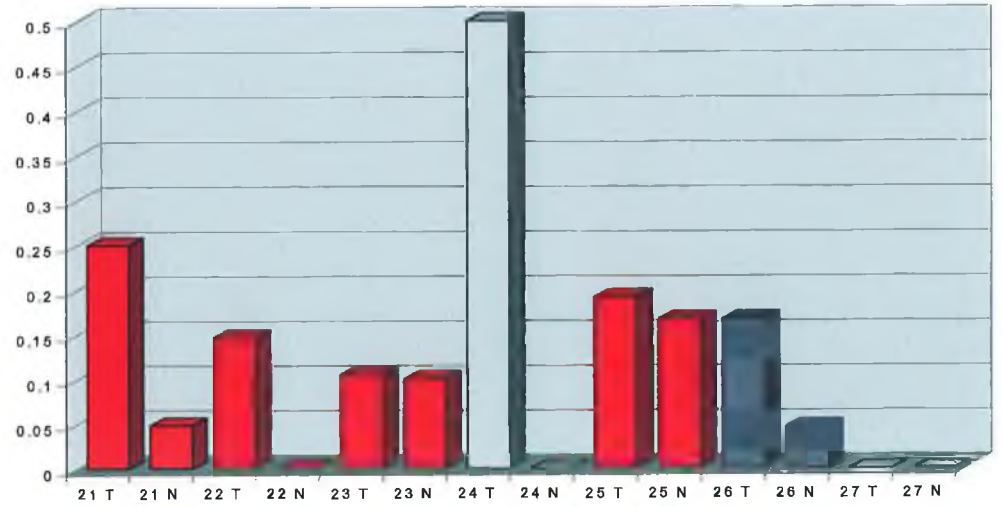

Fig. 3.6.29a: Gel electrophoresis photograph of Bcl-$x_{L/S}$ RT-PCR results on Lung Primary (RED), Oesophagus Primary (ORANGE), Metastatic (GREY) & Non-carcinoma (NAVY) tissue samples; Fig. 3.6.29b: Densitometric analysis of Bcl-x_L RT-PCR results; Fig. 3.6.29c: Densitometric analysis of Bcl-x_S RT-PCR results.

Fig. 3.6.30: Bcl-$x_{S/L}$ RT-PCR on Tumour tissue samples

Fig. 3.6.30a:

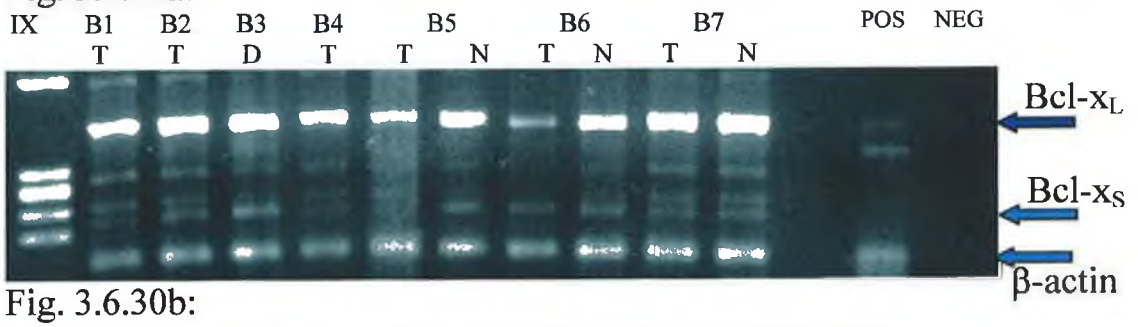

Fig. 3.6.30b:

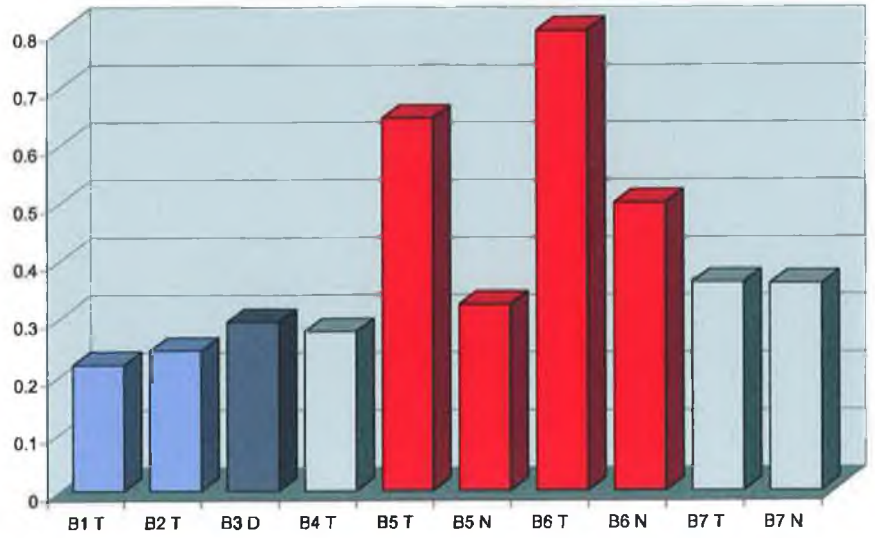

Fig. 3.6.30c:

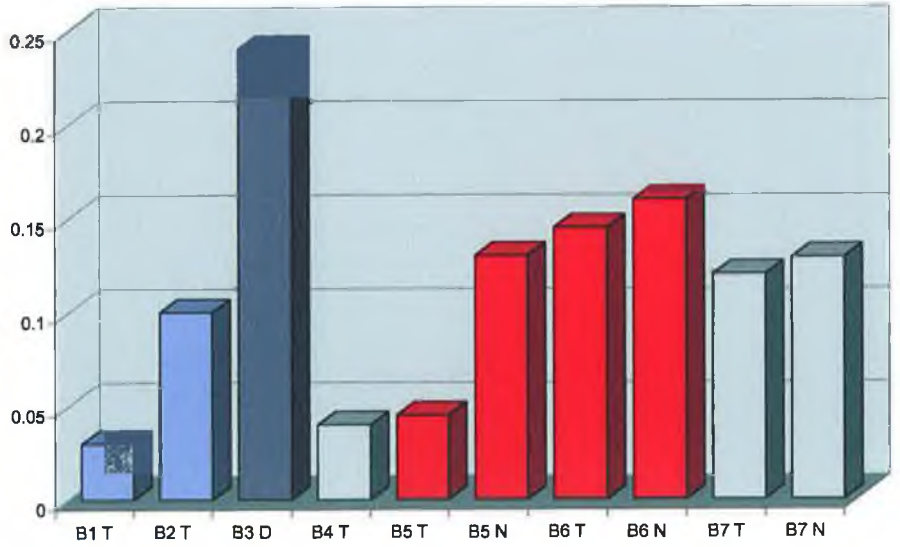

Fig. 3.6.30a: Gel electrophoresis photograph of Bcl-$x_{L/S}$ RT-PCR results on Lung Primary (RED), Oesophagus Primary (ORANGE), Metastatic (GREY) & Non-carcinoma (NAVY) tissue samples; Fig. 3.6.30b: Densitometric analysis of Bcl-x_L RT-PCR results; Fig. 3.6.27c: Densitometric analysis of Bcl-x_S RT-PCR results.

remaining two sample pairs (25%) expressed higher amounts in the normal tissue relative to its tumour equivalent.

3.6.2.16 Bcl-2α

The results of the anti-apoptotic Bcl-2α RT-PCRs can be seen in Figs. 3.6.31 and 3.6.32. All twenty-four lung tissue samples assayed for Bcl-2α expression were observed to express the gene to some degree. Two of the unpaired tumour samples expressed the gene at a low level, while the other two expressed much higher amounts of the gene. Of the ten tumour/normal sample pairs which expressed the gene, six (60%) expressed higher amounts of the anti-apoptotic Bcl-2α in the tumour sample relative to its normal equivalent. A further three sample pairs expressed equal amounts of the gene in either tissue, while only one sample pair expressed relatively higher levels in the normal tissue sample.

3.6.2.17 BAG

The results of these RT-PCRs can be seen in Figs. 3.6.33 and 3.6.34. Expression of the anti-apoptotic BAG gene was observed in twenty-three of the twenty-four lung tissue samples assayed (>95%). Expression was also observed to be quite high in most samples. All four unpaired tumour samples expressed the gene. Of the ten tumour/normal sample pairs, only three (30%) were observed to express higher amounts of the gene in the tumour sample relative to the normal. Six (60%) sample pairs expressed higher amounts of the gene in the normal sample. The remaining sample pair expressed similar amounts of the gene in both tissue samples.

3.6.2.18 Survivin

The results of these RT-PCRs can be seen in Figs. 3.6.35 and 3.6.36. The anti-apoptotic Survivin gene was observed expressed in twenty-one of the twenty-four (>87%) lung

Fig. 3.6.31: Bcl-2α RT-PCR on Tumour tissue samples

Fig. 3.6.31a:

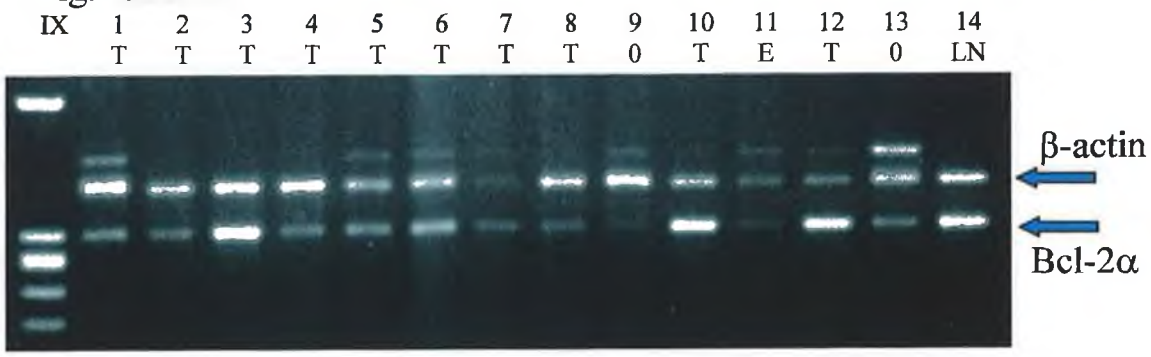

Fig. 3.6.31b:

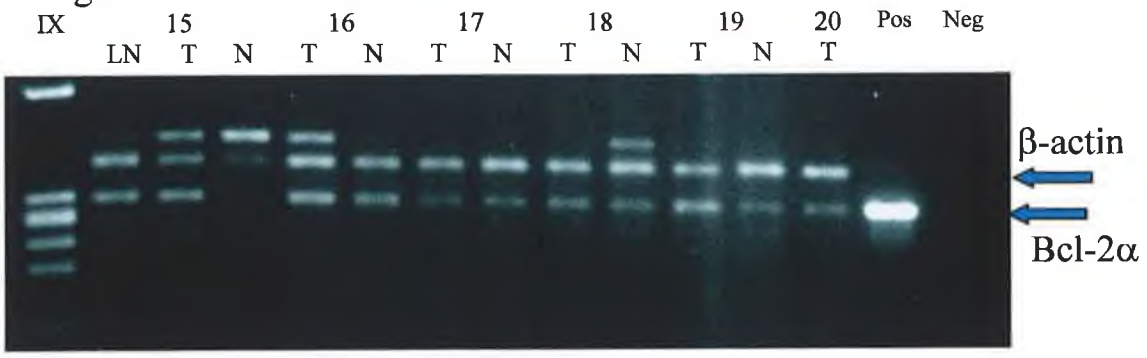

Fig. 3.6.31c:

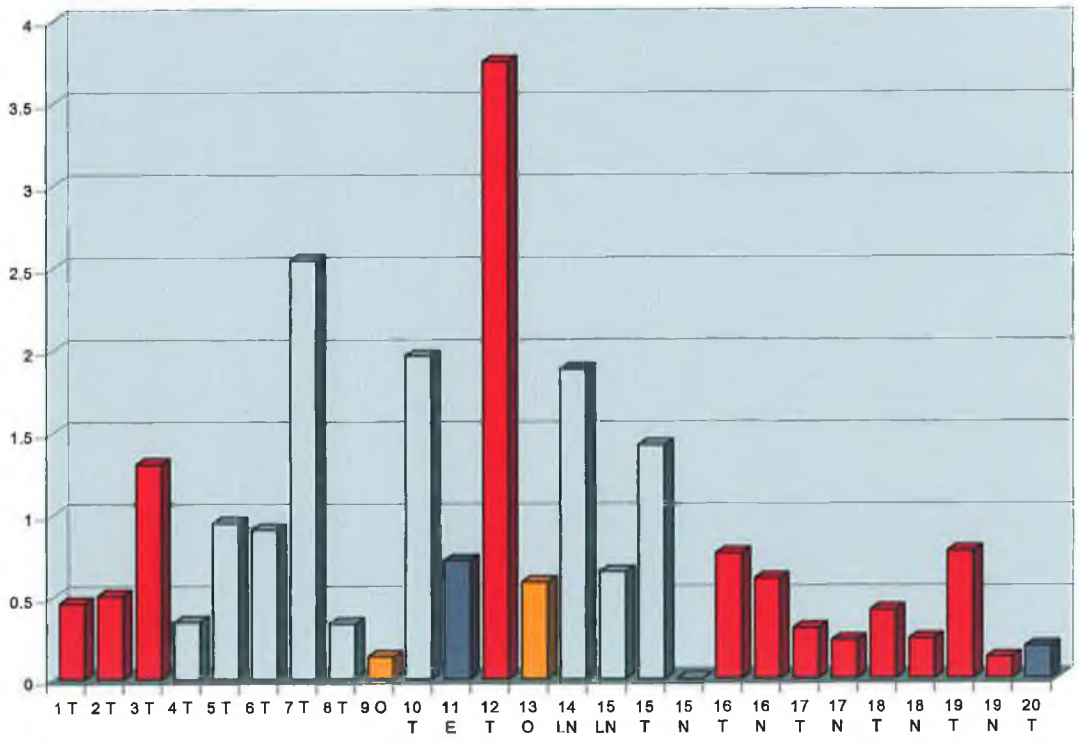

Figs. 3.6.31a & b: Gel electrophoresis photographs of Bcl-2α RT-PCR results on Lung Primary (RED), Oesophagus Primary (ORANGE), Metastatic (GREY) & Non-carcinoma (NAVY) tissue samples; Fig. 3.6.31c: Densitometry of RT-PCR results.

Fig. 3.6.32: Bcl-2α RT-PCR on Tumour tissue samples

Fig. 3.6.32a:

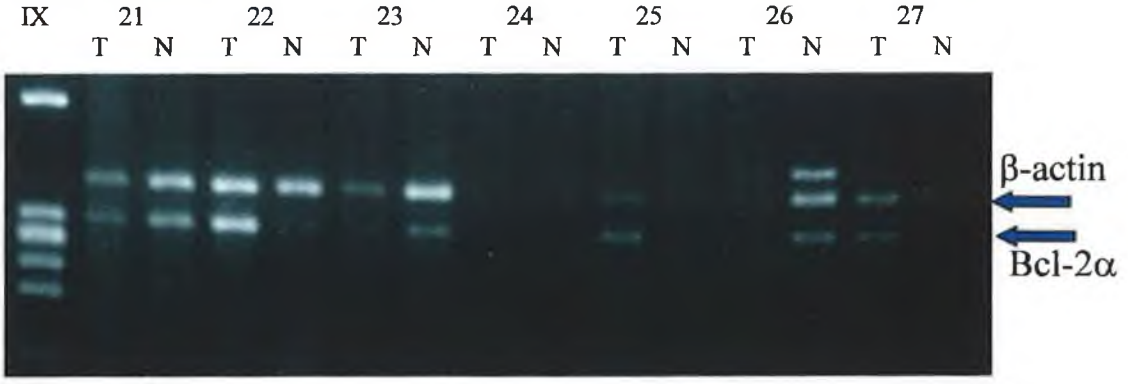

Fig. 3.6.32b:

Fig. 3.6.32c:

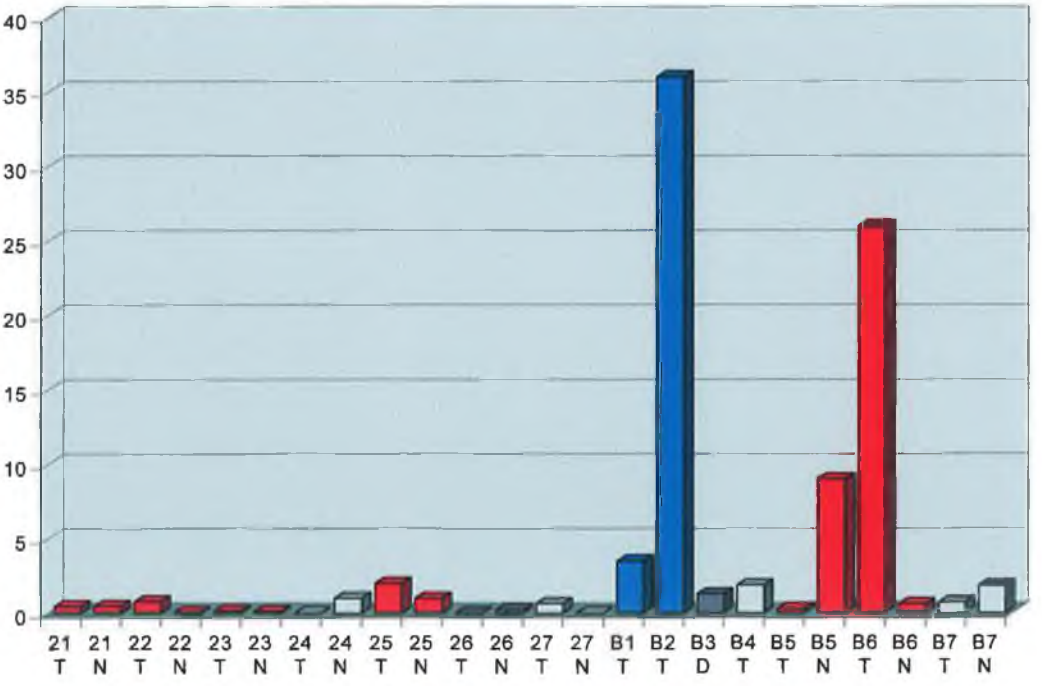

Figs. 3.6.32a & b: Gel electrophoresis photographs of Bcl-2α RT-PCR results on Lung Primary (RED), Breast Primary (BLUE), Metastatic (GREY) & Non-carcinoma (NAVY) tissue samples; Fig. 3.6.32c: Densitometry of RT-PCR results.

Fig. 3.6.33: BAG RT-PCR on Tumour tissue samples

Fig. 3.6.33a:

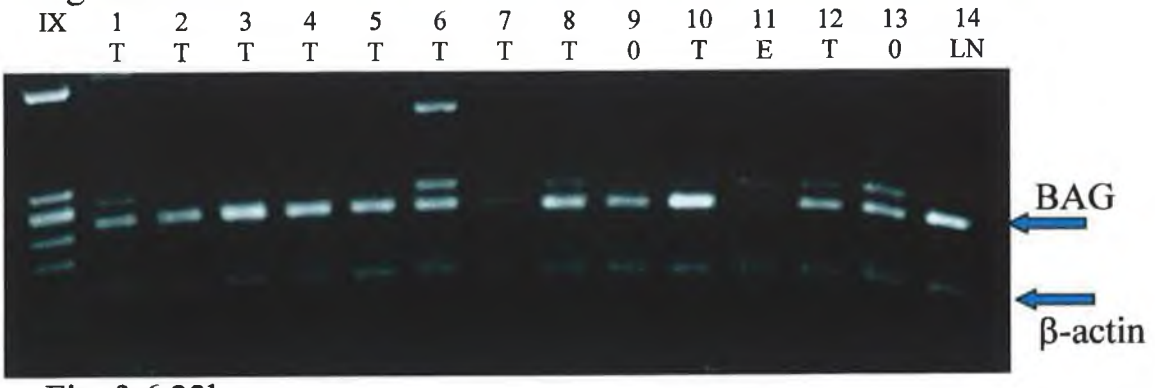

Fig. 3.6.33b:

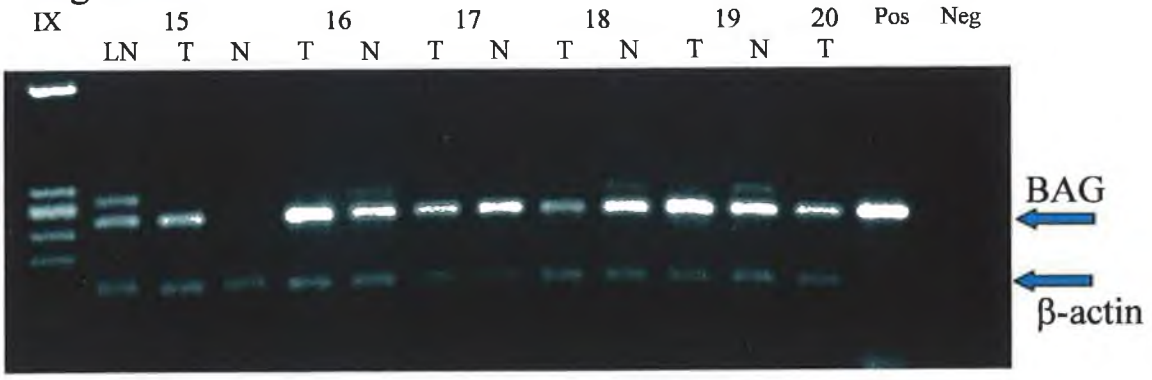

Fig. 3.6.33c:

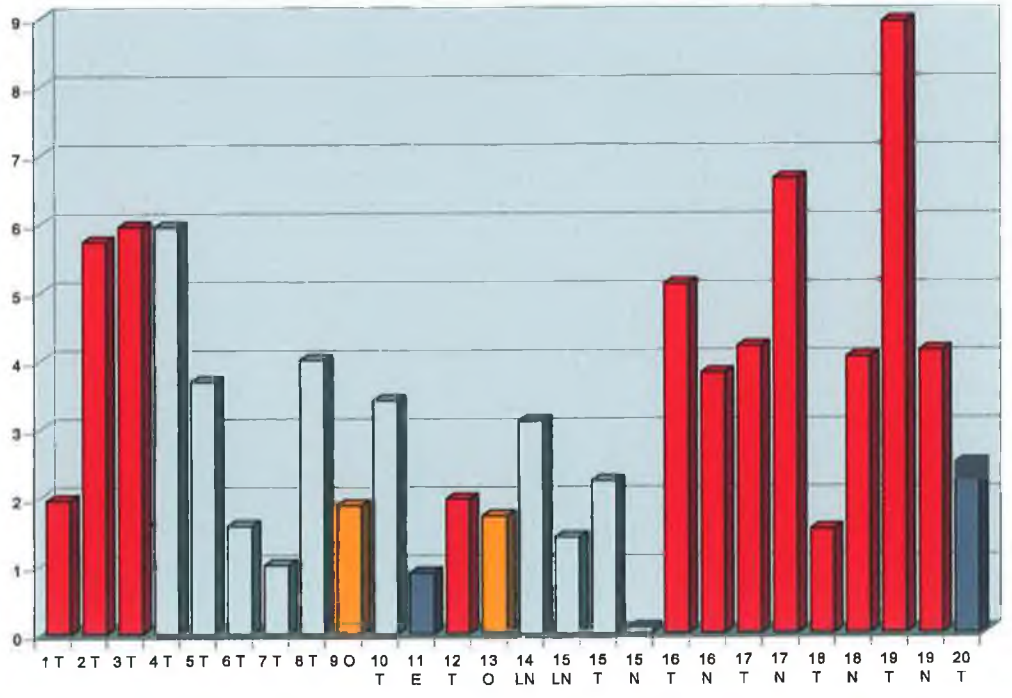

Figs. 3.6.33a & b: Gel electrophoresis photographs of BAG RT-PCR results on Lung Primary (RED), Oesophagus Primary (ORANGE), Metastatic (GREY) & Non-carcinoma (NAVY) tissue samples; Fig. 3.6.33c: Densitometry of RT-PCR results.

Fig. 3.6.34: BAG RT-PCR on Tumour tissue samples

Fig. 3.6.34a:

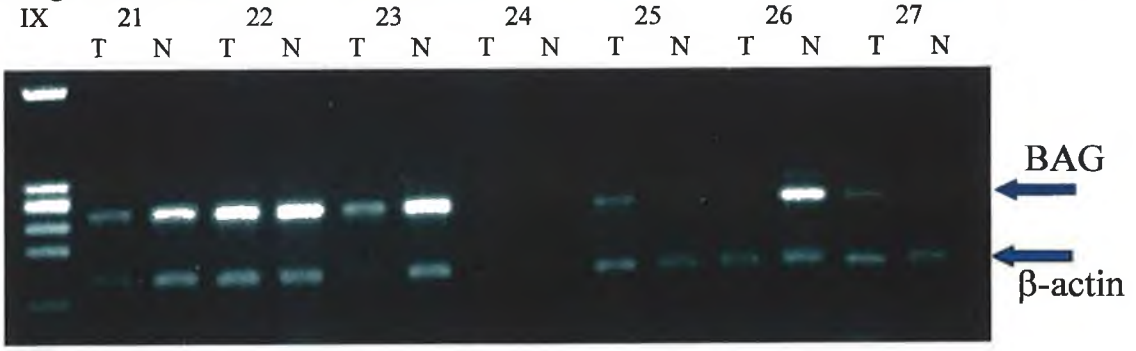

Fig. 3.6.34b:

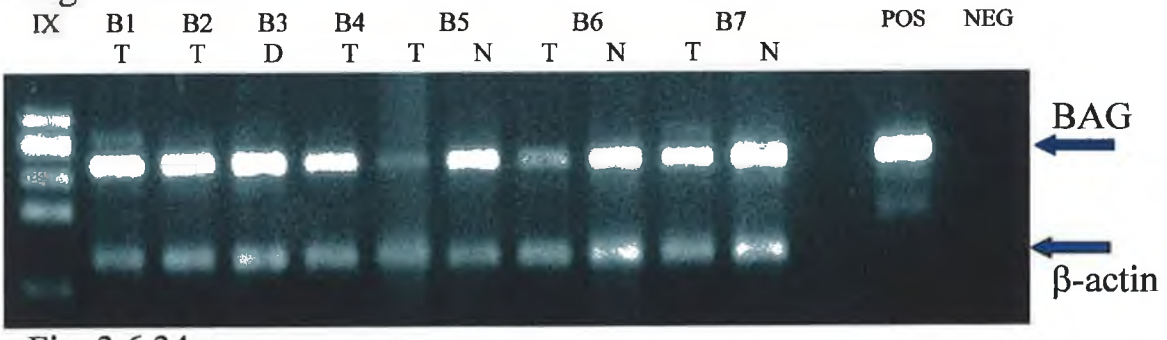

Fig. 3.6.34c:

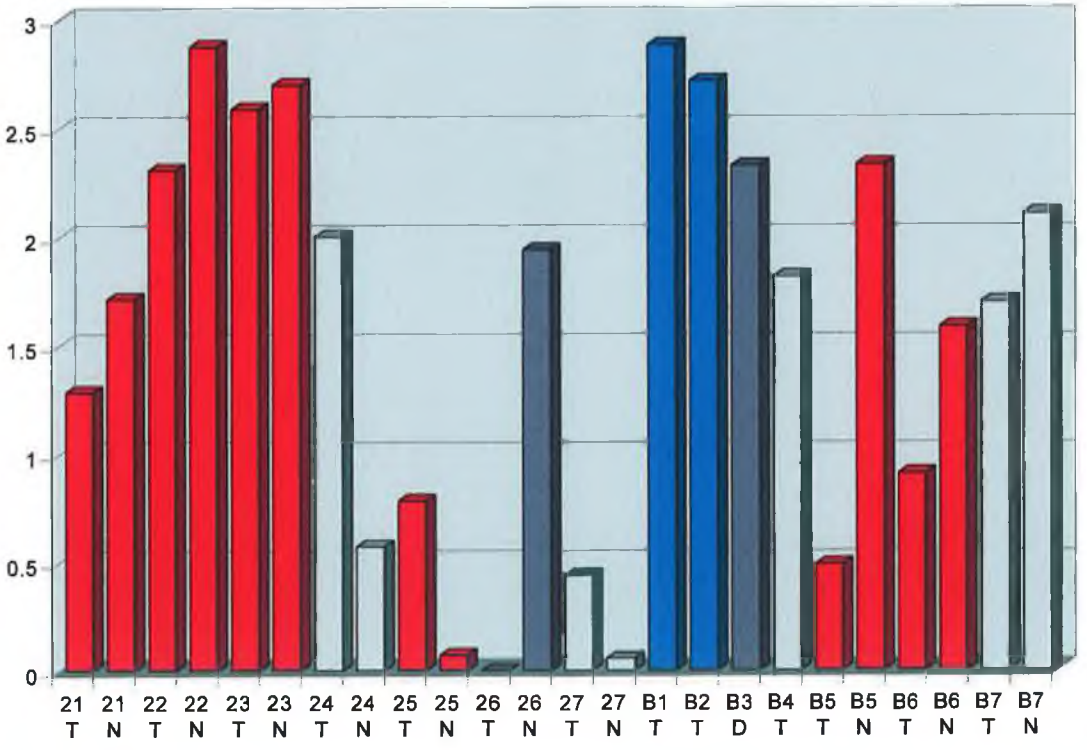

Figs. 3.6.34a & b: Gel electrophoresis photographs of BAG RT-PCR results on Lung Primary (RED), Breast Primary (BLUE), Metastatic (GREY) & Non-carcinoma (NAVY) tissue samples; Fig. 3.6.34c: Densitometry of RT-PCR results.

Fig. 3.6.35: Survivin RT-PCR on Tumour tissue samples

Fig. 3.6.35a:

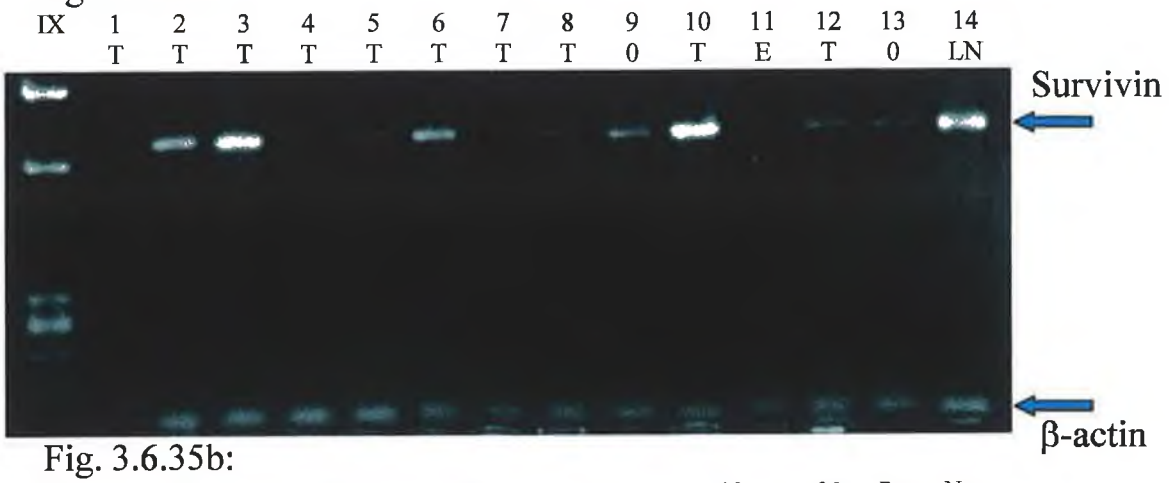

Fig. 3.6.35b:

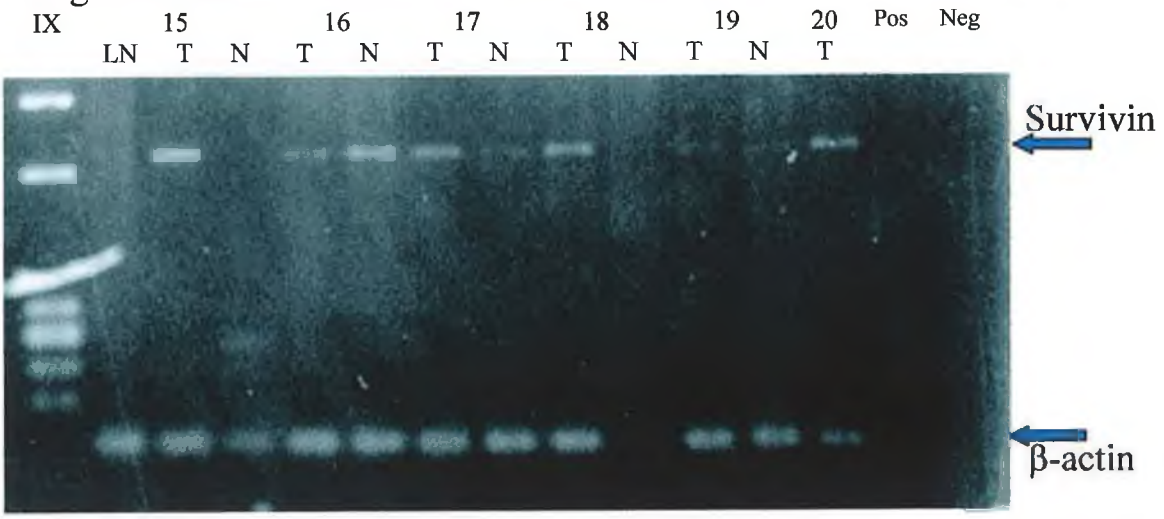

Fig. 3.6.33c:

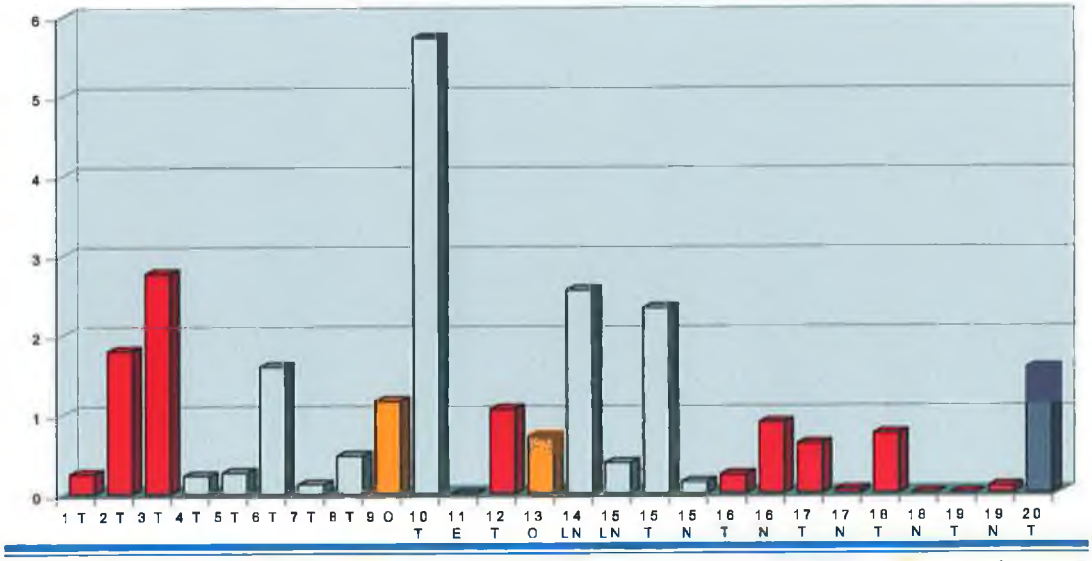

Figs. 3.6.35a & b: Gel electrophoresis photographs of Survivin RT-PCR results on Lung Primary (RED), Oesophagus Primary (ORANGE), Metastatic (GREY) & Non-carcinoma (NAVY) tissue samples; Fig. 3.6.35c: Densitometry of RT-PCR results.

Fig. 3.6.36: Survivin RT-PCR on Tumour tissue samples

Fig. 3.6.36a:

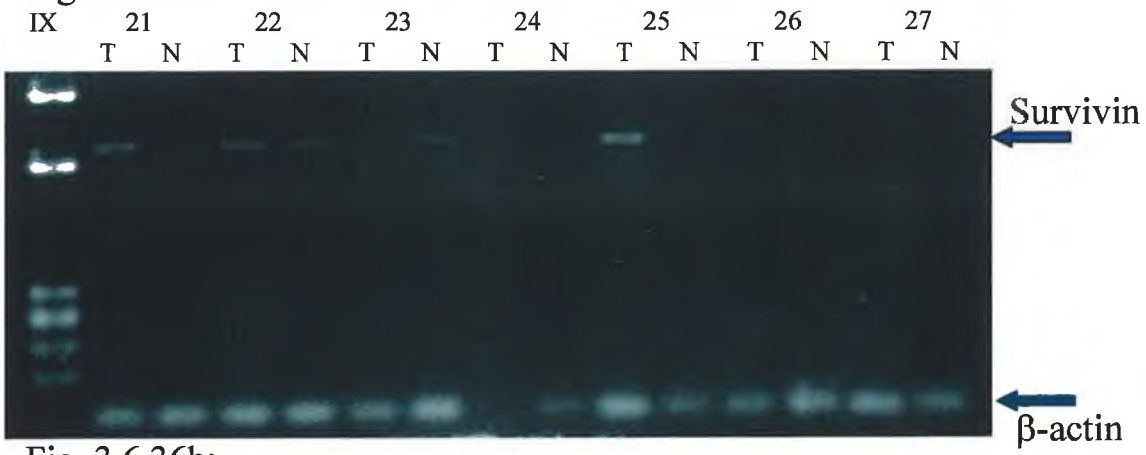

Fig. 3.6.36b:

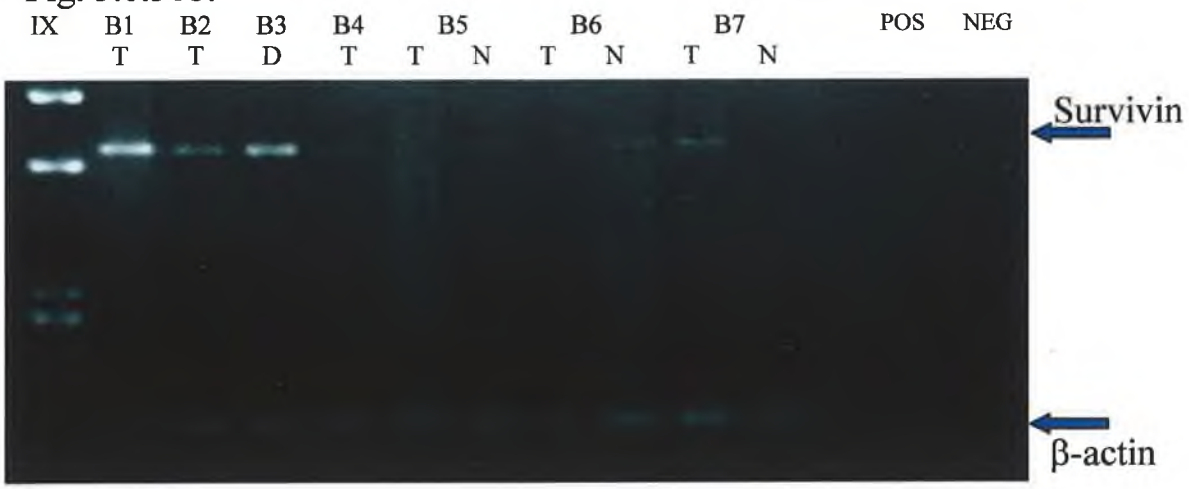

Fig. 3.6.36c:

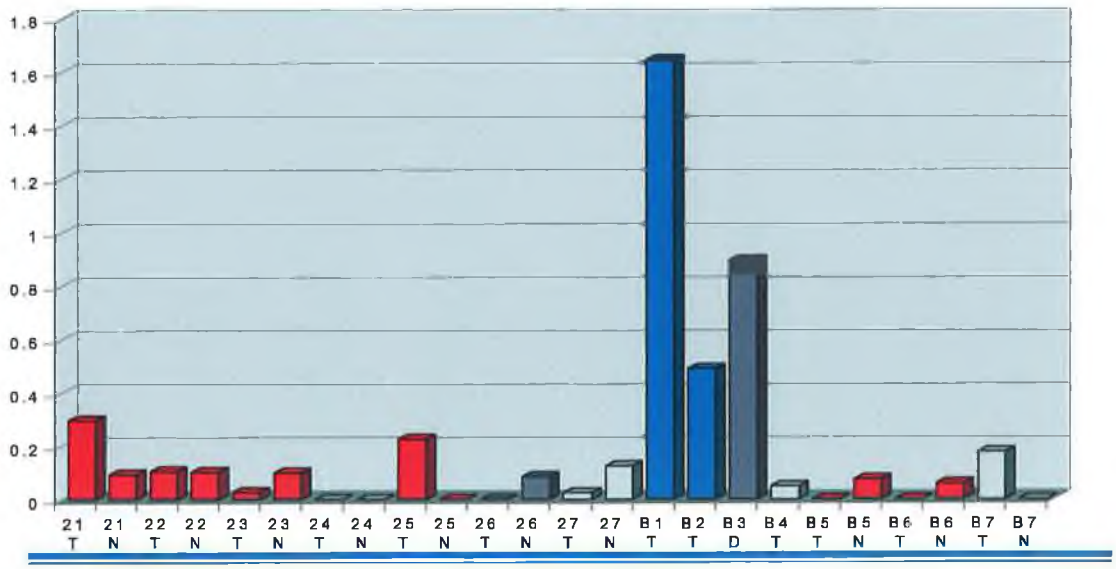

Figs. 3.6.36a & b: Gel electrophoresis photographs of Survivin RT-PCR results on Lung Primary (RED), Breast Primary (BLUE), Metastatic (GREY) & Non-carcinoma (NAVY) tissue samples; Fig. 3.6.36c: Densitometry of RT-PCR results.

tissue samples studied. Expression was detected in at least one tissue sample in each of the ten tumour/normal sample pairs. All four unpaired tumour samples were observed to express the gene. However, only five (50%) of the paired sample sets expressed higher levels of Survivin in the tumour, relative to the normal, tissue. One sample pair expressed similar amounts of the gene, while the remaining four (40%) sample pairs expressed more Survivin in the normal tissue. This result indicates that Survivin expression is divided roughly equally between tumour and normal tissue in human lung cancer.

3.6.2.19 eIF-4E

The results of these RT-PCRs can be seen in Figs. 3.6.37 and 3.6.38. As with Survivin, eIF-4E expression was detected in twenty-one of twenty-four lung tissue samples studied. Expression was observed in all four unpaired tumour samples assayed and in nine out of ten (90%) tumour/normal sample pairs. Of these nine pairs, only two (22%) expressed higher levels of eIF-4E in the tumour sample relative to the normal. A total of six (>66%) sample pairs expressed more eIF-4E in the normal sample relative to the corresponding tumour sample. The remaining sample pair expressed identical amounts of the gene in both tissues.

3.6.2.20 eIF-2α

The results of these RT-PCRs can be seen in Figs. 3.6.39 and 3.6.40. All twenty-four lung tissue samples assayed for eIF-2α expression were observed to express the gene. Expression levels in the unpaired tumour samples was generally at a medium level, while much greater variance was observed in the tumour/normal sample pairs. Of the ten paired sample sets, seven (70%) expressed higher amounts of the gene in the tumour sample relative to the normal equivalent. The remaining three sample sets expressed higher amounts of eIF-2α in the normal tissue sample relative to the tumour.

Fig. 3.6.37: eIF-4E RT-PCR on Tumour tissue samples

Fig. 3.6.37a:

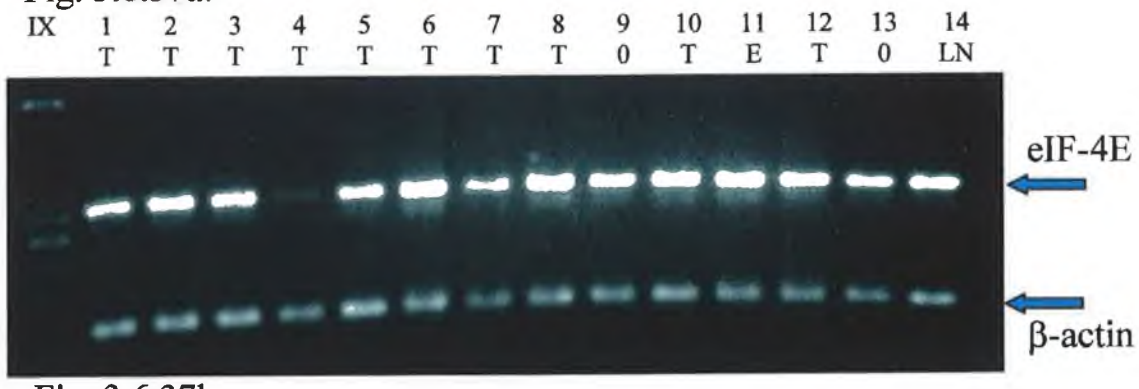

Fig. 3.6.37b:

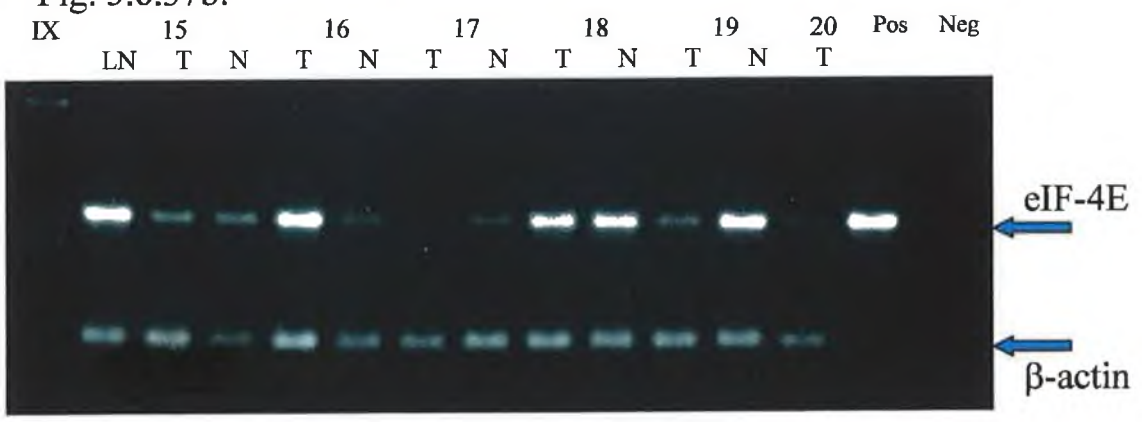

Fig. 3.6.37c:

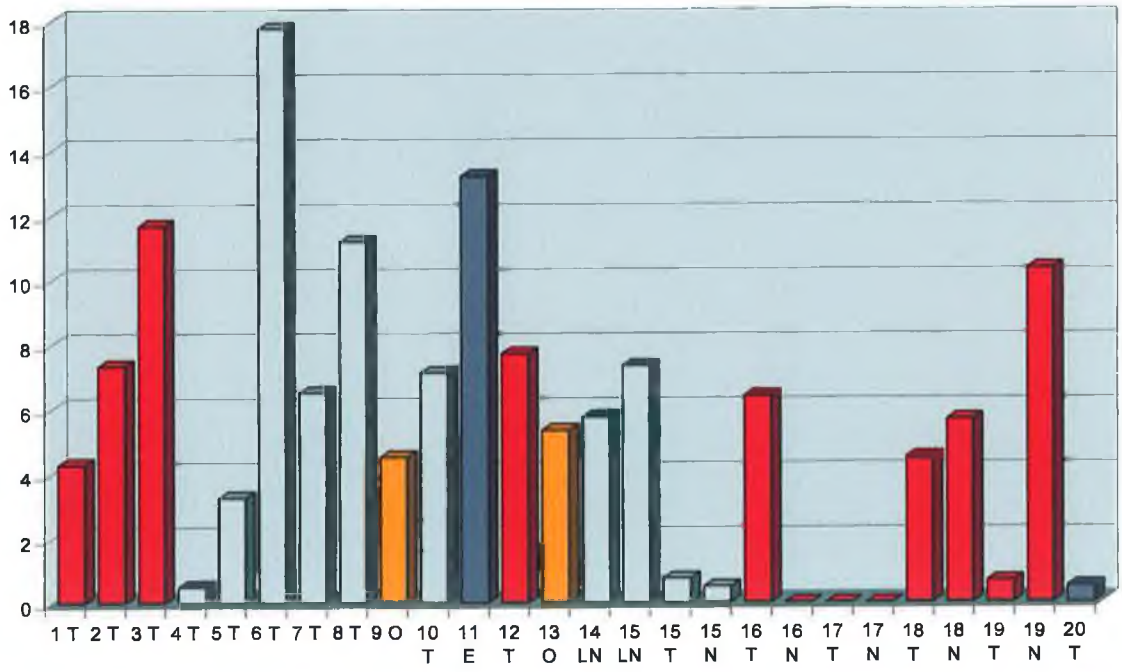

Figs. 3.6.37a & b: Gel electrophoresis photographs of eIF-4E RT-PCR results on Lung Primary (RED), Oesophagus Primary (ORANGE), Metastatic (GREY) & Non-carcinoma (NAVY) tissue samples; Fig. 3.6.37c: Densitometry of RT-PCR results.

Fig. 3.6.38: eIF-4E RT-PCR on Tumour tissue samples

Fig. 3.6.38a:

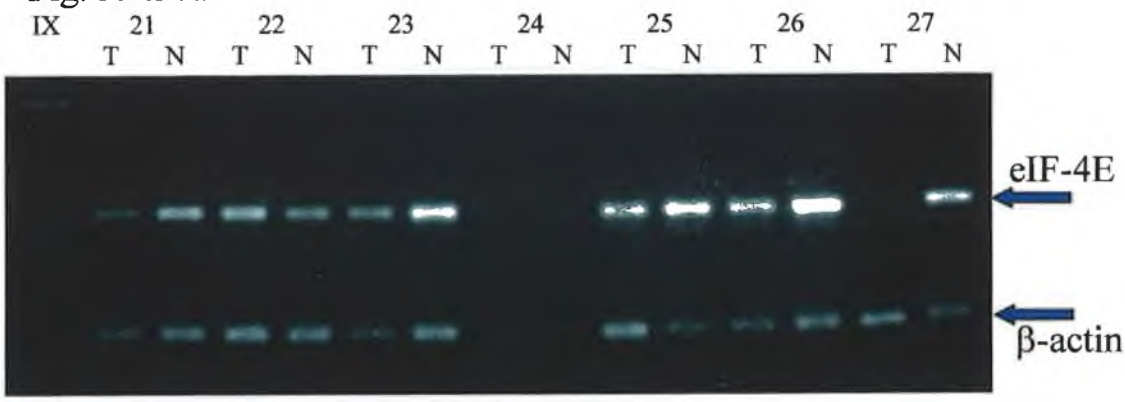

Fig. 3.6.38b:

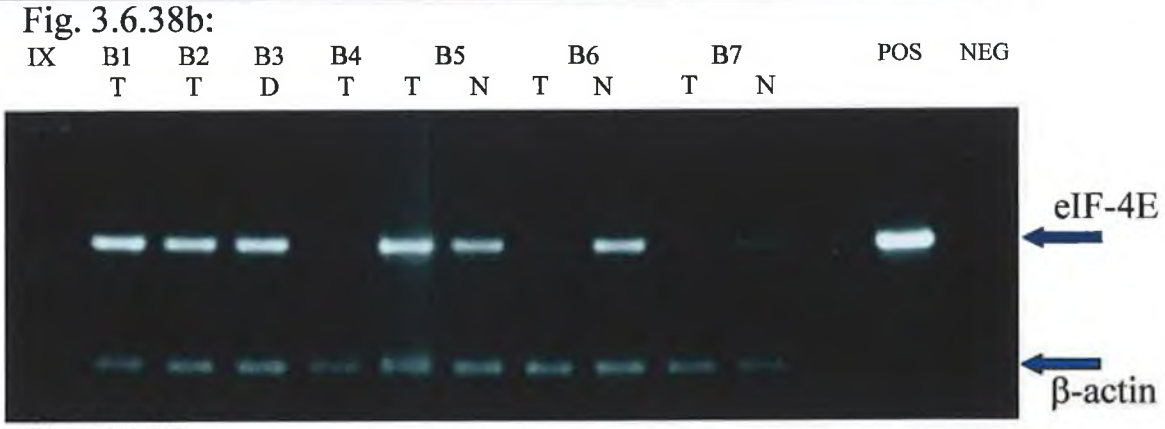

Fig. 3.6.38c:

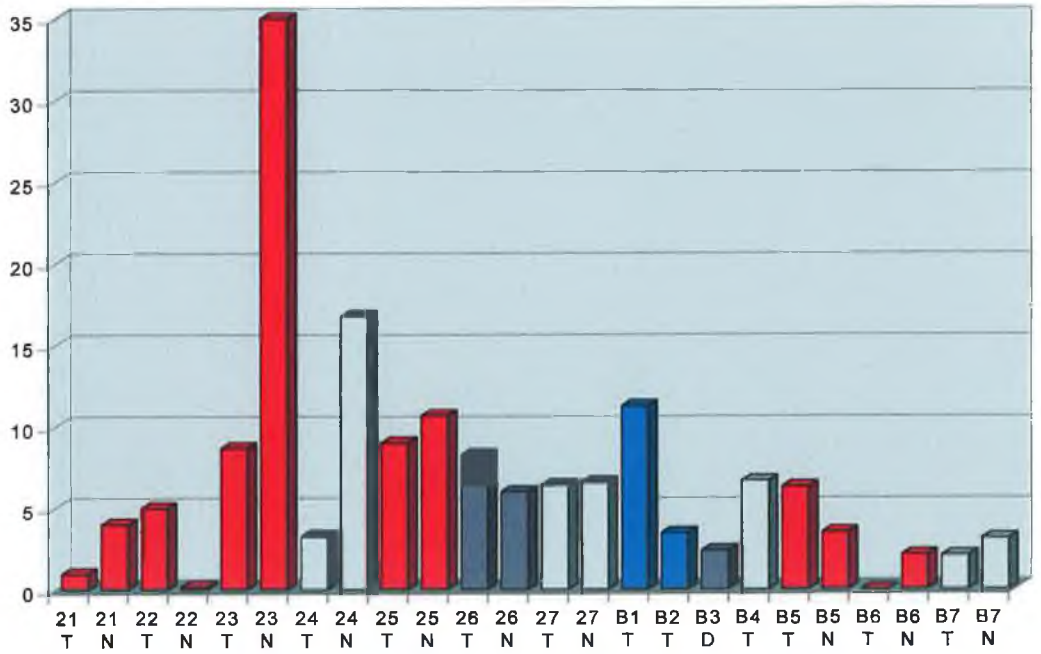

Figs. 3.6.38a & b: Gel electrophoresis photographs of eIF-4E RT-PCR results on Lung Primary (RED), Breast Primary (BLUE), Metastatic (GREY) & Non-carcinoma (NAVY) tissue samples; Fig. 3.6.38c: Densitometry of RT-PCR results.

Fig. 3.6.39: eIF-2α RT-PCR on Tumour tissue samples

Fig. 3.6.39a:

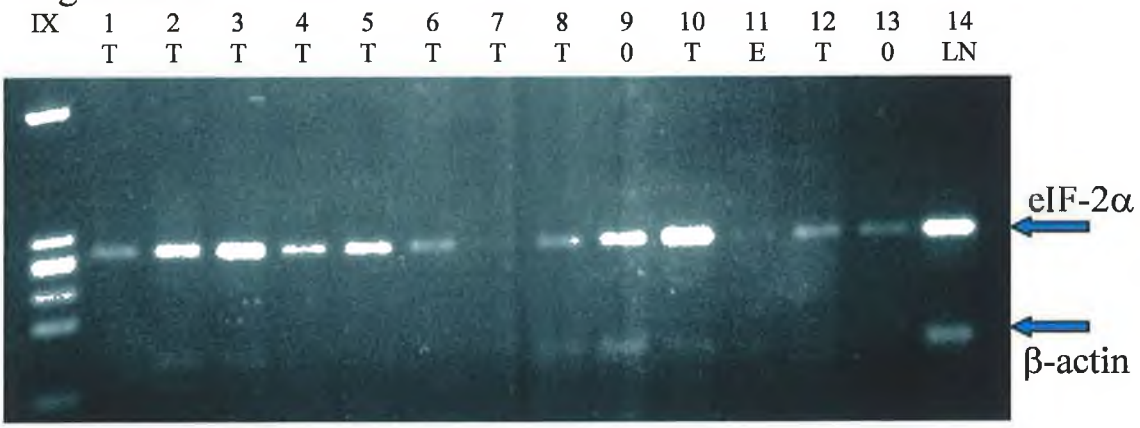

Fig. 3.6.39b:

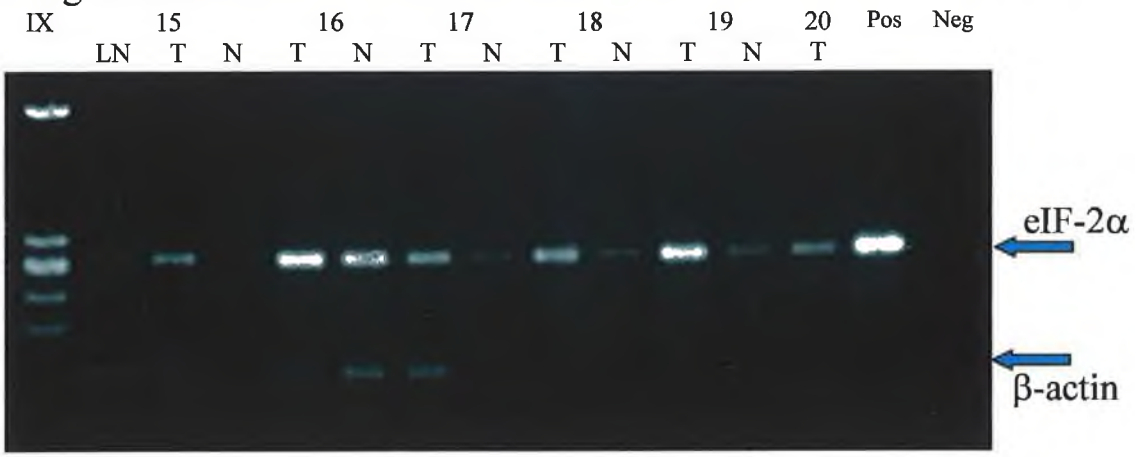

Fig. 3.6.39c:

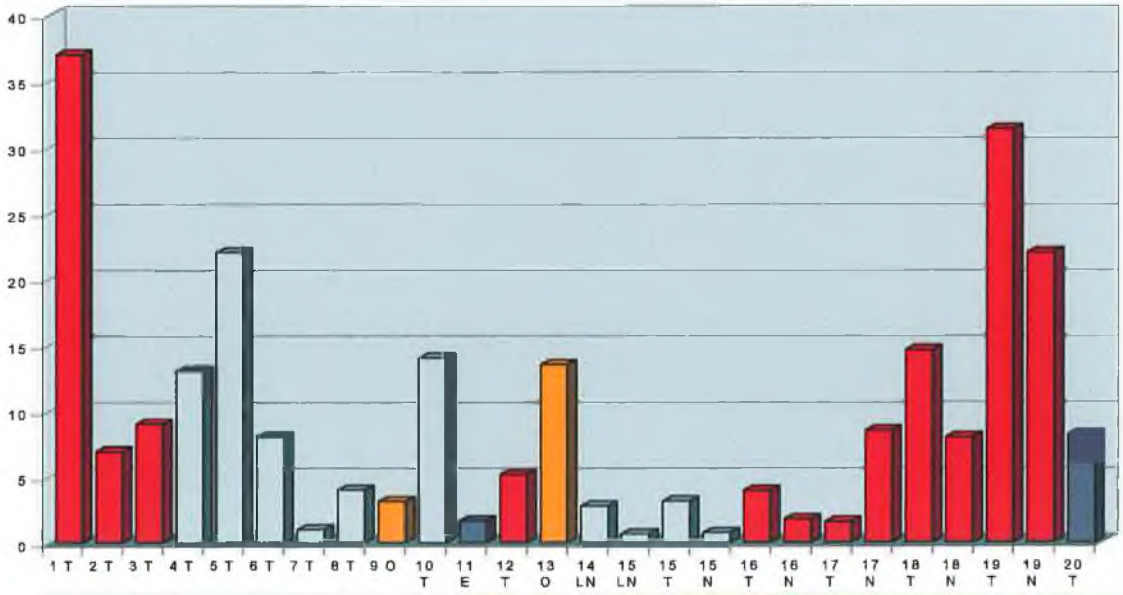

Figs. 3.6.39a & b: Gel electrophoresis photographs of eIF-2α RT-PCR results on Lung Primary (RED), Oesophagus Primary (ORANGE), Metastatic (GREY) & Non-carcinoma (NAVY) tissue samples; Fig. 3.6.39c: Densitometry of RT-PCR results.

Fig. 3.6.40: eIF-2α RT-PCR on Tumour tissue samples

Fig. 3.6.40a:

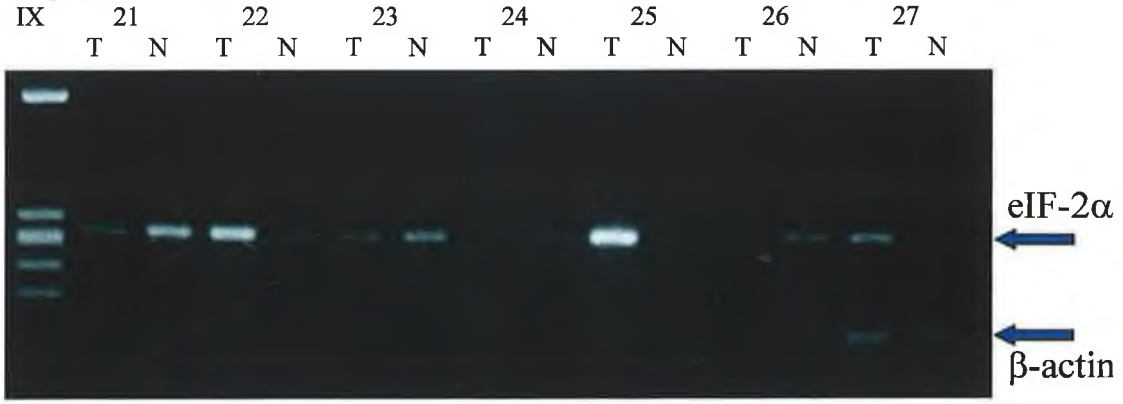

Fig. 3.6.40b:

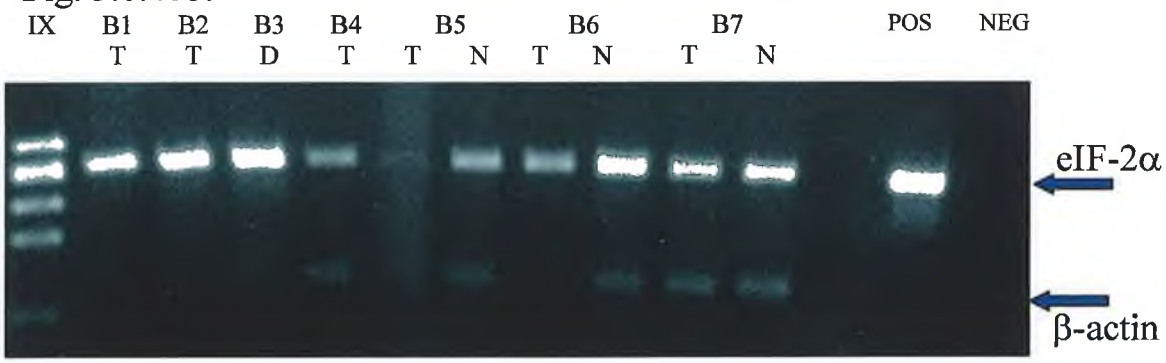

Fig. 3.6.40c:

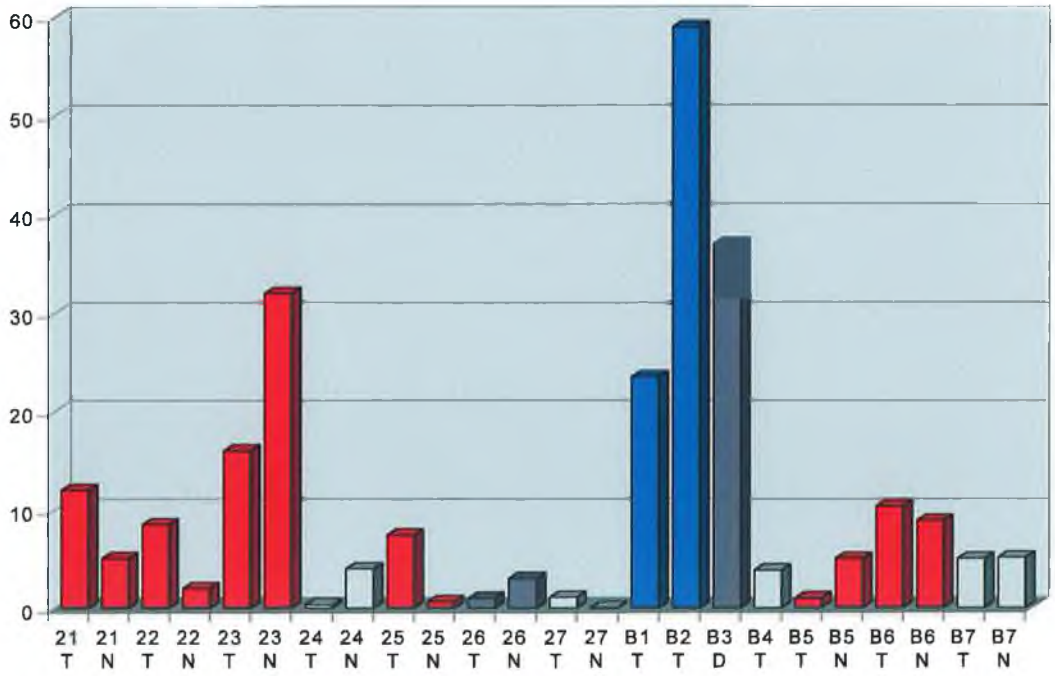

Figs. 3.6.40a & b: Gel electrophoresis photographs of eIF-2α RT-PCR results on Lung Primary (RED), Breast Primary (BLUE), Metastatic (GREY) & Non-carcinoma (NAVY) tissue samples; Fig. 3.6.40c: Densitometry of RT-PCR results.

3.6.2.21 c-*myc*

The results of these RT-PCRs can be seen in Figs. 3.6.41 and 3.6.42. c-*myc* expression was observed in only eleven (46%) of the twenty-four lung tissue samples studied. Most of these samples also expressed only quite low levels of the gene. Expression was detected in two of the unpaired tumour samples, while six of the ten tumour/normal sample pairs (60%) expressed the gene in at least one of the supplied tissue samples. Of these six pairs, only two expressed higher amounts of c-*myc* in the tumour sample. Three others expressed higher amounts in the normal sample, while another sample expressed equal amounts of the gene.

3.6.3 Correlation of Primary lung RT-PCR expression data with clinical data

The largest obstacle to meaningful interpretation of the primary lung cancer gene expression results with regard to their clinical diagnosis is the limited clinical information available on the tumours. Data was sought on a total of twenty-two distinct clinical parameters which are summarised in the clinical data information form (Clinical Data Questionnaire) included in Appendix B. This form was supplied to the clinicians at St. Vincent's for completion on each sample sent. Age, Gender and Tumour size were the only parameters where 100% availability of information was obtained. The other parameters obtained a compliance rate of between 7% and 78%. The clinical information relating to the primary lung samples only is displayed in Table 7.2B. All information was obtained from patient medical files and the tables presented in this Section reflect the totality of information obtained. As can be seen from a comparison of the Clinical Data Questionnaire with the aforementioned tables, information was not available for all parameters sought.

3.6.3.1 Age

Age was one of the most easily obtained of all the clinical parameters and was readily available for all primary tumour and normal samples supplied. The average age of the

Fig. 3.6.41: c-*myc* RT-PCR on Tumour tissue samples

Fig. 3.6.41a:

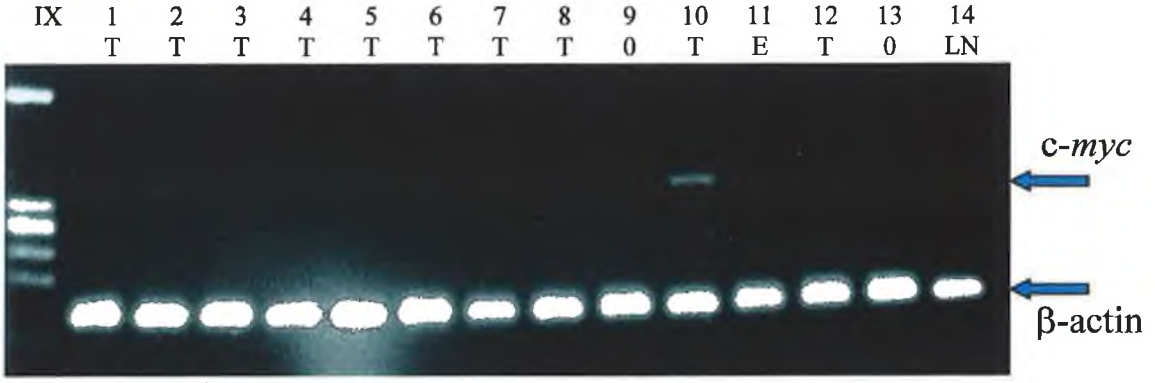

Fig. 3.6.41b:

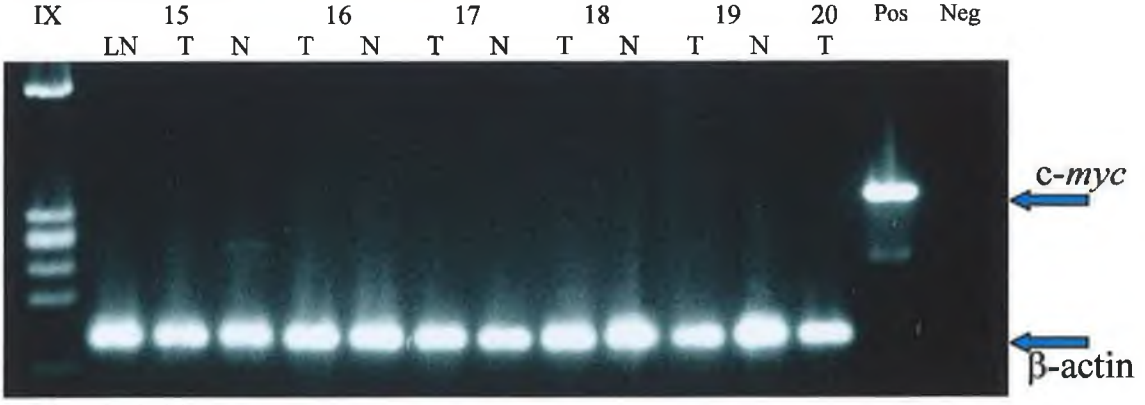

Fig. 3.6.41c:

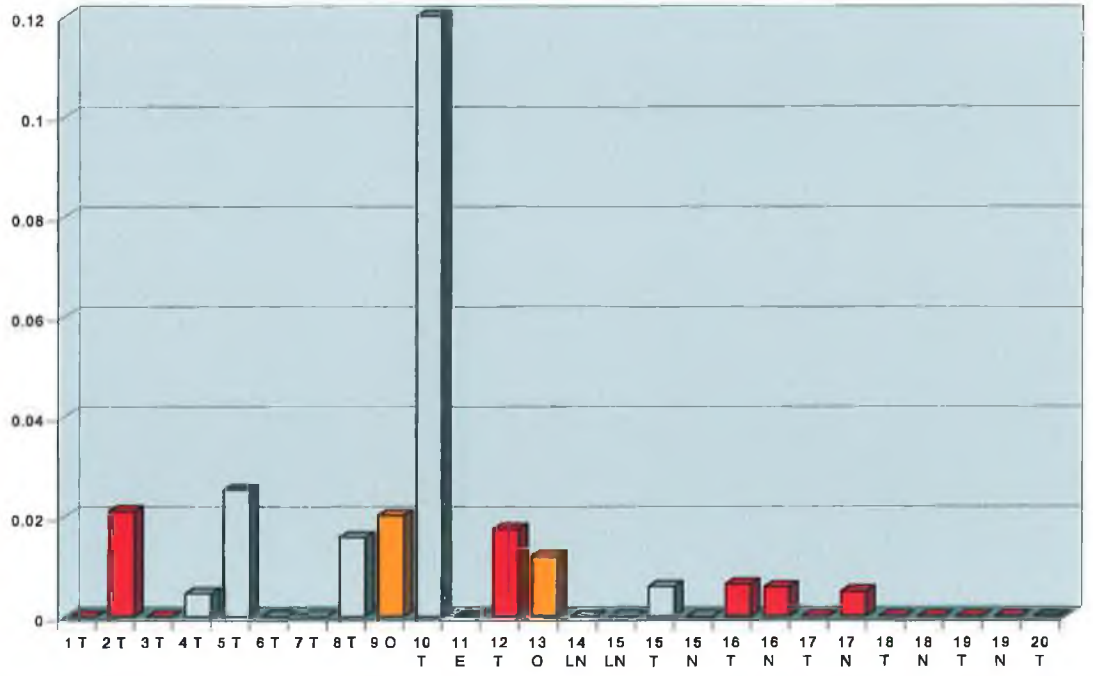

Figs. 3.6.41a & b: Gel electrophoresis photographs of c-*myc* RT-PCR results on Lung Primary (RED), Oesophagus Primary (ORANGE), Metastatic (GREY) & Non-carcinoma (NAVY) tissue samples; Fig. 3.6.41c: Densitometry of RT-PCR results.

Fig. 3.6.42: c-*myc* RT-PCR on Tumour tissue samples

Fig. 3.6.42a:

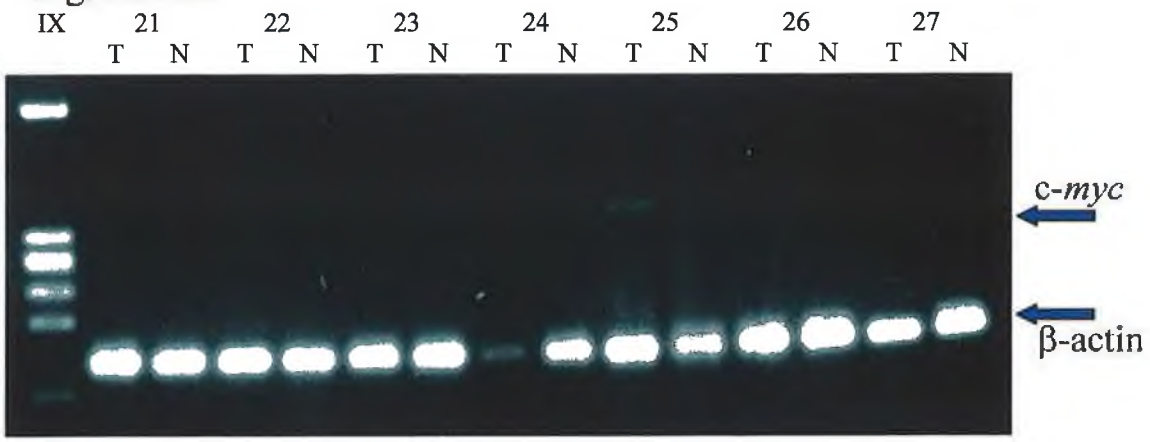

Fig. 3.6.42b:

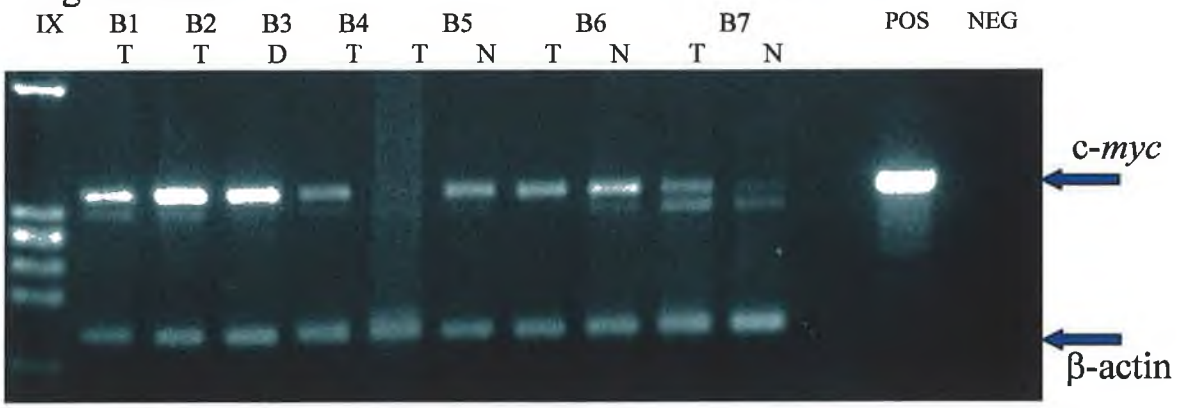

Fig. 3.6.42c:

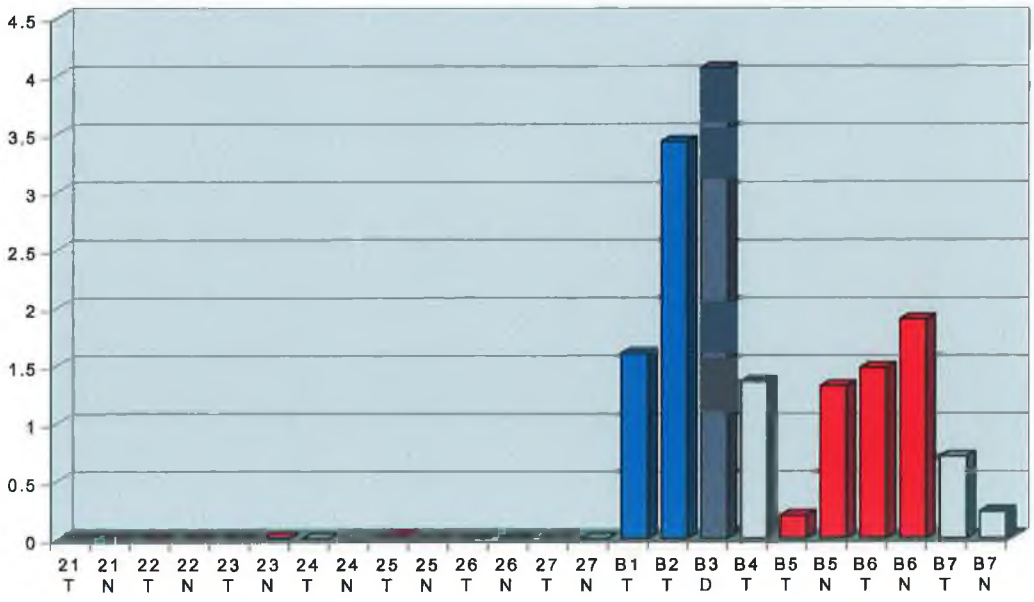

Figs. 3.6.42a & b: Gel electrophoresis photographs of c-*myc* RT-PCR results on Lung Primary (RED), Breast Primary (BLUE), Metastatic (GREY) & Non-carcinoma (NAVY) tissue samples; Fig. 3.6.42c: Densitometry of RT-PCR results.

male patients at time of surgery was 62.6 years. Average age for the female patients was eight years younger, at 54.6 years.

Although the study group involved was too small to divide up the samples into categories of patient age, several inferences may be drawn from the data. For instance, it was noted that the older the patient at the time of surgery, the larger the removed tumour size. Also, despite the fact that a number of the treated patients had expired at the time of writing (November 2001; two years after surgery), these were not the oldest patients to undergo surgery. None of the genes examined revealed a particular preponderance for the age of the patient, although expression of the MRP-related genes were notably absent from tumours removed from younger patients.

3.6.3.2 Gender

As has been previously explained, samples were taken from a total of fourteen patients undergoing surgery for removal of primary lung carcinomas. Seven patients were male, seven were female. Two of the unpaired tumour samples were obtained from male patients, two from female. Also, there were five tumour/normal sample pairs for each gender, yielding an identically divided study group along gender lines. A list of the sample numbers divided along gender lines is provided in Table 3.6.4.

Table 3.6.4 Primary lung tumour patient nos. listed by gender

Male	Female
1 T	2 T
12 T	3 T
16 T/N	19 T/N
17 T/N	21 T/N
18 T/N	23 T/N
22 T/N	B5 T/N
25 T/N	B6 T/N

When the samples are divided up by gender, an analysis of expression of the various genes reveals a number of interesting correlations. Firstly, MRP1 is predominantly expressed in tumours isolated from male patients. MRP1 overexpression was observed in six of the seven tumour samples (>85%) taken from males. Four of the five (80%) tumour/normal sample pairs expressed higher MRP1 in the tumour sample relative to the normal. For the female patients, MRP1 overexpression is largely confined to the normal samples, with four of the five normals expressing higher MRP1.

The expression of MRP5 also appeared to be slightly sex-linked. The gene was also expressed in higher amounts in the tumour sample in four of the five (80%) tumour/normal sample pairs taken from male patients. Other interesting results observed when the tumours were segregated according to gender of donor were those seen for COX-1, MRIT, Bcl-2α and eIF-2α. Bcl-2α and eIF-2α were both observed to be overexpressed in the majority of tumours extracted from male patients with an incidence rate of six out of seven samples. In tumours donated from female patients, COX-1 was observed to be expressed in only one unpaired tissue sample, and then only at a very low level. By contrast, MRIT was overexpressed in all seven female tumour tissue samples, the highest rate of expression seen on a gender basis.

Comparison of the other clinical parameters by gender also reveals another interesting anomaly. The average tumour size for specimens isolated from male patients is 2.0cm. By contrast, the average tumour size from female patients is almost triple this at an average of 5.4cm. This is the only clinical parameter which appeared to be affected by gender classification.

3.6.3.3 Tumour size

Tumour size was the third and last clinical parameter for which data was received on all tissue samples supplied. As has been already outlined (Section 3.3.3.2), tumours from female patients were generally larger than those obtaind from male donors. None of the other clinical parameters revealed any significant correlation with tumour size. Also, no significant correlation with any of the gene expression data was noted, although it was

noted that expression of BAXα was largely confined to smaller tumour sizes, while MRP1 tended to be overexpressed slightly in the larger tumours.

3.6.3.4 All other clinical parameters

None of the other clinical parameters mentioned as relevant to the primary lung tissue group contained enough information to make any rational observation about their relevance to any other parameter within the group or to any gene expression results. For this reason, data from these parameters will not be discussed further in relation to this tissue study group.

3.6.4 RT-PCR gene expression results for Primary Human Breast Tissue samples

After analysis of the clinical data, the group was reduced to just two unpaired primary specimens. As this small group is not statistically significant, the general trends will be discussed here. The complete RT-PCR results, as well as clinical data, for each of these samples is presented on Table 7.3B in Appendix B. A list of the clinical data for these samples is displayed in Table 7.4B in Appendix B. The two primary breast tumour samples are listed in Table 3.6.5.

Table 3.6.5 List of Primary Breast tumour samples

Sample Name	Sample Tissue Type
B1 T	Single Tumour only
B2 T	Single Tumour only

The PCR results for both tumour tissue specimens were observed to be largely similar. Both tissue samples expressed low amounts of the MRP genes 1, 2, 3, 5 and 6. No expression for MRP4 was observed in either tissue. Mdr-1 and BCRP were also expressed in these samples to a low degree, although expression of mdr-3 was not seen. Expression of the pro-apoptotic genes BAP, BAX α and MRIT was observed to be quite high in these tissues, although no expression of the Bcl-x_S gene was observed.

Similarly, Bcl-x_L expression was not detected in these samples although the other anti-apoptotic genes surveyed, Survivin, BAG and Bcl-2α were all expressed at medium to high levels. Finally, high levels of expression of the eIF-4E and eIF-2α genes was also observed, along with high expression of the c-*myc* gene.

3.6.5 RT-PCR gene expression results for Primary Oesophageal tissue samples

Two unpaired oesophageal tumour samples were received and analysed in the course of this study. Due to the small sample size, no significant correlations may be drawn between gene expression and clinical data. However, the results obtained for these two samples will be outlined here. All gene expression data on these samples are included in Table 7.5B, while the clinical information is displayed in Table 7.6B, both of which are located in Appendix B. The two primary oesophageal tumour samples are listed in Table 3.6.6.

Table 3.6.6 List of Primary Oesophageal tumour samples

Sample Name	Sample Tissue Type
9 O	Single Tumour only
13 O	Single Tumour only

RT-PCR analysis of the oesophageal tumour samples reveal high expression of Bcl-x_S and medium expression levels of the genes BAXα, Bcl-x_L, BAG and eIF-4E. Low expression levels was observed for MRPs 1, 4, 5 and 6, as well as for COX-1, COX-2, and c-myc. Variable expression levels were observed for all other genes studied. The clinical data available on these samples was especially sparse, with only four criteria completed. Overall, there was little correlation to be made from such a small group; both donors were male, in their mid-to-late 70s and both tumours appeared poorly differentiated.

3.6.6 RT-PCR gene expression results for Metastasised tumour samples

The metastasised tissue group was the second largest group in the study, comprising a total of seventeen tissue samples, yielding a total of 374 individual gene expression results. As the origin of these tumours is unknown, it is impossible to group these tissues under any category resembling tumour type and so these samples will therefore be analysed in one distinct grouping. All expression data are included in Table 7.7B, while the clinical information on these samples is shown in Table 7.8B, both of which are in Appendix B. A list of the seventeen metastasised tissue sample numbers is given in Table 3.6.7.

Table 3.6.7 List of Metastsised human tissue samples

Sample Name	Sample Tissue Type
4 T	Single Tumour only
5 T	Single Tumour only
6 T	Single Tumour only
7 T	Single Tumour only
8 T	Single Tumour only
10 T	Single Tumour only
B4 T	Single Tumour only
14 LN	Mediastinal Lymph Node tissue
15 LN	Mediastinal Lymph Node tissue
15 T/N	Tumour with Normal tissue control
24 T/N	Tumour with Normal tissue control
27 T/N	Tumour with Normal tissue control
B7 T/N	Tumour with Normal tissue control

As outlined already, the metastasised tissue sample group was made up of five single tumour samples from lung, three tumour/normal sample pairs from lung and two mediastinal lymph nodes as well as two single tumour samples from breast and one tumour/normal sample pair from breast. An analysis of the clinical details for this group reveals a number of details which may be of potentially relevance to the clinical profiling of metastasised tumour tissue.

From the clinical results that were available, the lung samples were excised from five male and two female patients. There was an even distribution of ages over the samples included, and only one patient was deceased at the time of writing. An analysis of the RT-PCR gene expression results revealed a very different expression profile to that obtained from primary tumours of the lung, breast or oesophagus. Most of the twenty-two genes assayed were expressed at widely varying levels over the samples studied. Only MRP2, COX-1 and eIF-2α which were generally expressed at low to medium levels in these tissues showed any pattern of expression at all. The expression levels of the other genes varied too widely for general classification. Overall, only expression of the MRP1 gene in these tissues was deemed significant. MRP1 was strongly overexpressed in the tumour sample of all the tumour/normal sample pairs analysed as well as being significantly expressed in every unpaired tumour specimen.

3.6.7 Expression results for non-carcinoma tissue samples

The non-carcinoma tissue group was made up of five tissue samples as already outlined (see Section 3.6.1). The complete RT-PCR results are presented in Table 7.9B in Appendix B, along with the clinical data in Table 7.10B. The five non-carcinoma tissue sample nos. are listed in Table 3.6.8.

Table 3.6.8 List of non-carcinoma human tissue samples

Sample Name	Sample Tissue Type
11 E	Empyema strip decortication
20 T	Non-malignant bronchial reSection
B3 D	Duodenal tissue sample
26 T/N	Non-malignant bronchial reSections

As this sample group is taken from non-malignant tissue, the information obtained is of relevance only so far as it may indicate expression levels of the various genes for normal human tissue.

3.7 Identification of a cell system for further research into MRP1 inhibition

As shown in Sections 3.1-3.4, expression of the MRP1 gene appears to be an important factor in the study of cell responses to outside stimuli. It was found that MRP1 gene expression increased following exposure to the differentiating agent BrdU in the DLKP and A549 cell lines (Section 3.1), in response to short-term exposure to cisplatin and taxol (Section 3.2), also in DLKP and as well after long-term selection into drug-resistant DLKP-variant cell lines (Section 3.3). Promoter analysis of the MRP1 gene has indicated that it may be transcriptionally controlled by the action of at least some of these agents (Section 3.5). Expression of MRP1 was also shown to be expresed in tumour biopsies (Section 3.7).

It was felt that this gene may prove to be an important target for gene therapy. The twin gene therapy techniques of Antisense and Ribozyme technology were chosen in an attempt to modify or eliminate the expression of the MRP1 gene and its protein product in the cell system of choice. Before using these technologies, it was firstly considered necessary to identify a cell system in which expression of the MRP1 gene has already been identified and which would be amenable to treatment with gene therapy. It was then essential to demonstrate the basal level of activity of the MRP1 gene product in this system. If the normal, functioning, activity of the MRP1 protein was interrupted following treatment with either antisense or ribozymes, the doenregulation could then be considered to have been achieved.

Significant increases in MRP1 gene expression in response to BrdU and certain chemotherapeutic drugs were observed in the DLKP cell line. Therefore, it was decided to continue the research into the activity of MRP1 using this cell system. As outlined in Section 1.3.4, DLKP is a poorly differentiated human lung carcinoma cell line, which was established in the NCTCC (Law *et al.*, 1992) and is found to be composed of three clonal cell lines, DLKP-I, -M and -SQ. It has been found to express low levels of MRP1 at both the mRNA and protein level.

In order to properly examine the effect of gene therapy on expression and function of MRP1, it was felt that examination of the role of the protein in one of the clonal cell lines would be more advantageous. While treating the uncloned DLKP cell line with

antisense oligonucleotides and monitoring the effect on the gene and protein expression of MRP1 would be feasible, effective ribozyme treatment required the establishment of stable ribozyme-expressing clones to accurately ascertain the effect of this particular gene therapy technique. As DLKP is a composite of three separate clonal cell lines, it would not be apparent which of the three cell lines was being examined.

For this reason, it was decided that one of the clonal variants of DLKP would be chosen for further study of MRP1. The squamous cell line variant of DLKP, DLKP-SQ, (see Section 2.2.2) was chosen as the cell line for further research. This cell line was chosen as it had already been characterised in this laboratory as expressing the same level of MRP1 RNA as the parent DLKP. This low level of gene expression was considered ideal for use in gene therapy experiments that would attempt to reduce or knock-out the effect of the MRP1 gene, as any observed reduction in the expression of the gene at either the mRNA or protein level should have a significant knock-on impact on the toxicological profile of the cell line.

The proceeding sub-sections will refer to the characterisation of the DLKP-SQ cell line, repeated in order to confirm the expression of the MRP1 gene in the cell line. A number of other cell lines were also utilised during these characterisations; these are outlined in Section 2.2.2. These cell lines were chosen for a number of reasons; these are outlined in Table 3.7.1.

Table 3.7.1 Selected cell lines examined in study

Cell Line	Reason for inclusion in study
COR L23R	Expresses high levels of MRP1; use as a Positive control
COR L23S	Expresses very low levels of MRP1; use as a Negative control
A549	Included to give an indication of the difference between a clonal and parent cell line response to gene therapy
A549 C9	

While reference will be made in the following Sections to results obtained for the inhibition of MRP1 in DLKP from other studies, all results shown from here on will refer exclusively to those obtained for the DLKP-SQ cell line.

3.7.1 Characterisation of the DLKP-SQ cell line using RT-PCR

MRP1 RT-PCRs were carried out on the DLKP-SQ cell line as outlined in Section 2.4.2.5. This was done, firstly to confirm the earlier characterisation data; that the cell line expressed MRP1 at a low level, and secondly to compare this expression level with other cell lines, including its parental DLKP cell line.

The results of the PCRs can be seen in Figs. 3.7.1 and 3.7.2. As can be seen, expression of MRP1 in the DLKP-SQ cell line is generally low, although slightly higher than that obtained for the A549 cell line. This is surprising as previous work in this laboratory had identified higher MRP1 gene expression levels in the A549 cell line, than for DLKP-SQ (M. Heenan, Personal communication). MRP1 gene expression was highest for COR L23R (positive control) and almost non-existent for COR L23S (negative control). In Fig. 3.72, the relative expression levels of MRP1 in both the DLKP cell line and its clonal variant, DLKP-SQ, were compared. As can be seen from the figure, expression levels for the gene were almost identical for both cell lines.

3.7.2 Characterisation of the DLKP-SQ cell line using Northern blotting

Northern blotting of the selected cell lines was also carried out to examine the level of MRP1 gene expression using this method. The probe was prepared and the procedure carried out as outlined in Section 2.4.3.3. A GAPDH Northern blot was also carried out to standardise the MRP1 expression levels detected. The results of this blot can be seen in Fig. 3.7.3. As can be seen, the COR L23R RNA sample expressed the highest levels of the gene, at almost double that of the A549, A549 C9 and DLKP-SQ samples. Expression levels were generally high also for the DLKP-SQ cell line and for the negative COR L23S control.

It was decided that RT-PCR would be commonly used in future to measure changes in MRP1 gene expression as it was a more convenient method of analysis. Northern blotting could be used as a secondary method, to back up any RT-PCR results which proved promising.

Fig. 3.7.1: MRP1 RT-PCR on selected cell lines

Fig. 3.7.1a:

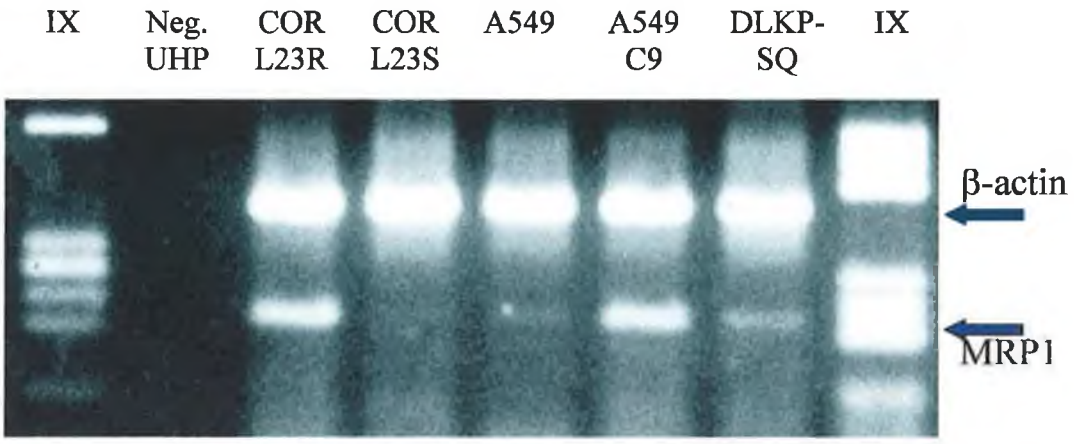

Fig. 3.7.1b:

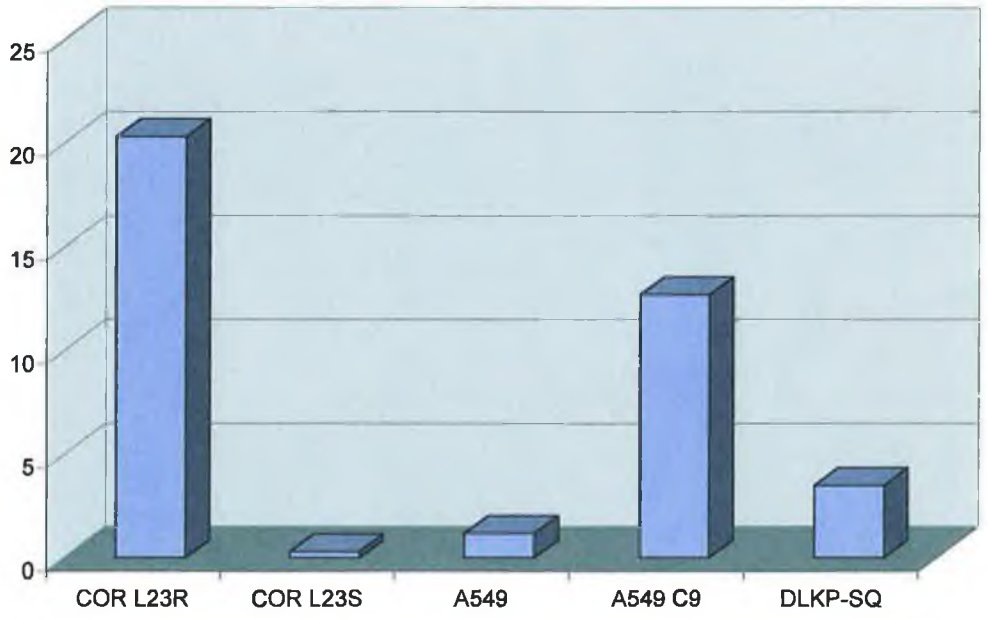

Fig. 3.7.1a: Gel electrophoresis photograph of MRP1 RT-PCR results selected cell lines; Fig. 3.7.1b: Densitometric analysis of RT-PCR results.

Fig.3.7.2: MRP1 expression in DLKP & DLKP-SQ cells

Fig. 3.7.2a:

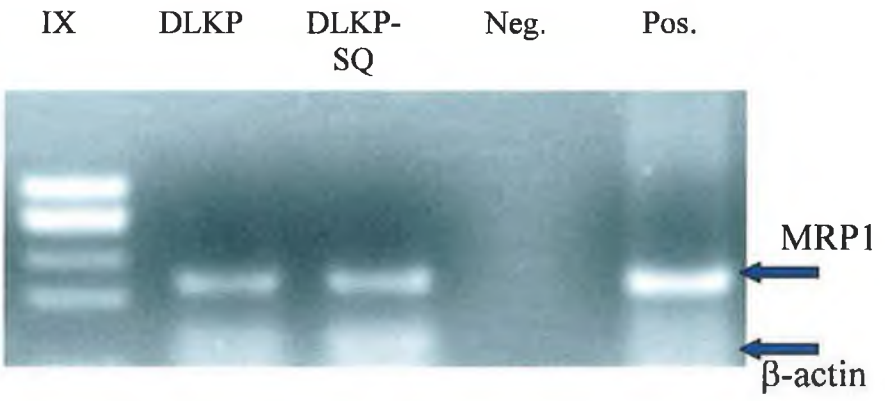

Fig. 3.7.2a:

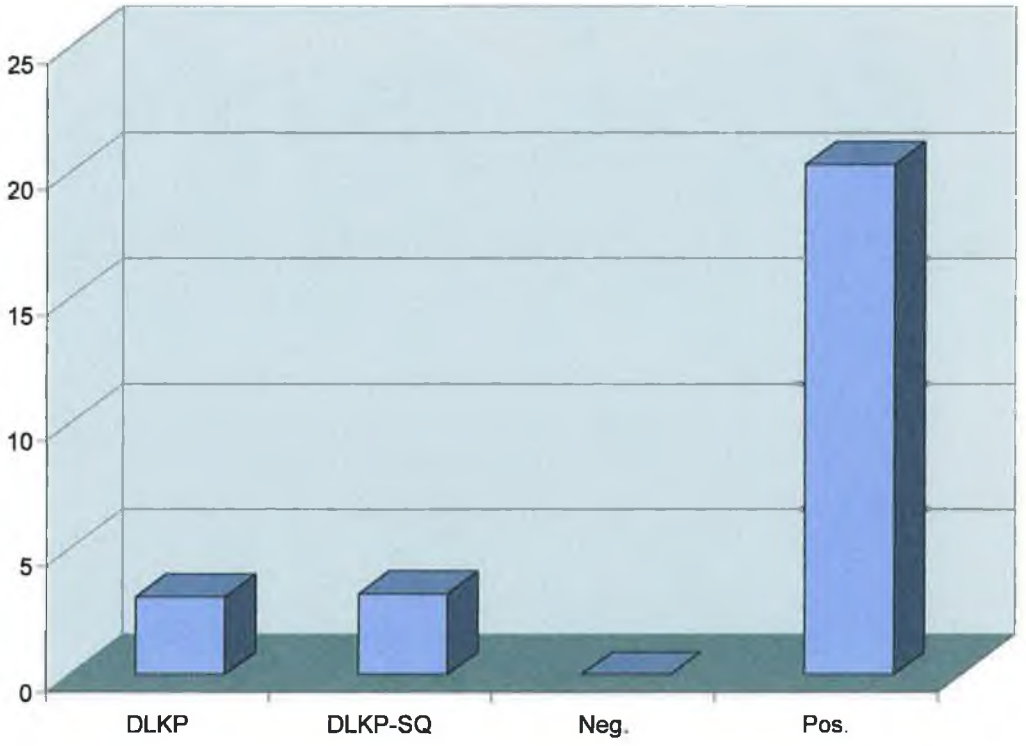

Fig. 3.7.2a: Gel electrophoresis photograph of MRP1 RT-PCR results on DLKP & DLKP-SQ cells; Fig. 3.7.2b: Densitometric analysis of RT-PCR results.

Fig. 3.7.3: MRP1 Northern blot of selected cell lines

Fig. 3.7.3a:

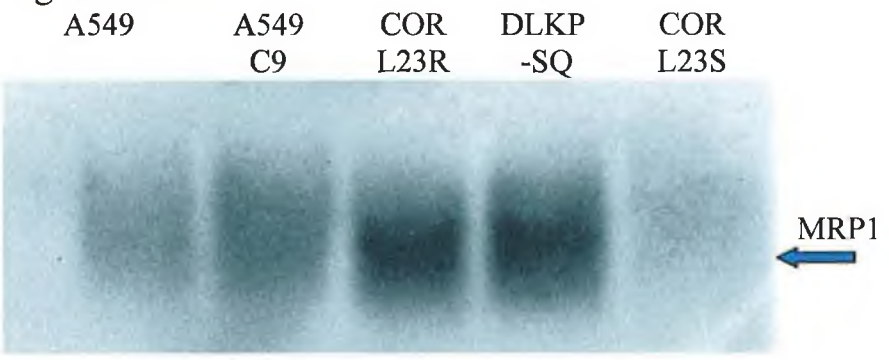

Fig. 3.7.3b:

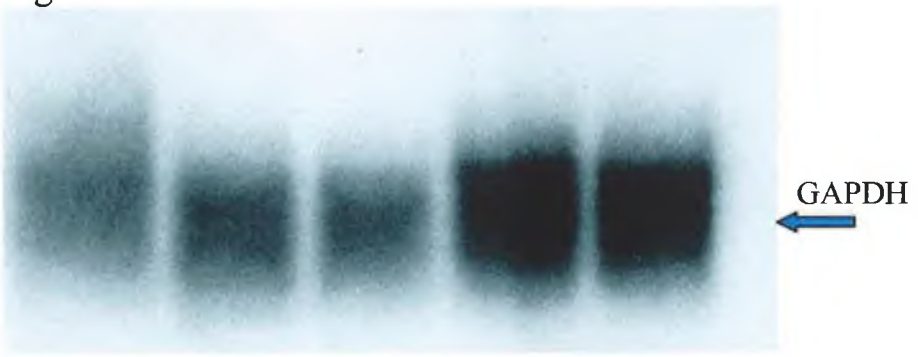

Fig. 3.7.3c:

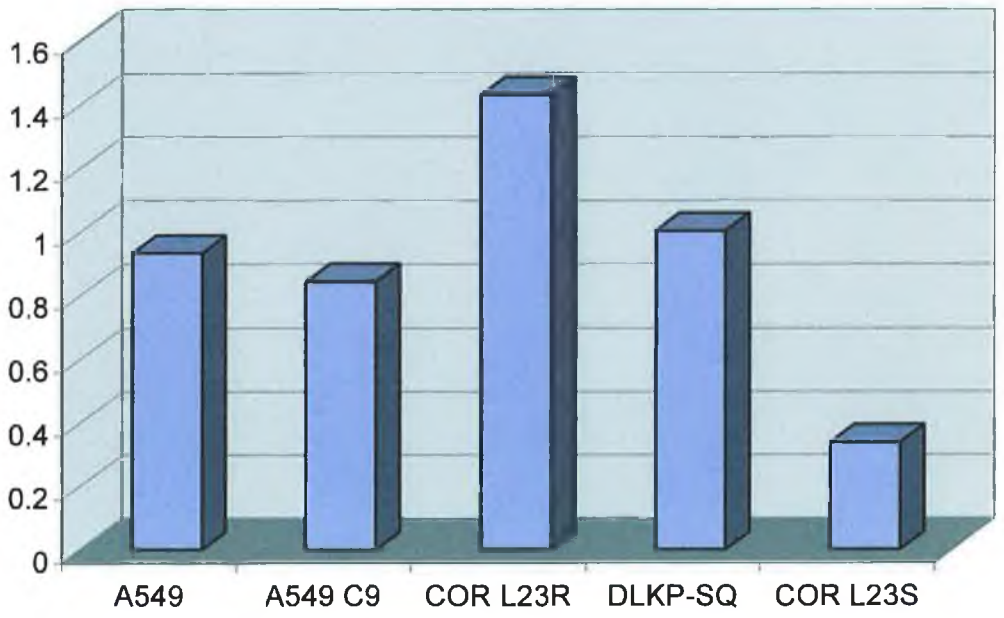

Autoradiogram showing the relative expression of MRP1 (Fig. 3.7.3a) and GAPDH (Fig. 3.7.3b) in the selected cell lines using Northern blotting; Fig. 3.7.3c: Densitometric analysis of autoradiogram results.

MRP1 protein (see Section 1.7.1.2.4). All five selected cell lines were again assayed in this study. The *in-vitro* toxicity results presented in Figs. 3.7.5 and 3.7.6 are the results obtained for one assay of each type which was successfully repeated twice.

As can be seen in Fig. 3.7.5, COR L23R, which expresses the highest levels of MRP1 protein, exhibits the highest level of resistance to vincristine, while its MRP1-negative parent, COR L23S exhibits the lowest level of resistance. Both A549 and its C9 clone express identical resistance levels to the drug, while DLKP-SQ reveals the second lowest level of resistance to vincristine of the five cell lines tested. Fig. 3.7.6 examines the relative resistance levels of the five cell lines to the non-MRP1 substrate vinblastine. Resistance levels (μg/ml) are much lowered for this drug, although a relatively similar pattern of resistance is observed for the cell lines. One significant difference is for A549 C9, which expresses a resistance to the drug of roughly half that of its parent cell line, A549.

Fig. 3.7.5: Relative IC50 Vincristine (VNC) values of selected cell lines

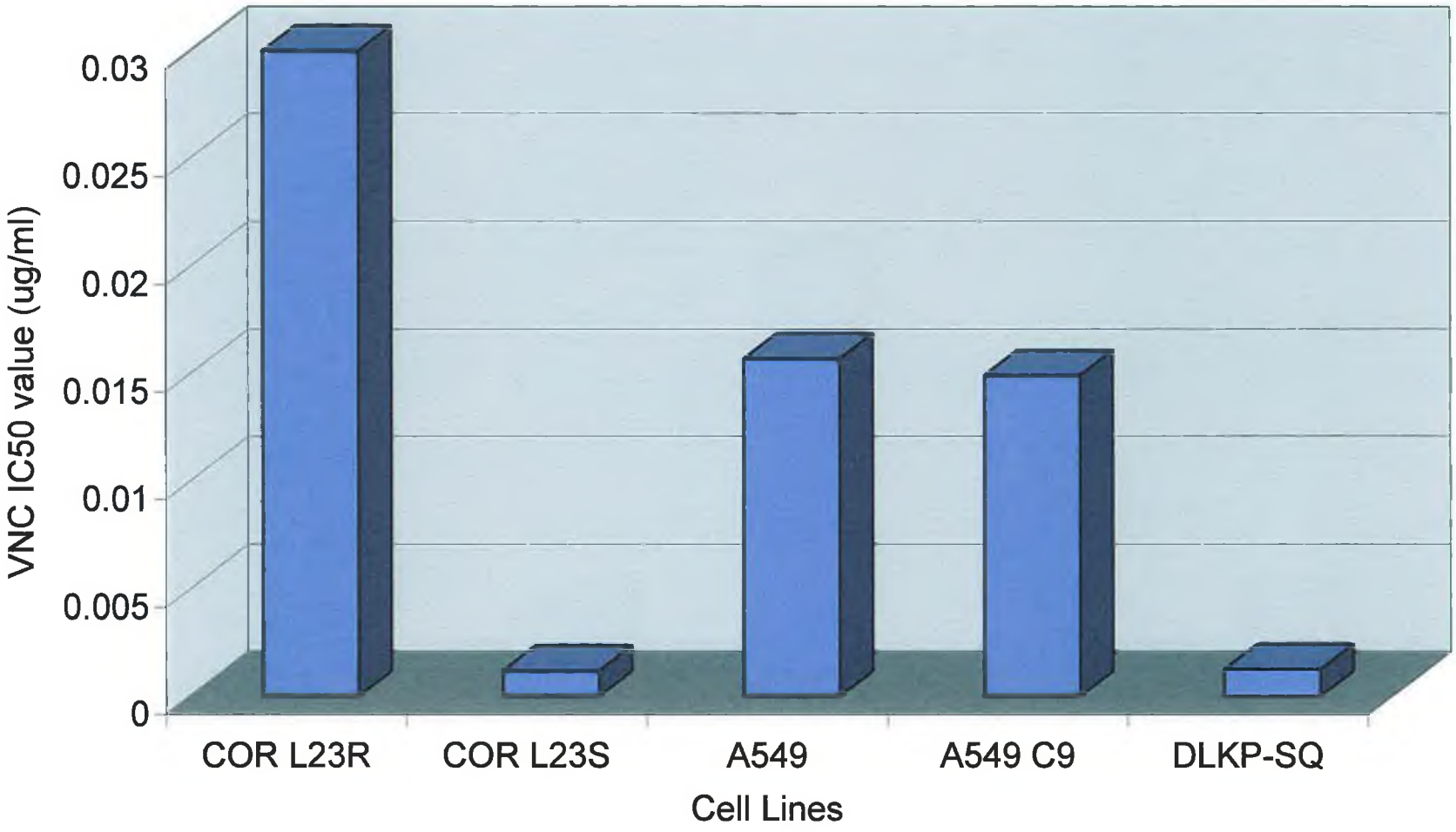

3.8 Assessment of the functionality of the MRP1 gene product in DLKP-SQ cells

Two techniques were employed to examine the role played by MRP1 in conferring multidrug resistance in this cell line; Indomethacin-mediated Combination assays and Inside-Out Vesicle (IOV) assays.

3.8.1 Examination of MRP1 expression using Combination assays

Several nonsteroidal anti-inflammatory drugs (NSAIDs), have been reported (Duffy *et al.*, 1998; Draper *et al.*, 1997; Kobayashi *et al.*, 1997) to have the ability to enhance the cytotoxicity of anti-cancer drugs *in-vitro* when co-administered to a multidrug-resistant cell line which overexpresses MRP1. Indomethacin is a compound which has been shown to be very active as an MRP1 inhibitor (Duffy *et al.*, 1998). The structure of Indomethacin, which was subsequently chosen to inhibit MRP1 activity in DLKP-SQ cells here, is shown in Fig. 3.8.1.

Research carried out in this laboratory (Duffy *et al.*, 1998; S. Touhey, PhD. Thesis, 2000), indicated the ability of Indomethacin to potentiate the toxicity of adriamycin in DLKP cells using the miniaturised *in-vitro* toxicity assay as described in Section 2.3.1. It was postulated that indomethacin potentiated the toxicity of adriamycin in the cancer cells by inhibiting the action of the MRP1 pump in those cells, and in so doing, decreasing the level of chemotherapeutic drug being pumped out of the cell. An enhancement of chemotherapeutic drug toxicity, caused as a direct result of the presence of the NSAID, was regarded as significant if the level of cell kill achieved by the combination was significantly greater than that obtained by either the toxicity of the drug or NSAID individually.

Two anticancer drugs were chosen for this assay; Vinblastine (VNB), which has been shown to be poorly transported by MRP1 and Vincristine (VNC), which is a substrate for the MRP1 pump protein (see Section 1.7.1.2.4). Both of these are widely used chemotherapeutic agents and are detailed in Sections 1.5 and 2.3.1. Two concentrations of both drugs were used in the combination assay experiment, and given the monikers MED and HIGH. The "HIGH" drug concentration was the IC_{50} concentration of drug

Fig. 3.8.1: Structure of Indomethacin

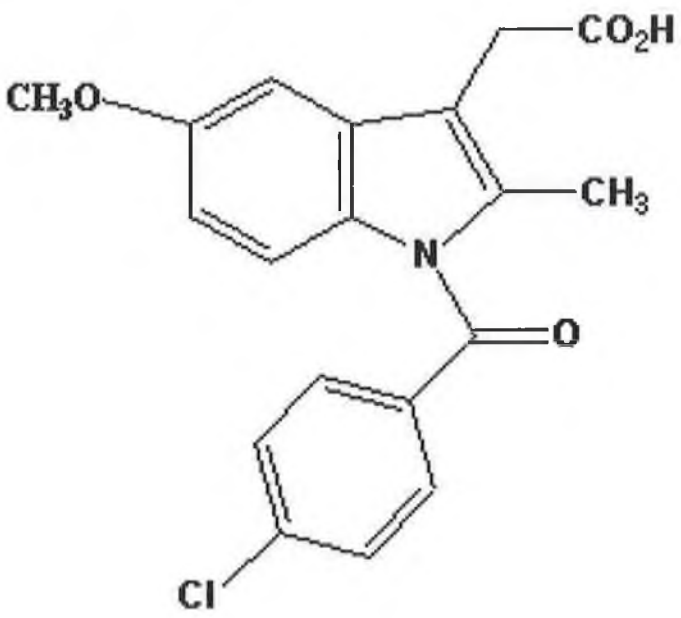

Fig. 3.8.1: Schematic structure of the NSAID Indomethacin

for the DLKP-SQ cell line, which was calculated from triplicate *in-vitro* toxicity assays (data not shown). The "MED" drug concentration was this concentration divided by two. The concentrations for these two drugs are outlined in Table 3.8.1. The concentration of indomethacin used was also varied, in order to determine if the level of inhibition was concentration-dependant. Three concentrations were chosen for inclusion in the combination assay and were given the monikers LOW, MED and HIGH. The "HIGH" concentration of the NSAID was that determined to be the highest concentration which constituted a non-toxic dose on the DLKP cell line. The "MED" and "LOW" concentrations were this concentration divided by two and four, respectively.

It was thought that for the indomethacin to exert the effect as expected, a significant decrease in the level of cell survival would be seen when vincristine and indomethacin were combined in the assay. It was hypothesised that this would be as a result of the indomethacin inhibiting the transport of vincristine by the MRP1 protein. Also, a variable level of this inhibition would be seen when varying amounts of both the drug and the NSAID were used on the DLKP-SQ cell line, i.e. the combination of the highest concentrations of both indomethacin and vincristine would result in the greatest amount of cell kill. To ensure that the method of action of indomethacin was via inhibition of the pumping action of MRP1 and not through another unrelated method of inhibition, duplication of the combination assay using vinblastine was carried out. In order to verify that the method of inhibition was MRP1-related, it was hypothesised that no significant alteration in cell survival would be observed following combination of vinblastine and indomethacin at any concentration of either drug or NSAID. Finally, as a further control, the different concentrations of indomethacin were also added to the cells in the absence of drug, to ascertain cell survival following exposure to the NSAID alone. An untreated plate was also included in the experiment against which all treatments, combination or otherwise, could be compared.

All assays were carried out in triplicate and all results shown here are representative of those triplicates. The amount of indomethacin required to provide a non-toxic dose in DLKP cells which inhibited MRP1 function had already been determined using data from three separate experiments (Touhey, Samantha, PhD. Thesis, 2000) and these

concentrations are listed in Table 3.8.1. These concentrations were also used in the combination assays carried out here on the DLKP-SQ cell line.

Table 3.8.1 Highest non-toxic concentration of Indomethacin, Vincristine and Vinblastine used in combination assay experiments in DLKP-SQ

Compound	ηg/ml	Molar Conc. (nM)
Vincristine High	1.25	-
Vincristine Med	0.625	-
Vinblastine High	0.6	-
Vinblastine Med	0.3	-
Indomethacin High	2500	7
Indomethacin Med.	1250	3.5
Indomethacin Low	625	1.75

The combination assays were carried out as outlined in Section 2.3.1.2 and cell survival was assayed using the acid-phosphatase assay (Section 2.3.1.4). The results of the assays are outlined in Figs. 3.8.2 – 3.8.6.

3.8.1.1 Effect of indomethacin on drug toxicity of Vincristine in DLKP-SQ cells

Fig. 3.8.2 shows the results of the combination of the NSAID and vincristine at half the IC_{50} concentration for the cell line (VNC MED). As can be seen, roughly 20% of the cells were killed by the action of the drug alone at this concentration. Following inclusion of the NSAID, the level of toxicity of the drug rose sharply, yielding a cell kill of over 60% at low indomethacin concentration, finally rising to over 90% at the highest concentration of the NSAID. Concomitant exposure of these concentrations of NSAID to the cells without drug revealed only a slight decrease in cell survival of roughly 5%. Fig. 3.8.3 shows the results for the same concentrations of indomethacin on the DLKP-SQ cells at the higher concentration of vincristine (VNC HIGH). In this plot, the initial level of cell kill without NSAID is far greater, at over 60%. However, the toxicity of the drug is again increased following inclusion of the NSAID, increasing the amount of cell kill to 90% at all concentrations of the NSAID. Again, exposure of the cell line to the NSAID only revealed a slight decrease in cell survival (<5%).

Fig. 3.8.2: Effect of Indomethacin on Vincristine (Med.) resistance in DLKP-SQ

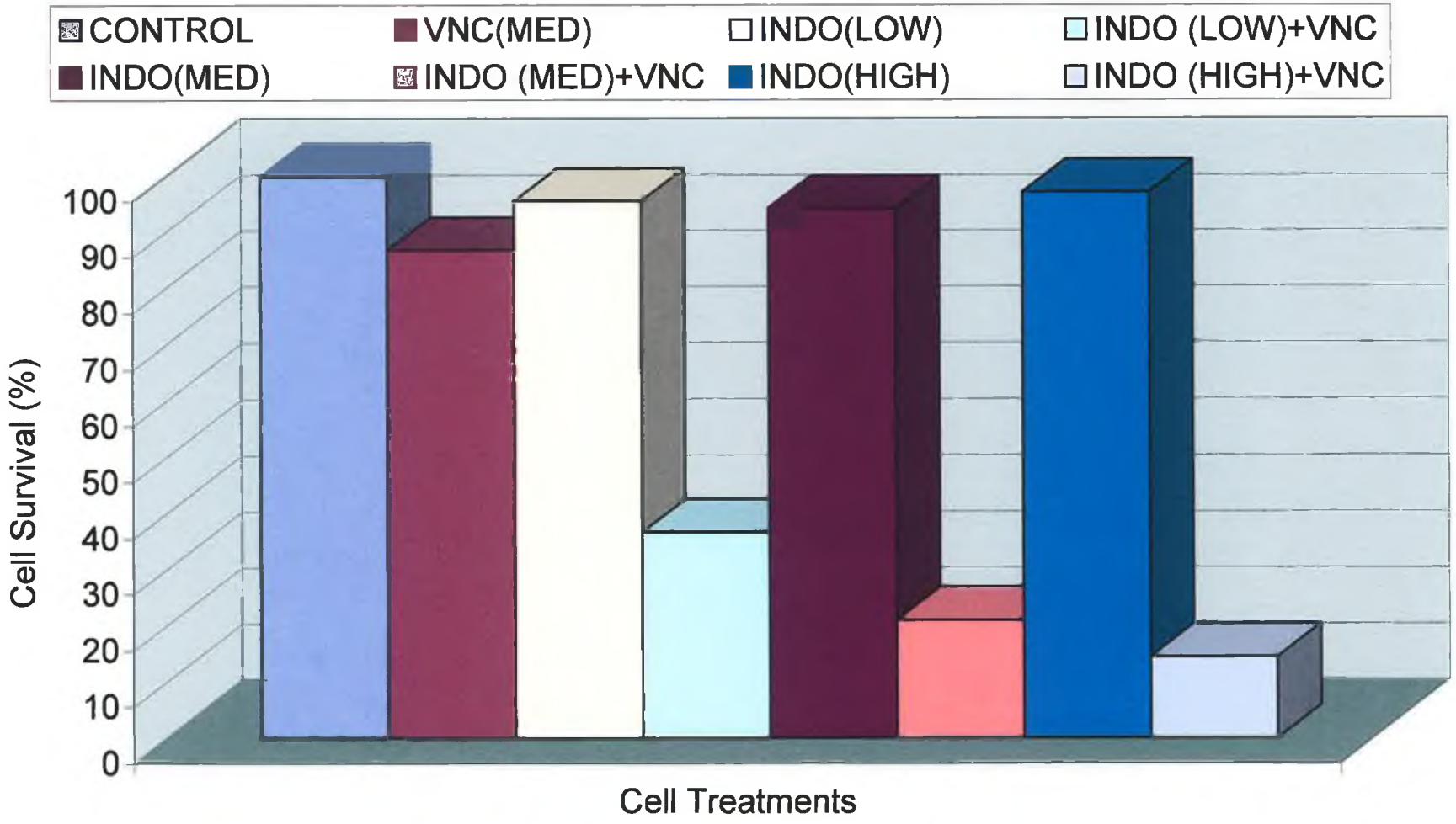

Fig. 3.8.3: Effect of Indomethacin on Vincristine (High) resistance in DLKP-SQ

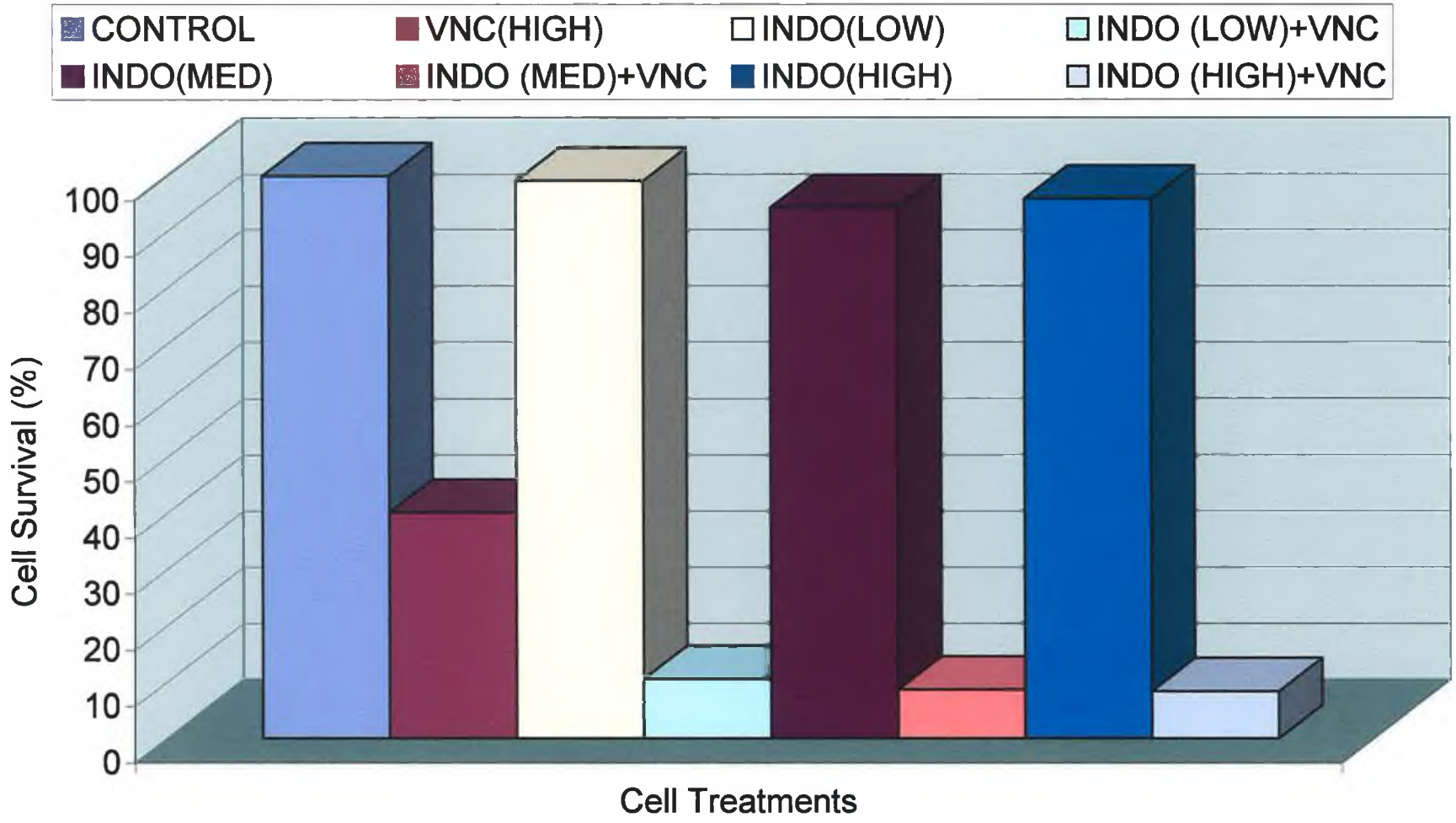

3.8.1.2 Effect of indomethacin on drug toxicity of Vinblastine in DLKP-SQ cells

Figs. 3.8.4 and 3.8.5 show the effect of exposure to indomethacin on the toxicity of vinblastine in the DLKP-SQ cell line. It is clear from both plots that the combination of the NSAID with the drug does not produce any significant effect. In Fig. 3.8.4, the combination of both MED drug concentration and NSAID produces a barely perceptible (1-2%) decrease in cell survival at any NSAID concentration. At the higher concentration of vinblastine (Fig. 3.8.5), the amount of initial cell kill without NSAID (roughly 60%) is augmented a further 10% following combination with the NSAID. However, a roughly 10% level of cell kill is seen in this plot following exposure to the NSAID without drug, so it can be concluded that this increase in toxicity is non-MRP1-related. Table 3.8.2 shows the actual levels of cell survival obtained for each of the different treatments as well as the standard deviation (S.D.) of those results.

Fig. 3.8.4: Effect of Indomethacin on Vinblastine (Med.) resistance in DLKP-SQ

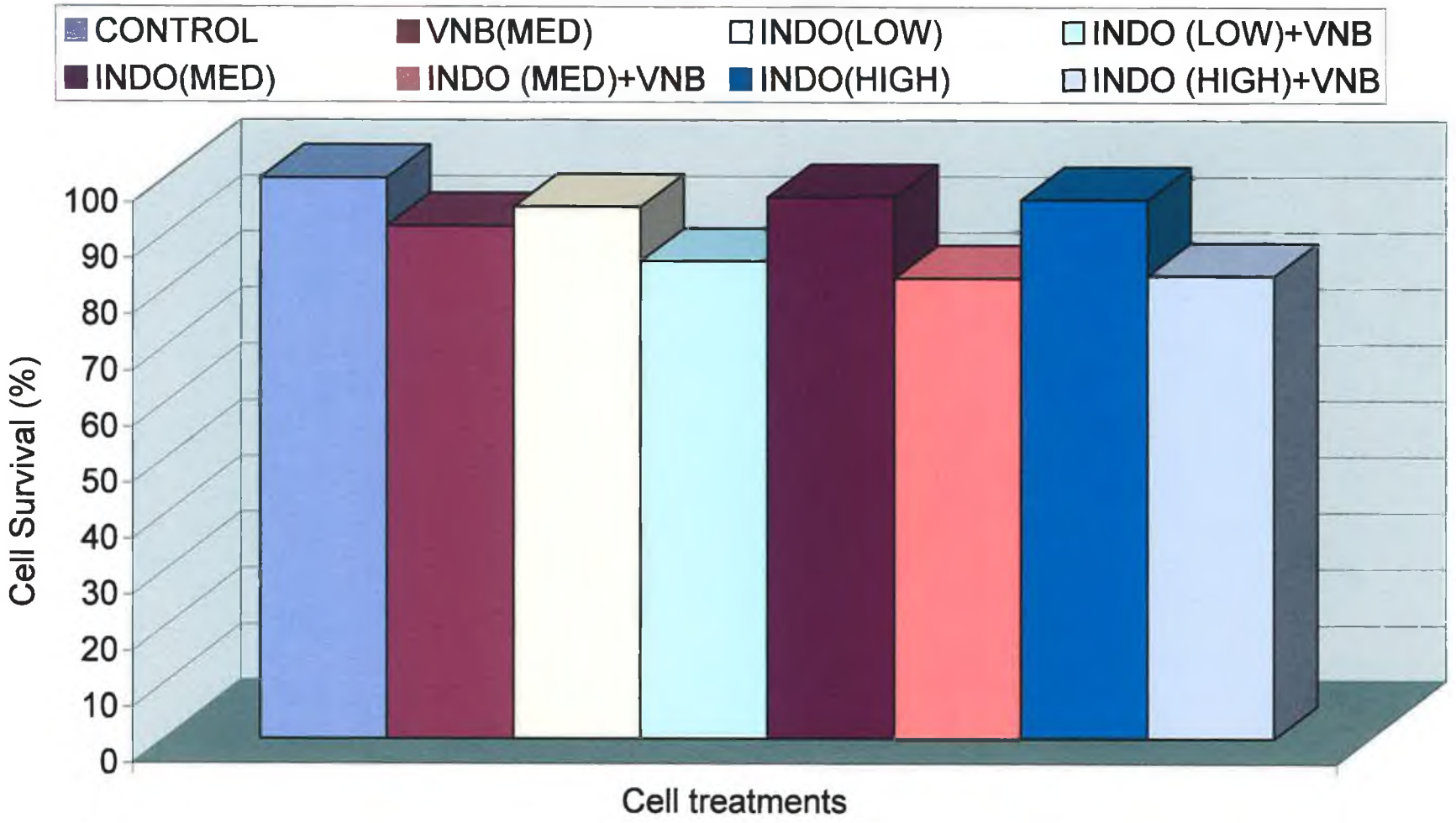

Fig. 3.8.5: Effect of Indomethacin on Vinblastine (High) resistance in DLKP-SQ

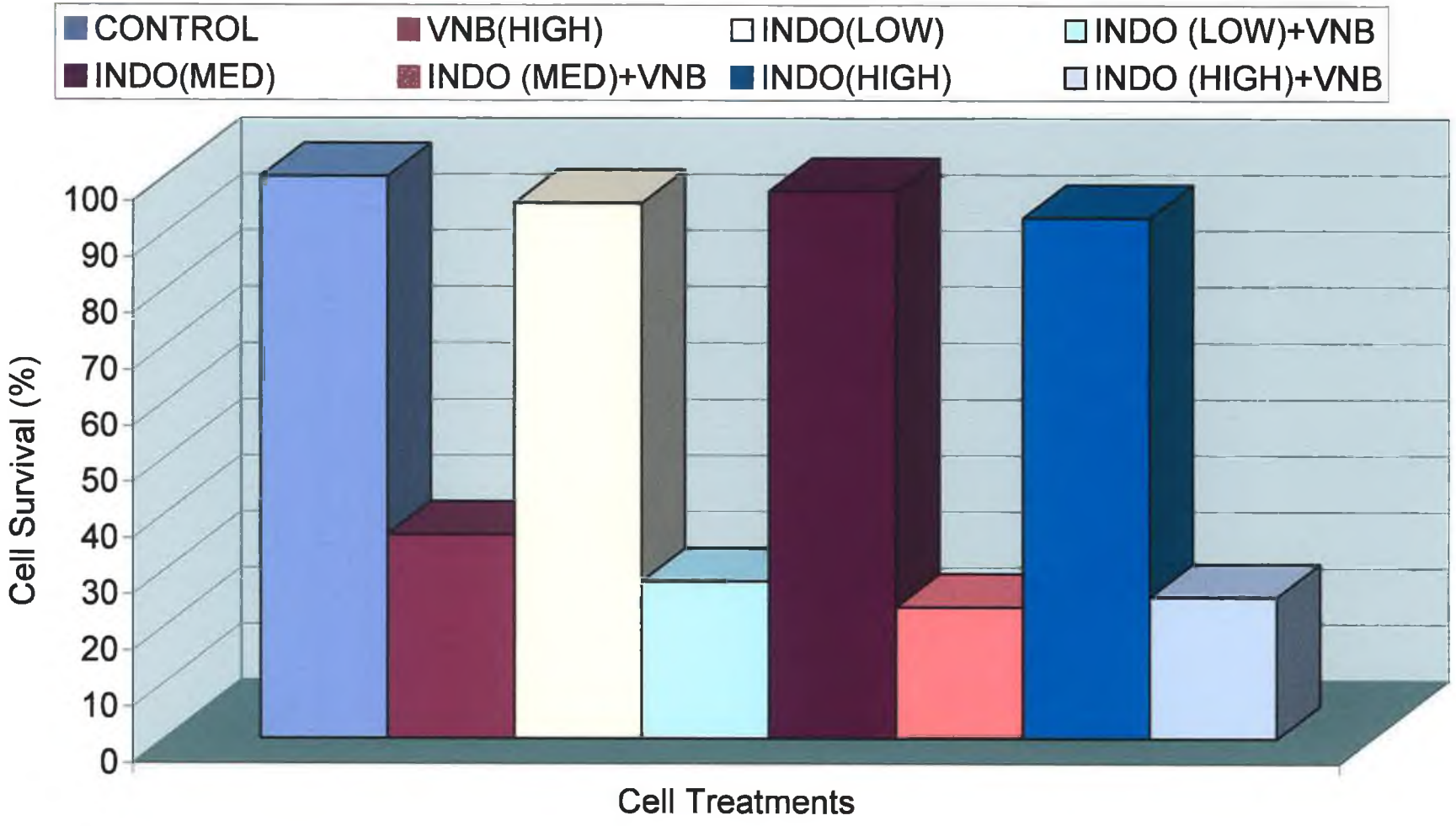

Table 3.8.2 Results of effects of NSAID concentrations on drug toxicity in DLKP-SQ cells

	Treatment	% Cell survival	S.D.
DLKP-SQ Control	Untreated	100	0
VNB MED	VNB (MED)	91.394	3.054
	INDO (LOW)	94.812	3.281
	INDO (LOW) + VNB	85.033	5.929
	INDO (MED)	96.591	1.021
	INDO (MED) + VNB	82.04	6.059
	INDO (HIGH)	96.166	4.341
	INDO (HIGH) + VNB	82.486	5.994
VNB HIGH	VNB (HIGH)	36.224	3.606
	INDO (LOW)	95.248	2.342
	INDO (LOW) + VNB	27.927	1.826
	INDO (MED)	97.383	5.287
	INDO (MED) + VNB	23.351	2.629
	INDO (HIGH)	92.605	3.964
	INDO (HIGH) + VNB	25.125	1.166
VNC MED	VNC (HIGH)	86.809	3.968
	INDO (LOW)	95.615	6.04
	INDO (LOW) + VNC	36.674	3.143
	INDO (MED)	90.306	10.508
	INDO (MED) + VNC	20.969	2.115
	INDO (HIGH)	87.268	10.306
	INDO (HIGH) + VNC	14.452	0.306
VNC HIGH	VNC (HIGH)	40.114	2.141
	INDO (LOW)	99.123	2.738
	INDO (LOW) + VNC	10.488	0.872
	INDO (MED)	92.323	1.838
	INDO (MED) + VNC	8.584	0.688
	INDO (HIGH)	92.97	2.002
	INDO (HIGH) + VNC	8.27	0.195

3.8.2 Examination of MRP1 expression using Inside-Out Vesicle (IOV) assays

Western blotting analysis studies failed to show the existence of MRP1 protein in whole-cell extracts of DLKP, although MRP1 protein expression was detected in whole-cell preparations from DLKP-SQ (Section 3.7.4). It had been demonstrated that all other cell lines, in which the toxicity enhancement effect had been found to occur, expressed MRP1 (Duffy *et al.*, 1998). The drug profile, for which the NSAID-mediated toxicity enhancement effect was found to occur, was exactly similar to the range of drugs believed to be transported by MRP1. This suggested that co-treatment of MRP1-expressing cells with an MRP1-substrate drug and an NSAID with the ability to interfere with the drug pumping ability of MRP1 may have resulted in an increased retention of drug within the cell. This would ultimately cause an enhancement of cytotoxic drug-induced cell kill. This toxicity enhancement effect which had been found to occur in DLKP (S. Touhey, PhD. Thesis, 2000), was also found to occur in DLKP-SQ in this study. It was suggested that DLKP expressed MRP1 at levels undetectable by Western blotting in whole cell extracts. In order to isolate the plasma membrane from these cells and specifically target Western blotting analysis to the area in which the MRP1 protein may have localised, Inside-out Vesicles were prepared from the DLKP cells as outlined in Section 2.3.2. It was found that MRP1 was detected in IOVs isolated from DLKP (S. Touhey, PhD. Thesis, 2000).

Duffy *et al.* (1998), also determined that Indomethacin inhibited the transport of the MRP1 substrate, LTC_4 in IOV (Inside-Out Vesicle) assays prepared from DLKP cells. The glutathione conjugate, LTC_4, was found to be transported into vesicles in an ATP-dependent manner (Jedlitschly *et al.*, 1994; Leir *et al.*, 1994). Duffy *et al.* (1998), demonstrated the influence of various NSAIDs on MRP1 activity in HL60/ADR (a strongly MRP1-overexpressing cell line) IOVs by measuring the ability of the compounds to inhibit the transport of LTC_4. The authors reported that the positive NSAIDs, especially sulindac and indomethacin, exhibit strong MRP1 pump inhibitory activity on the IOV preparations.

Although the combination assay results had already indicated a functioning MRP1 protein in the DLKP-SQ cell line and demonstrated that the action of the protein could be inhibited by exposure to indomethacin, it was decided to carry out an inside-out

vesicle assay on the DLKP-SQ cells. This was carried out to demonstrate the pumping ability of the MRP1 protein in the DLKP-SQ cell line. MRP1 has been localised to the membrane vesicles of certain cell types (Leier *et al.*, 1994) and this was investigated in the DLKP-SQ cell line with this experiment. Also, MRP1 has been reported to be a GST pump (see Section 1.7.1.2.4) and it was considered necessary to investigate if this was a potential mode of action of the protein in this cell line.

A pure preparation of MRP1 IOVs (see Section 2.3.2) was used in a standard IOV assay along with the radiolabelled MRP1 substrate, LTC_4. This pure preparation of MRP1 was contained within vesicles, prepared from actively growing DLKP-SQ cells, which were subsequently turned inside out. This procedure was carried out to allow measurement of the transport of LTC_4 – instead of the MRP1 protein pumping the radiolabelled substrate out of the vesicle, it now pumped it into the vesicle using ATP as an energy source. A repeat of the procedure was also carried out in the presence of AMP to provide a negative control for the experiment. The results of the IOV assay on the DLKP-SQ cell line is shown in Fig. 3.8.6.

From the results presented in Fig. 3.8.6, it is evident that the level of radiolabelled LTC_4 transported into the DLKP-SQ vesicle preparation increases over time. It was also demonstrated that this transport was an ATP-dependent mechanism. This result proves that MRP1 is functioning in the DLKP-SQ cell line and that its mode of action (i.e. ATP-dependent glutathione-conjugate, vesicle-localised pump) is as described in the literature previously mentioned.

Fig. 3.8.6 Time course of LTC4 transport into DLKP-SQ IOVs

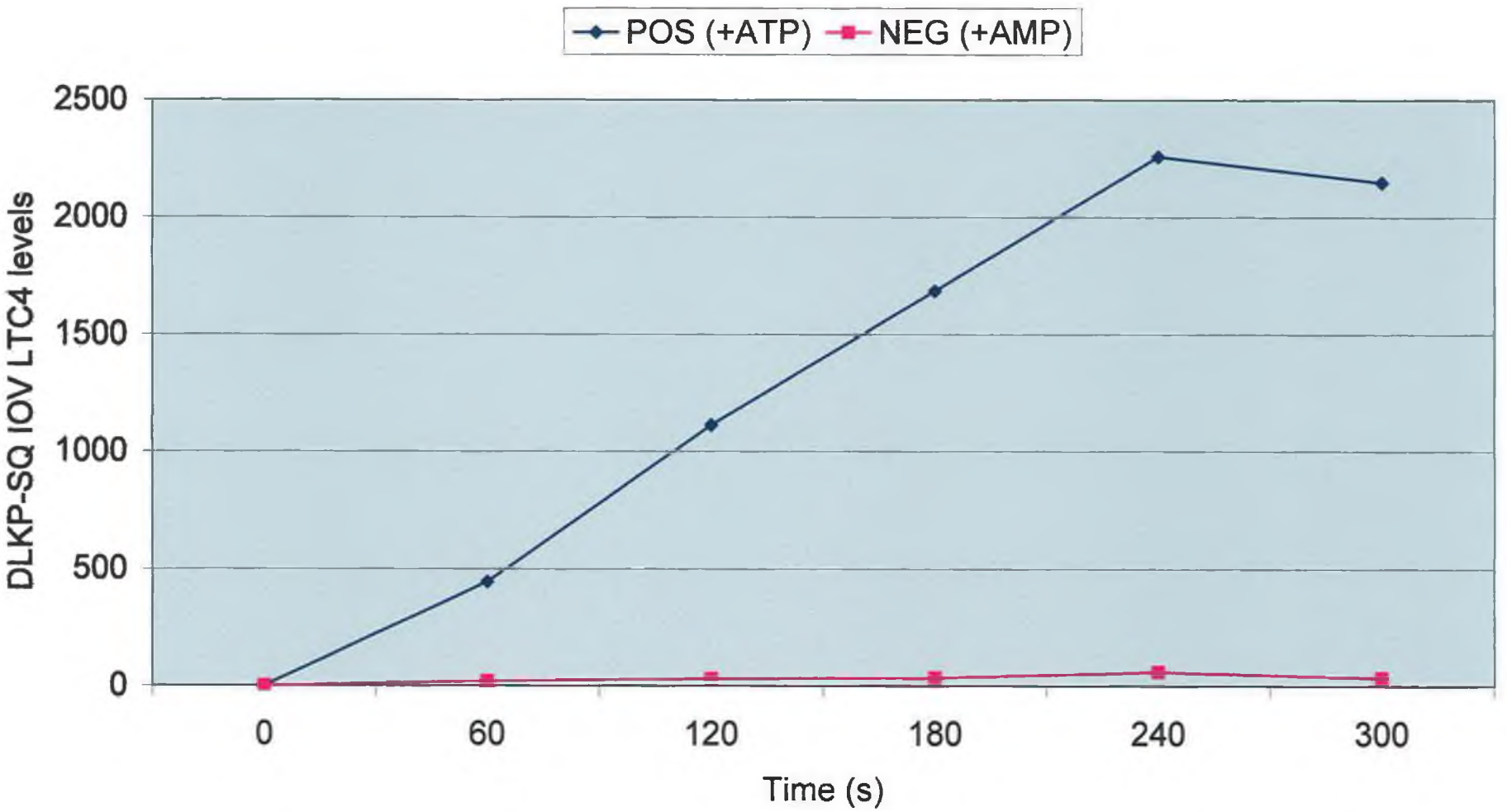

3.9 Analysis of the use of MRP1 ribozyme to downregulate expression of the gene

In order to more accurately examine the effect of transfection of the MRP1 ribozyme on MRP1-expressing cells, stable transfections were carried out to establish banks of MRP1 ribozyme-expressing clonal cell lines which could be used for further study. The DLKP-SQ cell line was transfected with a pHβ (pHβApr-1-neo) plasmid containing the MRP1 ribozyme which was a generous gift from Prof. Kevin Scanlon. This plasmid expresses the neomycin phosphotransferase gene under a Simian-Virus (SV) promoter (*SV-neo*) which enables mammalian cells expressing the plasmid to grow in the presence of Geneticin (Promega, G418). Expression of the MRP1 ribozyme was regulated by a β-actin promoter. A BLAST™ homology search (http://www.ncbi.nlm.nih.gov/blast/Blast.cgi) revealed that the MRP1 ribozyme shared 100% complementarity only with the MRP1 coding sequence. The ribozyme was, however, >85% complementary to a number of additional genes in humans. These genes are summarised in Table 3.9.1.

Table 3.9.1 List of human gene sequences which share over 85% complementarity with the MRP1 ribozyme

Gene
Faciogenital dysplasia (Aarskog-Scott syndrome) (FGD1)
Heparan sulfate (glucosamine) 3-O-sulfotransferase 2
Ubiquitin associated and SH3 domain containing gene
Cadherin-associated protein-related (CTNNA2)
α-catenin

The pHβ construct is shown in Fig. 3.9.1. A schematic of the MRP1 ribozyme and target is illustrated in Fig. 3.9.2. The cells were transfected with the ribozyme-containing plasmid and stable geneticin-resistant clonal cell lines were isolated from the parent cell line as outlined in Section 2.4.5.3. A total of fifteen clonal cell lines were isolated from this transfection and these were subjected to further analysis to examine the effect of MRP1 ribozyme expression on expression of the MRP1 gene. A list of the fifteen isolated clones are shown in Table. 3.9.2. This analysis will comprise of RT-

Fig. 3.9.1: Schematic map of pHβ-Apr-1-neo plasmid

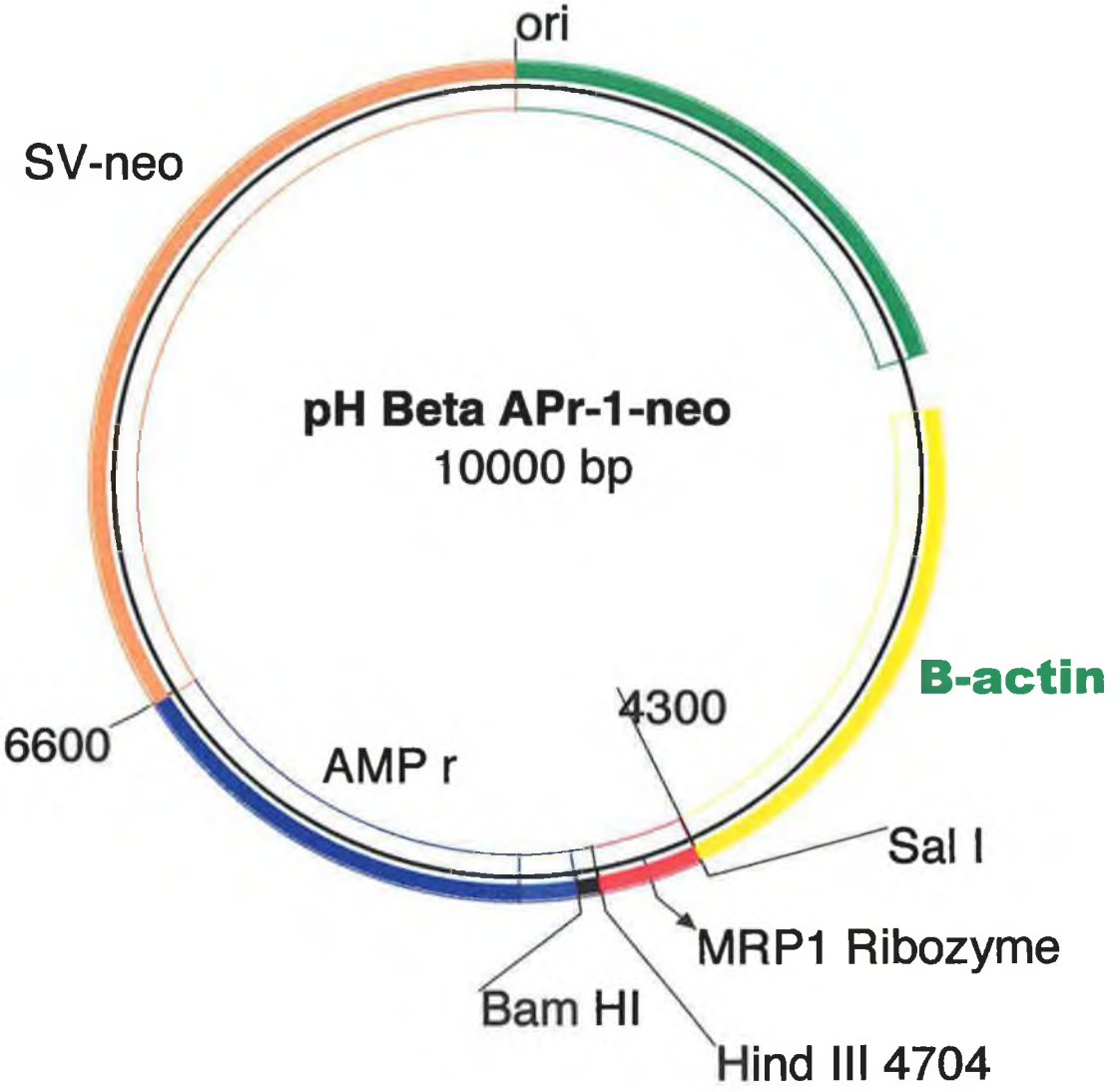

Fig. 3.9.1: Schematic map of pHβ plasmid, showing location of cloning site and ampicillin & neomycin resistance genes

Fig. 3.9.2: Schematic of MRP1 Ribozyme and RNA Target

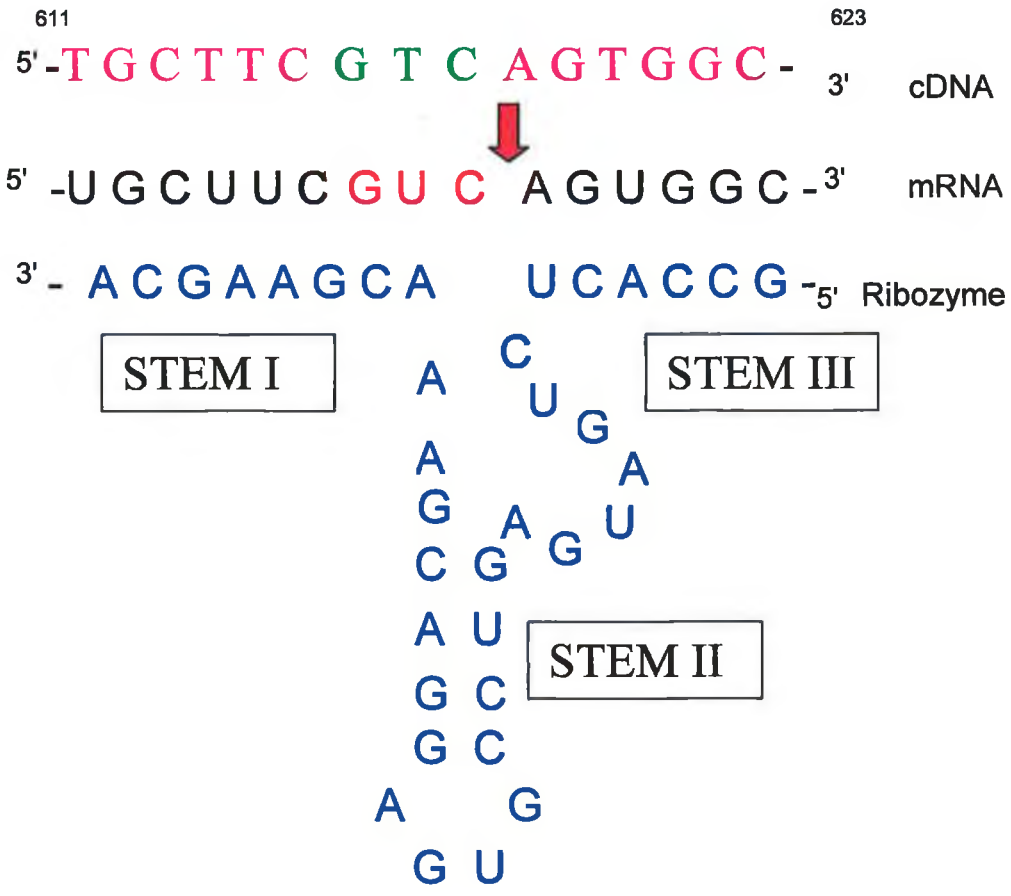

Fig. 3.9.2: Schematic of MRP1 ribozyme and RNA target sequence, showing the location of Stems I, II & III, as well as the cleavage site immediately 3' to the GUC site (RED ARROW)

PCR, Western blotting and *in-vitro* toxicity assays to determine the effect, if any of transfection and expression of the MRP1 ribozyme in the DLKP-SQ cell line.

Table 3.9.2 List of successfully isolated clones from DLKP-SQ

Clone Name
DLKP-SQ R1
DLKP-SQ R2
DLKP-SQ R3
DLKP-SQ R4
DLKP-SQ R6
DLKP-SQ R7
DLKP-SQ R9
DLKP-SQ R11
DLKP-SQ R16
DLKP-SQ 2R1
DLKP-SQ 2R3
DLKP-SQ 2R4
DLKP-SQ 2R5
DLKP-SQ 2R9
DLKP-SQ 2R10

3.9.1 RT-PCR analysis of DLKP-SQ cells transfected with MRP1 ribozyme

RT-PCR analysis of the clonal cell lines isolated from the transfection of the MRP1 ribozyme into the DLKP-SQ cells was divided up into two distinct segments. It was considered necessary to firstly identify which of the clones expressed the pHβ-MRP1 ribozyme expression plasmid at the RNA level. pHβ expression primers were designed to detect expression of the plasmid from total RNA isolated from the clonal cell lines. Once expression of the plasmid had been detected in a cell line, it was considered reasonable to assume that clonal cell line was also expressing the MRP1 ribozyme. The sequences of these primers are included in Appendix A (Table 7.1A).

The second part of the RT-PCR analysis was to investigate if the expression of the MRP1 gene was affected by expression of the MRP1 ribozyme in a ribozyme-expressing clone. This was also achieved by the use of MRP1 expression primers used to examine MRP1 expression in the ribozyme-expressing clones.

Also, it was considered important to examine the expression of the MRP1 homologues (Section 1.7.1.2) in the ribozyme-expressing cells relative to the normal DLKP-SQ cell line, in case of non-specific activity of the MRP1 ribozyme.

3.9.1.1 pHβ plasmid expression in the MRP1 ribozyme-transfected clones

pHβ RT-PCR analysis of the untransfected DLKP-SQ control and the geneticin-selected clonal cell lines was carried out as outlined in Section 2.4.2.5. The results from the expression PCR are shown in the gel electrophoresis photograph as outlined in Fig. 3.9.3. From the results shown, it was apparent that expression of the pHβ plasmid was observed in ten of the fifteen (66.7%) isolated cell lines. A list of these ribozyme-expressing clones is given in Table 3.9.3. The level of expression of the plasmid was also observed to vary between the different clones. As expected, pHβ plasmid expression was not observed for the negative (untransfected DLKP-SQ) control. A strong positive was observed for the pHβ cDNA positive control. From the RT-PCR analysis, the ten ribozyme-expressing clones were selected for further study, along with two non-ribozyme-expressing cell lines DLKP-SQ R1 and DLKP-SQ 2R10, which were included as negative controls.

Table 3.9.3 List of MRP1 ribozyme-expressing clones

Clone Name	
DLKP-SQ R2	DLKP-SQ R16
DLKP-SQ R3	DLKP-SQ 2R1
DLKP-SQ R6	DLKP-SQ 2R4
DLKP-SQ R7	DLKP-SQ 2R5
DLKP-SQ R9	DLKP-SQ 2R9

Fig 3.9.3: pHβ expression RT-PCR on DLKP-SQ clones

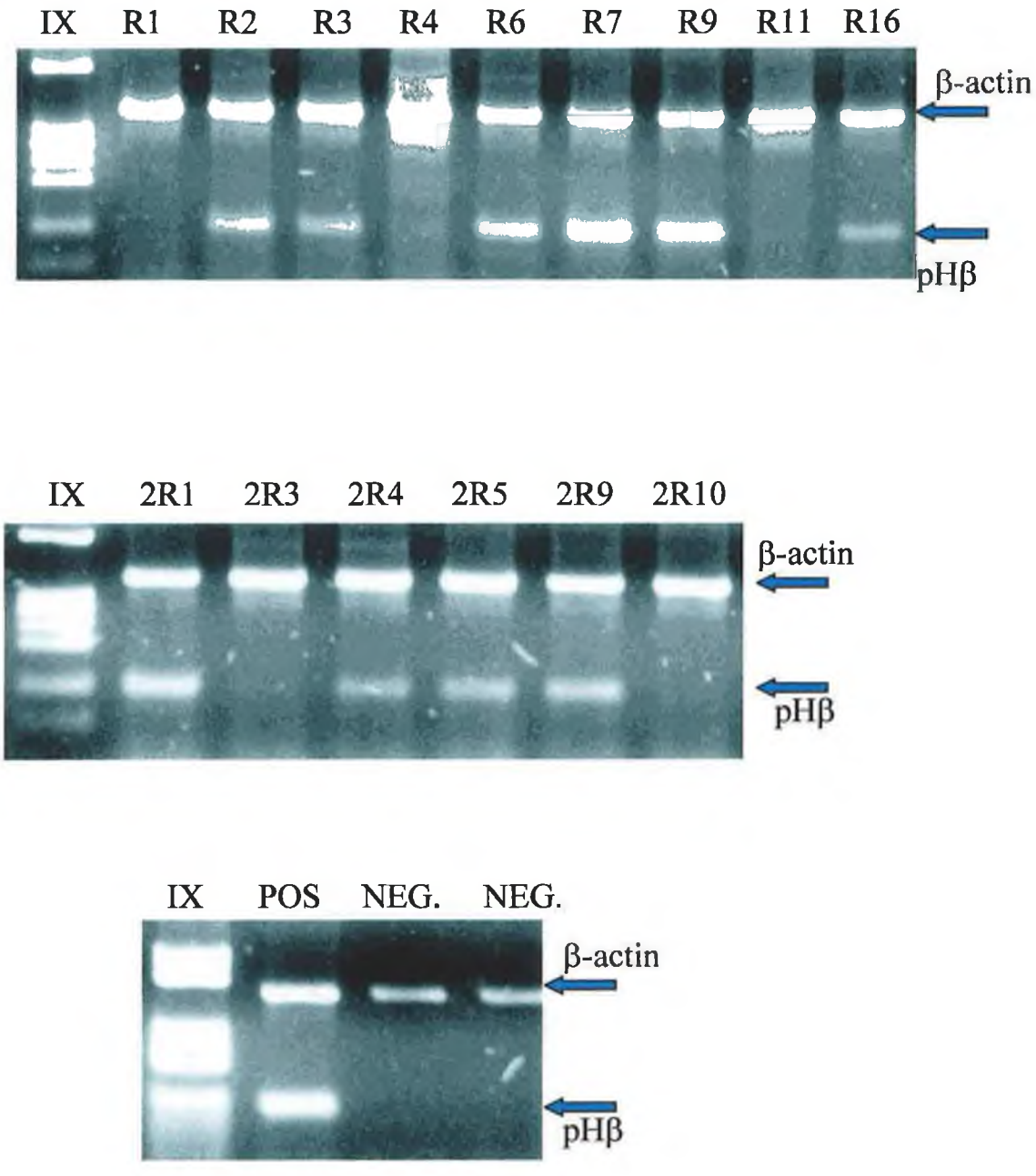

Fig. 3.9.3: Gel electrophoresis photographs of pHβ expression RT-PCR on all MRP1 ribozyme-transfected DLKP-SQ clones.

3.9.1.2 Analysis of MRP1 gene expression in the MRP1 ribozyme-transfected clones

MRP1 RT-PCR analysis of the ribozyme-transfected clones was carried out as outlined in Section 2.4.2.5. The results for the PCR are shown in Fig. 3.9.4. As can be seen from the plot and accompanying densitometry, no significant decrease in MRP1 gene expression was observed in any of the clones, whether they were ribozyme-expressing or not. On the contrary, expression of the MRP1 gene was increased in almost all RNA samples assayed. The PCR results displayed are an average of three separate RT-PCRs carried out on these samples.

3.9.1.3 Expression of MRP homologues in MRP1 ribozyme-transfected DLKP-SQ

The sequence similarity of MRP1 and its homologues has already been elucidated (see Section 1.7.1.2). It was considered that the MRP1-targetted ribozyme might also downregulate the expression of the other MRP1 homologues in a non-sequence-specific manner. A number of additional RT-PCRs for the MRP homologues 2 to 6 were carried out to examine the expression of these genes in the ribozyme-expressing cells relative to the normal DLKP-SQ cell line. These PCRs were carried out in duplicate to confirm the results displayed in Figs. 3.9.5 to 3.9.8. As can be seen from these plots, expression of the MRP1 homologues MRP2 and MRP4 only were detected in the DLKP-SQ cell line.

From the MRP2 RT-PCR results (Figs. 3.9.5 and 3.9.6), it was observed that cMOAT expression levels varied widely in the clonal cell lines relative to the parent. Expression for the most part was decreased in the clones, with 70% of the ribozyme-expressing samples showing decreased expression, with one clone retaining identical expression levels. Only two of the MRP1 ribozyme-expressing clones exhibited higher expression levels of the gene. The expression pattern for the non-ribozyme-expressing clones was quite different, with the majority of the clones (60%) expressing higher levels of the cMOAT gene than did the parent. The most dramatic increase in expression was observed in DLKP-SQ clones 2R3 and 2R10 where expression was increased by more than 50% when compared to the parent cell line. Only two of the five clones not expressing the ribozyme showed decreased expression levels of cMOAT.

Fig. 3.9.4: MRP1 RT-PCR analysis of DLKP-SQ clones

Fig. 3.9.4a:

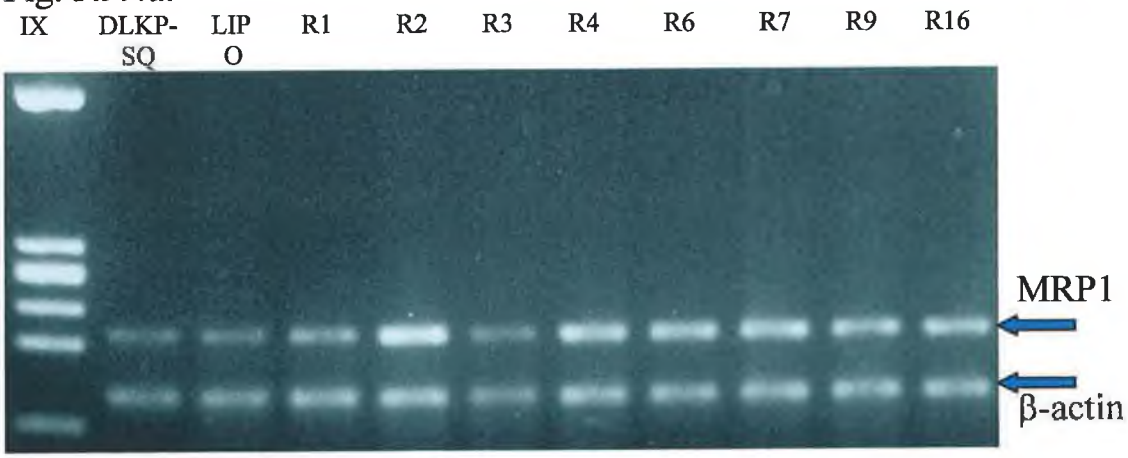

Fig. 3.9.4b:

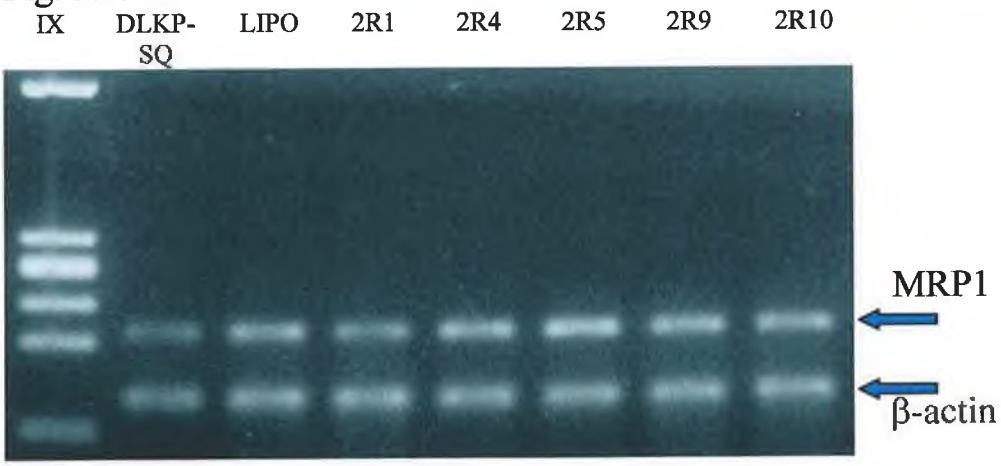

Fig. 3.9.4c:

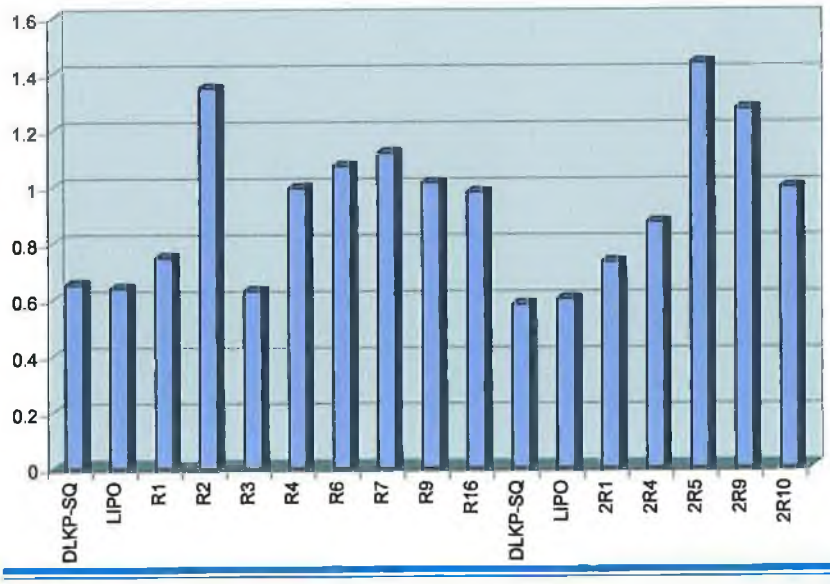

Figs. 3.9.4a & b: Gel electrophoresis photographs of MRP1 RT-PCR results on ribozyme-transfected DLKP-SQ clones; Fig. 3.9.4c: Densitometric analysis of RT-PCR results.

Fig. 3.9.5: MRP2 RT-PCR analysis of DLKP-SQ clones

Fig. 3.9.5a:

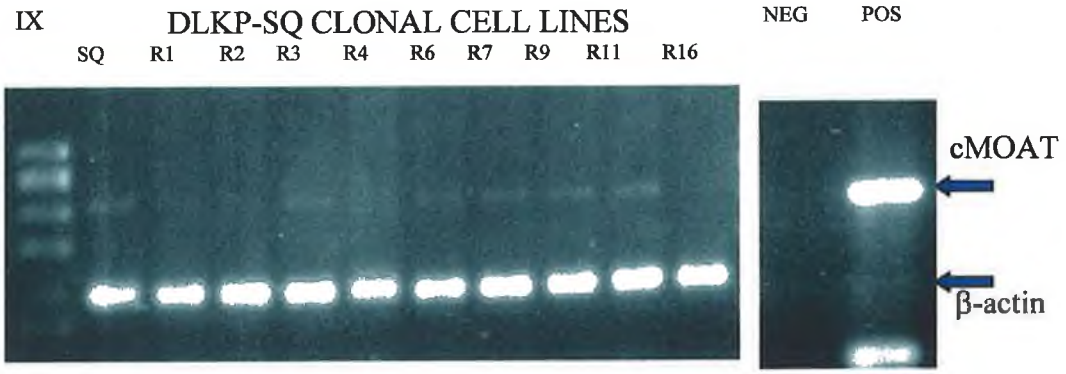

Fig. 3.9.5b:

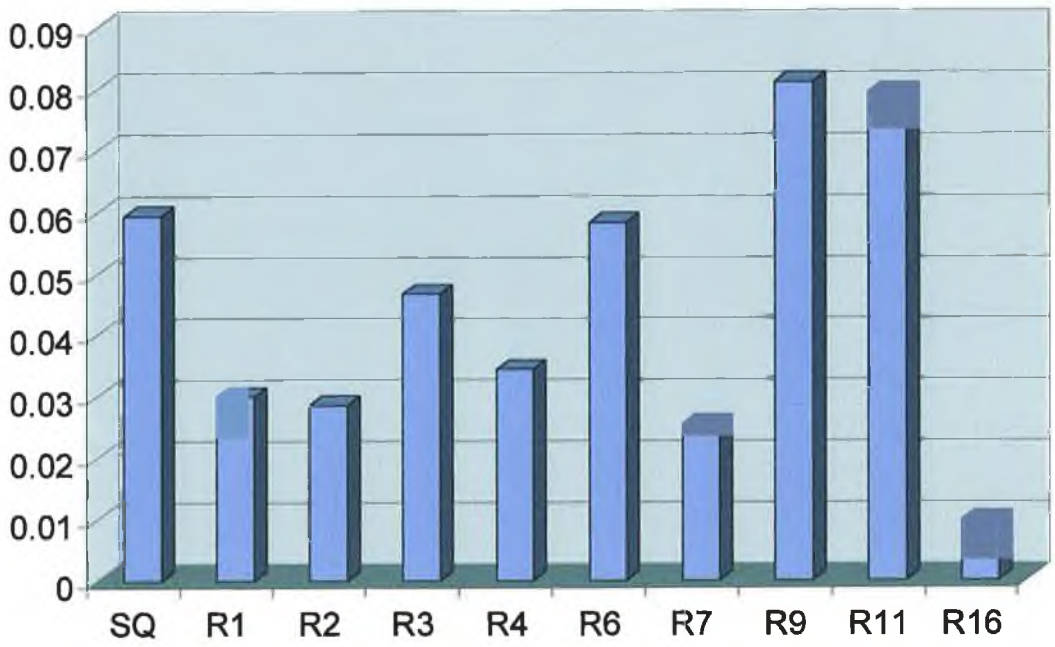

Fig. 3.9.5a: Gel electrophoresis photograph of cMOAT RT-PCR expression levels of MRP Ribozyme-transfected DLKP-SQ clones; Fig. 3.9.5a: Densitometric analysis of RT-PCR results.

Fig. 3.9.6: MRP2 RT-PCR analysis of DLKP-SQ clones

Fig. 3.9.6a:

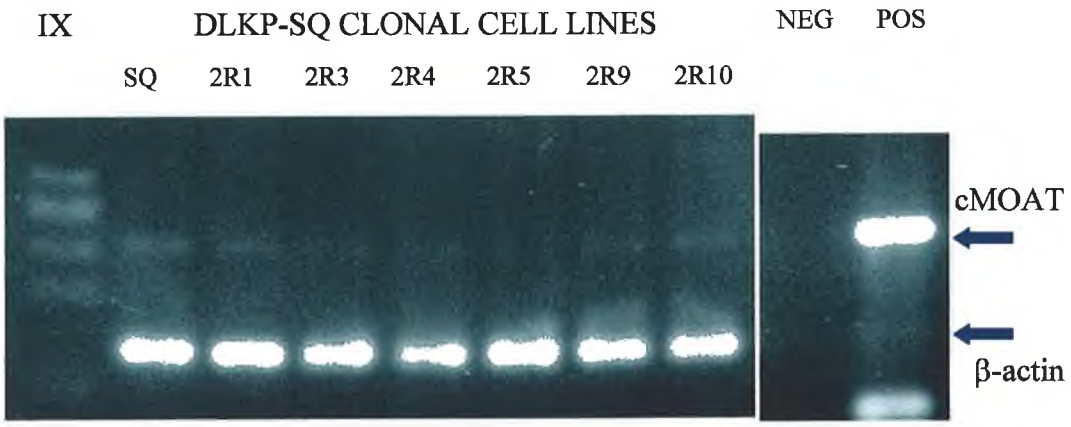

Fig. 3.9.6b:

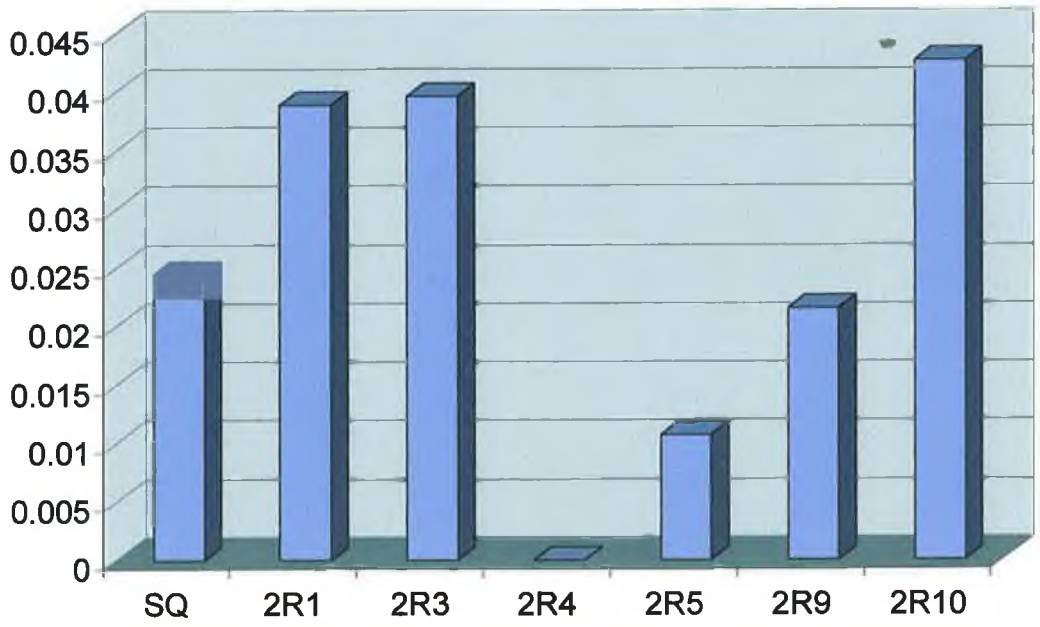

Fig. 3.9.6a: Gel electrophoresis photograph of cMOAT RT-PCR expression levels of MRP Ribozyme-transfected DLKP-SQ clones; Fig. 3.9.6b: Densitometric analysis of RT-PCR results.

In contrast to the MRP2 PCR results for the MRP1 ribozyme-transfected clones, all of the clones generated showed decreased levels of MRP4 gene expression (Figs. 3.9.7 and 3.9.8). The transfection was repeated transiently, to investigate if the downregulation of the gene was time-dependant. However, the result was not transiently repeatable.

From the pHβ and MRP1 expression RT-PCRs detailed above, a number of non-ribozyme-expressing clones were discarded to make subsequent analysis easier. The discarded clones were DLKP-SQ R4, R11 and 2R3. All analysis from here on will just involve the remaining twelve clones.

3.9.2 Western blotting analysis of MRP1 ribozyme-transfected DLKP-SQ clones

The results from the Western blotting analyses are shown in Figs. 3.9.9 and 3.9.10. Fig. 3.9.9 shows the results for the DLKP-SQ clones R1 – R16. Three of the ribozyme-transfected clones expressed significantly lower levels of the MRP1 protein than either the DLKP-SQ parent or the untransfected DLKP-SQ R1 control. In all other samples, MRP1 protein expression had either increased or decreased slightly after transfection. In Fig. 3.9.10, there was no decrease in MRP1 protein expression observed for either the ribozyme-expressing or non-ribozyme-expressing clones. One clone, DLKP-SQ 2R3, expressed almost twice as much MRP1 protein than the parental DLKP-SQ control.

3.9.3 *In-vitro* toxicity analysis of MRP1 ribozyme-transfected DLKP-SQ clones

From the results already presented, it was apparent that while no effect had been observed at the RNA level, it was possible that the MRP1 ribozyme was exerting an effect at the protein level of expression. In order to test whether this effect had any influence on the drug resistance profiles of the ribozyme-expressing clones, a series of *in-vitro* toxicity assays were set up as outlined in Section 2.3.1. Each toxicity assay was carried out in triplicate; the results presented here are an average of those three separate assays. Fig. 3.9.11 shows the Vincristine (VNC) resistance profile of the DLKP-SQ cell line as well as the profiles for the ribozyme-expressing and non-ribozyme-expressing

Fig. 3.9.7: MRP4 RT-PCR analysis of DLKP-SQ clones

Fig. 3.9.7a:

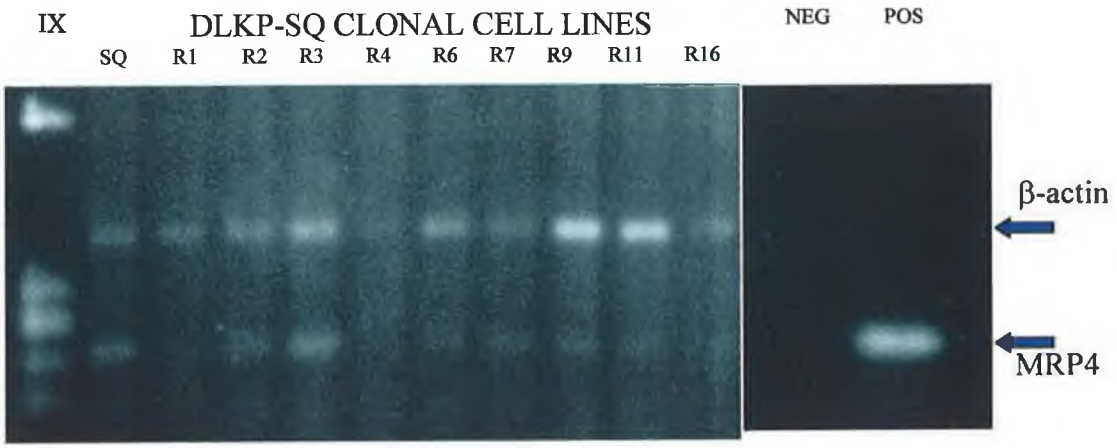

Fig. 3.9.7b:

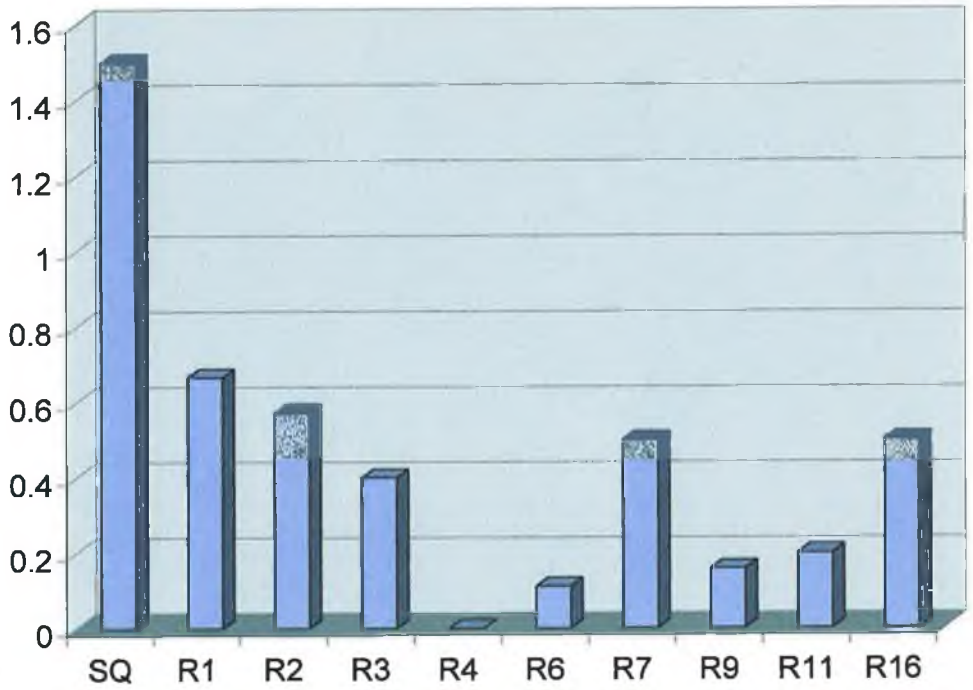

Fig. 3.9.7a: Gel electrophoresis photograph of MRP4 RT-PCR expression levels of MRP1 Ribozyme-transfected DLKP-SQ clones; Fig. 3.9.7b: Densitometric analysis of RT-PCR results.

Fig. 3.9.8: MRP4 RT-PCR analysis of DLKP-SQ clones

Fig. 3.9.8a:

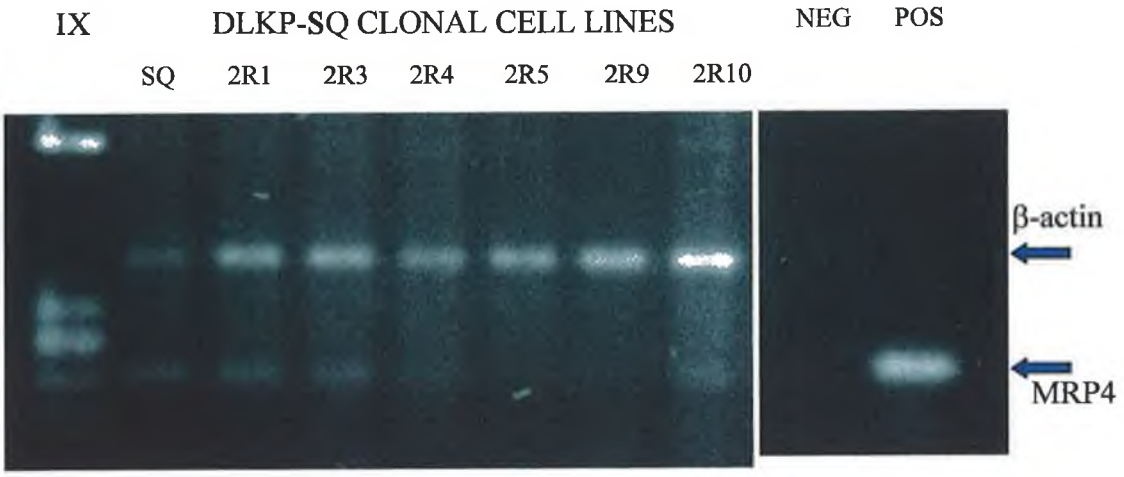

Fig. 3.9.8b:

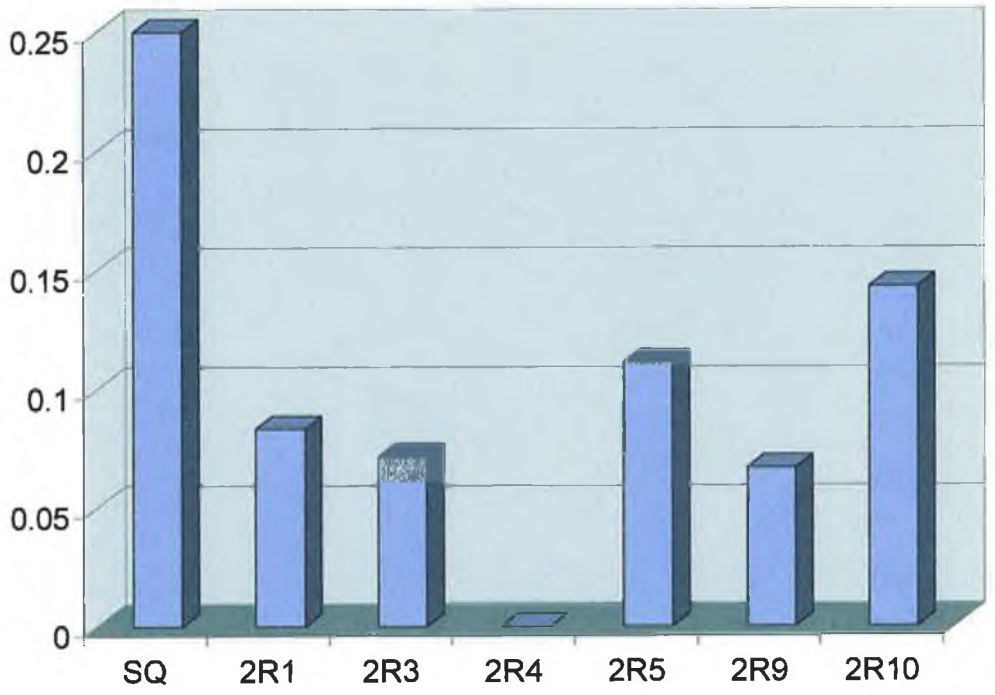

Fig. 3.9.8a: Gel electrophoresis photograph of MRP 4 RT-PCR expression levels of MRP Ribozyme-transfected DLKP-SQ clones; Fig. 3.9.8b: Densitometric analysis of RT-PCR results.

Fig. 3.9.9: MRP1 Western on transfected DLKP-SQ clones

Fig. 3.9.9a:

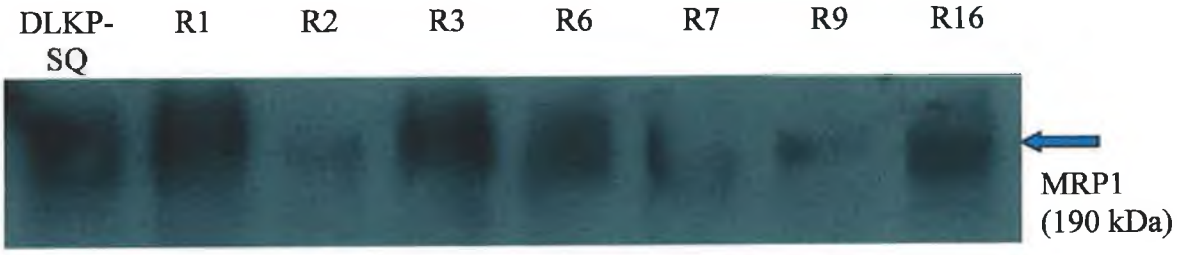

Fig. 3.9.9b:

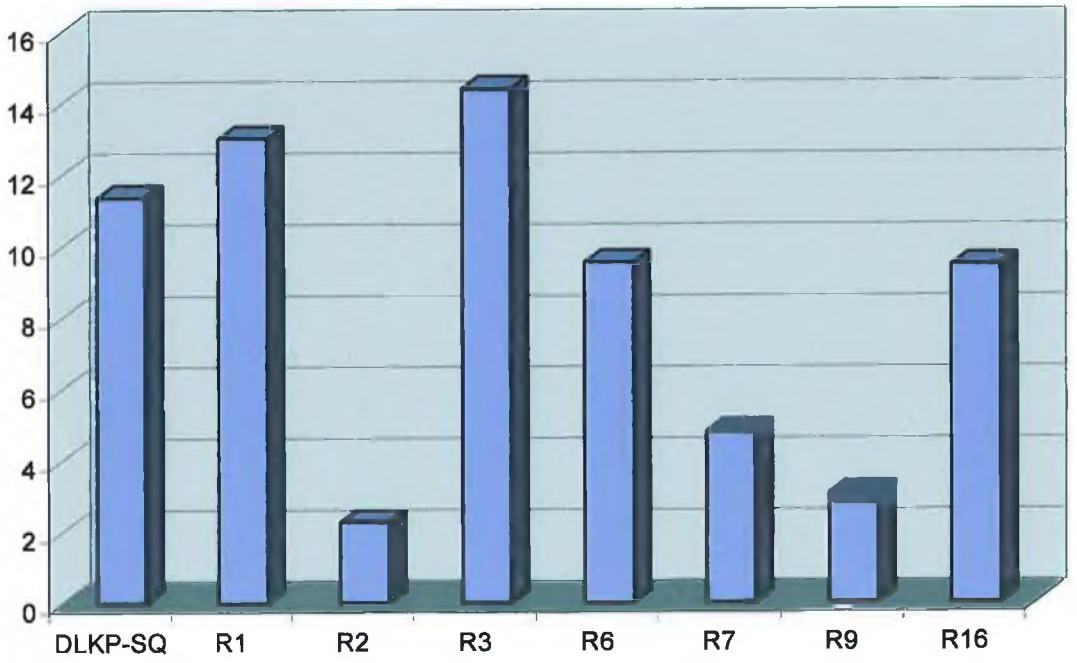

Fig. 3.9.9a: Western blot of MRP 1 results on ribozyme-expressing and non-expressing clones; Fig. 3.9.9b: Densitometric analysis of Western blot results.

Fig. 3.9.10: MRP1 Western on transfected DLKP-SQ clones

Fig. 3.9.10a:

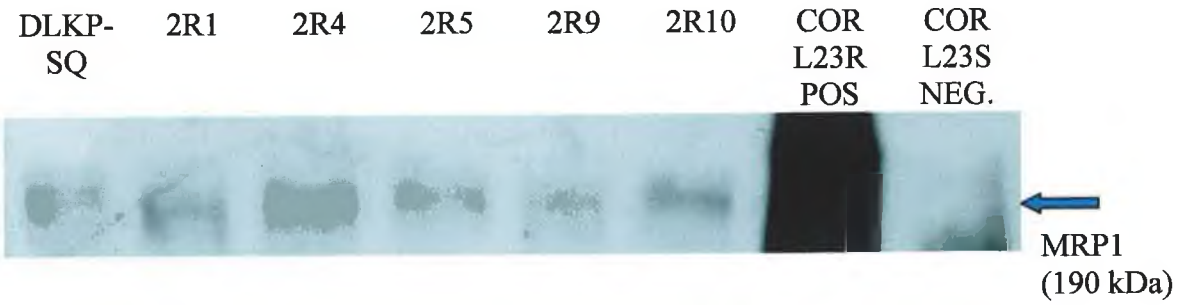

Fig. 3.9.10b:

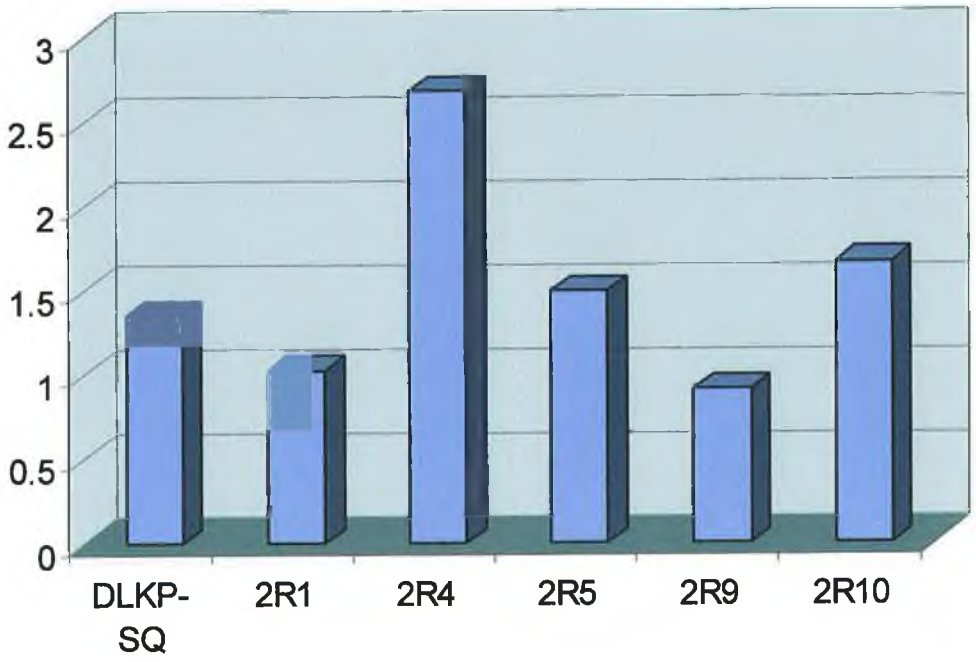

Fig. 3.9.10a: MRP1 Western blot analysis of ribozyme-expressing and non-expressing DLKP-SQ clones; Fig. 3.9.10b: Densitometric analysis of Western blotting results.

Fig. 3.9.11: Relative Vincristine (VNC) IC50 values for the MRP1 ribozyme-transfected DLKP-SQ clones

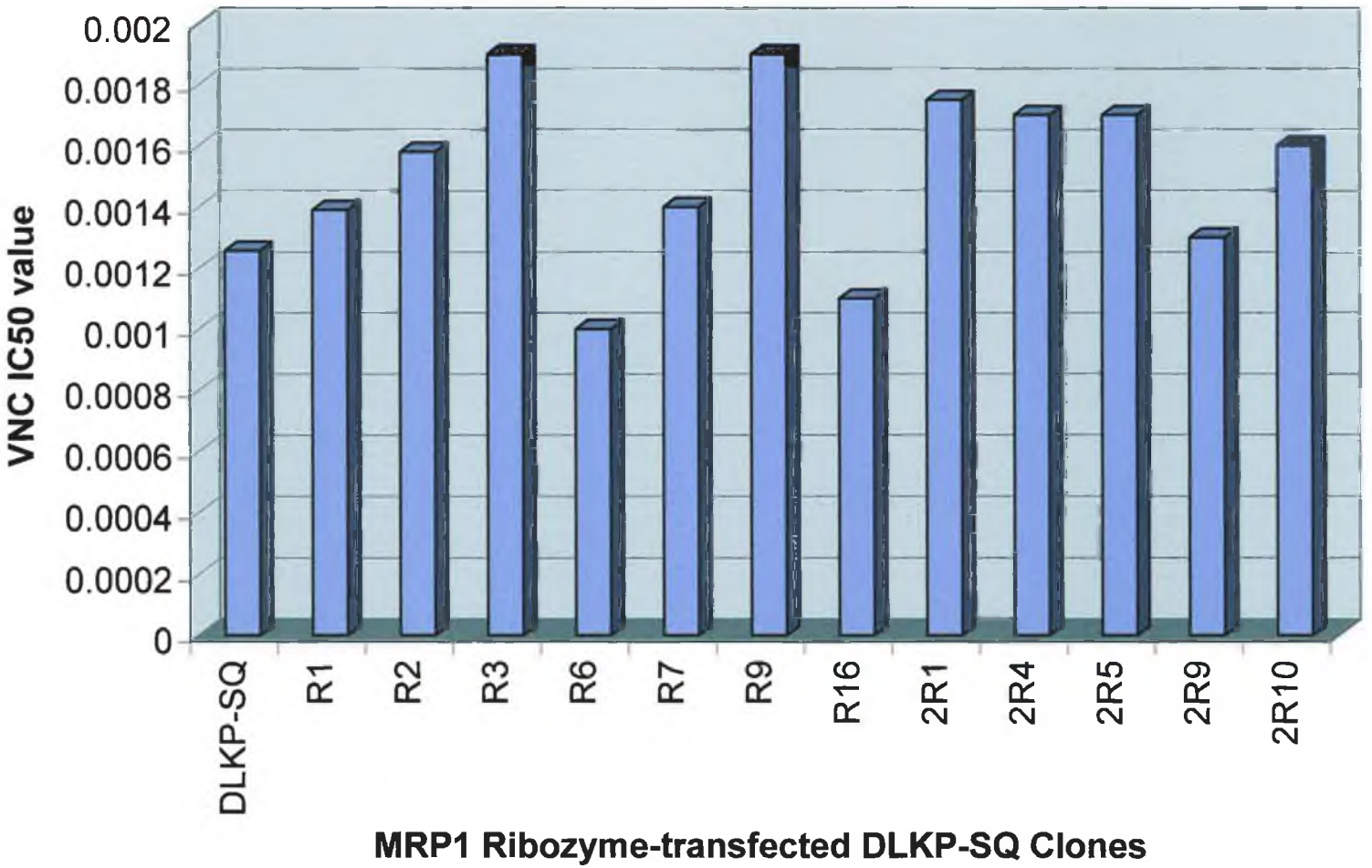

clones. If the ribozyme was exerting the specified effect in downregulating expression of the MRP1 protein, as was seen in the DLKP-SQ R2, R6 and R7 clones, an attendant effect of a decrease in resistance to vincristine, an MRP1 substrate, would be expected, particularly for these cell lines. As can be seen from Fig. 3.9.11, resistance to vincristine increased slightly in most of the ribozyme-expressing clones, although not significantly so. Slight decreases in resistance to the drug were observed in clones DLKP-SQ R6 and R9, although neither of these were felt to be of significance. The three non-ribozyme-expressing clones did not display any significant change in resistance to vincristine. The clones were also analysed for any change in resistance to the drug, Vinblastine (VNB). The results of these *in-vitro* toxicity assays are shown in Fig. 3.9.12. As expected, the resistance of the DLKP-SQ cells, ribozyme-expressing or otherwise, to vinblastine was not altered following transfection with the ribozyme.

3.9.4 *In-vitro* cleavage (IVC) analysis of the MRP1 ribozyme

From the results presented in the previous sub-Sections, it was apparent that while no reduction in MRP1 RNA was observed in the ribozyme-transfected DLKP-SQ cells, a reduced level of expression of MRP1 protein was observed which, however, did not affect significantly the drug resistance profiles of those cells. It was therefore considered necessary to investigate whether the ribozyme was actually capable of cleaving the MRP1 mRNA. If the ribozyme was observed not to be involved in the downregulation of the RNA, and hence, the protein product of the MRP1 gene, the decreases would have to attributed to some other factor. As already outlined, one of the non-ribozyme-expressing clones, DLKP-SQ R4, exhibited slightly decreased levels of the MRP1 RNA; a phemonenon attributable possibly to the selection process of the clonal cell lines from the parent. The IVC assay was carried out to investigate if this was also a potential cause for the decreases in MRP1 protein expression in the ribozyme-expressing cell lines.

As outlined already in Section 2.4.8, the IVC protocol involved a lengthy process which had previously been demonstrated by Kashani-Sabet *et al.* (1992). To manufacture the radiolabelled ribozyme, two PCR primers were designed which would anneal to one another and amplify a forty base-pair fragment with a T7 RNA polymerase promoter

Fig. 3.9.12: Relative Vinblastine (VNB) IC50 values for the MRP1 ribozyme-transfected DLKP-SQ clones

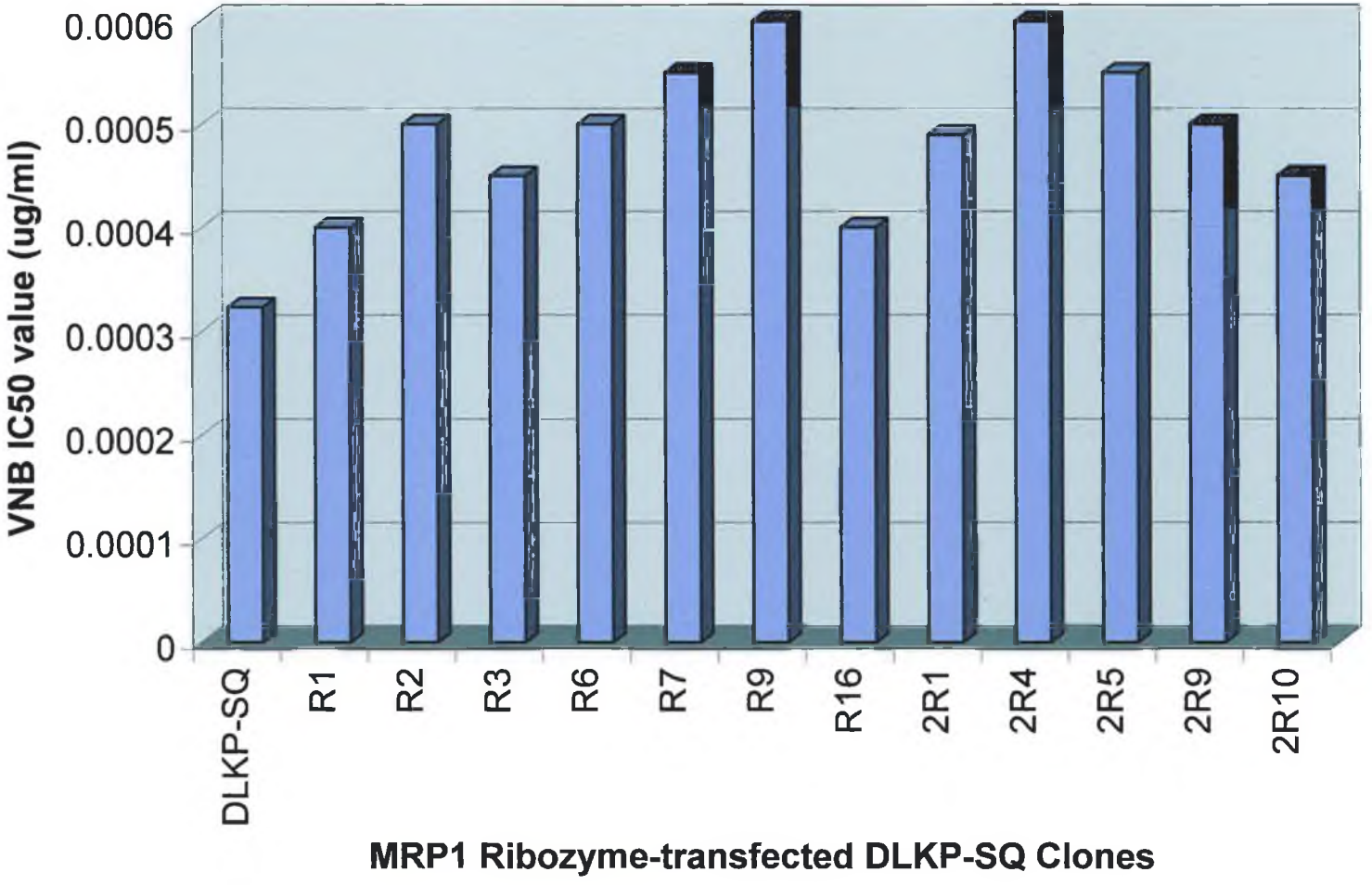

and leader sequence. This PCR product was used in a T7 polymerase Riboprobe™ kit to produce the radiolabelled ribozyme. To manufacture the target sequence, the procedure was altered and the protocol as outlined by Kashani-Sabet *et al.* (1992) was not used. Instead, a second pair of RT-PCR primers were chosen which amplified across the cleavage site of the MRP1 ribozyme. The PCR product was purified and sub-cloned into the expression vector pTarget™, which also contains a T7 RNA polymerase promoter sequence. This cloned DNA was then transformed into JM109 bacteria and from single transformed colonies a number of "miniprep" purifications were isolated. These were analysed using restriction digestion to ascertain the orientation of the insert in a particular isolate. Once the correct orientation was confirmed and a particular colony identified as desirable, a "maxiprep" isolation of the bacteria was sequenced to confirm correct orientation as well as the inclusion of the target sequence. Once this was confirmed, the plasmid DNA was digested with a single-cutting site enzyme and subjected to the same riboprobe™ procedure to generate the radiolabelled target RNA. Both the radiolabelled ribozyme and target RNA were then combined in the *in-vitro* cleavage (IVC) reaction and the products eluted on a polyacrylamide gel. The results for each Section will be illustrated here. The technical details of these experiments are outlined in Section 2.4.8.

3.9.4.1 Selection and amplification of PCR primers encoding the MRP1 ribozyme

The PCR primers selected to amplify the DNA template for production of the MRP1 ribozyme are listed in Appendix A (Table 7.3A). The PCR and subsequent transcription labelling of the ribozyme were carried out as outlined in Section 2.4.8. Once transcription and purification was complete, the ribozyme was eluted on a 12% polyacrylamide gel to ensure that the fragment was of the correct size. Fig. 3.9.13 shows the forty-two base radioactively labelled ribozyme. The ribozyme was sized using the migrating dye front as a marker, as outlined by Sambrook *et al.* (1982).

Fig. 3.9.13: *In-vitro* transcription of MRP1 ribozyme

Fig. 3.9.13: Autoradiogram showing presence of the *in-vitro* transcribed MRP1 ribozyme

3.9.4.2 Restriction digestion of cloned pTarget™ plasmids

The pTarget™ Mammalian Expression Vector System (Promega, A1410) was the mammalian expression system chosen for the radioactive-labelling of the MRP1target fragment as the plasmid can be expressed in both in bacterial as well as mammalian cells, and also contains a T7 polymerase promoter immediately 5' to the cloning site. A map of the pTarget™ vector, expressing the MRP1 cleavage target sequence, is shown in Fig. 3.9.14.

The RT-PCR primers selected to amplify the MRP1 fragment containing the ribozyme cleavage site are listed in Appendix A (Table 7.3A). These primers amplified a 477-bp fragment from the cDNA of any MRP1-expressing cell line. A standard RT-PCR was carried out on a COR L23R RNA sample and the PCR product was purified and cloned into pTarget™ as outlined in Section 2.4.4.2.1. Restriction enzyme analysis of the insert sequence using the DNA *Strider*™ 1.3 computer package revealed a number of single-cutting enzymes which could be used for digestion. Upon further consultation with the pTarget™ Mammalian Expression Vector System Technical Manual (Promega, TM044), *Pst*I was the enzyme chosen for digestion, as it cuts twice in the pTarget™ plasmid and once in the insert. Depending on the presence and orientation of the insert, the banding pattern obtained for the digest would be different for each ligation. An illustration of the plasmid containing inserts and the resultant banding pattern expected from either orientation of insert is shown in Figs. 3.9.15 to 3.9.17. As can be seen, the banding pattern observed for each isolate will reveal the presence and orientation of the MRP1 insert in the pTarget plasmid.

The digestion with *Pst*I (Sigma, R7023) of the miniprep plasmid DNA isolated from JM109 bacteria transformed with this cloned DNA and selected as outlined in Section 2.4.3, is shown in Fig. 3.9.18. As can be seen, DNA isolated from a total of fifteen colonies were selected for digestion. The selection of transformed colonies was made on the basis of the colour of those colonies. The pTarget™ plasmid contains a sequence coding for the *lacZ* α-peptide, interrupted by a multiple cloning site. Non-recombinant plasmids produce a functional α-peptide, which, by complementing the product of the host cell *lacZ*M15 gene, leads to a production of functional β-galactosidase. Bacterial

Fig. 3.9.14: Schematic map of pTarget™ Vector

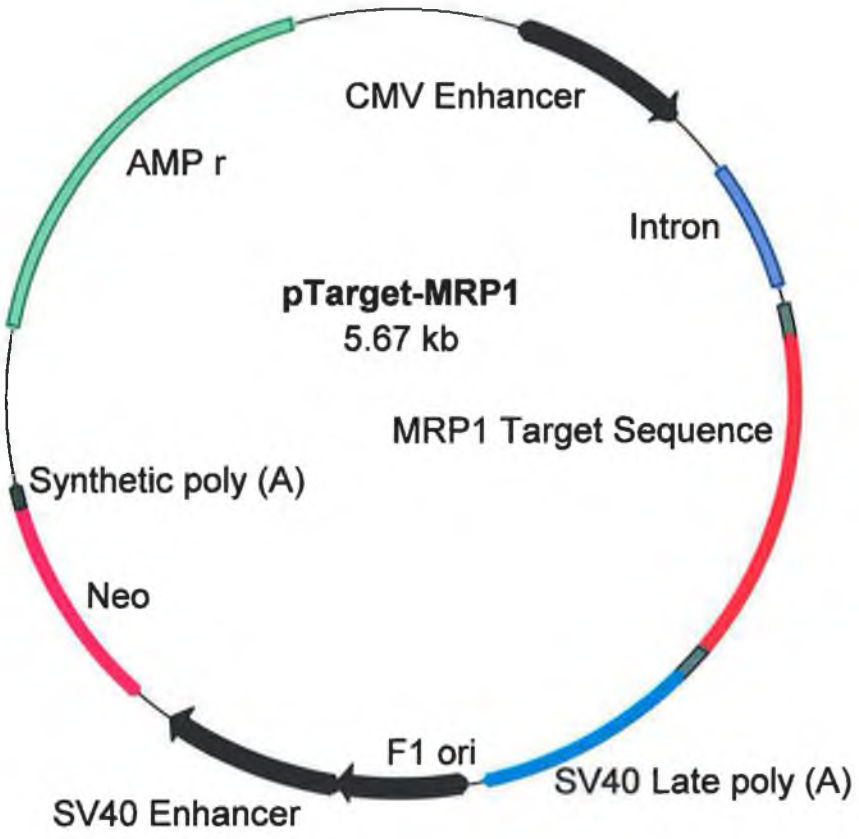

Fig. 3.9.14: Schematic map of pTarget™ Vector, showing location of promoter & insert, polyadenylation site and neomycin- & ampicillin-resistant genes

Fig. 3.9.15: MRP1-pTarget™ (FWD.) plasmid banding pattern following *Pst*I digestion

Fig. 3.9.15a:

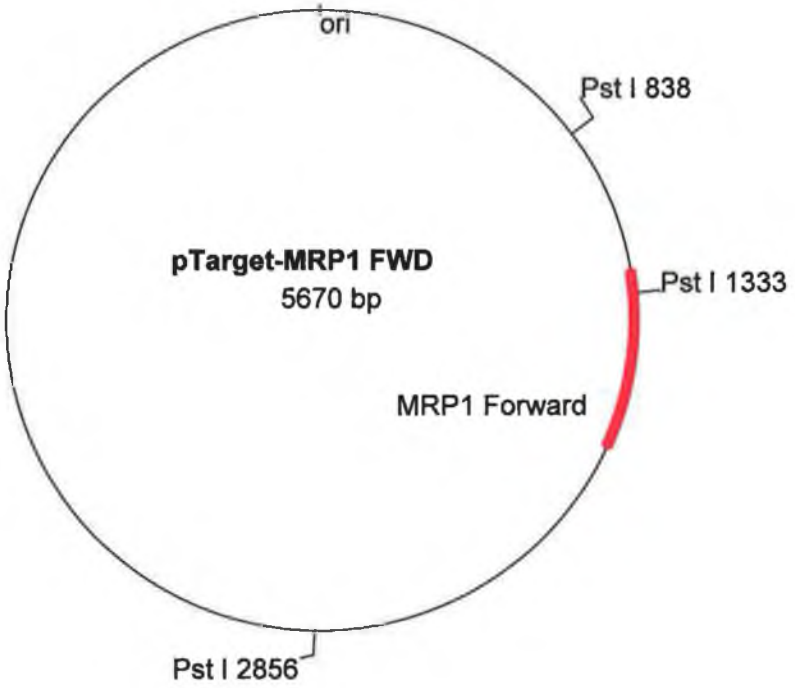

Fig. 3.9.15b:

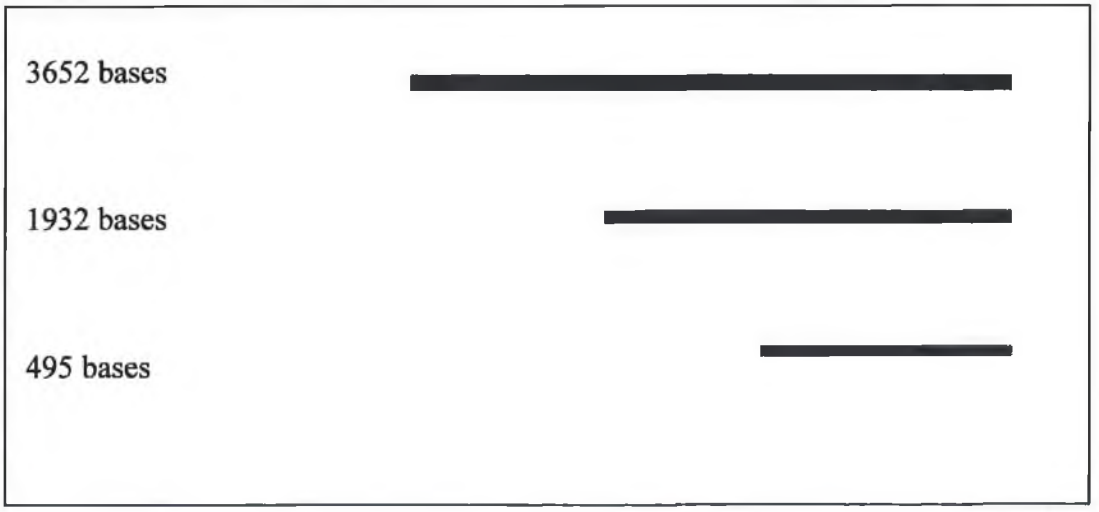

Fig. 3.9.15a: Schematic map of pTarget™ plasmid containing MRP1 target sequence insert in the Forward (FWD.) orientation. Location of *Pst*I sites are included.

Fig. 3.9.15b: Banding pattern of plasmid obtained when digested with *Pst*I.

Fig. 3.9.16: MRP1-pTarget™ (REV.) plasmid banding pattern following *Pst*I digestion

Fig. 3.9.16a:

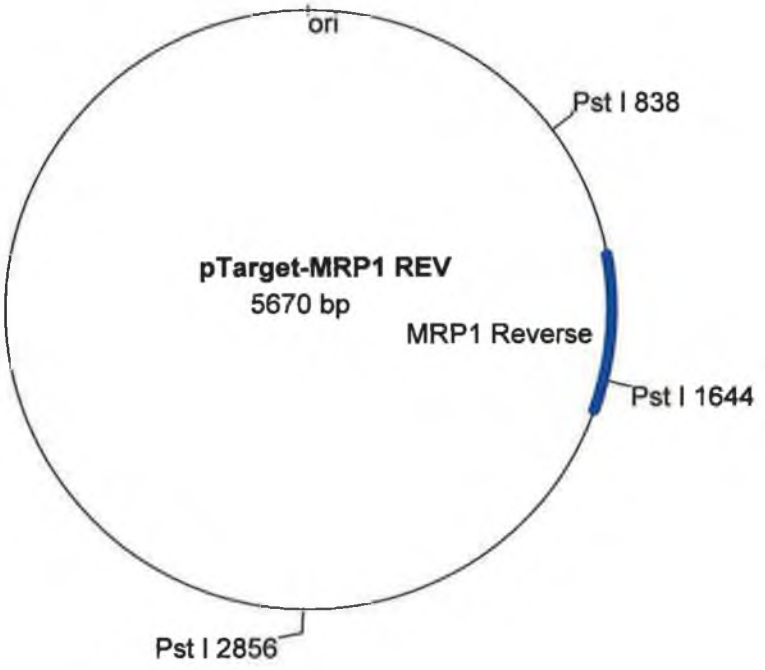

Fig. 3.9.15b:

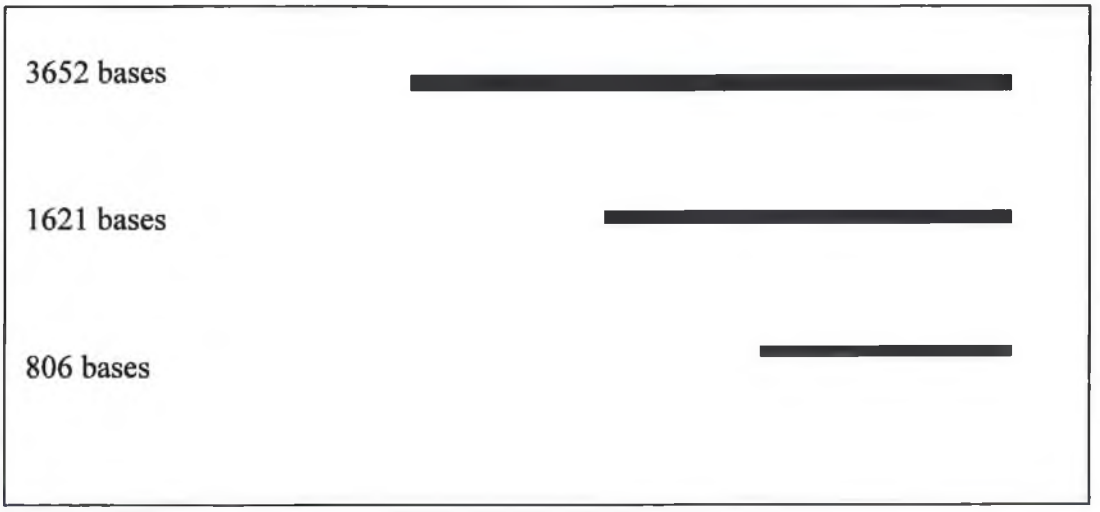

Fig. 3.9.16a: Schematic map of pTarget™ plasmid containing MRP1 target sequence insert in the Reverse (REV.) orientation. Location of *Pst*I sites are included.

Fig. 3.9.16b: Banding pattern of plasmid obtained when digested with *Pst*I.

Fig. 3.9.17: pTarget™ plasmid banding pattern following *Pst*I digestion

Fig. 3.9.17a:

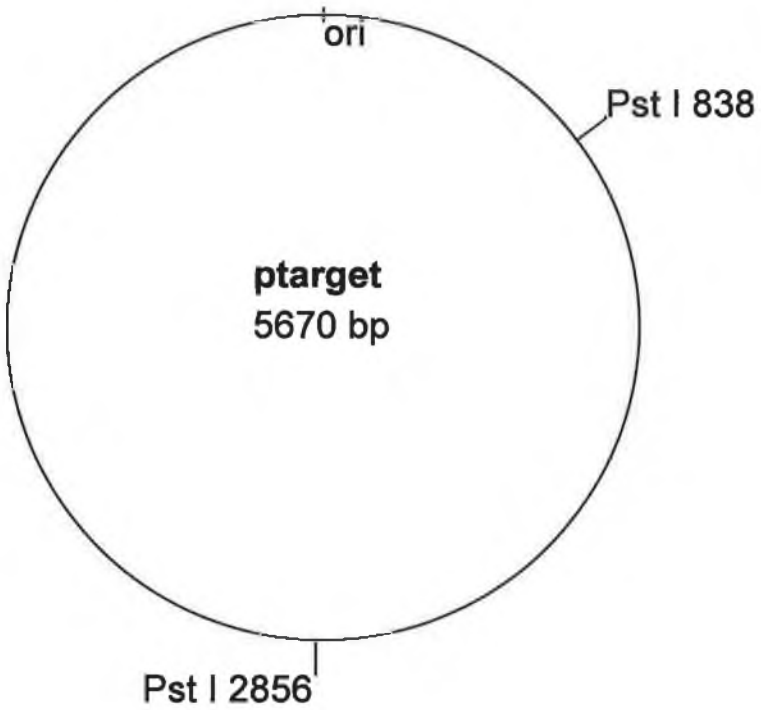

Fig. 3.9.17b:

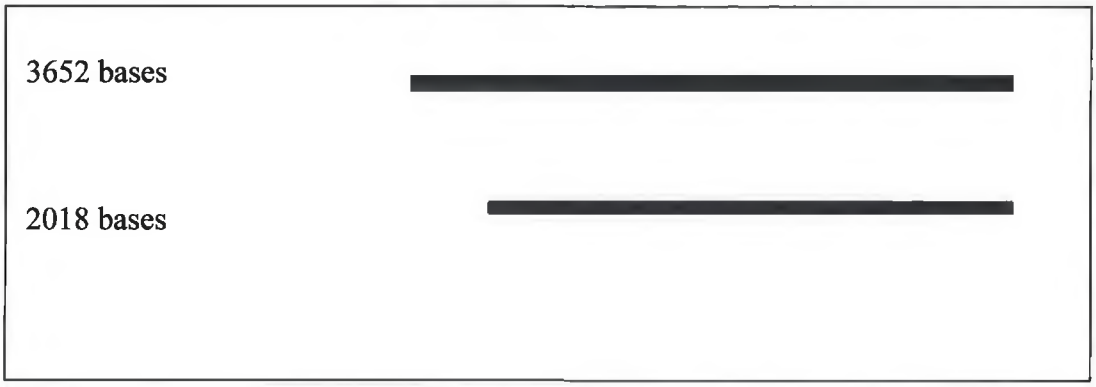

Fig. 3.9.17a: Schematic map of naked pTarget™ plasmid. Location of *Pst*I sites are included. Fig. 3.9.15b: Banding pattern of plasmid obtained when digested with *Pst*I.

Fig. 3.9.18: *Pst*I digest of pTarget™ plasmid DNA

Fig. 3.9.18a: Banding pattern for Samples 1, 3, 4, 9-13 & 15

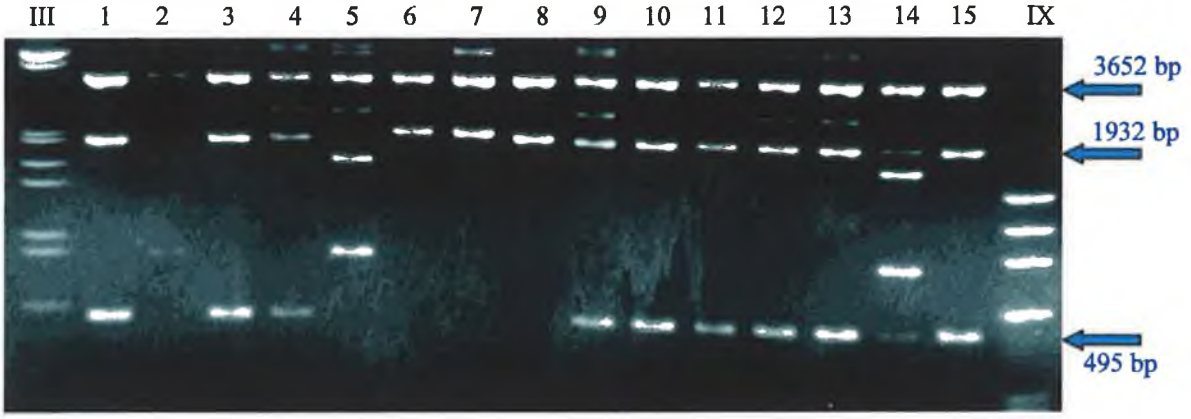

Fig. 3.9.18b: Banding pattern for Samples 2, 5 & 14

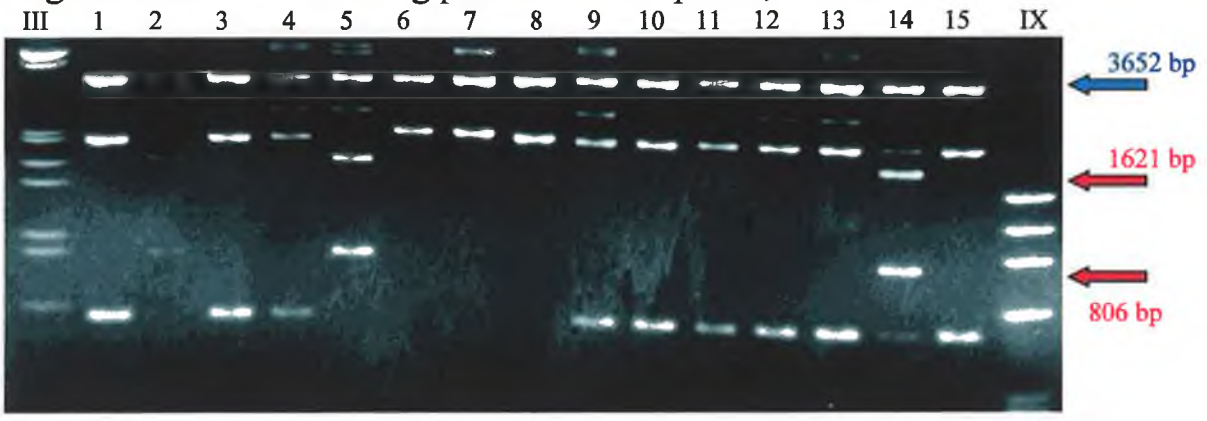

Fig. 3.9.18c: Banding pattern for Samples 6, 7 & 8

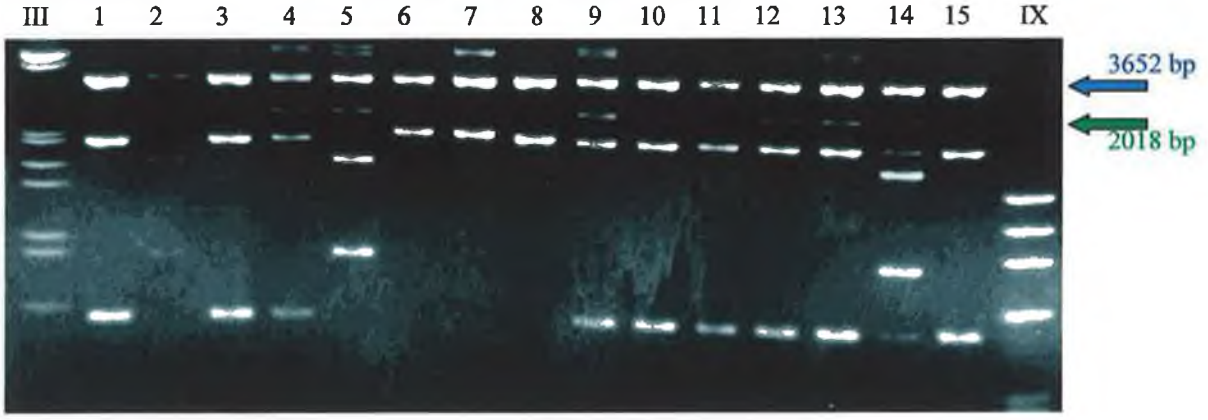

Fig. 3.9.18a: Banding pattern obtained for plasmids expressing MRP1 insert in the forward orientation. Fig. 3.9.18b: Banding pattern obtained for plasmids expressing MRP1 insert in the reverse orientation. Fig. 3.9.18c: Banding pattern obtained for naked pTarget™ plasmids.

colonies harbouring the naked recircularised pTarget™ vector are blue in colour when plated on indicator plates containing IPTG and X-Gal as outlined in Section 2.4.4.4. However, when the *lacZ* α-peptide is disrupted by cloning into the pTarget™ vector multiple cloning region, complementation does not occur and no β-galactosidase activity is produced. Colonies harbouring recombinant pTarget™ vector constructs are therefore coloured white. Twelve of the selected colonies were white in colour, and three, samples 6-8, were blue. These last three colonies instead contained the recircularised plasmid, and were chosen to act as negative controls for the insert in the digestion. Nine of the twelve white transformed colonies (samples 1, 3, 4, 9-13 and 15) contained the insert in the correct (forward) orientation. Three colonies (samples 2, 5 and 14) contained the insert in the reverse orientation, while the remaining three colonies (samples 6-8) were observed not to contain the insert, as expected.

3.9.4.3 Sequence analysis of cloned fragment

Colony samples 1 and 14 were chosen for further cultivation of the expression plasmids containing the insert in the correct orientation (sample 1) and in the reverse orientation (sample 14). A plasmid maxiprep was carried out on these samples to provide DNA for sequence analysis to confirm both the orientation of the insert in both samples and also, in the case of sample 1, to confirm that the ribozyme cleavage site was contained within the insert. The isolated DNA from both samples was subjected to sequence analysis as outlined in Section 2.4.4.6 and the products were eluted on a polyacrylamide gel. Fig. 3.9.19 shows the relevant Section of sequence from sample 1 containing the ribozyme cleavage site, which was also obtained in the correct orientation for transcriptional production of the mRNA product. Sequence analysis of sample no. 14 also confirmed that the insert was reverse-oriented in the pTarget™ plasmid (data not shown).

3.9.4.4 Riboprobe™ production of Target sequence

Once orientation and presence of ribozyme cleavage site had been confirmed, the transcribed target mRNA was then generated from the isolated plasmid DNA along with

Fig. 3.9.19: Sequence analysis of MRP1 target

Fig. 3.9.19a:

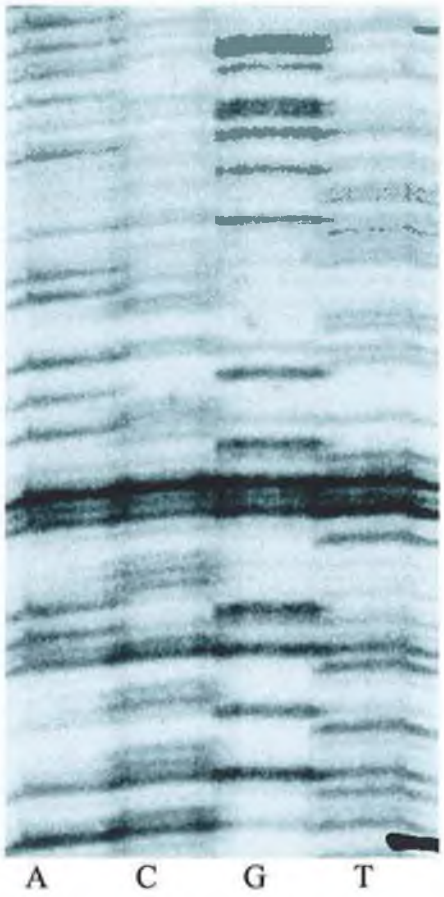

Fig. 3.9.19b:

AGT TGC TCA TCA AGT TCG TGA ATG ACC GAA
GGC CCC AGA CTG GCA GGG CTA CTT CTC TAC
ACC GTG CTG CTG CTG TTT GTC ACT GCC TGC
CTG CAG ACC CTC GTG CTG CAC CAG TAC TTC
CAC ATC TGC TTC GTC AGT GGC A

Fig. 3.9.19a: Autoradiogram showing sequence of the MRP1 target from sample 1 containing ribozyme cleavage site (Bases 1236 – 1373). Fig. 3.9.19b: Sequence data showing transcribed sequence (Black) including PstI site (Green) and ribozyme cleavage site (Red). An unreadable compression section is listed in Blue.

an *in-vitro* transcribed pGem positive control. In Fig. 3.9.20, the transcribed MRP1 target sequence can be seen, sized against a human apoptosis hAPO-2c multi-probe RNA marker (Promega, 45609P) (Fig. 3.9.20). It can be observed from this figure that the transcribed fragment was of the correct size (477 bases). In Fig. 3.9.21, the radioactively-labelled MRP1 target RNA fragment was placed beside the 1,065 base pGem RNA product. As can be seen in both figures, the *in-vitro* transcribed MRP1 target fragment did not suffer any non-specific degradation in its stability. Thus, this presentation will serve as the untreated control for all subsequent cleavage experiments involving the MRP1 ribozyme.

3.9.4.5 *In-vitro* cleavage of Ribozyme and Target

The radioactively-labelled MRP1 ribozyme and target sequence were combined in an *in-vitro* cleavage assay as outlined in Section 2.4.8.5. Cleavage reactions were incubated at 37°C and samples were removed for analysis at 30mins, 60mins, 3 hours and overnight. There are five expected cleavage reaction products;

1. 519 bases – the size of the bound MRP1 target sequence and ribozyme
2. 477 bases – unbound and uncleaved MRP1 target sequence
3. 348 bases - 1st and larger cleavage product
4. 129 bases – 2nd and smaller cleavage product
5. 42 bases – unbound MRP1 ribozyme

The reactions were eluted on a 12% polyacrylamide gel, the results of which are shown on Fig. 3.9.22. At the higher fragment sizes, it was difficult to discern the bound and unbound radioactively-labelled fragments. As a result, these two fragments will be analysed together here as one fragment. As can be seen from the autoradiogram and densitometric analysis in Fig. 3.9.22, the amount of the bound MRP1 target sequence decreases over time, while those of both cleavage products increase with time. This is entirely consistent with a time-dependent cleavage of the MRP1 target sequence by the MRP1 ribozyme. The radioactively-labelled MRP1 ribozyme was either run off the gel or remains bound to the remaining MRP1 target sequence.

Fig. 3.9.20: *In-vitro* transcription of MRP1 target

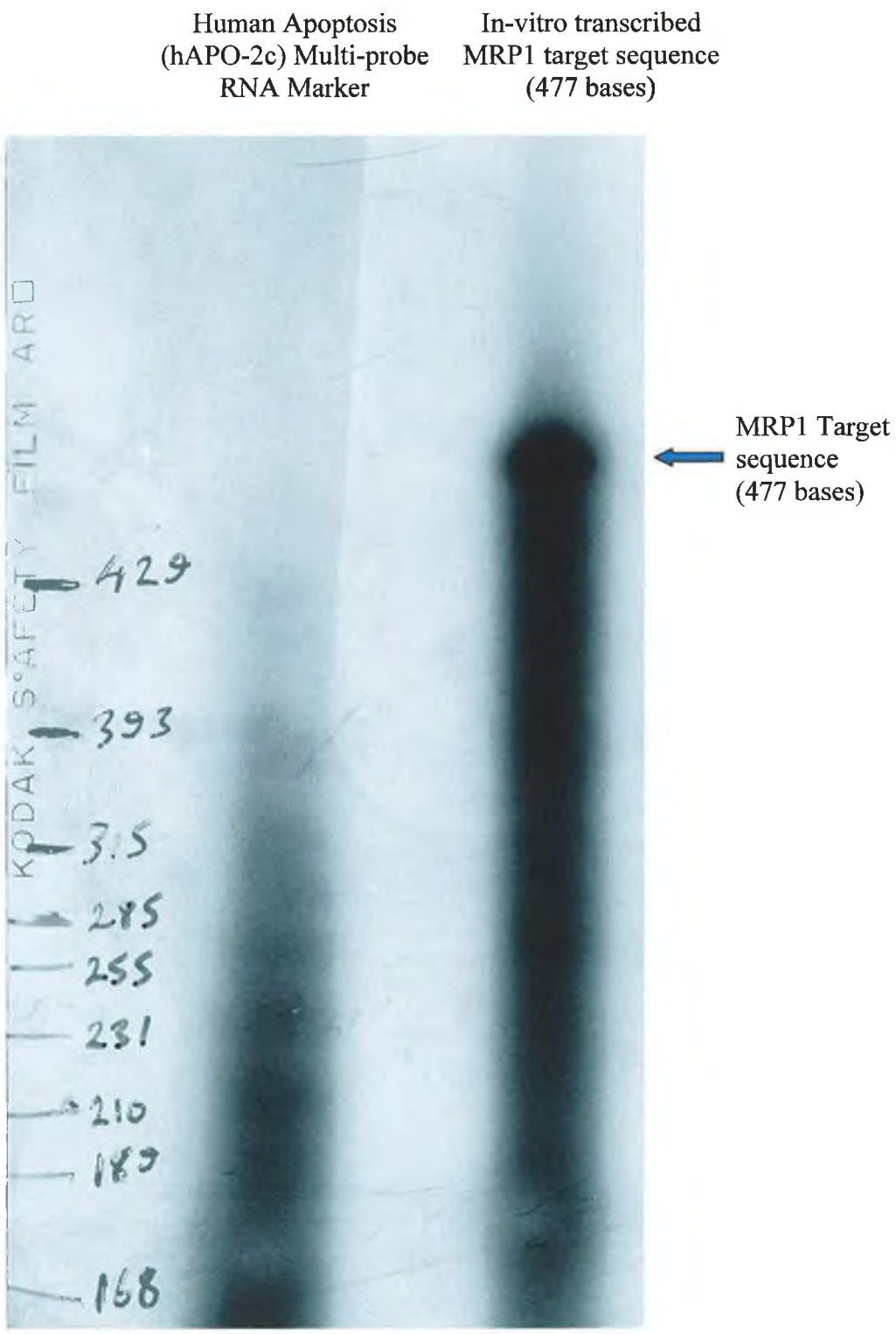

Fig. 3.9.20: Autoradiogram showing the in-vitro transcription of the MRP1 target RNA sequence sized against a commercially prepared marker (hAPO-2c)

Fig. 3.9.21: *In-vitro* transcription of MRP1 target

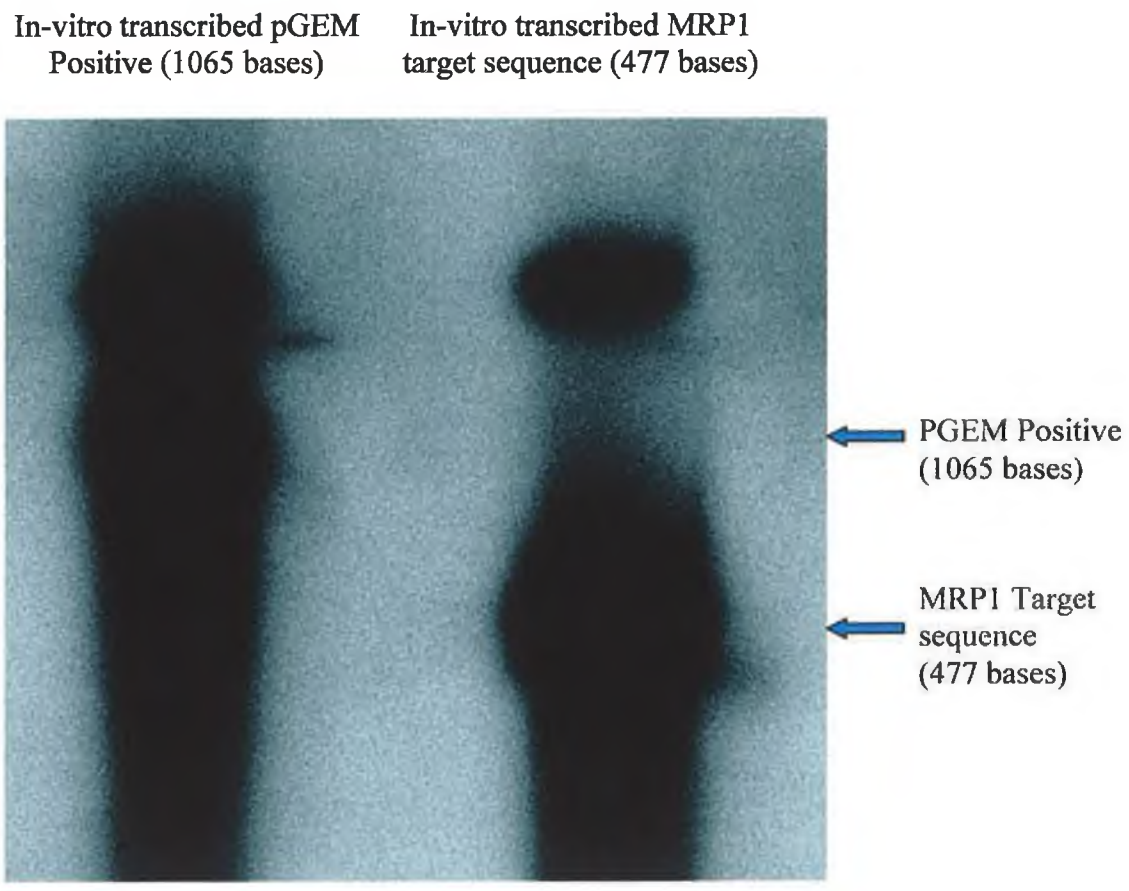

Fig. 3.9.21: Autoradiogram showing the in-vitro transcription of the pGEM positive control and the MRP1 target RNA sequence

Fig. 3.9.22: *In-vitro* cleavage of MRP1 target

Fig. 3.9.22a:

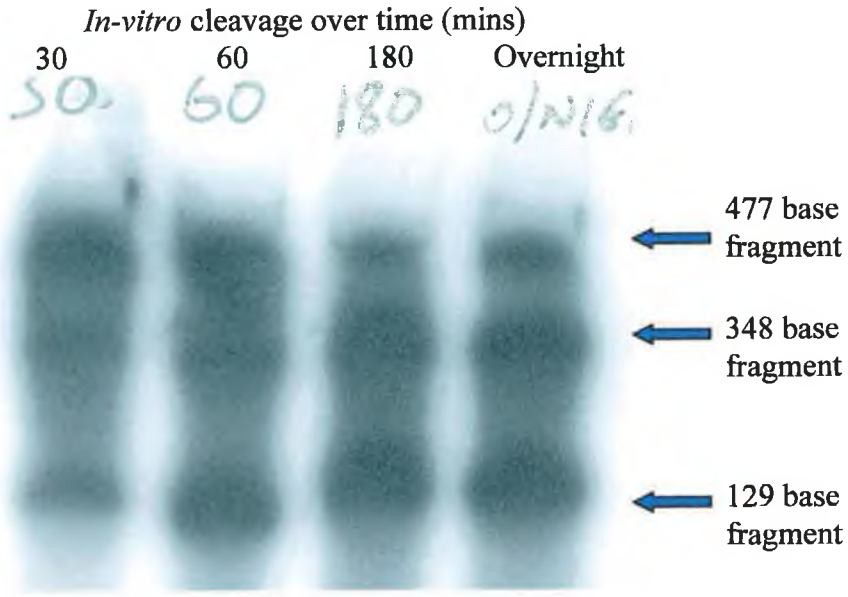

Fig. 3.9.22b:

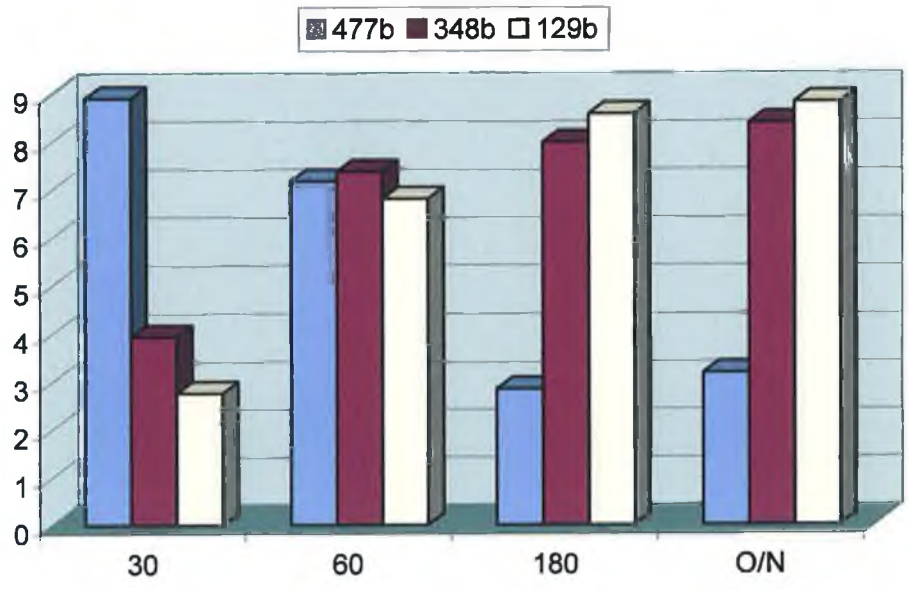

Fig. 3.9.22a: *In-vitro* cleavage of the MRP1 target sequence over time using the *in-vitro* transcribed MRP1 ribozyme; Fig. 3.9.22b: Densitometric analysis of autoradiogram results.

3.9.4.6 Cleavage of the MRP1 target sequence using cell extract

As outlined by Kashani-Sabet *et al.* (1992), a further test of the activity of the ribozyme was the cleavage of the MRP1 target sequence using cell extract taken from ribozyme-expressing clones. The protocol for isolating the cell extract from these clones is as outlined in Section 2.4.8.2. The radioactively labelled MRP1 target sequence was incubated in the standard *in-vitro* cleavage reaction (see Section 2.4.8.5) with solutions of cell extract taken from three ribozyme-expressing clones (DLKP-SQ 2R1, R7 and R9), one non-ribozyme-expressing clone (DLKP-SQ R1) and from the control DLKP-SQ cell line. The cleavage reaction was allowed to run overnight and the products eluted on a 12% polyacrylamide gel. The results of this reaction can be seen in Fig. 3.9.23. As can be seen, cleavage of the target sequence occurs in all three ribozyme-expressing clones, the highest level of cleavage occurring in the cell extract from the DLKP-SQ R9 sample. No cleavage was observed in the DLKP-SQ control cell line, although it must be noted that less MRP1 target sequence was incubated in this reaction. Slight cleavage was observed in the ribozyme-negative DLKP-SQ R1 control, although this was more likely due to non-specific RNA degradation due to the samples being incubated at 37°C overnight as no clear cleavage banding pattern was observed for this sample.

It was also considered interesting to investigate if the cleavage recorded for the cell extract was also time-dependant, as was observed for the *in-vitro* transcribed MRP1 ribozyme. Cell extract from one of the ribozyme-expressing clones examined in the previous cell extract cleavage experiment, DLKP-SQ R7, was incubated in a cleavage reaction with the radioactively-labelled MRP1 target sequence. The cleavage reaction was carried out as usual (see Section 2.4.8.5), and samples were removed from the reaction at 0hrs, 30 mins, 1hr, 3hrs and overnight (O/N). The samples were eluted on a 12% polyacrylamide gel, the autoradiogram and attendant densitometry of which is shown in Fig. 3.9.24. As can be seen, the large target sequence is degraded over time into the distinct smaller cleavage fragments characteristic of the action of the MRP1 ribozyme. However, significant cleavage of the target sequence is only obtained after the reaction has proceeded overnight, which indicates that the process from cell extract is slower than that observed for the purified MRP1 ribozyme.

Fig. 3.9.24: *In-vitro* cleavage with Clone No.7 Cell Extract

Fig. 3.9.24a:

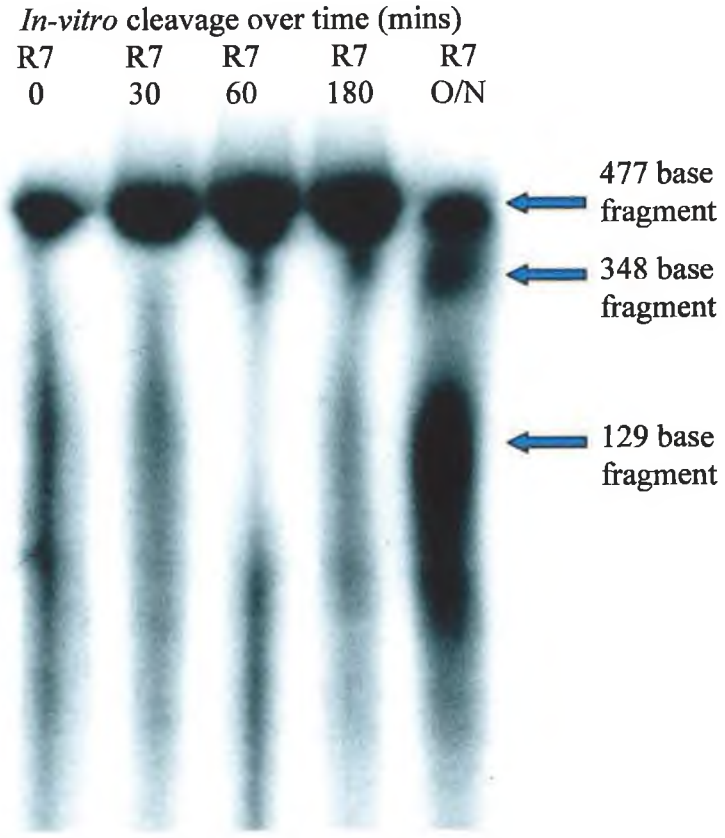

Fig. 3.9.24b:

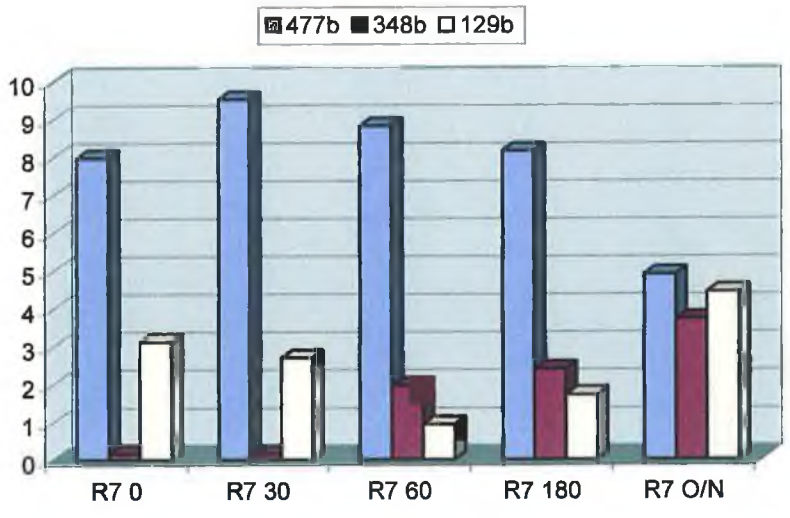

Fig. 3.9.24a: *In-vitro* cleavage of the MRP1 target sequence over time using cell extract from the ribozyme-expressing clone DLKP-SQ R7; Fig. 3.9.24a: Densitometric analysis of autoradiogram results.

3.10 Analysis of MRP1 downregulation using MRP1 antisense oligonucleotides

A decrease in MRP1 mRNA or protein expression was sought also through using antisense oligonucleotides targetted to the mRNA of the MRP1 gene. The analysis was begun by utilising an MRP1 antisense which had already been proven to downregulate expression of both the MRP1 mRNA and protein in HeLa cells. This antisense was transfected into DLKP-SQ cells and its effect on expression of both the MRP1 mRNA and protein, as well as the *in vitro* toxicity profile of the cell line was examined.

This was then followed up by the identification of nineteen novel potential MRP1 antisense oligonucleotides. These oligos were selected on the basis of inhibition studies carried out on the MRP1 mRNA and protein (see Section 1.7.1.2.2). These oligos were also transfected into DLKP-SQ and their effect on MRP1 mRNA expression and drug-resistance profile in the cell line was investigated. An RNaseH assay was also developed and optimised to investigate if the selected antisense were capable of cleaving the MRP1 sequence.

3.10.1 Use of MRP1 antisense oligonucleotide *ISIS 7597* to downregulate MRP1 expression

From the relevant literature (Stewart *et al.*, 1996; Canitrot *et al.*, 1996), a phosphorothioate antisense oligonucleotide, *ISIS 7597*, was chosen to be used to downregulate expression of the MRP1 gene in the DLKP-SQ cell line. From these previous studies, the oligo had been successful in decreasing MRP1 gene expression by 90% and protein expression by 49% in the HeLa cell line. Unfortunately, several transfections of the antisense including a sense control oligonucleotide into the DLKP-SQ cell line failed to induce any significant decrease in expression of either the MRP1 gene or protein (data not shown). Also, *in-vitro* toxicity assays carried out on the transfected cells with the MRP1 substrate chemotherapeutic drug, vincristine, failed to detect any effect on the resistance profile of the transfected cell line relative to the normal (data not shown). Subsequent discussion on the subject of this oligonucleotide with external colleagues revealed that the molecule was not as efficient at cleaving the

MRP1 mRNA as had been previously assumed (Dr. Finbarr Cotter, Personal communication).

3.10.2 Selection of novel MRP1 antisense oligonucleotides to downregulate gene expression

The decision was taken to design a number of novel antisense oligonucleotides to target and hopefully inhibit the action of the MRP1 gene. A total of nineteen potential oligos were designed from inhibition studies carried out in previous studies (see Section 1.7.1.2.2). Ten of these nineteen oligonucleotides were chosen for further use in downregulating the MRP1 gene in DLKP-SQ cells. These ten oligos, along with their sequence and the position on the MRP1 coding mRNA strand relative to the translational start are outlined in Table 3.10.1. The oligos are given the prefix *MA*, which stands for *M*RP1 *A*ntisense.

Table 3.10.1 List of novel antisense targetted to the MRP1 gene

Name	Target position	Antisense sequence
*MA*1	315-334	CCCACGGAACAAAAATGGAG
*MA*3	854-873	TGGAAGACCACCTAGTGTCC
*MA*5	2366-2385	CTTTTGTAGGAAAAACCTAC
*MA*8	3690-3709	CAGTGCGAAGCTCGGAAGCTCCTCGTCCGCACTG
*MA*9	569-588	GTCGACCTCTCCTCCTTCCC
*MA*10	1436-1455	CGGTCTTTTAGGAGGTGCCA
*MA*12	1775-1794	TTCCACGACCGGTAGTCCGT
*MA*13	4533-4552	CCTTCTGCTTCTAGGAACAC
*MA*14	2246-2265	TTCAACAGGGACGAGAGTCG
*MA*19	5' UTR	ACCCCGCCCCGGAGGCGTAG

All of the above oligos except *MA*19 were targetted to the coding mRNA strand of the MRP1 gene. *MA*19 was targetted to the gene itself. The oligos were selected for the reasons outlined below, although Section 1.7.1.2.2 contains the background to the studies which identified those areas of the MRP1 gene and protein which were more likely to have a significant effect on the functioning protein if successfully disrupted. BLAST™ homology searches revealed that none on the designed oligos shared 100% complementarity with any other known human genes (data not shown).

3.10.2.1 Reasons for selection of novel MRP1 antisense oligonucleotides

*MA*1 is targetted to the first transmembrane helix in the MSD1 region of the MRP1 gene, corresponding to the amino acid positions 41 – 46. Previous studies had already determined that removal or inhibition of this area of the gene (Stewart *et al.*, 1996) or protein (Gao *et al.*, 1998) resulted in disruption of MRP1 function.

*MA*3 is targetted to the L_o linker region of the MRP1 gene, identified as essential for activity in several previous studies (Bakos *et al.*, 1998; Gao *et al.*, 1998).

*MA*5 targets the NBD1 Section of the gene, at a position indicated by studies involving deletion mutations in the Yeast Cadmium Factor (YCF1) as being potentially important for MRP1 activity.

Deletion mutant studies involving YCF1 (Falcon-Perez *et al.*, 1999) were also the source of identification of the next antisense, *MA*8, which is targetted to the MSD3 area of the gene, also deemed a necessary part of the protein to ensure proper function (Stride *et al.*, 1999). This structure of this oligonucleotide was designed to act as a circular antisense (Niewiarowski *et al.*, Paper submitted).

Epitope insertion studies which inactivated the MRP1 protein (Kast *et al.*, 1997) identified sensitive sites for MRP1 function which are targetted by the following three antisense oligos; *MA*9, *MA*10 and *MA*12. *MA*9 is targetted to the MSD1 region of the gene, while the other two target MSD2.

Studies in the murine *mrp* gene (Lorico *et al.*, 1997) identified a deletion which disrupted the activity of the protein. *MA*13 was designed to target the equivalent region in the human MRP1 gene.

The identification of shared homology between the various MRP genes (MRPs 1 – 6) allowed for the selection of antisense which may target functionally important sequences. *MA*14 was designed with this in mind as it targets the Walker A motif in the NBD1 region of the MRP1 gene.

Finally, an attempt was made to design an effective "antigene", or antisense targetted to the MRP1 DNA sequence. Such antigenes bind to the DNA, forming stable triple-stranded structures and are sometimes effective in downregulating expression of the targetted gene. From the promoter analysis already carried out (Section 3.4.6.1), it has been determined that most MRP1 promoter activity in the DLKP cell line occurs in the –91 to +103 base Section of the promoter sequence (relative to the transcriptional start). It was considered that this Section of the promoter might also be the most utilised in the DLKP-SQ cell line. To this end, *MA19* was designed to target the transcriptional start site of MRP1 and the promoter region immediately 5' to it. The antisense was designed to bind to the Sp1 transcription recognition sequence which is the most prevalent motif in this Section of the MRP1 promoter.

Overall, three antisense were designed to target the first Membrane-spanning Domain (MSD1), two to target both MSD2 and Nucleotide-binding Domain 1 (NBD1) and one each against MSD3, NBD2 and the 5' Untranslated region (UTR).

3.10.2.2 Transfection of novel antisense into DLKP-SQ

The type of oligos used for all the antisense except *MA8* were Second-generation chimera™ antisense, rather than the simple phosphorothioates which had been previously used. A description of these chimeric oligos is included in Section 2.4.4.1. Two concentrations of each oligo were set up for transfection into the DLKP-SQ cell line, which were denoted by letters A and B. The concentrations used (in μm/ml) were 1.0 (A) and 1.5 (B) of oligonucleotide. Transient antisense transfections using the novel designed oligos into DLKP-SQ were set up as outlined in Section 2.4.5, and the cells were analysed for effects on MRP1 mRNA and toxicological response.

3.10.2.3 Analysis of antisense-transfected DLKP-SQ cells by MRP1 RT-PCR

The DLKP-SQ cells were taken down 24hrs after transfection with the antisense oligos and assayed by RT-PCR to examine any possible effect on the MRP1 gene expression

levels in the transfected cells. The results of these RT-PCRs can be seen in Figs. 3.10.1 and 3.10.2. As can be seen from these figures, none of the designed oligos were observed to reduce expression of the MRP1 gene in the transfected DLKP-SQ cells. In the main, MRP1 gene expression was increased in most of the transfected cells, the most significant increases observed for *MA* 13 (Conc. A), at eighteen-fold, and for *MA* 10 (Conc. A), at twelve-fold. Overall, expression of the MRP1 gene was observed increased in ten of the twenty (50%) transfections carried out, while no significant decreases in expression were observed.

3.10.2.4 *In vitro* toxicity analysis of antisense-transfected DLKP-SQ cells

In-vitro toxicity assays with the designed MRP1 antisense oligos were carried to examine if transfection with the oligos affected the drug resistance profile of the DLKP-SQ cells. DLKP-SQ cells were set up for transfection with the oligos and the results analysed as outlined in Section 2.4.5. The results of these toxicity assays are shown in Figs. 3.10.3 (1.0 μm/ml conc. antisense) and 3.10.4 (1.5 μm/ml conc. antisense). As can be seen, none of the designed oligos were effective in significantly decreasing the resistance of the DLKP-SQ cells to the MRP1-substrate vincristine. Transfection with the oligos was observed to adversely affect the ability of the cells to survive, although this lowered cell survival was also observed at zero vincristine concentration, so the toxic effect is not specifically MRP1-related. The most promising result was that obtained for *MA* 3 (at 1.0 μm/ml conc.) for which a negligible 13% non-specific rate of cell death was observed at zero vincristine concentration. This had increased to a cell death rate of almost 40% at 1μg/ml vincristine conc., at which the untreated DLKP-SQ control registers almost no cell death due to the action of the drug alone (Fig. 3.10.3). However, further transfections at the higher oligo conc. of 1.5 μm/ml (Fig. 3.10.4) revealed no significant effect of the oligo. The oligos which exhibited the most toxic non-specific effect were *MA*s 1 and 14. These oligos were targetted to the first transmembrane helix and the Walker A motif in nucleotide-binding domain 1 (NBD1), respectively.

Fig. 3.10.1:MRP1 RT-PCR on Antisense-transfected DLKP-SQ

Fig. 3.10.1a:

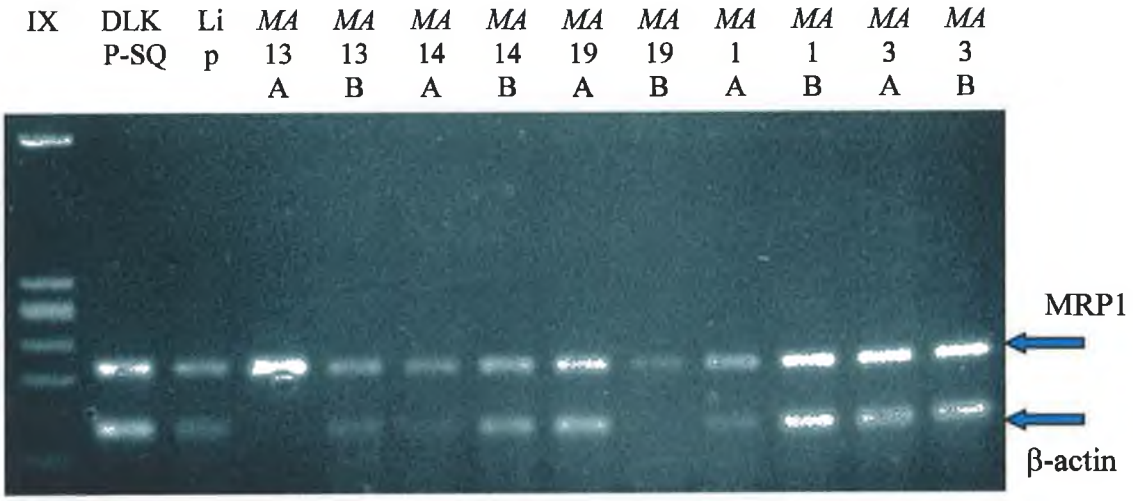

Fig. 3.10.1b:

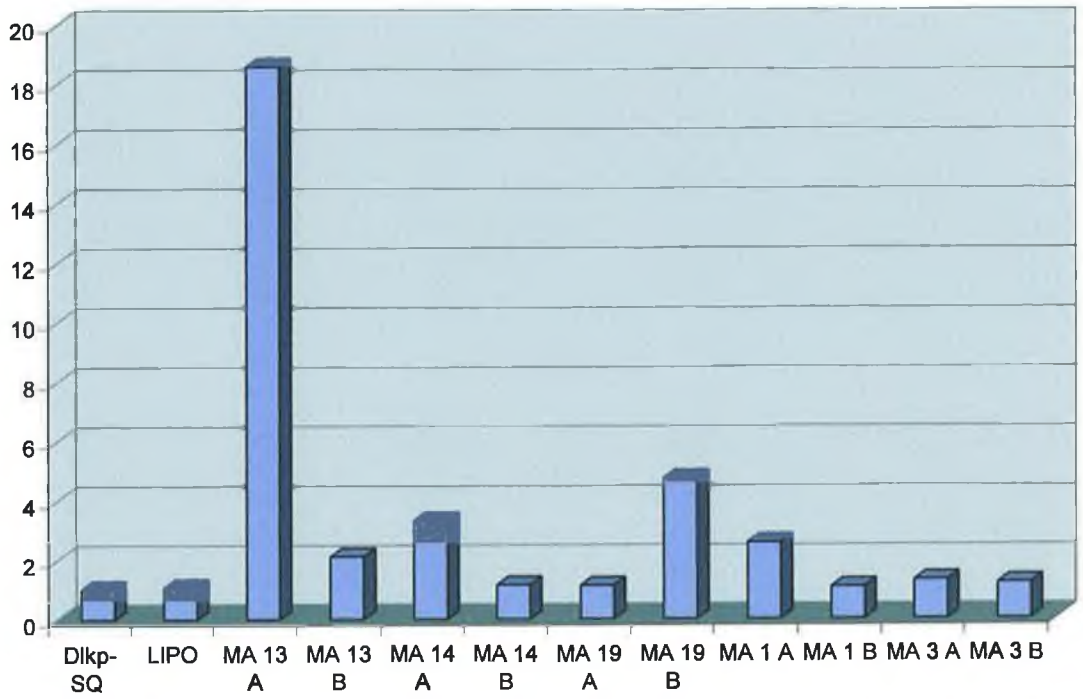

Fig. 3.10.1a: Gel electrophoresis photograph of MRP1 RT-PCR results on antisense-transfected DLKP-SQ cells; Fig. 3.10.1b: Densitometric analysis of RT-PCR results.

Fig. 3.10.2:MRP1 RT-PCR on Antisense-transfected DLKP-SQ

Fig. 3.10.2a:

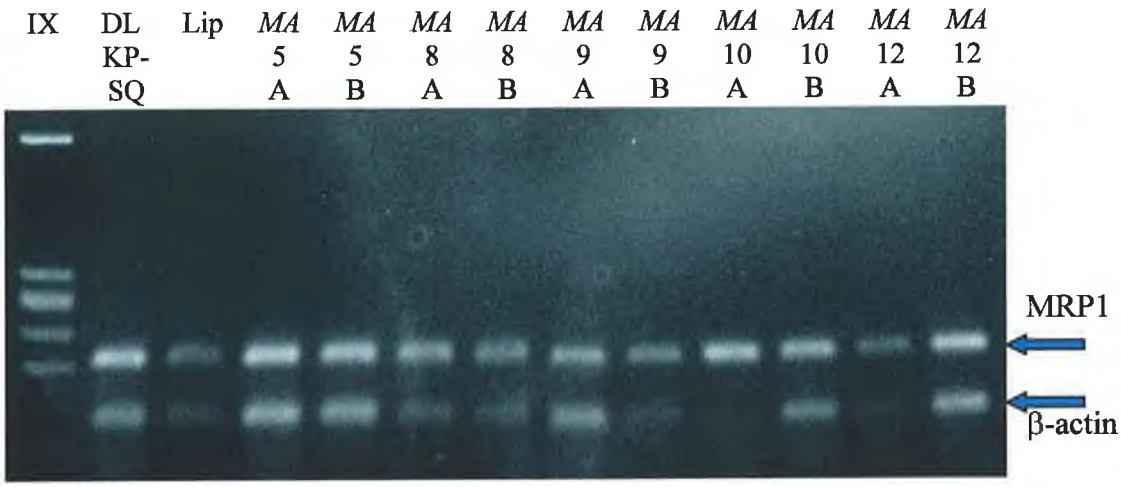

Fig. 3.10.2b:

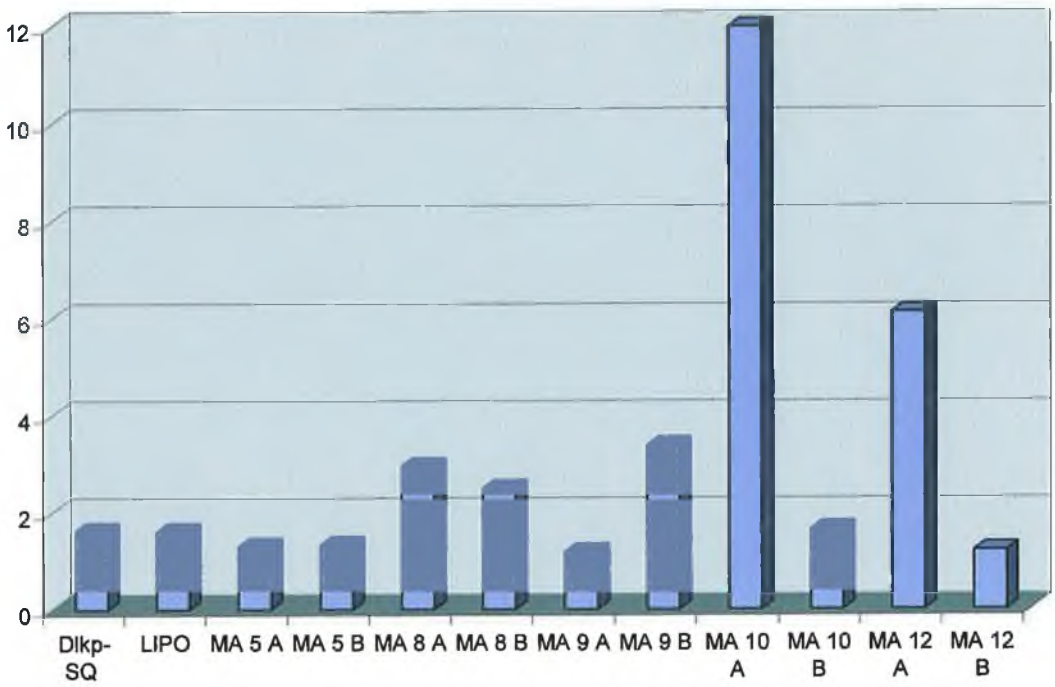

Fig. 3.10.2a: Gel electrophoresis photograph of MRP1 RT-PCR results on antisense-transfected DLKP-SQ cells; Fig. 3.10.2b: Densitometric analysis of RT-PCR results.

Fig. 3.10.3: Effect of MRP1 Antisense (1.0 um/ml) on Vincristine (VNC) resistance in DLKP-SQ cells

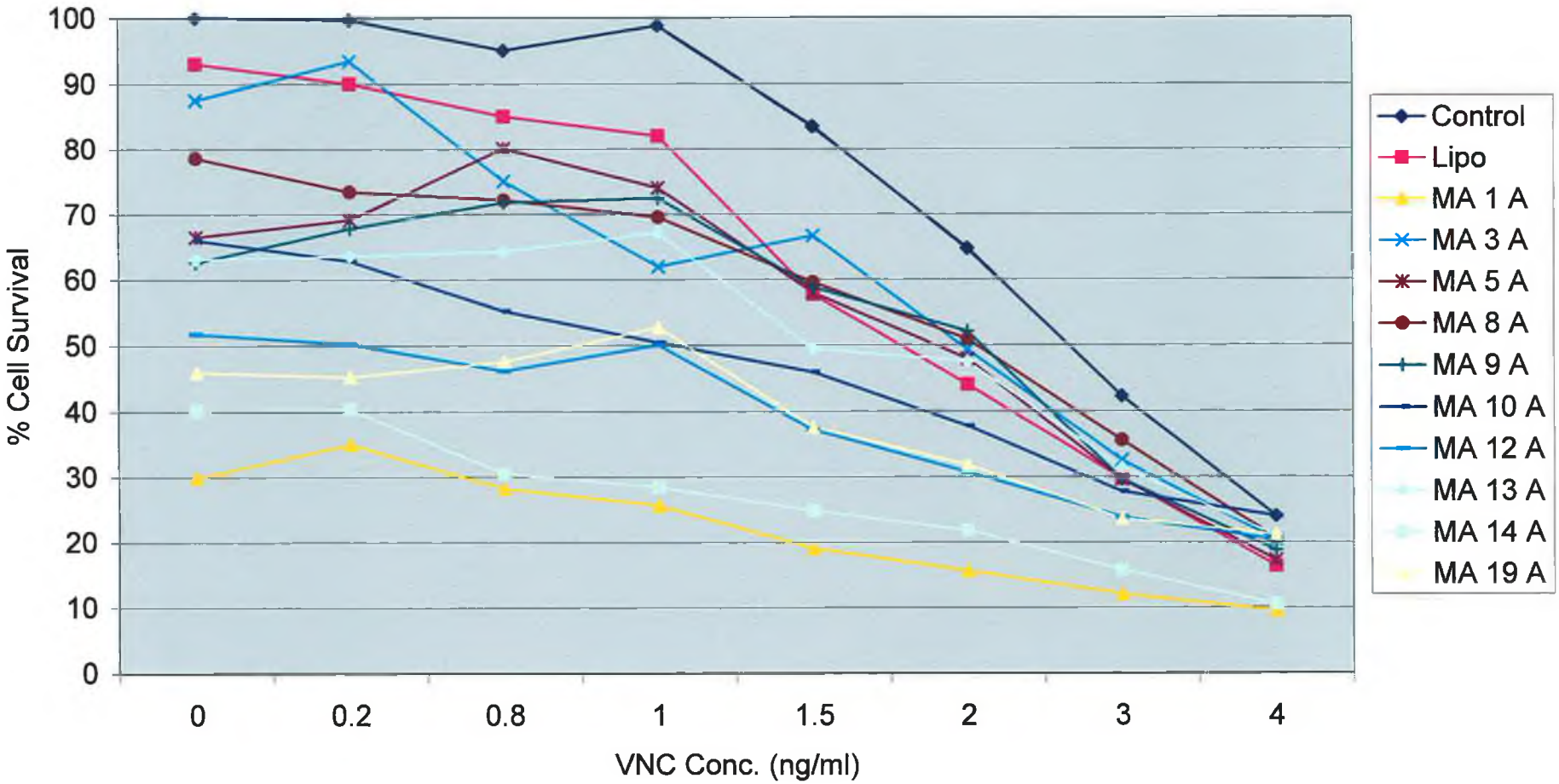

Fig. 3.10.4: Effect of MRP1 Antisense (1.5 um/ml) on Vincristine (VNC) resistance in DLKP-SQ cells

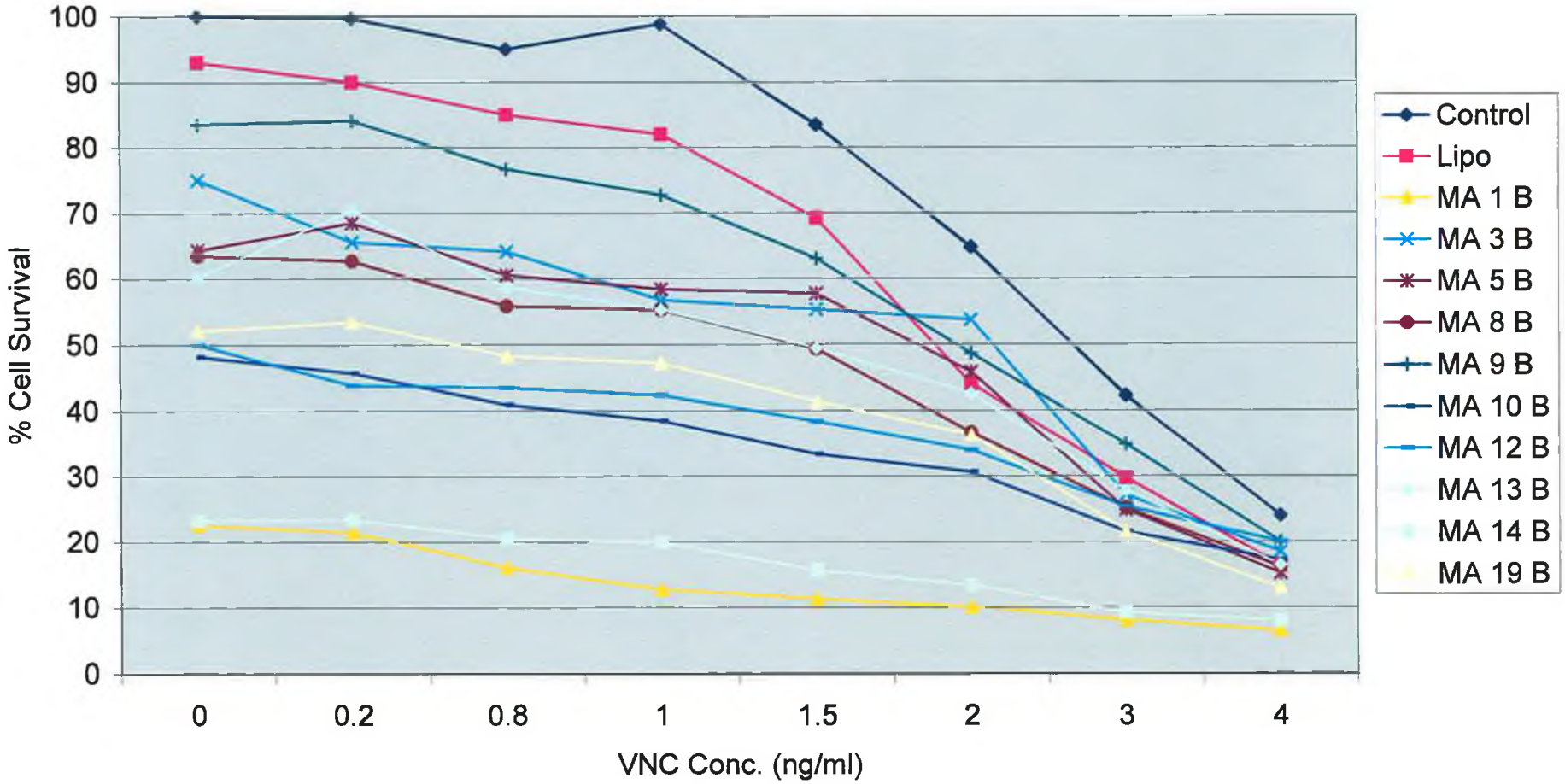

The effects of the antisense (at 1.5μm concentration) on the vinblastine resistance of the DLKP-SQ cells can be seen in Fig. 3.10.5. As can be seen, no significant MRP1-related effect was observed in the transfected DLKP-SQ cells. Again, *MA*s 14 and 19 exerted the most non-specific toxic effect of all the oligos tested.

3.10.3 Use of the RNaseH assay to examine MRP1 antisense cleavage

In Section 3.9.4.5, the ribozyme *in-vitro* cleavage assay had demonstrated the ability of the MRP1 ribozyme to cleave its target fragment and thereby indicated that the failure of the ribozyme to successfully affect the expression and/or activity of the gene *in-vivo* was due to some other factor. It was considered useful to develop a similar assay to examine whether the designed MRP1 antisense oligonucleotides were capable of cleaving their target fragments. To this end, an RNaseH assay was designed to investigate the cleavage properties of the antisense oligonucleotides examined here.

3.10.3.1 Optimisation of the RNaseH assay using an mdr-1 antisense oligonucleotide

In order to standardise the assay, and also to detect the desired cleavage, an antisense oligo which had been comprehensively proven to downregulate expression of its target gene was required. It was also necessary that this oligo recruited RnaseH for cleavage of the target mRNA. An mdr-1 antisense which targets the AUG codon (Alahari *et al.*, 1996) was chosen for this purpose, the sequence of which is listed in Appendix A (Table 7.5A). The type of chemical modification chosen for optimisation of the assay was phosphorothioate, as this type of antisense has been shown to recruit RNaseH to cleave DNA:RNA hybrids (Nakamura *et al.*, 1991; Peng Ho *et al.*, 1996; Milner *et al.*, 1997).

The RNaseH assay was carried out much the same way as for the ribozyme *in-vitro* cleavage assay. Two PCR primers were designed which would anneal to each other during a PCR cycle, amplifying a DNA fragment with a T7 RNA polymerase promoter attached. Once this fragment was purified, a radioactively-labelled RNA product would

Fig. 3.10.5: Effect of MRP1 Antisense (1.5 um/ml) on Vinblastine (VNB) resistance in DLKP-SQ cells

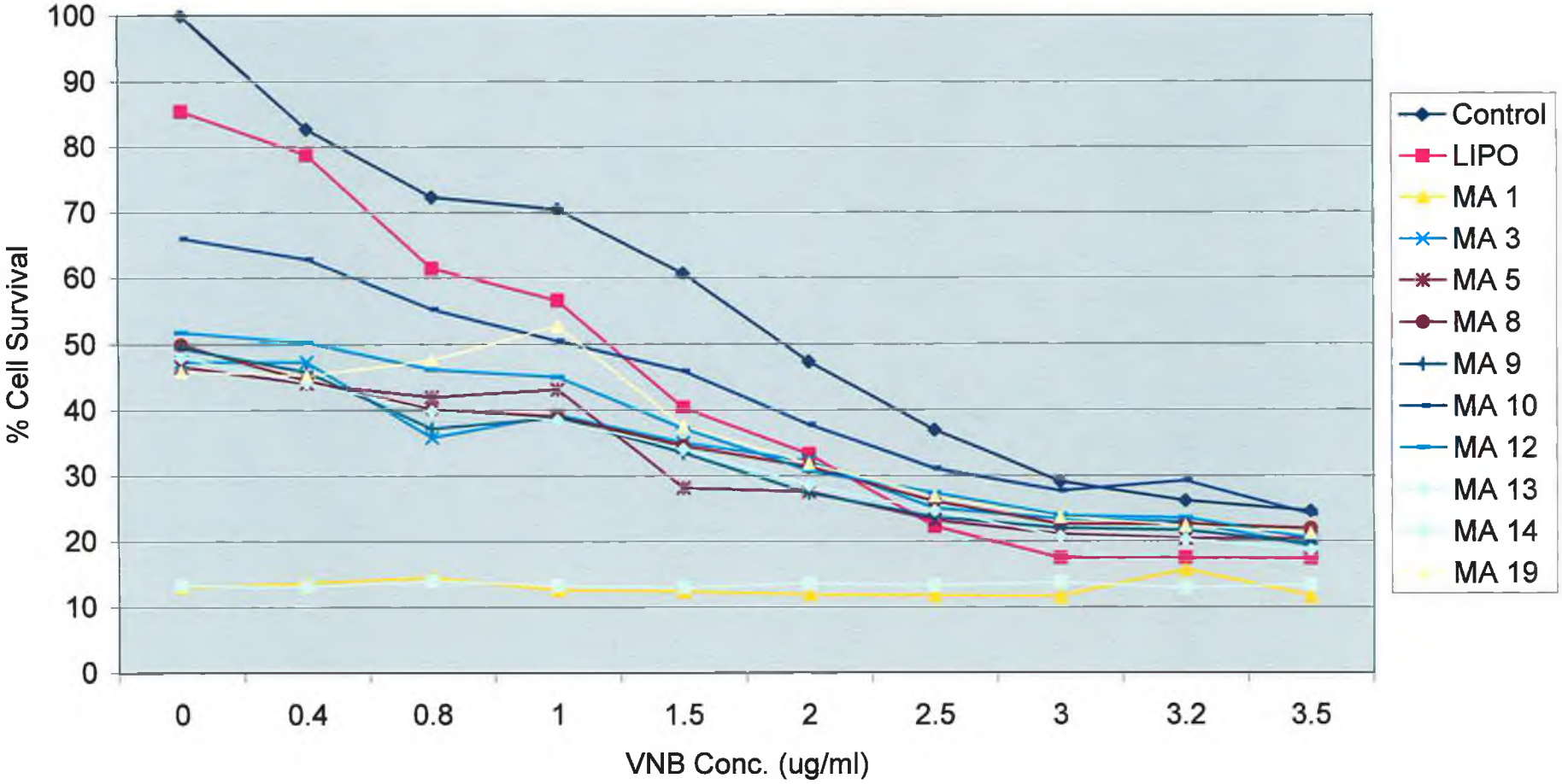

be generated from the DNA template using the Riboprobe™ kit. This radioactively-labelled target RNA could then be cleaved by the addition of the selected antisense oligo in a specifically-controlled RNaseH cleavage assay (see Section 2.4.7), the conditions for which were obtained from previous studies (Nakamura *et al.*, 1991; Peng Ho *et al.*, 1996). The fragments were eluted and sized in a similar fashion to the radioactively-labelled MRP1 ribozyme (see Section 3.9.4.5). A schematic of the expected cleavage and desired products is shown in Fig. 3.10.6.

3.10.3.2 Results of the mdr-1 RNaseH assay

The assay was carried out as outlined in Section 2.4.7. The results of the assay are shown in Fig. 3.10.7. As can be seen, the 38-base fragment of uncleaved target sequence becomes cleaved over time into the smaller 20-, 11- and 7-base fragments, which are observed to accumulate with time. RNaseH-mediated cleavage was observed to occur at a much faster rate than for the ribozyme, with all of the target sequence cleaved after one hour. After this hour, all of the larger fragments (38-base, 20-base) had been broken down into the smallest fragments (7-bases).

3.10.3.3 Use of the Second Generation Chimera™ antisense in the RNaseH assay

The designed MRP1 antisense oligos were used in the same way as the mdr-1 antisense in the RNaseH assay. Each oligo had its own particular target sequence designed and manufactured and each was subjected to analysis using the assay. The sequences for these target primers are listed in Appendix A (Table 7.6A). The procedure was again carried out as outlined in Section 2.4.7.

None of the Second Generation Chimera™ antisense were observed to effectively cleave their target RNA sequences. A typical result from the RNaseH assay is shown in Fig. 3.10.8. As can be seen, a similar-looking banding pattern of cleavage products is obtained. However, a much larger number of labelled bands were observed, most of which could not be sized accurately to those expected cleavage products.

Fig. 3.10.6: Schematic of RNaseH cleavage of mdr-1 target

Fig. 3.10.6a:

Fig. 3.10.6b:

Uncleaved labelled target (38-bases)	
Cleaved Primary fragment (20-bases)	
2nd Cleaved fragment (11-bases)	
3rd Cleaved fragment (7-bases)	

Fig. 3.10.6a: Schematic of binding of mdr-1 antisense (RED) to transcribed radiolabelled target sequence (BLACK) and the cleavage fragments generated by the recruitment of RNaseH; Fig. 3.10.6b: List of expected cleavage fragments.

Fig. 3.10.8: RnaseH cleavage using 2nd Generation Antisense

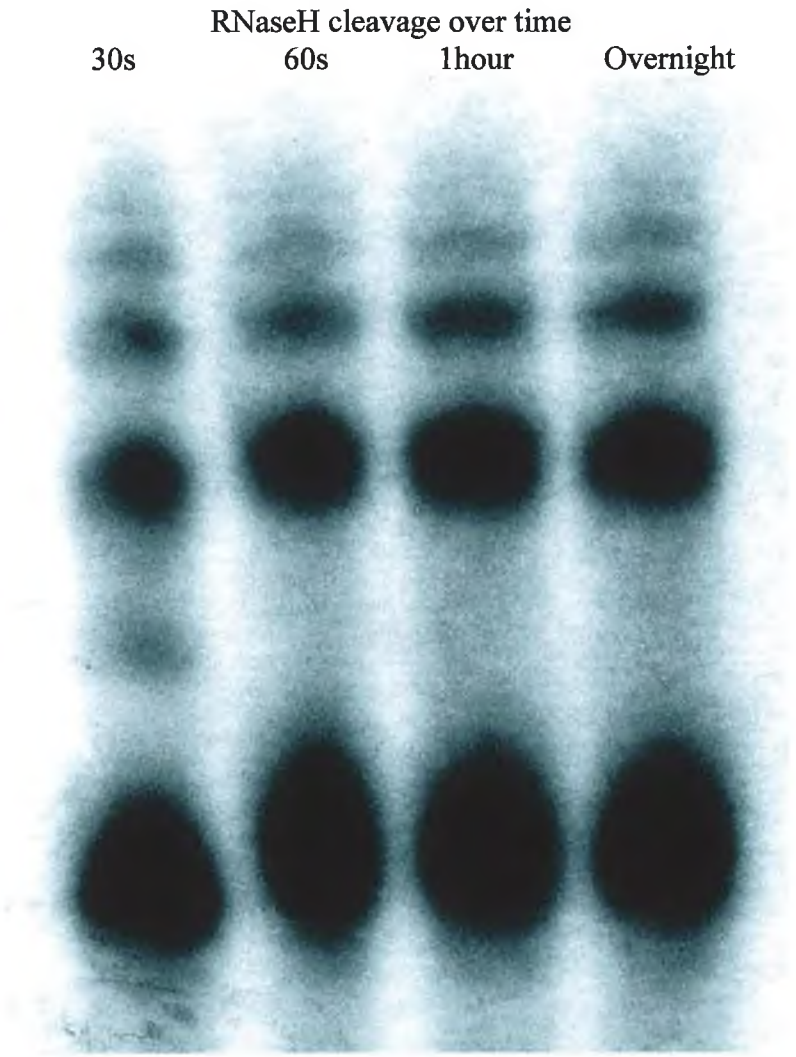

Fig. 3.10.8: Example of RNaseH-mediated cleavage using Second Generation™ antisense oligonucleotides.